AEROSPACE PROPULSION FROM INSECTS TO SPACEFLIGHT

Ulf Olsson

Volvo Aero Corporation
Vice president Technology (ret)

PREFACE

This book is an introduction to the theory and history of aerospace propulsion. It describes how this specific technology has reached its present form and how it may develop in the future.

To understand the technical parts, the reader is assumed to know about thermodynamics and aerodynamics at university level but no prior knowledge of aerospace propulsion technologies is required. For those wishing to go directly to the mathematics, a number of calculation schemes are given in the text as Appendices to various Chapters. They make it possible to write computer programs for performance estimates of the various types of engines.

A number of exercises are included at the end of the different chapters. Solutions to the examples are provided in a separate Chapter at the end of the book together with the relevant equations being used. This can be used as a short handbook to the most important equations.

For the reader specifically interested in the history of propulsion, a separate guide to the main topics and the most famous names is given under **Contents** below. Historical notes are also underlined in the text to be easily located.

Ulf Olsson
April 2012

CONTENTS

Preface

Appendices

Equations for the performance of ramjets, scramjets and pulse detonation engines are given in Chapter 19 and for rocket engines in Chapter 20. Performance estimates for combined engines for spaceplanes are treated in Chapter 21.

Historical Notes

0. INTRODUCTION

The passion to fly must have originated in prehistoric times. Stories of the flight of men, animals, and Gods abound in the myths, art, and religions of ancient civilizations and the magical ability to fly was often attributed to the Gods. Oriental and Western folklore abound with stories of magic carpets, witches on broomsticks, and other forms of movement through the air. As far back as 3500 BC the Babylonians engraved on semiprecious stones the adventures of **Etana**, a shepherd who flew on the back of an eagle. The legendary Chinese prince **Ki Kung-shi** flew a flying chariot and the Persian king **Kai Ka'us**, a flying throne. **Khonsu** was a winged Egyptian God and **Assur**, the main

Assyrian God, had an eagle's wings. In Arabic folklore a magic carpet glided over Baghdad, in a Greek myth Bellerophon rode **Pegasus**, the flying horse and in Roman mythology **Mercury** was the winged messenger of the Gods.

The best known ancient legend on the subject of flight is that of **Daedalus**, the engineer who built the labyrinth on the island of Crete in which the Minotaur lived, having the body of a man and the head of a bull. Daedalus was imprisoned by King Minos together with his son **Icarus**, but they escaped by making themselves wings of wax and feathers. With these Daedalus flew successfully all the way to Naples, but Icarus, excited by the thrill of the new experience, let his youthful exuberance deafen him to his father's warnings. He flew too close to the sun, which melted the wax and sent the boy crashing to his death in the sea below.

Long before men learned how to fly, they sent objects soaring through the air. The arrow dates from the Stone Age and the ancient Chinese flew kites. The early inhabitants of Australia invented the boomerang, with blades carved in the shape of an airfoil.

However, it took a long time before technology had advanced sufficiently to make the dreams of human flight come true. Then in 1783 the first men took to the air in a **balloon** using a principle first discovered by **Archimedes** two thousand years earlier. The balloons would reign the skies for more than a century but in the end it was the reaction principle giving thrust and lift from the accelleration of a jet that made controlled flight possible in a large scale. **Isaac Newton**´s equation for the the thrust of a jet is therefore one of the most important equations in history.

The first manmade object using the **reaction** principle for flight was the **rocket** invented by the Chinese some time before the 10th century. Long before that the insects had learnt how to fly using the reaction principle blowing an air flow downward by their flapping wings. Over many centuries, numerous attempts were made by daring adventurers to fly like insects and birds but the necessary power was much more than that of a man.

A breakthrough came with the discovery in the beginning of the 19th century of the **lifting wing** of the birds. This made it possible to separate lift and propulsion producing lift without flapping. From then on the main problems were to understand how the wings worked and to develop engines with sufficient power. It was not until in 1903, that man could make machines as powerful as a bird and the **Wright Brothers** could make their first flight using an internal combustion engine powering a propeller.

The **propeller** soon gave way to the **jet engine** and during the 20th century, air and space transportation grew into one of the world's most important industries. Modern society is inconceivable without it and it is an essential part of economic development. It is now possible to travel across the globe in a matter of hours rather than the weeks or months of fifty years ago.

For the nearest future, the priorities in propulsion will be on the gradual improvement of existing systems and technologies. For the civil aircraft, that means less fuel consumption for reasons both of economy and ecology. For the military, it means maintaining speed and agility while increasing stealth capabilities.

In the long term we will want to travel as swiftly and comfortably to space as we now do over the surface of the earth. This will eventually lead to radically new engine and aircraft shapes.

The machines used for flight are the most powerful of all produced by man. One hundred years after the first aircraft took off from Kitty Hawk we have raised the power density of our machines from that of a bird at 25 W/kg to that of a fighter aircraft at 2000 W/kg and a space launcher at 20000 W/kg. It took one thousand years of research and experiments to overtake the birds and another century to leave them far behind. Future propulsion systems will be even more powerful.

1. THE BALLOONS LIGHTER THAN AIR

The first controlled flight was made with a balloon in 1783 based on a scientific principle discovered by Archimedes nearly two thousand years earlier. For about 150 years the balloons reigned the skies before aircraft took over after the crash of the great airship Hindenburg in New Jersey in 1937.
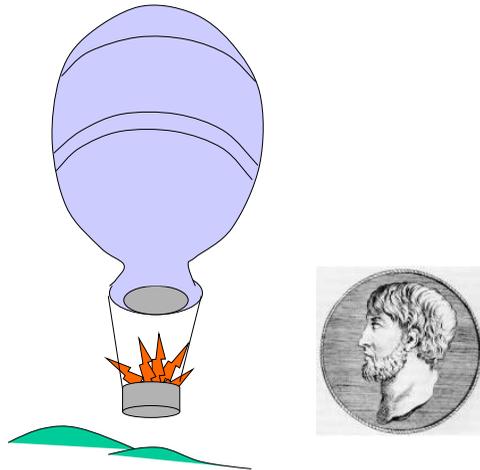
Fig. 1.1 The hot air balloon makes use of Archimedes principle.

The 21st of November 1783 is a remarkable date in human history. On this day a balloon carrying **Jean Pilatre de Rozier**, a physics lecturer, and **Francois Laurent the Marquis d'Arlandes**, a major in the French infantry, lifted a thousand meters into the air and

drifted nearly ten kilometers over Paris. This was the first time that human beings were flying in a "controlled way".

When they took to the air, it was nearly exactly two thousand years after the death of the Greek scientist **Archimedes (287-212 BC)**, the founder of the principle they used. At the side of Newton and Einstein, Archimedes is regarded as one of the most remarkable scientists of all times. He is the founder of the number "pi" and took the first steps towards an infinitesimal calculus. He was also the inventor of many practical machines like the Archimedes' screw that is still used today to raise water from wells.

Archimedes had been a student at the famous university of Alexandria in Egypt, founded by Alexander the Great, but he lived and worked in the Greek city of Syracuse on Sicily. His hometown became involved on the side of Carthage in the great war with Rome about the domination of the Mediterranean. As the Roman army attacked Syracuse, Archimedes made great contributions to defending the city by inventing many ingenious war machines. He was killed by a soldier as the Romans broke through the walls. This was a regrettable mistake because the Romans were very well aware of Archimedes and his works and the Roman commander Marcellus had given orders that he should be spared.

The law of hydrostatics, often called **Archimedes' principle**, states that a body immersed in a fluid is exposed to a lifting force equal to the weight of the displaced fluid and it is of course also valid for a balloon in the air. This discovery is said to have been made as Archimedes stepped into his bath and saw the displaced water overflowing.

The idea of filling a closed container with a substance lighter than air, causing it to rise through the atmosphere, was probably conceived in the thirteenth century. For lack of a substance to fill the balloons, nothing of practical value was achieved for several hundred years until in 1670 an Italian monk, **Francesco de Lana**, proposed a vacuum balloon. Four copper spheres, from which air had been exhausted, were to support a car equipped with oars and a sail. Of course, he overlooked the phenomenon of atmospheric pressure, which would have crushed the spheres.

A hundred years later, the first balloon was flown successfully in public. The two brothers **Étienne and Joseph Montgolfier** worked for the family's paper-making firm at Annonay, near Lyon, France. They also owned a washing business and they had watched shirts billow as they dried in the air rising from a fire. They then released scraps of paper over the hearth, watched them rise up into the chimney and came to the incorrect conclusion that smoke rather than hot air caused the lifting power. Maybe that is how they got the brilliant idea to attach a fire to a balloon. It worked, but not because of the smoke. Instead, the hot air rising up into the balloon, being less dense than the cool air outside, gave rise to the lifting force in accordance with the Archimedes principle. Thus the **hot-air balloon** powered by an attached fire pit was born.

The first living creatures to fly under a Montgolfier hot air balloon were a sheep, a duck, and a rooster on the 19th of September 1783, in the Montgolfiers' first demonstration flight for King Louis XVI before the two test pilots Rozier and d'Arlande took to the air two months later.

A few weeks after this first manned flight in a hot air balloon, two other Frenchmen, **J A C Charles and Noel Robert**, took off in a balloon filled with **hydrogen**. In a second flight that same day, Charles reached an altitude of three thousand meters. Such hydrogen filled balloons soon became dominant because of their higher lifting power.

Balloons came to be used for military reconnaissance purposes for the first time in June 1794 at the battle of Fleurus between the revolutionary French forces and the Austrian army. It was since used intermittently during the wars of the 19th century for instance for dropping bombs as at Venice in 1849 but with no great success.

The problem was that balloons were basically handicapped by a total lack of directional control. This proved to be disastrous in the Swedish balloon expedition to the North Pole in 1890 led by **S. A. Andree**. He planned to guide his balloon by the way of ropes trailing over the ground. Unfortunately, the ropes detached leaving the balloon uncontrollable and the expedition stranded and eventually perished in the polar ice.

The problem was solved with the introduction of power plants or engines on elongated-like balloons. In 1852 **Henri Giffard** of France flew such a **"dirigible"** powered by a steam engine and a propeller. The term "dirigible" in fact means controllable. The elongated shape also helped reduce the drag in order to decrease the power required. The shape could be kept by filling the balloon with gas instead of hot air.

The problem with such elongated dirigibles was that they would buckle or bend if they were carrying a heavy weight or in bad

weather. By adding a wooden keel along the bottom this problem was solved and larger dirigibles could be built.
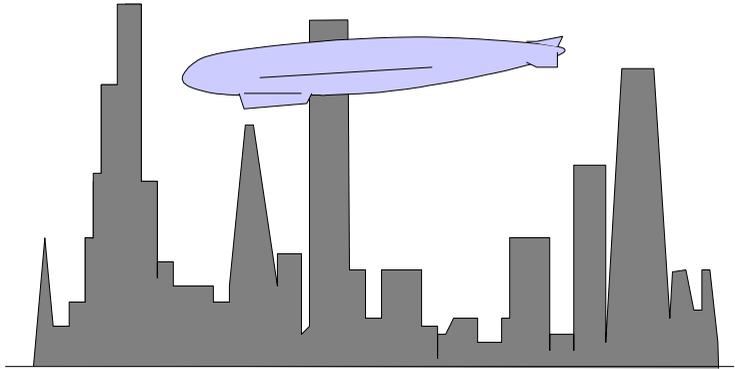
Fig. 1.2 The hot air balloon developed into gas filled dirigibles

The most successful builder of this type of lighter-than-air craft was a German, Count **Ferdinand von Zeppelin**, whose name is synonymous with large rigid dirigibles. He designed and built them around a steel frame. This made it possible to make much larger dirigibles, which were able to lift many people and much more weight.

Zeppelin got his idea about a long thin balloon while serving as a volunteer on the Union side in the American civil war in the 1860's. Returning to Germany he advanced to become a general of the cavalry. As a native from Wurtenberg, he openly criticized the

dominant role of Prussia, which put an end to his military career. Free from the military, he started to design and build airships based on the ideas of his youth.

In the early 1930's, the first Zeppelin machine was able to make a Trans-Atlantic flight to the United States. The large airships were very successful until one of them, the Hindenburg, was destroyed by fire while attempting a landing in **1937** in Lakehurst, New Jersey with many people onboard. Pictures of the huge machine breaking down in flames were spread over the world and for a long time afterwards no one dared to fly on a Zeppelin craft.

Zeppelins had in fact numerous flaws such as difficulty of control and vulnerability to the weather. They were also rather slow with a cruising speed of about 125 km/h. But the big mistake was to use hydrogen, which is a very flammable gas, to fill the balloon. Balloons are nowadays filled with **helium**, which does not burn. In any case, the Hindenburg accident put an end to the balloons for transportation in the air and left the field open to the aircraft, which soon came to dominate flight. It was based on a very different scentific principle from that of the balloons.

2. NEWTON AND THE REACTION FORCE

The 'heavier-than-air' flying machines are based on the reaction principle. It was first applied in practice to rockets by the Chinese sometime in the first millennium and later explained by the great scientist Isaac Newton. His equation for the reaction force of a jet $F = \dot{m}V_j$ is the basis for both aircraft and rockets. It is probably the most important equation of all times.

Apprehensive but with great expectations the young astronomer Edmund Halley arrived in Cambridge on a rattling coach. He had an appointment with the reclusive genius **Isaac Newton**.

Together with Einstein and Archimedes, Newton (1642-1727) is regarded as one of the greatest scientists of all times. However, he may also be the origin of the myth of the mad scientist, which has become such an important part of popular culture. This was the cause of Halley's apprehension.

Newton was really a very strange man. He was born into a farming family but proved to be an inept farmer and with eighteen he ended up in Cambridge to study for priesthood. While at Cambridge, he became interested in mathematics and physics. Suspicious of other people, he decided to live in celibacy and devote himself exclusively to science. However, he was forced to return to the countryside when the university closed because of a

plague. During this forced retirement, he made some of his most important discoveries.

After intense work on returning to the university, he became professor of mathematics at 28. He often forgot to eat, went about in shoes that were falling apart and with his unkempt hair falling to his shoulders. As suspicious as he was of human beings, he loved animals and when his cat had kittens he took up a hole for each kitten in his door with its name inscribed over it.

He was utterly impractical but his devotion to science was fanatic. He even experimented on himself by for instance poking his eye with a needle to observe the colored optical rings produced. He did not publish anything considering it a waste of time and fearing that he would be drawn into discussions with people, who anyhow were unable to understand his work. The university obliged him to give just one lecture a year but those lectures were such that the students preferred to stay away and he often talked to an empty hall.

Finally, he published a work on optics, where he proposed that the light was a stream of particles. Unfortunately, another professor, Robert Hooke, criticized this idea, saying that the light was a type of wave. Much later, Einstein showed that light could be both things but Newton became so incensed over the criticism of Hooke that he decided to leave science altogether.

For the next twenty years, Newton came to devote more and more time to alchemical research and attempts to date events in the bible. He wished to make gold out of mercury, but this proved impossible even for a man of his abilities and led to nervous break-downs.

This was the situation when Halley appeared in Cambridge. He had a specific question to Newton. What would be the orbit of a planet circling the sun?

To his relief, Newton welcomed him friendly and answered that the orbit would be elliptical. When Halley asked how he could know that, Newton replied that he had calculated that long ago. He promised to find the calculations among his papers and send them to Halley.

Once Newton had started to look at his old work, his interest in science returned and Halley persuaded him to write down all his findings over the years. The result, published in 1687, was the famous book *Philosophia Naturalis Principia Mathematica,* one of the most important and influential scientific works of all times. In it Newton formulated the classical theories of mechanics, optics and mathematical calculus.

The book made Newton an instant celebrity. He was elected to parliament and moved to London, where he became a very pompous president of the scientific academy, the **Royal Society**. In this position, he saw to it that the portrait of his archenemy Robert Hooke, himself a former president of the academy, got lost when the academy moved to a new site. He also became embroiled in a bitter feud with the German mathematician Gottfried Leibniz about who of them was the originator of the infinitesimal calculus. This scientific quarrel were continued by their respective supporters long after both of them had died.

Newton finally left science altogether and ended his life as director of the British Mint. After his death, it was discovered that his body

contained large amounts of mercury, probably as a result of his attempts to produce gold from that substance.

In *Principia Mathematica* Newton summarized his understanding of physical motion into three scientific laws:

1. A body in motion tends to remain in motion at a constant speed and in a straight line unless acted upon by some external force.
2. *The rate of change of* **momentum** *(mass x velocity) of a body is proportional to the impressed force and takes place in the direction of the force.*
3. For every action there is an equal and opposite reaction. The two actions are directed along the same straight line.
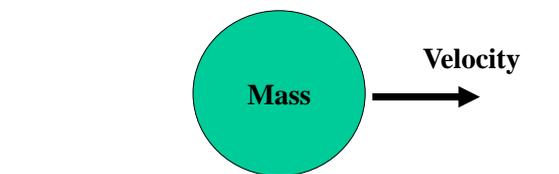
Fig. 2.1 Momentum is mass x velocity

The first law is only a special case of the second where the force F=0. In mathematical terms, the second law states that the force

required to increase the rate of momentum of a **mass m** and **velocity V** is:

$$F = \frac{d(mV)}{dt} \qquad\qquad (2.1)$$

It follows from the third law that if the rate of momentum is increased, a force in the opposite direction is produced on the mover. This so called **reaction force** was discovered in practice long before Newton. Aulus Gellius, a Roman, in his book "Noctes Atticae" from 170 B.C. tells a story of a Greek named **Archytas** who lived in the city of Tarentum, now a part of southern Italy. Somewhere around the year 400 B.C., Archytas is said to have mystified and amused the citizens of Tarentum by flying a pigeon made of wood suspended on a wire and propelled by escaping steam. The pigeon may thus have used the action-reaction principle.

Heron, a Greek scientist from Alexandria in Egypt, developed the first reaction machine about the year 60 A.D. Steam coming from a boiler entered through two hollow tubes supporting a sphere causing it to spin by the reaction forces. Heron is said to have used this invention to pull open temple doors without the aid of visual power thus giving the impression of an act of the Gods.

Having abundant access to slave labor, the Romans had no real incentives to develop machines other than for military purposes. Also, the Western Roman empire collapsed in the fifth century under the pressure of the Germanic tribes. Its engineering skills disappeared together with the institutions that had organized their use. The leadership in technology went over to China and to some extent to the Islamic world. It was in ancient China that the first

practical invention was made based on the reaction principle, the rocket.
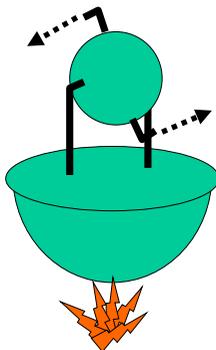
Fig 2.2 Heron's Aeolipile-the first reaction machine?

When you fire a gun, a small gunpowder explosion occurs in the shell causing the bullet and smoke to be pushed out the end of the barrel and there is a recoil into your shoulder. The same thing happens in a **rocket**, see Figure 2.3. Its combustion chamber is very much like a gun barrel with one end open. The burning releases gases and heat. The gases are pushed out of the exhaust nozzle and the reaction or push in the opposite direction drives the rocket forward.

Note that the jet does not have to push against the outside atmosphere as some people tend to believe. In fact, the rocket functions even better in a vacuum. It is the reaction principle and

not the pressure that produces the thrust. If not, flight in the emptiness of space would be impossible.
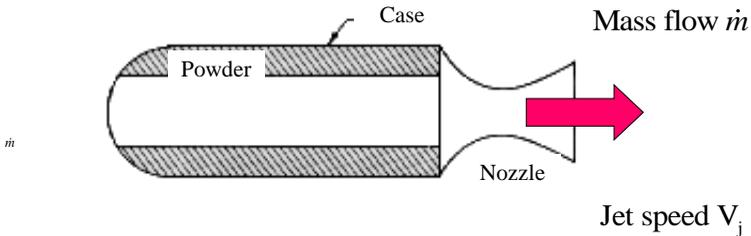
Fig. 2.3 The solid rocket-the simplest of all reaction engines

If mass is leaving the rocket at a **rate of mass flow "$\dot{m}$"** with a constant **jet speed "V_j"**, the rate of change of momentum of the rocket and therefore the force or **thrust "F"** acting on it is from Eq. (2.1):

$$F = \dot{m}V_j \qquad\qquad (2.2)$$

Forming the basis for aerospace propulsion, this expression of Newton for the force (or thrust) produced by a jet is perhaps the most important equation in the history of science. It has changed our world even more than Einstein's famous $E=mc^2$.

We do not know exactly when the rocket was invented but it was probably during the first half of the first millennium. The scientific understanding of the reaction principle through Newton thus came a long time after the invention itself. This is not unusual in the history of engineering. It is often said that science precedes technology. Many times, however, the invention is made first by clever and practical people. Science and scientists then explain why it works and provide the know-how for refinements.

Air in at V

Air out at V_j
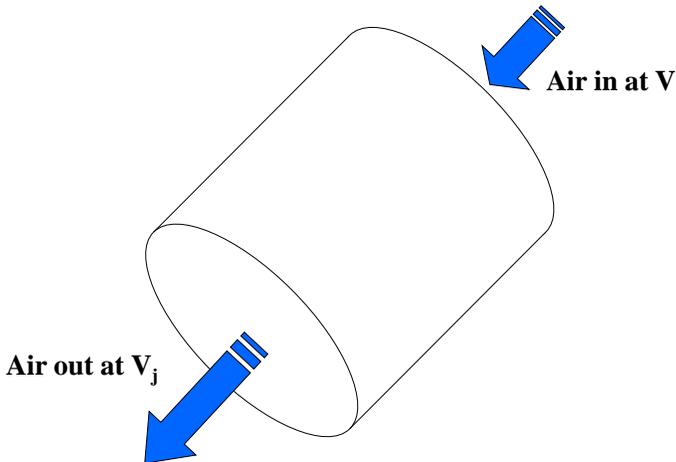
Fig. 2.4 The airbreathing engine.

The rocket, especially of the solid propellant type, is a relatively simple device. Many years later, the next step was taken. In the rocket, the jet that produces the reaction force is made up of the propellants carried in its tanks. However, one could also use the surrounding air to generate a lifting reaction force or a forward thrust. This is the basic idea behind aircraft and air breathing engines.

In the air breathing engine, air enters at the **flight speed V** and leaves at the **jet speed V$_j$.** The result is a thrust that according to Newton is the difference between the momentums leaving and entering the engine, that is:

$$F = \dot{m}(V_j - V) \qquad\qquad (2.3)$$

The main advantage of the air breathing engine is of course that most of the fluid necessary for the jet must not be carried in the vehicle itself but is taken from the surrounding atmosphere. However, as is seen from Eq. (2.3), such an engine could never fly faster than its jet speed without losing its thrust. This is the main disadvantage of air breathing engines compared to rockets. In the latter, no air is allowed into the engine, the jet consists entirely of the propellants, and there is no speed limit.

3. INSECTS AND THE LIFT OF WINGS

The insects were the first to use the reaction force for flying and a study of the insects discloses many secrets about flight. Of great importance is Bernoulli's expression for the dynamic pressure $q=\rho V^2/2$ first formulated in 1738. It can be used to calculate the lifting and resisting forces on bodies moving through the air such as an insect. Together with Newton's equation, it is at the foundation of aeronautics.
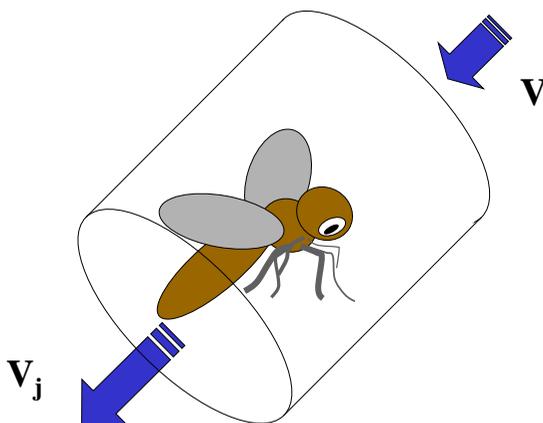
Fig. 3.1 The insect falls forward on a flow of air

But how to produce the jet? Nature never invented the wheel so the solution became the flapping of wings. The first creatures to make use of the reaction principle for flight were the insects.

The first appearance of winged insects is shrouded in the past but they probably lifted into the air about 300 million years ago. They first used extensions of the body for gliding and these gradually evolved into wings for powered flight.

Insect flight is easier to understand than bat and bird flight because the required forward thrust is not very large. Basically, the insect falls forward on a flow of air that it blows downwards with its flapping wings, Figure 3.1. The tilt angle is relatively small (around 20 degrees) and the jet speed is typically 2-3 times the flight speed. According to Newton's equation this creates a reaction force that carries the insect along.

Insects come in a huge variety of shapes. It is not at all certain, that natural selection leads to the most optimized aerodynamic performance. Many non-technical factors like courtship and mating influence the natural selection in the animal world as it does for human beings. The striking difference in shape between for instance a butterfly and a wasp, see Figure 3.2, can, however, be explained from Newton's equation.

Nothing can be produced without **work** and this is also so for the insects. Technically, work is defined as the acting force multiplied by the distance over which it acts. The amount of work required to bring a mass m from a velocity V to another velocity V_j is called the increase of **kinetic energy** stored in the mass. From Eq. (2.1) it is:

$$W = \int_V^{V_j} F ds = \int_V^{V_j} \frac{d(mV)}{dt} ds = \int_V^{V_j} mV dV = m\frac{V_j^2 - V^2}{2} \quad (3.1)$$

The **power** is defined as the work per unit of time so the power that is needed to produce a continuous mass flow with a certain jet speed is:

$$\dot{W} = \dot{m}\frac{V_j^2 - V^2}{2}$$

(3.2)

To fly fast we need a high jet speed but this equation shows that the required power grows much more rapidly than the thrust as the jet speed increases. High flight speed therefore comes at the cost of lots of power. This consequence from Newton´s equation helps to explain the different shapes of butterflies and wasps as well as of civil and military jet engines.

$$Power = \frac{1}{2}\dot{m}V_j^2$$

$$Thrust = \dot{m}V_j$$
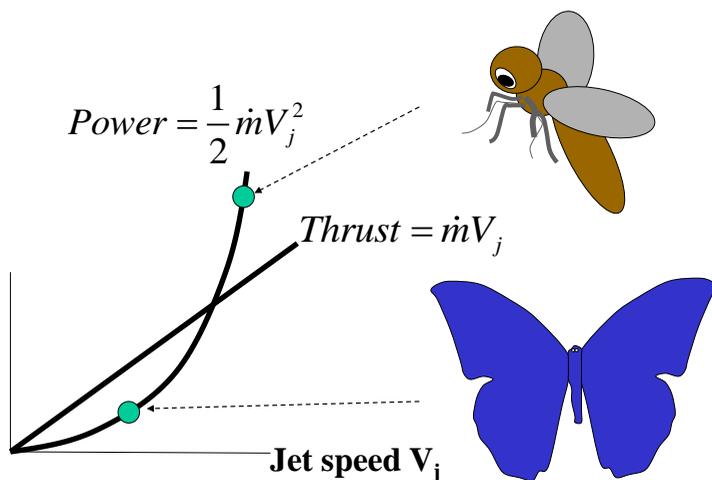
Jet speed V_j

Fig. 3.2 Insects come in many different shapes

The **butterfly** wants to fly over large distances. Some butterflies even cross the Mediterranean. To minimize its effort it should fly

with a low jet speed according to Eq. (3.2). To carry its weight, it then needs a high mass flow as is seen from Eq. (2.2). To summarize, the butterfly should have a low wing speed and consequently a high wing area.

A problem with a large wing area is that the flight gets wobbly and exposed to winds and turbulent air. The **wasp**, that wants a swift and stable flight, therefore contrary to the butterfly uses a high wing speed and a low wing area. The effort is larger and the range is less but it can fly at a much more variable speed and with higher stability. We will see later on that a civil jet engine is shaped like the butterfly and a military one like the wasp.

One disadvantage of having a small wing span is obviously that the wings must be able to beat very rapidly. Many small insects such as midges have beat frequencies of up to 1000 per second, which is impossible using normal nerve-muscle interaction.

In insects employing a low wing beat frequency, the thorax muscles act directly on the wing base as in butterflies. In insects with high wing beat frequencies, the wing is a lever structure acting through muscular control of external body plates, the movement of which is transferred to the wing. The muscles moving the body plates are like vibrating strings stimulated by nerve impulse. A small movement of the body plates causes a large movement of the wing.

Dragonflies, are remarkable because they are able to move their large wings with a relatively high frequency. They are hunters that rely on their ability to make swift dashes to catch their prey, which calls for high power. Dragonflies were among the first insects to

take to the air. One has found dragonflies with a wingspan up to 70 cm from the times of the dinosaurs.

The dragonfly is also unusual because it has two wing pairs, which may operate in 180 degrees phase shift, see Figure 3.3. This is an advantage in order to stabilize the flight. All insects had basically two pairs of wings but most modern insects have lost one pair or coupled the wings together. In some insects such as flies, the second pair has modified into a pair of balancing structures called halteres. These provide positional and motional feedback to the fly.
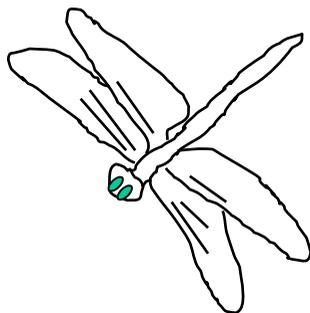
Fig. 3.3 The dragonfly is one of the most advanced insects.

Dragonflies' flight capabilities are prodigious. Though counter-stroking is the normal mode, synchronized stroking is used in order to maximize thrust when changing direction quickly.

Dragonflies may also practice updraft gliding by adjusting their wing positioning to float in the air without beating of the wings.

To make things more impressive, dragonflies can fly with different wings doing quite different things, even using different methods to generate thrust. Asymmetric wing stroking permits wings on one side to drive forward, and the other side to drive back, spinning the animal on its axis in a single combined stroke.

All dragonflies achieve their mastery of flight by varying what their wings are doing in a coordinated fashion. They can adjust wing shape, stroke length, angle of attack, move a wing forward or backward from its "usual" position, stop one or two wings, adjust relationships between any two wings on either side of the body and so on. Their flight is very powerful. Accelerations to 4g in a straight line and 9g in turns are documented. Dragonflies are also able to accelerate very fast. In short bursts they may reach speeds of 7 m/s. The wasp is also relatively rapid at 6 m/s while the bumble bee reaches 3 m/s

It is obvious that a lot can be explained by Newton's equations. However, it is difficult to calculate the mass flow and jet speed produced by the wing. Therefore, in order to understand the flight of an insect, we need to study what happens at its wings in more detail. Obviously, the reaction force from the downwash jet is balanced by the pressure under the wing as it moves down. If we knew this pressure, we would also know the lifting force of the wing. To find this pressure, we need to turn to the science of hydrodynamics.

The science of hydrodynamics was born in 1738 when **Daniel Bernoulli (1700-1782)** published his famous textbook "*Hydrodynamica*". Daniel was from Basel in Switzerland and he

had a good scientific family backing. His father Jakob was an excellent mathematician and his uncle Johann even better, being credited as the inventor of the integral.

After having won the great Nordic War against King Charles XII of Sweden in the early 1700's, Tsar Peter had founded a new Russian capital, Saint Petersburg, to secure the access to the Baltics. He and his successors wanted to make it a leading European center so they invited leading scientists to come and work in their new capital.

Daniel started to work on his book on hydrodynamics in 1729 while a professor of mathematics in St Petersburg. He tried to understand the relationship between pressure and velocity in a fluid. This was further developed by his father, Johann, in another book, "*Hydraulica*", of 1743.

In fact, none of the Bernoullis derived the equation that has been named after them. This fell to another Swiss, **Leonhard Euler**, who is one of the most important mathematicians of all times. Euler, also from Basel, was seven years younger than Daniel whom he followed to St Petersburg, where he also became a professor of mathematics and finally derived the Bernoulli equation in 1764. This equation appears in many physics textbooks, as well as in fluid mechanics and airplane textbooks and it has formed the basis for the study of fluids in motion and the forces acting on flying bodies.

Assume now that the wing of the insect with area S moves downward with the speed V in a frictionless tube, see Figure 3.4. Consider an element of a fluid of density ρ moving along the tube. The fluid changes its velocity from V to V+dV and the pressure changes from p to p+dp.
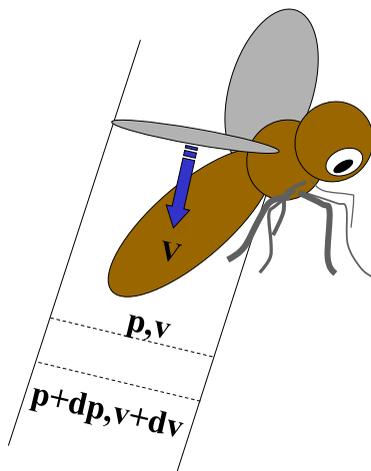
**Fig. 3.4 The reaction force is balanced by a
pressure force below the wings.**

The mass flow is the same at inlet and outlet of the element.
According to Newton's reaction principle, the force acting on the
end surfaces of the tube element is the mass flow through it
multiplied by the velocity of the jet. This must be balanced by the
net force due to pressure so:

$$\rho S v(v+dv) - \rho S v v = \rho S v dv = -S dp \qquad (3.3)$$

This relation can be integrated along the stream tube to give for
compressible fluids:

$$\int \frac{dp}{\rho} + \frac{v^2}{2} = const \qquad (3.4)$$

Note, that in the derivation of this equation, the dissipation of energy by viscous forces was neglected (inviscid flow), and there was no introduction of energy (no heat addition).

Relative to the wing in Figure 3.4, there is a flow of air with the velocity V at the surrounding pressure p coming to rest at the wing. In incompressible flow, which is a good approximation provided that the speed is not too high, the pressure at the wing becomes:

$$p_{tot} = p + \frac{1}{2}\rho V^2 \qquad\qquad (3.5)$$

In other words, if a flow is stopped by an obstacle such as a wing, the pressure will increase by an amount:

$$q = \frac{1}{2}\rho V^2 \qquad\qquad (3.6)$$

This is often called the **dynamic pressure** and Eq. (3.6) is called **Bernoullis equation**. At the side of Newton's equation, it is one of the fundamental equations in aeronautics. It is used to calculate the lifting and resisting forces on wings and bodies.

For a long time, Bernoullis equation for the dynamic pressure, as derived by mathematicians, was regarded with considerable suspicion by more practical engineers. The reason for that was the Scot **John Smeaton**, one of the most famous civil engineers of the 18th century. In 1759 he presented a paper on the power of water and wind and since then, engineers for more than 150 years tried to use the following relation for the dynamic pressure:

$$q = K\rho V^2 \qquad\qquad (3.7)$$

where K was given by Smeaton as a constant around 0.4 instead of the mathematically correct value 1/2. Much later this was to create considerable problems to the Wright Brothers. Not until 1913, was it established by **John Airey** at the University of Michigan that the constant was indeed equal to 1/2 and the mathematicians were proved to be right.

The square dependence on velocity had been established earlier experimentally by among others the Frenchman **Henri Pitot (1695-1771).** Six years before the "*Hydrodynamica*", he invented the famous Pitot tube, now used to measure the speed of airplanes. His basic idea was to compare the pressure in two tubes. One of the tubes was straight so that the water could flow unimpeded, the other was bent at a straight angle so that the water stagnated. Pitot found that there was a difference and concluded more or less intuitively that it was related to the square of the water velocity. Using this instrument, he found that the speed of the water in the river Seine decreased with depth while the contemporary assumption was that the speed should increase with depth.

Let us now apply Bernoulli´s equation to the moving wing. The lifting force produced by the pressure under the wing should according to Newton correspond to the reaction force of the downwash. Introducing the mass flow of the downwash into Eq. (2.2) and using Eq.(3.6), the lifting force should be:

$$L = \dot{m}V = \rho S V^2 = 2q \qquad\qquad (3.8)$$
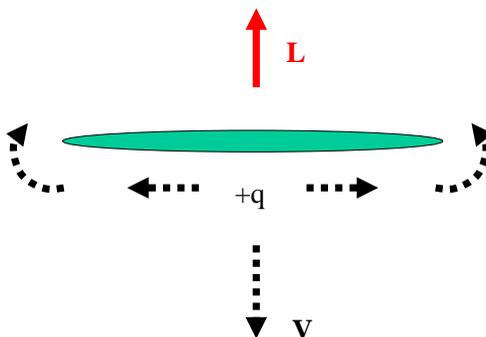
Fig. 3.5 Air leaking around a wing moving down

In reality, it is not so simple because of air leaking around the wing. Also, in real flight, the air is meeting the wing at a certain so called "angle of attack". To take such effects into account, it is common to introduce a **"lift coefficient"** $C_L < 2$ so that the lift of the wing having a surface area S becomes:

$$L = C_L \frac{1}{2} \rho V^2 S \qquad\qquad (3.9)$$

Eq. (3.9) may be used to find out how much weight an insect wing can carry. Some lifting force is produced also during the upstroke due to twisting of the wing. If this is neglected and if the summary force perpendicular to the wings is L during the down stroke with α as the angle of the wing to the horizontal, then the average

vertical force of the two wings may be found. This is balanced by the weight of the insect so that:

$$mg = 2\frac{L}{2\Phi} \int_{-\Phi/2}^{\Phi/2} \cos\alpha\, d\alpha = 2L\frac{\sin\Phi/2}{\Phi} \qquad (3.10)$$

If the beating wing makes a period of 2Φ radians with a frequency of ω periods/sec and if "**b" is the length of the wing**, then the average speed of the geometric center at half-wing b/2 is approximately V=$\Phi\omega$b. From Eqs. (3.9) and (3.10), the weight of an insect in flight is then:

$$m = \frac{\Phi\sin\Phi/2}{4g}\rho\omega^2 b^2 SC_L \qquad (3.11)$$

A measure of the effort of the insect in flight is the power it must use per body weight. The average **power of each wing** over a wing beat cycle is LV/2. Solving for L from Eq. (3.10), this leads to the following expression for the effort required for the two wings:

$$\frac{\dot{W}}{m} = \frac{\Phi^2}{2\sin\Phi/2} g\omega b \qquad (3.12)$$

where from Eq. (3.11):

$$\omega b = \sqrt{\frac{4}{\rho C_L \Phi\sin\Phi/2}\frac{mg}{S}} \qquad (3.13)$$

Those relatively simple equations provide many interesting insights into the life and circumstances of the insects. An interesting consequence of the equations is that it would be possible to fly with less effort and with more weight in a low gravity environment. If we ever create an artificial biosphere on for instance the moon or at a space station, we can expect the insects there to be very much larger than on earth.

The lift coefficient C_L is perhaps the most important parameter in aeronautics and its size is a measure of the aerodynamic efficiency of the wing. A high lift coefficient helps the insect to support a large weight as is seen from Eq. (3.11).

There is a popular story that **bumblebees** could not fly. The reason for that is that calculations on real insects show that the lift coefficient needs to be considerably higher than the theoretical maximum $C_L = 2$ to lift the insect, see Example 3.1. It is therefore obvious that they must employ some high-lift mechanisms. In fact, researchers have found that insects use three distinct but interacting techniques to gain extra lift.

Insect wings come in a huge variety of shapes, sizes, and appearance but in essence they are passive membranous foils that depend largely on the arrangement of their supporting framework for many of their aerodynamic properties. In flight, the wings are distorted by the changing forces acting on them, but in an effective and efficient way. The leading edge of the wing has a much stronger and stiffer structure than the other regions of it, which are more flexible and capable of twisting. The joints between wing and body are remarkable for the complex movements they allow and their ability to store and release energy appropriately at different stages in the flapping cycle.

One of the mechanisms employed to gain lift is called "**delayed stall**". This occurs as the insect sweeps its wings forward at a high angle of attack cutting through the air at a steeper angle than that of a typical airplane wing. On a fixed wing, like that of an airplane or bird, the flow would separate from the wing and break down into vortices (stall) at such a high angle, lose lift, suffer increased drag and end in disaster. Under some conditions, however, a structure called a **"leading edge vortex"** can form and sit on the top surface of the wing. The insects use this to delay stall and create extra lift.

Another technique used by insects is called "**rotational circulation**". As the insect wing nears the end of its stroke, it rotates backward, creating backspin. Just as backspin lifts a tennis ball making it fly longer, so it can provide extra lift for an insect.

From a third mechanism called "**wake capture**" an insect gains lift by recapturing the energy lost in the wake behind the wing. As the wing moves through the air, it leaves vortices of air behind it. If the insect rotates its wing before starting the return stroke, the wing can intersect with its own wake and capture extra lift to keep the insect aloft.

Blood is supplied to the wing through longitudinal vessels, which makes for very noticeable **corrugations** over the wing surface. Such corrugations are sometimes used on glider wings and are being investigated for airliners. They decrease the drag by delaying the separation of the flow over the wing through the creation of turbulence. It is possible that insects are able to generate very high lift-to-drag ratios with the help of this mechanism.

In addition, studies of insects have revealed another mechanism of lift generation. With the body nearly vertical, the wings are brought into flat contact behind the back and are then flung open as one opens a book. This creates a temporary vacuum on the upper side of the wings, which increases the lift force. This **clap and fling** mechanism can generate lift coefficients up to 6-8 times that of a flat plate in an equivalent steady flow. It was originally observed in very small insects with a wingspan of around 2 mm but is also found in some medium sized and large insects such as butterflies and moths. Some dragonflies use it for take-off. It is not generally used, maybe because of the wear and damage of the wings caused by the repeated clapping.

Finally, the **bee** is said to have a line of breathing holes along its body. Air passes in and out of these holes, which produces the loud buzzing noise typical for bees. The noise is at the same frequency as that of the wing beats because valves in the holes are synchronized with the wings by the nervous system. The compression pulses coincide with the downbeat of the wing generating extra lift.

It is obvious that the aerodynamics of the insects are still beyond most of our own knowledge. Calculations using the previous equations also show that the power of insects is awesome compared to human beings, see Example 3.1 below. The specific power of insects may reach 100 W/kg of body weight while a man can perform a mere 3 W/kg. The beautiful butterfly is a very powerful creature indeed.

Ex 3.1

A typical bumblebee has a weight of 175 mg, a wing length of 13 mm, a wing area of 50mm^2 and a wing beat angle of 114° with a frequency of 150 periods/s. The air density on a standard day is 1.225 kg/m^3 . Calculate the lift coefficient it requires.

4. BIRDS LIFT-TO-DRAG

The equations governing the flight of birds are also valid for aircraft. In their evolution, the birds made important discoveries that allow them to fly with less effort than the insects. They found that there is a certain speed that minimizes the power and that long wings give better lift but also that a wing in the form of an airfoil can produce lift without flapping just by moving forward through the air. This made it possible to separate lift from propulsion and led to the invention of the aircraft.
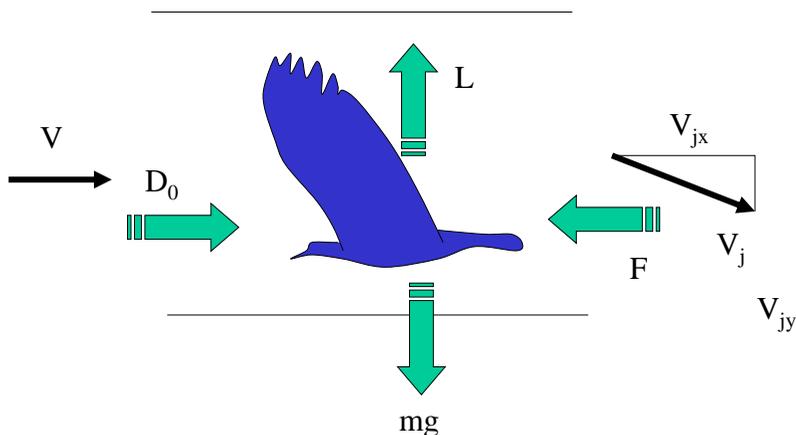
Fig. 4.1 Birds make use of the living force of a large air flow

<u>With a 60-million odd years of history, the birds probably evolved their flying skills from a gliding tree-living ancestor.</u> They go one step further than insects in the complexity of their wings. Instead of a membrane stretched elastically between the skeletal elements, they have numerous feathers, each shaped and equipped for a number of functions. This greatly increases the range of geometries over which an aerodynamically effective foil can be maintained. Although birds' wings share similar structures and composition, different species have emerged with sophisticated adaptations for different modes of flight such as long range, high speed, hovering or short take-off to give just a few examples.

Unlike insects, a bat´s or a bird's flight is characterized by a significant forward speed. This type of flight makes it possible to make use of the living force or momentum of a large air flow by deflecting it downward, letting the reaction provide the required lift. Most importantly, however, the birds and to some extent the bats, have learnt how to take advantage of this momentum of the forward speed to minimize the power to fly.

Intuitively, we understand that it should take a lot of power to fly very fast but also very slowly. Somewhere in between there should be a speed that requires least effort and this fact is used by the birds. To understand this, we may assume that the bird is flying on the spot within an imaginary tube with a diameter corresponding to the wing span, see Figure 4.1. The air flow within the tube meets the bird with a **speed "V"** and the flapping wings angle part of it down to a **jet speed of "V_j"**. The power spent by the bird to accelerate the air flow is then:

$$\dot{W} = \dot{m}\frac{V_j^2 - V^2}{2} = \dot{m}\frac{V_{jx}^2 - V^2}{2} + \dot{m}\frac{V_{jy}^2}{2} = \dot{m}(V_{jx} - V)\frac{V_{jx} + V}{2} + \frac{(\dot{m}V_{jy})^2}{2\dot{m}}$$

$$(4.1)$$

The air flow exposes the bird to a **drag force D_0,** that is balanced by the reaction force from the jet in the horizontal direction so that:

$$D_0 = \dot{m}(V_{jx} - V) \qquad\qquad (4.2)$$

while the lift force on the bird from the vertical component of the jet is:

$$L = \dot{m}V_{jy} \qquad\qquad (4.3)$$

The **drag "D"** is always defined as the component of the force parallel to the relative wind while the **lift "L"** is the component perpendicular to the relative wind.

If the angle of the jet is relatively small so that $V_{jx} \approx V$, the power from Eq. (4.1) becomes:

$$\dot{W} = D_0 V + \frac{L^2}{2\dot{m}} \qquad\qquad (4.4)$$

All of the mass flow in the "tube" of Figure 4.1 can not be used to provide lift. For a final wing span, some part of the air flow is leaking out around the wing tips and is not deflected downwards, see Figure 4.2.

The wing tip vortex displaces air upward behind and outside the wing. This upward displacement of air creates an upwash beyond a bird's wing tips that enables the bird beside or behind it to fly with less energy, like a hang-glider who catches an updraft of warm air. The V-form is therefore a natural choice for migrating birds.

Researchers have discovered that a flock of birds in formation can fly 70 percent farther than a single bird using the same amount of energy. Pelicans flying in formation have also been shown to have heartbeats 15 % lower than pelicans flying alone. NASA scientists have demonstrated that fuel savings of 15% are possible in aircraft flying in a V-formation.
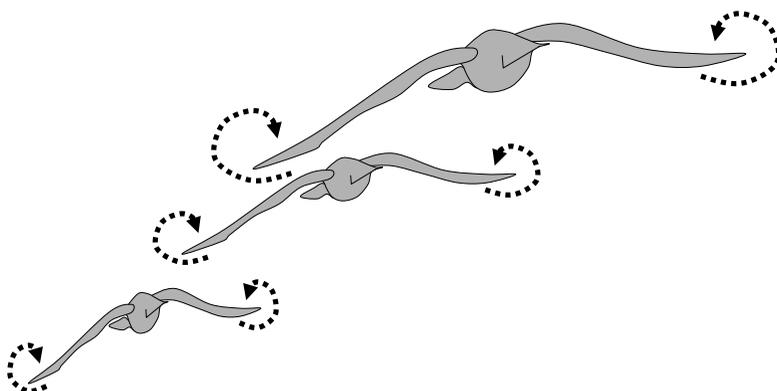
Fig. 4.2 The wing tip vortex creates an upwash

The most efficient wings are those which supply lift with the minimum amount of vortices. This is the case with the crescent shaped wings of swallows and terns. Wing theory also shows that **winglets** can reduce the kinetic energy left in the vortex sheets, and hence the induced drag. The feathers at the wing tips of most birds that soar over land separate both horizontally and vertically and bend upwards in flight to form slotted tips. The slotted tips

resemble the winglets used on the wing tips of some aircraft and reduce the induced drag.

To take the wing tip leakage into account, we may introduce an **efficiency factor "e"** (also called the **Oswald factor** after **W. Bailey Oswald** who first used this terminology in 1932). The useful mass flow is therefore with the **wing span "b":**

$$\dot{m} = e\rho\frac{\pi b^2}{4}V \qquad (4.5)$$

We now get the following expression for the total **power** that is required for flight:

$$\dot{W} = D_0 V + \frac{2L^2}{\rho\pi b^2 Ve} \qquad (4.6)$$

The first part of the right hand side corresponds to the power required to overcome the drag on the bird while the second part is the power required to stay in the air.

Power is force multiplied by speed so the total resistance or drag ($D = \dot{W}/V$) that is felt by the bird is:

$$D = D_0 + \frac{L^2}{\pi b^2 eq} \qquad (4.7)$$

where we recognize the **dynamic pressure "q"** from Bernoullis equation.

The second term is commonly called the **induced drag** or the drag due to lift. The drag D_0 is sometimes called the **profile drag** and consists of both friction and pressure forces (drag due to pressure

alone is sometimes called **form drag**). It is customary to express it through a **friction coefficient "c_f"** acting on the total exposed area of the body, called the **wet area "S_w"**, so that:

$$D_0 = c_f S_w q \tag{4.8}$$

and therefore:

$$D = c_f S_w q + \frac{L^2}{\pi b^2 eq} \tag{4.9}$$

The relation between drag and lift is very important. Assume that the bird is gliding in a downward slope, see the Figure 4.3 below. It is then seen that all the forces are in equilibrium if $D = mg\sin\alpha$ and $L = mg\cos\alpha$ that is $\tan\alpha = D/L$. When it is flying at this angle, the bird feels no effort at all but glides downward at the angle α.
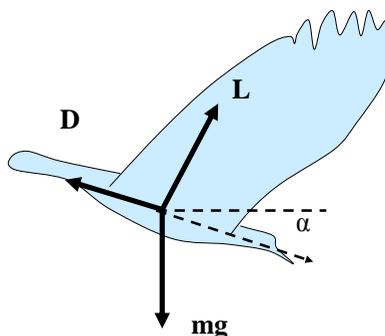
Fig. 4.3 Forces on the bird and the gliding angle

The minimum gliding angle is obtained when D/L is a minimum or

L/D a maximum. The lift "L" must balance the weight of the bird and is fixed at L=mg. Maximum L/D is therefore obtained where the drag "D" is a minimum and from Eq. (4.9), it is seen that this happens at a certain dynamic pressure or speed. Differentiating with respect to "q", it is found that the **Lift-to-Drag ratio L/D** has the following maximum value:

$$\lambda = \left(\frac{L}{D} \right)_{\max} = \sqrt{\frac{\pi e b^2}{4 C_f S_w}} \tag{4.10}$$

The corresponding speed that makes the total resistance a minimum or the L/D a maximum is found to be:

$$V_{d0} = \sqrt{\frac{mg}{\rho C_f S_w \lambda}} \tag{4.11}$$

Let us now go back to the equation for the power. To simplify the treatment it proves advantageous to introduce the **non dimensional velocity "v"**:

$$v = \frac{V}{V_{d0}} \tag{4.12}$$

A good measure of the effort of the bird in flight is the power it must develop per body weight. From Eq. (4.6), the variation of power with speed for a lift force of L=mg can be written:

$$\frac{\dot{W}}{m} = \frac{\dot{W}_{d0}}{2m} \left(v^3 + \frac{1}{v} \right) \tag{4.13}$$

Solving for the friction coefficient from Eq. (4.10) and introducing it in Eq. (4.11), the minimum power per body mass required for flight with the least total resistance or drag becomes:

$$\frac{\dot{W}_{d0}}{m} = \frac{gV_{d0}}{\lambda} = 2g\sqrt{\frac{mg}{\pi e \rho \lambda b^2}} \qquad (4.14)$$

The shape of the **power curve** of Eq. (4.13) is as below:
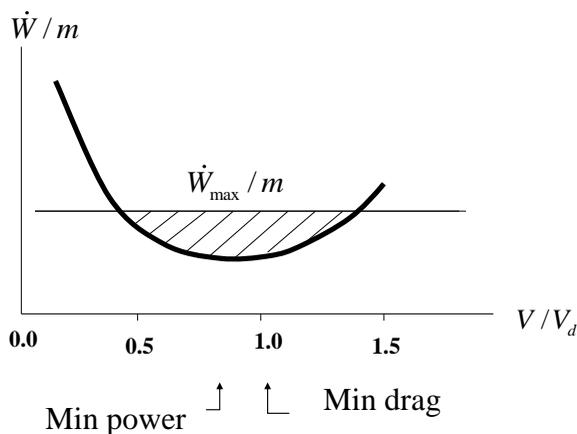
Fig. 4.4 The flight power curve

In order to fly, the bird must produce a power per body weight that is higher than the curve in Figure 4.4. There is therefore a certain flight domain as shown by the dashed area above. In the end points of this domain only level flight is possible but within the domain, the bird has sufficient extra power to accelerate upwards.

It is also seen from Figure 4.4 that there is a speed where the effort of flying is the least. This is the most fundamental discovery of the birds and it distinguishes their type of flight from that of the insects. The insects fly at a low speed, where they need a lot of power. The birds are able to find a higher speed, where their effort is minimized.

The left hand side of the power curve of Figure 4.4 rises very steeply so becoming airborne requires a large amount of power. Some birds must therefore run along the ground or jump from a perch to gain sufficient speed for entering the flight domain and take-off.
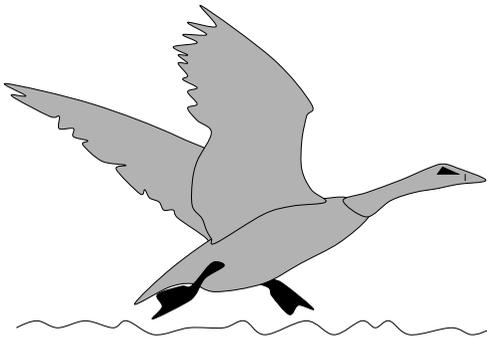
Fig. 4.5 It may be difficult to enter the flight domain

The living habits of some birds require them to fly very slowly or to stand still in the air, which requires a lot of power. Hummingbirds' flight techniques are more similar to insects' than

to birds'. The humming bird is the smallest warm blooded animal on earth. Their bodies are held upright, rather than horizontal and they make up to 200 wing beats per second. The wings do not move up and down, but sweep back and forth, pushing the air downwards instead of backwards. Each time the wings change direction, they also twist 90 degrees, so the air is pushed downward in whatever direction they move. This is like the horizontal rotor of a helicopter. In order to hover, the wings move in a figure of eight holding the bird stationary in the air. The hummingbird can even fly backwards.
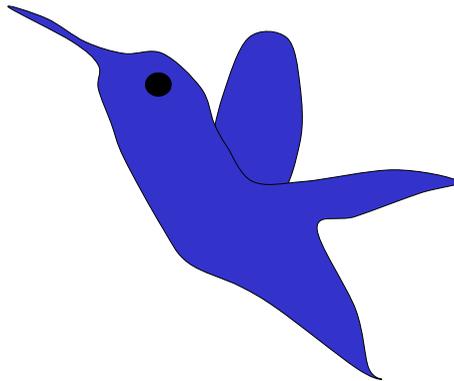
Fig. 4.6 The powerful hummingbird.

The top speed of the hummingbird in level flight is about 15 m/s, indicating that it produces about 75 W/kg. The weight of a hummingbird is around 2 grams though there is a giant humming bird weighing about 20 grams. Large humming birds can lift twice

their body mass for about half a second. They then perform a burst of muscle power of about 300 W/kg.

The small and beautiful hummingbird is is in fact the most powerful creature on earth, much more powerful than any man. To support its vast amount of power, the heart beat of the hummingbird is 500 and it breaths 250 times a minute. It eats twice its own weight in nectar (25% pure sugar) each day.

$$D = \frac{\dot{W}t}{Vt} = \frac{\text{Energy}}{\text{Distance}}$$
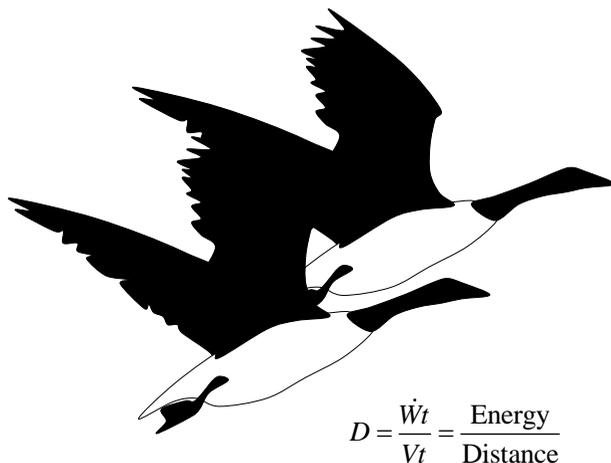
Fig. 4.7 Migrating geese are minimizing drag

Birds may also find a speed where they are **minimizing the energy** they would spend on long distance flights. Note that the energy spent per distance flown is the power divided by the speed which is in fact the drag, see Figure 4.7. Therefore, the speed, where energy per distant is minimized, is also the speed, where the total drag is a minimum. This speed V_{d0} as derived in Eq. (4.11) is found to be higher than the speed for minimum power V_{p0} , see Figure 4.4. For level flight L=mg the relation is:

$$V_{p0} = \frac{V_{d0}}{3^{1/4}} \qquad (4.15)$$

The **minimum power** required for flight is lower than the power for minimum drag as derived in Eq. (4.14). The relation is:

$$\dot{W}_{p0} = \frac{2}{3^{3/4}} \dot{W}_{d0} \qquad (4.16)$$

The Lift/Drag ratio at minimum power is lower than at minimum drag, where L/D is at its maximum λ:

$$\left(\frac{L}{D}\right)_p = \frac{\sqrt{3}}{2} \lambda \qquad (4.17)$$

At the speed of minimum drag, the energy spent per distance flown is at a minimum, see Figure 4.7. Migrating birds therefore tend to fly at this **economic speed**, which is approximately 30% higher than the most **leisurely speed**.

As is seen from Eq. (4.11), the economic flight speed tends to increase with decreasing air density. On the other hand, the total drag, that is the energy per distance flown, is not dependent on air density, see Eq. (4.10) for L=mg. It is therefore an advantage for migrating birds to fly at a high altitude and they have even been observed from traffic aircraft.

However, it is also seen from Eq. (4.14) that it takes more power to fly when the air is thin. Birds that fly for long distances at high altitude need to be stronger than birds living in sea level conditions. Birds have to use more and more power the higher they fly so there is clearly a limit to the altitude they can reach. It is also

easier to fly in cold weather because the air density is higher. This is so not only for birds but also for aircraft. Aircraft with too little engine power will climb very slowly when it is warm.
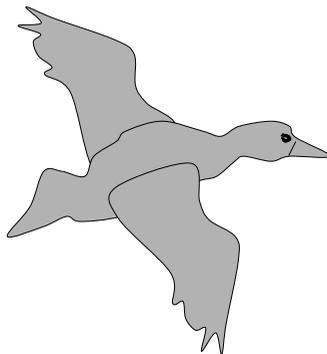
Fig. 4.8 The duck is one of the swiftest birds

The rising right hand side of the power curve limits the flight speed of the birds. Generally, the larger and more powerful the bird, the faster it flies. At very high speeds, friction drag becomes dominant in Eq. (4.9). A swift bird should have short, stubby wings and a streamlined body to give low total wet area. A typical example is the duck, which is one of the swiftest birds. Of course, a drawback with stubby wings is that the beat frequency must be very high.

There is, however, a way to increase the flight speed beyond that given above. An interesting feature of birds that is sometimes

recognized is the **bounding flight**. It is a special type of flight where they periodically fold their wings falling through the air as shown in Figure 4.9.
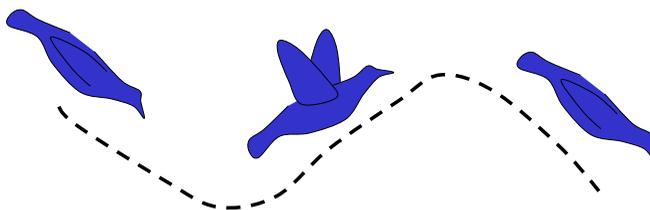
Fig. 4.9 Bounding flight

Assume that the bird starts flapping at the altitude h=0 when the vertical downward speed is "U". If the lifting acceleration is a=L/m-g then at the end of the flapping flight which is assumed to take t_1 seconds:

$$u = at_1 - U \qquad\qquad (4.18)$$

The bird then folds its wings and glides over the top and into free fall. At the end of the free fall flight, the vertical downward speed is again U. If this part of the flight takes t_2 seconds then:

$$-gt_2 + u = -U \qquad\qquad (4.19)$$

From these equations it is found that $t_2 = t_1 a/g$. Therefore the relative time spent in flapping flight is:

$$\tau = \frac{t_1}{t_1 + t_2} = \frac{mg}{L} \qquad (4.20)$$

The power in gliding flight is only to overcome the zero lift drag with folded wings so that:

$$\dot{W}_{glide} = \frac{S_b}{S_w} D_0 V = \alpha D_0 V \qquad (4.21)$$

Where α is the relation between body wet and total wet area and the drag D_0 is based on the total wet area.

The average power over one cycle is then:

$$\overline{\dot{W}} = \tau D V + (1 - \tau) \alpha D_0 V \qquad (4.22)$$

And the power equation describing the effort of the bird in flight now becomes:

$$\frac{\dot{W}}{m} = \frac{\dot{W}_{d0}}{2m} \left[\left(v^3 + \frac{1}{v\tau^2} \right) \tau + (1 - \tau) \alpha v^3 \right] \qquad (4.23)$$

With $L = mg$ we revert to the equation for continuous flight.

The relative time in flapping that minimizes the power in bounding flight is found to be:

$$\tau = \frac{1}{v^2 \sqrt{1 - \alpha}} \qquad (4.24)$$

Then the effort required for intermittent flight becomes:

$$\frac{\dot{W}}{m} = \frac{\dot{W}_{d0}}{2m}\left[\alpha v^3 + 2v\sqrt{1-\alpha}\right]$$ (4.25)
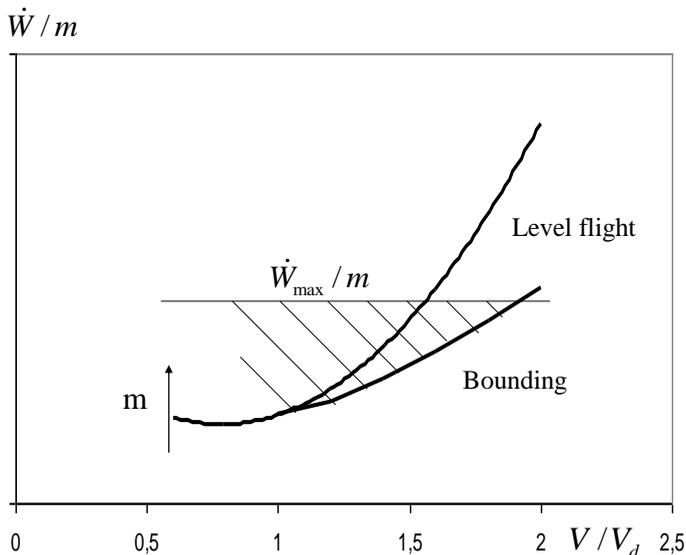
Fig. 4.10 The flight power curve is lower in bounding flight

It is now seen, Figure 4.10, that the optimum curve for bounding flight is a tangent to the curve for level flight at the point where:

$$v = \left(\frac{1}{1-\alpha}\right)^{1/4}$$ (4.26)

Obviously, the flight domain is now wider and the bird can fly faster. Because the relative time in flapping must be <1, it follows

from Eq. (4.25) that this type of flight can not be used below the speed given by Eq. (4.26).

As is seen from Eq. (4.14), the minimum effort required for flight increases with the weight "m" of the bird. Since the maximum muscle power W_{max}/m can be assumed to be more or less the same for different birds, this means that the flight domain in Figure 4.4 decreases for a heavier bird. For the same reason, it is seen from Figure 4.10 that bounding flight is most advantageous for smaller birds.

Also, a bird carrying a catch will be reduced to flying at the most leisurely pace. This is a problem for the pelican transporting its catch back to its nest. The frigate bird is fond of attacking the slow pelican in the air forcing it to vomit the fish it carries, which is then caught in flight by the attacker.

Anyhow, because of the shrinking of the flight domain with weight, there is obviously a limit to how heavy a bird can be while still flying. As we will see in the next chapter this also constitutes a hindrance for human flight.

5. MICRO AIR VEHICLES AND THE NEED FOR POWER

All animal flight are based on the flapping of wings and it was natural that man tried to copy that during the early attempts at flight. All such attempts failed because the remarkable physiological capabilities of insects and birds can never be matched by human beings. Also, the power required to move in the air increases with weight. This led to the most important discovery of the birds, the lifting wing.
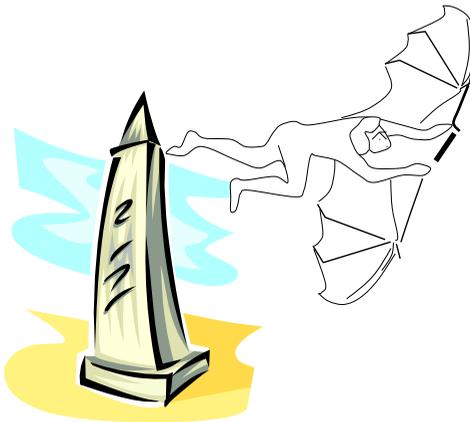
Fig. 5.1 Many early attempts were made to fly like insects or birds.

Accounts from the early centuries A.D. tell of a Chinese engineer, Chang Heng who designed and constructed a small model of a mechanical bird that actually flew. Such birds may nowadays be bought as toys. The Chinese also developed man-carrying kites and can therefore claim to have invented the gliders.

But the first historically documented attempt to fly with wings is attributed to a Roman magician named **Simon**, who tried to demonstrate his proficiency by jumping from a tower with his hand-made wings in front of the Roman emperor Nero. Simon survived the resulting crash landing but died the day after. From what we are told about the said emperor, he probably enjoyed the performance.

In the eleventh century, **Oliver of Malmesbury**, an English Benedictine monk built some wings and sprang from the top of a tower. According to the annals he succeeded in sailing a distance of 125 paces but either through impetuosity or whirling of the wind, or through nervousness resulting from his audacious enterprise, he fell to the earth and broke his legs. He is said to have made his attempt against the wind, which shows that he had some understanding of the task.

In 1178, a '**Saracene**' of Constantinople undertook to sail into the air from the top of the tower of the Hippodrome in the presence of the emperor, Manuel Comnenus. The attempt is recounted in several 19th century books on Aerial Navigation. He was clothed in a white robe, very long and very wide, whose folds, stiffened by willow wands, were to serve as sails to receive the wind. The Emperor, not the same type as Nero, attempted to dissuade him from this vain and dangerous enterprise but the Saracene kept extending his arms to catch the wind. At last, when he deemed it

favorable, he rose into the air like a bird but his flight was as unfortunate as that of Icarus, he fell and broke his bones.

The first to consider the technological means for flight may have been the Fransiscan scholar **Roger Bacon**, who in 1260 coined the designation ornithopter (from the Greek words *ornithos* "bird" and *pteron* "wing") for an aircraft that flies by flapping its wings. Over the next centuries, many were those, who tried to make such flying a reality. Various people fashioned wings and met with sometimes disastrous and always unsuccessful consequences in leaping from towers or roofs, courageously and desperately flapping their home-made wings.

In the late fourteenth century there are reports of partial success by an Italian mathematician **Giovanti Dante**. Starting from the highest tower in the city of Perugia, he sailed across the public square and balanced himself for a long time in the air. Unfortunately, the iron forging which managed his left wing suddenly broke. He fell upon the main church of the city and had one leg broken. Upon his recovery he wisely gave up flying and went to teach mathematics at Venice.

Perhaps the most famous among the early flight pioneers was the great **<u>Leonardo da Vinci</u> (1452-1519).** Leonardo was a Florentine artist and one of the great masters of the High Renaissance, celebrated as a painter, sculptor, architect, engineer, and scientist. His profound love of knowledge and research was the keynote of both his artistic and scientific endeavors and made him anticipate many of the developments of modern science.

Leonardo was possessed by the idea of human flight and he devised vast numbers of flying machines. He grasped that humans are too heavy, and not strong enough, to fly using wings simply

attached to the arms. Therefore he proposed a device in which the aviator lies down on a plank and works two large, membranous wings using hand levers, foot pedals, and a system of pulleys.

In his surviving manuscripts more than 500 sketches deal with flight. However, it is not known whether he ever built or tested any of his designs. This was probably just as well because it might have risked the life of one of mankinds greatest geniuses.

But what about machines? During the latter part of the 1800's, steam power seemed to offer a hope. The first flapping machines capable of flight were constructed in France in the 1870s. **Hureau de Villeneuve** of France designed and made nearly 300 artificial birds. They were powered by rubber bands but he also built a machine in the shape of a bird with a wing span of about 15 m supplied by steam from a stationary boiler on the ground. Turning on steam he was able to make the wings beat. Sitting on the machine he rose a few meters into the air, then fell to the earth.

Another Frenchman, **Alphonse Pénaud**, pioneered the use of rubber band-powered motors in a small machine built and flown in 1874. Then, the French inventor **Gustave Trouvé** designed a flapping wing machine that was powered by an internal combustion engine with gunpowder activating a bourdon tube, which flapped the wings. In 1870, Trouvé's unmanned model successfully flew a distance of 70 meters in a demonstration before the French Academy of Sciences.

Many attempts with flapping gliders have been made, some of which were successful. A famous glider developer in the 19th century was **Jean Marie Le Bris**, a Frenchman who tested a glider with movable wings. Lawrence Hargrave's, a British-born Australian inventor, experiments with powered experimental

models were of great interest to people then involved with aeronautics. He introduced the use of small flapping wings providing the thrust for a larger fixed wing. This eliminated the need for gear reduction, thereby simplifying the construction. His rigid-wing aircraft with flapping blades operated by a compressed-air motor flew about 100 m in 1891.

After the success of the fixed-wing Wright Flyer, the experiments with ornithopters died for a while. Then, in 1929, a human-powered flapping machine designed by the German aviation pioneer **Alexander Lippisch** was towed into the air and, upon release, flew a distance of 250 to 300 meters. The flight duration was short due to the limitations of human muscle power.

In 1942, **Adalbert Schmid** flew a motorized, manned ornithopter in Germany. It was driven by small flapping wings mounted at the sides of the fuselage, behind a larger fixed wing and fitted with a motorcycle engine. It made flights up to 15 minutes in duration. Schmid later constructed a 10 horsepower machine based on the Grunau-Baby IIa sailplane, which was flown in 1947.

In 1959, in England, **Emil Hartman** also built a human-powered ornithopter that was towed into the air by a car, and then released to perform powered glides. From 1990-1995, **Vladimir Toporov** and students built a tow-launched ornithopter that reportedly could be made to climb as a result of the pilot's muscular effort.

Yves Rousseau of France attempted his first human-powered flight with flapping wings in 1995. Mounting his patented flapping mechanism on a 'Vector' ultralight airplane, he succeeded in flying a distance of 64 metres in 2006. Unfortunately, on his next flight

In this equation we have referred the drag to the wing area S instead of the total wet area S_w as in Chapter 4. The coefficient C_{D0} is often called the zero lift drag coefficient and obviously:

$$C_f S_w = C_{D0} S \qquad\qquad (5.3)$$

From those equations it may be seen that a gull in full flight reaches a specific power of about 30 W/kg, see Ex. 5.1. This is less than most insects but still much more than a man at about 3 W/kg.

Larger creatures that would attempt to fly would require still more power. All else equal, it follows from the Eq. **Fel! Hittar inte referenskälla.** that the specific power required increases as the square root of the weight making it more and more difficult to reach into the air.

Scientists did not like to abandon their hopes of manned flight although a professor at the university of Florence, **Giovanni Alphonso Borelli**, had demonstrated in 1680 that humans simply lacked the muscle power. From Leonardo da Vinci onwards a lot of studies were devoted to birds. <u>Many of those studies were concentrated on the so called **"Law of Two Thirds"**</u>. This is a general law in nature, which tells that the weight increases with the linear dimension in the power of three while the area carrying the load increases only in the power of two. Therefore, the wing area should increase more slowly than the weight, which to the early pioneers looked very promising for man's possibilities to fly.

**Fig. 5.2 The Law of Two Thirds shows that the weight grows
faster than the area**
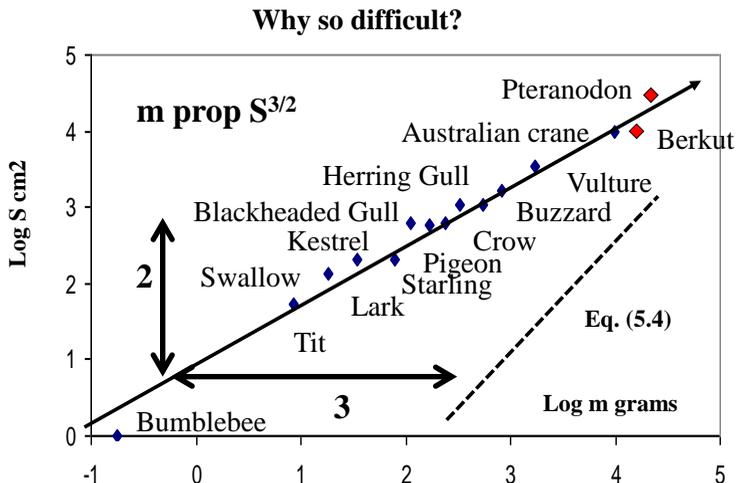
In 1873, the German scientist **Hermann Ludwig von Helmholtz** reported to the government of Preussen concerning the possibilities for human flight. He applied the Law of Two Thirds to flying animals and Figure 5.2 above is based on his data. The straight line in the Figure indicates that the Law is indeed valid for birds. Subsequent studies have shown that birds do not follow the Law exactly but without doubt, the tendency is right.

From the Law of Two Thirds, the wing area needed to lift a man could be predicted. If one draws out the line in Figure 5.2, then a man should be able to lift himself in the air with a wing area of about 10 m^2. However, it is also seen from Figure 5.2 that there is no proof or confirming evidence indicating any bird much larger than albatrosses and a few of the largest condors and eagles. All birds of greater weight seem to be incapable of flight.

Helmholtz therefore concluded that it would be very improbable that a human being could lift itself into the air by his own power only. Obviously then, there is a limit to the size of a flying creature. From Eqs. (5.1) and (5.2), the maximum weight is obtained when the minimum power required for flight equals the maximum power available, that is:

$$m = \frac{3\sqrt{3}}{4g^3}\left(\frac{\dot{W}_{max}}{m}\right)^2 \rho\lambda^3 C_{D0}S \qquad\qquad (5.4)$$

Obviously from Eq. (5.4), the maximum weight is directly proportional to the wing area and must stay to the left of the line indicated in Fig. 5.4. This line crosses the law of two-thirds somewhere and this constitutes the maximum possible weight. The specific power available to biological creatures seems to limit this weight to about 10 kg.

An interesting fact is that this maximum weight is strongly dependent on the **gravity constant "g"** so that on a planet or a space station, where gravity is smaller than on earth, the line would move to the right and birds could carry a much larger body with the same wings at the same air density. It is also seen that it is more easy to fly in high density air.

Inspite of all the efforts by nature, there is obviously a limit to how heavy a bird can be while still flying. There have always been tales, stories, and legends of giant birds. The heaviest flying creature in existence happens to be the Andean **condor**, averaging 9 to 11 kg. Another very heavy and powerful bird is the **Berkut** eagle which has an average weight of between 7 and 9 kg.

The killing powers of the Berkut are out of proportion to its size. In the Asian equivalent to falconry, Berkuts are normally flown at wolves, deer, and other large prey. Their talons are so forceful that they can bury into a wolves back, snapping its spine. Hunters therefore would like to have as large Berkuts as possible and efforts to breed larger such birds have been an obsession since the time of Genghis Khan. However, in over 700 years, one has not been able to breed any Berkut beyond about 11 kg gross weight.

In fact, although admittedly more complex than a fixed wing design, there are many reasons to explore the possibilities of flapping wing flight. After all, throughout creation, all terrestrial life that is capable of initiating lift-generating flight, does so through the flapping of wings. From general aerodynamic considerations, small size ornithopters appear also to make more efficient use of power than a helicopter. Propellers below about 10 cm in diameter have poor efficiency.

A small size flapping vehicle is more energy-efficient than a larger one. It might be possible for instance to design a small flying machine, a Micro Air Vehicle (MAV). Such an aircraft could be an efficient and inexpensive tool for collecting information in dangerous or hostile environments. Equipped with a sensory device, it could be used to detect the presence of poisonous gases in an environmental disaster area or if equipped with a camera, it could be used in reconnaissance missions of interest to the military. A swarm of MAVs could co-ordinate through sensing, communication and mobility to form a virtual "super-organism" that could penetrate any structure and find targets of interest.

The smaller the vehicle the less reasonable is a fixed wing solution because fixed wing vehicles rely strictly on lift generated by

airflow from the vehicle moving through the air to support the weight of the vehicle. This lift is directly proportional to wing area and velocity of air flow over the wing. Thus, the smaller the vehicle, the less lift it can supply. Presently, most designs counter this effect by increasing the velocity of the vehicle. This increase in velocity is unacceptable in situations such as indoor missions where the turning radius may be too large to navigate tight spaces. In such cases, an MAV makes the most sense.

An advantage to wing flapping also relates to the ability to perform short takeoffs and landings. Provided with enough power for hovering, a vehicle with flapping wings could actually take off and land vertically.

Flapping includes the ability to vary wing beat kinematics and generate large peak lift coefficients and hence large control moments. This allows rapid transition between flight modes including hover. Such characteristics are beyond the capability of conventional fixed-wing or rotary-wing systems.

The low speed capabilities of flapping vehicles could become important for flight on other planets. Fixed wing aerial Mars rovers would have to fly at over 400 km/h just to stay aloft in the rarefied Mars atmosphere. This makes landing on a rocky surface almost impossible and reduces dwell time on any particular area. A flapping vehicle could fly slowly over the Martian landscape, and could land and then take off during a survey mission.

The power that is required from an MAV may be calculated from Eqs. (4.13) and (4.14) as:

$$\dot{W} = mg\sqrt{\frac{mg}{\pi e\rho\lambda b^2}}\left(v^3 + \frac{1}{v}\right)$$ (5.5)

The speed where the total resistance is a minimum or the L/D a maximum is from Eq. (4.11) and (5.3):

$$V_{d0} = \sqrt{\frac{mg}{\rho C_{D0}S\lambda}}$$ (5.6)

In order to estimate the power requirement for a MAV, statistical data for birds could be used. According to Azuma the drag coefficient for small birds is $C_{D0} = 0.035$ while the wing span and wing area vary with mass as:

$$b = 1.1m^{1/3}$$ (5.7)

and

$$S = 0.2m^{2/3}$$ (5.8)

The resulting variation of the power with speed is shown in Figure 5.3 below for a larger sparrow-sized vehicle and a smaller one more like an humming-bird.
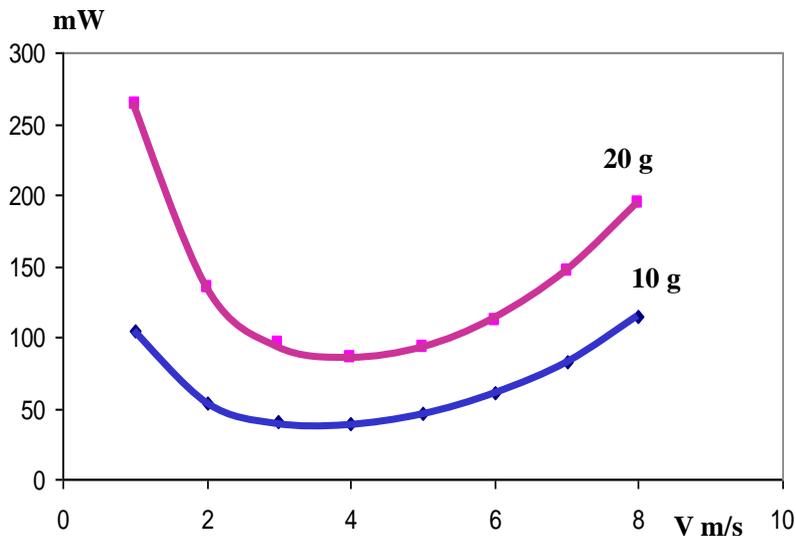
Fig. 5.3 Micro Air Vehicle power vs speed

Even if the power required is modest, the biggest challenge facing MAV designers is the same problem encountered by early pioneers of manned flight, that is finding a sufficiently lightweight powerplant.

Piezoelectric motors are efficient, but still require electricity. Wings covered with photoelectric materials ultimately reach the point at which they have too little light-capture area to produce enough power to flap wings or run electronics. Batteries can provide power for short flights, but are too heavy for missions extending beyond a few minutes. The consensus among experts is that MAVs will need some sort of fuel as an energy carrier and an engine, maybe a small gas turbine, to produce the power on board.

Even if it would be possible to find sufficient power to create the necessary lift, maintaining control once airborne, involves a lot of problems For maneuvering a MAV and deal with the wild heaving the craft must endure, a capacity similar to that developed by nature over many millions of years would be called for.
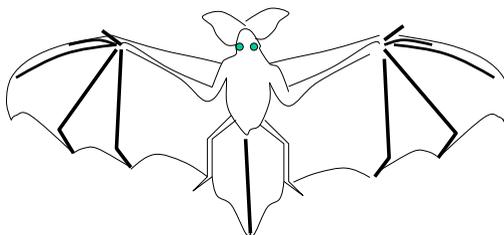
Fig. 5.4 The bats are masters of controlled flight

Maybe such a MAV would like a mechanical bat. Many bats are adept and agile flyers even in complete darkness because they have a system to orientate themselves using ultrasound. When they fly, their wings undergo large amplitude motions and deformations. During the down stroke, the wings are fully extended and sweep downwards and forwards until the tips are ahead of the bat's nose. The leading edge is tilted down during this

phase, particularly towards the tip. The down stroke produces lift and forward propulsion. During the upstroke, the elbows and wrist flex so the wing partially folds, and the leading edge tilts upwards.

The difficulties in developing an agile flapping vehicle are obviously tremendous. With the small size of the MAV comes high surface-to-volume ratios and severely constrained weight and volume limitations. The challenge to integrate all the physical elements and components will require a large level of multi functionality among the system components.

Controlling the wings is a special problem. The remarkable maneuverability of insects and birds is enabled by active control of the three-dimensional shape of the wings during the beat cycle. The wings combine the features of levers, oscillating airfoils and cantilevered beams and are able to perform and withstand shifting patterns of bending and twisting forces. The wing is an integrated structure, combining sensors, materials and actuators in order to achieve the structural control and adaptability required by highly maneuverable flapping flight. In the future, new technologies like contractile polymers could maybe make it possible to design something similar to that.

It is obvious from Eq. (5.4) that one way to increase the weight in the air is to increase the specific power as much as possible. In this respect, birds are extreme among all living creatures.

Let us first look at their bodies. Birds have fewer bones than most animals and many are hollow and filled with air sacs to make them lighter than solid tissue. Some bones have diagonally placed struts for added strength. A bird's wing consists almost entirely of feathers, with only a few bones along the leading edge. The

feathers have a very low weight and the wing bones are long and thin but very strong.

Another weight reduction scheme is reducing the number of muscles a bird needs. In birds many bones are fused together so that muscles are not needed to hold them in position. There are fewer joints, which makes the skeleton very ridged.

If very few muscles are found in the wing itself, the most powerful muscles in a bird are its chest muscles. These are the most highly developed because they must raise the entire body weight into the air. If we spread our arms sideways, push-ups become more and more difficult but that is what a bird must be able to do routinely. A man's chest muscles equal 1% of his body weight compared to 15% for the birds.

In conjunction with the skeletal and muscular adaptations for flight there are structural adaptations. The entire shape of a bird's body is streamlined. Feathers create a smooth, hard, streamlined surface. There are even bays for the feet to be withdrawn during flight to decrease drag.

Birds also have natural mechanisms for supplying energy to their bodies, while maintaining lightness. All internal organs of a bird run at high speed. This produces high energy, but also shortens the life span of the bird. Therefore, small birds live only a few years.

The kinds of food consumed by birds such as seeds, nuts, fruits, fish, and rodents are high in calories and produce a high amount of energy. The food is used up quickly, and some birds must eat more than their weight every day. The speed at which a hummingbird burns its food is 50 times higher than a man's. Most birds eat

during the day and at night their body functions slow down in order to conserve energy. A hummingbird would starve to death in the night if its heart, respiration, and body temperature did not slow down in something approaching hibernation.

In order to maintain the high energy levels necessary in a bird, the oxygen in the blood is very concentrated. The more oxygen available, the faster the food burns. Therefore, a flying bird breathes about 450 times/min while a man in hard activity breathes only about 80 times/min.

The heart is the key for pumping all the blood through the system. In general, a bird's heart is larger than that of other animals. It also beats much faster under normal circumstances than in other animals. Under stress the heart makes about 1000 beats/min and ordinarily about 400. This rapid pumping system produces large amounts of heat. The average of a bird's body temperature is 7 or 8 degrees higher than that of a man. This is approaching the upper limit for living things, so it is very important that birds have a cooling system to get rid of excess body heat.

In a man, body heat is eliminated through perspiration from the skin. A bird is cooled down through a system of air sacs that extend throughout the body and into the hollow portions of the larger bones. Those air sacs are also used to store air so that the bird always have fresh air in the lungs, both during inhale and exhale.

Inspite all the efforts by nature, there is still a limit to how much specific power that can be produced. But as is seen from Eq. (5.4), it is also possible to increase the maximum weight of a flying creature by having a large lift-to-drag ratio $\lambda=L/D$.

There is in fact a tendency for large birds to have higher L/D than small birds. Examples of L/D values for some birds are:

Sparrow	4
Pigeon	7
Herring Gull	10
Tern	12
Albatross	20

As everyone knows, gulls are excellent gliders and can ride right up to their nests on their stiff unmoving wings. A seagull in still air can glide quite efficiently, losing only 1 meter in altitude for every 10 meters it travels. Albatrosses that spend nearly all their life in the air are even better. They can glide 20 meters for the loss of only 1 meter in altitude. This is about the same as the best airliners of today as seen from Figure 5.5 below.

Increasing the lift-to-drag ratio means changing the physical shape. As is seen from Eq. (5.2) and (5.3), the L/D ratio is dependent on the friction coefficient and the so called **wetted aspect ratio** $A_w = b^2/S_w$ Long, slender, high aspect ratio wings have higher L/D than short, thick, low aspect ratio wings. If one wants to glide well, it also helps to have a small body compared to the wing area. Then the ratio S_{wet}/S will be low, which increases the wetted aspect ratio and the L/D.

L/D
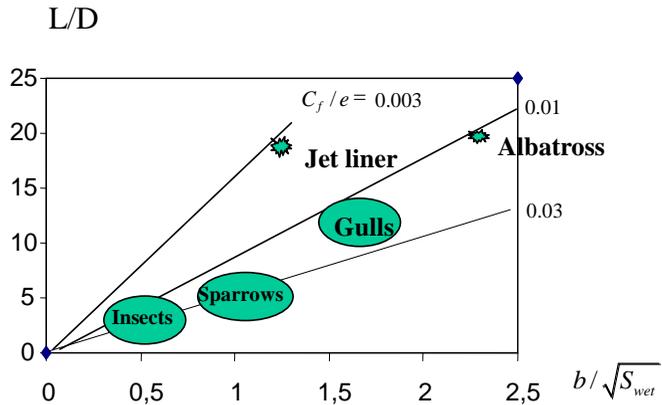
Fig. 5.5 The Lift-to-Drag ratio of birds

In Figure 5.5, the L/D ratios for birds are compared to that of aircraft. The lower L/D values for birds are explained by their higher friction coefficient. In spite of the feathers, the surface roughness is higher than for a smooth plate. Also, the friction coefficient generally tends to decrease with size. Small birds therefore tend to have a higher friction coefficient than large birds and therefore also a lower L/D-ratio.

For insects, the aspect ratio varies between approximately 5 and 12 with 7 as a fairly typical value. They also have low values of S_{wet}/S (with the exception of the dragonfly) so their L/D is very low and they are practically incapable of gliding flight.

Small birds, water birds or pheasants have low aspect ratios of around 3 to 6 that allow their owners to explode into flight suddenly and are quite adequate for relatively slow powered flight, but not good for gliding.

Waders have medium length wings with an aspect ratio of around 12. They also tend to be pointed and directed backwards after the first half. These wings are slower in takeoff but allow for a faster top speed and a little gliding. They are good for long distance migrants.
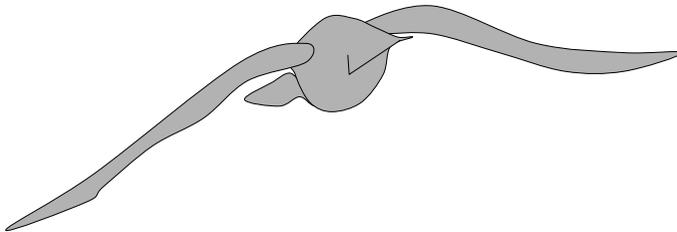
Fig. 5.6 Large birds tend to have large wing span

Eagles and vultures have broad, long wings with an aspect ratio of around 9 and the feathers at the ends are separated into fingers which help with detailed control while the birds are gliding. These

are basically terrestrial birds riding high above the ground using a variety of updrafts to avoid flapping.

Sea birds have long, thin wings without fingers and an aspect ratio of around 14 and higher. These are good for gliding over the sea, close to the surface, using small changes in wind direction to maximum advantage.

Thus, as the birds grow larger their weight tends to grow faster than their wing area, increasing the power they require to fly. They may try to compensate for this and increase the lifting capacity of their wings by increasing the **wing span** in relation to the wing area.

The largest known flying bird is the now extinct American **Teratorn** with a wingspan of five meters. However, the largest creature that ever flew, the **Pteranodon** was a flying reptile that lived during the time of the dinosaurs. It was not a dinosaur, but was a close relative of them. Pteranodon's wing-span was larger than that of any known bird. One pterosaur found in Texas had a wingspan of ten meters. Pteranodons lived about 85-75 million years ago. Some pteranodons had very typical, long, light-weight, bony crests on their heads that may have acted as a rudder or stabilizer when flying.

Pteranodon, was not a flapping creature. Its long, thin albatross-like wings betray it as a glider, the most advanced glider the animal kingdom has produced. Its estimated weight was a mere 20 kg. The low weight combined with an enormous wing span meant that Pteranodon could glide at ultra-low speeds. Therefore, take-off would have been relatively easy. All Pteranodon needed was a breeze when it would face the wind, stretch its wings and be lifted

into the air like a piece of paper. No effort at all would have been required. Again, if it was forced to land on the sea, it had only to extend its wings to catch the wind in order to raise itself gently out of the water.

A large wing span creates considerable problems for very large birds because the wings become very cumbersome to handle. Besides increasing their aspect ratio, such birds must therefore find other methods to increase the lifting capacity. This leads to the most important discovery of the birds, the lifting wing.
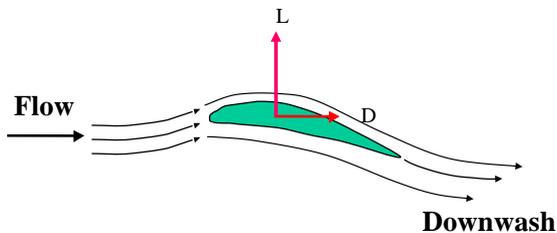
Fig. 5.7 The lifting wing

To be able to fly without moving their wings, the wings of the birds have the very characteristic **airfoil** shape that the airplane wing came to be modeled after. In this way, the birds are able to generate lift without even moving their wings, just by the forward

movement itself. The birds' wings are honed into perfection by natural selection to give a maximum amount of lift. This "invention" is probably the most fundamental ever made in aeronautics. To understand how such a wing works we may look at the Figure 5.7 above.

Consider two stream tubes approaching the wing. Because of the shape of the wing, the upper stream tube senses a larger obstruction than the lower one and consequently it is flattened more as it moves over the top. Because of the law of mass continuity, the speed will be higher on top and the pressure lower. This makes the pressure pushing up from under the wing greater than the pressure pushing down on the top so the wing moves up as soon as it moves forward. It allows birds to generate lift with less flapping of the wings. The more curved the aerofoil the greater the lift, provided that the degree of curvature does not impede the flow of air.

An alternative explanation to the generation of lift is that the wing deflects the airflow slightly downward behind the wing creating a downwash. Because of the reaction principle, this gives rise to a lifting force.

There are a lot of hot discussions going on which of the pressure or downwash explanations are the most correct. In fact, because there are no other forces present, the pressure and reaction forces must balance each other. They are two sides of the same thing and both explanations are equally valid. To deflect the air downward, the wing must exact a pressure on the air and because of the reaction principle this pressure force gives rise to an equally large lifting force on the wing.

It is sometimes proposed that the higher velocity on top would occur because a fluid element approaching the edge of the blade

will split in two that have to come together again at the trailing edge. This is not true. Experiments and calculations show that a fluid element passing over the top will leave the trailing edge long before the bottom element arrives.

For similarly shaped flyers, the weight increases as the cube of linear dimensions, while the lift-producing surface area increases only as the square of linear dimensions. Thus as the weight gets larger, the wings must increase in size disproportionately. These much larger wings are then more difficult to flap. In bird species, increase in size results in a trend away from flapping flight and toward gliding.

Birds do not separate lift from propulsion. By flapping its wings down, together with the forward motion of the body, a bird can tilt the lift of its wings forward for propulsion. The relative wind comes from below the wing during the down stroke and from above the wing during the up stroke. The wing must therefore constantly twist around its long axis so it has the appropriate angle of incidence at each point in the flapping cycle.

In addition to the basic movements described here, birds can do a lot of other things with their wings to allow them to maneuver in the air. Instead of using their tails for flight control, they move their wings forward and backward for balance. To make a turn, they can twist the wings or apply more power on one side. The wing can also flex considerably providing a very controllable flight and allowing birds to glide for extended periods.

The unique property of the lifting wing is that it will provide lift once it is made to move forward by for instance a propeller. Attempts have been made to design flying machines that are manually powered at a mere 3 W/kg.

The wing span required can be obtained from Eq. (5.1) as:

$$b = \frac{4g}{3^{3/4}\left(\dot{W}_{max}/m\right)}\sqrt{\frac{mg}{\pi e \rho \lambda}} \qquad (5.9)$$

where $\lambda = L/D$ is the maximum lift to drag ratio.

In 1977, it proved possible to cross the English channel in such a manually powered machine but as shown in Ex. 5.2, the wing span was prohibitively large and the speed from Eq. (4.11) is very low.

As was is seen above the size of the vehicle is strongly dependent on the gravity. As shown in Example 5.3, the wing span of a Mars flyer would have to be more than twice that on Earth due to the very low density of the atmosphere even though the gravity is lower.

Ex 5.1
What would be the power density of a gull flying at twice the minimum drag speed if the wing span is one meter and the weight 0.4 kg? The lift-to-drag ratio of a gull is (L/D=10). Air density is 1.225 kg/m3 and the Oswald factor e=0.85.

Ex 5.2
What would be the wing span of a man weighing 100 kg flying at minimum power assuming that he can reach the lift-to-drag ratio of a gull (L/D=10) and has a specific power of 3 W/kg. Air density is 1.225 kg/m3 and the Oswald factor e=0.85. What would be the flight speed?

Ex 5.3
The Mars atmosphere is mostly CO_2 and is at about 1/100 the density of the Earth. The gravity is 0.38 times that of Earth. What would be the wing span of a Mars flyer compared to one on Earth?

6. THE EVOLUTION OF THE FIXED WING AIRCRAFT

The Wright Brothers reached the power density of a bird in 1903 more than one hundred years after George Cayley discovered the fixed lifting wing and invented the aircraft. In the meantime, great contributions to the understanding of wings had been made by Otto Lilienthal and other pioneers.

Fig. 6.1 George Cayley invents the aircraft in 1799

As was said in Chapter 5, the unique property of the lifting wing is that a fixed wing can produce lift just by moving through the air. It

is then possible to separate lift from propulsion and **<u>George Cayley (1773-1857)</u>** <u>was the first to understand this, thus inventing the fixed wing aircraft.</u>

In 1799 he made a very important discovery. He looked closely at birds' wings and found that air flowing over curved, fixed wings created a downwash flow and lift. In 1799, he engraved his concept of such an aircraft on a silver disk to preserve it to future generations. This disk is now in the Science Museum in London. It shows on one side a crude type of aircraft, see Figure 6.1, and on the reverse side the resultant aerodynamic force on a wing resolved into lift and drag components indicating his understanding of the function of a fixed lifting wing.

Cayley lived all his life as a typical English gentleman on his country estate Brompton Hall, which he had inherited from his father. Typical in all respect save for his interest in the problem of human flight.

In 1804, he built a whirling-arm machine for the testing of airfoils. Cayley also wrote about his experiences. In 1809 and 1810 he published three papers, which are regarded as the first treatise on theoretical and applied aerodynamics. In them he described his scheme for the separation of lift and propulsion. He noted that a surface inclined at some angle to the direction of motion would generate lift and that a cambered surface was more efficient in this respect. He also noted for the first time that lift was generated by a pressure difference over the wing.

One of his most important papers was published in 1852 and describes a large human carrying glider with all the features of a modern airplane. His publications were very important because

people interested in flight would study his writings and continue his work. In this way, he started a process that ended one hundred years later in the first successful powered flight.

At around 1853 when he was 80 years old, he built the first human carrying glider. According to several eyewitnesses, it flew for a couple of hundred metres across a valley at Brompton Hall with one of Cayley's coachmen onboard before landing rather abruptly.

Unfortunately, Cayley never solved the propulsion problem. On his silver disk Cayley shows some paddles just behind the wing. He was obsessed with such flappers from 1799 until his death in 1857 and he gave little attention to other propulsion schemes such as the propeller.

Cayley's ideas were further developed by other people throughout the 19th century. In 1842 **William S. Henson**, a British inventor, patented an "aerial steam carriage," the *Ariel*. He and **John Stringfellow**, a lace machinery manufacturer, organized the Aerial Transit Company, a world-wide airline service, but to their surprise a model of Henson's airplane failed to fly. However, Stringfellow continued to experiment. He built several small steam engines and attempted without success to power model airplanes off the ground by using crude propellers.

Alphonse Pénaud of France also made models but powered by rubber bands. His models of the airplane, orthopter, and helicopter were successful. His *Planaphore* model of 1871 was a single-stick pusher monoplane that looks like the models built today.

In 1874 the French naval officer and engineer **Felix du Temple** achieved the world's first powered take-off. It was a monoplane

with swept forward wings powered by some sort of hot air engine. Piloted by a young sailor, the machine was launched down an inclined plane at Brest in France and left the ground for a few moments.
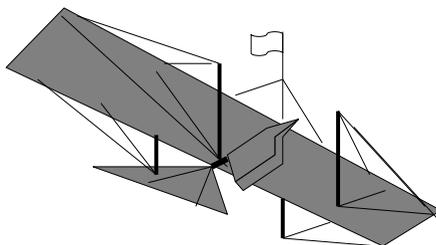
Stringfellow & Henson 1842
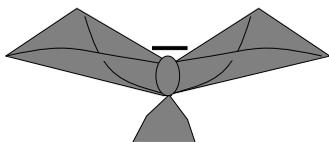
Felix du Temple 1874
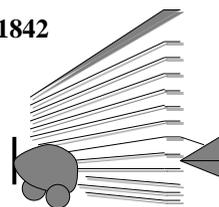
Horatio Phillips 1893

Fig. 6.2 Early aircraft designs

A similar hop was achieved in St Petersburg in 1884 with a steam powered monoplane designed by **Alexander Mozhaiski** launched down a ski ramp.

Clement F. Ader built batlike monoplanes powered by steam engines. He claimed he flew his Eole in 1890 and his Avion in

1897. However, there were some discussions about whether he hopped rather than flew.

In 1893, **Horatio Phillips** constructed a strange steam-powered multiplane with 50 narrow wings that resembled a Venetian blind. Tethered and without a pilot, it rose a few feet off the ground.

Sir **Hiram Maxim**, an American-born inventor who lived in England, constructed another curious machine, in 1893. It was a three ton multiplane monster powered by a steam engine. In a test flight on a circular track, it rose, ripped up a guard rail, and then crashed.

None of those projects were successful so some people understood that a better scientific understanding of the art of flying was required. Of particular interest during this period is the creation in London in 1866 of the Aeronautical Society of Great Britain, which later developed into the respected **Royal Aeronautical Society**. It soon attracted scientists of vision and stature working on the problems of flight.

Cayley had separated the problem into lift and propulsion and scientists first concentrated on understanding the lifting wing. To better understand how the wings worked, gliding experiments were very important and George Cayley, who first noticed the lifting properties of birds´ wings, started working on gliders already in 1810. In France **Jean Marie le Bris** built the *Artificial Albatross,* a birdlike glider, in 1857. **Louis Pierre Mouillard**, also a Frenchman, in 1881 wrote a book on gliding, which applied bird flight to aviation.

In Germany **Otto and Gustav Lilienthal** contributed greatly to aeronautics. Otto Lilienthal, who was the most active, continued his studies of aerial navigation for over 20 years. In the history of aeronautics, he has a place at the side of George Cayley and the Wright Brothers. Otto Lilienthal was born in 1848 and had graduated with a degree in mechanical engineering from the Berlin Technical Academy. After work as an engineer and salesman at a machine factory, he founded his own business in Berlin manufacturing spiral-tube boilers.
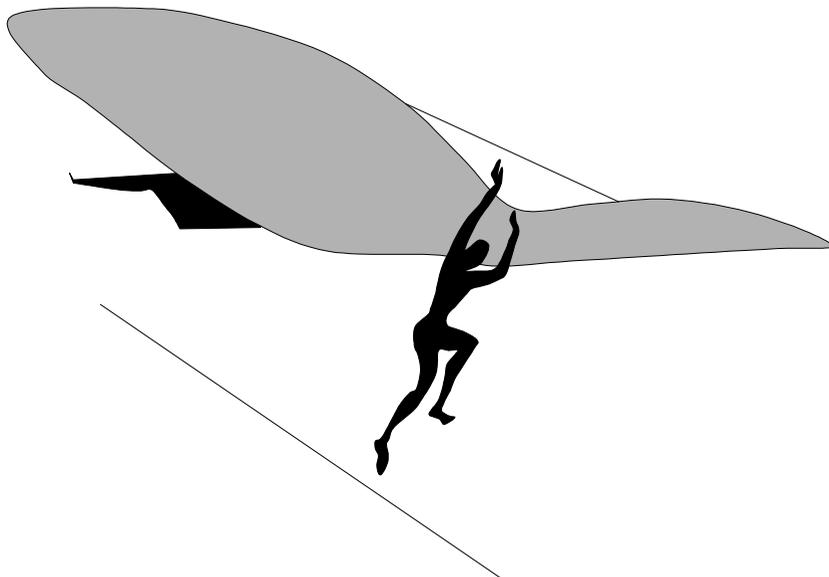
Fig. 6.3 Otto Lilienthal made gliding experiments from a hill

This gave him economic resources and practical means to work on his hobby, aeronautics. He flew off a hill near his home. His glider

was a wing with a hole in the middle and he patterned his designs from large birds. Lilienthal would stick his head up through the hole, hold on to the wing and run down the hill. He could glide like that for fifty meters or more. He did this more than 2000 times.

He learned that he needed a tail on the glider. The tail helped keep it steady. He learned about roll - tipping from side to side, pitch - the nose moving up and down and yaw - turning right to left. This helped him control the glider much better. In 1889, he created tables that gave airlift values at varying angles of incidence. He published this in a book entitled "*Der Vogelflug als Grundlage der Fliegekunst*", which contained some of the most detailed aerodynamic data available at the time.

He also discovered an important property of wings. At the end of each flight the glider would suddenly dive down into the ground. Lilienthal didn't know why. He finally learned that it was because of the angle of the wing to the wind. This is called a **"stall"**.

Why does an aircraft stall? We have already seen that the lift force on the wing can be written as:

$$L = C_L \frac{1}{2} \rho V^2 S \qquad (6.1)$$

It also proves practical to refer the lift and the drag to the same area and it is common to use the **wing area S**. It is therefore convenient to introduce the profile drag as:

$$D_0 = C_{D0} \frac{1}{2} \rho V^2 S \qquad (6.2)$$

The coefficient **C_{D0}** is often called the **zero lift drag coefficient** and referring to Eq. (5.3) $C_f S_w = C_{D0} S$.

Therefore and with the aspect ratio A=b^2/S, the total drag coefficient is, see Eq. (4.9):

$$C_D = C_{D0} + \frac{C_L^2}{\pi A e} \qquad\qquad (6.3)$$

And the total drag may be obtained from:

$$D = C_D \frac{1}{2} \rho V^2 S \qquad\qquad (6.4)$$

It was shown by **Ludwieg Prandtl** in the 1920's that the simple expression we have derived for the induced drag of flapping wings is indeed also valid for stationary wings and that the efficiency or **Oswald factor is e**=1 for infinite wings of elliptical planform. Typical values of the **Oswald factor** is e=0.85-0.95 since in the real world most wings are neither elliptical nor infinite. We will come back to Prandtl and his work later.

Plotting the relation between the lift and drag coefficients of Eq. (6.3) constitutes the so called drag polar. This method of graphic results of airfoil tests was used first by Otto Lilienthal in the end of the 19th century. He plotted the lift and drag forces of his experimental results as lift versus drag, as we still use it today (using coefficients instead of the actual forces). However, he did not use the term "polar" for the diagrams he produced. This term was first used by Gustave Eiffel, the designer of the Eiffel tower, in 1909.

To stay in the air, the lift of an airplane must equal its **weight m** so that L=mg. Then the wing area necessary for flight will be:

$$S = \frac{2gm}{\rho V^2 C_L} \tag{6.5}$$

Alternatively, for a given wing, in order to lift off the ground or keep flying we must reach a speed of:

$$V = \sqrt{\frac{2gm}{C_L \rho S}} \tag{6.6}$$

Note that this is the speed relative to the aircraft. A head wind will decrease the aircraft speed needed for take-off. Indeed, if it is blowing sufficiently hard an aircraft may lift straight up from stand-still.

Obviously, for low speed, the aircraft should have a high lift coefficient. The Figure 6.4 below shows the **drag polar**, that is a plot of the lift coefficient versus the drag coefficient. Note that the angle of attack is indicated along the polar curve. It shows how the lift coefficient C_L varies with the angle of attack of the wing.

For an uncambered wing, the minimum drag is at zero angle of attack with zero lift. For a cambered wing, a negative angle of attack is required to obtain zero lift. The variation of the lift coefficient with angle of attack is nearly linear except for high angles.

The theoretical minimum of $D/L = C_D / C_L$ is found as the tangent to the drag polar. Differentiating C_D / C_L of Eq. (6.3) with respect to C_L it is found that this happens when:

$$C_L = \sqrt{\pi A e C_{D0}} \tag{6.7}$$

The **maximum lift-to-drag ratio** $\lambda = L/D = C_L/C_D$ is then found to be:

$$\lambda = \sqrt{\frac{\pi}{4}\frac{Ae}{C_{D0}}}$$

(6.8)

This could also have been obtained from Eq. (4.10) using Eq. (5.3)
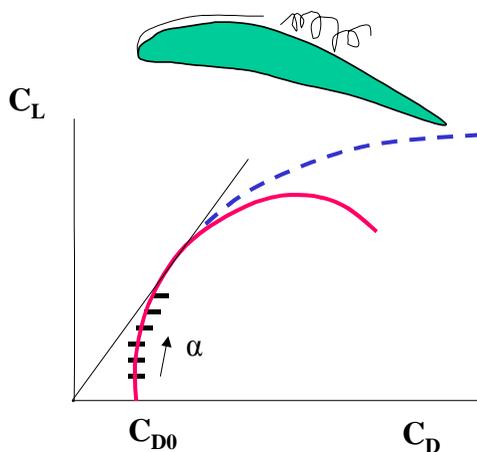
Fig. 6.4 The maximum L/D is at the tangent to the drag polar

Theoretically from Eq. (6.3), the lift coefficient should continue to grow with the drag coefficient as is shown by the dashed line in Figure 6.4. However, in reality that is not the case. The rapid fall in lift beyond a certain angle is referred to as **stall** and occurs when the boundary layer separates from the upper surface of the wing.

The result of this loss of lift is that the aircraft starts to fall. For stable aircraft, the aerodynamic center of pressure is behind the center of gravity. That way the aerodynamic forces tend to realign the aircraft with the direction it is moving. If it is falling then it tips forward around its center of pressure and dives.

Nowadays, to be sufficiently far away from stall, the angle is controlled so that typically $C_L < 1.6$, sufficiently far away from the maximum value of $C_L = 2$. Lilienthal did not understand this and died on August 9, 1896 when his glider stalled and dove to the ground while gliding from the Gollenberg hill near Stollen in Germany.

Meanwhile in the United States, **Samuel P. Langley**, a prominent American scientist and director of the Smithsonian Institution, attempted to solve the problem of flight with large powered models after years of scientific research. He called his models aerodromes, meaning "air runners." In 1896 his *Aerodrome* No. 5, powered by a steam engine, flew for a minute and a half and covered more than half a mile.

In 1898 while at war with Spain the United States government granted Langley fundings to build a man-carrying aerodrome for aerial observation. In 1903 a gasoline-engined model flew successfully and **Charles M. Manly**, Langley's assistant, was aboard a full-scale aerodrome in two attempted flights this year. It was catapulted from the roof of a houseboat on the Potomac but plunged into the river both times. The last attempt was made on 8th of December 1903.

None of those aircraft had enough power for take-off. At take-off the **thrust F** of an aircraft is usually much larger than the drag and

the friction on the ground. Then the take-off distance s can be approximated by:

$$s = \frac{mV_{to}^2}{2F} \tag{6.9}$$

To ensure a margin of safety, the take-off speed V_{to} is typically chosen to be 20% higher than the stall speed so that:

$$V_{to} = 1.2\sqrt{\frac{2mg}{\rho SC_{L\max}}} \tag{6.10}$$

and:

$$s = 1.44 \frac{gm^2}{\rho SC_{L\max}F} \tag{6.11}$$

It is interesting to note that it is harder to take-off on hot summer days when the air density is low, or for the same reason from airports located at high altitudes. The equation also shows that in order to take-off you need a low weight, a large wing area, good aerodynamics i.e. high maximum lift coefficient and an engine that can give sufficient thrust.

Note also that as the weight is doubled the take-off distance is quadrupled. Many heavy water birds – such as geese and swans - need very long runs along the surface of the water before they are able to get into the air. Their large, webbed feet make running on water possible. They then tend to accelerate along the water surface taking advantage of the so called **ground effect**, see Chapter 7.

Birds with large wings and light bodies like sea gulls will lift into the air with one stroke of the wings. Alternatively, they could take advantage of upwinds close to a steep rock or something like that. This is the method used by the albatross, which spends nearly all its life in soaring flight. The South American condors, with wing spans of nearly 3 meters, cannot flap their wings while on the ground. They must use some sort of outside help to take off. They need a very strong head wind or they land only on cliffs which they can leap off to begin their next flight.

The most comical takeoff and landing is made by the albatrosses in the South Pacific also called "Gooney Birds". They run, flap, hop, and finally with the aid of a head wind manage to get airborne. Landing is another problem. Thermals and breezes are great high up, but the closer the bird gets to the water, the slower the wind moves and the weaker the updrafts. The gooney bird therefore looses altitude very rapidly until it comes in for a crash landing on its nose!

Unknown or at least neglected by Langley, two brothers, **Orville and Wilbur Wright**, from Dayton, Ohio began to develop a machine that would combine all the features required. They were self-educated mechanics and in 1892, they had opened a shop in Dayton selling and repairing bicycles. It was a profitable business because bicycles were becoming more and more popular and by 1895 they were manufacturing them on their own.

In 1896, they heard about the death of Otto Lilienthal and became interested in aviation. They started to experiment with gliders and built them in their own manufacturing shop using the results of experiments conducted by Lilienthal. However, most of their flights turned out to be failures.

They blamed the failure on the data provided by Lilienthal. In fact, their main mistake was to have used, like Lilienthal, the so called Smeaton coefficient. As we have already described in Chapter 3, the civil engineer **John Smeaton** had developed an experimental expression for the dynamic pressure that led to somewhat lower values than the mathematically correct expression given by Bernoulli's equation.

As a result, the Wright Brothers failed to estimate correctly the wing area they needed. In 1901, they decided to gather their own wing data by conducting systematic experiments on different types of wing configurations. In their bicycle shop in Dayton, Ohio, they built a wind tunnel and started to work.

The Wright brothers did not invent the wind tunnel. It had already been mentioned by Leonardo da Vinci in the 1500s and wind tunnells had been built in many countries at the end of the 1800s. The first wind tunnel in history was built by **Francis Wenham** in Greenwich, England, in 1871. **Gustave Eiffel**, the designer of the Eiffel tower in Paris, built two wind tunnels and carried out extensive aerodynamic testing from 1909 to his death in 1923. However, the Wright brothers were the first to use wind tunnels in concentrated product development work.

They tested more than 200 different airfoil shapes made from steel. From their work came the 1902 Glider, a machine with a wing span of 10 m and wing width of 1.5 m. This was the first aircraft with three-axis control. This means that the aircraft could go up or down, left or right, and could also roll about its longitudinal axis.

Filled with confidence, they went back to the place where they had tested their first glider, Kitty Hawk in North Carolina, a place

carefully selected for its high prevailing winds and soft ground for landings. At Kitty Hawk, they performed over 800 flights to solve the problem of aircraft control and stability.

The most important parameter defining a wing is the aspect ratio which is defined as the square of the span divided by the carrying area i.e. $A=b^2/S$. We already know from Eq. (6.8) that the lift-to-drag ratio is proportional to the square root of the aspect ratio. The Wright brothers were the first persons to investigate the influence of the aspect ratio in detail using their wind tunnel. They verified that a long thin wing (high aspect ratio) gives more lift for a given drag than a short broad wing (low aspect ratio). In their 1902 glider they also solved the problem of lateral control with vertical rudders and wing tips that could be warped or twisted up and down.

But the Wright brothers did not want to limit themselves to gliders. They wanted to make a machine that could take off under its own power. And as we have seen, the power density this requires is considerable. The birds generate about 25 W/kg of body weight and in the age of the cast iron and steam engine, this was very difficult to achieve.

To take-off and fly, an aircraft must be light. The easiest way not to be heavy is to be small. Another way to make an object lighter is to use light weight materials to build it. However, these light weight materials must also be strong enough for flight. To decrease the weight as much as possible, the design of the Wright aeroplane looked very flimsy and to obtain a stiff and light wing, it was made as a biplane from cloth and wooden spars. This biplane wing also gave a high wing area, which is needed for short take-off, see Eq. (6.11).

As for propulsion, it was clear that the Wrights would have to use a propeller to harness the reaction principle for producing the thrust needed. By means of a propeller mechanical energy of a rotating shaft is transferred to the mechanical energy of the jet. The unique advantage of the propeller is that it represents a continuous process. Other mechanical devices such as pistons pumping air were tested in the early development of aircraft engines but without much success due to their intermittent nature.

The propeller as such was an old invention. In the 12th century windmills were invented and rapidly spread over Europe providing a more flexible source for power than the old water wheels. They were used well into the 20th century. It was close at hand to think of the reverse, i.e. powering the blades to produce a wind to give thrust.

Leonardo da Vinci made drawings of a propeller and a helicopter. Already one year after the first balloon flight in 1783, a hand-driven propeller was used on a balloon but it did not succeed due to the lack of an engine to power it. However, in 1852 a propeller connected to a steam engine was successfully used in an airship by **Henri Giffard** and allowed him to fly over Paris at the fantastic speed of 10 km/h. Also, propellers for marine applications were developed by the Swedish inventor **John Ericsson** and successfully used by the Union forces in the American Civil War.

The early aeronautical propellers were very crude paddle-like devices and the marine propellers could not easily be used in air. It fell to the Wright brothers to take the first steps towards the propeller as an efficient tool for aircraft propulsion.

The propeller is not 100 percent efficient, because, like any airfoil, it has losses from skin friction drag, induced drag, tip losses due to

near sonic speeds at the tip, etc. The **efficiency η_p=FV/P** of a propeller is defined as the thrust power divided by the shaft power. This is related to what is called the efficiency of a propulsion system. Marine engineers call it the Froude efficiency after **William Froude (1810-1879)** who first used it. For flight, the propulsive efficiency expresses how much of the energy supplied that is available for thrust work.

The propeller designed by the Wright brothers after extensive experimenting reached the remarkably high efficiency of 70% and was one of their most valuable contributions to aeronautics.

Aircraft designers everywhere adopted the Wright propeller. It reached its final form thanks to work carried out at NACA. The theory and design of propellers were laid down in all its essentials in a NACA report in 1917 by **William Durand.** His propellers reached an efficiency of 75 to 80%. The typical aircraft propeller of today might have a cruise efficiency close to 90%, with lower efficiency at lower airspeed. This means that 90 percent of the shaft power is converted to propulsive power by the propeller.

To power the propeller, the Wright Brothers needed an engine light weight enough to be lifted up into the air while powerful enough for the aircraft to reach the take-off speed. The main obstacle facing them was the problem of finding a sufficiently light weight power source in a time dominated by steam power. The external combustion steam engines were in no way able to produce sufficient power per kg to make flight possible.

Now, another recently made invention came to their help. This was the internal combustion engine. About 1660, the first person to experiment with an internal combustion engine was the Dutch

physicist **Christian Huygens**. But no effective gasoline-powered engine was developed until 1859, when the French engineer **J. J. Étienne Lenoir** built a double-acting, spark-ignition engine that could be operated continuously. In 1862 **Alphonse Beau de Rochas**, a French scientist, patented but did not build a four-stroke engine. Sixteen years later, when **Nikolaus A. Otto** built a successful four-stroke engine, it became known as the "Otto cycle." The first successful two-stroke engine was completed in the same year by Sir **Dougald Clerk** in a form which remains in use today though somewhat simplified by Joseph Day in 1891. **George Brayton**, an American engineer, had developed a two-stroke kerosene engine in 1873, but it was too large and too slow to be commercially successful.

In 1885 **Gottlieb Daimler** constructed what is generally recognized as the prototype of the modern gasoline engine. Small and fast, with a vertical cylinder, it used gasoline injected through a carburetor. In 1889 Daimler introduced a four-stroke engine with mushroom-shaped valves and two cylinders arranged in a V, having a much higher power-to-weight ratio than previous engines. With the exception of electric starting, which would not be introduced until 1924, most modern gasoline engines descend from Daimler's engines.

The other main type of reciprocating internal combustion engine is the diesel engine, invented by **Rudolf Diesel** and patented in 1892. The diesel uses the heat produced by compression rather than the spark from a plug to ignite an injected mixture of air and diesel fuel (a heavier petroleum oil) instead of gasoline. Diesel engines are heavier than gasoline engines because of the extra strength required to contain the higher temperatures and pressures. The Wrights decided they needed a gasoline engine.

Unable to find an engine manufacturer to meet their specifications, the Wrights decided to design and build their own gasoline engine. Aided by their bicycle mechanic **Charlie Taylor**, they were able to build an engine that produced 12 horsepower at 900 rpm. It was a four cylinder in-line water-cooled engine.

In 1903, after redesigning the airframe of their 1902 Glider, the Wright Flyer was born. The weight of the aircraft was 340 kg and the area of the wings 15 m^2 with a wing span of 12 m. The two propellers rotated in opposite directions and were chain driven from the engine at the rear.
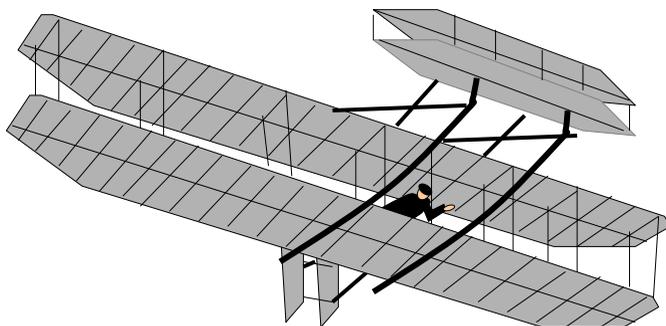
Fig. 6.5 The Wright Flyer was the first machine to reach the power density of a bird

In the fall of 1903 the Wright brothers shipped their airplane to Kitty Hawk, on the coast of North Carolina. The Flyer was launched from a trolley on rails. On December 17, 1903, Orville made the first manned controlled flight in a machine heavier than air. It lasted 12 seconds and covered 40 m. The speed of the first flight was 15 m/s. This was nine days after Langley's disaster with his Aerodrome. So close was the race and so small the margin between failure and success. Langley had never taken much interest in the two obscure brothers from Ohio while the Wrights were keenly aware of Langley's work. Langley died in 1906, a broken man while the Wrights toured the US and Europe with their machine.

It is an interesting observation that the power per aircraft weight of the Wright Flyer was 26 W/kg which is approximately the same as that of a gull in full flight. Thus, man had now designed a machine that could match nature …

Once the take-off was achieved, man rapidly outpaced nature. The power of a modern aircraft like the Swedish Gripen is at about 2500 W/kg and a space launcher like the Ariane is at 20000 W/kg. This gives an idea about the progress in 100 years of human flight.

It is a remarkable fact that a pair of brothers were behind both the two great inventions of manned flight, the balloons and the aircraft. Perhaps a close-knit family provides the atmosphere of competition and interaction that is required for developing new ideas. Certainly, a great deal of persistance is also required and the Wrights would soon be required to prove that they were very well equipped in that respect.

The Wrights improved their machine so that by 1905 they could fly more than 40 km in 38 minutes. In 1909 the War Department purchased an improved machine. The Wright Brothers started the Wright Company in 1909 to produce their aircraft and promptly became involved in bitter patent fights with people that tried to copy their inventions. Lastly, in 1914, they won the right to royalties from their competitors.

At that time Wilbur Wright was dead since two years of typhoid fever and Orville had sold out his interest in the Wright Company. He lived on until 1948 and his natural obstinacy grew with the years. When his sister Kathrine, who herself had participated in some tests of the early Flyer, married, he took it as an act of treason to the family and refused to see her until she was dying.

 He also became entangled in a dispute with the Smithsonian as the museum tried to honor its former director Langley as the true pioneer of powered flight. In revenge, Orville sent the original Wright Flyer to the Science Museum in London. There it stayed from 1928 until Orvilles death in 1948 when it was sent back to the Smithsonian, where it now remains.

Ex 6.1

Accelerating an airplane to take-off speed is risky. To keep the speed down, the lift coefficient should be high which can be achieved with a high angle of attack. On the other hand there is an angle beyond which the aircraft stalls. The Wright Flyer weighed 340 kg with the pilot. Its wing span was 12 m and the wing area was 46 m2. What would be the take-off speed required to avoid stall?

Ex 6.2

Another indication of the standard of technology is wing loading, which is a measure of the sofistication of the wings. The wing loading of the Wright Flyer was 72 N/m2 from the figures in Ex. 5.1. What is the wing loading required for a modern aircraft at take-off when the standard take-off speed is 90 m/s?

7. THE GOLDEN AGE OF THE PROPELLER

After the Wright Brother's first flight in 1903, the development went very fast. Many different types of aircraft were built and tested and the science of aerodynamics was born. It was shown how the air flow over flying bodies could be modelled and applied to practical designs. Charles Lindbergh's solo flight over the Atlantic in 1927 was a big media event and accelerated the development. Gradually, the speed limit of the propeller was approached.
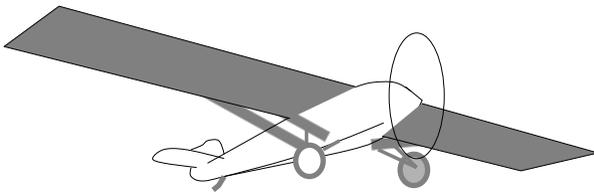
Fig. 7.1 Charles Lindbergs Spirit of Saint Louis 1927

When the young American **Charles Lindbergh** landed at Le Bourget outside Paris on the 21st of May 1927 greeted by thousands of people, neither he nor anyone else had any idea of the

fantastic impact his solo flight over the Atlantic would have on the future of air transport.

However, in the emerging age of mass media, Lindbergh overnight became the most famous man in the world. In the months following his flight, hundreds of new aircraft companies sprang up. It was the break-through of aviation. Yet, although Lindbergh was the first to cross the Atlantic nonstop he was far from being the first to cross it in air. And behind him there was 25 years of development that finally resulted in his famous aircraft, the *"Spirit of Saint Louis"*.

The Wright Brother's first flight had been in 1903. After that the development went very fast. From 1900 to 1910 many pioneer airmen in many nations flew airplanes. Cash prizes for record flights stimulated the development of aviation. Fliers were particularly active in France and in 1909 **Louis Blériot** was the first to cross the English Channel in his *Blériot XI*.

After 1910, European aeronautics rapidly caught up with America and the Wright brothers. The main reason was that all the Wright aeroplanes were controlled by a nose wing and statically unstable. This meant that they could not fly by themselves but had to be constantly controlled by the pilot. Modern test pilots regard it as a miracle that the Wright brothers were able to fly their machine at all. European inventors instead developed inherently stable tail controlled aeroplanes that were safer and easier to fly. This was to remain the dominant philosophy for about a century until the advent of "fly-by-wire" electrically controlled aircraft of the 1990's.

The first commercial airline began in 1910 in Germany. Passengers and cargo could now fly from city to city day and night, on seaplanes, planes with landing gear, and even over long distances.

Of course, the military in several countries were interested in using aeroplanes in war. The Italian army was the first to use aircraft for military purposes and they also dropped the first bombs, took the first aerial photographs and were the first to have one of their aeroplanes shot down.

World War I accelerated the expansion of aviation. Airplanes were first used for observation and later for aerial duels, bombing, and other purposes. A multitude of aircraft types were tested in combat in the war period 1914-18, and literally hundreds of prototypes were built and flown. Those numbers become believable when one considers that the prototype of a fighter aircraft could be designed, built and test flown within a period of a few weeks. In contrast to the earlier home-made approach to aircraft construction that prevailed prior to 1914, an aircraft industry was developing, nurtured by large sums of money from the belligerent governments.

Aircraft types of amazing varieties were built in the continual quest for better fighting machines. Monoplanes, biplanes, and triplanes were employed in military operations in various stages of the war, and several quadruplanes were tested in prototype form. The wings of most of these aircraft were supported externally by a combination of wires and struts, although several designers developed aircraft with internally braced cantilever wings. Perhaps the most notable was the Dutch designer **Anthony Fokker**, who supplied many cantilever-wing fighter aircraft to the German airforce. Both pusher- and tractor-type engine installations were

employed, and multiengine bombers frequently utilized a combination of pusher and tractor powerplant installations.

The pusher-type configuration was used extensively for fighters, particularly by the British, in the early stages of the war because the propeller was out of the way of the machine gun. This changed when **Anthony Fokker** synchronized the engine and the machine gun.

The internal structure of most of the aircraft consisted of a wooden framework braced with wire and covered externally with cloth. Some aircraft employed a mixture of metal and wood in their construction, and experiments were conducted with all-metal aircraft whose wings were internally braced. **Dornier** and **Junkers** in Germany were among the pioneers in all-metal aircraft construction. The types of alloys available at the time, however, did not lend themselves to the light weight required in aircraft design, and the concepts of a light, stressed-skin metal construction lay in the future.

Two vastly different engine types were employed in the World War I aircraft, the stationary engine and the rotary engine. The stationary water-cooled engines of 4, 6, 8, and 12 cylinders were not unlike the automobile engine of today. A few of the engines were aircooled. The rotary engine had cylinders arranged radially around a crankshaft; but unlike the modern radial engine, the crankshaft was fixed to the aircraft, and the cylinders and crankcase, with propeller attached, rotated around it. This engine type was of relatively light weight and was easily cooled by engine rotation, advantages that accounted for its extensive use. The rotary engine was perfected in France. It had a primitive control system and introduced undesirable gyroscopic moments in the aircraft that adversely affected flying characteristics. The rotary engine is a curiosity that rapidly vanished from the scene.

Aircraft design during World War I was more inventive, intuitive, and daring than anything else. Prototypes were frequently constructed from full-size chalk drawings laid out on the factory floor. The principles of aerodynamics that form so important a part of aircraft design today were relatively little understood by aircraft designers during those days.

Basic studies of the airfoil shaped wings of birds had started much earlier and scientists were now slowly beginning to understand how they functioned. We have mentioned before that the wing causes the air to flow more rapidly above than below the wing. The difference in air speed creates a downwash at the end of the wing which gives a lifting force. It is a remarkably simple and ingenious invention.

Relative to the average velocity, the air is moving forward below the wing and is accelerated backward over the wing. Thus, relative to the average velocity, the air circulates around the airfoil. To be able to understand the flow of air around the wing, scientists concentrated on this circulation.

It is complicated to analyse the flow around an airfoil. It is much easier to understand what happens around a circular cylinder. We are all familiar with the fact that a ball given a spin will drift to the side. Obviously, the rotation has created a force on the ball.

Next to any surface, the molecules of the air will stick to it. This thin layer of molecules will entrain or pull the surrounding flow in the direction that the surface moves. If we put a cylinder that is rotating about the longitudinal axis (a line perpendicular to the circular cross section) into a fluid, it will eventually create a spinning, vortex-like flow around the cylinder. If we then set the

fluid in motion, the uniform velocity flow field can be added to the vortex flow.

In Figure 7.2 we can see that the streamlines around the cylinder are distorted because of the spinning. The speed will be higher above the cylinder than below. If the cylinder were not spinning, the streamlines would be symmetric at top and bottom. Because of the change to the velocity field, the pressure field will also be altered around the cylinder. The net turning of the flow has produced an upward force. The magnitude of the force can be computed by integrating the surface pressure times the area around the cylinder. The direction of the force is perpendicular to the flow direction.

In fact, in the early 1920's the force from a rotating cylinder was used to power a sailing ship. The idea, proposed by **Anton Flettner** of Germany, was to replace the mast and cloth sails with a large cylinder rotated by an engine below deck. The idea worked, but the propulsive force generated was less than the motor would have generated if it had been connected to a standard marine propeller!

The incompressible flow around a rotating cylinder was known since a long time but how could it be used to analyze the much more complicated shape of the airfoil? In 1906, the Russian mathematician **Joukowski** found the key. In this year he published two papers in which he gave a mathematical expression for the lift on an airfoil. He had developed a mapping function using complex variables that converted a circular cylinder into an airfoil shape.
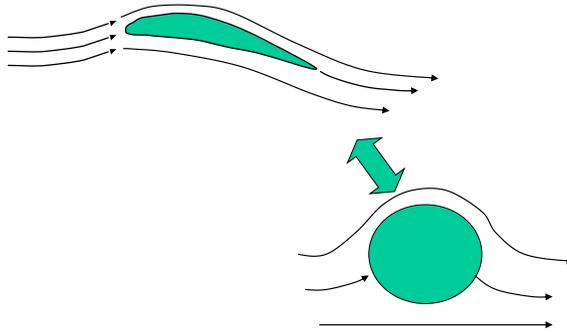
**Fig.7.2 Joukowski transformed the flow around an airfoil
to that around a cylinder**

The mapping function also converted the entire flow field around
the cylinder into the flow field around the airfoil. Since he knew
the velocity and pressures in the plane containing the cylinder, he
could derive the velocity and pressures around the airfoil using the
mapping function. Knowing the pressure around the airfoil, he
could then compute the lift. Today this is known as the Kutta-
Joukowski theorem, since the German scientist **Kutta** pointed out
that the equation also had appeared in his 1902 dissertation.

Nikolai Egorovich Joukowski was born in 1847 and obtained a
doctorate from Moscow University in 1882 for a dissertation on
the stability of motion. He continued to work at the university and
became Head of its Department of Mechanics in 1886.

In 1891, he began to study the dynamics of flight and in 1895 he visited Lilienthal in Berlin. Joukowski observed several of Lilienthal's flights and was very impressed. Joukowski also purchased one of the eight gliders which Lilienthal sold to members of the public.

His mapping function gave Joukowski a means of designing airfoils. Those Joukowski airfoils were actually used on some aircraft, and today these techniques provide a mathematically rigorous reference solution to which modern approaches to aerofoil design can be compared for validation.

The **circulation** around the airfoil created an important theoretical problem when it was first proposed. From fluid conservation laws, if a fluid initially had no vorticity, then when an airfoil moved through the fluid the net vorticity within the domain had to remain zero. With a bound vortex around the airfoil, there should be another vortex of opposite strength present within the flow domain. Then the sum of the two vortices, one spinning clockwise, the other counter clockwise, would be zero as required by the conservation laws.

It took some very careful experimental work by **Ludwieg Prandtl** to actually "catch" the other vortex on film. In his experiment he placed an airfoil in a tunnel with no flow. He then started the flow and photographed the flow field at the trailing edge of the airfoil. What he saw was a vortex shed from the trailing edge, spinning opposite to the predicted bound vortex in the airfoil. The shed vortex was transported downstream and eventually mixed out due to viscous effects in the real fluid. Theoretically, the shed vortex would remain with constant strength and would be carried

downstream away from the airfoil. This is depicted by the vortex at the right of the Figure 7.3.

Flow **Shed vortex**

Downwash
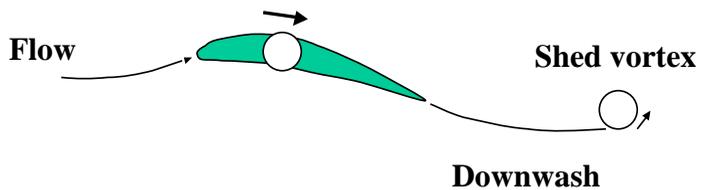
Fig. 7.3 Prandtl detected the shed vortices from an airfoil

Ludwieg Prandtl is without much doubt the most important aeronautical scientist. He was born in Freising, Germany, in 1875. In 1904, 29 years old, Prandtl was appointed professor of applied mechanics at Göttingen University, where he remained until his death in 1953. In Göttingen he founded the world-famous Kaiser-Wilhelm Institute for the study of fluid flow. He made notable innovations in the design of wind tunnels and other aerodynamics equipment. His advocacy of monoplanes greatly advanced the heavier-than-air aviation. His influence was spread not only by

published papers but also by many brilliant students, who worked with him and then moved on.

Prandtls greatest contribution to fluid mechanics is the so called boundary layer theory. In August of 1904, a small group of scientists gathered in the picturesque German city of Heidelberg for the Third International Mathematics Congress. One of the speakers of the congress was the 29 year old Ludwieg Prandtl. In just ten minutes he managed to present one of the most important breakthroughs in fluid mechanics of all time.

Before Prandtl's description of the **boundary layer** in 1904 scientists had tried to construct potential flows, i.e., incompressible, irrotational flows, over bodies. It was recognized that such flows failed to model real flows and frequently resulted in zero drag, a prediction in clear contradiction with everyday experience.

Prandtl's contribution was to realize that the flow could be divided into two regions. Only in a small region near the body, the boundary layer, do viscous effects dominate. The bulk of the flow can be regarded as a potential flow. A proper understanding of the boundary layer is the key to understanding flow separation, transition into turbulence, skin friction and heat transfer.

Originally, Prandtl studied mechanical engineering in Munich. For his doctoral thesis he worked on a problem on elasticity under **August Föppl**, who himself did pioneering work in bringing together applied and theoretical mechanics. Later Prandtl became Föppl's son-in-law. It is said that on turning 40, he suddenly decided that it was time to get married and wrote a letter to Föppl requesting the hand of one of his daughters but he did not mention

which one. The Föppl family decided which of the two daughters that should marry Prandtl and they lived happily ever after.

One of Ludwieg Prandtl's most notable contributions to aeronautics was to explain the **induced drag**. The total coefficient of drag on the airplane is as we have already seen given by Eq. (6.4). The second term on the right hand side of this equation is called the induced drag and is manifested in the tip vortices from the wing.
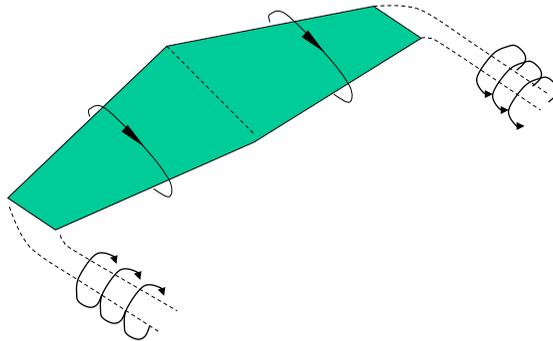
Fig. 7.4 Trailing vortices from wingtips give rise to induced drag

With a finite wing span, the circulation created around the wing tends to spill over the wingtip. This creates the **trailing wingtip**

vortices found with all aircraft in flight, see Figure 7.4. Sometimes they are visible when an aircraft flies at a high angle of attack creating a high pressure difference over the wing. The water in the air condenses in the low pressure vortex and two curled lines extend backwards from the wingtips. The energy that is stored in those vortices is lost and is experienced as induced drag. It is as if the aircraft had to pull these vortices with it through the air, which of course will take some extra effort.

In addition to producing induced drag, the trailing vortices create considerable turbulence, which can be very dangerous for nearby aircraft. The trailing vortices of a large jet can actually flip a small aircraft which approaches too closely. These considerations are important in air traffic control. With large planes such vortices may persist for several kilometres.

Although it is not possible to eliminate the induced drag, it is possible to minimize it by suitably choosing the shape of the wing. In fact, it was shown by Prandtl that the induced drag is minimized if the lift per unit span along the wing is elliptical. This can be achieved in a number of ways - for instance, making the chord vary elliptically along the wing (known as an elliptical planform). The outstanding aerodynamic performance of the Spitfire of World War II was partially attributed to its elliptic shaped wing.

In this way Prandtl explained the experimental results by e.g. the Wright brothers that the amount of induced drag is dependent on the span wise lift distribution and the aspect ratio of the wing. A high aspect ratio wing has lower induced drag than a low aspect ratio wing since its wingtip vortices are weaker.

Thus, much of the work in aerodynamics at the time aimed to understand vortices. The mathematical theory describing the

alternately shed vortices behind a bluff body was developed by **Theodore von Karman** in 1911. This was later called "The Karman Vortex Street".

Von Karman was born in Hungary and became interested in aeronautics while visiting a girlfriend in Paris who dragged the not very interested Theodore to a flight display of the French aviator **Henri Farman**. Getting interested in aeronautics, Von Karman then came to work with Prandtl in Göttingen and went on to become one of the leading personalities in the US aeronautics scene as a professor at the California Institute of Technology. He also founded an aeronautical institute in Brussels that carries his name. Among other things his work at Caltech resulted in the so called "fillets". In the 1930's it was found that the sharp corner where the wing joined the fuselage resulted in shed vortices which increased drag and buffeted the tail. Von Karmans solution was to smooth out the corner with fairings. Since that time, such "fillets" are standard on airplanes.

There is another effect associated with the vortices. Ever since the beginning of manned flight, pilots have experienced something strange when landing an aircraft. Just before touchdown it suddenly feels like the aircraft wants to go on and on due to the air that is trapped between the wing and the runway, forming an air cushion. The air cushion is best felt in low-winged aircraft with large wing areas. This is called the **ground effect** and you can see water birds taking advantage of it to gain speed to take off. The Wright brothers probably never flew out of ground effect in their early flights. They benefited from it without even knowing it existed.

Around 1920 this effect was first described and some (theoretical) research was carried out. The reason for the effect is that there is not enough space for the vortices to fully develop when a wing is approaching the ground. Therefore the amount of "leakage" of pressure from the lower to the upper side is suppressed and the vortices become weaker. The vortices are also pushed outward by the ground so that the effective aspect ratio of the wing becomes higher than the geometric aspect ratio reducing the induced drag.

Over the years there have been many proposals to take advantage of the ground effect for making long distance aircraft that could cross the Atlantic or even the Siberian tundra. The flying boat Dornier DO-X could only cross the Atlantic when it was flying with its hull just above the wave crests.

After the War (in 1918), the military started to make use of the new ideas. The aircraft carrier was developed. At the same time helicopters were tested. But the war's pilots found little use for their skills. Many of them bought surplus warplanes and offered rides in their craft or did stunt flying at county fairs and carnivals. These courageous and often foolhardy fliers promoted interest in aviation.

Nonetheless, the pace of aircraft development and production was extremely slow in the first years after the war. The military were exhausted and the requirements of civil aviation during this period presented little incentive for advanced aircraft. Only by the middle of the 1920's did aircraft development begin to accelerate and the aircraft industry started to grow.

At the same time, the results of research began to play an increasingly important role in providing the new technology necessary for the development of advanced aircraft. Wind tunnels, laboratories, flight research, and analytical studies were the means

by which new technology was developed. The US National Advisory Committee for Aeronautics (NACA) began to play an increasingly important part in providing new technology

The Atlantic Ocean fascinated the airmen. In 1919 **Raymond Orteig** of France had offered $25,000 for the first nonstop flight between New York City and Paris. Several French and American fliers made unsuccessful and often tragic attempts. In 1919 three huge United States Navy flying boats attempted the first Atlantic crossing. Only one, the NC-4, succeeded. In 1924 the first round-the-world flight was made. United States Army airmen took off in four Douglas World Cruisers from Seattle in the USA but only two completed the trip. It took them 15 days, 3 hours, and 7 minutes flying time.

Finally, in 1927, Charles A. Lindbergh succeeded in his Ryan monoplane, the "*Spirit of St. Louis*". His brave solo flight of 33 1 /2 hours not only conquered the Atlantic but also made the world more air-minded.

The Spirit of St. Louis" was designed with one thought in mind: to get to Paris. Extra fuels tanks were added and the wing span increased to accommodate the additional weight. In his efforts to cut down the plane's weight, Lindbergh considered every detail. Any item considered too heavy or unnecessary was left behind. These included a radio, parachute, gas gauges, and navigation lights. Lindbergh even designed for himself special lightweight boots for the flight, and went so far as to cut his maps down to include only those reference points he would need. Instead of a heavy leather pilot's seat, Lindbergh would be perched in a far lighter wicker chair.

Why was it so important to cut down on the weight? The reason is

the so called Brequet range equation. **Louis-Charles Brequet** was a French aircraft designer born in 1880, who built his first aircraft in 1909. During WWI he mass produced aircraft for the French army. It is not clear whether he had anything to do with the equation that came to be named after him but anyhow it is one of the most important equations in aeronautics.

The engine efficiency is defined as the thrust power divided by the power supplied by the fuel i.e.

$$\eta = \frac{FV}{\dot{m}_f h} \tag{7.1}$$

where **"h" is the heat content** of the fuel in J/kg.

Now since F=D and L=mg

$$-\frac{dm}{dt} = \dot{m}_f = \frac{FV}{\eta h} = \frac{DV}{\eta h} = \frac{D}{L}\frac{mgV}{\eta h} = \frac{D}{L}\frac{mg}{\eta h}\frac{ds}{dt} \tag{7.2}$$

Thus the **range "s"** for a given amount of fuel is:

$$s = \eta \frac{L}{D}\frac{h}{g}\ln\frac{1}{1 - m_f / m_0} \tag{7.3}$$

The Brequet equation shows that the range of an aircraft is directly proportional to the product of the engine efficiency, the lift-to-drag ratio and the heat content of the fuel. However, and this was the most important to Lindbergh, the equation also shows that the range increases very rapidly with the so called "fuel factor" that is the weight of the fuel relative to the weight of the aircraft. Thus he had to keep down the weight as much as possible.

The equation assumes that the L/D remains constant. This is not the case since the weight of the aircraft decreases as the fuel is consumed, which decreases the lift L. To keep L/D constant, D must also decrease and this can be achieved by rising to a higher altitude with decreased air density. Therefore, the Brequet range equation assumes that the aircraft climbs slowly during the flight while traffic control normally requires a constant altitude. Nevertheless, the Brequet equation shows that weight, L/D and engine efficiency are important characteristics of an aircraft.

The monoplane Spirit of St. Louis popularized the monoplane configuration and marked the beginning of the decline of the biplane. The motivation for the biplanes was that they gave sufficiently high wing area to keep down the take-off speed. At the same time they produced a lot of drag . The drag coefficient of the Spirit of Saint Louis was about half that of the biplane Wright aircraft.

Before Lindbergh made his flight, engine technology had also advanced very much. The Wright Flyer's engine developed 12 hp and the aircraft weighed 340 kg which represented 26 W per kg of aircraft. The Spirit of Saint Louis was equipped with a 220 hp engine that gave 170 W per kg of aircraft so the relative engine power had increased more than six times.

Fighting fog, icing, and sleep deprivation, Lindbergh finally landed safely at Le Bourget Field in Paris at 10:22pm on May 20, 1927. "The Spirit of St. Louis" had carried him nearly 6000 km in 33.5 hours. A new aviation hero was born, and the "Spirit of St. Louis" attained legendary status.

He was soon followed by others. **Amelia Earhart** flew over the Atlantic as the first woman passenger in 1928 in the Fokker Friendship. In 1932, she became the first woman to fly alone over the Atlantic in a Lockheed Vega setting a new record of 12 hours and 30 minutes. In 1935 she also became the first woman to cross the Pacific Ocean. She and her navigator, **Fred Noonan** then disappeared on a flight over the Pacific in 1937 during an attempt to circumnavigate the earth.

Civil aviation now started to take off. In the United States many airline companies started business to deliver mail. These same companies also carried passengers and other cargo. Some of them are still in business today. **Pan American** Airways became the leader in flying across the Atlantic and the Pacific.

The engineering principles of aircraft design were beginning to take shape. Government laboratories, such as the Royal Aeronautical Establishment in England, contributed greatly to the foundation of aeronautical engineering. Scientific and engineering laboratories also existed in France, Italy, and Germany and were behind the European domination of aeronautical sciences during the early decades of the 1900's. In 1915, the National Advisory Committee for Aeronautics (**NACA**) was established in the United States by an act of Congress. The results of NACA research did not begin to have a significant impact on aircraft design until the second half of the 1920's but since then America has dominated the scene.

The high-wing monoplane, the **Ford Trimotor**, formed the mainstay of the infant U.S. airline industry in the late 1920's and early 1930's. It was an all-metal construction. The internal structure of the aircraft was entirely of metal, and the skin was a corrugated aluminium alloy. The corrugations provided stiffness in the skin panels and were aligned with the direction of air flow in

order to minimize the drag. This type of construction had been pioneered by **Hugo Junkers** in Germany.

The **Lockheed Vega** was another very high-performance monoplane that first flew in 1927. A new feature, which appeared on this aircraft, was a circular cowling surrounding the 450-horsepower Pratt & Whitney Wasp air-cooled engine. This cowling concept was one of NACA's early contributions and reduced the drag of the aircraft dramatically, in some instances by more than 50%. The maximum speed of the Lockheed Vega was increased from 260 km per hour to 300 km per hour by the addition of the NACA cowling.

The **Wasp** was one of the most used engines of the days and it came to have a colourful history in Sweden during WW2. Before the war, Sweden had ordered a number of aircraft from the US. The aircraft were equipped with the Twin Wasp engine but only a small number was delivered before the war broke out and export to Sweden was interrupted. Since no licence for production could be obtained, Sweden decided to copy the American engine. This was done by the Svenska Flygmotor AB now the Volvo Aero Corporation. This engine was called the Swedish Twin Wasp (STW). After the war, Sweden payed a royalty to Pratt & Whitney for the engines produced.

The Lockheed Vega had a very low zero-lift drag coefficient obtained through careful attention to the aerodynamic design of the aircraft and by the absence of drag-producing struts, wires, and other external drag-producing elements. The fixed landing gear, however, remained as a significant drag-producing feature of the airplane. The maximum lift-drag ratio of the Vega was 11.4, which was unusually high for that time period. This means that after 30 years of development, man had reached the same aerodynamic

efficiency as a sea-gull but still had some way to go before overtaking the albatross at an L/D close to 20. This was not achieved until by the Boeing 747 in the 1970's.

In the 1930's, the propeller-driven aircraft reached its final form. The power of reciprocating engines tends to fall with altitude as air density decreases. A supercharger compresses the incoming air increasing its density. Without a supercharger the altitude is limited to below 5000 m. Early work on such superchargers was performed by NACA in the 1920's. In 1929 an airplane powered by a supercharged Pratt & Whitney Wasp engine reached a record altitude of nearly 10000 m.

Another feature was an effective high-lift flap system for increasing the maximum lift coefficient and reducing the stalling speed. The use of effective high-lift flaps became standard practice on high-performance configurations later in the decade.

Finally, the use of wood as a primary material for construction had many disadvantages so some form of light, stiff, all-metal structure was desired. One of the first aircraft developed in the United States to employ an all-metal stressed-skin type of structure was the **Northrop Alpha**. In this type of structure, the metal skin is smooth, not corrugated, and contributes significantly to the stiffness and load-carrying capability of the structure. The stability of the thin metal skin is usually enhanced by numerous internal stringers attached to it. Various forms of stressed-skin metal construction were destined to become the norm for propeller-driven aircraft in the years ahead.

The Alpha also employed a low wing of cantilever construction and a full NACA-type cowling around the radial engine, but had an anachronistic fixed landing gear together with an open cockpit for the pilot. The zero-lift drag coefficient for the aircraft was about the same as that for the Lockheed Vega.

Thus in the 1930's, vintage aircraft design included:

1. Cantilever wings

2. Retractable landing gear

3. Efficiently cowled, light radial engine

4. Supercharger

5. All metal, stressed-skin construction

The first aircraft that assembled most of these features in a single configuration was the **Boeing 247**. This aircraft did not employ wing flaps and had a relatively low wing loading. Its maximum lift-drag ratio was 13.5. About 75 Boeing 247's were built but the type was not developed further, perhaps because of Boeing's preoccupation with bomber aircraft development during that period of time.

A contemporary and very similar aircraft, the **Douglas DC-2**, employed all the features mentioned for the Boeing machine and, in addition, had a higher wing loading and split-type landing flaps. The **Douglas DC-3** was developed from the DC-2 and it incorporated all the advanced technical features of the Boeing 247 and the Douglas DC-2 but, in addition, was sufficiently large to carry 21 passengers. With this number of passengers and a cruising speed at 3 000 meters of 300 km per hour, the aircraft set a new standard for air travel and made it possible for airlines to make a profit in passenger service independent of subsidy or mail contracts.

The DC-3 is, by any measure, one of the best-known aircraft ever produced anywhere in the world. The aircraft first flew in December 1935 and was in airline operation by the summer of 1936. Seventy years later, more than 1,000 DC-3s are still operating.
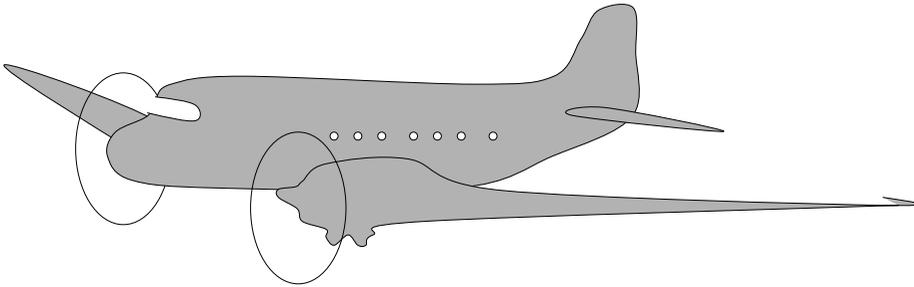
Fig. 7.5 DC3- the first modern passenger aeroplane 1935

 The timing of the introduction of the DC-3 to the market was nearly perfect and the growth was phenomenal. From 1936 to the start of World War II in 1939, U.S. air travel increased up to 500 percent. Airline response was swift. The DC-3 was what they needed to continue their growth. Outside the U.S., there was a similar surge in commercial aviation. The Douglas aircraft were available to meet the need and generate profits, and were in service with 30 carriers in Europe and Asia. License agreements for building the DC-3 were granted to manufacturers in Holland, Japan and Russia.

A distinctive identification feature of the DC-3 was the sweptback wing, which was inherited from the DC-2 and was used to position

the aerodynamic centre of the aircraft in the proper relationship to the centre of gravity.

The design of the DC-2 wing did not initially employ sweepback but had a highly tapered straight wing. As the design of the aircraft progressed, however, it became evident that the centre of gravity was farther aft than had been anticipated. Sweepback offered a simple means for moving the aerodynamic centre into the correct position. The higher aspect ratio of the DC-3 increased the maximum lift-drag ratio to 14.7 as compared with 13.5 for the Boeing 247. Later, it would be proved that a swept wing also increased the high speed performance of aircraft.

Thus in the late 1930's, the aircraft had found a shape that remains more or less the same today. But propulsion stood before a revolution. As the world approached WW2, the inability of the **propeller** to provide speed became a serious obstacle to the further development of fighter aircraft. The propeller was also becoming an obstacle to the increasing demands for civil transportation, which required higher speeds to increase the transportation capacity.

The details of propeller propulsion are very complex because the propeller acts like a rotating wing creating a lift force by moving through the air. The blades are usually long and thin. A cut through the blade perpendicular to the long dimension will give an airfoil shape. Because the blades rotate, the tips move faster than the hub so the angle of attack of the airfoils at the tip is lower than at the hub making it necessary to twist the blades. Of course, this makes analyzing the airflow through the propeller a very difficult task. However, a general understanding may be obtained relatively easy, see Figure 7.6.
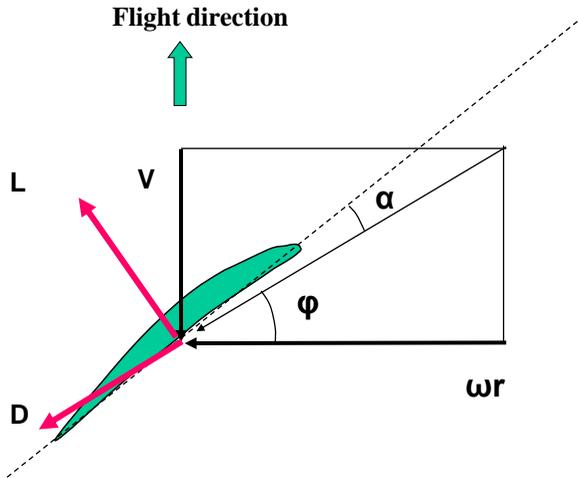
Fig. 7.6 Forces on a propeller

Assume that the propeller rotates with an **angular velocity "ω"** while the **airspeed is "V"**. When the plane of the propeller is normal to the airspeed, the resulting speed at a blade element at the **radius "r"** will have the effective **pitch angle "φ"** where:

$$\varphi = \arctan \frac{V}{\omega r} \qquad (7.4)$$

By pushing air aft, the propeller converts the power exerted by the crankshaft into propulsive power. With L as the lift of the blade perpendicular to the relative wind and D as the drag parallel to the relative wind, the axial and circumferential forces are:

$$F_{ax} = L\cos\varphi - D\sin\varphi \qquad (7.5)$$

$$F_c = L\sin\varphi + D\cos\varphi \qquad (7.6)$$

The former is given to the air jet by the propeller, the second is provided to the propeller by the crankshaft. Then the local efficiency at any radius "r" with which the propeller produces thrust becomes:

$$\eta_p = \frac{F_{ax}V}{F_c\omega r} \qquad (7.7)$$

or with Eqs. (7.4) to (7.6):

$$\eta_p = \frac{V}{\omega r}\frac{\dfrac{L}{D} - \dfrac{V}{\omega r}}{1 + \dfrac{L}{D}\dfrac{V}{\omega r}} \qquad (7.8)$$

Obviously, the efficiency is zero at V=0. This is natural because when there is no motion of the aircraft there is no power available. But there is also a maximum speed, where the pitch angle φ becomes so large that the axial force of the propeller vanishes, see Eq. (7.5). Between those two extremes there is a speed, where the efficiency passes through a maximum. It is not so simple to find the efficiency variation of a propeller because the L/D is itself dependent on speed. However, for a given L/D, the speed that gives maximum efficiency is:

$$(\frac{V}{\omega r})_{opt} = \sqrt{1 + \frac{D^2}{L^2}} - \frac{D}{L} \qquad (7.9)$$

Operating the propeller at this speed gives the maximum efficiency at radius "r" as:

$$\eta_{p\max} = (\sqrt{1 + \frac{D^2}{L^2}} - \frac{D}{L})^2 \qquad (7.10)$$

Thus the propeller efficiency is directly dependent on the lift-to-drag ratio of the blade. A good propeller has L/D>10, which means a maximum efficiency above 80 %.

The **angle of the blade "β"** is the **pitch angle "φ"** in addition to a certain **incidence angle "α"**, that is β=α+φ. It follows that the blade angle has to vary with speed as:

$$\beta = \alpha + \arctan\frac{V}{\omega r} \qquad (7.11)$$

From the drag polar diagram of an airfoil, Fig. 6.4, it is seen that L/D is a maximum for a certain incidence angle α. For a given speed, the blade angle should therefore decrease along the blade, that is with increasing radius "r", in order to maintain the optimum incidence angle. For this reason propeller blades always have a built-in twist angle along the blade.

Optimum conditions cannot be maintained at all sections of the blade at all speeds. To characterize propellers, it is therefore common to use the so called **advance ratio**:

$$J = \frac{V}{nd} \qquad (7.12)$$

Here **"d" is the diameter of the propeller** and **"n" is its number of rotations per second**. It is usual to take the advance ratio at 75% of the radius as representative for the propeller. This represents about half of the propeller surface. The advance ratio which gives maximum efficiency is approximately from Eq. (7.9) if D<<L:

$$J_{opt} \approx \frac{3\pi}{4} \qquad (7.13)$$

It is also seen from Eq. (7.8) that the efficiency is zero both at J=0 and at a certain highest value of J.

For a preset blade angle β, the incidence angle α will vary with speed, see Eq. (7.11). Since the L/D of the blade is dependent on the incidence angle, the efficiency of the propeller will follow one of the curves in Figure 7.7 according to Eq. (7.8). For each speed, there is a blade angle that will give maximum efficiency. To let the propeller operate optimally at each speed, it must therefore be possible to adjust the blade angle.
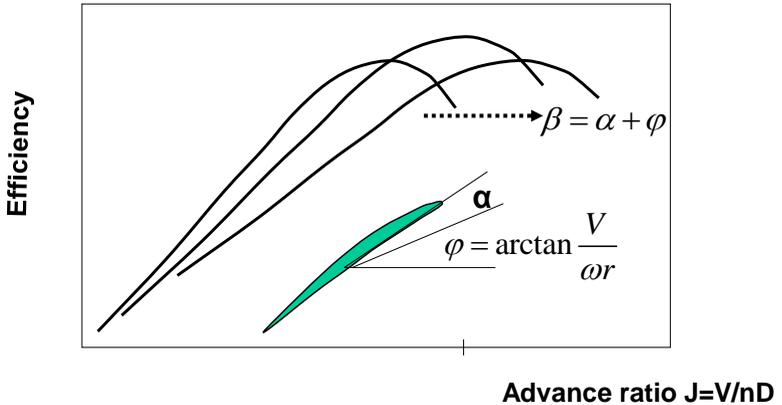
Fig. 7.7 The propeller has maximum efficiency for a certain advance ratio

As far back as the 19th century the French pioneer **Alphonse Penaud** proposed adjustable propeller blades and they were patented in 1924 by **H S Hele-Shaw** and **T E Beacham** in England. They came into practical service around 1935 after pioneering work by **Frank Caldwell** and the Hamilton Standard Company. The propeller blade is fixed to a mechanism in the hub, which rotates the entire blade. When the Boeing 247 was introduced in 1933, it had difficulties flying over the Rocky Mountains at 2000 m because of the fixed propeller. With adjustable propellers, the performance of the aircraft improved to such an extent that since that time it is generally used.

With this concept, it was possible to vary the pitch angle so that the engine could operate at a constant speed over a range of flight velocities. This allows the pitch to be varied automatically to maintain the proper torque on the engine while the speed of the engine is kept constant. For each flight speed the propeller blade angle is automatically adjusted so that the efficiency of the engine is a maximum.

When an object moving through air reaches a certain speed, shocks start to appear in the air due to compressibility effects. Propellers encounter such adverse effects of compressibility before the aircraft configuration itself because portions of the blades of the propeller, particularly near the tip, are traveling at a higher speed relative to the air than the aircraft.

The propeller tip speed is the resulting velocity of the propeller tip relative to the airflow so that:

$$V_{tip}^2 = V^2 + \left(\pi n d \right)^2 \qquad\qquad (7.14)$$

This means that the tip speed of the propeller is always higher than the flight speed and will have to increase with flight speed if the engine speed is maintained. It is then obvious that the tip speed can become very high while the flight speed is still relatively low.

When shock waves start to occur, the drag of the blade starts to increase, the L/D ratio falls and the maximum efficiency of the propeller decreases. This was what happened in the 1930's as the speed of aircraft increased.

A disturbance in air propagates at a certain speed, the so called speed of sound. Such disturbances spread through the air as rings on a water surface. Assume, see Figure 7.8, that the blade tip at a certain instance created such a disturbance, that moves away from the blade at a speed "a" m/s. Assume also that the blade tip moves through the air at a higher speed than that, say V>a. Then after one second when the first disturbance has moved a distance "a", the blade tip has moved a larger distance "V" and has caused a series of disturbances that move away from at the speed of sound. The result is that the blade leaves behind a shock wave that it has to pull through the air as shown in Figure 7.8.
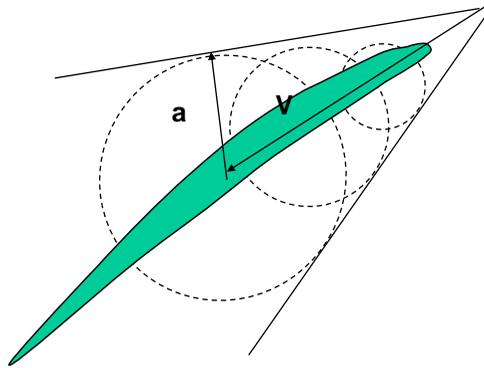
Fig. 7.8 Shocks at a blade tip at supersonic speed

The speed of sound is a very important property in aeronautics. Consider a shock wave moving at the **speed of sound "a"** through a tube as shown in Figure 7.9 below:

P   P+dp

ρ   ρ+dρ

a   a+da
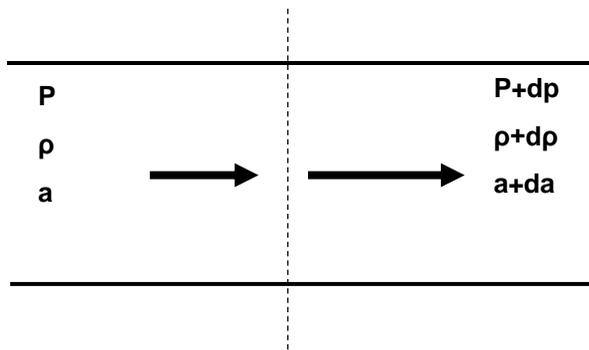
Fig. 7.9 Shock moving through a tube

The law of conservation of momentum gives:

$$\rho a da + dp = 0 \qquad (7.15)$$

Conservation of mass flow means that:

$$\rho a = const \qquad (7.16)$$

This gives the speed of the wave as:

$$a = \sqrt{\frac{dp}{d\rho}}$$ (7.17)

The English natural philosopher and chemist **Robert Boyle**, 1627-1691, made important contributions to experimental chemistry. The so called Boyle's law states that the volume of a given amount of gas varies inversely with **pressure "p"** so that for one kilogram $\rho = 1/v = k_1 \, p$. This made it possible for <u>**Isaac Newton** to make the first calculations of the speed of sound</u> in air and he found a value of 290 m/s.

Unfortunately, this was considerably below the value of 340 m/s that could be measured by observing the difference in time between the lightning bolt and the thunder from a cannon. Newton explained the difference by dust and water vapor in the atmosphere. However, he had made an incorrect assumption. As pointed out more than a century later by the great French mathematician **Pierre Laplace**, the sound wave is adiabatic (no heat loss) and not isothermal as Boyle's law assumes and this explains the error in Newton's calculations.

To understand the meaning of this we have to go back some time in the history of thermodynamics. The science of thermodynamics is the basis for the understanding of all machines involving heat and it is a landmark of 19th Century science. In the early 1800's, two French scientists, **Jacques Charles** and **Joseph Gay-Lussac** discovered that the volume of a gas is directly proportional to the **total temperature "T"** of that gas so that $\rho = k_2 / T$. It is possible to

combine their law with Boyle's law so that $\rho = k_3 \, p/T$. This can be rewritten into one simple relationship, the **Ideal Gas Law**.

It has been experimentally verified that for many gases including air at reasonable temperatures and pressures:

$$p = \rho RT \tag{7.18}$$

where $R = \Re/M$ is the **gas constant** in which $\Re = 8314$ is the universal gas constant and M is the molecular weight of the gas. For air $R = 287 \ m^2/s^2 \ K$.

An ideal gas is a substance that follows this equation. Despite its simplicity, this law is remarkably good at predicting the behavior of real gases at ordinary temperatures and pressures.

James Prescott Joule (1818-1889) was an English physicist who established that the various forms of energy (mechanical, electrical, and heat) are basically the same and can be changed, one into another. This is the law of conservation of energy, the first law of thermodynamics. He also established that heat was a form of energy regardless of the substance that was heated.

In 1852 Joule and William Thomson (later Lord **Kelvin**) (1824-1907) discovered that when a gas is allowed to expand without performing external work, the temperature of the gas falls. This "Joule-Thomson effect" was used to build a large refrigeration industry in the course of the 19th century. The value of the mechanical equivalent of heat is generally represented by the letter *J*, and a standard unit of work is called the "joule" in the honor of James Prescott.

dq=du+pdv
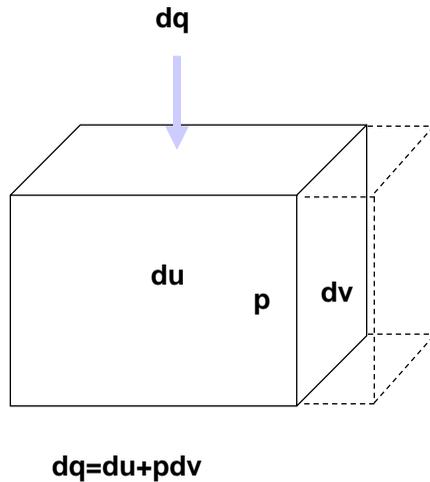
Fig. 7.10 The first law of thermodynamics

The first law states that for a closed system dq=du+dw, where "dq" is the quantity of **heat energy "q"** entering the system through its walls, "du" is the change of the **internal energy "u"** and "dw" is the **external work "w"** per unit mass. If the system is closed but allowed to increase its **volume "v" per unit mass**, where v=1/ρ and where **"ρ" is the density**, then the work performed is dw=pdv so that dq=du+pdv. This can also be written dq=d(u+pv)-vdp=dh-vdp where the so called **enthalpy h**=u+pv is a group of properties, that is frequently used in thermodynamics.

It is common to introduce specific heat coefficients dq/dT at constant pressure and constant volume. The temperature is a

measure of the state of the system. Taking absolute zero temperature as a reference state where everything freezes to zero gives $u = C_v T$ and $h = C_p T$ where **"C_v" is the specific heat at constant volume** and **"C_p" the specific heat at constant pressure**. According to the ideal gas law $pv = RT$. Then from the definition of enthalpy $h = u + pv$ one obtains $C_p - C_v = R$.

The first law of thermodynamics states that one type of energy can be transformed into another. However, this can not be made without a loss. The second law of thermodynamics was formulated in the middle of the last century by the German physicist **Rudolf Clausius** (1822-1888) and Lord Kelvin and it states that once energy has been lost, it can never be regained. All spontaneous processes are irreversible.

According to the second law, heat is always leaking away, that is the potential to do work decreases in all thermodynamic processes such as the spontaneous mixing of hot and cold gases, the uncontrolled expansion of a gas into a vacuum, and the combustion of a fuel. Clausius coined the term **entropy "s"** in 1865 to refer to the exchange of heat q in a process relative to its state, that is the absolute temperature "T". The second law states that the change of entropy in a process is always positive that is $ds = dq/T > 0$ that is heat is always leaking away from the process.

The active nature of the second law is intuitively easy to grasp and to demonstrate. If a glass of hot water is placed in a colder room a flow of heat is spontaneously produced from the cup to the room until it is minimized (or the entropy is maximized) at which point the temperatures are the same and all flows stop. No spontaneous change takes place in the other direction. Active work must be spent if we want to regain the heat in the glass.

Since the potential to do work is decreasing, the entropy change is a measure of a system's loss of potential to do useful work. Since work is obtained from order, the amount of entropy is also a measure of the disorder, or randomness, of a system. Since according to the second law, the entropy of the universe is increasing, more and more energy becomes unavailable for conversion into mechanical work, and because of this the universe is said to be "running down" like a clock!

In one statistical interpretation of entropy, it is found that for a very large system in a thermodynamic equilibrium state, entropy "s" is proportional to the natural logarithm of a quantity "W" representing the maximum number of microscopic ways in which the macroscopic state corresponding to "s" can be realized so that $s = k \ln W$, in which "k" is the Boltzmann constant. According to this interpretation, the increase in entropy that the universe is undergoing, can not avoid to lead to an increase of the available states, which means that the disorder of a closed system left to itself will always increase, an interpretation that is in good agreement with general experience.

Fortunately, we do not need to trouble ourselves much more with the entropy because what we are interested in are the temperatures and pressures in the process. The concept of entropy is useful, however, to clarify the thermodynamic processes and the losses in the different parts of them.

The change in entropy "ds" is obtained from the definition of entropy by **Gibb's** equation:

$$ds = dq/T = (du + pdv)/T = (dh - vdp)/T \qquad (7.19)$$

Or using dh= C_pdT and the ideal gas law pv=RT that is v/T=R/p:

ds=dq/T=C_pdT/T-Rdp/p   (7.20)

A closed system is said to be **adiabatic** if there is no heat interaction with the rest of the world so that **dq=0** externally. This is a good approximation for propulsion systems where the gas often passes so rapidly through the machine that the leakage of heat can be neglected. We will also restrict ourselves to cases where there is no heat exchange internally in the gas during the process. This means for instance that there must be no friction. With those assumptions, **ds=0** and the process is said to be **isentropic**, i.e. there is no change of entropy. Of course, all real processes involve an increase in entropy so that ds > 0.

It is common to introduce the **ratio of specific heats γ=C_p/C_v** . For air γ=1.4. Since from the above C_p-C_v =R:

$$C_p = \frac{\gamma}{\gamma - 1} R$$ (7.21)

So that ds=0 leads to the following isentropic relation between temperature and pressure:

$$T / p^{(\gamma - 1)/\gamma} = const$$ (7.22)

Then, the ideal gas law gives that ρ=p/RT=$p^{1/\gamma}$ /(Rxconst) so if there is a negligible exchange of heat across the wave, it can be shown that the speed of sound is:

$$a = \sqrt{\frac{dp}{d\rho}} = \sqrt{\gamma RT} \qquad\qquad (7.23)$$

As the speed of aircraft began to approach the speed of sound, the term **Mach number M**=V/a came to be used as a measure of speed. Mach 1 is the speed of sound. Mach 2 is twice the speed of sound and so on.

The Mach number is named after **Ernst Mach** (1838-1916), a philosopher and physicist from Austria. Mach was the first person to realize, that if matter traveling through the air moved faster than the speed of sound it drastically altered the quality of the space in which it moved. Mach's paper on this subject was published in 1877 and correctly describes the sound waves observed during the supersonic motion of a projectile. Mach deduced and experimentally confirmed the existence of a shock wave which has the form of a cone with the projectile in the top.

Compressibility problems on aircraft propellers were first encountered during the 1930's, and research studies were made in those years in an effort to improve propeller design. This work continued through World War II. New plan form shapes, new twist distributions, and new airfoil sections designed especially for propellers all combined to increase the Mach number to which the propeller could be operated.

It is the air flow normal to the leading edge of the blade that creates shocks in supersonic flow. Therefore the onset of shocks can be delayed if the air speed normal to the blades is reduced by sweeping the blades backwards (or forwards). The local velocity at the blade can also be reduced by decreasing its thickness. By using very thin and twisted blades it has been possible to stretch the

propeller to higher Mach numbers. However, well before Mach 1 it becomes uncomfortable to operate the propeller.
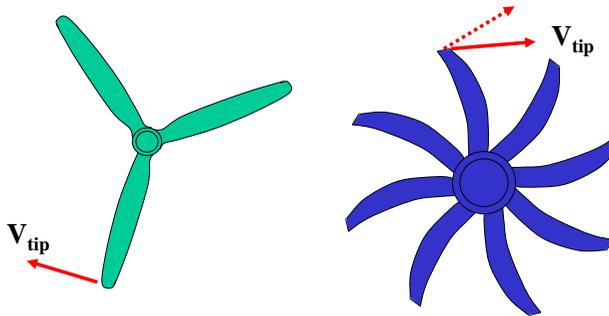
Fig. 7.11 The blades are swept to increase the speed of propellers

When the air speed at the tip approaches the speed of sound, blade element shock waves and boundary layer separation cause the noise level to increase beyond reasonable levels. For low speed propellers with relatively thick airfoils, the tip Mach number should be below 0.8 and for high speed propellers with relatively thin blades it could reach 0.85-0.9. This limits the flight Mach number to relatively low values as seen in Example 7.1. The time was ripe for a new invention.

Technological change is often incremental and gradual consisting of innovations that improve the efficacy and efficiency of technology. Characteristic of such change is engineering refinements, manufacturing process optimizations and

development of new variants of existing configurations. This was the case of the propeller engines in the years before WWII. Thus, during the time frame 1925-1945, through great cost and efforts, the power increased ten times from 350 HP to 3500 HP.

However, despite all the efforts, the speed of sound provided a barrier for the development of propeller aircraft. In such a situation, a revolutionary change must come and a classic example of such a revolution is the advent of the jet engine, which within a few years rendered propeller engines obsolete.

Ex 7.2

Tip speed is most important for the suppression of noise and for that reason, the tip Mach number is limited to below 0.85. What is the limit of the flight Mach number if the advance ratio is to be chosen for maximum performance? The speed of sound is 300 m/s.

8. THE JET ENGINE ARRIVES

The time was now ripe for a new type of engine. In 1930 Frank Whittle in England patented a jet engine but it was Hans von Ohain in Germany, who tested the first engine in 1937 and in 1939 the Heinkel 178 aircraft made the first jet flight. The turbojet engine and the swept back wing led to a rapid increase of speed and the sonic barrier was passed in 1947 by the American Chuck Yeager in a rocket plane. The maximum speed of the jet engine is close to Mach 3 and this limit was reached in 1962 by the American SR71 Blackbird.

As we have seen, the main disadvantage of the propeller was that the efficiency decreased as the relative speed of the blade tips approached the speed of sound. It is seen from Newton's equation for air breathing engines, Eq. (2.3), that to fly at supersonic speeds, what is required is a jet with a higher velocity than the speed of sound in ambient air. The slipstream of the propeller can never reach the speed of sound. This restricts the speed of a propeller driven aircraft to subsonic speeds.

That it would be possible to produce supersonic jets was shown by a Swedish engineer in 1888. **Carl Gustaf Patrick de Laval** was born in 1845 as the son of an army captain. After graduating from Uppsala University in 1866 he joined the Stora Kopparberg mining company and then the Kloster iron works in Germany. While at Kloster, he invented among other things the apparatus for separating cream from milk. In 1877 he moved to Stockholm,

started his own company and within 30 years sold more than one million separators.

During this time he started to experiment with steam turbines. In 1882 he constructed his first steam turbine using conventional convergent nozzles. This restricted the speed of the machine because the jet exhausting from the nozzle was restricted to subsonic speed. After several years of experimenting, in 1888 de Laval hit on the idea to add a divergent section to the original convergent shape. Suddenly, his steam turbines began to operate at incredible speeds as the jet emanating from the nozzle became supersonic and de Laval could develop his turbine business into a large corporation.

Interestingly enough, de Laval and other contemporary engineers were never quite sure that supersonic flow existed in the "**Laval-nozzles**". This was not shown until in 1903 by the Hungarian engineer **Aurel Boleslav Stodola**. As a professor in Zurich, he became the world's leading authority on the design of supersonic nozzles and came to be one of the leading figures behind the Swiss turbine company Brown Boveri, which later was to merge with the Swedish company ASEA into the ABB company.

To understand what happens in the Laval nozzle, we have to go back to thermodynamics. Assume that we are studying a nozzle as in Figure 8.1, where gas flows through a control volume increasing its speed but so rapidly that there is no exchange of heat.
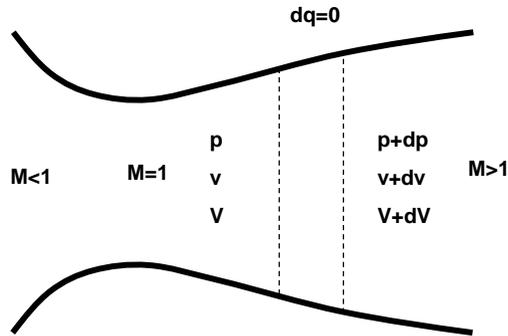
Fig. 8.1 The Laval nozzle produces a supersonic jet

We have already seen that the first law of thermodynamics may be written dq=dh-vdp where h=u+pv=C_pT is called the enthalpy. We also know that from Bernoullis equation dp+ρVdV=0 or vdp=-VdV so that dq =dh+VdV=d(h+V^2 /2). The group $\mathbf{h_t}$= h+V^2 /2 is often called the **total enthalpy**. If there is no heat exchange so that the process is adiabatic that is dq=0, the total enthalpy is constant so that the **stagnation temperature T_{t0}** at V=0 is obtained from:

$$C_p T_0 + \frac{V^2}{2} = C_p T_{t0} \tag{8.1}$$

Then with Eqs. (7.21) and (7.23) the stagnation temperature is:

$$T_{t0}/T_0 = \tau_0 = 1 + \frac{\gamma-1}{2}M^2 \qquad\qquad (8.2)$$

Cp and therefore γ is strongly dependent on both temperature and pressure as is seen from Figure 8.2 for different mixtures of kerosene in air.
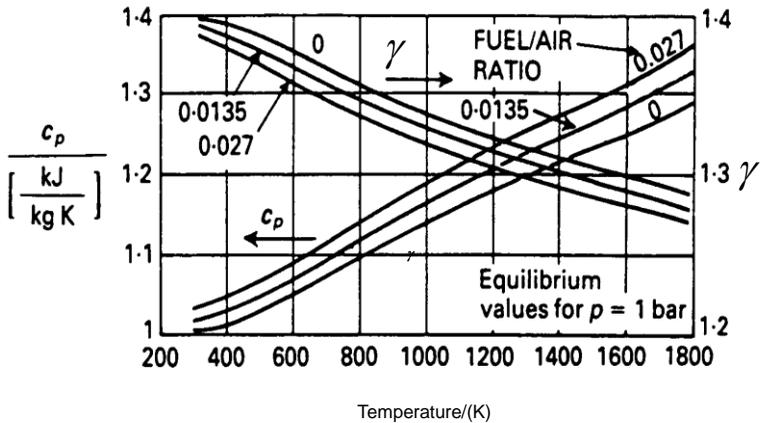
Fig. 8.2 The specific heat and the adiabatic constant vary with temperature.

In the relations, Cp and γ should therefore be given values representative of the respective thermodynamic state.

The conservation of mass flow ρVA=const in the flow in the Laval nozzle leads to:

$$\frac{d\rho}{\rho} + \frac{dV}{V} + \frac{dA}{A} = 0 \qquad (8.3)$$

The Bernoulli equation Eq. (3.4) means that:

$$\rho V dV + dp = 0 \qquad (8.4)$$

Using Eq. (7.23) for the speed of sound:

$$a^2 = \frac{dp}{d\rho} \qquad (8.5)$$

it may then be found that:

$$\frac{dV}{V}(1 - M^2) = -\frac{dA}{A} \qquad (8.6)$$

If M<1, an increasing area will decrease the speed as is well known. However, if M>1, the opposite is the case and the speed will increase with increasing area. It is also seen that if M=1, dA=0 so that the area is a minimum at this speed. This means of course that in a canal, the speed will be sonic where the area is a minimum. However, this requires that the pressure difference over the canal is above a certain critical value as we will now show.

Using Eq. (8.1), the mass flow per area becomes:

$$\frac{\dot{m}}{A} = \rho V = \frac{p}{RT}\sqrt{2C_p(T_t - T)} \qquad\qquad (8.7)$$

Since the air flows very rapidly through the nozzle, the heat exchange with the walls is negligible. The flow could then be regarded as isentropic and with Eq. (7.22) and (8.2) it may be shown that the mass flow through an orifice in compressible flow is given by the following non dimensional form where "i" is the inlet state to the orifice:

$$\frac{\dot{m}\sqrt{C_p T_{ti}}}{A p_{ti}} = \frac{\gamma}{\sqrt{\gamma - 1}} M \left(1 + \frac{\gamma - 1}{2} M^2\right)^{-(\gamma+1)/2(\gamma-1)} \qquad (8.8)$$

This equation describes the variation of the nozzle area with Mach number for a certain mass flow. The non dimensional left hand part of the equation has a maximum at M=1 so for a given mass flow, the area is a minimum there. This means that as the Mach number increases, the area will first decrease until M=1 and then increase again.

When the pressure ratio over the nozzle is increased, the mass flow through the nozzle increases until the velocity in the throat reaches its maximum sonic value and remains there. From then on the mass flow remains constant even if the pressure is increased further, see Figure 8.3.
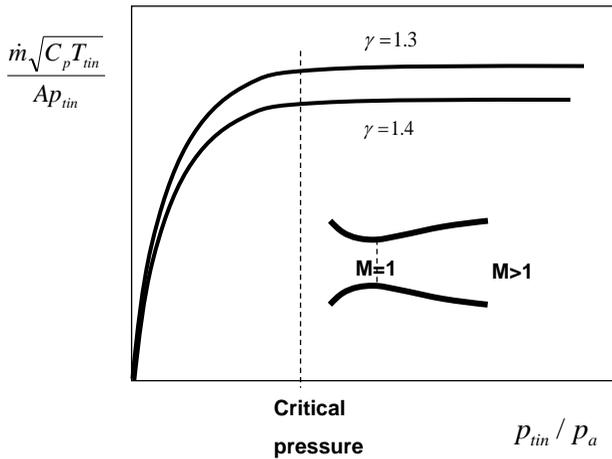
Fig. 8.3 The variation of the mass flow with pressure in a nozzle

From the relation for the stagnation temperature Eq. (8.2), the ratio between the stagnation temperature before the nozzle and the temperature at the sonic throat is:

$$\frac{T_{ti}}{T_c} = \frac{\gamma + 1}{2} \tag{8.9}$$

And the corresponding critical pressure ratio required to obtain sonic flow at the throat is using Eq. (7.22):

$$\frac{p_{ti}}{p_c} = \left[\frac{\gamma+1}{2}\right]^{\gamma/(\gamma-1)} \tag{8.10}$$

At $\gamma=1.4$ the critical pressure ratio is 1.89. If the pressure ratio over the nozzle is increased beyond this value, the nozzle becomes **choked** and the mass flow with the **throat area A^*** is given by:

$$\frac{\dot{m}\sqrt{C_p T_{ti}}}{p_{ti}A^*} = \bar{m}(\gamma) = \frac{\gamma}{\sqrt{\gamma-1}}\left(\frac{2}{\gamma+1}\right)^{\frac{\gamma+1}{2(\gamma-1)}} \tag{8.11}$$

This non dimensional value is often called the **mass flow parameter** and we will use it many times in the following.

From Eqs. (7.22) and (8.2), the Mach number at any section of the nozzle can be found as a function of the pressure. Then using Eqs. (8.8) and (8.11), the area ratio at any pressure is obtained as:

$$\varepsilon = \frac{A}{A^*} = \frac{\left(\dfrac{2}{\gamma+1}\right)^{\frac{1}{\gamma-1}}\left(\dfrac{p_{ti}}{p}\right)^{\frac{1}{\gamma}}}{\sqrt{\dfrac{\gamma+1}{\gamma-1}\left[1-\left(\dfrac{p}{p_{ti}}\right)^{\frac{\gamma-1}{\gamma}}\right]}} \tag{8.12}$$

This makes it possible to calculate the area and diameter of a nozzle exhausting to the ambient pressure.

It was thus known that it was possible to produce supersonic jets with a very simple device, the Laval nozzle, provided that the

pressure before the nozzle was more than about twice the atmospheric pressure. The question now was how to produce the gas with sufficient pressure and in sufficient amounts. The answer to this problem was the **gas turbine**.

In the beginning of the 20th century, experiments were made with steam boilers and piston engines but the resulting engines were much too heavy for use in aircraft. However, for a long time people had already used turbines to drive compressors. The first actual turbine is thought to have been built by the Italian **Giovanni Branca** in 1629. Water was heated in a boiler and the steam was expelled in a jet to impinge upon buckets around the periphery of a wheel.

In 1791 **John Barber**, an Englishman. was the first to patent a design that used the thermodynamic cycle of the modem gas turbine with a compressor, a combustion chamber, and a turbine driving the compressor. The main difference in his design compared to present gas turbines is that his turbine was equipped with a chain-driven reciprocating type of compressor. He intended its use for jet propulsion but it was almost 100 years before the necessary materials, designs, and manufacturing techniques made it possible to build one.

Aegidus Elling of Norway built the first successful gas turbine using both rotary compressors and turbines in 1903. In his system, part of the air leaving a centrifugal compressor was bled off for external power use. The remainder, which was required to drive the turbine, passed through a combustion chamber and then through a steam generator where the gas was partially cooled. This gas was further cooled to a temperature of 400ºC, the maximum

temperature that Elling's turbine could handle. The turbine was then used to drive the compressor.

Elling continued his development work reaching efficiencies of 82% and an inlet temperature of 550ºC. However, due to a lack of support and financial help, he had to stop his work on gas turbines and no commercial units were ever built. Nevertheless, he continued his employment with the Norwegian company Kongsberg, which later developed into a gas turbine factory and is now part of the Volvo Aero Company

Numerous gas turbines were built in Europe between 1905 and 1920 for the purpose of driving air compressors. The earliest applications of gas turbines for aircraft were for superchargers for the reciprocating engines driving the propeller. The turbosupercharger emphasized the development of materials capable of operating at high temperatures. This was a very important factor in making possible the gas turbine as a power plant for aircraft.

The gas turbine engine is essentially a heat engine using air as a working fluid. To provide thrust, the air passing through the engine has to be accelerated. This means that the velocity or kinetic energy of the air must be increased. First, the pressure energy is raised, then heat energy is added and finally the energy is converted back to kinetic energy in the form of a high velocity jet.

The basic mechanical arrangement of a gas turbine jet engine is relatively simple. It consists of the following basic components, see Figure 8.4:
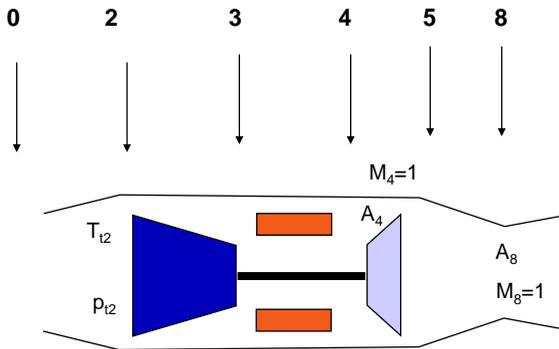
Fig. 8.4 The principle of the jet engine

- The **intake** (0-2) where air enters at ambient pressure and in a constant volume and leaves at an increased pressure and decreased volume.
- The **compressor** (2-3), which is used to increase the pressure (and temperature) of the inlet air.
- One or a number of **combustion chambers** (3-4) in which fuel is injected into the high-pressure air as a fine spray, and burned, thereby heating the air. The pressure remains (nearly) constant during combustion, but as the temperature rises, each kilogram of hot air needs to occupy a larger volume than it did when cold and therefore expands through the turbine.

- **The turbine** (4-5), which converts some of this temperature rise to rotational energy. This energy is used to drive the compressor. The inlet to the turbine, section 4, is usually choked so that M=1. This determines the mass flow through the engine in accordance with the equation for the Laval nozzle.
- The **exhaust nozzle** (5-9), which accelerates the air using the remainder of the energy added in the combustor, producing a high velocity jet exhaust. The nozzle throat, section 8, is also choked, which means that that its area must vary if conditions change before the nozzle.

Simple as the basic idea is, translation of the turbojet concept into a useful aircraft propulsion system presented formidable problems that required technical innovation and engineering of the highest order. Among the many problems were the design of turbines and compressors of sufficiently high efficiency and the proper matching of these components. If the efficiency of these units was not sufficiently high, the turbine would drive the compressor but have a low velocity exhaust incapable of producing useful thrust. Compressor and turbine efficiencies higher than those of other applications of these components were necessary to produce a usable jet engine.

Technological revolutions are often initiated by outsiders working outside the established manufacturers. The turbojet revolution was pioneered by Frank Whittle in England and Hans von Ohain in Germany. Both had their revolutionary ideas as students and developed them without the help of the established companies.

Frank's Whittle Patent Drawing
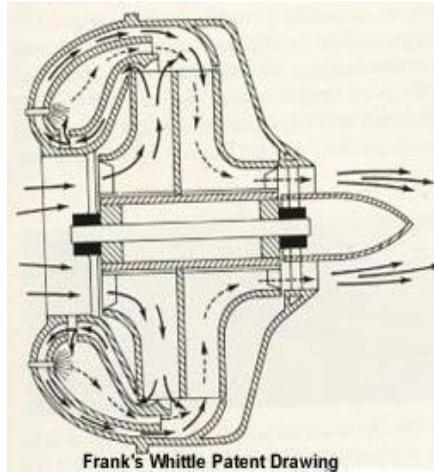
Fig. 8.5 Frank Whittle patented the jet engine in 1930

Frank Whittle is often regarded as the father of modern jet propulsion systems. He was born in 1907 and at the age of 16 became an apprentice with The Royal Airforce and later a cadet in the RAF College in Cranwell. There he became interested in advanced forms of aircraft propulsion and prepared his thesis laying the groundwork for the turbojet. He tried without success to obtain official support for study and development of his ideas. In the end he persisted on his own initiative and received his first patent on jet propulsion in January 1930. Although rotating turbines and compressors had been in use for various purposes for many years, the idea of coupling the two components, with burners

in between, and utilizing the resultant turbine exhaust to propel an aircraft was unique.

Unaware of Whittle´s work a young scientist at Goettingen University, **Hans von Ohain**, was investigating a new type of aircraft engine that did not require a propeller and patented a jet propulsion engine in 1936 together with **Max Hahn**. At the same time the German aircraft manufacturer **Ernst Heinkel** was searching for new concepts in aircraft propulsion. Ohain joined Heinkel in 1936 and continued with the development of his concepts of jet propulsion. A successful bench test of one of his engines was accomplished in September 1937. To avoid the combustor development problems associated with the use of liquid fuel, gaseous hydrogen was employed in this early test demonstration.

By 1939 after intense efforts and pushed by Heinkel, Hans von Ohain and his mechanic Max Hahn had designed, built and tested a jet engine. The Heinkel Aircraft Company adapted their ideas and flew the second aircraft engine of this development in an **HE-178** aircraft on August 27, 1939. The HE-178 was the first true jet-propelled aircraft. The pilot on this historic first flight was Flight Captain Erich Warsitz. The engine, known as the Heinkel HES-36, developed 5 kN of thrust and pushed the HE-178 to speeds of over 650 km/h. This engine used a centrifugal flow compressor. The aircraft was destroyed during an Allied air raid in 1943.

Later development produced a more advanced turbine engine, the **Junkers JUMO 109-004B**. This engine was used to power the **ME262** jet fighter to 800 km/h. These planes were introduced in the closing stages of World War II. Modern engine features of blade cooling, ice prevention, and a variable-area exhaust nozzle were incorporated into the JUMO engine. The aircraft had two

such engines each with a thrust of 9 kN. About 8000 JUMO engines were produced between 1943 and 1945.

Both Whittle and von Ohain had based there designs on centrifugal compressors. The JUMO featured an axial flow compressor, which has become the basis for modern jet engines relegating the centrifugal compressor to smaller turboprop engines. Thus the JUMO may be regarded as the first modern type jet engine.
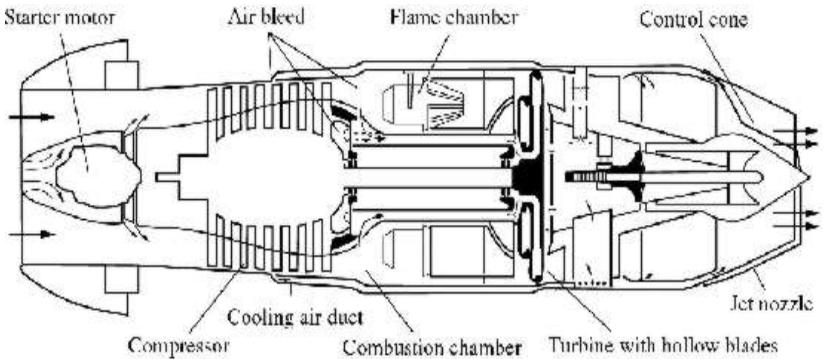
Picture from the RAF museum at Cosford, Wolverhampton, England

Fig. 8.6 WW2 JUMO 109-004B

It was developed and built by the Junkers Aircraft Corporation of Dessau, Germany. It used an eight stage axial flow compressor, six individual can type combustion chambers, a single stage turbine and a variable area outlet utilizing an axially adjustable inner cone.

To be noted is that 7% of the air was used for cooling purposes. In spite of this, the engine had a service life of only 10 hrs.

Meanwhile, with private financial support, Whittle began the construction of his first engine in 1935. This engine, which had a single-stage centrifugal compressor coupled to a single-stage turbine, was successfully bench tested in April 1937. It was only a laboratory test rig, never intended for use in an aircraft, but it did demonstrate the feasibility of the turbojet concept.

The firm of Power Jets Ltd., with which Whittle was associated, received its first official support in 1938. It received a contract for a Whittle engine, known as the W 1, on July 7, 1939. This engine was intended to power a small experimental aircraft known as the **Pioneer**.

The historic first flight of the Pioneer took place on May 15, 1941, nearly two years after that of the Germans. The aircraft was used for a number of years in the exploration of the problems of flight with jet propulsion and was finally placed in the Science Museum in London in 1947.

Britain emerged from World War II as the only Allied power to have had a jet fighter operational in squadron strength before the German surrender on May 8, 1945. This was the **Gloster Meteor**, which first flew on March 5, 1943. Appropriately, the Meteor's first duty was to defend Britain from attacks by German V-1 pulse jet-powered guided bombs, of which it destroyed 13 by the end of the war. Meteor IIIs were committed to Continental Europe in the last months of the conflict, but they never got the opportunity to meet the Me-262A in battle. Powered by two Rolls-Royce Welland I engines, generating 8 kN of static thrust, the Meteor I was a pleasant plane to fly, and for the next 12 years, upgraded models would serve in the RAF and other Air Forces around the world.

The present main manufacturers of jet engines, **Rolls-Royce**, **Pratt & Whitney** and **General Electric** all started their work after the World War II based on the Whittle concept of the centrifugal compressor then gradually switching to the German concept of axial compressors. The Whittle engine was used by Rolls Royce to launch the Welland followed by the Derwent, Nene and Tay.

In 1941, the U.S. Army Air Corps picked General Electric's plant in Lynn, Massachusetts to build a jet engine based on the Whittle design. Six months later, on April 18, 1942, GE's engineers successfully ran their I-A engine. With a modest thrust of 6 kN, the I-A engine launched America into the jet age.

PWA entered gas turbines soon after the war using the Nene to form the basis of their J42. Then PWA took the lead in the industry with the revolutionary J-57 jet engine, producing twice the thrust of any other engine.

Soon, the J-57 powered the new generation of fighters. Meanwhile, the new generation of jetliners, such as the Boeing 707, turned to the commercial version of the J-57 to open a new era in passenger service. Its dual-rotor axial-flow compressor allowed lower fuel consumption and improved acceleration over earlier jet engines. Entering production in 1953 the last production was finally ended in 1970, with more than 21000 of the J57 and its civilian equivalent the JT3 being produced.

Soviet work in turbojet engines had begun in the 1920's with the experiments of **Arkhip Lyulka** and his assistants **I.F. Kozlov** and **P.S. Shevchenko**, on the VRD-1, an axial-flow engine with an eight-stage compressor and a projected thrust capability of 7 kN.

The German invasion on June 22, 1941, postponed Lyulka's experiments, but they resumed at the end of 1942, and by the end of 1944 he had developed the TR-1, a more advanced power plant capable of producing 14 kN of thrust. In February 1945, Soviet forces advancing into Germany discovered the first BMW 003 and Junkers Jumo 004 turbojets. Josef Stalin, perceiving Western advances in military aircraft as a potential threat to Soviet security, placed maximum priority on the development of Soviet turbojet fighters and bombers.

Four design teams took up the challenge. Two of them delivered prototypes for flight testing a bare six months after the Me-262's first trials. The first to fly (by the outcome of a coin toss) was **Artem Mikoyan** and **Mikhail Gurevich's MiG**-9, which took off on April 24, 1946, with MiG test pilot **Alexei Grinchik** in the cockpit. It was followed by the Yakovlev Yak-15 flown by **Mikhail I. Ivanov**.

In 1946, to Stalin's delighted surprise, the British government allowed the export of Rolls-Royce Derwent and Nene engines as well as technical drawings to the USSR, which the Russians promptly placed in license production as the RD-500 and RD-45, respectively. Renewed efforts were then made to take advantage of these new developments. Yakovlev simply stuck to the RD-500 in a final refinement of the basic Yak-15 formula, the straight-winged Yak-23, which featured the first ejector seat in a Soviet fighter and entered service in 1948. Mikoyan and Gurevich, on the other hand, built an original sweptwing fighter around one of the imported British Nenes, the I-310, which first flew on December 17, 1947. Production using the RD-45 engine quickly followed, under the designation of MiG-15.

Sweden emerged from World War II with one of the world's largest air forces. Recognizing the challenge that the Cold War would present to its policy of neutrality, Sweden embarked on a crash program to modernize its air defences. On November 9, 1945, the Swedish government instructed the *Svenska Aeroplan Aktie Bolaget* (**Saab**) to adapt its twin-boom, piston-engine 21A fighter to use the British de Havilland Goblin turbojet engine. Although its configuration resembled the de Havilland Vampire's, the **Saab 21R**'s maximum speed of 800 km/h was about 150 km/h faster than the 21A's.

In October 1945, the Saab design team had tentatively laid out a new turbojet fighter whose corpulent appearance led the team's leader, **Lars Brising**, to dub it the *Tunnan* ("Barrel"). By January 1946, a revised design incorporating the de Havilland Ghost engine and a 25-degree wing sweepback had been finalized, and the first prototype, designated the Saab 29, was flown in1948. The 29 proved to be an excellent airplane and was the first of a proud line of Saab fighter planes with names like *Lansen*, *Draken, Viggen and Gripen*.

After the war, Sweden also embarked on the development of jet engines of its own. The Swedish pioneer was **A.J. Lysholm**, who began working on aero-turbine concepts in the mid-1930s while with the Bofors defence company. He then went on to work at Svenska Flygmotor (now the **Volvo Aero** Corporation), which was the Swedish company manufacturing the Goblin engine on license from the British De Havilland company.

PROJEKT R 102
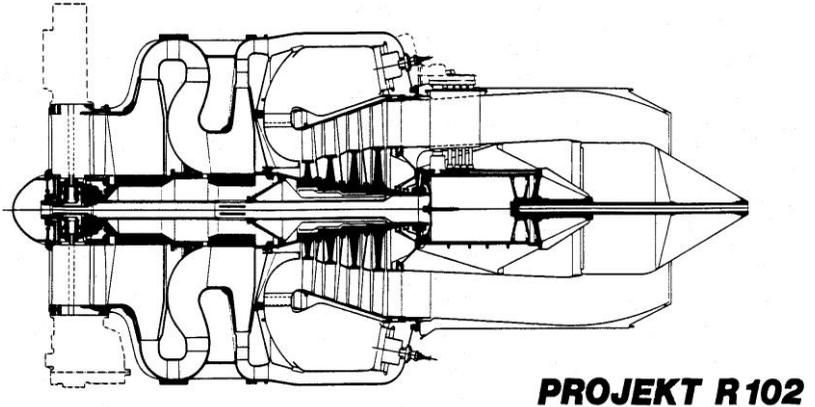
Fig. 8.7 Volvo's first jet engine

Svenska Flygmotor went on to bench-test a turbojet, the **R102,** in 1947. This was a straightforward centrifugal-flow engine, with a two-stage centrifugal compressor, an annular reverse-flow combustion chamber, a four-stage turbine, and a thrust of 15 kN, see Fig. 8.7.

However, the Swedish Air Material Board, wanting more competition, ordered another company with experience in gas turbines, Svenska Turbinfabriks AG Ljungstrom (STAL), to begin work on axial-flow turbojets of similar performance. STAL bench

tested their first model, the "*Skuten*", in 1948. It had an eight-stage axial compressor, can-type combustors and a single-stage turbine.

It was then realized that the thrust must be doubled, which led to the projects "**R201**" and the"*Dovern*". Those engines were to have a thrust of 33 kN and were intended for the SAAB 32 Lansen fighter aircraft. The work was conducted in parallell at the two companies until in 1949 "Dovern" was chosen to be developed by STAL but manufactured by Svenska Flygmotor. Finally, for cost reasons, in November 1952, the development was cancelled for good. Instead, British and later American engines adapted and developed under license by Volvo Aero to Swedish requirements were chosen for the SAAB fighters.

A summary of the Swedish jet engines produced under license is given below:

Original	Swedish designation	Thrust kN With A/B	Thrust kN Without A/B
DH Goblin 1	RM1	-	13.6
DH Goblin 3	RM1A	-	15.0
DH Ghost 50	RM2	-	22.7
DH Ghost 48	RM2B	28	21.6
RR Avon Mk21A	RM5	47	34.6
RR Avon 47A, 48A	RM6A,B	65.2	48.4
RR Avon 60	RM6C	77.55	59.5
P&W JT8D	RM8A	117.9	67.9
	RM8B	127.5	73.5
GE F404-400	RM12	82.1	55.1

France, recovering from a devastating German occupation, was understandably late in entering the jet age, although the Rateau

firm had been experimenting with jet turbines as early as 1939. During the occupation, the *Societé Nationale de Constructions Aéronautiques de Sud-Ouest* (SNCASO) began clandestinely to design a jet test-bed called the SO 6000 Triton. Wind tunnel tests with models were conducted in 1944, and after the liberation, construction of five prototypes began early in 1945.

With two crewmen side by side within a corpulent fuselage, the SO-6000 was to have been powered by a Rateau SRA-1 axial-flow engine with 16-stage compressor and two-stage turbine embodying the bypass principle. At the time the airplane was completed, however, the SRA-1 was still not fully developed, so the modified prototype, SO-6000J No.1, used a German-built 5 kN Junkers Jumo 004B-2 engine when it made its first flight on November 11, 1947. Subsequent Triton prototypes were built around the British Rolls-Royce Nene engines and were designated SO-6000N. The fourth airplane in the series crashed in 1949, but much was learned from the Tritons, and SO-6000N No. 3 survives at the *Musée de l'Air et l'Espace* at le Bourget.

Let us now see in more detail how the jet engine works. With a thermodynamic cycle of a machine we mean the transformations that a fluid undergoes while it is handled by that machine. The thermodynamic cycle of the gas turbine is the so called "**Brayton cycle**". This is a varying-volume, constant-pressure cycle of events and is also commonly called the "constant-pressure cycle" or "open cycle." A more recent term is "continuous-combustion cycle". This cycle is shown in Figure 8.8 in a so called T-s (temperature-entropy) diagram.
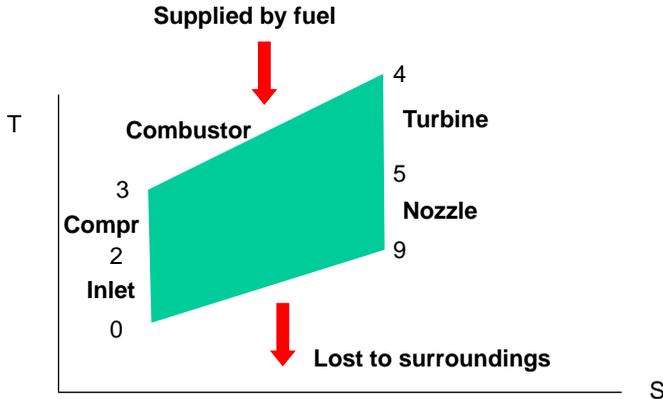
Fig. 8.8 The jet engine follows the Brayton cycle

In thermodynamic analysis, it is usually convenient to use temperature "T" and entropy "s" as the two independent variables used to describe the state of the gas. This is because the specific heats are dependent only on "T" (besides at very high temperatures where they are weakly pressure dependent). Because dq=Tds, it is also easy to find the heat exchanged in a process by integrating the temperature over the entropy. The heat added is then visualised as the area below the temperature line. In the integration, it is not any specific value of the entropy that is of interest but only the two end values between which the integration is made. We will therefore use T-s diagrams to depict the processes taking place in the components.

When the engine moves through the air, the air which is originally at rest at the condition "0" is exposed to adiabatic compression from stage "0" to "2" in the inlet and from "2" to "3" in a compressor inside the engine. Chemical energy is supplied to the engine by the fuel between stations 3 and 4 at constant pressure. Then there is an adiabatic expansion in a turbine between stage "4" and "5" followed by adiabatic expansion in a nozzle back to the surrounding pressure. After expansion the fluid in the machine is coming to rest at the temperature T_9, which is higher than the surrounding temperature T_0 so that energy is lost to the surroundings. Thus the cycle takes place between two constant pressures, the atmospheric pressure and the combustor pressure.

The amount of heat added to a control volume is the difference in total enthalpy $dq = dh_t = C_p dT_t$. The difference between the **power** supplied by the fuel and that lost to the surroundings is then:

$$\dot{W}_c = \dot{m} C_p \left(T_{t4} - T_{t3} \right) - \dot{m} C_p \left(T_9 - T_0 \right) \qquad (8.13)$$

This is the power available in the machine that can be transformed into useful work. Note that the air is coming to rest at static temperatures at states "0" and "9" at the same surrounding pressure.

If there is no pressure loss in the inlet or in the combustion chamber and as the jet is expanding adiabatically to the surrounding pressure:

$$\frac{T_{t4}}{T_9} = \left(\frac{p_{t4}}{p_9} \right)^{\frac{\gamma-1}{\gamma}} = \left(\frac{p_{t3}}{p_0} \right)^{\frac{\gamma-1}{\gamma}} = \left(\frac{p_{t3}}{p_{t2}} \frac{p_{t2}}{p_{t0}} \frac{p_{t0}}{p_0} \right)^{\frac{\gamma-1}{\gamma}} = \frac{T_{t3}}{T_{t2}} \frac{T_{t2}}{T_{t0}} \frac{T_{t0}}{T_0} \qquad (8.14)$$

Where with no losses in the inlet $p_{t2}=p_{t0}$, $T_{t2}=T_{t0}$ and:

$$\tau_0 = \frac{T_{t0}}{T_0} = 1 + \frac{\gamma-1}{2}M_0^2 = \pi_0^{\frac{\gamma-1}{\gamma}} \qquad (8.15)$$

$$\tau_c = \frac{T_{t3}}{T_{t2}} = (\frac{p_{t3}}{p_{t2}})^{\frac{\gamma-1}{\gamma}} = \pi_c^{\frac{\gamma-1}{\gamma}} \qquad (8.16)$$

So that :

$$T_9 = \frac{T_{t4}}{\tau_c \tau_0} \qquad (8.17)$$

Also with adiabatic compression and no losses in the inlet:

$$T_{t3} = \frac{T_{t3}}{T_{t2}} \frac{T_{t2}}{T_{t0}} \frac{T_{t0}}{T_0} T_0 = \tau_0 \tau_c T_0 \qquad (8.18)$$

With

$$\theta_t = \frac{T_{t4}}{T_0} \qquad (8.19)$$

we then obtain the following expression for the power produced by the cycle.

$$\frac{\dot{W}_c}{\dot{m}C_p T_0} = \theta_t - \tau_0\tau_c - \frac{\theta_t}{\tau_0\tau_c} + 1 \qquad (8.20)$$

This power can be used in different ways. One way would be to use all of it to increase the kinetic energy of the air flowing through the engine. The jet speed would then be obtained from:

$$\frac{V_j^2 - V^2}{2} = \frac{\dot{W}_c}{\dot{m}} \qquad (8.21)$$

The **specific thrust** (thrust per mass flow) is from the momentum principle, neglecting the fuel flow:

$$\frac{F}{\dot{m}} = V_j - V \qquad (8.22)$$

It is clear that the thrust tends to decrease with speed and vanishes as the jet velocity equals the flight speed. The aircraft then flies away from the jet so there is no thrust. From the expression for the power, it is seen that this occurs when:

$$\tau_0 = \theta_t / \tau_c \qquad (8.23)$$

Using the expression for the stagnation temperature, the maximum Mach number becomes:

$$M_{max} = \sqrt{\frac{2}{\gamma - 1}(\frac{\theta_t}{\tau_c} - 1)} \qquad (8.24)$$

Of course, this speed can never be reached because it means that the thrust goes to zero while the drag of the aircraft increases with speed in the power of two. However, one important conclusion from this relation is that high speed engines need to have low compressor temperature ratios. If we assume that it would be

possible to successively decrease the compressor temperature ratio, the absolute speed limit of the turbojet is at $\tau_c=1$. This means that there is no internal compression in the engine. All the compression is taking place in the inlet through ram pressure. This is a so called **ramjet** engine.

The turbine inlet temperature is seen to be very important and obviously we should try to increase it as much as possible. Note that it is the temperature ratio that is involved so that at high altitude when the inlet temperature is low, a high temperature ratio can be obtained with relatively low turbine temperature.

There is a highest combustion temperature, the so called **stoichiometric temperature**, reached in complete combustion of fuel in air and this sets the absolute limit of the flight speed. For kerosene in air this temperature is around 2300 K. There is of course also a limit to the turbine inlet temperature as regards materials. This is lower than the stoichiometric temperature. The maximum value with present materials and cooling systems is about 1900 K.

The most important limit in practice is often the material temperature in the compressor. This is usually made from titanium, which can sustain a maximum temperature of $T_{cm}=875$ K. This limit is given by:

$$\tau_0 \tau_c = \theta_{cm} = T_{cm}/T_0 \tag{8.25}$$

so that:

$$M_{max} = \sqrt{\frac{2}{\gamma - 1}(\theta_{cm} - 1)} \qquad (8.26)$$

Example 8.2 below shows that the maximum speed of the jet engine is very much higher than the propeller regardless of which limit is considered. The jet engine therefore became the basis for all high- performance aircraft developed after about 1945.

However, even with access to this new engine, very soon it was realized that an invisible "barrier" was preventing aircraft from surpassing the speed of sound. This famous **"sound barrier"** became a new big obstacle to higher speed. By the mid-1940's, much had been written in the popular press about this problem. Many knowledgeable engineers thought, that reasonably safe and controllable flight past the "barrier" was highly unlikely, if not completely impossible.

When the aircraft exceeds the speed of sound, it continuously produces shock waves similar to the water waves caused by a ship's bow. The aircraft is pulling this shock cone, attached to its nose, with it through the air. As the air passes through the Mach cone, it experiences a very sudden drop in pressure. This gives rise to the **sonic boom** that someone on the ground experiences as a bang as the Mach cone passes him.

The **critical Mach number** of a wing is the flight Mach number of the aircraft at which the local Mach number at some point of the wing becomes supersonic. At a Mach number slightly in excess of this critical value, usually at around M 0.7, further increases in speed cause large changes in the forces, moments, and pressures on the wing. This created the difficulties as one tried to increase the speed towards Mach 1.

Extensive investigations were undertaken in the United States and Europe in an effort to better understand the compressibility phenomena and to devise design methods for increasing the value of the critical Mach number and reducing the adverse effects of compressibility that occur beyond the critical Mach number.

Those efforts were hampered by fundamental difficulties in both theoretical and experimental methods of investigation. The governing equations for flows near Mach number 1 proved intractable to solution by the then existing methods. Adequate solutions to these nonlinear equations were not possible until the advent of the large-capacity, high-speed digital computers in the late 1960's and 1970's.

Practical theoretical approaches to the compressibility problem during the war years therefore usually involved the application of relatively simple correction factors to results obtained under the assumption of incompressible flow. These correction factors worked fairly well up to Mach numbers relatively close to the critical value but broke down completely at higher Mach numbers. One was therefore to a large extent forced to rely on experiments to understand what happened in the air close to the "sonic barrier".

The wind tunnel which had proved so useful in past aerodynamic investigations also became of questionable value at Mach numbers somewhat in excess of the critical value. At some Mach number, not too much higher than the critical value for the airfoil or body, the tunnel "choked," which meant that no higher free-stream Mach numbers could be obtained. A Mach number range between the subsonic choking value and some supersonic value, such as 1.2 or 1.3, was not available for wind-tunnel investigations. Supersonic tunnels operating beyond a Mach number of 1.2 or 1.3 were possible but were of little practical interest during the World War II time period. The solution to the problem of wind tunnel choking

was not found until the advent of the slotted and perforated- throat wind tunnel in the early 1950's.

In spite of these experimental and theoretical difficulties, a good deal of progress was made. In the wind tunnels one could easily visualize the "**sonic barrier**" by the large increase in drag close to Mach 1, see the Figure 8.9 below. The laminar-flow airfoil sections inherited from the birds and described previously clearly did not achieve the desired objectives of increasing the critical Mach number. New configuration concepts were needed.
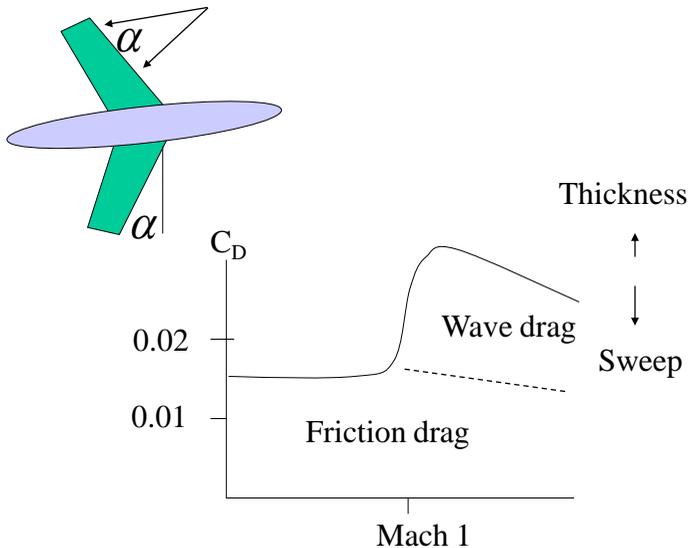
Fig. 8.9 The sonic barrier is seen as a large increase in drag

As early as 1935, Professor **Adolf Busemann** of the German Luftfahrtforchungsamt (aeronautical research establishment) suggested that sweptback wings would reduce drag at the "sonic

barrier". He did this at the famous Volta Conference in Rome where the world's leading experts in high-speed aerodynamics had gathered to discuss flight at very high speeds. This was a series of conferences organized by Italy during the 1930's to discuss the most important scientific areas of the day. Despite this prestigious gathering Busemanns ideas got very little attention and were largely ignored outside Germany. (Calculations on the centre of gravity had dictated the use of sweptback wings on the DC-3 but their aerodynamic benefits were not realized until later).

During World War II, however, the Germans tried to put Busemann's principles into practical use on such revolutionary aircraft as the Messerschmitt **Me-163** rocket fighter This aircraft saw limited operational use towards the end of World War II but it was not particularly effective as a fighter because of the capricious nature of its rocket propulsion system.

The way in which sweep back increases the critical Mach number is illustrated in Figure 8.9 above. If the swept wing is of infinite aspect ratio, the flight Mach number at which the critical Mach number is reached on the wing is:

$$M = \frac{M_{c0}}{\cos \alpha} \qquad\qquad (8.27)$$

This relationship is based on the assumption that the critical Mach number of the wing is controlled only by the flow normal to the leading edge and is independent of the Mach number parallel to it. Thus, the free-stream Mach number, that is, the flight Mach number of the aircraft, is resolved into components normal and parallel to the leading edge of the wing. The assumption of independence of the two components of the stream Mach number is strictly true only for inviscous flow, but the assumption works reasonably well in predicting the effect of sweep on the critical

Mach number of wings operating in real flows with viscosity. As compared with a straight wing, the swept wing offers significant increases in cruising Mach number.

According to the simple theory in which the streamwise velocity is resolved into components normal and parallel to the leading edge of the wing, the wing could just as well be swept forward. The experimental Junkers Ju 287-1, built in Germany during World War II had swept forward wings.

 Swept forward wings, however, have a fundamental aero elastic problem that has prevented their use. Simply stated, an increase in load on the wing twists the outer portions of the swept forward wing to higher angles of attack. This may result in the wing twisting off the aircraft. The critical condition at which this catastrophic failure occurs is called the divergence speed, or divergence dynamic pressure. The advent of composite materials, however, seems to offer the possibility of constructing stiff enough swept forward wings with little or no weight penalty.

A variation on the swept wing theme is the delta wing first proposed by the German aerodynamicist **Alexander Lippisch** in the years prior to World War II. This wing derives its name from the Greek letter, which describes its plan form shape. The delta wing is particularly well suited to tailless, all-wing configurations since the flap-type longitudinal controls can be located on the wing trailing edge, far behind the aircraft centre of gravity.

Dozens of courageous test pilots lost their lives trying to break through the "sound barrier". By early 1947, the British had thrown in the towel when their plane, a unique tailless design called "The Swallow," self-destructed close to the speed of sound. The pilot, **Geoffrey De Havilland**, was killed instantly.

That an aircraft could successfully fly past Mach 1 was convincingly demonstrated that same year by Captain **Charles E. Yeager**. Under US Army Air Forces and NACA contract, engineers at Bell Aircraft Corporation designed and built a unique airplane for the task of surmounting the "barrier". It was called the **X-1**. Painted a brilliant orange for better visibility, the X-1 was unlike other aircraft of its day. It was shaped like a bullet with wings sharpened to a razor edge. Its rocket engine was fueled by a mixture of liquid oxygen and dilute ethyl alcohol. The airplane was built for one thing only, to conquer the speed of sound by breaking through the "barrier" and beyond it into supersonic flight.

On October 14, 1947, Chuck Yeager and the X-1 were carried aloft for the most famous flight since the Wright Brothers had taken off at Kitty Hawk. At 20,000 feet, the little orange rocket plane was released and Yeager ignited two of its four rockets. Smoothly, he accelerated to Mach 0.88 and climbed to 42,000 feet. Once there, he began the dramatic assault on the "sonic barrier", igniting one after another of the little plane's rocket thrusters. Pressing ahead, the buffeting of transonic flight disappeared. The faster he flew, the smoother it became. The world's first man made sonic boom marked his passage of the "barrier". Once past, it was an easy ride. Ground data would show later that the plane had reached Mach 1.07. In the end, the "barrier" was a myth.

This historic event set the stage for an intensive research and development effort, which had as its objective the production of jet fighters capable of passing through Mach 1 and into the once forbidden supersonic speed range.

In the early 1950's, **Richard T. Whitcomb** of the NACA Langley Memorial Aeronautical Laboratory first experimentally

demonstrated an aerodynamic principle that has had a profound and far-reaching effect on the entire process of airplane configuration synthesis. It is known as the transsonic "area rule".
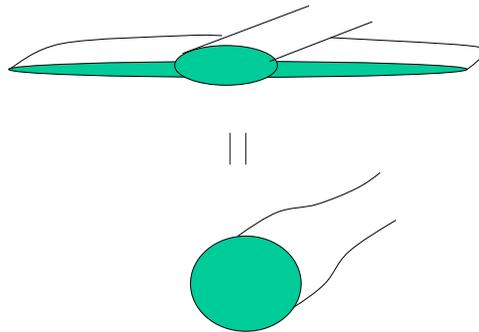
Fig. 8.10 The area rule for the design of supersonic aircraft

The concept known as the "**area rule**" is one of the great success stories of airplane design. It says very simply that the transonic wave drag of an aircraft is essentially the same as the wave drag of an equivalent body of revolution having the same cross-sectional area distribution as the aircraft, see the Figure 8.10. This fact, coupled with the knowledge of the shape that minimizes drag shows designers how to reshape the fuselage and other components of an airplane to reduce the drag of the total configuration.

This procedure is correct only for a Mach number of 1.0, but with a relatively simple modification it can be applied at supersonic speeds. The area-rule principle is now an accepted part of aircraft configuration synthesis and must be regarded as one of the cornerstones of transonic and supersonic aircraft design. It clearly differentiates these aircraft from their subsonic ancestors. A typical configuration will frequently have a fuselage with a local minimum of area near the middle of its length, sometimes referred to as "coke-bottling". Thus, the era of the "wasp waist" or "Coke bottle" airplane with indented fuselage began.

Since the rule was formulated and verified experimentally, attempts have been made to estimate aircraft wave drag by a theoretical analysis of the equivalent-body area distributions. The transonic area rule was considered so valuable that attempts were quickly made to extend the results to higher Mach numbers. This theoretical effort culminated in the development of the so called "Supersonic Area Rule", which is more complicated than the transonic rule. The supersonic area rule depends on computing areas intercepted by oblique cuts through a configuration and requires a considerable amount of computations.

The use of wing sweepback, together with small thickness ratios and high fineness ratios, and later combined with the transonic and supersonic area rule, provided the basic configuration elements needed for the successful design of aircraft of high subsonic and transonic speed.

During the fifties and sixties a lot of tests were made with higher speed. One example is the French turboramjet-powered Griffon flying at Mach 2. The first jet fighter that passed Mach 2 was the US F104 in the late fifties. The go ahead for the Concorde, the only Mach 2 passenger aircraft until this day, was given in 1962.
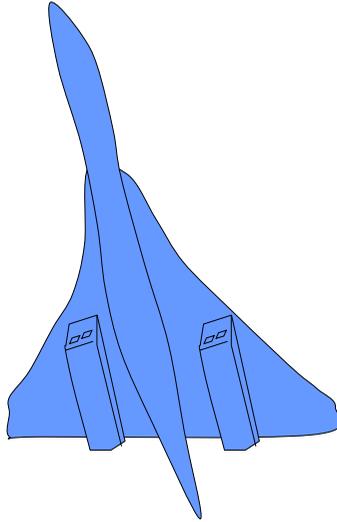
**Fig. 8.11 The Concorde- Still looking like an
airplane from the future**

One spring day in 1962 a test pilot named **Louis Schalk**,
employed by the Lockheed Aircraft Corporation, took off from the
Nevada desert in an aircraft the like of which had never been seen
before. The aircraft had been designed and built for reconnaissance
and its development had been carried out in profound secrecy.
Despite the numerous designers, engineers, skilled and unskilled
workers, administrators and others who had been involved in the
affair, no authentic accounts had leaked to the outside world.
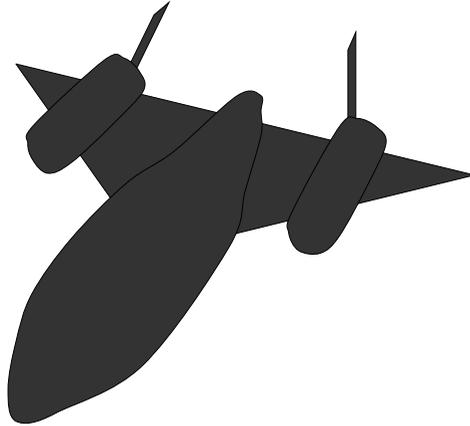
Fig. 8.12 The SR71- the highest speed aircraft ever

Unofficially nicknamed the "Blackbird," the SR-71 was developed as a long-range strategic reconnaissance aircraft capable of flying at speeds over Mach 3 or more than three times the speed of sound and at altitudes of over 25000 m. The first SR-71 to enter service was delivered in 1966 and it was retired in 1990.

In flying through the atmosphere at its designed speed the skin of this aircraft would be subjected to a temperature of more than 300 degrees Centigrade. Aluminium commonly used in aircraft production would not stand this temperature. During the design phase Lockheed evaluated many materials and finally chose an alloy of titanium.
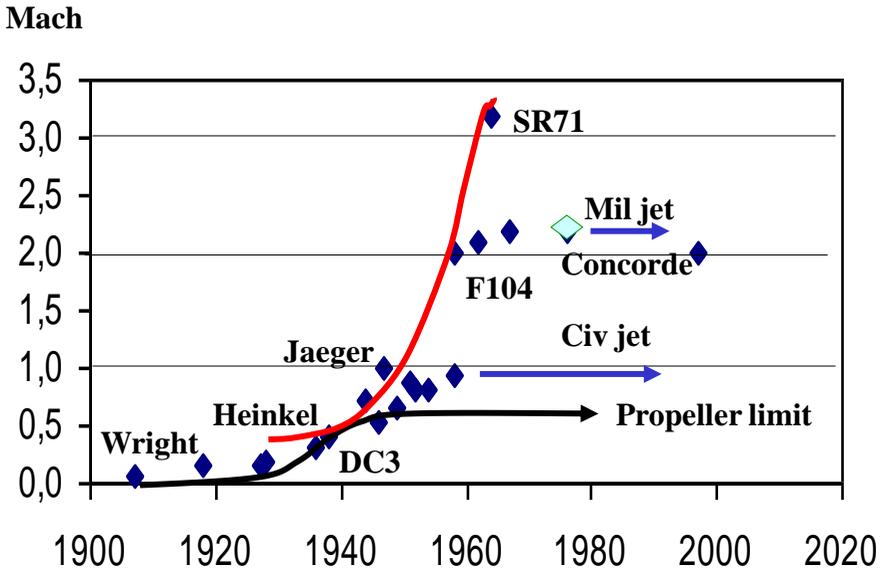
Mach

Fig. 8.13 The revolutionary 1960's

The only aircraft ever to come close to the SR-71's speed besides the rocket powered X-15 is the Russian MiG-25 Foxbat. The MiG-25 could only reach speeds of over Mach 3 for a few minutes. The Anglo-French Concorde is the only aircraft besides the SR-71 that can fly at supersonic speeds for hours at a time. Both of them are now taken out of operation.

If we look at how speed has developed over the years, Figure 8.13, we see that there was a very rapid development in the first half of the century culminating in the 1960's. Then the speed of commercial flight stagnated at just below Mach 1 and for military

aircraft at around Mach 2. The reasons for this is that air combat between opposing fighter aircraft quickly degenerates to subsonic speeds because of enhanced manoeuvrability at those lower speeds. Also, the drag and therefore the fuel consumption tend to increase with the speed, which makes supersonic aircraft uneconomical. Finally, as we have seen above, there is a limit to the speed of jet engines set by the temperature in the engine and the SR71 is already close to this limit.

Ex 8.1

The stagnation temperature equation, together with the isentropic relation can be used to measure the flight speed of aircraft from the stagnation pressure in a Pitot-tube. Assume that an aircraft is flying at a speed of 700 km/h in air with a temperature of 15 C and a pressure of 101.4 kPa. What is the pressure measured by a Pitot-tube relative to the aircraft if the adiabatic constant is 1.4 and the ideal gas constant 287 J/kg K?

Ex 8.2

A jet engine is flying at an altitude of 11 km where the ambient temperature is 216 K. What is the maximum speed if the maximum temperature in the titanium compressor is 875 K and the maximum turbine inlet temperature 1900 K while the maximum combustion temperature is 2300 K?

9. THE BYPASS ENGINE AND THE REVOLUTION IN AIR TRAVEL

The jet engine was first used in military aircraft during WW2 but already in 1947 the first civil jet airliner, the de Havilland Comet, was introduced. The first airliners used military type jet engines with a high jet speed to keep down the mass flow and the engine size. To maximize the efficiency, civil engines need a jet speed matched to the flight speed and a high mass flow, which led General Electric to develop the bypass engine. Because of its higher efficiency, the advent of this type of engine in the 1960's gave rise to a rapid growth in traffic and aircraft size.

One Sunday evening in the early 1960's, **Gerhard Neumann**, German auto mechanic graduated to general manager of GE's Flight Propulsion Division, phoned the head of the US Air Force's research and development at his home asking for a meeting "in strictest privacy". What was disclosed to the general the following day was a new type of jet engine more than twice as powerful as any other engine then flying. It was the high by-pass engine that was to revolutionize air transport.

Gerhard Neumann, one of the most renowned engineers in the history of jet engines, was born in 1917 in Frankfurt an der Oder, Germany. After completing a mandatory 3-year apprenticeship as an engine mechanic, Neumann entered Germany's oldest technical

college, Mittweida. After graduation, being of Jewish origin, in May of 1939, he accepted a position with a Chinese company, as an advisor and instructor in the use of German military equipment.

Neumann arrived in Hong Kong to find that his employer contact had disappeared without a trace. Worse yet, on September 1, Hitler invaded Poland, touching off World War II and making Neumann an "enemy alien" in (then British) Hong Kong. But with some help from a Pan American vice president, Neumann avoided being shipped to an internment camp. Instead, he flew to mainland China, where he joined the Flying Tigers, an American volunteer contingent of the Chinese Air Force, as an aircraft mechanic.

By the end of the war in 1946, Gerhard Neumann won his citizenship to the US because of his services in the war, married an American and settled in China. But soon, the threatened Communist takeover of mainland China persuaded Neumann and his wife to leave. They built a working jeep from two broken ones, and the young couple made an adventure-filled, three-month journey overland to Palestine, then sailed to Europe and flew to America. In 1948, Neumann began a 32-year career with General Electric, where he rose to the rank of Vice President and Group Executive of the Aircraft Engine Group.

The basic idea disclosed by Neumann to the US military was to use part of the power of the core engine to drive a fan at the front of the engine via a separate turbine, see Figure 9.1. The huge airflow from this fan would give an aircraft lots of extra thrust during take-off and lower fuel consumption in cruise.
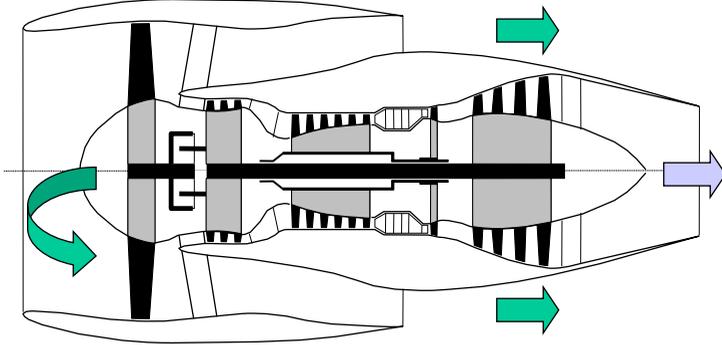
Fig. 9.1 In the bypass engine part of the power is used to drive a fan

Why was this so important for the military? The answer is in the Brequet equation:

$$s = \eta \frac{L}{D} \frac{h}{g} \ln \frac{1}{1 - m_f / m_0} \tag{7.3}$$

It shows that the range of an aircraft is directly proportional to the engine efficiency for a given amount of fuel. The range of new transports could be dramatically increased with the help of the bypass engine and the US was just starting the development of the

Galaxy C-5A, that was to transport one thousand troops over long distances.

The engine **thrust efficiency** is the ratio between the thrust work and the energy supplied to the cycle by the fuel. If the kinetic energy of the fuel is neglected compared to its heat content, the efficiency is:

$$\eta = \frac{FV}{\dot{Q}_c} = \frac{FV}{\dot{m}_f h} \qquad (9.1)$$

It is also common to use the **specific fuel consumption**:

$$SFC = \frac{\dot{m}_f}{F} \qquad (9.2)$$

or the **specific impulse**:

$$I_s = \frac{F}{\dot{m}_f} = 1/SFC = \eta \frac{h}{V} \qquad (9.3)$$

The efficiency of an engine consists of two parts. Some of the energy supplied by the propellant is lost inside the engine due to the thermal efficiency η_t of the thermodynamic cycle. Another part is lost outside the engine because when the jet has left the vehicle it still has a velocity higher than the flight speed and therefore a kinetic energy that is not utilized for driving the vehicle. This is expressed in the propulsion efficiency η_p so that the total efficiency is:

$$\eta = \frac{FV}{\dot{Q}_c} = \frac{\dot{W}_c}{\dot{Q}_c}\frac{FV}{\dot{W}_c} = \eta_t \eta_p \qquad (9.4)$$

The **thermal or cycle efficiency** is the ratio between the work output and the heat supplied to the cycle, see Fig. 9.2:

$$\dot{Q}_c = \dot{m}C_p\left(T_{t4} - T_{t3}\right)$$

Combustor

Power $\dot{W}_c$
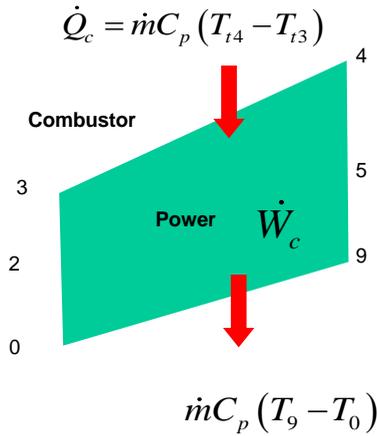
$$\dot{m}C_p\left(T_9 - T_0\right)$$

Fig. 9.2 High pressure for high thermal efficiency

$$\eta_t = \frac{\dot{W}_c}{\dot{Q}_c} = \frac{\dot{W}_c}{\dot{m}C_p\left(T_{t4}-T_{t3}\right)} = \frac{\dot{m}C_p\left(T_{t4}-T_{t3}\right)-\dot{m}C_p\left(T_9-T_0\right)}{\dot{m}C_p\left(T_{t4}-T_{t3}\right)} = 1 - \frac{T_9-T_0}{T_{t4}-T_{t3}}$$

$$(9.5)$$

Using Eqs. (8.17) and (8.18), this reduces to:

$$\eta_{th} = 1 - \frac{1}{\tau_0 \tau_c} = 1 - \frac{1}{\tau_0 \pi_c^{\frac{\gamma-1}{\gamma}}}$$ (9.6)

It is then seen that the thermal efficiency increases with speed as stagnation pressure builds up in the engine. This is the main advantage of the gas turbine as compared to a piston engine. A consequence of this is that a civil engine, where efficiency and fuel consumption is of high importance, should have the highest possible pressure ratios. This is contrary to what we found in Chapter 8 for high speed engines, which were seen to need low pressure ratios.

The **propulsive efficiency** is the relation between the thrust work and the power given to the jet by the engine:

$$\eta_p = \frac{FV}{\dot{W}_c} = \frac{\dot{m}V(V_j - V)}{\dot{m}(V_j^2/2 - V^2/2)} = \frac{2V}{V_j + V}$$ (9.7)

In order to achieve a high propulsive efficiency, the jet velocity, or the velocity of the gas stream exiting the engine, should be close to the flight speed of the aircraft. Slow aircraft should have engines with low jet velocities and fast aircraft should have engines with high jet velocities.

Remember the reaction equation:

$$F = \dot{m}\left(V_j - V\right)$$ (9.8)

It may be seen that a required level of thrust can be produced at a certain flight velocity, either by the addition of a small increment

of velocity to a large mass flow of air or by the addition of a large increment of velocity to a small mass flow of air. Military engines will typically be designed with high jet speeds to keep the mass flow and the engine size and weight down.

At the same time, this creates a problem at lower speeds because if all the available power of the engine is used to create a jet, then the jet speed is much higher than the flight speed and consequently the propulsive and total efficiencies are low even if the thermal efficiency of the cycle itself is high. This dilemma led to the invention of the bypass engine.

When high efficiency is the most important, the jet speed should be close to the flight speed and the mass flow must therefore be high to give sufficient thrust. The idea of the GE engineers was to use some of the available power to drive a fan. This is the bypass or turbofan engine, see Fig. 9.1, which through the fan provides the propulsive power of a bypass stream in addition to the remaining propulsive power of the core stream.

Taking into account efficiencies in the fan and the LP turbine, the cycle **power** that must be supplied by the core is:

$$\dot{W}_c = \frac{1}{2}\dot{m}_c (V_{jc}^2 - V^2) + \frac{1}{2}\dot{m}_b (V_{jb}^2 - V^2)/\eta_f \eta_{lt} \qquad (9.9)$$

It is now possible to minimize the work the core must deliver for a given amount of thrust :

$$F = \dot{m}_c (V_{jc} - V) + \dot{m}_b (V_{jb} - V) \qquad (9.10)$$

Differentiating both equations with respect to the two unknown **bypass and core jet speeds** V_{jb} and V_{jc} and putting them to zero results in the following condition for the matching of the core and bypass streams:

$$V_{jb} = V_{jc} \eta_f \eta_{lt} \tag{9.11}$$

With ideal 100 percent efficiencies, the jet speed from the bypass canal should be the same as from the core, but in real engines it should be a bit lower.

Overall **P**ressure **R**atio

Bypass flow

Core flow

By**P**ass **R**atio $\alpha = \dfrac{\dot{m}_b}{\dot{m}_c}$

Fan **P**ressure **R**atio
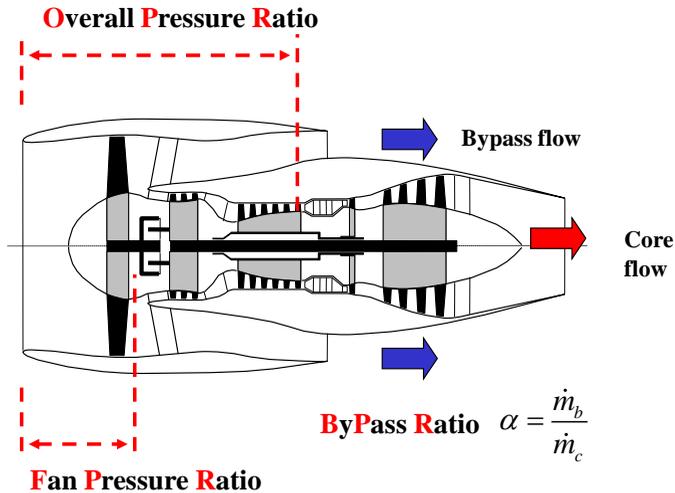
Fig. 9.3 Important performance parameters

We will now introduce some important parameers that determine the performance of an engine. First of all the **bypass ratio** α, that is the ratio between the bypass mass flow and the core mass flow:

$$\alpha = \frac{\dot{m}_b}{\dot{m}_c} \qquad (9.12)$$

so that with ideal components, that is $V_{jb}=V_{jc}$:

$$\dot{W}_c = \frac{\alpha+1}{2}\dot{m}_c(V_{jb}^2 - V^2) \qquad (9.13)$$

With no losses, the propulsive power of the bypass flow is α times the power of the core flow. Since for large bypass engines, the bypass ratio is commonly more than 6, it is seen that for such engines, the fan provides the dominant part of the propulsive power. The role of the core is to provide the power but not propulsion.

Now, if all the propulsive power per air flow added in the fan is used with no losses to accelerate the bypass flow, then since the power is the specific heat times the pressure difference over the fan with τ_f as the fan temperature ratio:

$$\frac{1}{2}(V_{jb}^2 - V^2) = C_p T_0 \tau_0 (\tau_f - 1) \qquad (9.14)$$

so that using the expression for the core work of Eq. (8.20) we obtain:

$$\frac{\dot{W}_c}{\dot{m}_c C_p T_0} = \theta_t - \tau_0 \tau_f \tau_c - \frac{\theta_t}{\tau_0 \tau_f \tau_c} + 1 = (\alpha+1)\tau_0(\tau_f - 1) \qquad (9.15)$$

from which the fan temperature ratio is obtained as expressed in the overall temperature ratio $\tau_f \tau_c$:

$$\tau_f = 1 + \frac{\theta_t - \tau_0 \tau_f \tau_c - \dfrac{\theta_t}{\tau_0 \tau_f \tau_c} + 1}{(1+\alpha)\tau_0} \tag{9.16}$$

The **specific thrust** per total of airflow is often used as a measure of how powerful the engine is. For an ideal bypass engine:

$$\frac{F}{\dot{m}_c(1+\alpha)} = V_{jb} - V \tag{9.17}$$

With the jet speed from Eq. (9.13), a general expression for the **specific thrust** of the ideal bypass engine is with the total airflow $\dot{m} = \dot{m}_c(1+\alpha)$:

$$\frac{F}{\dot{m}a_0} = \sqrt{\frac{2}{\gamma-1}\frac{\dot{W}_c/\dot{m}_c C_p T_0}{1+\alpha} + M^2} - M \tag{9.18}$$

Using Eq. (9.15) and the expression for the fan pressure ratio just derived in Eq. (9.16), we then obtain the specific thrust of the ideal bypass engine as:

$$\frac{F}{\dot{m}a_0} = \sqrt{\frac{\theta_t - \theta_t/\tau_0 \tau_f \tau_c - \tau_0(\tau_f \tau_c - 1) + \alpha(\tau_0 - 1)}{(1+\alpha)(\gamma-1)/2}} - M \tag{9.19}$$

There is a relation between the efficiency and the specific thrust. From the definition in Eq. (9.1), the total **efficiency** is:

$$\eta = \frac{FV}{\dot{Q}_c} = (\gamma - 1)(1 + \alpha)M \frac{F/\dot{m}a_0}{\dot{Q}_c/\dot{m}_c C_p T_0} \qquad (9.20)$$

where the power added in the combustion chamber is:

$$\dot{Q}_c / \dot{m}_c C_p T_0 = \theta_t - \tau_0 \tau_f \tau_c \qquad (9.21)$$

Looking at the equations for specific thrust and efficiency, it is obvious that the specific thrust should decrease with bypass ratio. On the other hand, the efficiency contains the specific thrust multiplied by $(1+\alpha)$, which means that the efficiency should increase with the bypass ratio. The general behaviour of specific thrust and efficiency with bypass ratio is shown in Figure 9.4. Note that the total thrust level is actually increasing with the bypass ratio because the mass flow increases very much. It is therefore easy to understand the enthusiasm of the US Air Force generals as Gerhard Neumann presented the GE ideas.

For military engines, where specific thrust is the most important, the bypass ratio should be low. Civilian engines, where efficiency is important, should have high bypass ratios. This means that the jet speed gets closer to the flight speed. The jet speed approaches the flight speed asymptotically with increasing bypass ratio, which explains the behaviour of the efficiency curve in Figure 9.4.
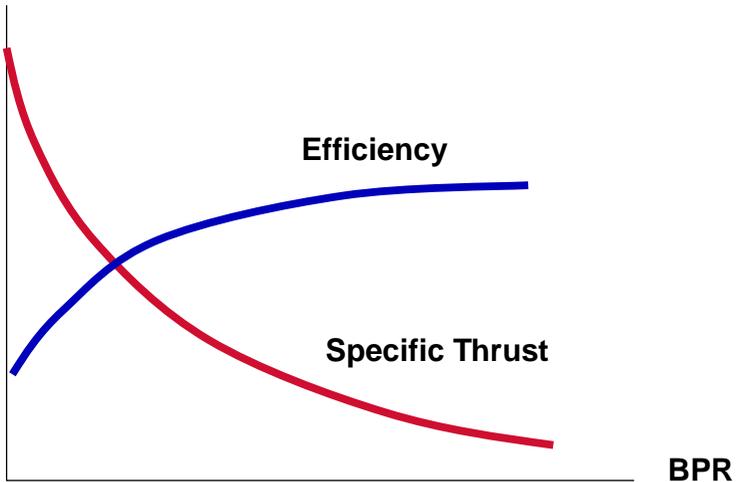
Fig. 9.4 The behaviour of specific thrust and efficiency with bypass ratio

The general behaviour of specific thrust and efficiency with overall pressure ratio is shown in Figure 9.5 below. For military or other high speed engines it is often required to have a significant excess thrust available for accelerations etc. This can of course be achieved by a larger engine, but one often wants the engine to be as small and light weight as possible. Therefore, for military engines we need a high jet speed that is high specific thrust. Looking at Figure 9.5 and the expression for the specific thrust above, it is seen that there is a total compression temperature ratio that maximizes the specific thrust, namely:

$$\tau_f \tau_c = \frac{\sqrt{\theta_t}}{\tau_0} \qquad (9.22)$$

Note that if the turbine inlet temperature is increased, then the overall pressure ratio should also increase and vice versa.
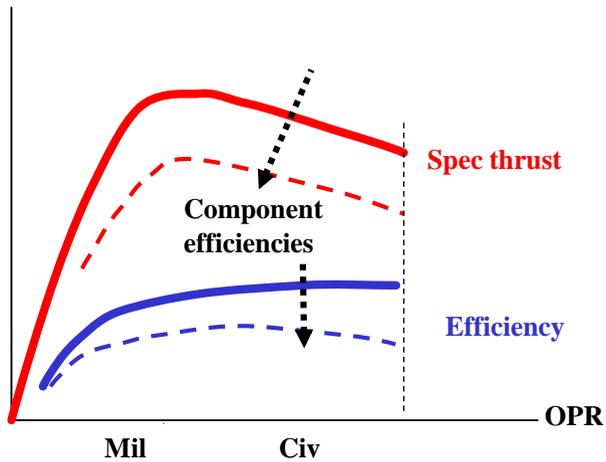
Fig. 9.5 The behaviour of specific thrust and efficiency with pressure ratio

For the ideal cycle, contrary to the specific thrust, the efficiency increases continuously with increasing pressure ratio. Note that

there is a maximum permitted pressure ratio set by the material temperatures at the end of the high pressure compressor.

Component efficiencies will lower both curves and also cause a maximum in efficiency which is not there with ideal components. An interesting consequence of Figure 9.5 is that civil engines should have high pressure ratios to obtain high efficiency while military or other high speed engines, which require high specific thrust, should have low pressure ratios.

The pressure ratio cannot fall below unity, which means that the maximum Mach number that can be reached by a jet engine of maximum specific thrust is:

$$M_{max} = \sqrt{\frac{2}{\gamma - 1}(\sqrt{\theta_t} - 1)} \qquad (9.23)$$

This is lower than the maximum speed obtained in Eq. (8.24), where the pressure ratio was allowed to vary independently of the turbine temperature.

The relation between fan pressure ratio and bypass ratio in Eq. (9.16) can also be written:

$$\alpha + 1 = \frac{\theta_t - \theta_t / \tau_c - \tau_0 \tau_f (\tau_c - 1)}{\tau_0 (\tau_f - 1)} \qquad (9.24)$$

Note that the bypass ratio decreases with increasing fan pressure ratio. This is natural since the limited turbine power can either provide a high pressure or a large airflow.

 Typical variations of fan pressure and bypass ratio are shown in Figure 9.6.
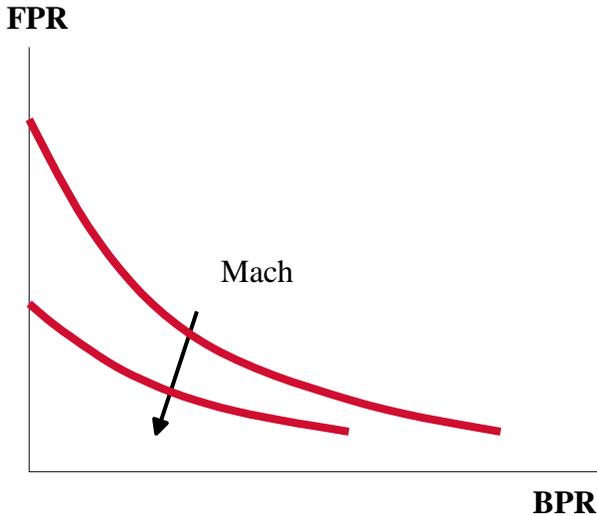
Fig. 9.6 The variation of fan pressure ratio with bypass ratio and Mach number

If the fan pressure ratio is too high, the LP turbine is not able to drive the fan and the bypass ratio falls to zero. In this case the turbofan becomes a straight turbojet. It is also seen that both the bypass ratio and the fan pressure ratio should decrease with speed so that high speed engines tend to be straight turbojets. Bypass engines on the other hand are for low speed.

The components of the **turbofan** is shown in Figure 9.7 below. The fan is somewhat like a propeller being driven by the turbo

machinery. Unlike the propeller, however, a single fan stage may contain from 20 to 50 blades, is surrounded by a shroud, and is more like a single-stage compressor than a propeller. For example, the pressure ratio across a single fan stage is usually in the range of 1.4 to 1.6 whereas the pressure ratio across a propeller disc in cruising flight is somewhat less than 1.02.
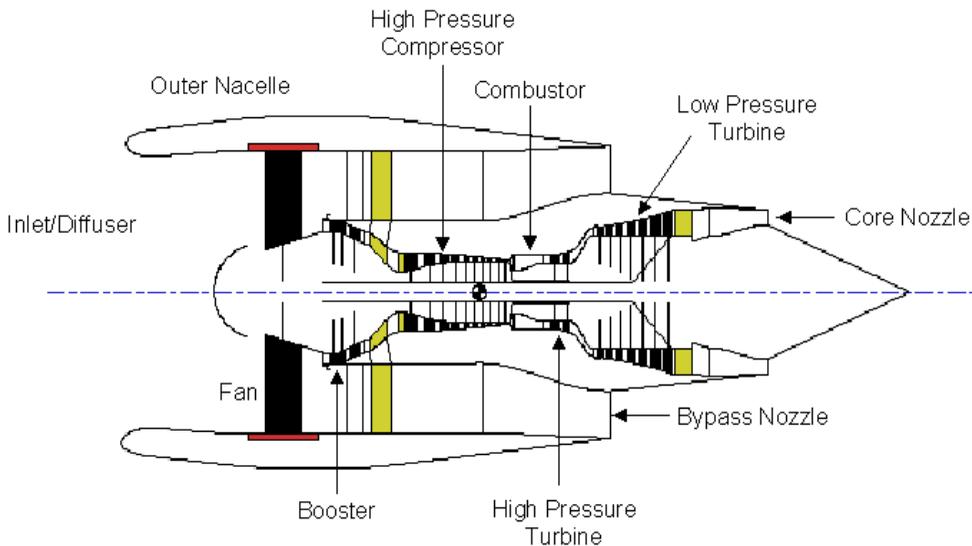
Fig. 9.7 The components of the bypass engine

Bypass ratios between 1 and 2 were typical of the first turbofan engines introduced in the early 1960's. The more modern turbofan engines for transport aircraft have bypass ratios that usually fall between 4 and 6 and higher. The Trent and the PW4084 have

bypass ratios about 6 while GE90 is at about 9. The larger the bypass ratio, the greater the amount of energy extracted from the hot exhaust of the gas generator. More than 80 percent of the total thrust of a turbofan engine may be attributed to the fan.

Some turbofan engines are of the **three-spool** type. The hot gas generator employs two spools and a third spool that is independent of the other two contains the fan and its own turbines. Only Rolls Royce has three shafts. This configuration has aerodynamic advantages but at a higher complexity.

Sometimes, as in the Figure 9.7, there is a booster stage just behind the fan to compress the core air before it enters the HP compressor.

Fans of more than one stage have also been used, as have aft-mounted fans. The aft-fan design is one in which the fan blades form an extension of an independently mounted turbine situated in the hot exhaust of the gas generator. This was originally promoted by GE while PWA favoured front fans.

There are several advantages of the turbofan. The fan is not as large as a propeller, so the tip speed at the blades is less. Also, by enclosing the fan inside a duct or cowling, there is a stagnation of the inlet air so the air speed meeting the fan is less than for a propeller. This means that the aerodynamics is better controlled. There is less flow separation at the higher speeds and less trouble with shocks developing.

A turbofan engine can fly at transonic speeds up to Mach 0.9. While the fan is smaller than the propeller, it uses much more air flow than the turbojet engine, so it gets more thrust at a lower fuel consumption. The turbofan engine is therefore the engine of choice for high-speed, subsonic commercial airplanes.

Soon after the first turbojets were in the air the **turboprop** engine was developed. The turboprop is a turbojet with an additional

turbine which uses the energy remaining in the gas stream to drive a propeller after sufficient energy has been absorbed to drive the compressor. In essence, it is a bypass engine without a nacelle around the fan. The nacelle results in a stagnating flow and makes it possible to avoid the compressibility effects at the blades at higher speed. This is not the case in the turboprop. Because the turbine needs to operate at a high speed, a large gear box is needed in the turboprop to avoid high Mach numbers at the propeller tips.

Because only a small part of the air flow is actually burned inside the engine, the turboprop engine can generate a lot of thrust with a low fuel consumption compared to a turbojet engine. When an airplane is designed to fly at lower speeds, the turboprop is usually the engine chosen. At flying speeds up to M=0.6 the propulsive efficiency of the turboprop is superior to that of the turbojet engine.

The turboprop produces two thrusts, one with the propeller and the other through the jet exhaust. What is the right distribution between these two?

Assuming that the shaft power is P the total propulsive power of the turboprop is, including the propeller efficiency:

$$\dot{W}_{tp} = \eta_{pr}P + F_{jet}V$$

The shaft power is the difference between the total cycle power and the jet power.

The jet thrust is:

$$F = \dot{m}\left(V_j - V\right) \qquad\qquad (9.26)$$

Then:

$$\frac{\dot{W}_{tp}}{\dot{m}} = \eta_{pr}\left(\frac{\dot{W}}{\dot{m}} - \frac{V_j^2 - V^2}{2}\right) + V\left(V_j - V\right) \qquad (9.27)$$

Differentiating, the jet speed that gives maximum total propulsive power is found to be:

$$\frac{V_j}{V} = \frac{1}{\eta_{pr}} \qquad\qquad (9.28)$$

This means that if the propeller efficiency is high then the jet speed should be close to the flight speed so that the thrust from the turbine engine vanishes and all the propulsive power is shifted to the propeller. In reality the propulsive power from the exhaust gases is about 10 to 20% of that of the propeller. However, as the propeller efficiency decreases at higher speeds, more propulsive power should be shifted to the jet.

A recent trend in turboprop design has been the evolution of propellers for efficient operation at flight speeds up to Mach numbers of 0.85. This usually involves a higher disk loading (that is a higher discharge velocity from the propeller) in order to permit the use of a smaller diameter. This trend has been accompanied by an increase in the number of blades in the propeller (from six to twelve instead of the more common two to four blades in lower-speed propellers). The blades are scimitar-shaped, see Fig. 9.8, with swept-back leading edges at the blade tips to accommodate

the large Mach numbers encountered by the propeller tip at high rotative and flight speeds. Such high-speed propulsors are called propfans.
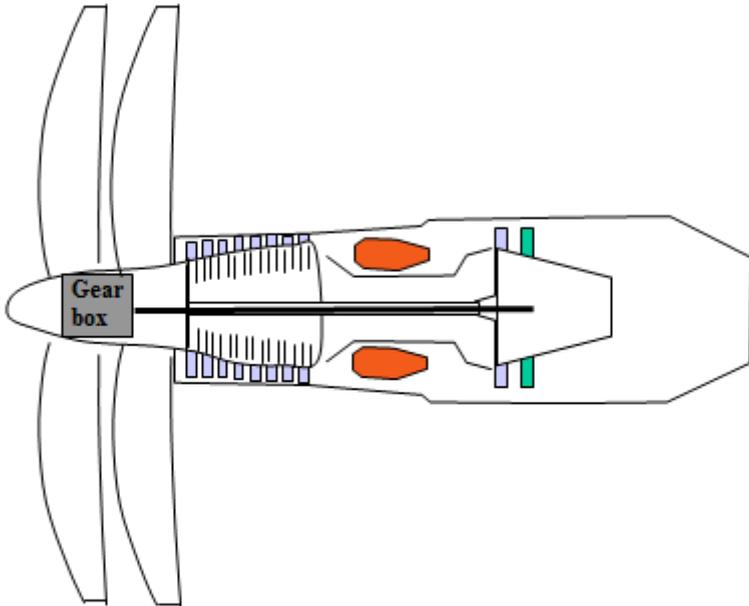
Fig. 9.8 In the turboprop engine, the propeller is exposed to the full air flow

Another variation of the propulsor involves the application of two concentric propellers driven by the same prime mover through a gearbox that causes each propeller to rotate in a direction opposite the other. Such counter-rotating propellers are capable of significantly higher propulsive efficiency and higher disc loading than conventional propellers.

In most turboprop installations the prime mover is mounted on the wing, and the plane of the propeller is forward of the prime mover

(the so-called "tractor" layout). Modern high-speed aircraft may find it more advantageous to mount the engine more toward the rear of the aircraft, with the plane of the propeller aft of the engine. These arrangements are referred to as "pusher" layouts. The so called unducted fan (or UDF), provides a set of very high-efficiency counter-rotating propeller blades, each blade mounted on one of either of two sets of counter-rotating low-pressure turbine stages and achieving all the advantages of the arrangement without the use of a gearbox.

The turbofan with its increased efficiency caused a revolution in commercial air traffic and a spectacular increase in the size of civil aircraft. This is seen very clearly in Figure 9.9 below, which shows the largest size of aircraft in the number of passengers each decade.

Some of the aircraft in this figure have a colourful history. Sir **Frederick Handley Page** founded Handley Page, Ltd. in 1909, the first British aircraft manufacturing corporation. During World War I, he produced the first twin-engine bomber, which was capable of carrying 800 kg of bombs. He then designed the V-1500 four-engine bomber, built to fly from England to Berlin with a bomb load of three tons. The war ended before it could be used.
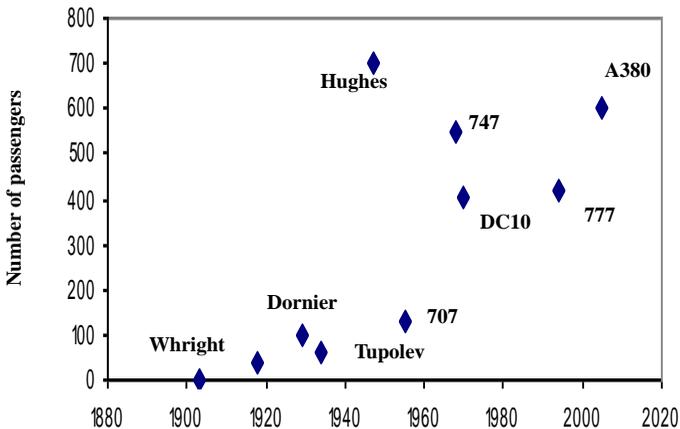
Fig. 9.9 The bypass engine led to a rapid increase in the size of aircraft

In the 1920's it was realized that the technology at the time did not permit the building of very large aircraft starting from the ground. This was the reason for the flying boats of which the Dornier "Do X" and the Hughes "Spruce Goose" were the largest.

Claude Dornier completed his education in 1907 at Munich's technical college and three years later began working for Ferdinand von Zeppelin, at the Zeppelin airship factory at Friedrichshafen. In 1911 he designed the first all-metal plane, and Zeppelin permitted him to found a separate division of the company, the Dornier aircraft works at Friedrichshafen. Wooden and metal fighters designed by Dornier were used by Germany in World War I.

During the 1920s Dornier built widely used seaplanes, and in 1929 he introduced the "**Do X**", at the time the world's largest aircraft. With a wingspan of 48 m and length of 40 m, the "Do X" was powered by 12 engines and carried 169 passengers. In 1931 it flew from Germany to New York. Because of its great cost, however, the "Do X" was abandoned.

In the 1930's, Joseph Stalin fixated on convincing the world that Russia was a leader in the new technology of aviation. He drove his designers to set distance and endurance records, and he sent them off to the Gulags when they failed. In 1932 Russia entered on the development of a great passenger plane. It was named after its famous writer Maxim Gorky, whom Stalin had persuaded to return to Russia after he had fled the country during the revolution.

Russia's leading designer, **Nikolaevich Tupolev**, got the project. A whole airplane factory, with 800 workers, was assigned to it. Complex as the project was, the "*Maxim Gorky*" flew already two years later. It had eight engines. Its wingspan was greater than a 747's. It cruised at 200 km per hour and had a range of 2000 km.

The "*Maxim Gorky*" made a great publicity flight two months after its test flight. It was staffed with 23 people, and it was to carry forty special passengers, farmers who had made their quotas, highly productive factory workers, and other heroes of the Revolution. Flashing lights on the undersides of its wings were to blink slogans at the people below. It was also equipped with a printing press for leaflets and an aerial loudspeaker system to make propaganda. Maybe this gave rise to the expression "Propaganda Machine".

This remarkable aircraft had a sad end, crashing during an exhibition flight over Moscow. The "Maxim Gorky" had lumbered into the air accompanied on each wingtip by a little biplane. One was there to take pictures. The other, even smaller, was simply there to emphasize the vast size of the "Gorky". Its pilot began showing off for a kid looking out through a window on board the big airplane. He did a loop, and then he drifted as he came out of it straight into the "Maxim Gorky's" wing. Forty-nine people died in the crash. The Russians had another "Maxim Gorky" built by 1939, but it was useless in a world that needed fast-moving military airplanes.

The **Howard Hughes** Flying Boat is commonly called the "*Spruce Goose*". The aircraft was a cargo-type flying boat designed to transport men and materials over long distances. Originally conceived by Henry Kaiser (famous for the production of liberty ships for transports over the Atlanic in WWII) the aircraft was designed and constructed by the flamboyant Hollywood millionaire Howard Hughes and his staff. The Hughes Flying Boat was of a single hull, eight-engine design, with a single vertical tail, fixed wing-tip floats, and full cantilever wing and tail surfaces. The entire airframe and surface structures were composed of laminated wood (primarily birch).

On November 2, 1947, Howard Hughes and a small engineering crew thrilled thousands of on-lookers with an unannounced flight. With Howard Hughes at the controls, the Flying Boat lifted 25 m off the water, and flew for about one minute at a top speed of 120 km per hour before making a perfect landing.

The "Spruce Goose" is now a tourist attraction in a museum in Mac Minnville, Oregon after a long spell at Long Beach in Los

Angeles. It is still the largest aircraft ever built, and it was decades ahead of its time in the early 1940s. It revolutionized jumbo flying bodies and large lift capability, shaping modern flight. It was born of a critical national need to fly over the enemy submarines ravaging shipping lanes during World War II.

By July 27, 1949, the first jet airliner, the "*de Havilland DH 106*", took to the air from Hatfield, England powered by four Ghost turbojet engines. However, it was no commercial success. The Comet was grounded for an extended period after a series of crashes and meanwhile the US manufacturers developed jetliners that were larger, faster and more economical.

There are larger aircraft than those shown in Fig. 9.9. The "*C-5 Galaxy*" is the worlds biggest troop transporter and can carry 1000 soldiers in a triple deck version. Construction of the prototype began in August 1966. The first "C-5A Galaxy" was "rolled out" on 2 March 1968.

Until the introduction of the Russian "*Antonov 124 Condor*" (1982), the "C-5A Galaxy" was the largest and heaviest aircraft in the world. The Antonov ASTC based in Kiev in the Ukraine, is now the world's largest cargo capacity aircraft in production. Like the "C-5 Galaxy" it is not a passenger aircraft. The largest passenger aircraft for the present is the "Airbus A380" with a possibility to grow into 800 passengers. It made its first flight in 2006.

Ex 9.1

It is common to operate a civil engine at its design point, where it will have the same pressure ratio at all conditions. The material temperature at the compressor outlet must stay below the maximum permitted, which for titanium is at 875 K, in all conditions. What is the maximum design pressure ratio for an engine operating in cruise at 10 km altitude and Mach 0.85 where ambient temperature is 223 K if at take-off in Sea Level Static standard atmosphere the temperature is 288 K? Is cruise or take-off the most critical for the compressor? The adiabatic constant for air is 1.4

Ex 9.2

Compare the non dimensional specific thrust and the efficiency for a straight turbojet and a turbofan with bypass ratio 8 at conditions and overall pressure ratio as in Ex 9.1. The turbine inlet temperature is 1560 K.

Ex. 9.3

Calculate values on the curves in Fig. 9.2 for the overall pressure ratio of Ex. 9.1 to verify the trend shown. The turbine inlet temperature is 1560 K and the specific heat is 1005 J/kgK.

Ex 9.4

Assume that we want to design an engine for max specific thrust. Calculate the variation of total compression ratio at Mach numbers 0, 1 and 2 to show that an engine requires much less pressure ratio at high speeds. The turbine inlet temperature is 1560K and the ambient temperature is 223 K.

Ex 9.5

Calculate the variation of the non dimensional specific thrust and the efficiency with overall pressure ratio for a turbofan with bypass ratio 1 to verify the general behaviour of Fig. 9.3. The turbine inlet temperature 1560 K. Assume Mach 2 conditions with ambient temperature 223 K.

Ex. 9.6

Calculate the variation of fan pressure ratio with bypass ratio at Mach numbers 1 and 2 to verify the curves in Fig. 9.4. The turbine inlet temperature is 1560K. The overall pressure ratio is designed for max specific thrust at Mach 1, see Ex.9.4.

10. ECONOMY AND ECOLOGY AS NEW LIMITS

Since the introduction of the bypass engine, air travel has grown by about 5 % a year. Environmental concerns are now emerging as a potential threat to this growth rate. Ultraviolet radiation has increased by 4% in Europe during the last 30 years due to the depletion of the ozon layer. The earth has also been heated up 0.3-0.6 C in the 1900s because of the so called greenhouse effect. Aviation contributes only by a few percent of the damaging emissions but this will increase due to the rapid growth in air travel. Therefore, the fuel consumption will dictate the shape of future aircraft for both economic and environmental reasons.

The revolution in air travel following the advent of the jet engine is reflected not only in the size of aircraft but also in traffic and the number of aircraft. This growth is largely driven by economy. There is a direct relationship between economic development and flying. Therefore, the world traffic will most certainly continue to grow at a high rate as a consequence of the economic growth in many parts of the world.

As shown in Figure 10.1, the sales of the civil aviation industry has grown rapidly and future projections suggest that the demand for air travel will continue to rise, in line with the growth in the world economy. The long term trend is a growth of 5 % per year, which means that the traffic will be nearly three times as high twenty years from now.
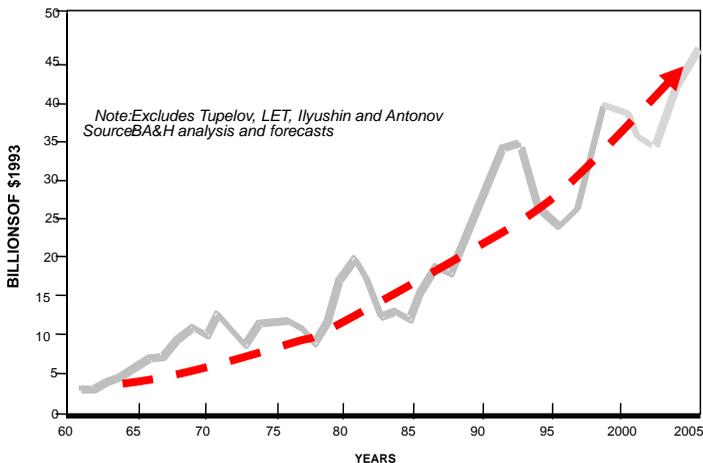
**Fig. 10.1 The sales of aircraft shows a long term
growth rate of 5 % per year**

The growth of the world's economy is certainly favourable for a future expansion of aviation. But there are also forces that work in the other direction. Chief among them are environmental concerns.

For a further expansion of aviation, it is necessary to open up new airports or to increase the traffic at existing ones. The main problem here is noise.

 The primary impact of the <u>high **noise** levels</u> associated with jet propulsion systems has been felt by people living in communities surrounding airports from which jet-powered transport aircraft

operate. Not only were the early jet transports noisier than contemporary aircraft powered with reciprocating engines, but the increased airline traffic that resulted from the widespread adoption of the jet transport resulted in an increased frequency of aircraft operations at most major airports.

The present certification process for transport aircraft involves experimental measurements of aircraft noise under controlled conditions. The noise level is measured at specified positions under the approach and climb paths of the aircraft and at a specified position to the side of the runway. The allowable noise levels vary to some extent with the gross weight of the aircraft and thus reflect what is technically possible and realistic. Lower allowable noise levels will no doubt be specified at some future time to reflect advancements in the state of the art.

In the 1970s, ICAO established international noise certification standards. The initial standards for jet aircraft designed before 1977 are known as Chapter 2. Newer aircraft certified before 2006 are required to meet the stricter standards contained in Chapter 3. Aircraft certified after 2006 are requested to meet the even tougher Chapter 4 standard.

Aircraft noise reduction has been the subject of intensive research and development for the past two decades. The aircraft and engine manufacturing companies as well as various government research and regulatory organizations have been involved in this work. As a result, much has been learned about methods of noise reduction, and a considerable literature exists on the subject. The noise levels have also been substantially reduced, see Figure 10.2.

Four approaches have been followed in the various studies aimed toward reducing aircraft noise. First, much work has been directed toward obtaining an understanding of the basic noise generation and propagation process. Second, new concepts in engine design have been developed to reduce the amount of noise generated at the source. Third, methods for suppressing and absorbing a portion of the noise emanating from the engine have been found. Fourth, aircraft operational techniques have been devised for minimizing noise impact on communities surrounding the airport.
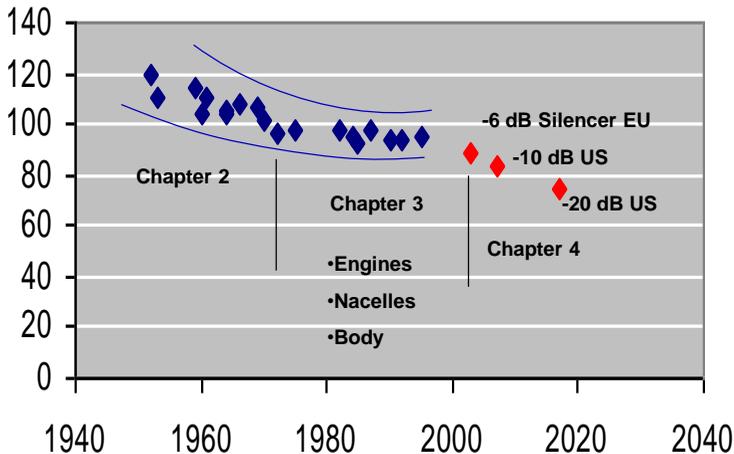
Fig. 10.2 Noise has been substantially reduced

The early jet transports were powered with straight turbojet engines. The hot, high-velocity exhaust is the primary source of noise in this type of propulsion system. The amount of energy in the exhaust that is transformed into noise varies as approximately the eighth power of the exhaust velocity, and the noise-frequency spectrum is related to the circumference of the exhaust jet. The relative amount of noise energy in the lower frequencies increases as the circumference of the jet increases.

Many of the early noise suppressors employed on turbojet propulsion systems were based on the concept of effectively breaking the large exhaust jet into a number of small jets so that the relative amount of noise at the lower frequencies is reduced. The amount of attenuation that accompanies transmission of the noise through the atmosphere increases as the noise frequencies increase. Thus, by breaking up a large jet into a number of small jets, the amount of energy transmitted as noise over a given distance is reduced.

Another type of noise suppressor proposed for the early turbojet powered transports entrains free-stream air, which is then mixed with the high-velocity exhaust. The velocity of the resulting mixed exhaust is therefore lower than that of the free exhaust of the engine alone, and the noise is accordingly reduced at the source.

A great deal of information has accumulated on the manner in which the various components of the engine should be designed so as to reduce the noise generated by it. The turbofan engine and the beneficial effects of increasing the bypass ratio on the propulsive efficiency have been discussed earlier. The advent of the turbofan type of propulsion system had an important effect on the nature of the aircraft noise problem. The extraction of energy from the gas generator for the purpose of driving a fan in a high-bypass-ratio engine would be expected to reduce the noise of the fan engine as

compared with a turbojet for the same thrust level. The fan itself, however, was found to constitute a new and highly disturbing source of noise. Studies of the relatively low-bypass-ratio, first-generation fan engines showed that the noise that was propagated from the inlet and the fan discharge ducts was greater than that associated with the high-velocity exhaust from the gas generator.

The noise associated with the fan can be greatly reduced by proper detail design of the fan and by the use of acoustic treatment in certain key areas of the inlet and fan discharge ducts. Acoustic treatment consists in the application of sound absorbing material to the interior passages of the nacelle. Most modern high-bypass-ratio engines employ some form of acoustic treatment.

During its history, the air transport industry has achieved major reductions in the noise made by typical commercial jet aircraft. An aircraft entering the fleet today is typically 20 dB quieter than a comparable aircraft of 30 years ago. In practice this corresponds to a reduction in noise annoyance of around 75%. Current research programs are expected to deliver the technology for a further 10 dB reduction within the next decade. A reduction of 10 dB is perceived by the human ear as a halving of the noise experienced.

However, it is also seen in Figure 10.1 that the sales of aircraft has fluctuated quite a lot. This indicates that the air traffic is very sensitive to economic conditions. The **direct operating cost** is a common measure of the economy of an aircraft. It can be shown to typically consist of the elements shown in Figure 10.3 below.

The residual, spares and insurance costs would all be proportional to the initial aircraft cost. The initial aircraft cost is very dependent on the series size, concessions etc. Maintenance, crew and other costs contain a fixed part but are also assumed to grow with the

utilization and size of the aircraft. Maintenance and crew are hourly costs scheduled according to the number of flight hours.
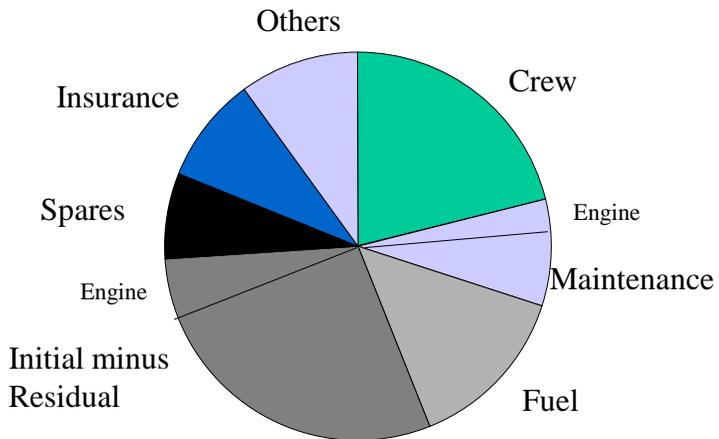
Fig. 10.3 The typical distribution of costs for an aircraft

Other costs directly related to operation are landing and handling costs at airports affected by landing weight, traffic servicing per flight proportional to the number of passengers or payload and reservation, sales, advertising and general administrative expenses proportional to revenues.

Although the cost of fuel takes up a minor part of the overall aircraft cost, it is very difficult to predict how it will develop. Since the 1970's the price of fuel has fluctuated quite a lot. It is very probable that the fuel price will increase due to increased

scarcity of oil. On the other hand a gradual transition to hydrogen in the economy as a whole means that more of the oil production capacity will move into aviation fuel which will keep the price down. The future of the fuel price is also much dependent on environmental concerns about NOX and CO2, which could drive up the costs of fuel by taxation etc. The future fuel price therefore constitutes a considerable economic risk. The aviation industry operates with very small margins and fluctuations in the fuel price could therefore imperil the growth predicted in Figure 10.1. To reduce this risk, the fuel consumption of aircraft should be decreased.

The fuel consumption also needs to come down for another reason. When the jet engine started the revolution in air travel in the 1960's, there was virtually no interest in the environment. Since then the growing environmental concerns have become an important factor blocking the road to air travel in general and high speed flight especially.

While the excessive airport noise levels of earlier times have been largely amended, engine exhaust gas emissions remain a major problem requiring special attention especially as regards its influence on the earth's climate.

The earth's climate is exposed to natural changes over extended periods of time. Thus, temperatures have been much higher for most of the last 500 million years than they are today. The polar ice caps, for example, were formed 15 to 20 million years ago in the Antarctic and perhaps as recently as 3 to 5 million years in the Arctic.

The climate is still dominated by **natural cycles** of warming and cooling of about 180 years. The bottom of the last cycle was in the early 1800s, which suggests that we may now be leaving a period of coldness and entering a natural warming trend. At the same time, the effects of pollutions are expected to add to this effect. Therefore, atmospheric temperatures could reach their highest level during the last 100,000 years by mid-century.

These changes could have an enormous impact. Attendant to a rise in the mean global temperature is a melting of a small but significant portion of the polar ice caps. This would result in a rise in sea level which would flood coastal areas including major population centers.

The earth is protected from the surrounding space environment by a very thin layer of atmosphere. It is in this thin layer that air traffic takes place and it is only very recently that we have begun to understand how vulnerable this system is.

With the advent of ballooning in 1783, people suddenly became interested in the properties of the **atmosphere**. However, a compelling reason for such knowledge did not arise until the coming of aircraft in the 20th century.

The atmosphere consists of layers with very different properties. Manned flight takes place in the two lower layers. The atmosphere up to about 10 km altitude is called the **troposphere**. In this layer, the temperature decreases almost linearly from room temperature to about -60 C. Above 10 km altitude is the **stratosphere** where the temperature starts to increase gradually until at about 50 km it reaches 0 C. Then it starts to decrease again.

The variation of the temperature, pressure and density within the atmosphere is shown in the table below:

Altitude km	Temp T/T_0	Pressure p/p_0	Density ρ/ρ_0
0	1.0	1.0	1.0
10	0.775	0.261	0.338
11 (tropopause)	0.752	0.224	0.298
15	0.752	0.120	0.159
20	0.752	0.055	0.073
30	0.786	0.012	0.015
50 (stratopause)	0.939	0.008	0.008
75	0.72	0.0002	0.0003

Standard atmospheric sea level conditions are T_0=288.15 K, p_0=101.3 kPa, ρ_0=1.225 kg/m3.

This remarkable behaviour of the atmosphere is due to a very small concentration of **ozone** (less than ten parts per million) in the stratosphere which absorbs solar energy leading to increasing temperatures there. The increase of temperature with altitude makes the stratosphere stable to vertical movements in contrast to the troposphere which is mixed vertically.This is a prerequisite for the formation of a stable ozone layer in the stratosphere protecting people on earth against the harmful effects of the suns radiation. The thickest part of the **ozone layer** is at about 20 km altitude.

The inverse temperature gradient makes the stratosphere hydrostatically stable so that pollutions left there will stay for a considerable time. The **tropopause**, the separating layer between

the troposhere and the stratosphere then serves as an invisible ceiling so that there is little exchange between the two layers.

The potential damage to the atmosphere from engine emissions is perhaps the largest cause for opposition to a new high speed aircraft. This is because there is a unique relation between the flight altitude and the speed of an aircraft.

If the dynamic pressure q is too large, the drag (and the structural forces) may become excessive while if q is too small the wing area may become unreasonably large. For hypersonic vehicles 50 kPa is a usual value while for aircraft q is at about 15 kPa.

Now:

$$q = \frac{1}{2}\rho V^2 = \frac{1}{2}\rho a^2 M^2 \qquad\qquad (10.1)$$

where the speed of sound a is:

$$a = \sqrt{\gamma \frac{p}{\rho}} \qquad\qquad (10.2)$$

The equilibrium of a thin layer of the atmosphere demands that

$$dp = \rho g dh \qquad\qquad (10.3)$$

and the perfect gas law means that:

$$\rho = p / RT \qquad\qquad (10.4)$$

which can be integrated to give the variation of the ratio of the static pressure p to the sea level value of p_0 with **altitude h**:

$$p = p_0 e^{-\frac{g}{R}\int_0^h \frac{dh}{T}} \tag{10.5}$$

For isothermal regions, this relation is exactly exponential so that the atmospheric pressure varies with the altitude as:

$$p = p_0 e^{-\frac{h}{h_0}} \tag{10.6}$$

It is also valid approximately in the gradient regions where the temperature varies only gradually with altitude. In average $h_0=7200$ m is the so called **scale height** of the atmosphere.

It follows from these equations that the flight altitude for a given dynamic pressure is:

$$h = h_0 \ln \gamma \frac{p_0 M^2}{2q} \tag{10.7}$$

Thus the flight altitude will increase with speed. For the Concorde at Mach 2+ for example, the preferred altitude was between 19-24 km while a subsonic aircraft has a preferred altitude of about 10 km. This means that the Concorde was flying in that part of the atmosphere where the ozone layer is at its thickest.
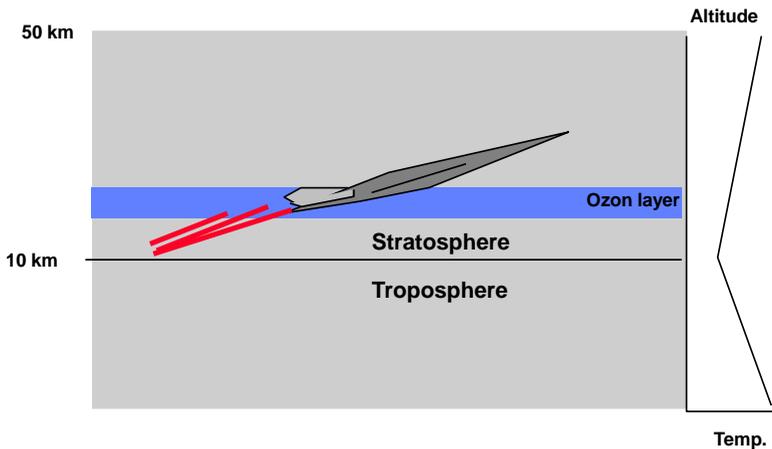
Fig. 10.4 High speed leads to high altitudes

The present state of knowledge of the impact of aircraft emissions on the global atmosphere is characterized by a high degree of uncertainty, concerning both the phenomena involved and their extent. However, there are two effects that are most important namely **ultraviolet radiation** and **global warming**.

It is now considered as a fact (according to a report from the UN body International Panel on Climate Change, **IPCC** 1999) that there has been an increase in ultraviolet radiation of about 4% at European levels during the last thirty years leading to an increased risk for skin cancer.

Also, the temperature of the earth atmosphere has increased between 0.3 and 0.6 degrees Centigrade in the 1900's (or maybe even higher according to IPCC 2007), with potential impact on the climate.

In environmental terms the most important emissions from aircraft are **carbon dioxide (CO2), water vapor (H2O),** in the form of condensation trails, and **nitrogen oxides (NOX)**. Aircraft emissions of **carbon monoxide (CO),** unburned **hydrocarbons (HC)** and smoke have almost disappeared due to better technology. CO2 and H2O can affect the global climate by contributing to the "greenhouse effect" directly while NOX contributes indirectly by interacting with the "greenhouse gases" ozone and methane. Jet aircraft produce 2-3% of global man-made NOX emissions and CO2 from the burning of fossil fuels.

In the past, environmental concern with aircraft emissions has focused on ground level pollution. The aircraft operations of interest close to the ground are defined as the **landing and takeoff (LTO) cycle**. The cycle begins when the aircraft approaches to the airport on its descent from cruising altitude, lands and taxis to the gate. It continues as the aircraft taxis back out to the runway for subsequent takeoff and climb-out as it heads back to the cruising altitude.

Emission standards for smoke, unburnt HCs, CO and NOX from LTO cycles have been set by the **International Civil Aviation Organization (ICAO)**. Each aircraft and engine combination has its own particular emissions profile, worked out according to the LTO cycle, and employing specific emission factors (grams of pollutants per kilogram of fuel) for each operating mode. For calculation purposes, each plane of a given aircraft category is

assumed to spend typical amounts of time in each mode of the LTO cycle on every flight and to operate its engines at standard and specified power setting for each mode. The various emission loads worked out for each pollutant in each mode are then averaged out to produce typical emissions per LTO cycle.
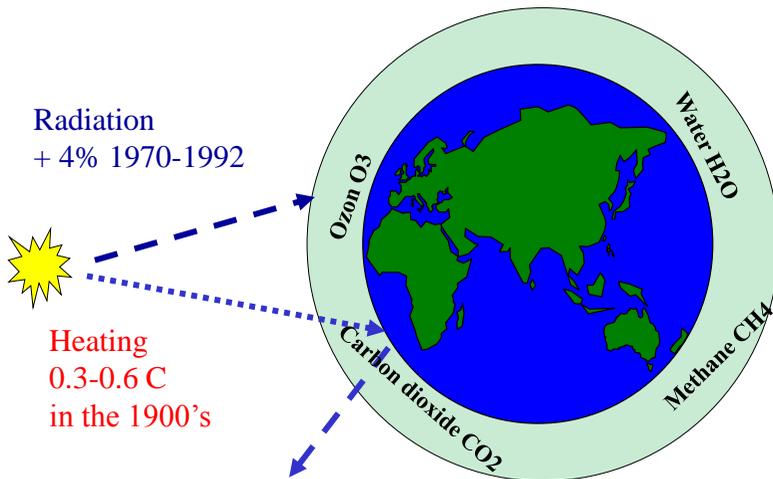
Fig. 10.5 Aircraft contribute to ultraviolet radiation and climate change

However, it is only NOX among the important emissions which is regulated presently and then only at ground level. Airports are usually situated in densely trafficated areas and it is probable that the NOX emissions from aircraft make up a small proportion of

the total NOX emissions there. On the other hand, aviation is the sole contributor to emissions at high altitude.

Efforts are therefore being made to modify the ICAO emissions standards to specifically address emissions of greenhouse gases at all phases of flight, including climb and cruise. However, it is very difficult to regulate this because flight characteristics vary enormously according to the distance to be covered. Jet engines work at 100 % during take-off, at around 60% of capacity in cruise mode and at 30 % during approach. Normal cruise speed for today's subsonic jets ranges between 750 km/h to 1000 km/h depending on the type and range (medium-haul, long-haul) of the aircraft. Flight altitude again varies from aircraft to aircraft and each aircraft has an optimum level according to the design and the weight.

As concerns the radiation problem, **ozone** is valuable as it blocks harmful ultra-violet radiation. NOX emissions are a key factor here. NOX is produced as soon as air is used for combustion irrespective of the fuel. Aircraft NOX emissions are considered to be about 2% of the total world NOX emissions (IPCC, 1990) and the effect on the atmosphere varies according to the altitude and latitude at which the emissions occur.

Thus, **NOX** emissions in the troposphere (below about 12 to 15 km) contribute to the formation of ozone. In the upper troposphere, ozone is created much more efficiently and is destroyed less easily than at ground level. It is thought that NOX concentrations along the busiest air routes may have doubled in recent years. As a result, the air lanes over the North Atlantic and Europe may have about 20% more ozone than other areas.

Stratosphere-
Decrease of Ozone
due to H2O, NOX

$$D \propto \frac{1}{2}\rho V^2$$

10 km

Troposphere-
Increase of Ozone
due to NOX
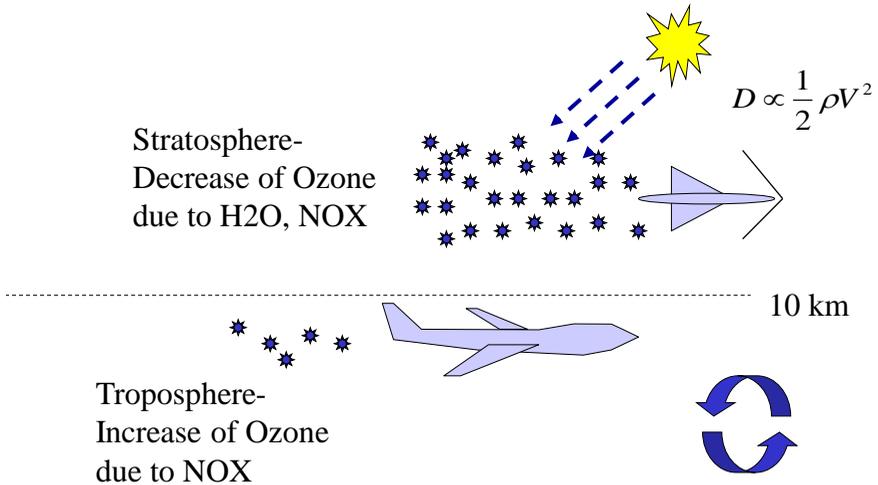
**Fig. 10.6 The influence on ultraviolet radiation
depends on flight altitude**

Thus, NOX emissions from subsonic aircraft have if any a positive effect on radiation. But unfortunately the chemistry higher up in the atmosphere reacts quite the opposite. NOX emissions from supersonic aircraft (such as Concorde) in the stratosphere (above 15 km) contribute directly to the depletion of the ozone layer there. The small volume of supersonic traffic at present ensures that this contribution is small. Available estimates suggest that the contribution of aircraft emissions to local destruction of stratospheric ozone is at present less than 1%. However, it is regarded as one of the most serious obstacles for a successor to the Concorde since NOX emissions from such an aircraft will directly affect photochemical processes which control the ozone layer.

Another issue with a new Concorde is the **radiation exposure** in the aircraft itself. High-altitude radiation can be very intense for short period of times as it is produced by solar flares. Biological damage may therefore be imposed depending on the radiation dosage. At supersonic cruise altitudes, the dose is double that of a subsonic airliner flying at lower altitude. Because the trip time is halved the total radiation dosage for passengers is roughly the same. The main concern, therefore, is for the exposure levels of flight crew members.

The **greenhouse effect** is a result of the absorption of infrared radiation by the atmosphere of the earth. Specifically, the atmosphere allows 50% of the incoming solar radiation to reach the surface but only 10% of the long wave radiation from the surface to escape. This natural greenhouse effect causes the temperature of the earth-atmosphere system to be maintained at a level where life as we know it can survive. Without it, the earth would be a much cooler place. It is this delicate balance that is at risk due to emissions into the atmosphere, which block the outward radiation leading to an increase of the temperature.

As temperatures increase, atmospheric circulation patterns are altered which will change local weather patterns. Also, the warming of the atmosphere will cause the sea temperature to rise as well. This will result in more tropical storms being generated. The polar ice caps would begin to melt, raising the sea level. This will be a slow process, but one that will be irreversible once the greenhouse threat is fully realized. Coastal regions would be flooded causing tremendous destruction of property.
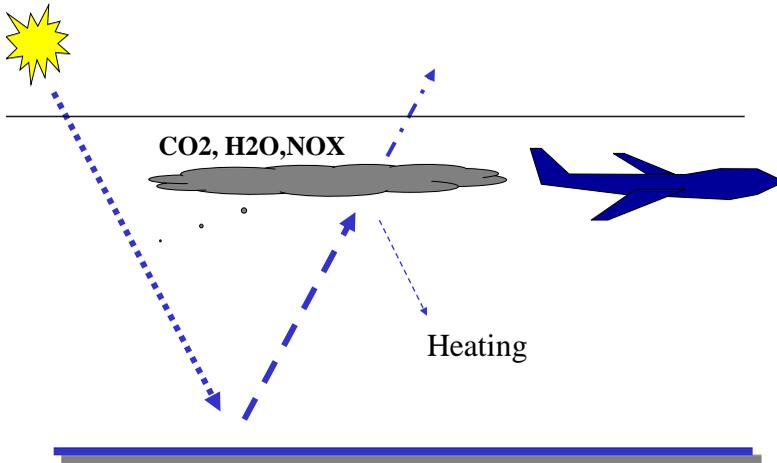
Fig. 10.7 Atmospheric warming is the most important environmental problem

There are three gases emitted by aircraft which contribute to global warming, namely H_2O, CO_2 and NOX**.** The most visible is the water vapor created by burning jet fuels. Jet-fuel - **kerosene** - is a mixture of substances produced by distilling crude oil, which can be represented by $C_{13}H_{28}$. The chemical equation for burning it is $2C_{13}H_{28} + 40O_2 =>26CO_2 + 28H_2O$. For every 13 carbon dioxide molecules the aircraft also produces 14 water molecules.

Long, thin condensation trails, **contrails**, are formed when the warm, humid exhaust gases from jet planes mix with the cold, dry air of high altitudes. The particles in the exhaust plumes allow the

formation of clouds by acting as the nuclei around which ice crystals can form. Since the air in the upper troposphere (the level at which most commercial planes fly) is naturally very dry, water vapor emitted by aircraft can make a big difference. Sometimes the contrails cover the whole sky and the average coverage in Europe is about 6%. Unfortunately, the more efficient the engine, the lower the exhaust temperature and the more ice crystals are formed.

Although these contrails reflect a little sunlight away from earth, they reflect back to earth much more of the invisible infra-red (heat) radiation, which would otherwise escape to space, and therefore they have an overall warming effect. This is hard to measure accurately, because the contrails eventually spread out and become indistinguishable from natural cirrus clouds. Not all of the water vapour forms contrails, but water is itself a "greenhouse gas", which also traps this outgoing infra-red radiation. Each water molecule traps much more heat and also survives much longer at altitude than it would do at sea-level.

Carbon dioxide accumulation in the atmosphere is regarded as the most dangerous pollution problem today. The fact that changes in CO_2 concentrations in the atmosphere could cause changes in the earth's climate has been known for over one hundred years. However, it is only in the last decades that significant research has been done in this field.

Since the Industrial Revolution, man has spewed tremendous amounts of carbon dioxide into the earth's atmosphere. Overall, the use of carbon-based fuels has increased at an exponential rate of more than 4 % per year from the mid 1800's. Aircraft emissions of CO_2 were about 514 million tons in 1992. This represents 2.4% of

total CO2 emissions from the burning of fossil fuels or 2% of total man-made CO2 emissions. While some of this CO2 is assimilated into natural reservoirs, approximately 50% remains airborne and stay in the atmosphere for hundreds of years.

Airlines have doubled their fuel efficiency over the last 30 years. Continuous efficiency improvements are expected to keep aviation's fuel use growth rates at around 3% a year while air traffic is forecast to grow by about 5% a year. The IPCC Special Report on Aviation and the Global Atmosphere suggests that aviation will reach 3% of the projected total man-made emissions of CO2 by 2050.

The annual increase of carbon dioxide in the atmosphere is dependent on several factors. First is the amount of carbon dioxide produced by consumption of carbon-based fuels. Subtracted from this amount is the carbon dioxide that is removed from the atmosphere and stored in reservoirs, or **sinks**. The most prominent sinks of carbon dioxide are the atmosphere, the oceans, and the biosphere. Approximately 50% of the CO2 produced from fossil fuel remains in the atmosphere. The rest is absorbed into sinks. **Reforestation** on a massive global scale or the growth of bio mass for energy production could serve as a method of reducing CO2 accumulation.

Nitrogen Oxides (NOX) are a by-product of combustion, created by the oxidation of nitrous oxide (N_2O) in the air. Normally, the higher the temperature and pressure in the aircraft engine, the higher the amount of NOX, which is produced. This runs contrary to the H2O and CO2 emissions, which decrease with increased temperature and pressure due to better efficiency of the engine. Therefore, it is difficult to decrease all emissions at the same time.

As was said before, NOX emissions at lower altitudes tend to increase the formation of ozone by a chemical reaction chain similar to smog-formation. In this reaction chain nitrogen oxides act as a catalyst under the influence of sunlight. This has the positive effect of decreasing the ultra-violet radiation but at the same time ozon is in itself a greenhouse gas.

To make matters even more complicated, NOX emissions also catalyse the destruction of methane (CH_4), another greenhouse gas, although this cooling effect is much smaller than the ozone warming effect (see Figure 10.8). Aircraft emissions of sulphate aerosols also have a slight cooling effect, but also contribute to acid rain.

As the climate becomes warmer, positive feedback mechanisms tend to exacerbate the problem. Elevations in temperature decrease the solubility of CO2 in the oceans. Therefore, as temperature increases, the oceans release more CO2 into the atmosphere, which causes another increase in temperature.

Even more threatening is the greenhouse water vapor coupling. The atmosphere tends to attain a definite distribution of relative humidity in response to a change in temperature. If the temperature is increased, the relative humidity, which is a measure of the amount of water vapor in the atmosphere, is also increased. At the same time, the vapor pressure of water is raised. The result is more water vapor in the atmosphere, which causes more greenhouse effect, which raises temperatures even higher, which again increases the water vapor in the atmosphere. This positive feedback mechanism approximately doubles the sensitivity of the surface temperature to changes in the amount of energy absorbed by the earth.

Radiative forcing is the term used by the IPCC to express the change to the energy balance of the earth atmosphere system in Watts per square meter (W/m2). Positive values of radiative forcing imply a net warming, while negative values imply cooling.

For the mean global temperature to stay constant, the earth-atmosphere system must be in radiative equilibrium with the sun. In other words, the incoming **solar radiation** must match the outgoing thermal radiation from the earth. Of the incoming solar radiation, 35% is reflected back into space. Of the remaining 65% of solar radiation that is not reflected back, 47% is absorbed by the surface and 18% is absorbed by the atmosphere. For the temperature of our system to remain constant, the energy that is absorbed by the atmosphere must be radiated back out.

The solar radiation absorbed in the atmosphere is in the average about 50 W/m2. In 2005, it is estimated that greenhouse gases of human origin prevented 2.3 W/m2 to be radiated back into space thus resulting in a heating up of the atmosphere. Aviation contributes about 0.05 W/m2 or about 2.5% of this total radiative forcing due to human activities.

It is not easy to quantify the exact greenhouse warming due to emissions from aircraft, but a scientific consensus is now emerging, that the total warming effect of all emissions (CO_2, H_2O and NOX) put together, is in the range 2-5 times greater than that of CO_2 alone. This is confirmed by analysis in the "Special Report on Aviation" recently published by the IPCC in April 1999. Figure 10.7, based on the summary of this report, shows the relative effect of the most important greenhouse gases ozone, CO2, water vapour and methane.
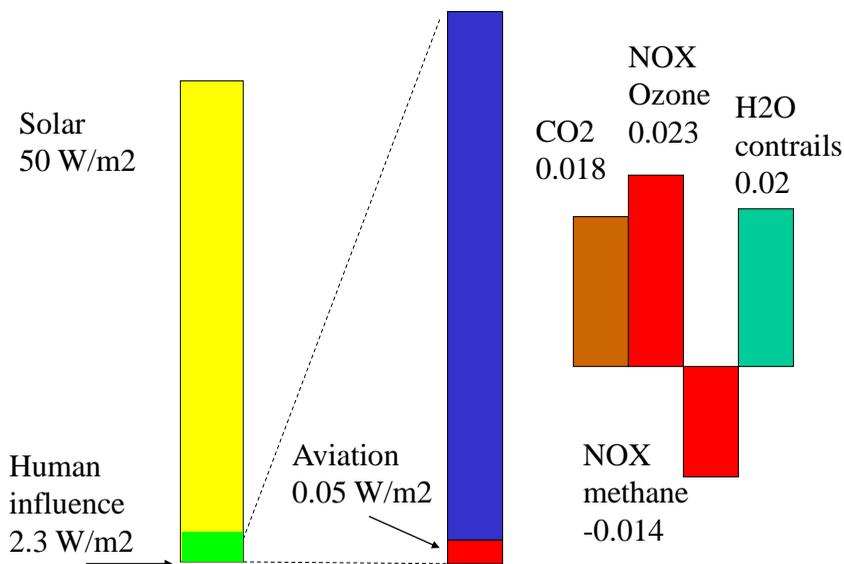
Fig. 10.8 Radiation contributions in 2005 (ICAO)

The amount of carbon added to the atmosphere depends on the type of fuel being burned. Fuels with a high hydrogen- to-carbon ratio produce the most energy for each unit of carbon released. Kerosene ($C_{12}H_{26}$) releases more CO_2 into the atmosphere per unit of energy produced than does natural gas or methane (CH_4), which contains much more hydrogen. Natural gas is the cleanest of the fossil fuels and large reserves of gas have been found.

It is fortunate then that seen over several centuries, the world seems to be moving slowly and inevitably towards pure **hydrogen**, which is found in abundance in e.g. sea water. However, both methane and hydrogen are gases at ordinary temperatures and for

use in aircraft they must be cooled down to low temperatures to reach a liquid state.

Their use would require new aircraft designs and substantial changes to the underlying fuel supply, delivery and storage infrastructure. Their handling in aircraft will also meet with some problems such as isolated high pressure fuel tanks and larger fuel volume leading to increased aircraft drag. An advantage could be that the lower fuel weight would mean less aircraft weight and engine thrust and therefore less noise. As always, safety must be the first and principal consideration in the development of new fuel technologies.

Aviation depends today entirely on low sulphur-based petroleum type fuels and it consumes 2-3% of all fossil fuels burnt. The whole transportation sector uses 20-25% of all fossil fuel consumption. Of this share, aviation consumes 12%, compared to 75% consumed by road transport. If a hydrogen economy based on fuel cells for cars develops it would be a strong incitement for the introduction of hydrogen in aircraft.

However, from an environmental point of view, **kerosene** may still be the best fuel for aviation. Kerosene may in fact produce less radiative forcing than the main alternatives, methane and hydrogen, because of the water produced by these.

A solution could be to use synthetic kerosene produced from biomass. The CO_2 released would then be absorbed by the biomass over a period of about 30 years avoiding its accumulation in the atmosphere. A mixture of ethanol and standard jet kerosene has also been flown. All such new fuels will have to meet the stringent performance and safety restrictions of aviation.

As there do not appear to be any practical alternatives to kerosene for aviation at present, efficiency will continue to be the key to controlling fuel use from aviation. In the past 30 years, aircraft fuel efficiency per passenger-km has improved by about 50% through enhancements in airframe design, engine technology and rising load factors. More than half of this improvement has come from advances in engine technology.

In time, the introduction of new technologies will bring about further reductions in fuel consumption, directly helping to decrease emissions of CO2 and H20. Although the technologies needed to do this are not operational today, there appears to be potential for a further 40-50% improvement in fuel efficiency. Current research goals include a reduction of NOX levels by 50% from today's regulatory limits in 5 to 10 years from now.

To decrease the amount of fuel consumption, the efficiency of the engines must be pushed up. The way to do this is to increase the pressure in the engines. It is then also necessary to increase the temperature for an optimal cycle. The problem is that the production of nitrogen oxides then increases exponentially. If the combustor is designed for constant residence time then from Kerrebrock p.175:

$$NOX \propto \sqrt{p_{t3}} \exp(-2400/T_{t3}) \qquad (10.8)$$

ICAO regulations also restrict the amount of NOX dependent on the pressure ratio, see Figure 10.9.

Hence, paradoxically, the key to efficient engines with low emissions of CO2 and H2O is to develop combustors with low emissions of NOX. Innovative combustion systems are developed to do this.
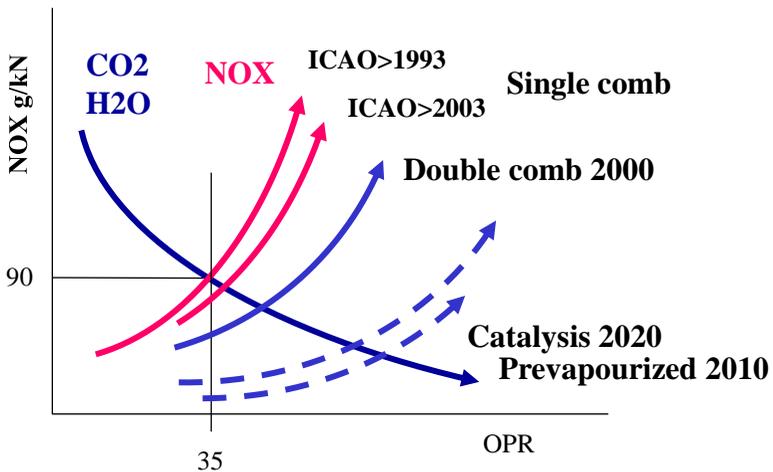
Fig. 10.9 Why NOX must decrease

In the so called **Rich Burn-Quick Quench** combustors, burning first takes place in a fuel-rich zone. The combustion is then quenched rapidly with copious amounts of secondary air. This technology limits the maximum flame temperature, which is a key factor in reducing NOX.

The **Lean Pre-mixed Pre-vaporized (LPP)** system relies on vaporization of the fuel to stop local stoichiometric combustion

which produces high levels of NOX. This approach prevaporizes the fuel and injects it into the air in a premixing passage, delivering a uniform droplet-free mixture to the combustion zone. The fuel/air ratio is set as low as possible, but above stability or inefficiency thresholds.

For both combustor types, liner material is a challenge, as active cooling (with air) negatively influences the mixing and chemistry critical for low NOX .

Important for all the low emission combustors is that no air should be allowed to enter the interior where it interferes with the combustion process. Thus, a non-cooled burner liner is required. This can only be met with ceramic composites.

Ex. 10.1

Subsonic aircraft typically fly at an altitude of 10 km at Mach 0.85. What would be the altitude of a Mach 2 aircraft flying at the same dynamic pressure as the subsonic aircraft?

11. THE FUTURE CIVIL AIRCRAFT

The fuel consumption of an aircraft is determined by the engine efficiency and the aircraft lift-to-drag ratio L/D. They may be predicted from their earlier development for a new generation of aircraft for the 2020's. The engine efficiency has been growing steadily but the gas turbine cycle is approaching its limits. The L/D ratio has stagnated as the friction coefficient of the aircraft skin has approached that of a turbulent flat plate but it could be made much higher with laminar flow and new aircraft shapes like flying wings. It falls rapidly beyond Mach 1, though, making supersonic aircraft uneconomical.

The fuel consumption of aircraft has decreased very much since the breakthrough of the jet engine, see Figure 11.1. Maybe contrary to what most people believe, it is now comparable to that of a car if both are occupied to 70% of the maximum, which is normal for aircraft though not for cars. Still, to reduce the economic risks and for environmental reasons, it is very important that the fuel consumption continues to decrease.

The **fuel fraction f_{cr},** that is the weight of fuel spent in cruise relative to the total weight at beginning of cruise, is from the Brequet equation, Eq. (7.3):

$$f_{cr} = \frac{m_{fc}}{m_{0c}} = 1 - \exp(-\frac{gR}{h\eta L/D}) \qquad (11.1)$$

Litres/10 km/passenger

Source DLR/EC 99
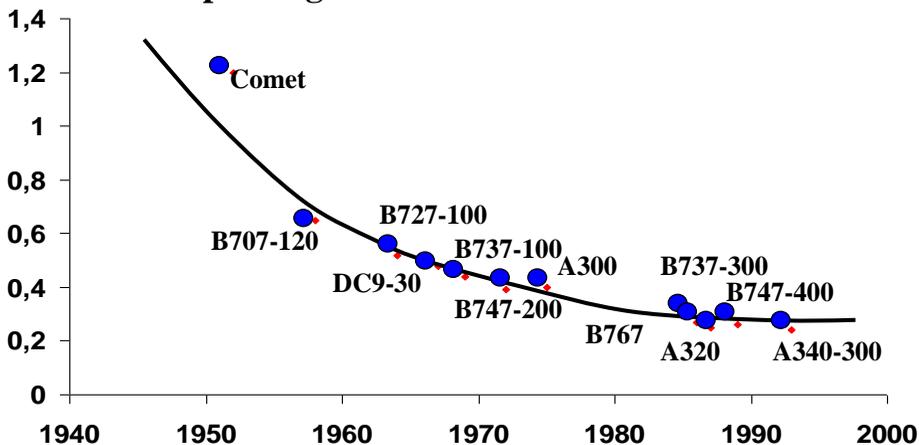
Fig. 11.1 The fuel consumption of aircraft has decreased

The **total weight m_{0c}** at beginning of cruise is obtained by adding the **empty weight m_e**, the **payload weight m_{pl}** and the fuel weight **m_{fcr}** spent in cruise in addition to fuel for landing and a fuel reserve, which is typically 10% of the total weight:

$$m_{0c} = m_e + m_{pl} + m_{fcr} + m_{fres} \qquad (11.2)$$

Therefore with Eq. (11.1), the **total weight at start of cruise is:**

$$m_{0c} = \frac{m_e + m_{pl}}{1 - f_{cr} - f_{res}}$$ (11.3)

where $f_{res}=0.1$.

The total take-off weight is typically about 4% higher than that given by Eq. (11.3) due to fuel spent in climb.

It is now seen from Eqs. (11.1) and (11.3) that the fuel consumption depends on the empty and payload weights and the so called Brequet factor $\eta L/D$. The payload weight is directly proportional to the number of passengers "N". Statistically each passenger takes up about 110 kg. Therefore, it is the development of the **empty weight m_e**, the **engine efficiency η** and the **lift-to-drag ratio L/D** that will decide the shape of aircraft and what may happen with the fuel consumption in the future.

As is seen from Figure 11.2 below, the empty weight of existing aircraft increases progressively with size. This means that for a larger aircraft, more weight is carried around with each passenger.

That the weight should behave like this is not surprising since it is a general law in nature that very large things tend to break down under their own weight. This law holds for all mechanical structures and it halts the ultimate growth in size provided the technology is static. This is because the weight tends to be proportional to the volume i.e. the length in power of three while the carrying capacity tends to be

proportional to the area i.e. in power of two. This is the so called **"Law of Two-Thirds".**
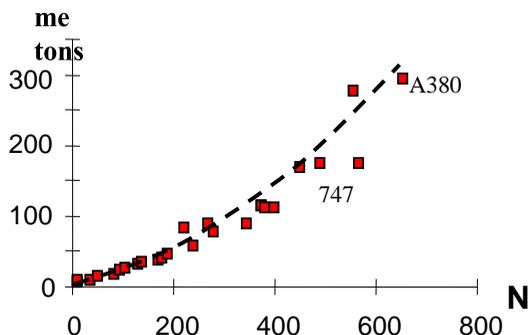
Fig. 11.2 The empty weight of aircraft vs the number of passengers

Since the number of passengers should be proportional to the floor space i.e. to the surface area, the empty weight of aircraft should grow according to:

$$m_e \propto \frac{\rho}{\sqrt{\sigma}} N^{3/2} \qquad\qquad (11.4)$$

As seen from Figure 11.2, Eq. (11.4) models the empty weight of aircraft relatively well provided that the technology and the design remains the same. This is roughly the case for aircraft during the last fifty years.

However, it may be assumed that the empty weight is inversely proportional to the **specific strength $\sqrt{\sigma}/\rho$** of the aircraft skin material. The motivation for this is that the thickness of a plate exposed to a bending moment is inversely proportional to the square root of the stress σ and the weight is therefore proportional to $\rho/\sqrt{\sigma}$, where ρ is the material density.

$\sqrt{\sigma}\,/\,\rho$
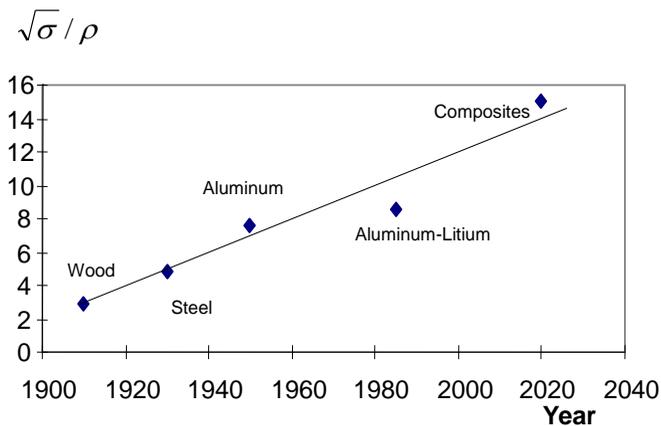
Fig. 11.3 The growth in strength of aircraft materials

Figure 11.3 shows the development of the specific strength of aircraft materials with time. The superiority of todays materials compared to those of 1903 is very clear as are the gains that could be obtained with composites. Composites generally have a much higher specific strength than the conventional aluminum.

In the very long term it seems possible to design fault free materials with ten times the present strength for the same density compared to today. The whisker crystals are possibly the most perfect specimen presently available. In some cases they contain no observable defects at all. The trick would be to achieve such perfection also with bulk materials. Maybe this could be obtained by building the materials atom by atom.

The efficiency of jet engines has more than doubled since their first appearance as is shown in Figure 11.4 below. The commercial jet engine era was initiated in the early 1950's with the **Ghost** engine from the De Havilland company, which was later to become a part of the Rolls-Royce company. The Ghost powered the De Havilland Comet DH106 Airliner. With minor modifications, under the name of RM2, it became the engine for the Swedish fighter SAAB J29 Tunnan.

The early engines like the Ghost were low pressure ratio, straight flow turbojets using centrifugal compressors. However, it was soon realized that the axial compressor provided both higher pressure ratio and lower frontal area than the centrifugal compressor. With the axial compressor it was also possible to use short annular combustors rather than can type combustors. Such turbojet engines, like the **JT3,** was used on the Boeing 707 and the KC135 US Air Force tanker.

Engine design gradually became polarized by companies featuring either two rotor spools (PWA) or three rotor spools (RR) with fixed geometry compressors or a single rotor with variable compressor vanes (GE). These advances paved the way for higher

bypass cycles reducing the jet velocity to closer match the aircraft flight speed.
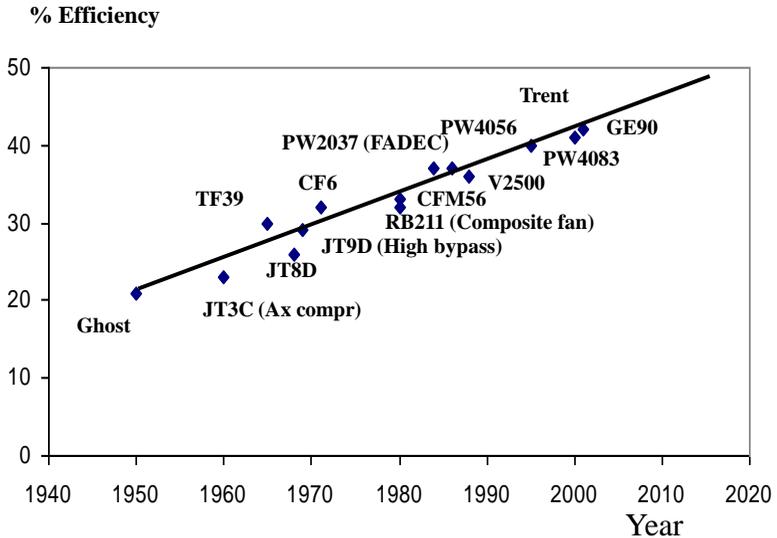
% Efficiency

Fig. 11.4 The engine efficiency has increased a lot

The late 1960's saw the emergence of such high bypass ratio engines. The GE **TF39**, the world's first high-bypass turbofan engine, was developed in response to the United States Air Force's desire for a new transport aircraft. The high-bypass turbofan was a giant leap in aircraft engine design, offering such pioneering technological accomplishments as an 8-to-1 bypass ratio and a 25-to-1 compressor pressure ratio.

The TF39 became the parent of GE's highly successful **CF6** family of commercial engines for wide body aircraft. More CF6 engines have been produced and have flown more hours than any other high bypass engine. It has powered wide body aircraft such as the Boeing 747 and 767, the Airbus A300 and A310, and the McDonnell Douglas MD-11.

Pratt & Whitney's **JT8D** engine is the most popular modern commercial engine ever made. More than 14000 of them have been built, achieving more than half a billion service hours between 1964 and 2004. More than 350 operators use the JT8D to power more than 4500 aircraft, nearly a third of the world's commercial fleet, such as Boeing 727 and 737 and McDonnell Douglas DC-9 and MD-80.

Pratt & Whitney's **JT9D** opened up a new era in commercial aviation, the high-bypass ratio engine powering wide-body aircraft. It introduced many advanced technologies in structures, aerodynamics and materials to improve fuel efficiency and reliability. Since entering service on the Boeing 747 in 1970, the JT9D has proven itself to be the workhorse for early 747, 767, A300, A310 and DC-10 aircraft models. The JT9D has flown more than 150 million hours.

The **CFM56** is presently the most popular engine in the world for narrow-body aircraft, including the Boeing 737 and Airbus A320 families. It is produced through a joint venture between Snecma Moteurs of France and GE. In 1971, Snecma selected GE as a partner in the development of a smaller commercial turbofan engine. The companies established CFM International to build engines based on Snecma's fan technology and the core technology of GE's F101 engine. The GE/Snecma collaboration was founded

on a desire to gain a share of the short-to-medium-range aircraft market, dominated in the early 1970s by low bypass engines. GE wanted to develop a powerplant to compete with the low bypass Pratt & Whitney JT8D engine on the Boeing 737 and McDonnell Douglas DC-9, as well as the Boeing 727.

With the emergence of the widebody airliners in the late 1960s, Rolls-Royce launched the **RB211** for the Lockheed L-1011 Tri-Star. Failed attempts to introduce composite fan blades on the RB211 led to the Rolls Royce Company being taken into state ownership with the separation of the motor car business in 1973. However, the three-shaft turbofan concept of the RB211 has now established itself at the heart of the Rolls-Royce world-class family of engines. An advanced version features extensive use of advanced computer-designed aerodynamics, particularly in its wide-chord fan.

The **PW2000** family was the first to offer Full-Authority Digital Electronic Control (**FADEC**). This engine entered service in 1984 on the Boeing 757. The **PW4000** has been selected to power more Boeing 777 aircraft than any of its competitors. It was the launch engine for the 777, entering service in 1995. Using hollow titanium, shroudless fan blades, the PW4000 provides high efficiency and low noise.

The Rolls Royce **Trent** family is designed to power the new generation of wide-bodied jets including the Airbus A380. The Trent 500 has been specifically designed to meet the requirements of the four-engined Airbus A340. With its design derived from the reliable RB211 family of three-shaft engines, the Trent's advanced layout provides lighter weight and better aircraft payload or range.

The **GE90** is the world's most powerful jet engine. Its high-flow swept fan blades are manufactured from composite materials (fibers and resin system). The swept fan blades add approximately one ton to the engine's thrust capability and provides better fuel burn.

As is seen from Figure 11.4, the engine efficiency has gradually increased over time and it would be tempting to assume that it could continue like this. However, it is important to understand that in reality there are always physical or other limits that make such curves bend downwards sooner or later.

Thus a technology developing towards a physical limit tends to follows an **S-curve**. This is a phenomenon that is noticeable for every kind of technology. Typically, see Figure 11.5, there is an initial period of slow growth followed by a period of rapid, sometimes exponential growth, with a tailing off towards some limit.

Since the growth rate should be small at the lower and upper asymptotes, it is natural to describe the shape of the curve by:

$$\frac{dy}{dt} = ay(1 - \frac{y}{y_c}) \tag{11.5}$$

with the solution:

$$y = \frac{y_c}{1 + Ce^{-at}} \tag{11.6}$$
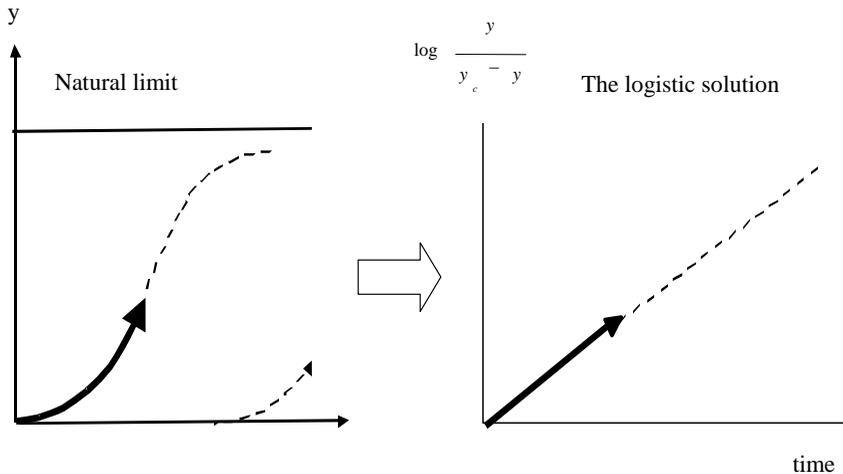
Fig. 11.5 The technology life cycle

The S-shaped curve obtained from the previous equation is the so called **logistic curve**, a term that appears to have been used first by **Edward Wright** in 1599. It was used to study population growth already in the 18th century.

To predict the future of a certain technology we should therefore determine the upper limit and then plot the logarithmic expression $\log \frac{y}{y_c - y}$ on a straight line in time. Because of the logarithmic type of this expression, earlier parts of the diagram are magnified

which means that good predictions can be made even if we are still far from the upper limit.
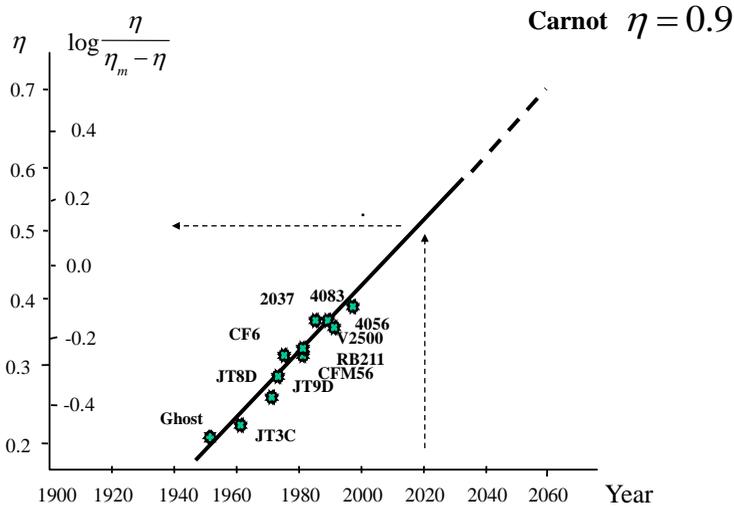
Fig. 11.6 A logistic prediction of the engine efficiency

The highest possible efficiency in a thermodynamic cycle is the **Carnot** efficiency $\eta_{max} = 1 - \dfrac{T_{min}}{T_{max}}$. For a cycle operating between the atmospheric and stoichometric temperatures the maximum efficiency therefore is about 90%. This makes it possible to construct a logistic diagram, see Figure 11.6, from which the future development of the jet engine efficiency may be predicted. As is seen from Ex. 9.2 and 9.3, the gas turbine bypass engine is

probably limited to efficiencies not much higher than 50 %. Continued development beyond about 2020 therefore requires some sort of new cycle.

The **transportation capacity** for a given number of aircraft is the number of passenger kilometers that can be produced in any given time i.e. N x V, where **N is the number of passengers** and V is the speed.

The increased traffic can therefore be met either with larger aircraft or with more aircraft and higher speed, which both would lead to more frequent flights. Historically, the solution has been more aircraft. Technically, there is a limit to the jet engine as high as Mach 4. Still, the only high speed civil aircraft has been the Concorde and as yet no successor to it is in sight.

Aviation has increased our capability to move around the globe tremendously. But long distance travelling is still a rather tedious business because we are limited to flight speeds below the local speed of sound. Any person who has spent 20 hours on a flight to Australia may be forgiven for wanting higher speeds. It would be fine if the the problem of meeting the increasing demand for travel could be solved by higher speed. So why did the speed of transport aircraft remain at subsonic speed?

Besides the engine efficiency, the lift-to-drag ratio is the most important parameter for airliners, affecting essential economic-related performance such as maximum range, payload and fuel consumption. It very much determines the shape and speed of the aircraft. The L/D for some existing and proposed aircraft for different speeds is shown in the Figure 11.7 below.
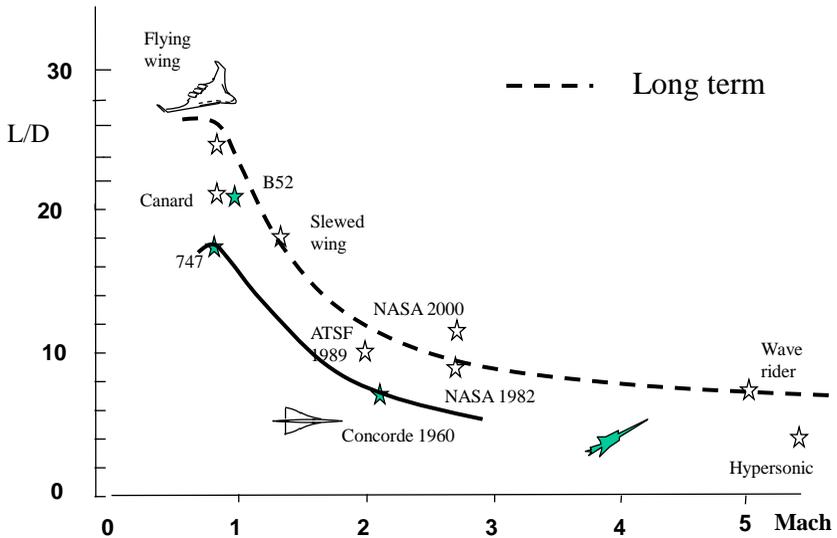
Fig. 11.7 The L/D falls rapidly at higher Mach numbers

The lift-to-drag ratio is seen to fall rapidly at higher speeds due to the supersonic wave drag. This drag begins to appear locally at the body of the aircraft even below Mach 1. At the drag divergent Mach number, the formation of shocks begins to substantially affect the drag. This Mach number is at about Mach 0.85 and therefore beyond this Mach number, the L/D starts to drop and it is because of this that the condition for cruise has been set at around 0.85.

For a Mach 2 aircraft like the Concorde, the L/D will be less than half the value for a subsonic aircraft like the 747. The Concorde which represents early 1960s technology has a L/D of about 7 at

Mach 2. For modern supersonic transports, such as the 1989 design ATSF, the lift-to-drag ratio is expected to be about 10. This would be accomplished by increasing the wing span and refining the fuselage shape and the landing gear stowage. Still larger increases may be obtained by laminar flow control of the wing boundary layer.

Current studies indicate a further improvement of about 30% by the year 2000 using arrow-wing technology and partly laminar flow control. For the longer term, improvements over the present technology could be possible with innovative body concepts such as a 3-body fuselage. Special configurations for flight at Mach 1.2-1.4 such as the slewed flying wing could realize values up to 12 or 14 at low supersonic speeds. However, such technologies could also be used to increase the subsonic performance and it is a safe assumption that supersonic aircraft always will have significantly lower L/D values than subsonic ones.

Both the range and the fuel consumption are directly dependent on the lift-to-drag ratio and the inferiority of supersonic flight then becomes pronounced. The engine efficiency η increases somewhat with speed but not very much beyond Mach 1 while the lift-to-drag ratio L/D decreases significantly. Thus the factor ηL/D is about 6 for a 747 but only about 3 for the Concorde. Therefore the potential range of the 747 is about twice that of the Concorde. To be able to compete with subsonic airraft over distances where speed really counts the factor ηL/D must be increased significantly for high speed aircraft. Technologies to decrease the wave drag are therefore a key to the success of supersonic transportation.

Consequently, we should not expect supersonic aircraft to become economical even in the very distant future. The direct operating

cost per passenger km of the Concorde of the 1980´s is two times that of a subsonic aircraft like the 747 and the fuel cost is three times as much. This difference will probably remain for the future because of the lower L/D for supersonic aircraft.

Moreover, because of its higher relative fuel consumption, a supersonic aircraft is more sensitive to environmental fees that translate into fuel price and also to the price of the aircraft itself. The environmental fees will sooner or later be based on how much the aircraft pollute the atmosphere instead of as landing fees, which decrease the pollution around airports only marginally because others contribute so much more to the pollution there.

Minimizing fuel consumption per kilometer corresponds to a flying manner where the drag, that is thrust, is minimized for a given weight, that is lift. This L/D is $2/\sqrt{3}$ times the L/D for minimum power and the corresponding speed is about 30% higher, see Chapter 4. Usually, one makes a compromise and flies somewhere in between the two extremes. A usual average value is to use:

$$\frac{L}{D} = \frac{2\sqrt{2}}{3}\left(\frac{L}{D}\right)_{max} \qquad (11.7)$$

Max L/D
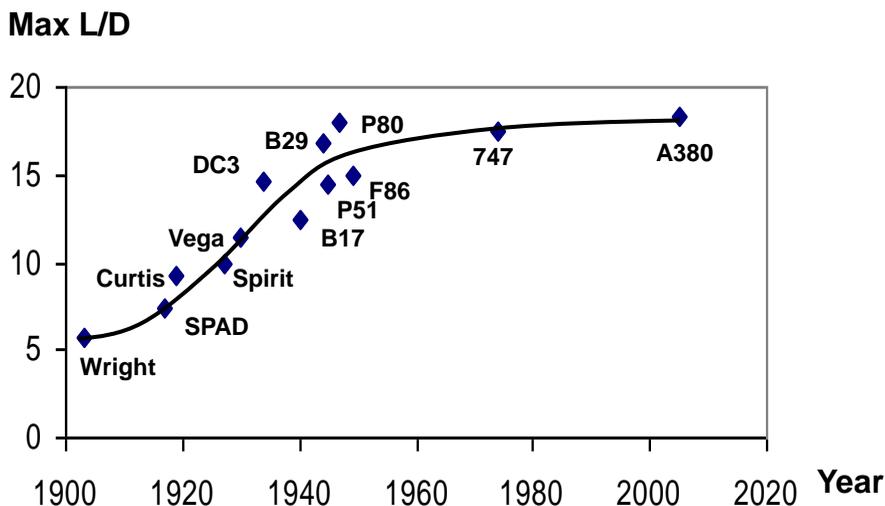
Fig. 11.8 Stagnating Lift/Drag ratio

As is seen from Figure 11.8, <u>the maximum L/D has stagnated at below 20</u>. The reason for this is that in subsonic cruising flight of a well designed aircraft, the parasite drag consists mostly of skin-friction drag. The maximum L/D for a subsonic aircraft is given by Eq. (4.10):

$$\left(\frac{L}{D}\right)_{max} = \sqrt{\frac{\pi e}{4C_{fp}} \frac{b^2}{S} \frac{S}{S_{wet}}} \qquad (11.8)$$

where C_{fp} is the so called **parasite skin friction coefficient**.

As is shown in Figure 11.9, modern aircraft are approaching the theoretically best attainable values for skin friction drag in turbulence. At the same time, the shape of aircraft has remained more or less the same since the DC3. This means that the L/D has not grown very much during the last 40 years.
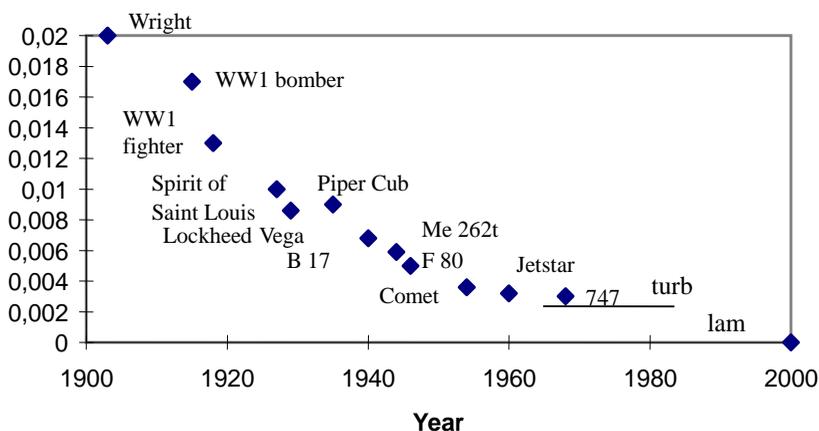
Fig. 11.9 The aircraft parasite drag is approaching that of a turbulent flat plate

The drag caused by flowing fluids was long an enigma. **Isaac Newton** was probably the first to formulate an equation for aerodynamic drag. In his book"*Principia*" of 1687, he assumed that the flow was a stream of particles impacting upon a surface. If the surface is inclined at an angle α, then the flow area is

proportional to sinα. Also if the particles are assumed to follow the surface after impact upon it, they lose the velocity component Vsinα perpendicular to it. Therefore the normal force on the surface would be proportional to sinα in square.

Newton's flow model is not correct at ordinary speeds because the streamlines are not straight and parallel until they hit the body. However, it is more useful at very high speeds. Newton's "sine square-law" is therefore used to estimate the aerodynamics of hypersonic vehicles, a type of machine that was not even dreamt of in Newton's time. A fluid following Newton's assumptions is often called a newtonian fluid.

Further attempts to understand the fluid dynamics drag were made by the French mathematician **Jean Le Rond d'Alembert** (1717-1783). d'Alembert was given the name Jean Le Rond because as an infant he was found abandoned on the steps of the St. Jean Baptiste le Rond church. He was placed in the care of foster parents, to whom he remained loyal all his life, even after it was discovered that his natural mother was an aristocratic lady, Madame de Tencin, and his natural father the artillery general Chevalier Destouches. d'Alembert grew up to become a famous mathematician and scientist, notable for his development of partial differential equations.

During the years from 1751 to 1772 he collaborated with **Denis Diderot** on the famous "Encyclopedia", to which he contributed the preface and most of the articles on science and mathematics. This was an ambitious attempt to gather and present to the general public all the then existing knowledge. It was a revolutionary undertaking because the power of church and state at the time relied more on traditions and beliefs than on scientifically proved

knowledge. Aided by the most celebrated writers of the day, including Voltaire and Montesquieu, the skeptical, rationalist Diderot used the "*Encyclopédie"* as a powerful propaganda weapon against the authorities of the time. In 1759 the first ten volumes were suppressed and further publication forbidden. Nevertheless, Diderot continued working on the remaining volumes and had them secretly printed.

D'Alembert solved the equations for an incompressible frictionless flow around a sphere. In a frictionless flow, the velocity field is symmetrical before and after the sphere. D'Alembert therefore expected that the force would approach zero for very small viscosities and he performed a series of experiments to prove this. However, to his astonishment, the net force seemed to converge on a non-zero value even though the viscosity approached zero. This became known as the **d'Alembert paradox**.

The reason for this is that any non-zero viscosity, no matter how small, will result in the velocity dropping to zero at the surface and therefore to a force on the sphere. It was not until a century later that the effect of friction was introduced in the equations describing fluid flow by Claude-Louis Navier and George Stokes. However, the d'Alembert solution of frictionless flow is important because of the Joukowski transformation, that makes it possible to transform the flow around a cylinder to that around an airfoil.

A specialist in road and bridge building, **Claude-Louis Navier** was the first to develop a theory of suspension bridges. He lived through a period when there were great political movements throughout Europe and in France in particular. Navier believed in an industrialised world in which science and technology would solve most of the problems. He also took a stand against war and

against the bloodletting of the French Revolution and the military aggression of Napoleon. The two men who had the most influence on Navier's political thinking were Auguste Comte, the French philosopher known as the founder of sociology and of positivism, and Henri de Saint-Simon who started the Saint-Simonian movement which proposed a socialist ideology based on society taking advantage of science and technology.

However, he is remembered not for his political interests or as the famous builder of bridges, but rather for the so called **Navier-Stokes equations** which today form the very foundation of fluid dynamics. Navier developed those equations for an incompressible fluid in 1821 and in 1822 he gave the equations for viscous fluids. The irony is that although Navier had no conception of shear stress and did not set out to obtain equations that would describe motion involving friction, he nevertheless arrived at the proper form for such equations. He did this by taking into account forces between the molecules in the fluid.

George Stokes was an English mathematician at Cambridge interested in hydrodynamics. After he had deduced the correct equations of fluid motion, Stokes discovered that he was not the first to obtain the equations since Navier and other French scientists had already considered the problem. This duplication of results was brought about by the lack of knowledge of the work of continental mathematicians at Cambridge at that time. Stokes decided that his results were obtained with sufficiently different assumptions to justify publication in 1845 and he has since been awarded by having his name added to that of Navier as founder of the equations.

The study of fluids was certainly not the only area in which George Stokes was making major contributions. In 1845 Stokes had also published an important work on the aberration of light. This was the first of a number of important works concerning the wave theory of light, such as a paper on diffraction in 1849. He also used his work on the motion of pendulums in fluids to consider the variation of gravity at different points on the earth. This led to a fundamental paper on hydrodynamics in 1851 where he published his law of viscosity, describing the velocity of a small sphere through a viscous fluid. Stokes also named and explained the phenomenon of fluorescence in 1852.

Stokes was appointed Professor of Mathematics at Cambridge in 1849 and became secretary of the Royal Society in 1854. The professorship at Cambridge paid very poorly so Stokes needed to earn additional money and he did this by accepting an additional position namely that of Professor of Physics at the Government School of Mines in London. After marrying in 1857 he tired of science and moved from his highly active theoretical research period into better paid occupations, where he became more involved with administration and experimental work.

The next break-through came in 1883 when **Osborne Reynolds,** a professor of engineering at the University of Manchester for 37 years until his retirement in 1905, discovered that a fluid could have two modes of motion, **laminar** and **turbulent**. In the former, the particles of the fluid follow defined and orderly paths. In the latter the motion is quite random and unpredictable. Reynolds showed that the transfer from laminar to turbulent flow occurred when the dimensionless parameter $\rho V c / \mu$ reached a certain value. This parameter is called the **Reynolds number Re**. It is proportional to the ratio of inertia forces to viscous forces in a

fluid flow. For air it is about 10^6. The mean aerodynamic length of the overflown body is "c", the so called dynamic viscosity is "μ" while the density is "ρ".

Reynolds is said to have had a very interesting approach to problem solving. He never began by reading what others had thought about the matter, which is the established method of scientific work. Instead, he first thought it out for himself. In this way he often reached very original solutions to difficult problems. The drawback was that it took a lot of time and required him to be very devoted to his work. This was sometimes a problem for his students. He was known to come up with new ideas in the course of a lecture and to spend the rest of the hour working them out on the board seemingly unaware of the students in the classroom.

The Navier-Stokes equations are highly nonlinear and very difficult to solve even for laminar flow. Then in 1904, **Ludwieg Prandtl** conceived the idea of **boundary layer**, which adjoins the surface of a body moving through a fluid. It is perhaps the brightest idea in the history of fluid mechanics. He reasoned that the flow velocity was zero at the surface of a body and increased to free flow speed within a thin layer. The influence of friction is limited to this thin layer, which allows the Navier-Stokes equations to be greatly simplified. By 1908, Prandtl and Blasius, one of his students, had solved these simplified equations for laminar flow. They found that the skin friction coefficient is inversely proportional to the square root of the Reynolds number. For a flat plate in laminar flow

$$C_f = \frac{1.328}{\sqrt{\mathrm{Re}}} \tag{11.9}$$

However, real flow is more often turbulent than laminar. A typical Reynolds number for a large aircraft is Re=3*10^7, which is substantially higher than the critical value of 10^6 where transition to turbulence occurs according to Reynolds. To this day no exact theoretical results have been given for turbulent boundary layers. Turbulence remains one of the major unsolved problems in physics and we must rely on experimental results. However, the flat plate skin friction coefficient in turbulent flow can be approximated from experiments by:

$$C_f = \frac{0.455}{(\log \text{Re})^{2.58}(1+0.144M^2)^{0.65}} \qquad (11.10)$$

With a typical Reynolds number for a large aircraft of Re=3*10^7, the turbulent skin friction coefficient is about 0.0025. The laminar drag proves to be considerably lower than the turbulent one. For the same Reynolds number the laminar skin friction coefficient is about 0.00025, that is ten times lower than the turbulent value. This can be taken as the lowest possible value of the skin friction coefficient on an aircraft.

The fully laminar aircraft will never be reached of course. A certain amount of air turbulence occurs on the surface of aircraft regardless of shape and size. Air often flows smoothly across the surface for a while but even if the surface is perfectly smooth, it eventually breaks off and creates a turbulent wake increasing the drag. Much of the work to reduce drag concerns methods to delay this break off of the flow.

Paradoxically, making a surface perfectly smooth would not necessarily help to decrease drag. This is because the break off of the flow is delayed if the boundary layer is made turbulent by

surface roughness. This may be seen in a golf ball where the dimples reduce drag significantly by creating turbulence.

Wind and water tunnel tests have shown that **riblets** can reduce viscous drag by as much as eight percent. Riblets are small, grooved channels manufactured in the skin of flow-bearing surfaces such as the skin of a wing. This models the rough surface of a shark's skin, which has been found to significantly reduce the drag of the shark in the water.

A **shark**'s skin is quite rough in a very particular way. It is embedded with millions of tiny, sharp, tooth-like scales, giving it a texture like sandpaper. The skin actually looks like a series of stripes that cause water to circulate in a particular way. The overall result is that the skin creates less drag in the water, an extremely important energy-saving device for a swimming creature. Hammerheads and some other kinds of sharks can swim up to 75 km/h with the help of these denticles.

The shark's denticles are attached to tiny subskin muscles. Sharks may be using these muscles to move the denticles in patterns that optimize drag reduction according to water pressure, turbulence, and other conditions. A similar idea is now being investigated on aircraft. It consists of micro-electromechanical systems consisting of an array of sensors for detecting air drag, a set of magnetically controlled microactuators (millimeter-long silicon membranes that resemble gnat wings) for deflecting surface air eddies, and circuitry that analyzes the sensor input and sends control signals to the actuators. An alternate technique is pulse blowing or suction through millions of laser-drilled holes at frequencies tailored to unstable fluctuations in the location of boundary-layer transition. Interaction of the secondary flow with the primary airflow

stabilizes the boundary layer and maintains laminar flow. Shock control with passive porosity or thermal boundary layer control may also be used.

The next big stride in aerodynamic drag reduction may come from one of these areas or it may emerge from research in other fields, such as, electromagnetics or magneto-hydrodynamics (MHD). In the very long term it has for instance been proposed to use beamed micro wave energy to alter the properties of the atmosphere in front of the vehicle in order to decrease the drag.

As is seen from Eq. (11.8) the L/D ratio depends both on the friction coefficient and on the shape of the aircraft. The shape of aircraft has remained more or less the same since the DC3. This may now be about to change. The body of the conventional aircraft makes for a lot of drag but very little lift. It would therefore be a good idea to abolish the body and put the passengers in the wings. This is a so called "**Flying Wing**" or "**Blended Body**" aircraft.

Of course, each of the wings could continue on their own. All that is required is that the sweep angle is maintained. A good rule for all design is that the most beautiful shape is also the most efficient one. This is probably something that is built into our brains. The ellipse is supposed to be one of the most beautiful shapes. It is no surprise, therefore, that a narrow elliptic flying wing has the highest lift-to-drag ratio both at subsonic and supersonic speeds. This leads us to aircraft shapes reminiscent of the famous "Flying Saucers" though they would not be round but elongated.
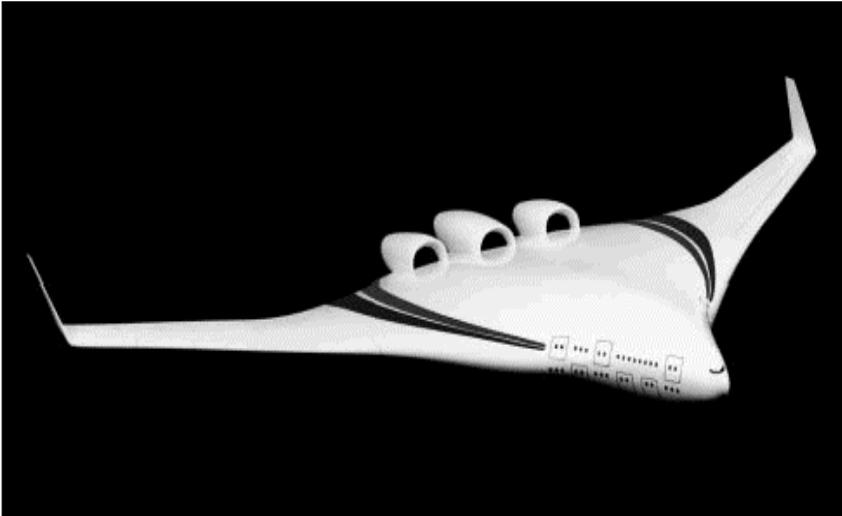
Fig. 11.10 The blended body aircraft

The search for higher lift to drag ratios obviously leads to strange and unorthodox configurations. Many such configurations may be ruled out by the adverse effects of their geometry on the weight ratios and the passenger comfort. It is invariably true that the requirements of stability and control, structure, and flight operation all contribute to reducing the design lift-to-drag ratio considerably below those exotic values which can be predicted from unrestricted aerodynamic theory. Nontheless, the future will see aircraft much different from those of today.

An example of such an aircraft is shown in Figure 11.10. This blended body flying wing is widely regarded as the most promising new configuration for an environmentally friendly airliner. It has been used in bombers such as the AVRO Vulcan, the B-2 and the B-49. The reason why this type of aircraft has not been used commercially is its aerodynamic instability. This may be solved with modern control technology.

In Eq. (11.8), the shape of the aircraft is represented by the wetted aspect ratio $\dfrac{b^2}{S}\dfrac{S}{S_{wet}}$.

For a triangular blended body with span b and chord c, the wetted aspect ratio becomes b/c provided that the body is so thin that S_{wet}/S is close to 2. For the Vulcan, it was 2.8. If the span is twice the chord, the wetted aspect ratio becomes about 2 while for large conventional transport aircraft, it is about 1.2. With the same friction coefficient, a blended body could therefore have a maximum L/D of 25-30 compared with 17-18 for a conventional aircraft.

Even higher wetted aspect ratios could be achieved with the elliptical shape for which the aspect ratio is 2b/πc. For an elongated fully laminar elliptic shape with the span five times the chord, the maximum L/D could be as high as 100. Adopting this as a maximum, a logistic diagram for the development of L/D can be constructed from historical data, see Figure 11.11. The limit of L/D=19 has been assumed for the present conventional aircraft with turbulent flow and the future development of laminar unconventional aircraft is assumed to follow the same pace.

Max L/D Turbulent/Conventional

Max L/D Laminar/Unconventional
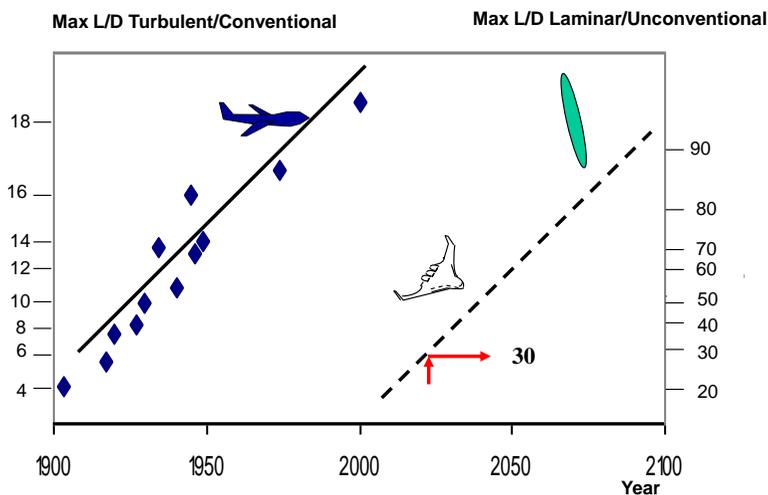
Fig. 11.11 Predicted L/D

Now assume that we want to design an aircraft and an engine for the 2020s. Such an aircraft would have a L/D ratio of 30 compared to 19 for the A380. This can be used to find the thrust of the engine.

Commercial engines are usually designed for lowest fuel consumption at end of climb as the aircraft is still rising to cruise altitude, see Figure 11.12. If the aircraft is climbing at an angle α, the lift at end of climb has to be:

$$L = gm_{0c} \cos \alpha \qquad\qquad (11.11)$$

where the total weight of the aircraft at end of climb and beginning of cruise is given by Eq. (11.3).
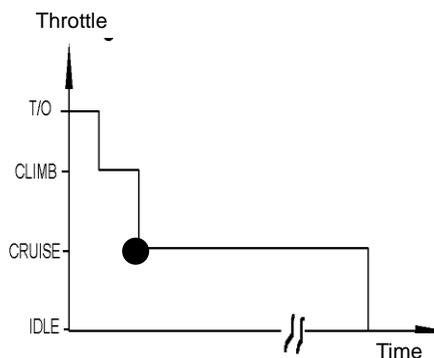
Fig. 11.12 The engine is designed for beginning of cruise

The thrust needed to balance the drag and the component of the weight in the direction of travel is:

$$F = D + gm_{0c} \sin \alpha \qquad\qquad (11.12)$$

Since α is small, the thrust-to-weight ratio is:

$$\frac{F}{gm_{0c}} = \frac{D}{L} + \frac{V_{c\lim b}}{V} \qquad (11.13)$$

There are operational advantages if the aircraft can climb to its cruising altitude as fast as possible. The **minimum rate of climb** in cruise for safety reasons is usually given at 100 m per minute, which corresponds to about 1.5 m/s at cruise altitude. The engine has to be dimensioned so that it can provide this rate of climb as the aircraft enters its cruise altitude.

Of course, the engine must also provide sufficient take-off thrust. To keep take-off distance down, the thrust-to-weight ratio of the aircraft should be at least 0.25.

A summary of the calculations to find the engine cruise thrust for an aircraft with 2020's technology level is given in Appendix 11, From Figures 11.6 and 11.11, the expected 2020 engine efficiency is estimated to 50 % and the max L/D to 30 compared to todays values 40% and L/D=19. The circumference of the earth is about 40000 km and it is expected that the aircraft would be able to reach any point on earth so the range should be 20000 km. The cruise speed is Mach 0.85 at 10 km where the ambient temperature is 223 K. It is assumed that the aircraft will carry 600 passengers. The specific strength of the materials could be expected to increase from 12 to 14 as shown in Figure 11.3. The empty weight would then be 240 tons and the engine thrust with four engines about 50 kN.

Ex 11.1

The fuel fraction would be somewhat lower for a supersonic aircraft because of a heavier structure. Compare the range if the useful fuel fraction is 0.4 for a Mach 0.85 aircraft and 0.35 for a Mach 2 aircraft.

Appendix 11
Civil aircraft

Number of passengers N	600
Number of engines n	4
Engine efficiency η (Figure 10.6)	0,5
Maximum L/D (Figure 10.11)	30
Strength factor of material $\sigma/\sqrt{\rho}$ (Figure 10.3)	14
Heat content of fuel h J/kg	4,30E+07
Range R m	2,00E+07
Reserve fuel factor f_{res}	0,1
Climb rate V_c m/s	1,5
Cruise Mach number M	0,85
Cruise ambient temperature T K	223 K
Empty weight (Figure 10.2 and	240 tons

Eq.**Fel! Hittar inte referenskälla.**)	
Lift-to-Drag ratio: $\dfrac{L}{D} = \dfrac{2\sqrt{2}}{3}\left(\dfrac{L}{D}\right)_{max}$	28,3
Cruise fuel factor: $f_{cr} = \dfrac{m_{fcr}}{m_{0cr}} = 1 - \exp(-\dfrac{gR}{h\eta L/D})$	0.276
Payload weight: $m_{pl} = 110N$	66000 kg
Weight at end of climb: $m_{0c} = \dfrac{m_e + m_{pl}}{1 - f_{cr} - f_{res}}$	490000 kg
Speed of sound: $a = \sqrt{1.4 * 287 * T}$	299 m/s
Flight velocity V=Ma	254 m/s
Engine cruise thrust : $F_c = gm_{0c}(\dfrac{D}{L} + \dfrac{V_{climb}}{V})/n$	49.6 kN

12. THE THERMODYNAMIC DESIGN OF A CIVIL JET ENGINE

The future aircraft will require an engine with efficiency close to the limit for the gas turbine cycle. The first step in the design of such an Advanced Civil Engine for the 2020's is thermodynamic calculations to find out if the required efficiency can be reached. It will be seen that if the engine is optimized for a Turbine Inlet Temperature (TIT) in line with the technological tendencies, its Overall Pressure Ratio (OPR) will be nearly twice as high as today. The very high Bypass Ratio (BPR) would require heavy and complicated geared fans to keep down the tip speed and noise levels. The thermodynamic calculations will also give the temperatures and pressures in the different components to be used in mechanical design.

The basic components of the engine are the inlet, the fan powered by the low pressure turbine, maybe through a gear box, the low pressure compressor or booster powered by the low pressure turbine, the high pressure compressor powered by the high pressure turbine, the combustor, the low pressure and high pressure turbines and the nozzle. It is customary to designate the states in the different sections of the engine with numbers. In Figure 12.1, the internationally accepted numbering is used.

13

0   **1**   **2**   **21**   **23**   **3** **4** **45**   **5**   **9**
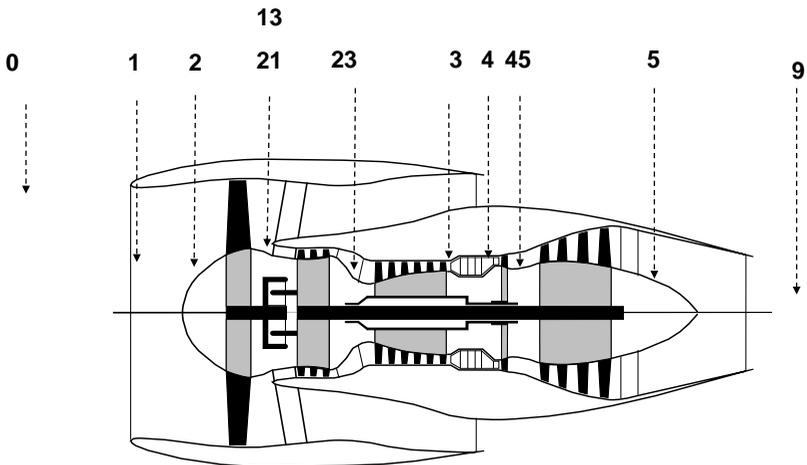
Fig. 12.1 Section numbering of a bypass engine

Note the gear box to keep down the fan tip speed and the booster or Low Pressure Compressor between sections 21 and 23. There are practical difficulties in using compressors with pressure ratios higher than about 20 on one shaft. The reason is the large difference in conditions between the inlet and outlet especially at parts load. The number of stages in the high pressure compressor is therefore limited and high pressure two-shaft engines usually employ some booster stages powered by the LP-turbine.

Before, we have restricted ourselves to ideal cycles without losses. We are now going to give the equations for a real cycle. The cycle

is still basically a Brayton cycle but the different components are no longer adiabatic so the loss of entropy must be taken into account in the individual components.

The inlet

Starting the calculations from the front of the engine, the inlet, or air intake, should provide the amount of air flow into the engine with minimum aerodynamic loss, turbulence, and flow distortion. High efficiency must be maintained for different engine-operating conditions, different aircraft speeds and altitudes, and for a wide spectrum of angles of attack.

As we have already seen, the relative stagnation temperature at the entrance to the inlet is:

$$T_{t0}/T_0 = \tau_0 = 1 + \frac{\gamma_c - 1}{2}M^2 \qquad (12.1)$$

And the corresponding stagnation pressure is:

$$\frac{p_{t0}}{p_0} = \pi_0 = \tau_0^{\gamma_c/(\gamma_c-1)} \qquad (12.2)$$

Since the flow through the inlet is very rapid, the heat losses in it can be neglected and the total temperature at the entrance to the fan is:

$$T_{t2} = T_{t0} = T_0\tau_0 \qquad (12.3)$$
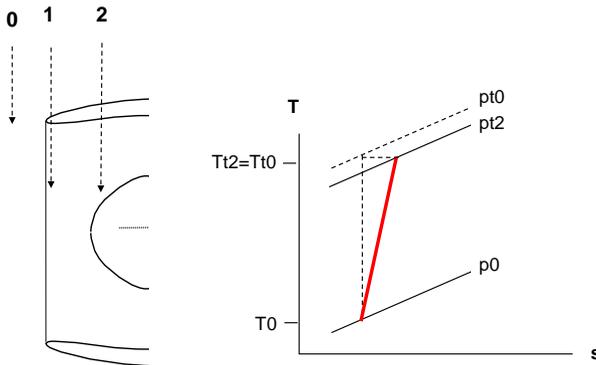
Fig. 12.2 The inlet has a small pressure loss

Inlet pressure losses arise because of wall friction, shock waves and separated flow. These are generally taken into account by using an inlet pressure coefficient. For high speed engines, the pressure losses in the inlet may be substantial and the inlet determines to a great extent the performance of such engines. For **subsonic** inlets, the losses are generally very small so that the pressure ratio over the inlet is $p_{t2}/p_{t0} = 0.97$.

Fans and compressors
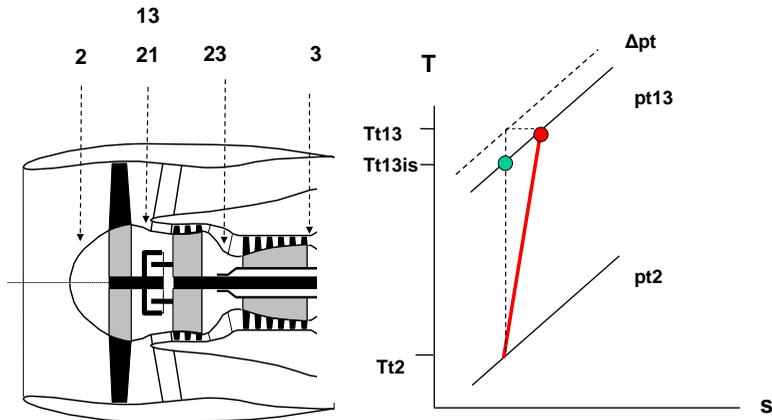
Fig. 12.3 Heat and pressure losses in fans and compressors

Fans and compressors are designed to give a certain pressure ratio. Thus, the pressure at the outlet from the fan, that is at the inlet to the bypass duct and the first stage of the Low Pressure Compressor is for an assumed fan pressure ratio:

$$p_{t13} = \pi_f \, p_{t2} \qquad (12.4)$$

The flow velocity in fans and compressors are lower than in the inlet so heat has time to leak away. Therefore they are only approximately adiabatic. Thus the temperature rise to achieve a certain pressure rise need to be somewhat higher than the ideal. This is taken into account by introducing efficiencies. Two types

of efficiencies are used. The **isentropic efficiency** is sometimes called the overall or adiabatic efficiency and is defined as the ideal or isentropic temperature rise divided by the real temperature rise, that is:

$$\eta_{is} = \frac{T_{t13is} - T_{t2}}{T_{t13} - T_{t2}} \qquad (12.5)$$

Where:

$$\frac{T_{t13is}}{T_{t2}} = \left(\frac{p_{t13}}{p_{t2}} \right)^{\frac{\gamma-1}{\gamma}} \qquad (12.6)$$

In dealing with multistage compressors it is useful to introduce another type of efficiency, the so called **polytropic** or small stage **efficiency** with which:

$$\tau_f = \frac{T_{t13}}{T_{t2}} = \left(\frac{T_{t13is}}{T_{t2}} \right)^{\frac{1}{\eta}} = \left(\frac{p_{t13}}{p_{t2}} \right)^{\frac{\gamma-1}{\eta\gamma}} = \pi_f^{\frac{\gamma-1}{\eta\gamma}} \qquad (12.7)$$

The polytropic efficiencies are more convenient algebraically in many instances. Thus for multistage machines it can be shown that the isentropic efficiency of each stage must be higher than that over the whole, while if all the stages had equal polytropic efficiency the efficiency of the overall machine would equal that of each stage. For an infinitely small stage the isentropic and polytropic efficiencies will be the same. The relation between

isentropic and polytropic efficiencies at different pressure ratios is shown in Figure 12.4 below:
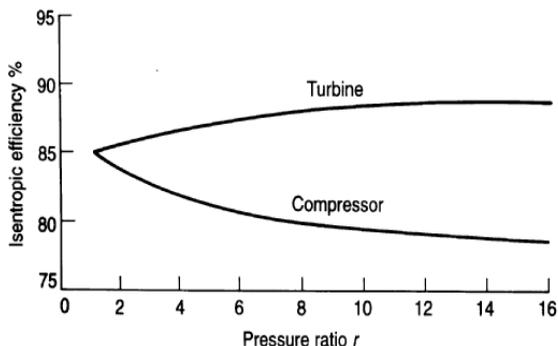
Fig. 12.4 **Isentropic efficiency for compressors and turbines at constant polytropic efficiency 0.85**

The higher the pressure ratio, the larger is the difference between the two types of efficiency. Using polytropic efficiency, the temperature ratio for the fan is:

$$\tau_f = \pi_f^{(\gamma_c-1)/\gamma_c\eta_f} \tag{12.8}$$

and the temperature after the fan is:

$$T_{t13} = T_{t2}\tau_f \tag{12.9}$$

With an overall pressure ratio (OPR), the pressure ratio over the booster is:

$$\pi_b = \frac{OPR}{\pi_c \pi_f} \tag{12.10}$$

and the pressure at inlet to the HP compressor is:

$$p_{t23} = \pi_b p_{t13} \tag{12.11}$$

The temperature ratio of the booster is :

$$\tau_b = \pi_b^{(\gamma_c - 1)/\gamma_c \eta_b} \tag{12.12}$$

and the temperature at inlet to the HP compressor:

$$T_{t23} = T_{t13}\tau_b \tag{12.13}$$

The pressure at the compressor outlet is:

$$p_{t3} = \pi_c p_{t23} \tag{12.14}$$

The corresponding temperature ratio is:

$$\tau_c = \pi_c^{(\gamma_c - 1)/\gamma_c \eta_c} \tag{12.15}$$

and the compressor outlet temperature:

$$T_{t3} = T_{t23}\tau_c \tag{12.16}$$
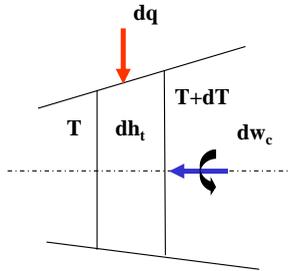
Fig. 12.5 Control volume of the compressor

Suppose that we are studying a control volume of the compressor as in Figure 12.5 to which is added heat and technical work "w_c". Then according to the first law of thermodynamics with mechanical work added to the system $dq + dw_c = dh_t$, where "dq" is the quantity of heat energy entering the system through its walls. The flow through the compressor is so rapid that there is very little exchange of heat with the surroundings. This means that the compressor is adiabatic with $dq=0$ so that $dw_c = dh_t$, where as defined in Chapter 7, the total enthalpy is $dh_t = C_p \, dT_t$.

The power that must be supplied to a compressor is then given by:

$$\dot{W}_c = \dot{m}_c \Delta h_t = \dot{m}_c C_p (T_{t3} - T_{t23}) = \dot{m}_c C_p T_{t23} (\pi_c^{\frac{\gamma-1}{\gamma\eta}} - 1) \tag{12.17}$$

This power must be supplied by the turbine. Note that for the same compression ratio and compressor efficiency, the lower the inlet temperature, the lower is the compressor work. Therefore a jet engine operating at high altitude or cold ambient temperature requires less compressor work when everything else remains the same.

Cooling flows

A part ε of the compressor flow is tapped off for cooling of the turbine parts of the engine. This air is transferred around the combustor and introduced into the turbine flow after having passed through cooling passages in the turbine. Since it does not participate in the combustion process it constitutes a loss in the cycle. The earlier the extraction point in the compressor, the lower the temperature and the lower the amount of cooling air required. However, the pressure difference between the point of extraction and reintroduction must be sufficient to get the air through the rather complicated cooling passages. The cooling air is therefore usually tapped off from the last stage of the high pressure compressor.

An accurate prediction of the amount of cooling flow required is complex. For turbine disk cooling and rim sealing approximately 1 % per stage is required in HP turbines and 0.5 % in LP turbines. In complex air systems an additional 2 % may leak back to the main flow. About 5 % may also be required to balance the bearings etc.

The amount of cooling air required for cooling the turbine blades and vanes could be estimated from a balance between the heat

flows to and from the wall material. For preliminary design purposes, the following equation could be used to find the cooling air flow:

$$\varepsilon = 0.05 + 0.05\frac{T_{t4} - T_m}{T_m - T_{t3}} \qquad (12.18)$$

The cooling flow should be designed for maximum thermal load, which is at take-off.

The combustor
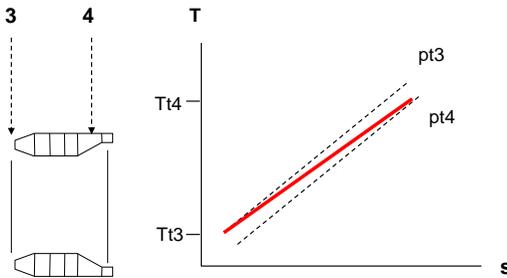
Fig. 12.6 Combustion takes place at nearly constant pressure

The combustion takes place at nearly constant pressure, see Figure 12.6, because the gas is free to expand as heat is released. There is a small pressure loss so that $p_{t4}/p_{t3} = 0.98$.

The relative mass flow rate of fuel $f = \dot{m}_f / \dot{m}$ needed to reach an outlet temperature T_{t4} for an inlet temperature of T_{t3} is for a fuel with a heating value "h" at 298K if a part ε of the compressor flow is tapped off for cooling:

$$f \eta_b h = (1 + f - \varepsilon) C_{pt}(T_{t4} - 298) - C_{pc}(1 - \varepsilon)(T_{t3} - 298) \quad (12.19)$$

The combustion efficiency is close to 100% at most engine conditions. However, if the pressure in the combustion chamber falls below about 100 kPa, the efficiency decreases markedly. This does not occur unless at very low power at high altitude.

A complication is that the specific heat will increase substantially when the temperature gets close to the so called stoichiometric temperature. Then, the amount of fuel needed to produce the rise in temperature will be substantially higher.

Heating values for different fuels are:

Kerosene   43 MJ/kg
Methane   50 MJ/kg
Hydrogen   120 MJ/kg

Hydrogen has the highest heating value but its density is so low that the fuel volume will be higher than for kerosene. Also, as was said in Chapter 10, the environmental advantages of the cryogenic fuels methane and hydrogen is dubious due to the larger emissions of frozen water crystals. It is therefore probable that kerosene, maybe of synthetic type, will continue to be used beyond the 2020 period.

The turbines
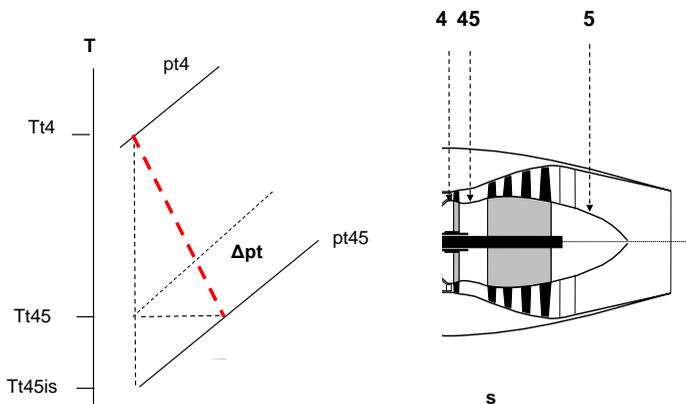
Fig. 12.7 Pressure and temperature losses in the turbine

After the combustion chamber, the hot gas expands through the turbine, see Figure 12.7. If the cooling air is mixed in after the HP turbine, the power balance with the HP compressor and HP turbine gives:

$$\dot{m}C_{pc}\left(T_{t3}-T_{t23}\right)=\dot{m}\left(1+f-\varepsilon\right)C_{pt}\left(T_{t4}-T_{t45}\right) \quad (12.20)$$

So that:

$$T_{t45}=T_{t4}-\frac{1}{\left(1+f-\varepsilon\right)}\frac{C_{pc}}{C_{pt}}\left(T_{t3}-T_{t23}\right) \quad (12.21)$$

No work is done in the stator so the stagnation temperature stays constant but there is a pressure loss due to friction in the cascade. There is then an expansion with additional losses to the pressure p_{t45}. Because the expansion is not isentropic there is a loss of stagnation temperature in the rotor. There is also a loss of stagnation temperature due to the pressure loss in the stator compared to an isentropic expansion from the original state.

The **isentropic efficiency** of the high pressure turbine is:

$$\eta_t = \frac{T_{t4} - T_{t45}}{T_{t4} - T_{t45is}} \tag{12.22}$$

where:

$$\frac{T_{t45is}}{T_{t4}} = \left(\frac{p_{t45}}{p_{t4}} \right)^{\frac{\gamma-1}{\gamma}} \tag{12.23}$$

And if **polytropic efficiencies** are used:

$$\tau_t = \frac{T_{t45}}{T_{t4}} = \left(\frac{p_{t45}}{p_{t4}} \right)^{\eta \frac{\gamma-1}{\gamma}} = \pi_t^{\eta \frac{\gamma-1}{\gamma}} \tag{12.24}$$

Note the position of the polytropic efficiency for the turbine as compared to that for the compressor in Eq. (12.7).

With a polytropic efficiency, the HP turbine pressure ratio is:

$$\pi_{th} = \frac{p_{t45}}{p_{t4}} = \left(\frac{T_{t45}}{T_{t4}}\right)^{\gamma_t/(\gamma_t-1)\eta_t} \qquad (12.25)$$

If a pressure loss in the combustor is included then the pressure after the combustor is:

$$p_{t4} = \pi_{bc}\,p_{t3} \qquad (12.26)$$

The pressure after the HP turbine:

$$p_{t45} = \pi_{th}\,p_{t4} \qquad (12.27)$$

The cooling air is assumed to be mixed in at constant pressure before the LP turbine, which gives the temperature after the turbine as:

$$T'_{t45} = \frac{\varepsilon}{1+f}\frac{C_{pc}}{C_{pt}}T_{t3} + \frac{1+f-\varepsilon}{1+f}T_{t45} \qquad (12.28)$$

To make the calculations a bit more complicated, part of the air could be mixed in after the LP turbine.

Now for an assumed bypass ratio and fan pressure ratio, a power balance over the low pressure shaft gives the temperature after the LP turbine as:

$$T_{t5} = T'_{t45} - \frac{1+\alpha}{1+f} \frac{C_{pc}}{C_{pt}} (T_{t13} - T_{t2}) - \frac{1}{1+f} \frac{C_{pc}}{C_{pt}} (T_{t23} - T_{t13}) \quad (12.29)$$

The pressure ratio over the LP turbine is:

$$\pi_{lt} = \left(\frac{T_{t5}}{T'_{t45}} \right)^{\gamma_t/(\gamma_t-1)\eta_t} \quad (12.30)$$

and the pressure after the LP turbine, that is before the core nozzle, is:

$$p_{t5} = \pi_{lt} p_{t45} \quad (12.31)$$

Matching of the exhaust streams

The pressure ratio over a jet engine nozzle will almost always be higher than the critical pressure so the nozzle is choked and the Mach number is unity at the throat. For pressure ratios over the nozzle up to about 5, experiments show that the convergent nozzle gives as much thrust as a fully expanded convergent-divergent nozzle because of the higher friction losses in the latter. This means that for civil engines with pressure ratios below 5, a simple convergent nozzle can be used. For the calculations, however, full expansion is a good and simple approximation for the jet speed and thrust.
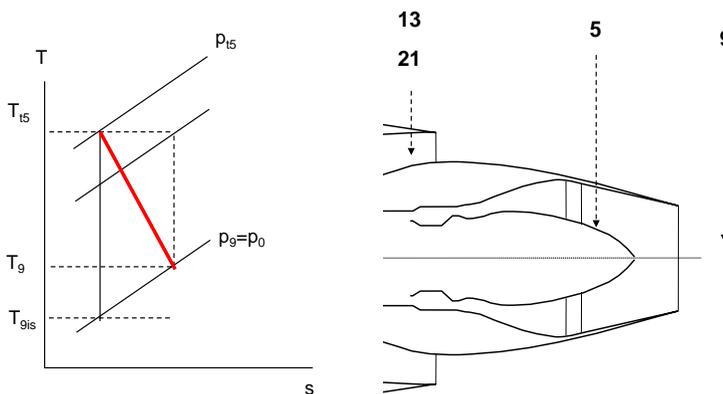
Fig. 12.8 Expansion with losses in the nozzle

The core jet speed for the assumed bypass ratio is with an ideally expanded nozzle:

$$V_{jc} = \sqrt{2\eta_j C_{pt} T_{t5}\left[1-\left(p_0/p_{t5}\right)^{(\gamma_t-1)/\gamma_t}\right]} \qquad (12.32)$$

The losses in the nozzle, see Figure 12.8, are taken into account by the nozzle efficiency η_j.

On the other hand, the bypass jet speed is:

$$V_{jb} = \sqrt{2\eta_j C_{pc} T_{t13}\left[1-\left(p_0/p_{t13}\right)^{(\gamma_c-1)/\gamma_c}\right]} \qquad (12.33)$$

With unmixed engines, in order to close the cycle calculations we need a matching condition between the exhaust streams. Such a matching condition may be obtained if we realize that the power of the core is to be used to provide the propulsive power of the core stream and to power the LP turbine, which through the fan provides the propulsive power of the bypass stream. As shown before, maximizing the core work leads to the following condition for the matching of the core and bypass streams:

$$V_{jb} = V_{jc}\eta_f\eta_{lt} \qquad\qquad (9.11)$$

where it can be shown that the isentropic efficiency in a turbine expansion is:

$$\eta_{lt} = \frac{1 - \pi_{lt}^{(\gamma_t - 1)\eta_t/\gamma_t}}{1 - \pi_{lt}^{(\gamma_t - 1)/\gamma_t}} \qquad\qquad (12.34)$$

While for the compression in the fan it is:

$$\eta_f = \frac{\pi_f^{(\gamma_c - 1)/\gamma_c} - 1}{\pi_f^{(\gamma_c - 1)/\gamma_c\eta_c} - 1} \qquad\qquad (12.35)$$

If the jet speeds are too far away from the matching criterion giving minimum core work, an **iteration is made in the bypass ratio** until the criterion is satisfied.

The uninstalled specific thrust is now with the bypass ratio α:

$$F_{s0} = \frac{F_0}{\dot{m}(1+\alpha)} = \frac{1+f}{1+\alpha}V_{jc} + \frac{\alpha}{1+\alpha}V_{jb} - V \qquad (12.36)$$

With a given gas generator, an increase in bypass ratio will result in a larger fan diameter and a larger wetted area of the engine nacelle. This gives rise to an installation drag that should be subtracted in order to obtain the real thrust the engine produces. This installation effect is very complicated to estimate. For present under the wing installations it seems reasonable to assume that the installed thrust is (Cumpsty p.72):

$$\frac{F_{si}}{F_s} = \frac{1}{1 + \dfrac{3 + \alpha}{100}} \tag{12.37}$$

The total mass flow can now be obtained from the required thrust and the installed specific thrust as:

$$\dot{m}_{tot} = \dot{m}(1 + \alpha) = F_{req} / F_{si} \tag{12.38}$$

The calculation scheme described above is given in the Appendix 12.

Optimizing the cycle

It follows from what we have said above that four cycle parameters determine the performance of an engine:
Bypass ratio (BPR)
Fan pressure ratio (FPR)
Overall pressure ratio (OPR)
Turbine inlet temperature (TIT)

A typical relationship between those parameters for an uninstalled engine (in a test rig but not in the aircraft) is shown in Fig. 11.9.
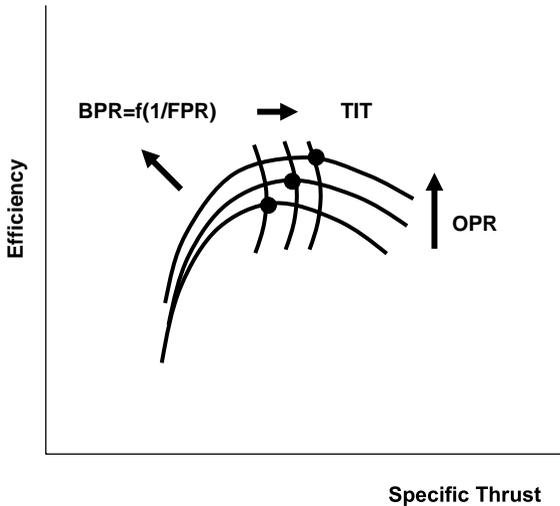
Fig. 12.9 Typical relationships between the main parameters

Two of the four cycle parameters, Bypass Ratio (BPR) and Fan Pressure Ratio (FPR), are coupled by a power balance over the low pressure shaft. Once one of them is chosen the other one is obtained. Generally speaking, the BPR increases with decreasing FPR because the LP turbine power can either be used to obtain high pressure or a high mass flow.

Higher bypass ratios will shift the whole map to the upper left increasing the efficiency but unfortunately also decreasing the

specific thrust. For civil engines, where low fuel consumption is more important than high specific thrust it seems that one should choose a high BPR which leads to a low FPR.

As is seen in Figure 12.9, a higher OPR will in general increase efficiency and decrease the fuel consumption up to a point where the compressor outlet air becomes too hot for efficient cooling of the turbine. It is therefore also necessary to find this optimum value of the OPR.

Looking at Figure 12.9, it is seen that a Turbine Inlet Temperature (TIT) value can be found that gives maximum efficiency for every Overall Pressure Ratio (OPR). This optimum TIT increases with increasing OPR. However, the influence of the TIT on the efficiency is relatively weak for a given OPR. There is therefore a tendency to choose the highest possible TITs because that will lead to higher specific thrust and therefore lower engine dimensions without losing too much in efficiency.

In the more than 50 years since the jet engine was first developed, materials technology has contributed more to the steady and dramatic progress in performance, durability, maintainability, and cost than any other technology. During various periods, as much as 50 percent of the improvements made in performance resulted from advances in materials technology, particularly improvements in high-temperature nickel-based superalloys for the hot section and high strength-to-weight titanium alloys for the cold section (less than 875 K). The original Whittle and Von Ohain engines were limited to turbine inlet temperatures of about 1000°K. Today's commercial engines operate at more than 1800°K. Although turbine airfoil cooling techniques have certainly contributed to this truly noteworthy improvement, most of the

increased capability continues to come from materials technology. An increase in turbine rotor inlet temperature is the single most powerful factor in maintaining the steady increase in specific core power generated.

The maximum turbine inlet gas and metal temperatures has increased very much since the early jet engines. Figure 12.10 below gives the temperatures that would typically be employed at take-off. The goal is to reach stoichometric turbine inlet temperatures of 2300 K. Demonstrator engines have been run on 2100 K. However, beyond that temperature the NOX pollutants will increase very rapidly. It has been assumed here that through low emission combustors a maximum temperature of 2300 K is the limit. This has been used to construct the logistic diagram in Figure 12.10.

An engine for the New Civil Aircraft of the 2020's should then have a turbine inlet temperature at take-off of 2000K. As will be shown in Chapter 17, the pressure ratios are maintained constant at different flight conditions if an engine is operating at its design point. It will then be shown that the ratio T_{t4}/T_{t2} is a constant. The ratio of inlet temperatures at take-off on a standard day to that at Mach 0.85 at 10 km is 1.13. If we were to operate at the design point, the turbine inlet temperature at cruise conditions should therefore be 1770 for a max temperature of 2000 K. Assuming that we need extra margin to avoid blade damage during sustained climb, the engine should be **designed for 1800 K**. A rule of thumb for blades limited by creep is that blade life is halved for each 10 K increase of metal temperature.
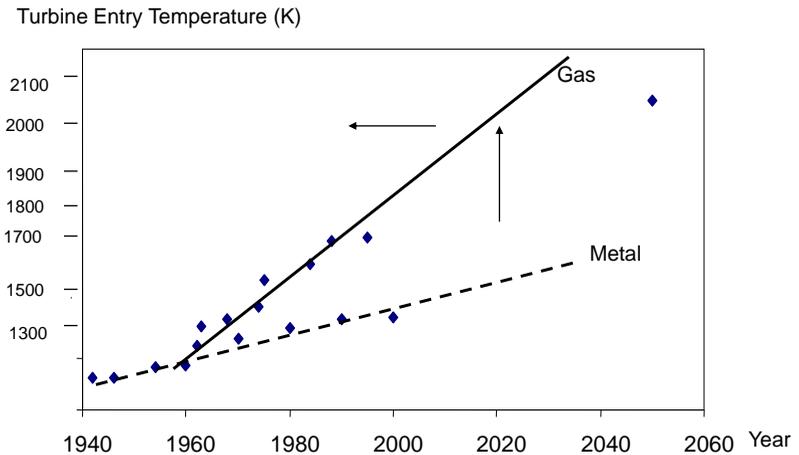
Fig. 12.10 The increase of the Turbine Entry Temperature

As is seen in Figure 12.10, there is a growing gap between the gas temperature and the metal temperature. This has been closed by advanced cooling systems. Cooling air is forced out of many small holes in the blade. This air remains close to the blade, preventing it from melting. Advanced high-temperature metals technology plus advanced turbine cooling and advanced thermal barrier coatings (TBC) on the turbine blades and vanes are critical for increased turbine temperatures until uncooled metal or non metal materials become feasible and practical.

Currently 10 to 20 percent of core flow is used to cool the turbine metal parts. This represents a substantial penalty when the air that

is compressed using turbine energy cannot be used in the cycle to produce thrust or shaft power.

The Advanced Civil Engine (ACE)

We can now make a preliminary thermodynamic design of an Advanced Civil Engine for the 2020's with the aim to reach at least 50 % total efficiency using the calculation scheme outlined in the Appendix at the end of this Chapter.

Assume that we want to design an engine for entering cruise at 10 km altitude with Mach 0.85. The polytropic efficiency of the fan, compressors and turbines are assumed to be 92 %. This is a few percent higher than present best technology especially as regards the turbines.

For simplicity we will assume that $\gamma_c = 1.4$ corresponding to a specific heat of 1005 J/kgK in all processes before the combustor and $\gamma_t = 1.3$ corresponding to a specific heat of 1244 J/kgK after the combustor. In reality γ would vary with the temperature in the different parts of the engine. The gas constant is R=287 J/kgK. The cooling flow is to be designed for take-off. We assume for the present that the LP turbine is uncooled. The SLS air temperature is $T_a = 288$ K.

As was said before, there is a direct coupling between the FPR and the BPR. If the calculations are carried out for different fan pressure ratios the results below, Figure 12.11, are obtained.
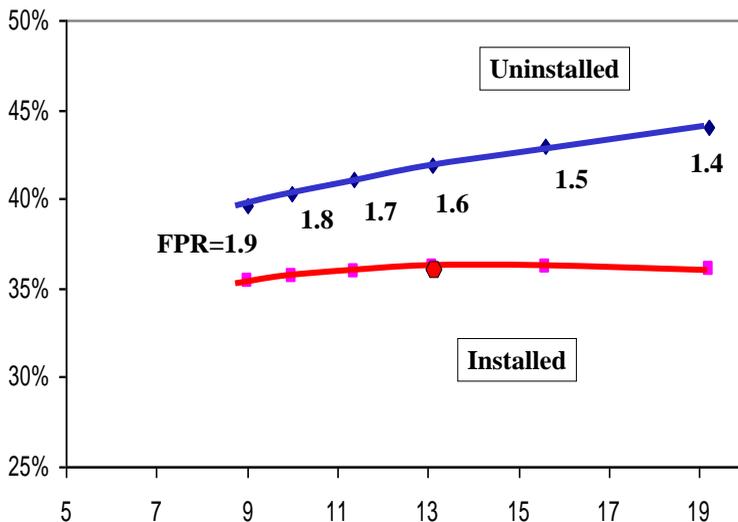
Fig. 12.11 The efficiency has a maximum for a certain Bypass Ratio (BPR)

It is mandatory to use a single stage fan for weight reasons. This limits the maximum value of the FPR to about 1.6 to 1.7. In the future it could increase to 1.8 to 1.9. However, because the influence of the FPR on the efficiency is not so significant, there is some freedom to choose it within rather wide limits. This leads to different philosophies. GE tends to design at higher pressure ratios to avoid the installation losses, while PWA seems to favor lower pressure ratios.

If the fan pressure ratio becomes too low along with a lower fan tip speed, a disparity is set up between the optimum speeds of the fan and the low pressure turbine that drives the fan because the LP

turbine spins faster than the fan. Solutions include adding more turbine stages (but that increases the length and weight of the engine) or adding a **gearbox** between the two components (but that is a heavy and expensive item).

A second problem is related to the thermodynamic cycle of the engine. As the design fan pressure ratio is reduced below about 1.4, a fan operational disparity is set up between high-altitude, high-speed flight and low-altitude, low-speed flight. In other words, there is too large a swing in several key fan parameters such as speed, flow, and pressure between takeoff and cruise for a fan to accommodate. Some sort of additional variable geometry somewhere in the engine is required to fix this problem. Such fixes include a variable area bypass nozzle or variable-pitch fan blades, but there are weight and complexity issues associated with any kind of variable geometry.

Of importance, particularly for an engine intended for application on a civil aircraft, are the noise characteristics of the engine. The fan is an important source of engine noise. In modern engines, part of the fan will work at transonic speeds which will cause an increase in noise. A high pressure ratio will lead to higher rotational speeds for a given mass flow. This means that the noise level increases. One could amend this by introducing a **geared fan** and let it operate at a lower speed than the LP-shaft. This solution is pioneered by PWA. An alternative would be to use **three shafts**, as does Rolls-Royce. However, all those solutions cause increased weight and mechanical complications.

A low FPR means a high BPR. Statistically, the engine weight seems not to be influenced significantly by the bypass ratio. However, if the bypass ratio is very large, the aircraft will be affected. The wings have to be higher above the ground and their

aerodynamic performance is impaired by the engines. Also, the installed drag due to the nacelle will increase with a higher BPR.

Taking the installation drag into account, it is possible to find a BPR (that is FPR) that gives maximum efficiency and least fuel consumption, see Figure 12.11. This bypass ratio of the future engine is very high at 13:1 compared to todays engines which are below 8:1. However, as was said before, the BPR (and the FPR) does not influence the efficiency very much and can be chosen within rather wide limits.

In response to the oil crisis in the 1970s studies were made of unshrouded **propfans** i.e. turboprops with multi-bladed propellers. The aim was to enable propfan driven aircraft to reach flying speeds in the region of Mach 0.8, i.e. comparable to jet aircraft, with less fuel consumption. It appeared that the two stage counter rotating fan was the most efficient. The studies revealed also, however, that the installation of the unshrouded propfan on the wing was impractical because of the requirements to soundproof the cabin. This gave rise to the shrouded or ducted propfan, i.e. a turbofan with very high bypass ratios above 10:1. This would require geared fans to keep down tip speed and noise level. Such engines have been studied by PWA and MTU in particular. From the present calculations, it appears that propfans with very high BPR may be needed in the future.
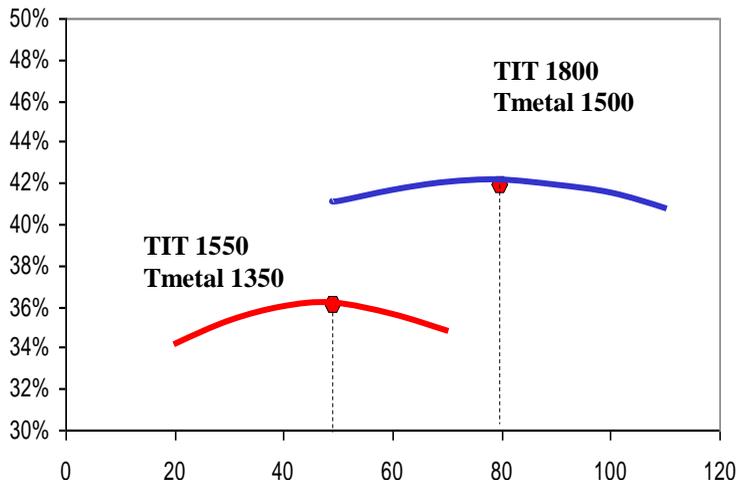
Fig. 12.12 There is an Overall Pressure Ratio (OPR) that maximizes the efficiency

It is the installed specific thrust that is used to dimension the engine. However, to be able to compare different engines, the uninstalled thrust efficiency, which is independent of the specific aircraft installation, is commonly used. The importance of OPR for the uninstalled efficiency is shown in Figure 12.12 where the 2020's engine is compared to an engine with todays technology. The OPR giving maximum efficiency is pushed to higher values by the higher permitted turbine inlet temperature in the 2020 engine. Beyond a pressure ratio of about 80, the large amount of

cooling air required, due to the increased compressor outlet temperature, leads to a decrease in total efficiency.

There is a tendency to keep OPR down because a higher pressure means more stages and a higher weight of the turbo machinery. There is also a maximum value of OPR dependent on the compressor outlet material temperature at take-off. Usually, titanium alloys are used in the compressor limiting the outlet temperature to 875 K. This leads to maximum OPR below 40 for todays most modern engines. For our future engine, assuming that the last stages in the compressor are made from titanium aluminides with a permitted temperature of 1150 K, maximum OPR up to 100 can be used without overheating the compressor. Superalloys could also be used but aluminides have the advantage of lower weight.

As is seen in Figure 12.12, the 2020 engine reaches an installed efficiency of 41.6 per cent which is about 6 per cent higher than present engines. As will be seen in the next Chapter, the higher pressures and temperatures will lead to differences in the mechanical design.

The importance of better component technologies for still higher efficieny is shown in the table below. The table shows the increase in engine efficiency for 1 % increase in component efficiencies. The compressor and turbine efficiencies are obviously the most important. Typically, the cruise efficiency with the engine in part load is 2-3 % higher than at entering cruise altitude. This means that the uninstalled cruise efficiency of the engine is around 45 % with those advanced components.

It is obvious then that to reach the goal of 50% engine efficiency in the year 2020 would require still more significant steps in component efficiencies. With ideal component efficiencies, the 1800 K and OPR 80 engine reaches a total efficiency of 53 % for a bypass ratio of 15:1, which means a cruise efficiency around 55 %.

	Effic
Datum engine (TIT=1800/OPR=80/FPR=1.6/ BPR=13.1)	41.6 %
+Fan efficiency +1 %	+0.4
+ Booster efficiency +1 %	+0.1
+Compressor efficiency +1 %	+0.5
+Combustor pressure loss −1 %	+0.1
+Turbine efficiency +1 %	+0.5
+Metal temperature +1 %	+0.1
Summary (FPR=1.6/ BPR=15)	43.3 %
Ideal engine (TIT=1800/OPR=80/FPR=1.6/BPR=20.1)	53.0 %

Ex 12.1

A jet engine has a maximum allowed turbine inlet temperature of 1700 K. What is the operating temperature at cruise conditions with M=0.85 at 11 km altitude where the temperature is 216 K if the ambient temperature at take-off is 293 K?

Ex 12.2

It must be checked that the New Civil Engine designed in Appendix 12 below can be used at all climates. What is the maximum ambient air temperature for which the engine can be used without overheating the compressor if its last stages are made from titanium aluminides that can take 1150 K?

Appendix 12
Thermodynamic design of a New Civil Engine
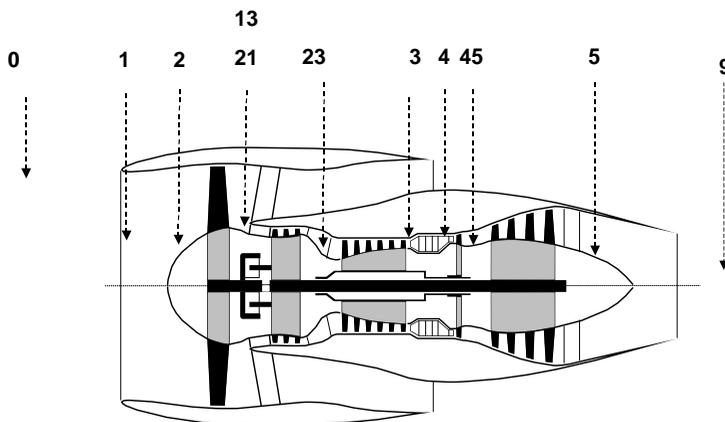
The indata to the calculation are:

Temperature Sea Level Static T_{SLS} K	288
Mach number M	0.85
Ambient temperature at 10 km T_0 K	223
D:o pressure p_0 Pa	2.64E+04
Fan polytropic efficiency η_f	0.92
LP Compressor polytropic efficiency η_{cl}	0.92
Overall Pressure Ratio OPR	80
LP compressor pressure ratio	16
Turbine Inlet Temperature T_{t4} K	1800

Turbine Inlet Temperature at take-off   K 2000
HP Turbine metal temperature T_m K 1500
Pressure recovery in combustion chamber π_b 0.97
Combustor efficiency η_b 1
Fuel heating value h J/kg 4.30E+07
HP Compressor polytropic efficiency η_{ch} 0.92
Specific heat in cold parts C_{pc} 1005
D:o hot parts C_{pt} 1244
Adiabatic constant in cold parts γ_c 1.4
Adiabatic constant in hot parts γ_t 1.3
LP and HP Turbine polytropic efficiency η_t 0.88
Nozzle efficiency η_j 0.95

Dry thrust F N   4.96E+04

Pos.	For 10 km altitude T_0=223 K and p_0 =26.4 kPa.	
0	**Assume Fan Pressure Ratio FPR**	**1.6**
1	Stagnation temperature ratio: $$T_{t0}/T_0 = \tau_0 = 1 + \frac{\gamma_c - 1}{2} M^2$$	1.145
2	Stagnation pressure: $\dfrac{p_{t0}}{p_0} = \pi_0 = \tau_0^{\gamma_c/(\gamma_c-1)}$	1.604
3	Inlet pressure recovery π_{in}	1
4	Inlet temperature ratio: $\tau_{in} = \pi_{in}^{(\gamma_c-1)/\gamma_c}$	1
5	The temperature at the inlet to the fan: $T_{t2} = \tau_{in} T_{t0}$	255 K

6	Pressure at fan inlet: $p_{t2} = \pi_{in} p_{t0}$	42.3 kPa
7	The pressure at the inlet to the bypass duct: $$p_{t13} = \pi_f p_{t2}$$	68 kPa
8	The temperature ratio for the fan: $$\tau_f = \pi_f^{(\gamma_c - 1)/\gamma_c \eta_f}$$	1.16
9	The temperature after the fan: $T_{t13} = T_{t2} \tau_f$	295 K
	Assume an overall pressure ratio of 80 and an HP compressor pressure ratio of 16.	
10	The pressure ratio over the booster: $\pi_b = \dfrac{OPR}{\pi_c \pi_f}$	3.125
11	The pressure at inlet to the HP compressor: $$p_{t23} = \pi_b p_{t13}$$	212 kPa
12	The temperature ratio of the booster: $$\tau_b = \pi_b^{(\gamma_c - 1)/\gamma_c \eta_b}$$	1.42
13	The temperature at inlet to the HP compressor is : $T_{t23} = T_{t13} \tau_b$	421 K
14	The pressure at the compressor outlet: $p_{t3} = \pi_c p_{t23}$	3390 kPa

15	The corresponding temperature ratio is: $$\tau_c = \pi_c^{(\gamma_c-1)/\gamma_c\eta_c}$$	2.36
16	The compressor outlet temperature: $T_{t3} = T_{t23}\tau_c$	995 K
17	The cooling flow: $$\varepsilon = \frac{\dot{m}_c}{\dot{m}} = 0.05 + 0.05\frac{T_{t4\max} - T_m}{T_m - T_{sls}\tau_f\tau_b\tau_c}$$	11.6 %
	The combustor efficiency is assumed to be 100 % and the heating value of the fuel is 43 MJ/kg.	
18	The fuel flow: $f = (1-\varepsilon)(C_{pt}(T_{t4}-298) - C_{pc}(1-\varepsilon)(T_{t3}-298))/(\eta_b h - C_{pt}(T_{t4}-298))$	0.025
19	Unmixed HP turbine outlet temperature: $$T_{t45} = T_{t4} - \frac{1}{(1+f-\varepsilon)}\frac{C_{pc}}{C_{pt}}(T_{t3} - T_{t23})$$	1289 K
20	HP turbine pressure ratio: $\pi_{th} = \dfrac{p_{t45}}{p_{t4}} = \left(\dfrac{T_{t45}}{T_{t4}}\right)^{\gamma_t/(\gamma_t-1)\eta_t}$	0.21
21	Pressure after the combustor: $p_{t4} = \pi_{bc}p_{t3}$	3290 kPa
22	The pressure after the HP turbine: $p_{t45} = \pi_{th}p_{t4}$	682 kPa

23	The mixing temperature after the turbine: $$T'_{t45} = \frac{\varepsilon}{1+f}\frac{C_{pc}}{C_{pt}}T_{t3} + \frac{1+f-\varepsilon}{1+f}T_{t45}$$	1234 K
24	**Assume that the bypass ratio is 13.1 for the fan pressure ratio 1.6.**	
25	Actual bypass jet speed is from: $$V_{jb} = \sqrt{2\eta_j C_{pc} T_{t13}\left[1-\left(p_0/p_{t13}\right)^{(\gamma_c-1)/\gamma_c}\right]}$$	374 m/s
26	The temperature after the LP turbine: $$T_{t5} = T'_{t45} - \frac{1+\alpha}{1+f}\frac{C_{pc}}{C_{pt}}(T_{t13}-T_{t2}) - \frac{1}{1+f}\frac{C_p}{C_p}$$	689 K
27	The pressure ratio over the LP turbine: $$\pi_{lt} = \left(\frac{T_{t5}}{T'_{t45}}\right)^{\gamma_t/(\gamma_t-1)\eta_t}$$	0.064
28	The pressure after the LP turbine: $$p_{t5} = \pi_{lt}\,p_{t45}$$	44.0 kPa
29	The core jet speed :	436

	$V_{jc} = \sqrt{2\eta_j C_{pt} T_{t5}\left[1-\left(p_0/p_{t5}\right)^{(\gamma_t-1)/\gamma_t}\right]}$	m/s
30	Isentropic efficiency in turbine: $\eta_{lt} = \dfrac{1-\pi_{lt}^{(\gamma_t-1)\eta_t/\gamma_t}}{1-\pi_{lt}^{(\gamma_t-1)/\gamma_t}}$	0.94
31	While for the compression in the fan: $\eta_f = \dfrac{\pi_f^{(\gamma_c-1)/\gamma_c}-1}{\pi_f^{(\gamma_c-1)/\gamma_c\eta_c}-1}$	0.91
32	Matching of the core and bypass streams: $V_{jb} = V_{jc}\eta_f\eta_{lt}$	374 m/s
	If different assume a new bypass ratio pos. 24	
33	Speed of sound: $a_0 = \sqrt{\gamma_c R T_0}$	299 m/s
34	Flight speed: $V = Ma_0$	254 m/s

35	The uninstalled specific thrust is: $$F_{s0} = \frac{F_0}{\dot{m}(1+\alpha)} = \frac{1+f}{1+\alpha}V_{jc} + \frac{\alpha}{1+\alpha}V_{jb} - V$$	125 m/s
36	The installed specific thrust for the bypass ratio 13.9: $$F_{\sin st} = \frac{F_{s0}}{1 + \frac{3+\alpha}{100}}$$	108 m/s
37	The total mass flow: $\dot{m}_{tot} = \dfrac{F_{req}}{F_{\sin st}}$	460 kg/s
38	The core mass flow is: $\dot{m} = \dfrac{\dot{m}_{tot}}{1+\alpha}$	32.6 kg/s
39	The fuel consumption: $\dot{m}_f = f\dot{m}$	0.82 kg/s
40	The uninstalled effciency is: $\eta_0 = \dfrac{F_s \dot{m}_{tot} V}{\dot{m}_f h}$	41.6 %
41	The installed efficiency of the engine is: $\eta = \dfrac{F_{req} V}{\dot{m}_f h}$	35.8 %

13. TURBO MACHINERY DESIGN FOR THE CIVIL JET ENGINE

After the pressures and temperatures at the interfaces of the different components have been defined, a detailed design of the turbo machinery itself can be made. The blade angles and flow areas are calculated so that certain empirical factors remain within prescribed values. The resulting design of the Advanced Civil Engine for the 2020's is characterized by small compressor blade dimensions and a high number of turbine stages due to the high overall pressure and bypass ratios.

The turbo machinery of a jet engine consists of the compressors and turbines as shown in Figure 13.1 below. The combustor that feeds the hot gas to the turbine is also a part of it. The inlet and nozzle are relatively simple for a civilian engine. They will be treated in more detail in connection with military engines where they are of central importance.

The cycle analysis has shown that the components in the turbo machinery of a jet engine are exposed to high temperatures. The temperatures in Figure 13.1 are those calculated in Appendix 12.

Materials typically used in the different components are also indicated. It is obvious that to reach beyond present material temperatures, very advanced materials will be needed combined with complex cooling systems. Nickel alloys are used to construct the turbine blades and the nozzle guide vanes because these materials demonstrate good properties at high temperatures.
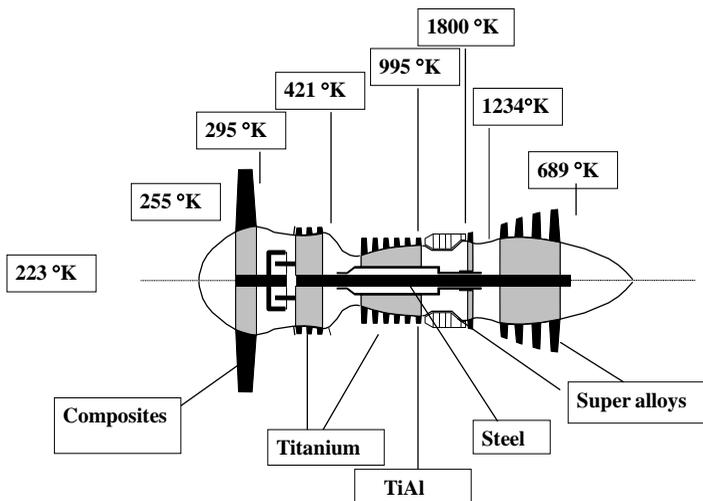
Fig. 13.1 The turbomachinery of the new civil engine

The temperature endurances of some other advanced materials are given below:

- Organic matrix composites   600 K
- Aluminum composites   700
- Titanium aluminides composites   1200
- Nickel aluminides composites   1400
- Niobium based composites   1700
- Ceramic and Carbon-Carbon   1500-1900

Organic matrix composites reinforced with carbon fibers may evolve as the material of choice for lower temperatures. Weight

savings up to 70% may result from using aluminum with high strength ceramic fibers in the direction of maximum stress. Intermetallic compounds containing aluminum promise high usage temperatures with reduced weight. Ceramic matrix composites use high specific strength fiber reinforcements to permit very high temperatures with less brittleness than monolithic ceramics. Carbon-carbon composites have enormous potential but need stable high temperature coatings to provide protection from burning.

The fan and compressor

The purpose of the fan and compressor is to increase the pressure of the incoming air. Situated at the front of the engine, they draw in air, pressurize it, then deliver it into the combustion chamber. At all flight conditions, the entering air must be decelerated to a low-speed, high-pressure state at the engine compressor face. The air should enter the first stage of the compressor at an **inlet Mach number** in the region of 0.4-0.5. From Eq. (8.8), the flow area could be obtained from:

$$A = \frac{\dot{m}\sqrt{C_p T_t}}{p_t \bar{m}}$$

(13.1)

where the **mass flow parameter**:

$$\bar{m} = \frac{\gamma}{\sqrt{\gamma - 1}} M \left(1 + \frac{\gamma - 1}{2} M^2\right)^{-(\gamma+1)/2(\gamma-1)}$$

(13.2)

To permit varying flight conditions, the mass flow per unit inlet area into the fan should not exceed about 85% of that required to choke the annulus.

There are two types of compressors. The **centrifugal flow compressor** consists of an impeller supported in a casing which houses a ring of diffuser vanes. The impeller is driven at high speed, by the turbine, and air is drawn through its center. Centrifugal action forces the air radially outwards and accelerates it into the diverging diffuser outlet, which further increases the pressure. The pressurized air then passes into the combustion system.

The **axial flow compressor**, see Figure 13.2, consists of a number of stages of alternately rotary and stationary airfoil-section blades, which force the incoming air through a convergent annular duct. The fan is always of an axial type but with few stages. The rotating blades are carried on discs or a drum and driven by a turbine via a connecting shaft. As the air passes through each stage it is accelerated by the rotating blades and forced rearwards through the static blades, known as vanes, which reduces the velocity and increases the pressure.

As the axial compressor needs more stages than a centrifugal compressor for the equivalent pressure rise, an engine designed with an axial compressor will be longer than one designed with a centrifugal compressor but an engine design using a centrifugal compressor will generally have a larger frontal area. This, plus the ability to increase the overall pressure ratio in an axial compressor by the addition of extra stages, has led to the use of axial compressors in most engine designs. However, the centrifugal compressor is still favoured for smaller engines where its

simplicity, ruggedness and ease of manufacture outweigh any disadvantages.
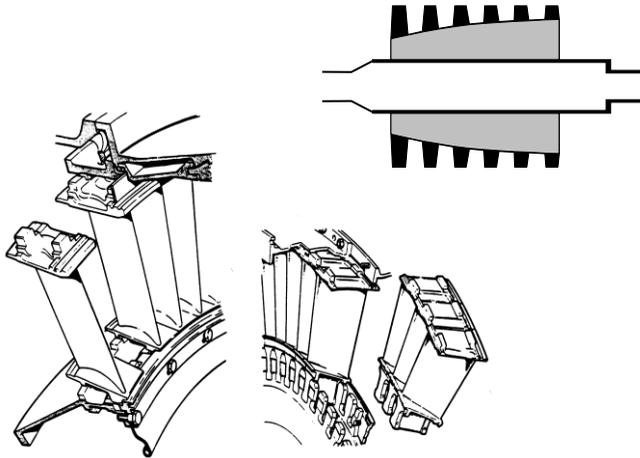
Fig. 13.2 Axial flow compressor blades and vanes

At high values of the hub/tip ratio, the clearance becomes a significant part of the blade height. This leads to reduced efficiency and surge margin. At low hub/tip ratios, disc and blade stresses become prohibitive. To balance these effects, the **compressor hub to tip** diameter ratio should be higher than 0.65. The **fan hub to tip** diameter ratio should be higher than 0.35 to avoid high hub stresses.

The design approach is to represent the blade-to-blade flow on cylindrical stream surfaces cutting through the blades and vanes as

shown in Figure 13.3. In preliminary design the blade-to-blade flow is treated as two-dimensional on these surfaces.
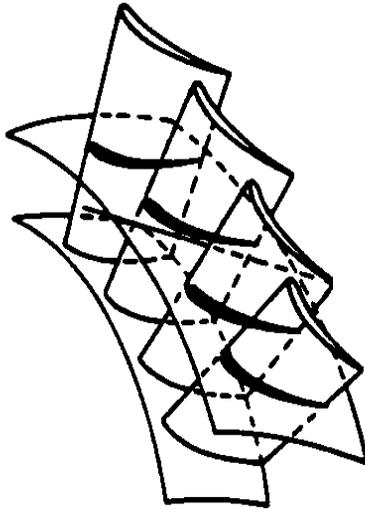
Fig. 13.3 Blade stream surfaces

 The shaft work of the axial compressor is transferred to the air by the blades and vanes of the compressor. The velocity triangles for a compressor stage, a cascade, is shown in Figure 13.4 below where **u is the circumferential blade speed** and **c and w are the real and relative air speeds**. From the law of momentum, the force on a blade in the circumferential direction is the mass flow times the velocity increase. The power is the force times the rim speed. Therefore the increase of enthalpy, i.e. the amount of work added to the air over the stage per unit of air flow, is:

$$\Delta h_t = \lambda u(c_{2u} - c_{1u}) = \lambda u(u - c_{2a} \tan \beta_2 - c_{1a} \tan \alpha_1) \quad (13.3)$$

This is the so called **Eulers equation** expressed in the outlet angles from the stator and rotor. The so called **work factor** $\lambda < 1$ is introduced to account for the blockage effect in the cascade due to wall boundary layers. Because of this the velocity profile becomes more and more "peaky" reaching a fixed profile at about the fourth stage.
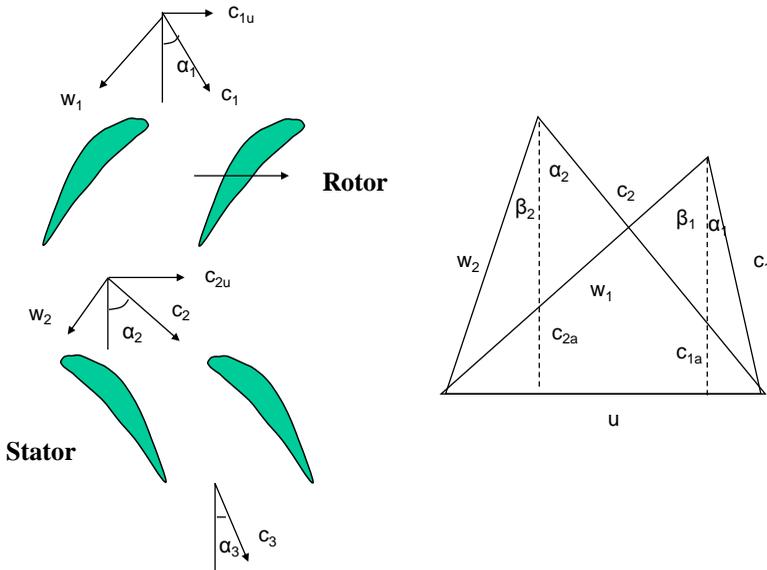
Fig. 13.4 Cascade flow and velocity triangles

When the enthalpy increase over the stage is known, the temperature ratio is:

$$T'_{t3} / T'_{t1} = 1 + \frac{\Delta h_t}{C_p T'_{t1}} \qquad (13.4)$$

For a given polytropic efficiency, this equation gives the pressure ratio over the stage as:

$$\pi'_c = \left(\frac{T'_{t3}}{T'_{t1}} \right)^{\frac{\eta\gamma}{\gamma-1}} \qquad (13.5)$$

Eq. (13.3) and Eq. (13.4) can be rewritten as:

$$\frac{T'_{t3}}{T'_{t1}} = 1 + \lambda \frac{u^2}{C_p T'_{t1}} \left(1 - \frac{c_{2a}}{u} \left(\tan \beta_2 + \frac{c_{1a}}{c_{2a}} \tan \alpha_1 \right) \right) \qquad (13.6)$$

With constant axial flow through the stage and with the tangential Mach number:

$$M_t = u / \sqrt{\gamma R T'_1} \qquad (13.7)$$

Eq. (13.6) may be rewritten as:

$$\frac{T'_{t3}}{T'_{t1}} = 1 + \lambda \frac{(\gamma-1) M_t^2}{1 + (\gamma-1) M_1^2 / 2} \left(1 - \frac{M_{1a}}{M_t} \left(\tan \beta_2 + \tan \alpha_1 \right) \right) \qquad (13.8)$$

When **N is the number of revolutions per second**, the tip Mach number is:

$$M_t \propto \frac{N}{\sqrt{T}} \qquad (13.9)$$

while the inlet Mach number is related to the mass flow equation (8.11):

$$\bar{m}(M_{1a}) = \frac{\dot{m}\sqrt{C_p T_t}}{A p_t} \qquad (13.10)$$

Therefore the pressure ratio is a function of the non dimensional speed and mass flow:

$$\pi = f(\eta, \frac{N}{\sqrt{T}}, \frac{\dot{m}\sqrt{C_p T_t}}{p_t}) \qquad (13.11)$$
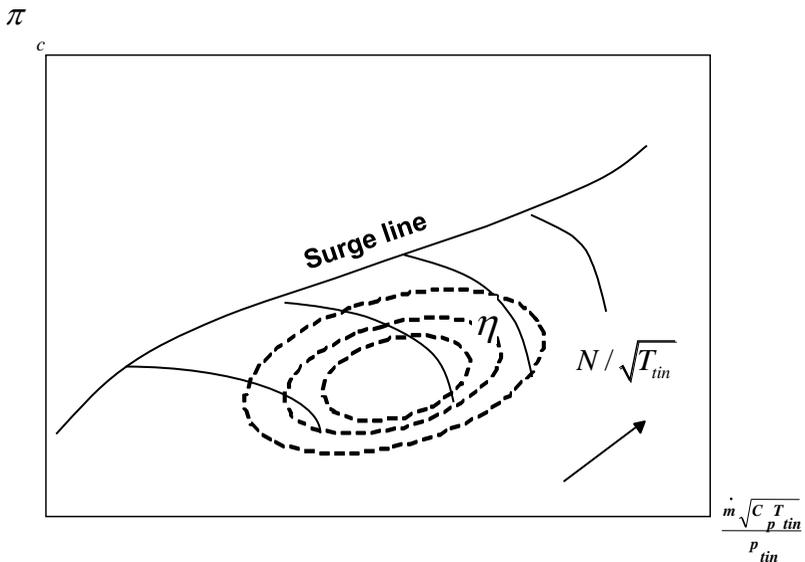
Fig. 13.5 A typical compressor characteristics

The variation of pressure ratio with non dimensional speed and mass flow of a fan or compressor may be found from testing. Usually, it is the inlet conditions that are used to characterize the machine and the result is a compressor map also called the characteristics of the compressor. A typical such **characteristic** is shown in Figure 13.5. Curves for constant efficiency are also shown.

The surge line indicated in the Figure 13.5 constitutes a limit beyond which the flow in the compressor breaks down when one tries to increase the pressure ratio.

One way to increase the work added to the air and therefore the stage temperature and pressure ratio is to increase the tangential Mach number or rim speed. As is seen from the velocity triangles, the relative velocity w_1 at the leading edge of the blade will increase and therefore the relative Mach number. When this Mach number approaches M=1, shocks and losses will occur as was described above for the propeller. In early compressors, the Mach number at the rotor tip was subsonic but in the early fifties it became possible to use transsonic Mach numbers up to 1.1 and even up to 1.3 for jet engine compressors. Much of the advancements in compressors have come from new materials and supersonic aerodynamics that made it possible to increase the tangential Mach number.

The fans are usually designed with higher tip Mach numbers than are the compressors. However, to reduce the damage caused by a potential bird strike and to keep down noise and root stresses, the tip speed of the fan must not be too high. The relative Mach number onto the tips should be below about 1.6 for fans. High

supersonic fan tip speeds are the cause of annoying "buzz saw" noise, especially from older turbofans with narrow chord fans.

It is also seen from Eq. (13.8) that reducing the outlet angle of the blade β_2 results in higher pressure ratio. This means that the relative velocity w_2 at the outlet from the blade decreases resulting in increased pressure gradients on the suction side of the blades. Making the compressor work against rising pressure in the flow direction increases the risk for massive boundary layer **separation**, see Figure 13.6.
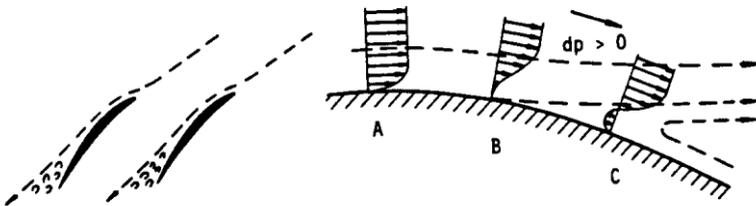
Fig. 13.6 Separation of a flow against increased pressure

The boundary layers on the pressure and suction sides merge at the end of the profile and cause a wake that disturbs the flow in the ensuing gitters. The losses in the flow are concentrated in this

wake. If the flow on the blade separates, reversed flow will occur in the boundary layer, the losses will increase and the wake will grow. Separation occurs more easily along the suction side of the blade, see Figure 13.7. On this side, the flow is first accelerated over the tip of the blade decreasing the pressure in the flow and then decelarated towards the rear end so that the flow meets a rising pressure, which may give rise to separation.
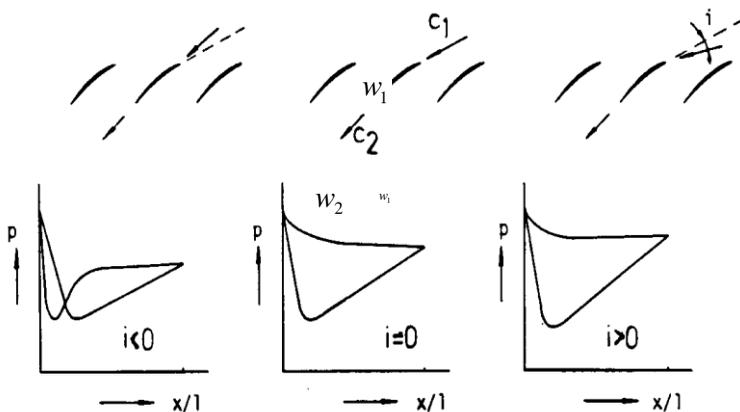
Fig. 13.7 Pressure variation at different incidence angles

At high negative incidence angles, separation may occur also on the pressure side. Negative incidence angles may occur if the inlet velocity is too high, see Figure 13.4.

Another way to increase the pressure ratio is to reduce the inlet flow velocity c_1, that is the Mach number M_1 in Eq. (13.8). Reducing the inlet velocity into the compressor means an increase

in **incidence**. This leads to an increased force on the blades and increased pressure. Further reduction of the mass flow leads to a collapse of the pressure ratio or violent oscillatory flow initiated by flow separation on the suction side of the compressor blades, see Figure 13.7. At high inlet flow velocities, the stage is more sensitive to variations in the incidence angle due to for instance erosion or dirt on the blades.

To avoid the risk for separated flow, the so called **de Haller number** w_2 /w_1 should be high. It is virtually impossible to avoid separation if the de Haller number is lower than 0.5 and it is usually assumed that it should not be above about 0.7. Separation also occurs more easily in laminar than in turbulent flow. To ensure turbulent flow, the Reynolds number should be sufficiently high and it is usually recommended that it should be at least $3*10^5$.

Because of the sensitivity of the compressor to separation of the flow in adverse pressures, the pressure rise per stage is to be relatively small. For axial compressors a typical pressure ratio per stage is below 1.4. Because of the low pressure ratio, an axial compressor may have a large number of stages. Then the front and back stages may be operating under very different conditions. Therefore it is not unusual to split the compressor into several parts each on a different shaft and different speed. For the same reason it is also common to have variable angle stators in the first stages. For fans the pressure ratio could be up to 1.8.
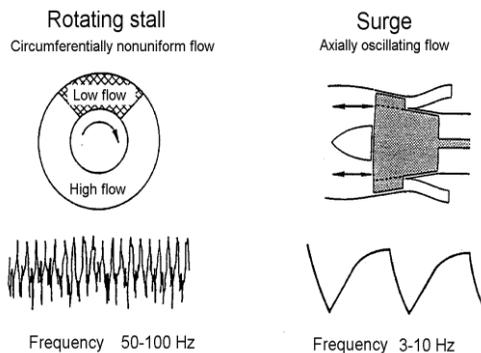
Fig. 13.8 Rotating stall and surge

When separation occurs, the performance of the compressor drops very distinctly and is said to stall or surge, see Figure 13.8. **Surge** is an oscillatory motion of the air in the axial direction, which is usually violent. **Rotating stall** is a non-uniform pattern with reduced flow rate and pressure rise tangentially. Both are unacceptable operating conditions which it is important to avoid. This has large influences on the off-design operation of the engine as will be explained later on.

In an axial compressor stage, there will be an increase in static pressure both in the rotor and the stator. The **degree of reaction** is defined as the relative contribution of the rotor to the pressure (enthalpy) rise in the stage. It is therefore:

$$\Lambda = \frac{\Delta h_t - (c_2^2 - c_1^2)/2}{\Delta h_t} \tag{13.12}$$

Now using Eq. (13.3) and the fact that:

$$c_2^2 - c_1^2 = c_{2a}^2 + c_{2u}^2 - c_{1a}^2 - c_{1u}^2 = c_{2u}^2 - c_{1u}^2 \tag{13.13}$$

we obtain the degree of reaction as:

$$\Lambda = 1 - \frac{c_{1u} + c_{2u}}{2u} = \frac{w_{1u} + w_{2u}}{2u} \tag{13.14}$$

For the most common case where the axial velocity component is constant throughout the stage and the air leaves the stage with the same absolute velocity as it enters, the degree of reaction can be shown to be:

$$\Lambda = \frac{c_a}{2u}(\tan \beta_1 + \tan \beta_2) \tag{13.15}$$

where for a constant axial velocity:

$$\frac{u}{c_a} = \tan \alpha_1 + \tan \beta_1 = \tan \alpha_2 + \tan \beta_2 \tag{13.16}$$

This makes it possible to calculate the angles of the velocity triangles for a given degree of reaction. Introducing the **flow coefficient** $\varphi = c_a/U$ we obtain:

$$\tan \beta_1 = 1/\varphi - \tan \alpha_1 \qquad (13.17)$$

and:

$$\tan \beta_2 = 2\Lambda/\varphi - \tan \beta_1 \qquad (13.18)$$

It is usually desirable to share the diffusion between rotor and stator. For 50% reaction, which is an important design case this leads to $\alpha_1 = \beta_2$ and $\alpha_2 = \beta_1$, that is to symmetrical velocity triangles.

In practice, the degree of reaction may vary considerably along the blade span increasing from root to tip especially in the first stages where the blades are relatively longer. Because of the lower blade speed at the root, more deflection, that is a greater diffusion, is required there for a given work input. The compressor is therefore usually designed with a high degree of reaction in the first stage. It is then gradually decreased so that it reaches 50% after three or four stages.

To obtain the radial variation of the blade angles, a very common design principle is the **"free vortex"**. If the axial velocity component is maintained constant, it can be shown that the radial equilibrium is satisfied if:

$$r c_u = const \qquad (13.19)$$

Since u=ωr this leads to a constant specific work in the radial direction. The radial variation of speed influences the shape of the blades at root and tip, see Figure 13.9.
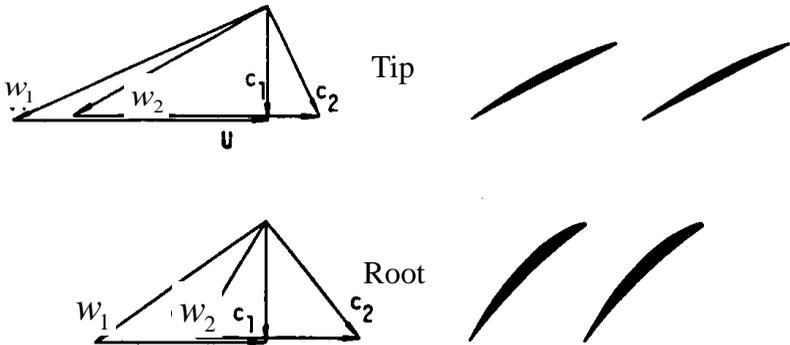
Fig. 13.9 Blade shapes at tip and at root.

The research in compressors is aimed primarily at reducing the number of stages by increasing the average stage temperature rise. The long term trend is to increase the temperature rise per stage by about one degree per year. A single stage fan having a pressure ratio of 1.6 today would then go to 1.8 in 25 years while a typical core compressor stage would increase in pressure ratio from 1.4 to 1.6. This means that the aerodynamic loads on the stage will increase.
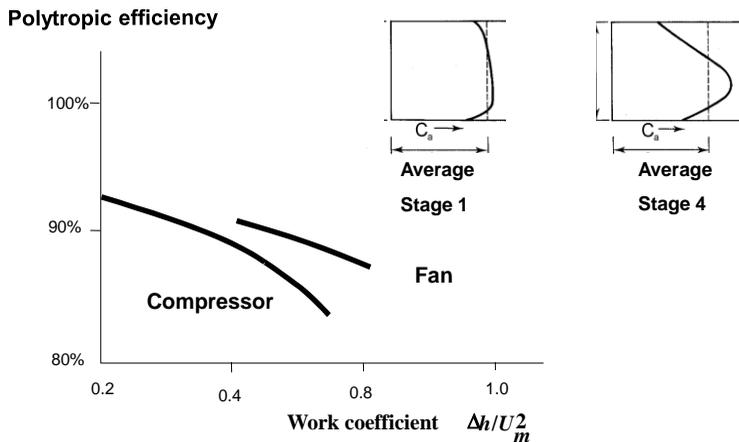
**Fig. 13.10 The efficiency decreases as the work
coefficient increases**

The **work coefficient** or blade loading coefficient (not the same as
the work factor above) is a measure of how much work the
compressor can perform. It is defined as the enthalpy increase per
unit mass flow divided by the square of the blade speed. Efficiency
decreases as more work is taken out of the compressor. Typical
values are shown in Figure 13.10. The work coefficient tends to
decrease with increasing number of stages. The reason is that the
axial velocity varies more radially further into the compressor.

It has been found that compressors and turbines work the best if
the non dimensional axial flow relative to the tangential speed at
mean radius, often called the flow coefficient, is in a restricted
range. The **work coefficient** $\psi=\Delta h_t/u^2$ is in most cases 0.35-0.5

and the **flow coefficient** $\varphi = c_a/u$ is normally 0.4-0.7 for compressors.

Combustion Chamber
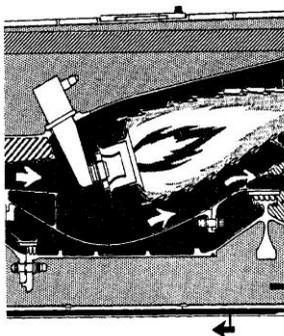
Fig. 13.11 Combustion chamber

The slow moving, high pressure air from the compressor is fed into the combustor or burner where it is mixed with a highly flammable fuel and ignited. This must be accomplished with the minimum loss in pressure and with the maximum heat release within the limited space available.

Two main types of combustion chamber are in use for gas turbine engines. These are the **multiple chamber** and the **annular chamber**. The multiple chamber type is used on centrifugal compressor engines and the earlier types of axial flow compressor engines. The annular type of combustion chamber consists of a single flame tube, completely annular in form, which is contained in an inner and outer casing.

The main advantage of the annular combustion chamber is that for the same power output, the length of the chamber is considerably shorter than that of a multiple chamber system of the same diameter, resulting in a considerable saving in weight and cost. Another advantage is the elimination of combustion propagation problems from chamber to chamber. All modern engines therefore use the annular type of combustor.

The complete **combustion reaction** of a hydrocarbon fuel ($C_x H_y$) with air follows the following formula:

$$C_x H_y + (x + \frac{y}{4})(O_2 + 3.76 N_2) \rightarrow x CO_2 + \frac{y}{2} H_2 O + 3.76(x + \frac{y}{4}) N_2$$
(13.20)
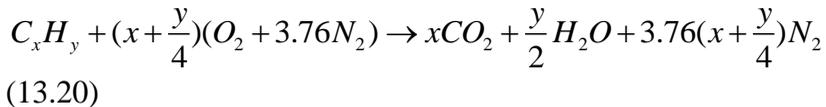
The result of the reaction is carbon-dioxide and water together with nitrogen.

The **stoichiometric** air to fuel ratio required for complete combustion is:

$$\frac{A}{F} = \frac{(x + y/4)32 + 3.76(x + y/4)28}{12x + y}$$
(13.21)

For kerosene the stoichiometric air to fuel ratio is A/F=14.7. This gives the highest possible combustion temperature, see Figure 12.12 below, where the temperature has been plotted versus the so called equivalance ratio.

As the mixture ratio is increased, the gas temperature increases and

theoretically should continue to increase until the stoichiometric mixture ratio is reached. In practice, it is found that there is a tendency for the gas temperature to reach some maximum value before the stoichiometric mixture depending on the chamber design and the combustor inlet temperature, see Figure 13.12. Beyond this point the efficiency of combustion is reduced.
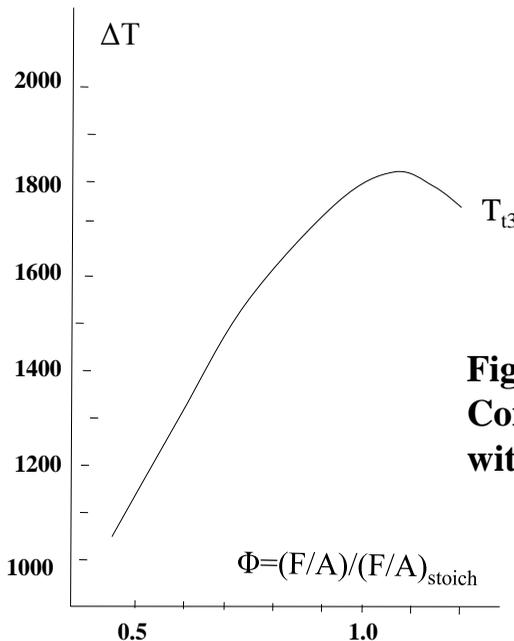
Fig. 13.12
Combustion temperature
with increasing fuel flow.

Since the gas temperature determines the engine thrust, the combustion chamber must be capable of maintaining stable and efficient combustion over a wide range of engine operating conditions. Experiments have shown that there are certain limits to

the fuel/air ratio for which combustion can be maintained, see Figure 13.13.
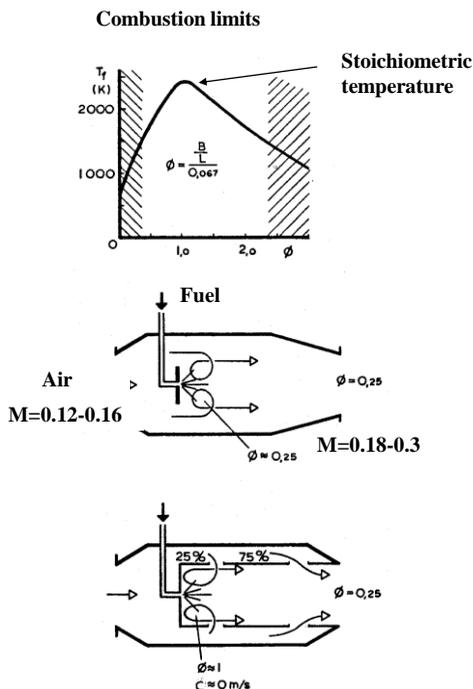
Fig. 13.13
Combustion limits

Fuel without oxygen will not burn, neither will oxygen without fuel. The two extremes of mixture ratio are termed the lean- and rich limit mixtures, the former when oxygen is in excess and the latter when fuel is in excess. The magnitude of these limits depends somewhat on the composition of the fuel but for ordinary hydrocarbons they are in the range A/F=5-25 that is the stoichiometric air to fuel ratio is somewhere in between.

The **lean blow-out** is usually at fuel flows well below those which

occur in the combustion zone during normal operation, though in a dive with the throttle in the idle position, difficulties in maintaining combustion may occur. However, it is the **rich blow-out** that gives most difficulties. As this limiting condition is approached, combustion becomes unstable and the flame starts to fluctuate giving rise to a resonant exhaust sound and vibrations.

The temperature of the gas after combustion is at about 1800 to 2000 °C, which is far too hot for entry to the nozzle guide vanes of the turbine. The air not used for combustion, which amounts to about 75%, is therefore introduced progressively into the flame tube. Normal mixture ratios in jet engine combustors are therefore 60-120. Approximately one third of the excess air is used to lower the temperature inside the combustor; the remainder is used for cooling the walls of the flame tube.

Attempts to reduce the chamber size results in reduced cross sectional areas and increased gas velocities. If the gas velocity exceeds some upper limit, the flame will be blown out. Therefore, the entrance velocity is a very important variable in combustion chamber design. **Entrance Mach numbers** of about 0.12-0.16 based on the local sonic velocity are possible, while **exit Mach numbers** of 0.18-0.30 appears to be common. This will establish an acceptable cross sectional area. The volume of the combustion zone is usually decided from experimental values of the heat release per unit volume. The rest of the design is determined by the arrangement of the compressor and the turbine together with the requirement to supply sufficient cooling air.

Turbines

Cooling air

Convection

Film

Impingement

Vane   Blade
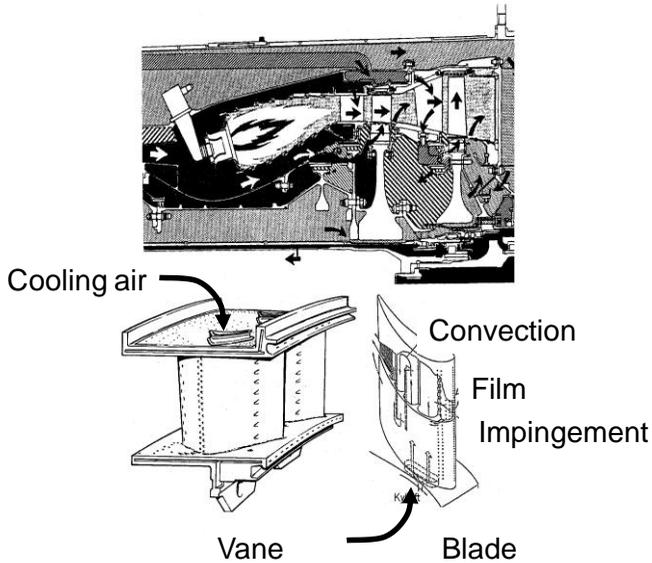
Fig. 13.14 Turbine with cooling flows

At a very high temperature, high pressure gases are released from the burner and passed into the turbine. As the pressure drops, the velocity of the flow of exhaust gases increases and power is

released. Part of this power is used to drive the compressor. As the gases leave the engine the rest of the power generates thrust.

Note that for the same turbine expansion ratio and the same turbine efficiency, the higher the turbine inlet temperature, the higher the turbine work output. Therefore it is always desirable to raise the turbine inlet temperature for higher specific power output.

The high temperatures mean that part of the compressor air must be used for cooling the turbine. Air bled from the compressor is carried aft and introduced in the vanes from the top and in the blades through their roots as shown in Figure 13.14. In a modern jet engine, 10-20 % of the air is bled off for this purpose. Most of this air is used to cool the first stage turbine blades and inlet guide vanes that are exposed to the highest temperatures. The air also cools the turbine discs and the casing. Impingement cooling, directing a jet against a surface, is used to cool the leading edges of the nozzle vanes and the first stage blades. The cooling air passes through complex internal passages and then penetrates through small holes in the wall inclined at an angle to the surface. This creates a film of cool air over the surface that protects the wall from the hot gases. Some heat is also released by radiation.

The **efficiency of the turbine cooling** system is usually defined as:

$$\phi = \frac{T_{gas} - T_m}{T_{gas} - T_{cool}} \qquad (13.22)$$

The level of the cooling efficiency is determined by the sofistication of the cooling system. A value around 0.65 is current state-of-the-art and values of 0.7 may be reached in future engines.

The cooling efficiency directly determines the metal temperature in the turbine.

To produce the driving torque, the turbine may consist of several stages such as the one shown in Figure 13.15, each employing one row of stationary guide vanes, and one row of moving blades. The number of stages depends on the relationship between the power required from the gas flow, the rotational speed at which it must be produced, and the permitted turbine diameter. The design of the nozzle guide vanes and turbine blade passages is broadly based on aerodynamic considerations.
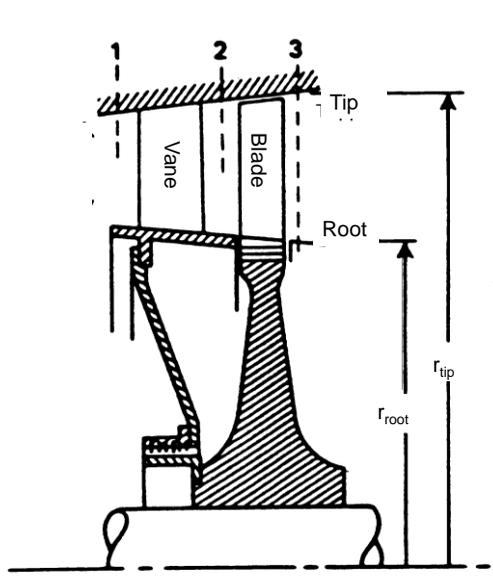
Fig. 13.15 Turbine stage

Unequal heating and cooling of the rotor and stator drives the need for larger **tip clearance** in order to prevent case rubbing and possible blade failure. But a larger gap between the rotor blade tips and the turbine case will lead to aerodynamic losses due to the leakage of the flow over the tips. By controlling the tip clearance throughout the operating engine, significant improvements in component efficiencies and thus in core engine performance could be achieved. Improvements in closed-loop flow path control could provide overall improvements in efficiency and operability, as well as smaller, lighter components.
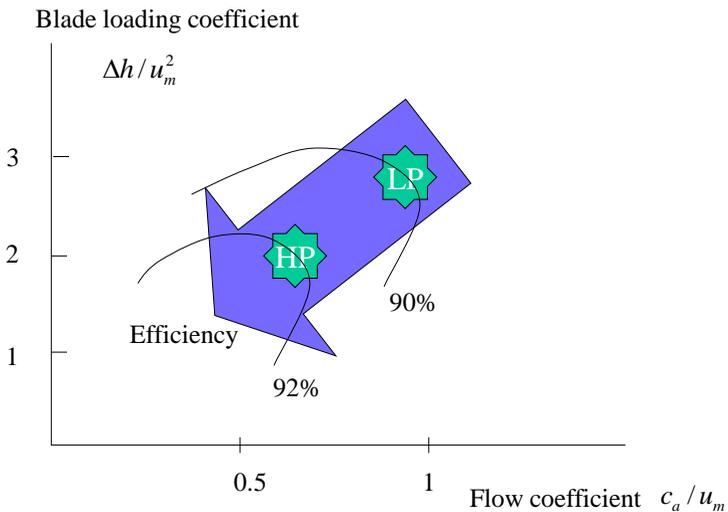
Fig. 13.16 Turbine efficiency versus flow and blade loading coefficients

The typical magnitude of the **polytropic efficiencies** for the LP and HP turbines are shown in Figure 13.16. The efficiencies

depend on the blade loading coefficient or temperature drop coefficient $\psi=\Delta h_t/u^2$ and the flow coefficient $\varphi=c_a/u$.

A long term increase of 1 % in polytropic efficiency is assumed to be reasonable. Todays standard for large civil turbofans seems to be 90% in fans and compressors and 88% in turbines.

Figure 13.16 provides guidelines for the design of turbines. The **blade loading coefficient** should be about 2.0 for HP turbines and 3.0 for LP turbines. The **flow coefficient** should be 0.5-0.65 for HP turbines and 0.9-1.0 for LP turbines. In general the efficiency can be made higher if the work load and the axial velocity is made to decrease. However, this means that more stages are required. LP turbines are generally made with more work load per stage in order to keep the number of stages down.

Because of the falling pressure throughout the machine, the risk for separated flow is lower for turbines than for compressors. Turbine efficiencies are therefore less sensitive to variations in operating conditions than compressors. Therefore, the magnitude of the flow turning and the specific work per stage can be much higher. The turning angle is typically 20 degrees for compressor blades and 60-90 degrees in turbine blades. Often one turbine stage can drive six or seven compressor stages.
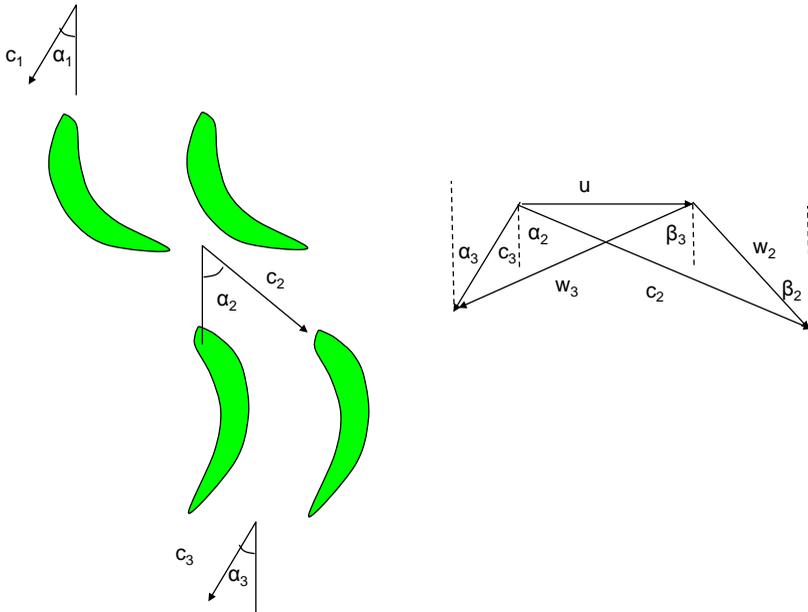
Fig. 13.17 Turbine cascade with velocity triangles

Like in the compressor, the blade-to-blade flow in a turbine stage is treated as two dimensional on cylindrical stream surfaces. A typical turbine cascade and its velocity triangles are shown in Figure 13.17. From the velocity triangles, the specific work becomes:

$$h_t = C_p(T_{t1} - T_{t3}) = u(c_{2a} \tan \alpha_2 + c_{3a} \tan \alpha_3) = u(c_{2a} \tan \beta_2 + c_{3a} \tan \beta_3)$$

$$(13.23)$$

The **degree of reaction** of the stage, i.e. the fraction of the stage expansion in the rotor, is:

$$\Lambda = \frac{w_3^2 - w_2^2}{2u(w_{3u} + w_{2u})} = \frac{w_{3u}^2 + c_{3a}^2 - w_{2u}^2 - c_{2a}^2}{2u(w_{3u} + w_{2u})} \qquad (13.24)$$

For a stage with constant axial velocity component through the stage, the degree of reaction can be shown to be:

$$\Lambda = \frac{c_a}{2u}(\tan \beta_3 - \tan \beta_2) \qquad (13.25)$$

while the Euler equation can be written:

$$\psi = \phi(\tan \beta_2 + \tan \beta_3) \qquad (13.26)$$

where:

$$\frac{1}{\phi} = \frac{u}{c_a} = \tan \alpha_2 - \tan \beta_2 = \tan \beta_3 - \tan \alpha_3 \qquad (13.27)$$

Now the flow angles are obtained from:

$$\tan \beta_2 = \tan \alpha_2 - \frac{1}{\phi} = \frac{\psi - 2\Lambda}{2\phi} \qquad (13.28)$$

$$\tan \beta_3 = \tan \alpha_3 + \frac{1}{\phi} = \frac{\psi + 2\Lambda}{2\phi} \qquad (13.29)$$

A typical value in gas turbines is 50% reaction at the mean diameter. The reaction will increase from root to tip of the blade.

The free vortex principle described above for compressors can also be used for the design of turbines.

The inlet guide vanes of the turbines behave very much as choked nozzles with sonic flow at the throat so that for each turbine:

$$\frac{\dot{m}\sqrt{C_pT_{ti}}}{p_{ti}A_i} = \frac{\gamma}{\sqrt{\gamma-1}}\left(\frac{2}{\gamma+1}\right)^{\frac{\gamma+1}{2(\gamma-1)}} \qquad (13.30)$$

1

It is shown in **Appendix 13** how the equations and design rules given above can be applied to find the main dimensions and the shaft speeds of an engine. The engine for the 2020's is designed with a high inlet Mach number to keep down the size of the engine. The air should enter the first stage of the compressor at a Mach number in the region of 0.4-0.5. For a Mach number of 0.5 when leaving the inlet and with temperatures and pressures from Appendix 12, the flow area is 5.8 m2. The hub to tip diameter ratio should be higher than 0.35 to avoid high hub stresses. This gives a diameter of 2.9 m.

To avoid too much noise and ensure containment the tip speed of the fan should have a relative Mach number below 1.6. The total temperature at the fan inlet is 255 K so the static temperature at Mach 0.5 is 243 K. The speed of sound in the inlet is then 312 m/s and the tangential tip speed becomes 474 m/s. With the tip diameter as above, the rotational speed is 3138 rpm.

 The inlet Mach number to the core compressor is M=0.5. The nondimensional mass flow parameter for M=0.5 becomes 0.96. The HP compressor inlet pressure is 212 kPa and the temperature

421 K. The core mass flow is 32.6 kg/s. The area is then 0.105 m2 and with the hub/tip ratio 0.65, the tip diameter is 0.48 m. The hub diameter is 0.31 and the blade length 84 mm.

With a Mach number at the inlet of 0.5 and a total temperature of 421K, the static temperature is 401 K so the speed of sound is 401 m/s and the axial velocity 200 m/s. The relative tip Mach number at inlet to the core compressor is assumed to be transsonic at M=1.1. The relative tip speed becomes 441 m/s, the tip speed 393 m/s and the rpm 15619. The flow coefficient is 0.51, which is in the recommended domain of 0.4-0.7.

The flow is axial at the inlet and the axial velocity is kept uniform through the compressor and the air leaves the stage with the same absolute velocity as it enters at 200 m/s. The Mach number at the compressor outlet is 0.32, the mass flow parameter is 0.67. The pressure at the outlet of the core compressor is 3390 kPa and the temperature 995 K and the flow area 0.014 m2. The mean diameter is constant at 0.4 m so the blade length is 11 mm.

The work or blade loading coefficient is given a high value of 0.5. The mean diameter is 0.4 m and the mean tangential speed 324 m/s at the 15620 rpm. The specific enthalpy rise in each stage is then 52.6 kJ/kg. The specific enthalpy rise of the whole compressor is from inlet and outlet temperatures 577 kJ/kg so the number of stages is 11.

With the axial inlet velocity 200 m/s and the mean tangential speed 324 m/s, the relative inlet velocity to the first stage is 381 m/s and the relative outlet angle β_2=37.4 deg. The axial velocity 200 m/s then gives a relative outlet speed of 253 m/s and a de Haller number w_2 /w_1 of 0.66. It is virtually impossible to avoid separation if the de Haller number is lower than 0.5 and it should preferably be above 0.7. There is therefore some risk for

separation at the mean radius in the first stage of the core compressor.

Since the specific enthalpy rise in each stage is 52.6 kJ/kg, the total temperature rise is 52.3 deg while the inlet temperature is 421 so the pressure ratio of the stage is 1.45, which should be within what could be expected in future engines.

The axial velocity is constant through the stage and the air leaves the stage with the same absolute velocity as it enters. Stage 1 air outlet angle at mean diameter is 40.4 deg and from the free vortex criterion the angles at root and tip become 47.2 and 35.1. The degree of reaction is 58% at the root and 82% at the tip.

With combustor inlet pressure 3390 kPa and temperature 995 K, we can calculate the flow area assuming an inlet Mach number of 0.12. The exit pressure is 3290 kPa and temperature 1800 K, the exit Mach number is assumed to be 0.18. With the mean diameter as in the HP compressor, the inlet and exit height of the combustor canal are both 26 mm.

To keep cost and weight down, the number of stages of the HP turbine is to be kept down and preferably limited to a single stage. For stress reasons, a rim speed of 400 m/s is usually assumed to be tolerable with HP turbines. This makes it necessary to use two stages in the HP turbine. The total temperature is constant through the turbine stator so the temperature at the rotor inlet is 1800 K while the unmixed outlet temperature is 1289 K from Appendix 12. The work in the turbine rotor is from the temperature difference 635402 J/kg. To maintain efficiency, the blade loading coefficient of the HP turbine should be about ψ_{th} =2. The mean tangential speed with a single stage then becomes 563 m/s which is

much higher than the recommended rim speed of 400 m/s. With two stages the mean tangential speed is 399 m/s. Since the rpm is 15619 this gives a mean diameter of 0.49 m.

Assume that the the flow coefficient (the axial to tangential velocity at the HP turbine inlet) is to be $\phi_{th}=0.55$ at mean diameter (see Figure 13.16 above). The axial inlet velocity will then be 219 m/s. The inlet is choked and the flow area becomes 0.01 m2. If the axial velocity component is kept constant through the stage then the flow angle out of the first stage stator blades is 75 deg. The area is

$$A = \pi Dh \cos \alpha_2$$

and the blade length becomes h= 24 mm in the first stage.

From the temperature drop in Appendix 12 from 1234 to 689 K, the LP turbine has to provide 677 kJ/kg. With six stages each stage must give 113 kJ/kg and if the blade loading is 3, the mean tangential speed is 194 m/s. The speed of the LP rotor is 3139 rpm. The mean diameter of the LP turbine is then 1.18 m. With four stages it would have been 1.45 m. The mean diameter of the LP turbine is then significantly higher than the HP turbine. Note that if the mean diameter is increased, the number of stages decreases as the square of the diameter. Six stages may be regarded as acceptable although cost and weight of having more than four is serious.

It is not clear if the LP turbine is choked so the method used in the HP turbine can not be used to find the flow areas. The blade loading coefficient is $\psi_{tl} = 3$ and the flow coefficient $\phi_{tl} = 1.0$ at mean diameter (see Figure 13.16 above). The degree of reaction there is $\Lambda_{tl} = 0.5$.

The relative velocity at inlet to the first stage rotor is assumed to be axial. The flow angle at exit from the first stator is then 63.5 deg from Eq. (13.28). From the definition of the flow coefficient and the mean tangential velocity, the axial velocity is 194 m/s. The absolute velocity out of the stator is then, see Fig. 12.17, 434 m/s. The total temperature is 1265 K, which gives the stationary temperature 1158 K or including the nozzle losses 1154 K. This is higher than the critical temperature, which is 1073 K, so the stage is not choked. The polytropic efficiency is 0.92, see Chapter 12, so the static pressure at the stator outlet is from the isentropic relation with losses 498 kPa and the density 1.5 kg/m3 which gives the height of the canal 27 mm and an inlet diameter of 1.21 m.

The air velocity is kept axial and similar at inlet and outlet of the turbine stage. If the relative velocity at exit from the last blade row is axial, then the flow angle is 45 deg from Eq. (13.29). The axial velocity is 194 m/s. The absolute velocity out of the turbine blades is 274 m/s which gives the stationary temperature 659 K. The total pressure at the outlet from the LP turbine is 43.4 kPa. The static pressure is from the isentropic relation with losses 35.1 kPa and the density 0.19 kg/m3 which gives the height of the canal 219 mm and the exit diameter is 1.4 m compared to the inlet diameter of 1.21 m.

The resulting design of the Advanced Civil Engine for the 2020's is shown in Figure 13.18. Note the small blade dimensions of the

last stages in the compressor (blade height 11 mm) and the high number of turbine stages (2+6) in this engine, which are due to the high overall pressure ratio of 80:1 and the high bypass ratio of 13.1.
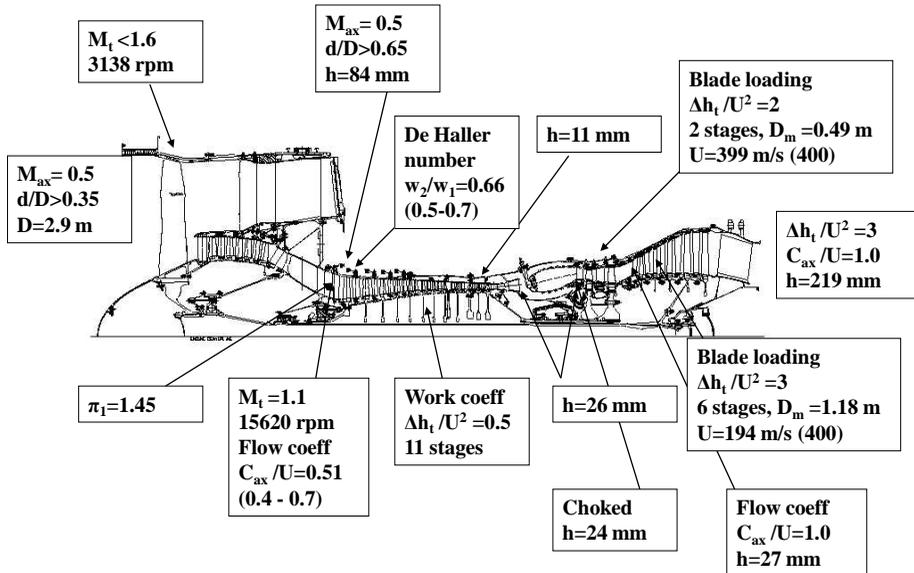
Figure 13.18 The Advanced Civil Engine 2020

Ex 13.1

The New Civil Engine was designed in Appendix 12 to give a compressor outlet temperature of 995 K at altitude. A deterioration of compressor performance takes place during the life time of the engine due to erosion, dirt etc. Assume that the polytropic

efficiency of the HP compressor falls from 92 to 85 %. What would be the compressor outlet temperature at altitude and at SLS +15 C?

Ex 13.2

Assume as in Ex 13.1 that for some reason the core compressor efficiency is reduced from 92 to 85%. How does that influence the HP turbine metal temperature. A rule of thumb for materials limited by creep is that a temperature increase of 10 K halves the creep life. What is the metal temperature

Appendix 13

Mechanical design of jet engines

Thermo data from App. 12   **Design data** (see text above)
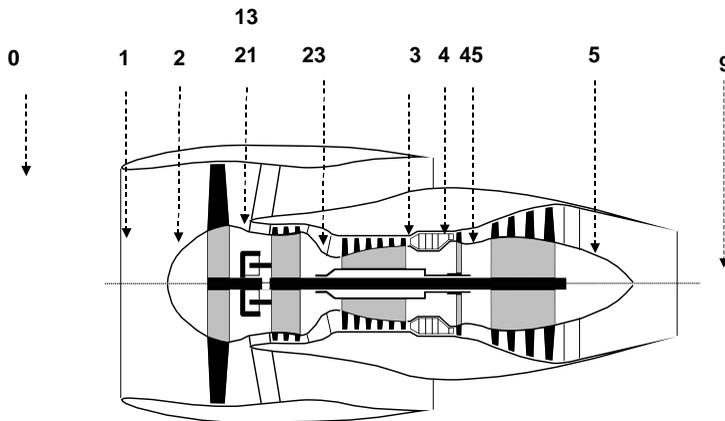
Thermo data from App. 12		Design data (see text above)	
Total mass flow $\dot{m}_{tot}$ kg/s	460	Fan hub/tip ratio r_f	0,35
Core mass flow $\dot{m}$ kg/s	32,6	Inlet Mach number M_2	0,5
Adiabatic constant in cold parts γ_c	1,4	Tip Mach number M_{2t}	1,6
Specific heat d:o C_{pc}	1005	Compressor hub/tip ratio r_c	0,65

Adiabatic constant in hot parts γ_t	1,3	Inlet Mach number M_{23}	0,5
Specific heat d:o C_{pt}	1244	Tip Mach number M_{23t}	1,1
Tt2 K	255	Total outlet/inlet velocity ν	1
pt2 Pa	42300	Work coefficient ψ_c	0,5
Tt23 K	421	Work factor λ	0,95
pt23 Pa	212000	Number of blades stage 1 n_1	52
Tt3 K	995	Combustor inlet Mach number M_{35}	0,12
pt3 Pa	3390000	Outlet Mach number M_{41}	0,18
Tt4 K	1800	HP-Turbine Blade loading coeff ψ_{th}	2
pt4 Pa	3290000	Flow coeff ϕ_{th}	0,55
Tt45 K	1289	LP-Turbine Blade loading coeff ψ_{tl}	3
Fuel flow ratio f	0,025	Flow coeff dito ϕ_{tl}	1
Coolant flow ratio ε	0,116	Turbine/Fan gear ratio G	1
Tt45p K	1234	Reaction stage 1 Λ_{tl}	0,5
pt45 Pa	682000	Efficiency η_{tl}	0,92
Tt5 K	689	Nozzle loss factor ζ_{tl}	0,05
pt5 Pa	44000		

Fan	
The air should enter the fan at a Mach number in the region of 0.4-0.5. For a Mach number of 0.5 to keep down the inlet diameter, the mass flow parameter is from Eq. **Fel! Hittar inte referenskälla.**: $$\bar{m}_2 = \frac{\gamma_c}{\sqrt{\gamma_c - 1}} M_{2a} \left(1 + \frac{\gamma_c - 1}{2} M_{2a}^{\,2}\right)^{-(\gamma_c + 1)/2(\gamma_c - 1)}$$	0.956
Fan **inlet diameter**: $D_2 = \sqrt{\dfrac{4A_2}{\pi(1 - r_f^2)}}$	2.9 m
Fan inlet static temperature: $T_2 = \dfrac{T_{t2}}{1 + \dfrac{\gamma_c - 1}{2} M_{2a}^2}$	243 K
Speed of sound: $a_2 = \sqrt{\gamma_c R T_2}$	312 m/s
To avoid too much noise and ensure containment the tips of the fan should have a relative Mach number below 1.6. Fan **tip speed**: $u_2 = a_2 \sqrt{M_{2t}^2 - M_{2a}^2}$	474 m/s
Fan **speed of rotation**: $N_2 = 60 u_2 / \pi D_2$	3139 rpm
HP compressor	
It is desirable to have a high inlet Mach number to the core compressor to minimize frontal area but this leads to high relative velocities and losses at the first stage blade tips. The flow is axial at the inlet. The mass flow parameter with the inlet Mach number 0.5: $\bar{m}_{23} = \dfrac{\gamma_c}{\sqrt{\gamma_c - 1}} M_{23} \left(1 + \dfrac{\gamma_c - 1}{2} M_{23}^{\,2}\right)^{-(\gamma_c + 1)/2(\gamma_c - 1)}$	0.956

The flow area: $A_{23} = \dfrac{\dot{m}\sqrt{C_{pc}T_{t23}}}{p_{t23}\bar{m}_{23}}$	0.105 m2
Compressor **inlet diameter**: $D_{23} = \sqrt{\dfrac{4A_{23}}{\pi(1-r_c^2)}}$	0.48 m
Inner diameter: $d_{23} = r_c D_{23}$	0.31 m
Inlet blade length: $l_{23} = (D_{23} - d_{23})/2$	0.084 m
Inlet static temperature: $T_{23} = \dfrac{T_{t23}}{1 + \dfrac{\gamma_c - 1}{2}M_{23a}^2}$	401 K
Speed of sound: $a_{23} = \sqrt{\gamma_c R T_{23}}$	401 m/s
The flow is axial at the inlet. Air speed: $c_{23} = M_{23}a_{23}$	201 m/s
Relative air speed at inlet: $w_{23} = M_{23t}a_{23}$	441 m/s
Tip speed: $u_{23} = \sqrt{w_{23}^2 - c_{23}^2}$	393 m/s
Compressor **speed of rotation**: $N_3 = 60u_{23}/\pi D_{23}$	15620 rpm
Flow coefficient: $\varphi_{23} = c_{23}/u_{23}$ The flow coefficient is in the recommended domain of 0.4-0.7.	0.51
The axial velocity is normally kept uniform through the compressor. Compressor air speed at exit: $c_3 = \nu c_{23}$	201 m/s
Static temperature at outlet: $T_3 = T_{t3} - \dfrac{c_3^2}{2C_{pc}}$	975 K
Speed of sound: $a_3 = \sqrt{\gamma_c R T_3}$	626 m/s
Compressor exit Mach number: $M_3 = c_3/a_3$	0.32

The mass flow parameter: $$\bar{m}_3 = \frac{\gamma_c}{\sqrt{\gamma_c - 1}} M_3 \left(1 + \frac{\gamma_c - 1}{2} M_3^{\,2}\right)^{-(\gamma_c + 1)/2(\gamma_c - 1)}$$	0.668
Compressor exit flow area: $A_3 = \dfrac{\dot{m}\sqrt{C_{pc}T_{t3}}}{p_{t3}\bar{m}_3}$	0.014 m2
The mean diameter is assumed to be constant through the compressor: $$D_{3m} = (D_{23} + d_{23})/2$$	0.397 m
Exit blade length: $l_3 = \dfrac{A_3}{\pi D_{3m}}$	0.011 m
Compressor **exit diameter**: $D_3 = D_{3m} + l_3$	0.408 m
Tangential speed at mean diameter: $u_{3m} = \pi D_m N_3 / 60$	324 m/s
The blade loading coefficient ψ_c (the enthalpy rise per stage divided by the mean tangential speed) is a measure of how much work is demanded from the compressor. The efficiency increases as the blade loading coefficient is reduced but more stages are required. The blade loading coefficient should be 0.5 so the enthalpy rise per stage is: $$\Delta h = \psi_c u_{3m}^2$$	52597 J/kg
The specific enthalpy rise of the whole compressor is from inlet and outlet temperatures: $h = C_{pc}(T_{t3} - T_{t23})$	577427 J/kg
The **number of stages**: $n_c = h / \Delta h$	10.98 (11)
Note that the flow is axial at the inlet to the stage. Relative speed at mean inlet diameter: $$w_{23m1} = \sqrt{c_{23}^2 + u_{3m}^2}$$	381 m/s

With axial inlet velocity, Eq. (13.3) gives the relative outlet angle from the first stage blades from: $$\beta_{23m2} = \arctan\frac{u_m - \Delta h/\lambda/u_m}{c_{23}}$$ The work factor λ is 0.95 and the axial velocity is constant through the stage.	0.654 rad
Relative speed at first stage exit: $w_{23m2} = c_{23}/\cos\beta_{23m2}$	253 m/s
De Haller number: $dH = w_{23m2}/w_{23m1}$ It is virtually impossible to avoid separation if the de Haller number w_2/w_1 is lower than 0.5 and it should preferably be above 0.7. There is therefore some risk for separation at the mean radius in the first stage of the core compressor.	0.66
Total power taken up by the first stage: $\Delta H = \dot{m}\Delta h$	1716794 J
Force per blade: $F = \Delta H/n_1 u_{3m}$	102 N
Temperature rise through the stage: $\Delta T_{t23} = \Delta h/C_{pc}$	52.3 K
Total exit temperature of stage 1: $T_{t232} = T_{t23} + \Delta T_{t23}$	473 K
Pressure ratio over the first stage: $$\pi = (T_{t232}/T_{t231})^{\eta\gamma_c/(\gamma_c-1)}$$ This should be within what could be expected in a future engine.	1.45
The axial velocity is constant through the stage and the air leaves the stage with the same absolute velocity as it enters. Stage 1 air outlet angle at mean diameter: $\alpha_{23m2} = \arctan(u_{23m}/c_{23} - \tan\beta_{23m2})$	40.4 deg 0.705 rad
D:o at root from the "free vortex" Eq. (13.19): $$\alpha_{23r2} = \arctan(\frac{D_m}{d_{23}}\tan\alpha_{23m2})$$	47.2 deg 0.824 rad

D:o at tip: $\alpha_{23t2} = \arctan(\dfrac{D_m}{D_{23}} \tan \alpha_{23m2})$	35.1 deg 0.612 rad
Tangential speed at root: $u_{23r} = \pi d_{23} N_3 / 60$	256 m/s
Relative air outlet angel at root: $\beta_{23r2} = \arctan(u_{23r} / c_{23} - \tan \alpha_{23r2})$	11 deg 0.191 rad
Tangential speed at tip: $u_{23t} = \pi D_{23} N_3 / 60$	393 m/s
Relative air outlet angel at tip: $\beta_{23t2} = \arctan(u_{23t} / c_{23} - \tan \alpha_{23t2})$ Note the **twist of the blade**.	51.5 deg 0.90 rad
Relative air inlet angel at root: $\beta_{23r1} = \arctan(u_{23r} / c_{23})$ Note axial flow at inlet.	51.9 deg 0.905 rad
Relative air inlet angel at tip: $\beta_{23t1} = \arctan(u_{23t} / c_{23})$	63 deg 1.1 rad
Reaction at root from Eq. (13.15): $\Lambda_{23r} = \dfrac{c_{23}}{2u_{23r}} (\tan \beta_{23r1} + \tan \beta_{23r2})$	0.58
Reaction at tip: $\Lambda_{23t} = \dfrac{c_{23}}{2u_{23t}} (\tan \beta_{23t1} + \tan \beta_{23t2})$	0.82
Combustor	
Assuming an inlet Mach number of 0,12, **t**he inlet mass flow parameter: $\bar{m}_{35} = \dfrac{\gamma_c}{\sqrt{\gamma_c - 1}} M_{35} \left(1 + \dfrac{\gamma_c - 1}{2} M_{35}^2\right)^{-(\gamma_c + 1)/2(\gamma_c - 1)}$	0.263
Combustor inlet flow area taking into account the coolant flow tap off: $A_{35} = \dfrac{\dot{m}(1 - \varepsilon)\sqrt{C_{pc} T_{t3}}}{p_{t3} \bar{m}_{35}}$	0.032 m2

The **inlet height** of the canal at mean compressor diameter: $l_{35} = \dfrac{A_{35}}{\pi D_{3m}}$	0.026 m
Assuming an exit Mach number of 0,18, **t**he exit mass flow parameter: $\bar{m}_{41} = \dfrac{\gamma_t}{\sqrt{\gamma_t - 1}} M_{41}\left(1 + \dfrac{\gamma_t - 1}{2} M_{41}{}^2\right)^{-(\gamma_t + 1)/2(\gamma_t - 1)}$	0.42
Combustor exit flow area taking into account the fuel flow: $A_{41} = \dfrac{\dot{m}(1 - \varepsilon + f)\sqrt{C_{pt}T_{t4}}}{p_{t4}\bar{m}_{41}}$ Note designed for maximum turbine inlet temperature.	0.032 m2
The **exit height** of the canal at mean compressor diameter: $l_{41} = \dfrac{A_{41}}{\pi D_{3m}}$	0.026 m
HP turbine	
The total power of the HP turbine: $h = C_{pt}(T_{t4} - T_{t45})$	635402 J/kg
To keep cost and weight down, the number of stages of the HP turbine is to be kept down and preferably limited to a single stage. This means a large diameter and a high tip speed since the rpm is fixed by the HP compressor. Assume the number of stages n:	2
Power per stage $\Delta h = h / n$	317701 J/kg

To maintain efficiency, the blade loading coefficient of the HP turbine should be about ψ_{th} =2. The mean tangential speed: $u_{m4} = \sqrt{\Delta h / \psi_{th}}$ With a single stage, the speed is 656 m/s. For stress reasons, a rim speed of 400 m/s is usually assumed to be tolerable with HP turbines. The design is therefore somewhat marginal even with two stages.	399 m/s
Mean diameter: $D_{m4} = u_{m4} / \pi /(N_3 / 60)$ With one stage, the diameter is 0.7 m so the diameter decreases with the number of stages.	0.49 m
Assume that the the flow coefficient (the axial to tangential velocity at the HP turbine inlet) is ϕ_{th}=0.55 at mean diameter (see Figure 13.15 above). The axial inlet velocity: $c_{1am4} = u_{m4}\varphi_{th}$	219 m/s
The air velocity is usually kept axial and similar at inlet and outlet of the turbine stage. Then, the stagnation enthalpy per stage is given by Eq. (13.23) with α_3 =0. If the axial velocity component is kept constant through the stage then the flow angle out of the first stage stator blades is: $\alpha_{2m4} = \arctan(\Delta h / u_{m4} / c_{2am4})$	74.7 deg 1.30 rad
The flow is choked at outlet from the stator blades. The mass flow parameter with M=1: $$\bar{m}_4 = \frac{\gamma_t}{\sqrt{\gamma_t - 1}}\left(1 + \frac{\gamma_t - 1}{2}\right)^{-(\gamma_t+1)/2(\gamma_t-1)}$$	1.39

The total temperature and pressure are constant through the stator. The flow area: $$A_4 = \frac{\dot{m}(1 - \varepsilon + f)\sqrt{C_{pt}T_{t4}}}{p_{t3}\overline{m}_4}$$	0.0097 m2
From the mean diameter and the flow direction, the **blade length** at inlet to the first rotor: $$l_{24} = \frac{A_4}{\pi D_m \cos\alpha_{2m4}}$$	0.024 m
HP turbine **diameter**: $D_4 = D_{m4} + l_{24}$	0.51 m
LP turbine	
Rotor speed: $N_5 = N_2 G$	3139 rpm
The total power of the LP turbine: $h = C_{pt}(T_{t45p} - T_{t5})$	677390 J/kg
Number of stages n:	6
Power per stage $\Delta h = h/n$	112898 J/kg
To maintain efficiency, the blade loading coefficient of the HP turbine should be about $\psi_{tl} = 3$, see Figure 13.15. The mean tangential speed: $u_{m5} = \sqrt{\Delta h / \psi_{tl}}$	194 m/s
Mean diameter: $D_{m5} = u_{m5}/\pi/(N_5/60)$	1.18 m
The diameter of the LP turbine is then significantly higher than the HP turbine. Note that if the mean diameter is increased, the number of stages decreases as the square of the diameter. Six stages may be regarded as acceptable although cost and weight of having more than four is serious. With 4 stages, the	

mean diameter is 1.45 m.	
It is not clear if the LP turbine is choked so the method used in the HP turbine can not be used to find the flow areas. The blade loading coefficient is $\psi_{tl}=3$ and the flow coefficient $\phi_{tl}=1.0$ at mean diameter (see Figure 13.15 above). The degree of reaction there is $\Lambda_{tl}=0.5$. The relative velocity at inlet to the first stage rotor is assumed to be axial. The flow angle at exit from the first stator is then from Eq. **Fel! Hittar inte referenskälla.**: $$\alpha_{245} = \arctan(\frac{1}{\phi} + \frac{\psi - 2\Lambda}{2\phi})$$	63.5 deg 1.11 rad
The axial velocity: $c_{2a45} = u_{m5}\varphi_{tl}$	194 m/s
The flow velocity: $c_{245} = c_{2a45} / \cos\alpha_{245}$	433 m/s
Static temperature at stator exit including 5% nozzle loss: $T_{45} = T_{t45p} - \dfrac{c_{245}^2}{2C_{pt}}(1+\zeta_{tl})$	1154 K
Critical temperature: $T_c = \dfrac{2T_{t45p}}{\gamma_t + 1}$ The static temperature is larger than the critical temperature so the stage is not choked.	1073 K
The polytropic efficiency is 0.92. Static pressure: $$p_{245} = p_{t45p}\left(\frac{T_{45}}{T_{t45p}}\right)^{\gamma_t/(\gamma_t-1)/\eta_{tl}}$$	498738 Pa
Density: $\rho_{245} = p_{245}/R/T_{45}$	1.50 kg/m3
Area: $A_{245} = \dot{m}(1+f-\varepsilon)/\rho_{245}/c_{2a45}$	0.102 m2

Inlet blade length: $l_{245} = \dfrac{A_{245}}{\pi D_{m5}}$	0.027 m
Inlet diameter: $D_{245} = D_{m5} + l_{245}$	1.21 m
If the relative velocity at exit from the last blade row is axial, then the flow angle is from Eq. (13.29): $$\alpha_{35} = \arctan(\frac{\psi + 2\Lambda}{2\phi} - \frac{1}{\phi})$$	45 deg 0.786 rad
Since the axial velocity component is constant through the turbine, the flow velocity: $c_{35} = c_{2a45} / \cos \alpha_{35}$	274 m/s
Static temperature at exit: $T_{35} = T_{t5} - \dfrac{c_{35}^2}{2C_{pt}}$	659 K
Static pressure: $p_{35} = p_{t5} \left(\dfrac{T_{35}}{T_{t5}} \right)^{\gamma_t/(\gamma_t-1)/\eta_{tl}}$	35618 Pa
Density: $\rho_{35} = p_{35} / R / T_{35}$	0.188 kg/m3
Area: $A_5 = \dot{m}(1 + f - \varepsilon) / \rho_{35} / c_{2a45}$	0.82 m2
Exit blade length: $l_{35} = \dfrac{A_{35}}{\pi D_{m5}}$	0.22 m
Exit diameter: $D_5 = D_{m5} + l_{35}$	1.40 m

14. ADVANCED CYCLES

To reach the efficiency needed for engines in the year 2020 more advanced cycles must be considered. As in commercial gas turbines, heat exchangers could increase the efficiency of a jet engine. A recuperator after the turbines increases the engine efficiency while intercooling in the compressor and reheating between the turbines reduces the efficiency. An even larger effect is obtained by combining recuperation and intercooling. This reduces the overall pressure ratio and increases the bypass ratio of the engine. Cooling of the coolant air also increases the engine efficiency. A fuel cell driving a fan or constant volume combustion in a wave rotor are other possible methods.

In land and marine applications where weight and size are not so important, heat exchangers are routinely used to increase the cycle efficiency. This may include cooling the cooling air in the bypass stream, introducing intercoolers in the main compressor and using a recuperator to transfer heat from the exhaust gas to the compressor discharge air. It has also been proposed to reheat the gas between the turbines. A ducted propfan layout featuring a cooling air cooler, intercooler, reheater and recuperator is shown in Figure 14.1.
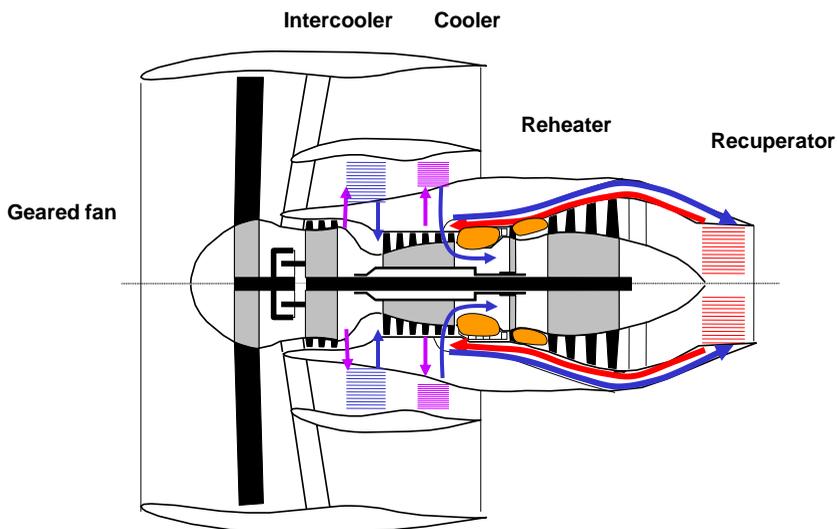
Fig. 14.1 Ducted propfan Intercooler-Reheater-Recuperator

Cooling the coolant flow by an heat exchanger in the bypass stream has two consequencies for the cycle. First, the heat added to the cycle decreases as the mass flow in the combustor decreases. The second effect is that the cooling air cools down the turbine flow. In cycle calculations this is usually taken into account by assuming a mixing in of the cooling air after the turbine or at several stations in the turbine.

The net effect is that the efficiency of the engine increases by some fraction of a percent. However, the installed efficiency

changes very little because the optimum bypass ratio tends to increase. Also, the specific thrust changes very little.

Some indirect effects are more important. Thus, the cooler coolant flow makes it possible to increase the turbine inlet temperature and this indirectly improves the engine efficiency. The reduced amount of cooling flow needed in the turbine because of the lower cooling air temperature will also increase the efficiency of the turbine. This is because the emerging cooling air increases the drag of the blades and also because the cooling air itself suffers a pressure loss in passing through the cooling passages. It is estimated that the turbine efficiency could increase by approximately 0.5 % for each 1 % decrease in turbine cooling air. As we saw in Chapter 13, this means about 0.25 % increased engine efficiency.

Intercoolers in the compressor may be required because of the high temperatures in the new engines. An intercooler is a heat exchanger that cools the compressor air during the compression process by heat exchange with the bypass flow. For instance, if the compressor consists of a high and a low pressure unit as in Figure 14.1, the intercooler could be mounted between them to cool the flow. Because of the diverging pressure lines in the T-s diagram, intercooling will decrease the work necessary for compression.

If a gas turbine has a high pressure and a low pressure turbine at the back end of the machine, a **reheater** (usually another combustor) can be used to "reheat" the flow between the two turbines as shown in Figure 14.1. Because of the diverging pressure lines in the T-s diagram, the turbine work for the same pressure drop should increase by such reheating.

Recuperators or **regenerators** can be used to transfer heat from the engine exhaust to the compressor as shown in Figure 14.1. A recuperator typically comprises corrugated metal sheets stacked together with the hot and cool streams flowing through alternate layers. Historically, there has been a problem with thermal fatigue in recuperators and this led in the 1960's to the development of regenerators consisting of a rotating ceramic disc with axial passages, which had better low cycle fatigue strength. However, owing to limitations on the disc diameter, regenerators are only practical for small mass flows so jet engines should use recuperators.

To understand how the different methods shown in Figure 14.1 influence the specific thrust and the efficiency, we may start by studying ideal cycles without losses.

It was seen from Eq. (9.4) that the thrust efficiency of an engine is the product of the thermal efficiency and the propulsive efficiency. The latter can always be increased by reducing the ratio of the jet speed towards the flight speed, that is by increasing the bypass ratio, see Eq. (9.7). The key idea behind modifications to the cycle of a jet engine is therefore to increase the thermal efficiency because this directly influences the performance for a given amount of heat input.

The thermal efficiency is defined as the ratio between the cycle work and the heat added to the cycle that is:

$$\eta_t = \frac{\dot{W}_c}{\dot{Q}} \qquad (14.1)$$

The cycle work increases the kinetic energy of the air passing through the engine. The specific thrust, or thrust per airflow, is the difference between the jet and inlet air velocities. Therefore the specific thrust directly depends on the cycle work. From Eq. (9.18):

$$\frac{F}{\dot{m}a_0} = \sqrt{\frac{2}{\gamma-1}\frac{\dot{W}_c}{\dot{m}C_pT_0} + M^2} - M \qquad (14.2)$$

To understand how heat exchangers influence the efficiency and specific thrust of an engine, we should look into what happens with the cycle work and the heat supplied to the cycle. An ideal Intercooled-Reheated-Recuperated cycle is shown in Figure 14.2. Note that total conditions are indicated by a "t" while stationary conditions are given by simple digits.

Theoretically, **intercooling** would decrease the compressor work. This is so because the lines of constant pressure in the T-s diagram of Figure 14.2 are diverging. The path to pass from the pressure p_{t0} to the pressure p_{t3} in Figure 14.2 is therefore shorter if intercooling is made from T_{t21} to T_{t22}.

In reality, a perfect exchange of heat can never be achieved because it would require a heat exchanger with an infinite area. It is customary therefore to define the heat exchanger effectiveness as the ratio between the really exchanged heat and the maximum

possible value. Taking the intercooler efficiency into account, the temperature after the intercooler is:

$$T_{t22} = (1 - \eta_{ic})T_{t21} + \eta_{ic}T_{t0} \qquad (14.3)$$

Fig. 14.2 Ideal IRR cycle

With adiabatic compression and an ideal intercooler:

$$T_{t3} = T_{t22}\left(\frac{p_{t3}}{p_{t22}}\right)^{\frac{\gamma-1}{\gamma}} = T_{t22}\left(\frac{p_{t3}}{p_{t0}}\frac{p_{t0}}{p_{t21}}\right)^{\frac{\gamma-1}{\gamma}} = T_{t22}\frac{\tau_c}{\tau_{c1}} \qquad (14.4)$$

where we have introduced a fictitious temperature ratio corresponding to the total compressor pressure ratio:

$$\tau_c = (\frac{p_{t3}}{p_{t0}})^{\frac{\gamma-1}{\gamma}} = \pi_c^{\frac{\gamma-1}{\gamma}} \qquad (14.5)$$

The power required in the compressor is now:

$$\dot{W}_c / \dot{m} C_p = T_{t3} - T_{t22} + T_{t21} - T_{t0} \qquad (14.6)$$

Using Eqs. (14.3) and (14.4), we then obtain the following expression for the compressor power:

$$\frac{\dot{W}_c}{\dot{m} C_p T_{t0}} = (\tau_c - 1)(1 - \eta_{ic}) + (\frac{\tau_c}{\tau_{c1}} + \tau_{c1} - 2)\eta_{ic} \qquad (14.7)$$

It is now seen that independently of the intercooler efficiency, intercooling provides a minimum of the compressor power when:

$$\tau_{c1} = \sqrt{\tau_c} \qquad (14.8)$$

This means that the compressor should be split into two parts with equal pressure ratios. This is not always possible for practical reasons and therefore the full effect of intercooling can not always be obtained.

The turbine work with **reheating** is:

$$\dot{W}_t / \dot{m} C_p = T_{t4} - T_{t41} + T_{t42} - T_{t5} \qquad (14.9)$$

where with a temperature ratio τ_t corresponding to the the the total pressure ratio over the turbine:

$$T_{t5} = T_{t42} \left(\frac{p_{t5}}{p_{t42}} \right)^{\frac{\gamma-1}{\gamma}} = T_{t42} \left(\frac{p_{t5}}{p_{t4}} \frac{p_{t4}}{p_{t41}} \right)^{\frac{\gamma-1}{\gamma}} = T_{t4} \tau_{t2} \frac{\tau_t}{\tau_{t1}} \quad (14.10)$$

Note that by definition, reheating can not take place at a lower pressure than the turbine exhaust pressure, that is $\tau_t < \tau_{t1} = <1$. On the other hand $\tau_{t2} =$ may take on values both larger and smaller than 1.

Now Eq. (14.9) may be rewritten as:

$$\frac{\dot{W}_t}{\dot{m} C_p T_{t4}} = 1 - \tau_{t1} + \tau_{t2} - \tau_{t2} \frac{\tau_t}{\tau_{t1}} \quad (14.11)$$

The maximum turbine work corresponding to an expansion from state "4" to state "5" is then obtained if the turbine as the compressor is divided into two parts so that:

$$\tau_{t1} = \sqrt{\tau_t} \quad (14.12)$$

If reheating is made to the turbine inlet temperature so that =1 then the turbine will be split into two equal parts. Like for the intercooling of the compressor, this ideal split is not always possible.

The fictitious temperature ratio over the turbine can now be obtained since the turbine work is used to power the compressor. For an ideal intercooler that is $\eta_{ic} = 1$:

$$\tau_t = \frac{\tau_{t1}}{\tau_{t2}}(1 - \tau_{t1} + \tau_{t2}) - \frac{\tau_0}{\theta_t}\left(\frac{\tau_c}{\tau_{c1}} + \tau_{c1} - 2\right)\frac{\tau_{t1}}{\tau_{t2}} \quad (14.13)$$

The energy contained in the exhaust gas after the LP turbine in the form of heat may be **recuperated** into the incoming air of the combustion chamber as shown in Figure 14.2. This would save part of the fuel that would otherwise be required

A recuperator effectiveness can be defined as the ratio of the temperature rise relative to the ideal value, the latter being the temperature difference between the two streams, that is:

$$\eta_r = \frac{T_{t35} - T_{t3}}{T_{t5} - T_{t3}} \quad (14.14)$$

This gives:

$$T_{t35} = T_{t3} + \eta_r (T_{t5} - T_{t3}) \quad (14.15)$$

An ideal recuperator with infinite heat transfer surface would raise the burner inlet temperature T_{t35} to T_{t5} the temperature of the inlet into the recuperator.

The heat added to the cycle is now:

$$\frac{\dot{Q}}{\dot{m}C_p} = T_{t4} - T_{t35} + T_{t42} - T_{t41} \qquad (14.16)$$

Using the previous equations:

$$\frac{\dot{Q}}{\dot{m}C_p T_0} = (1-\eta_r)(1-\tau_{t1}+\tau_{t2})\theta_t - \frac{\tau_c}{\tau_{c1}}\tau_0 + \eta_r\tau_0(2\frac{\tau_c}{\tau_{c1}}+\tau_{c1}-2)$$

$$(14.17)$$

The power of the cycle is:

$$\frac{\dot{W}_c}{\dot{m}C_p} = (T_{t55} - T_9) - (T_{t0} - T_0) \qquad (14.18)$$

Where for compression and expansion between the same pressures:

$$T_9 = T_{t55}\left(\frac{p_9}{p_{t55}}\right)^{\frac{\gamma-1}{\gamma}} = T_{t55}\left(\frac{p_0}{p_{t0}}\frac{p_{t0}}{p_{t3}}\frac{p_{t4}}{p_{t5}}\right)^{\frac{\gamma-1}{\gamma}} = \frac{T_{t55}}{\tau_0\tau_c\tau_t} \qquad (14.19)$$

The heat added to the compressor air is taken from the gas leaving the turbine. Therefore, the temperature of the core exhaust stream after the turbine will decrease to:

$$T_{t55} = T_{t5} - (T_{t35} - T_{t3}) = (1-\eta_r)T_{t5} + \eta_r T_{t3} \qquad (14.20)$$

So the cycle power becomes:

$$\frac{\dot{W}_c}{\dot{m}C_pT_0} = (1 - \frac{1}{\tau_0\tau_c\tau_t}) \left[(1-\eta_r)\theta_t\tau_{t2}\frac{\tau_t}{\tau_{t1}} + \eta_r\frac{\tau_0\tau_c}{\tau_{c1}} \right] - \tau_0 + 1$$

$$(14.21)$$

where the turbine temperature ratio τ_t is given by Eq. (14.13).

From the Eqs. (14.17) and (14.21), the thermal efficiency and the specific thrust could be calculated. For the basic case with no recuperator ($\eta_r = 0$), intercooler ($\tau_{c1} = 1$) or reheater ($\tau_{t1} = \tau_{t2} = 1$), the thermal efficiency reduces to Eq. (9.6) for the simple Brayton cycle:

$$\eta_t = 1 - \frac{1}{\tau_0\tau_c} \qquad\qquad (14.22)$$

and the power becomes:

$$\frac{\dot{W}_{c0}}{\dot{m}C_pT_0} = \theta_t - \tau_0\tau_c - \frac{\theta_t}{\tau_0\tau_c} + 1 \qquad\qquad (14.23)$$

For an ideal recuperator ($\eta_r = 1$) without intercooler or reheater, the thermal efficiency becomes:

$$\eta_t = 1 - \frac{T_0}{T_{t5}} = 1 - \frac{1}{\theta_t - \tau_0(\tau_c - 1)} \qquad\qquad (14.24)$$

and the power:

$$\frac{\dot{W}_c}{\dot{m}C_pT_0} = \tau_0(\tau_c - 1)(1 - \frac{1}{\theta_t - \tau_0(\tau_c - 1)}) \qquad (14.25)$$
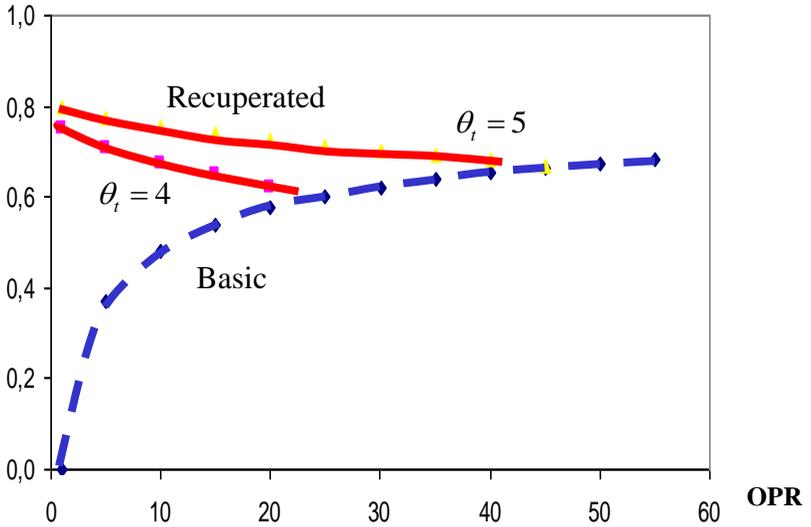
Fig. 14.3 Variation of recuperated thermal efficiency with pressure

Those equations are shown in Figure 14.3 for Mach=0 at take-off ($\tau_0 = 1$). For $\tau_c \rightarrow 1$, the efficiency with intercooler approaches the Carnot efficiency, which depends on the highest and lowest temperatures in the cycle, $\eta = 1 - 1/\theta_t$. It decreases with increasing compressor pressure ratio until it reaches the efficiency of the conventional jet engine at $\tau_c = (\tau_0 + \theta_t)/2\tau_0$.

At higher pressure ratios, the heat exchanger cools the air leaving the compressor instead of heating it so that more heat must be

added than in the conventional cycle and the efficiency is reduced. A consequence of this is that in the recuperated engine, the pressure is driven to low values. This is contrary to the simple Brayton cycle, where the pressure ratio should be as high as possible for maximum efficiency. It is also seen from Figure 14.3 that the temperature should be as high as possible in the recuperated engine. This is a difference from the simple Brayton cycle, where the thermal efficiency does not depend on the temperature but only on pressure.
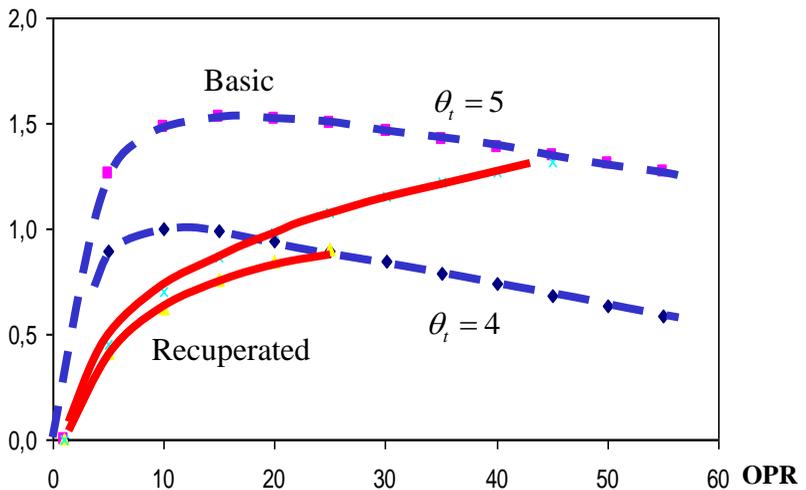
Fig. 14.4 Recuperated power with pressure

Thus, theoretically, a recuperator would lead to higher thermal efficiency. The higher thermal efficiency of a recuperated engine

is, however, accompanied by a reduction in the specific thrust or core power as is seen in Figure 14.4 as the pressure is driven to lower values. Contrary to the basic case, there is no optimum pressure for a recuperated engine.

From Eq. (14.17), the heat given to the cycle is with an <u>ideal</u> **<u>intercooler</u>** but without reheating and recuperation ($\eta_r = 0$, $\tau_{t1} = \tau_{t2} = 1$):

$$\frac{\dot{Q}}{\dot{m}C_pT_0} = \theta_t - \frac{\tau_c}{\tau_{c1}}\tau_0 \tag{14.26}$$

while from Eqs. (14.13) and (14.21), the power of the cycle becomes:

$$\frac{\dot{W}_c}{\dot{m}C_pT_0} = \theta_t - \tau_0(\frac{\tau_c}{\tau_{c1}} + \tau_{c1}) - \frac{\theta_t}{\tau_0\tau_c} + \tau_0 + 1 = \frac{\dot{W}_{c0}}{\dot{m}C_pT_0} + \tau_0(1 - \frac{1}{\tau_{c1}})(\tau_c - \tau_{c1})$$

$$\tag{14.27}$$

where the first part on the right hand side is the power without intercooling.

The thermal efficiency now becomes:

$$\eta_t = 1 - \frac{1}{\tau_0\tau_c} - \frac{(1 - 1/\tau_{c1})(\tau_0\tau_{c1} - 1)}{\theta_t - \tau_0\tau_c/\tau_{c1}} \tag{14.28}$$

It is seen that without intercooling ($\tau_{c1} = 1$), this expression reduces to the relation for the conventional Brayton cycle. The efficiency of the intercooled cycle is therefore always less than for the conventional cycle.

As is seen in Figure 14.5, the efficiency decreases successively the further into the compressor the intercooling is made. However, the power of the cycle is always higher with intercooling and highest if intercooling is made midstage in the compressor as said before. Thus, intercooling reduces the efficiency but increases the specific thrust of the engine. Note that if intercooling is made at $\tau_{c1} = 1$, that is before the compressor, there is no effect because the temperature there is the same as in the bypass canal being used for cooling. As a compromise between power and efficiency, intercooling should be made somewhere in the first half of the compressor.
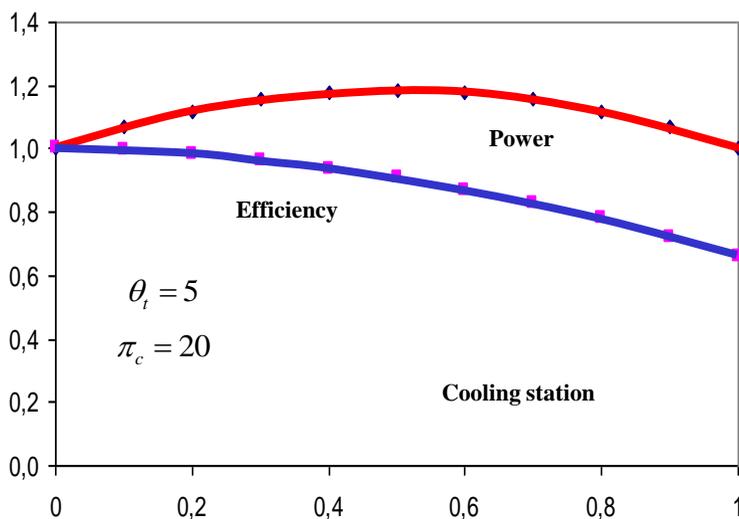
Fig. 14.5 Power and efficiency with intercooling

If a gas turbine has both a high and a low pressure turbine, a **reheater** (usually another combustor) can be used to "reheat" the flow between the two turbines.

From Eq. (14.17), the heat given to the cycle is with reheating in the turbine but without intercooling and recuperation ($\eta_r = 0$, $\tau_{c1} = 1$):

$$\frac{\dot{Q}}{\dot{m}C_p T_0} = (1 - \tau_{t1} + \tau_{t2})\theta_t - \tau_0 \tau_c \qquad (14.29)$$

From Eqs. (14.13) and (14.21), the power of the cycle can be written:

$$\frac{\dot{W}_c}{\dot{m}C_p T_0} = \theta_t(1 - \frac{1}{\tau_0 \tau_c \tau_t})\tau_{t2}\frac{\tau_t}{\tau_{t1}} - \tau_0 + 1 = \frac{\dot{W}_{c0}}{\dot{m}C_p T_0} + \theta_t(\tau_{t2} - \tau_{t1})(1 - \frac{1}{\tau_0 \tau_c \tau_{t1}})$$

$$(14.30)$$

while the thermal efficiency is:

$$\eta = 1 - \frac{1}{\tau_0 \tau_c}(1 + \theta_t \frac{\tau_{t1} + \tau_{t2}/\tau_{t1} - 1 - \tau_{t2}}{(1 - \tau_{t1} + \tau_{t2})\theta_t - \tau_0 \tau_c}) \qquad (14.31)$$

$\theta_t = 5 \quad \tau_{t2} = 1$

$\pi_c = 20$

Power

Efficiency

Heating station
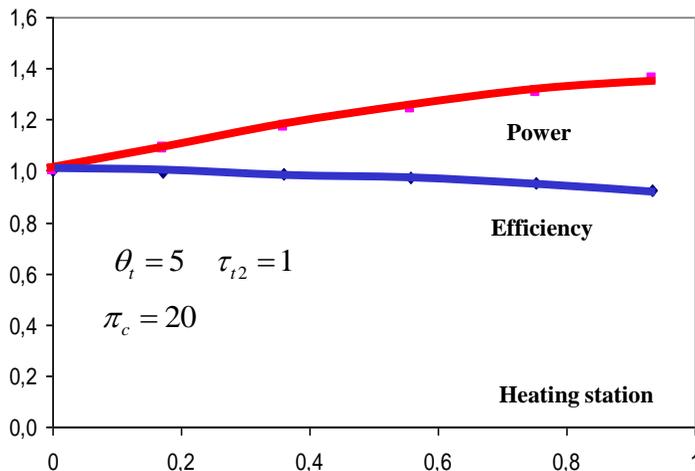
Fig. 14.6 Power and efficiency with reheating

Reheating leads to a reduction in thermal efficiency because of the hotter exhaust temperature that is essentially wasted. At the same time, the power of the cycle, that is the specific thrust, is increased. Obviously, the power effect is largest if reheating is made after the turbine, that is at station "1", where $\tau_{t1} = \tau_t$. This is the conventional **afterburner** and from Eqs. (14.13) and (14.30), the power is:

$$\frac{\dot{W}_c}{\dot{m}C_p T_0} = \theta_t \tau_{t2}(1 - \frac{\theta_t}{\tau_0 \tau_c(\theta_t - \tau_0 \tau_c + \tau_0)}) - \tau_0 + 1$$

$$(14.32)$$

It is seen in Figure 14.6 that afterburning gives a significant increase in power (that is in specific thrust) but a small reduction in thermal efficiency.

The optimum flight Mach number, that is τ_0, is higher with afterburning than without. Thus Eq. (14.32) has a maximum for:

$$\tau_0 = \frac{\theta_t}{2(\tau_c - 1)} \qquad (14.33)$$

while without afterburner, see Eq. (14.23), the maximum power is at:

$$\tau_0 = \sqrt{\theta_t} / \tau_c \qquad (14.34)$$

This means that an engine can operate optimally without afterburner at a lower Mach number and with afterburner at a higher Mach number, where a lot of thrust is needed. Such engines can be used on supersonic transports. An example is the Olympus engine for the Concord. Its compressor pressure ratio of 12, that is a compressor temperature ratio of 2, is near the optimum both at take-off without afterburner and also with afterburner at beyond Mach 2.

Take-off noise resulting from the high jet speed of such engines has made them unsatisfactory for civil supersonic aircraft, dictating the development of variable cycle bypass engines. Instead of using an afterburner such engines operate with a high bypass ratio and a low jet speed at take-off and a low bypass ratio with high jet speed in supersonic cruise.

Up till now, we have only considered ideal cycles without losses. Summarizing the results so far, we may conclude that recuperation tends to increase the efficiency and reduce the specific thrust while intercooling and reheating works the other way around. However, as is shown below, a combination of intercooling and recuperation could have a more positive effect on the cycle efficiency than either of them alone.

To investigate the combined effect of the different methods, we need to study real cycles with component losses rather than the ideal cycles above. The size of an heat exchanger efficiency, see e.g. Eq. (14.14), depends on the areas involved, a typical value being about 90%. Off-design, the efficiency varies with the mass flow of the heated stream. For first order accuracy, the loss $1-\eta$ could be assumed to be proportional to the mass flow. There will also be a pressure loss in a heat exchanger. Its size depends of course on the configuration and will increase with exchange efficiency.

Appendix 12 can be used to calculate the performance of a bypass engine with heat exchangers with the additional equations given in Appendix 14 below. The results for ideal heat exchangers are summarized in the Table 14.1 below, where the uninstalled efficiency is given relative to the basic engine without heat exchangers.

Engine	Basic	Cooled Cooling air	Recup	Interc	Reheat	Recup+ Interc	Recup+ Reheat	Interc+ Reheat	Rec+Int+ Reheat	Rec+Int+1% component
BPR	13,0	13,4	14,6	15,9	17,9	16,3	20,3	21,4	21,5	16,5
OPR	80,0	80,0	15,0	80,0	100,0	25,0	30,0	100,0	30,0	20,0
Efficiency	41,5%	41,7%	43,2%	40,8%	32,7%	47,1%	38,5%	30,4%	39,5%	48,0%
Fspec	126,2	125,6	124,6	133,4	124,3	130,4	123,6	130,9	128,5	128,8
Deltaeff	0,0%	+0,2%	+1,6%	-0,7%	-8,8%	+5,6%	-3,1%	-11,2%	-2,0%	+6,5%

Table 14.1

It was seen above that a recuperated engine with ideal components should have a higher efficiency at a much lower optimum pressure ratio. This is verified in the Table 14.1 for nonideal components. However, as seen in Figure 14.7, it is very dependent on the efficiency and pressure losses in the recuperator. At 90 % efficiency and pressure recovery, the efficiency of the recuperated engine is lower than the basic nonrecuperated one. But if the recuperator is well designed (i.e., the heat exchanger effectiveness is high and the pressure drops are small) the efficiency will be increased over the simple cycle value.
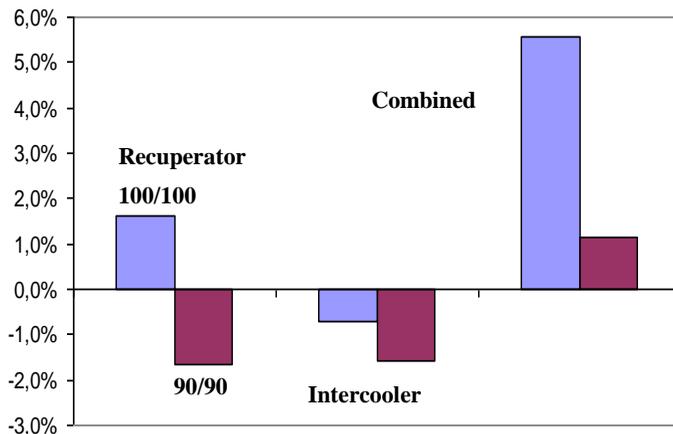
Fig. 14.7 Effect of heat exchangers on engine efficiency

The results of Figure 14.5 showed that even ideal intercooling would lead to reduced efficiency and increased fuel consumption. This is also verified in Table 14.1. For heat exchangers with losses, the effect is even more pronounced, see Figure 14.7. Intercooling in itself is therefore no way to increase the efficiency. However, intercooling is an efficient method to increase the specific thrust.

Reheating between the turbines has a negative effect both on efficiency and on specific thrust. It will also lead to somewhat

higher pressure and bypass ratio. Cooling the turbine cooling air has a small positive effect of a few fractions of a percent.

It is seen from Table 14.1 and Figure 14.7 that attempts to increase the performance should be based on combining recuperation and intercooling. With a recuperator, the fuel flow needed to raise the temperature to the turbine inlet temperature is reduced compared to an engine without recuperator. As is obvious from Figure 14.2, this means that the part of the heating supplied by adding fuel is reduced, leading to increased efficiency. It is also seen from Figure 14.2 that this effect is even more pronounced if recuperation is combined with intercooling. The result, see Table 14.1 and Figure 14.7, is an increase in efficiency beyond that of the recuperator alone even though the intercooler by itself has a negative effect on the efficiency.

A summary of the effects of introducing recuperators and an intercoolers in bypass engines is shown in Figure 14.8 below for the datum engine (TIT=1800/FPR=1.6) for both an ideal case of 100 % heat exchanger efficiency and pressure recovery and for a more realistic case of 90 %. An extra 1 % increase in component efficiencies is included. A separate cooler for the cooling air is not deemed to be necessary in the presence of the intercooler.

The most important effect of the recuperator is that the optimum overall pressure ratio is driven to very low values of about 20. Since efficient high-pressure compressors are complex and expensive, this is a great advantage. At the same time, the recuperator and the intercooler both tend to drive the bypass ratio to somewhat higher values. Note that the increased efficiency should be offset against the extra weight of the heat exchangers. This extra weight, which could be counted in tons, must of course

be added to the aircraft weight and would increase the fuel consumption.

Engine	OPR	BPR	Efficiency	Weight limit	Spec. thrust
Base	80	13	41.5 %	0 %	126
Ideal Heat exch.	20	16.5	48 %	27 %	129
90/90 % Heat exch.	20	15	44.5 %	13 %	129
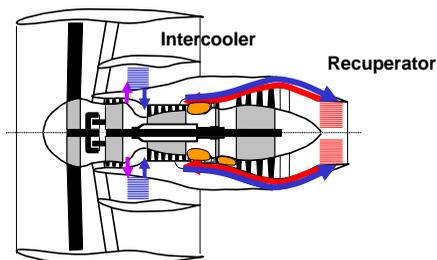
Fig. 14.8 Effect of combined recuperators and intercoolers

The gains shown in Figure 14.8 will of course be reduced substantially when the extra weight of the heat exchangers is taken into account. The influence on fuel consumption may well be negligible or negative.

To realize an engine with heat exchangers, major design changes must be implemented and an optimal design may imply a completely new configuration. Major difficulties will be to design ducts transferring the core flow to the heat exchanger and to

design light-weight and very efficient and durable heat exchangers.

Anyhow, it is obvious from Figure 14.8 that heat exchangers are not sufficient to reach the 50% engine efficiency expected for the 2020's. Constant volume combustion in a **wave rotor** could obtain a higher cycle work. The wave rotor consists of a rotating bank of passages inside a housing with ports bringing air in or taking air out like in revolver cartridges. It was invented by **Seippel** in 1940. Such engines are relatively complicated mechanically but by increasing the overall cycle pressure and allowing higher combustion temperatures, they offer a route to higher efficiency.

Basically, the wave rotor is a rotor with axially aligned blades in a stationary casing between the compressor and the burner. The result is a periodic closing and opening of the inlet to the combustor, where the gases are burnt at constant volume at a high pressure. A turbofan and turboshaft engine can incorporate a wave rotor component in place of a conventional combustor. Both General Electric and Rolls-Royce investigated the use of wave rotors for aircraft engines during the 1960s and showed that the concept was workable.

The wave rotor follows the so called Humphrey cycle as shown in Figure 14.9 below. The main difference from the Brayton cycle is that the temperature increase in combustion takes place at constant volume instead of constant pressure. According to the ideal gas law, the pressure reached is then directly proportional to the temperature.
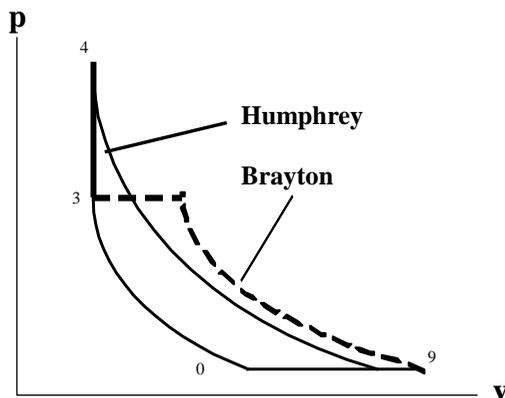
Fig. 14.9 The Humphrey and Brayton cycles

The thermal efficiency of the Brayton cycles is:

$$\eta_{tB} = 1 - \frac{C_p(T_9 - T_0)}{C_p(T_{t4} - T_{t3})} = 1 - \frac{T_0}{T_{t3}} \frac{T_9/T_0 - 1}{T_{t4}/T_{t3} - 1} \quad (14.40)$$

From Figure 14.9 for the Brayton cycle:

$$\frac{T_9}{T_0} = \frac{T_{t4}}{T_0}\left(\frac{p_0}{p_{t4}}\right)^{\frac{\gamma-1}{\gamma}} = \frac{T_{t4}}{T_{t3}}\frac{T_{t3}}{T_0}\left(\frac{p_0}{p_{t3}}\right)^{\frac{\gamma-1}{\gamma}} = \frac{T_{t4}}{T_{t3}} \quad (14.41)$$

we therefore obtain the simple expression:

$$\eta_{tB} = 1 - \frac{T_0}{T_{t3}} \tag{14.42}$$

Now, for the Humphrey cycle:

$$\eta_{tH} = 1 - \frac{C_p(T_9 - T_0)}{C_v(T_{t4} - T_{t3})} \tag{14.43}$$

and since:

$$\frac{p_{t4}}{p_{t3}} = \frac{T_{t4}}{T_{t3}} \tag{14.44}$$

and:

$$\frac{T_9}{T_0} = \frac{T_{t4}}{T_0}\left(\frac{p_0}{p_{t4}}\right)^{\frac{\gamma-1}{\gamma}} = \frac{T_{t4}}{T_{t3}}\frac{T_{t3}}{T_0}\left(\frac{p_0}{p_{t3}}\frac{T_{t3}}{T_{t4}}\right)^{\frac{\gamma-1}{\gamma}} = \left(\frac{T_{t4}}{T_{t3}}\right)^{\frac{1}{\gamma}} \tag{14.45}$$

we obtain:

$$\eta_{tH} = 1 - k\frac{T_0}{T_{t3}} \tag{14.46}$$

where:

$$k = \gamma_d \frac{(T_{t4}/T_{t3})^{1/\gamma_d} - 1}{T_{t4}/T_{t3} - 1} \tag{14.47}$$

The thermal efficiency of the Brayton cycle is obtained for k=1. Since for the Humphrey cycle k<1 it follows that its thermal efficiency always is higher than for the Brayton cycle.

For an engine with an overall compression temperature ratio of 3 and turbine inlet temperature ratio of 7, the thermal efficiency increases from 67 to 80 %. The difference may become even larger because it would be possible to maintain a higher turbine inlet temperature in the intermittent wave rotor turbine. The wave rotor, therefore seems to be a promising way to increase the efficiency

The early straight turbojets without bypass flow achieved overall thrust-work efficiencies of 20 %. Low bypass ratio engines which became available in the early sixties improved overall efficiency to 25 %. Current high bypass ratio turbofans because of improvements in both thermal and propulsive efficiency approach overall efficiencies of 40 %. There are still possibilities to increase the efficiency of jet engines somewhat by very high bypass and pressure ratios. However, the Brayton cycle as it is now known may soon be reaching its limits.

As shown in Figure 14.10, the bypass engine based on the Brayton gas turbine cycle cannot reach an efficiency higher than about 45 % even with very high bypass ratios. Heat exchangers, wave rotors or fuel cells may make it possible to reach around 50 % of total efficiency in the 2020's. New and as yet unknown technologies must therefore be found.
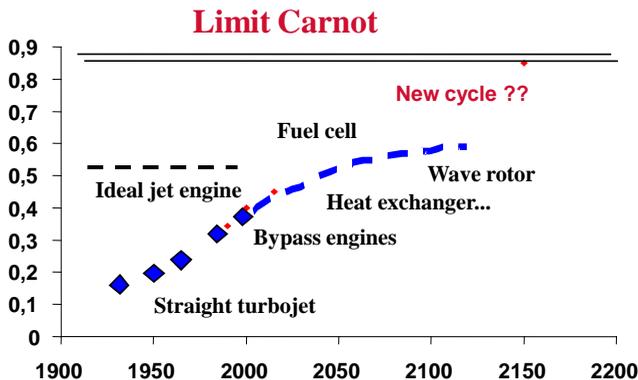
Fig. 14.10 Limits of the turbojet

It is interesting to note that a **fuel cell** has an efficiency of about 60 % and a fan could reach over 90% so this combination would be able to reach beyond the required 50% foreseen for the 2020's. A further advantage would be that this engine would operate without combustion, which would be an advantage for the environment.

But that is still far from the ultimate limit, the Carnot efficiency, as shown in Figure 14.10. The engine efficiency is the product of the internal or thermal efficiency of the thermodynamic process and the propulsive efficiency. The highest possible thermal efficiency is the Carnot efficiency, which is determined by the ratio between

the lowest and the highest temperature in the cycle, that is the ambient and stoichiometric temperatures, so that:

$$\eta_t = 1 - \frac{T_0}{T_{st}} \qquad\qquad (14.48)$$

Thus, the future types of engines will be characterized by very high temperatures and consequently pressures. For a stoichiometric Carnot engine, the thermal efficiency would be around 90 %.

Appendix 14

Additions to Appendix 12:

Indata (corresponding to conventional cycle of Ch. 12 used to check the calculations)

Intercooler efficiency η_{ic}	0
Intercooler pressure recovery π_{ic}	1
Recuperator efficiency η_{rc}	0
Recuperator pressure recovery π_{rc}	1
Reheater switch on K	0
Reheater temperature T_{tr} K	2000
LP Turbine metal temperature T_{lm} K	1500
Cooling air cooler efficiency η_{cc}	0

Pos.		
15.1	Temperature ratio before intercooler: $\tau_{ca} = \sqrt{\tau_c}$	1.54
15.2	Temperature before intercooler: $T_{t2a} = \tau_{ca} T_{t23}$	647 K
15.3	Temperature after the intercooler: $T_{t2b} = (1-\eta_{ic})T_{t2a} + \eta_{ic}T_{t0}$	647 K
16	The compressor outlet temperature: $T_{t3} = T_{t2b}\tau_{ca}$	995 K
16.1	Cooling air temperature: $T_{tc} = T_{t3} - \eta_c(T_{t3} - T_{t13})$	995 K
16.2	Cooling air temperature at take-off: $T_{c0} = T_{sls}\tau_f\tau_b\tau_c - \eta_c T_{sls}\tau_f(\tau_b\tau_c - 1)$	1123 K
17	The HP cooling flow: $\varepsilon_h = \dfrac{\dot{m}_c}{\dot{m}} = 0.05 + 0.05\dfrac{T_{t4\max} - T_m}{T_m - T_{c0}}$	0.116

17.1	The LP cooling flow: $\varepsilon_l = \dfrac{\dot{m}_c}{\dot{m}} = K(0.05 + 0.05\dfrac{T_{treheat} - T_m}{T_m - T_{c0}})$	0
18	**Assume main fuel flow f_h**	0.025
19	Unmixed HP turbine outlet temperature: $T_{t45} = T_{t4} - \dfrac{1}{(1 + f_h - \varepsilon_h - \varepsilon_l)}\dfrac{C_{pc}}{C_{pt}}(T_{t3} - T_{t2b} + T_{t2a} - T_{t23})$	1289 K
21	Pressure after the combustor: $p_{t4} = \pi_{bc}\pi_{rc}p_{t3}$	3290 kPa
23	The mixing temperature after the turbine: $T'_{t45} = \dfrac{\varepsilon_h}{1 + f_h - \varepsilon_l}\dfrac{C_{pc}}{C_{pt}}T_{tc} + \dfrac{1 + f_h - \varepsilon_h - \varepsilon_l}{1 + f_h - \varepsilon_l}T_{t45}$	1230 K
23.1	Temperature after reheater: $T'_{t45r} = T'_{t45} + K(T_{tr} - T'_{t45})$	1230 K
23.2	Pressure after reheater: $p_{t45r} = p_{t45}(1 - K + K\pi_b)$	682 kPa
24.1	Heated bypass flow: $T_{t135} = T_{t13} + (T_{ta} - T_{tb} + (\varepsilon_h + \varepsilon_l)(T_{t3} - T_{cool}))/\alpha$	295 K
25	Actual bypass jet speed is: $V_{jb} = \sqrt{2\eta_j C_{pc}T_{t135}\left[1 - (p_0/p_{t13})^{(\gamma_c - 1)/\gamma_c}\right]}$	374 m/s
25.1	**Assume total fuel flow f**	0.025

26	The temperature after the LP turbine: $$T_{t5} = T'_{t45r} - \frac{1+\alpha}{1+f-\varepsilon_l}\frac{C_{pc}}{C_{pt}}(T_{t13}-T_{t2}) - \frac{1}{1+f-\varepsilon_l}\frac{C_{pc}}{C_{pt}}(T_{t23}-T_{t13})$$	690 K
27	The pressure ratio over the LP turbine: $$\pi_{lt} = \left(\frac{T_{t5}}{T'_{t45r}}\right)^{\gamma_t/(\gamma_t-1)\eta_t}$$	0.064
28	The pressure after the LP turbine: $$p_{t5} = \pi_{lt}\,p_{t45r}$$	44 kPa
28.1	The mixing temperature after LP turbine: $$T'_{t5} = \frac{\varepsilon_l}{1+f}\frac{C_{pc}}{C_{pt}}T_{tc} + \frac{1+f-\varepsilon_l}{1+f}T_{t5}$$	690 K
28.2	Air temperature after recuperator: $$T_{t35} = T_{t3} + \eta_{rc}(T'_{t5}-T_{t3})$$	995 K
28.3	Exhaust temperature: $$T_{t55} = T'_{t5} - \frac{C_{pc}(1-\varepsilon_h-\varepsilon_l)}{C_{pt}(1+f)}(T_{t35}-T_{t3})$$	690 K
28.4	The pressure after the recuperator: $p_{t55} = \pi_{rc}\,p_{t5}$	44 kPa

29	The core jet speed : $$V_{jc} = \sqrt{2\eta_j C_{pt} T_{t55} \left[1 - \left(p_0 / p_{t55} \right)^{(\gamma_t - 1)/\gamma_t} \right]}$$	436 m/s
32.1	The main fuel flow: $$f_h = (1 - \varepsilon_h - \varepsilon_l)(C_{pt}(T_{t4} - 298) - C_{pc}(T_{t35} - 298))/(\eta_b h - C_{pt}(T_{t4} - 298))$$	0.025
32.2	The reheater fuel flow: $$f_l = K(1 - \varepsilon_l)(C_{pt}(T_{t4} - 298) - C_{pc}(T_{t35} - 298))/(\eta_b h - C_{pt}(T_{t4} - 298))$$	0
32.3	Total fuel flow: $f = f_h + f_l$. **If necessary assume new fuel flows pos. 18 and 25.1.**	0.025

15. MILITARY AIRCRAFT REQUIREMENTS

If low fuel consumption is the dictating goal of the future civil aircraft, military aircraft will continue to be driven by speed and turning capability in addition to new demands for stealth, unmanned operation and agility. A fighter aircraft is designed for supersonic penetration (supercruise) or for air superiority at close combat. A high aircraft thrust-to-weight ratio means higher acceleration, more rapid climb, higher maximum speed and a shorter take-off. Vectored thrust can be used to reduce drag and increase fuel economy or range.

Discussions about <u>stealth technologies</u> began in the 1940s but it was not until the 1950s that designs actually began to take into account an airplane's radar signature. The U-2 spy plane, which was built in the 1950's by the Lockheed Aircraft Company, was intended to be stealthy largely by flying at a very high altitude. However, the first U-2s to fly over Soviet territory were immediately detected. This prompted U.S. radar and aircraft experts to evaluate a number of ways to reduce the radar signature of the airplane. These included a fine wire mesh that was molded over the plane and covered with a paint that contained iron, and wires strung from the nose to the tail. However, none of these efforts reduced the airplane's radar signature very much. The high speed of the SR71, that replaced the U2, made the problem of detection less stringent but there was still a need to hide the plane from radar.
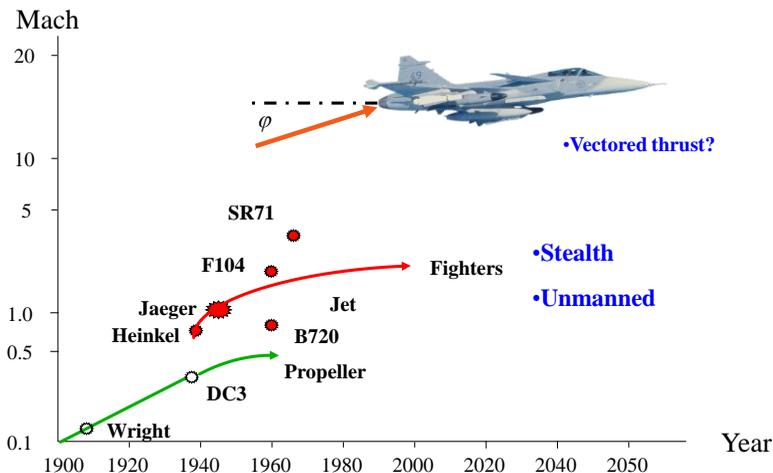
Fig. 15.1 Future military aircraft

The main problem was that significantly reduced radar reflection was very difficult to model mathematically. In the 1970s, a U.S. mathematician working for Lockheed Aircraft used a mathematical model developed by Russian scientists to develop a computer program that made it possible to predict the radar signature of an aircraft made with flat panels, called facets. In 1975, Lockheed Skunk Works engineers determined that an airplane with such faceted surfaces would have a remarkably low radar signature because the surfaces would radiate nearly all of the radar energy away from the receiver. This work marked a substantial change from the past, because for the first time, designers realized that it might be possible to make an aircraft that was virtually invisible to radar.

In early 1977, Lockheed got a contract to build and test two subscale models of a stealthy aircraft. The contract was known as Have Blue and was highly classified. Lockheed's plane looked like a low pyramid with wings and two tails angled inward. When it was placed on a tall pole outdoors and a radar was pointed at it, it was virtually invisible. Lockheed engineers soon developed the Have Blue into a larger bomber aircraft given the designation F-117.

Stealth is a complex design philosophy to reduce the ability of an opponent's sensors to detect, track and attack an aircraft. A variety of technologies may be combined such as a smooth surface, "flying wing" design, radar absorbent materials, and electronic countermeasures.

As propulsion contributes significantly to the signature of an aircraft, the engines are buried in the fuselage with air intake and exhaust ducts placed on the top of the aircraft. This reduces the heat trail, and hides the jet engine's compressor blades from radar detection. The inlets of the jet engines are covered with fine screens to prevent radar energy from reaching the face of the engines. To avoid heat detectors, the exhaust is channeled through long narrow ducts lined with heat-absorbing material so that it is cooled down by the time it exits the plane.

Like stealth, **Unmanned Air Vehicles (UAVs)** have been discussed for a long time but operating an unmanned airplane requires transmitting and processing a large amount of information. It is not until very recently that information technologies have developed sufficiently to make an unmanned aircraft realistic in hostile environments.
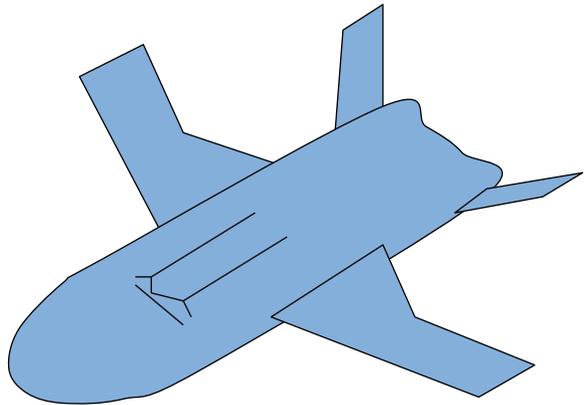
Fig. 15.2 Unmanned Air Vehicle (UAV)

It is expected that UAVs will be employed for a variety of missions, beginning with reconnaissance, surveillance, and targeting, and later expanding to include support tasks such as tanking, electronic warfare, antisubmarine warfare and airborne early warning. Some of these unmanned aircraft will fly from aviation ships and surface combat vehicles, whereas others may be based ashore at great distances from the supported battle group or expeditionary task force. An unmanned reconnaissance aerial vehicle can be employed either as an independent system or in conjunction with other airborne, ground-based, and spaceborne systems. It loiters subsonically at very high altitudes over the region of interest for extended periods of time without refueling.

As UAVs have become more reliable and gained operational acceptance, they have also been employed for air-to-air and ground attack. A strike UAV could loiter subsonically over the region of interest for long periods of time until directed to strike. A large capacity, long-loiter-time, unmanned subsonic air vehicle could be used to deploy and recover smaller combat UAVs. It also could replenish them with weapons and propellant.

The requirements on the propulsion system for a UAV are basically the same as for a stealth aircraft. Since the main source for detection is probably the exhaust jet, the engine must be designed so that infrared radiation from the exhaust is minimized. To keep down the temperature and mass flow of the exhaust, the engine must have a high efficiency. It is also easier to hide the jet in a low speed, cold jet aircraft, which keeps down the speed of stealthy aircraft. This means that the traditional reliance of military aircraft on high speed, high temperature jets must be modified. However, a low temperature jet makes for a larger nozzle area and increased risk for detection, which means that a trade-off must be made. A long exhaust duct to avoid detectors also means that the nozzle losses will increase. Finally, as regards UAV's, the acceleration levels of the aircraft can be much higher than in manned aircraft, which puts special demands on the engine.

The operation of a military aircraft, manned or unmanned, is quite different from a civil one. Most importantly, it has to function at conditions widely different from those it was designed for. This introduces the concept of off-design, which we will return to in a following chapter. But we will first describe how one can determine the required thrust and define the thermodynamic cycle of an engine for a military aircraft.

Figure 15.3 shows a typical **operating envelope** for a fighter aircraft. At the boundary to the left the aircraft stalls because it does not have sufficient speed to create the necessary lift. This boundary is dependent on the dynamic pressure and it flattens at high altitude, which gives the operational ceiling. Note the shrinking of the operating envelope because of the rapidly increasing drag close to Mach 1.

Usually one does not fly faster than Mach 1.2 at sea level because the high air density causes large structural loads on the aircraft. This constitutes the boundary to the right. At high altitudes the speed normally does not exceed Mach 2.3 because the high stagnation temperature makes it impossible to use aluminum in the aircraft skin. With other types of materials such as titanium, used in the SR71, this limit may be pushed beyond Mach 3.

A typical mission for an air-to-air fighter is also shown in Figure 15.3. The mission includes an acceleration to climb speed and a minimum time climb to cruise altitude and combat patrol followed by an acceleration and supersonic penetration to combat area at speeds at or beyond Mach 1.5. To conserve fuel such a dash should be carried out without afterburner. This is referred to as **supercruise.** It is believed that most of the fighting would take place at subsonic speeds between Mach 0.7 and 0.9 at low altitude. The combat will include a number of 360 deg turns. For **air superiority** at close combat, maneuverability is the key performance issue. After combat there is a minimum time climb-out and a descent to base. Note that most of the operations would take place at comparatively low speed below Mach 1.5 and 11 km altitude.
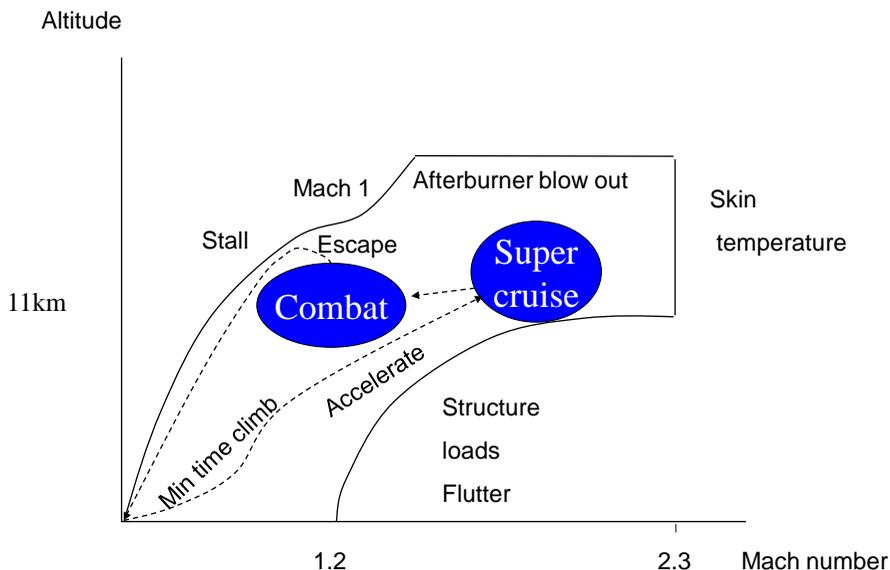
Fig. 15.3 The operating envelope for a fighter aircraft

The design process involves chosing a **design point**, either combat or supercruise, for which the engine is dimensioned. Then the performance of the engine **off-design** in the other parts of the mission is checked. The baseline engine design is then varied until satisfactory performance is obtained at all critical mission legs. Among the possible engines satisfying the mission specifications, the engine that gives the minimum fuel weight relative to the take-off weight of the aircraft is chosen.

The forces acting on a climbing aircraft are shown in Figure 15.4. The climb angle γ is the angle between the horizontal and the flight direction, which is the direction of the relative wind. Some modern fighter aircraft can change the angle of the thrust by using a movable nozzle. This ability to change the angle of the thrust is called **thrust vectoring**, or **vectored thrust**. The thrust vector in Figure 15.4 is assumed to be at an angle φ with the flight direction. Note that the aircraft itself has an angle of attack α with the flight direction. Therefore, the tilting angle of the nozzle relative to the aircraft is φ-α.

The concept of vectored thrust arose from projects designed to satisfy military requirements of short takeoff and landing. The Pegasus turbofan engine for the Harrier aircraft was the first engine to take advantage of this technology. It featured four swiveling nozzles which were all linked and could rotate through 90° between the vertically down and rear-facing horizontal positions. The bypass air is directed through the front two nozzles and the hot exhaust gases through the two rear nozzles.

Vectored thrust can be used to reduce drag and increase fuel economy or range as compared with conventional aerodynamic controls, which increase the drag forces acting upon the aircraft when used for trim. The only serious penalty for having vectored thrust is that the nozzle is heavier than a standard nozzle. Fluid thrust vectoring is a new design concept that could provide the same benefits as the mechanical thrust vectoring system without the added weight and expense.
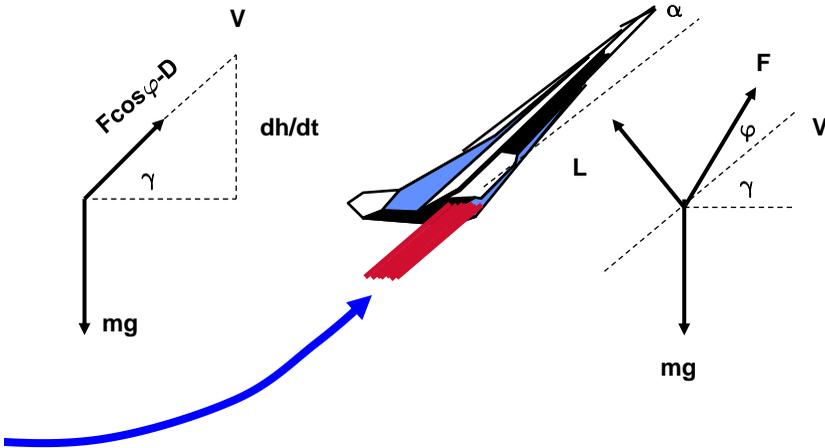
Fig. 15.4 Forces on a climbing aircraft

As the aircraft rises at a **climb angle γ** with a **thrust vector angle φ,** the forces that act on it are **lift L, weight mg, thrust F** and **drag D** as shown in Figure 15.4. The motion of the aircraft through the air depends on the balance between those forces in the flight direction and perpendicular to it, that is:

$$F \cos \varphi - D = mg \sin \gamma \qquad (15.1)$$

$$L + F \sin \varphi = mg \cos \gamma \qquad (15.2)$$

Lift and drag are not independent of each other. As was shown in Chapter 4, the drag on an aircraft consists of a zero lift drag and an induced drag due to lift. It was further shown that both the lift and drag forces can be expressed as coefficients multiplied by the wing area S and the dynamic pressure $q=\rho V^2/2$. With Eq. (6.4), the relation between drag and lift coefficient may be expressed by:

$$C_D = C_{D0} + KC_L^2 \qquad\qquad (15.3)$$

where the coefficient:

$$K = \frac{1}{\pi Ae} \qquad\qquad (15.4)$$

Here $A=b^2/S$ is the aspect ratio of the wing and "e" is the Oswald efficiency factor.

From Eq. (15.3), the relation between drag and lift becomes:

$$D = D_0 + \frac{K}{qS} L^2 \qquad\qquad (15.5)$$

Together with Eqs. (15.1) and (15.2) this relation can be used to calculate the performance of the aircraft.

Eq. (15.3) constitutes the so called "drag polar" of the aircraft as shown in Figure 15.5.
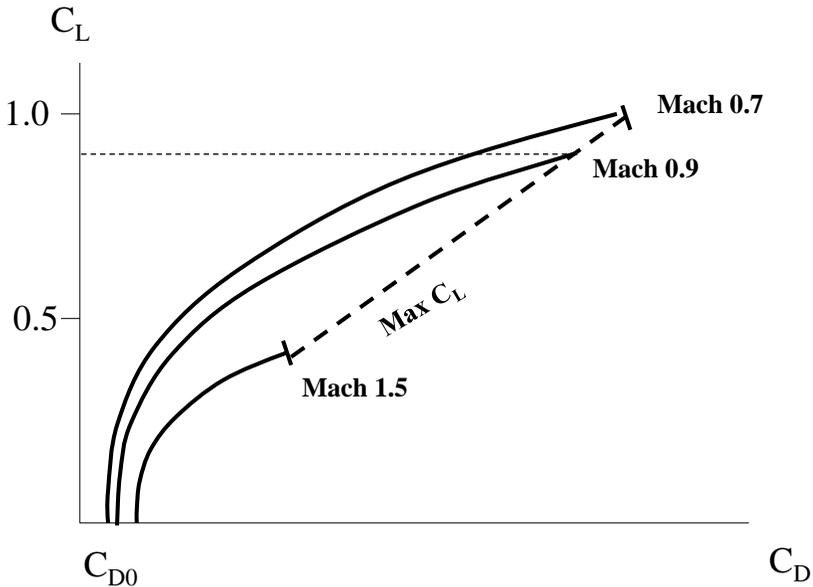
Fig. 15.5 Drag polar-lift versus drag coefficient

Aerodynamically there is an upper limit on the lift coefficient due to stall of the aircraft. A linear variation from 1 at Mach 0.7 to 0.4 at Mach 1.5 can be assumed to be representative, see Figure 15.5.

Both the zero lift drag coefficient C_{D0} and the induced drag coefficient K depend on the Mach number and the configuration of the aircraft. Typical variations based on a number of aircraft are shown in Figure 15.6. The zero lift drag coefficient increases rapidly in the transsonic region because of the wave drag. For the

next generation of aircraft, the drag at zero lift is expected to be about 0.015 below Mach 1, it then increases linearly in the transsonic region to about 0.03 and then remains level.
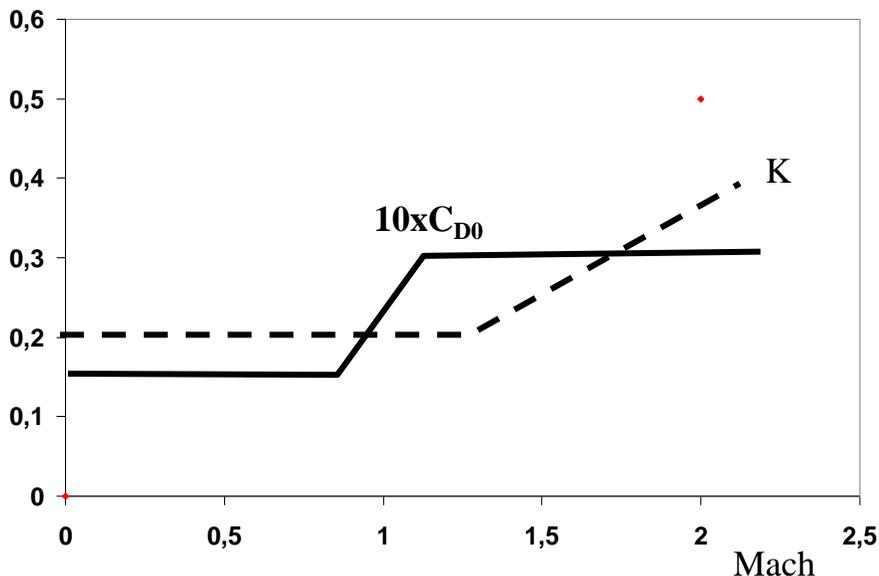
Fig. 15.6 Coefficients to calculate total drag

As for the K coefficent of Eq. (15.4), the sweep back angle of the wings should be higher for higher speed as mentioned in Chapter 8. This means a lower aspect ratio and therefore a higher value of K. The Oswald efficiency factor also decreases at supersonic speeds. This leads to a rapid increase of K with speed. The coefficient K will be about 0.2 below Mach 1.25 and varies then linearly to 0.4 at Mach 2.0.

The climb rate dh/dt of the aircraft is, see Figure 15.4:

$$\frac{dh}{dt} = V \sin \gamma = \frac{V(F \cos \varphi - D)}{gm} \qquad (15.6)$$

This expression is often called the "**Specific Excess Power**" (SEP) of the aircraft. The SEP is in fact the same as the vertical climb rate of the aircraft.

The climb angle is obtained from:

$$\sin \gamma = \frac{F \cos \varphi - D}{mg} \qquad (15.7)$$

or with the total drag from Eq. (15.5) and the lift from Eq. (15.2):

$$\sin \gamma = \frac{F}{mg} \cos \varphi - \frac{D_0}{mg} - K C_{L0} (\cos \gamma - \frac{F}{mg} \sin \varphi)^2 \; (15.8)$$

where the lift coefficient in level flight is:

$$C_{L0} = \frac{mg}{qS} \qquad (15.9)$$

To determine the lift coefficient at a certain speed we need to know the wing area. We must therefore select the **wing loading σ=mg/S**, that is the weight of the aircraft divided by the carrying wing area. For a fighter aircraft the wing loading is less than for an airliner to give high maneuverability. This means larger wings in relation to the aircraft weight. Large wings means shorter take-off

and lower speed at landing but also higher drag and empty weight. A typical value for the wing loading at take-off may be 3500 N/m2.

The **thrust-to-weight ratio F/mg** directly affects the performance of the aircraft. A high aircraft thrust-to-weight ratio means higher acceleration, more rapid climb, higher maximum speed and a shorter runway. On the other hand, a larger engine will consume more fuel. A probable requirement for future air superiority fighters is that at take-off there should be a thrust-to-weight ratio of 1.0 (i.e. an initial acceleration potential of 1g) with afterburner and 0.66 without afterburner. At combat conditions when some of the fuel has been burned, such a fighter would have thrust-to-weight ratios exceeding 1 and would be capable of accelerating straight up with afterburner.

It is seen from Eq. (15.8) that thrust vectoring tends to decrease the induced drag term but that it also decreases the direct thrust term. Differentiating with respect to the thrust vector angle φ, it is found that the maximum excess power is obtained for an angle that can be obtained from:

$$\tan \varphi = \frac{2KC_{L0}\cos\gamma}{1 + 2KC_{L0}\dfrac{F}{mg}\cos\varphi} \qquad (15.10)$$

Usually it is the **rate of turn** that sets the size of the engine. During a turn the aircraft has to bank as shown in Figure 15.7 below. The lift must balance both the weight and the centrifugal force.
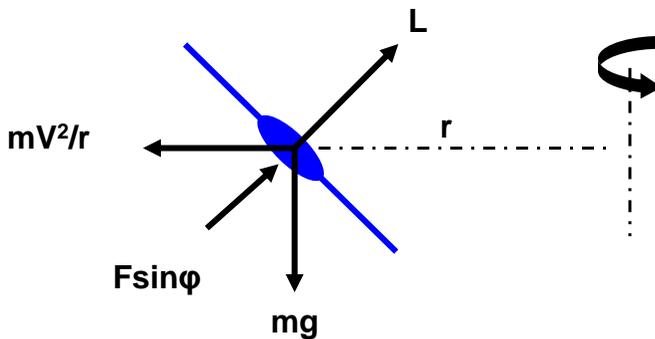
Fig. 15.7 Forces on a turning aircraft

The maximum lift is determined by the **maximum accelleration a_{max}** that the pilot can endure. Usually the max accelleration is given as 9g. It is then possible to calculate the **turning radius** r corresponding to max acceleration at the required flight speed. As the lift of the wings must balance not only the weight but also the centrifugal force this radius can be found from:

$$a_{max}^2 = g^2 + \frac{V^4}{r^2}$$
(15.11)

The balance between the forces acting on the aircraft leads to:

$$F \cos \varphi = D \tag{15.12}$$

$$L + F \sin \varphi = ma_{max} \tag{15.13}$$

The **loading n=a$_{max}$/g** is then with Eq. (15.5):

$$n = \frac{F}{mg} \sin \varphi + \sqrt{\frac{F \cos \varphi - D_0}{mg K C_{L0}}} \tag{15.14}$$

Differentiating with respect to φ shows that the accelleration is a maximum and the turning radius a minimum when the angle of the thrust vector is obtained from:

$$\tan \varphi = 2 \sqrt{K C_{L0} \frac{F \cos \varphi - D_0}{mg}} \tag{15.15}$$

Flight envelops for different loadings are shown in Figure 15.8.

At the contours, SEP=0 because Eq. (15.12) is satisfied. This gives the limit of sustained turn rate corresponding to flight at constant speed and constant altitude with the engine producing maximum thrust. Moving inside this contour, the value of SEP rises. Usually one wants a SEP>0 in order to break out of a turn. As the g-load on the aircraft is increased, that is as the turning radius decreases, the flight envelope shrinks as shown schematically in Figure 15.8.
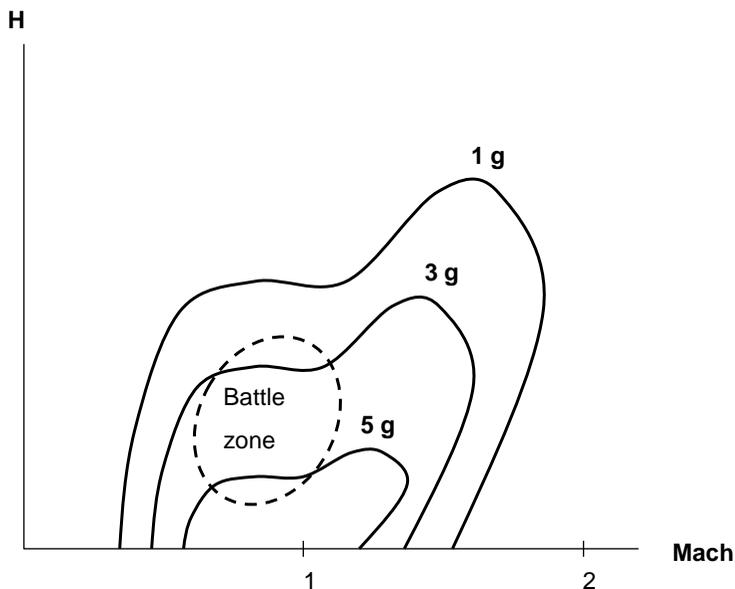
Fig. 15.8 Sustained turn flight envelops for different load factors

The thrust required for sustained turns with unvectored nozzle (φ=0) is obtained from Eq. (15.12) as:

$$F = D_0 + mgKC_{L0}n^2 \qquad (15.16)$$

The thrust for steady, level flight is obtained letting the radius be infinitely large (n=1).

The equations used to find the thrust of a military aircraft are summarized in Appendix 15. As an example the aircraft is

assumed to have a take-off weight of 18 tons and to weigh 15 tons at altitude. This determines the wing area from the wing loading 3500 N/m2. The thrust required is calculated for each engine of a twin engine aircraft for sustained turns at Mach number 0.9 and for supercruise in Mach 1.5 at 11 km altitude (air temperature 216 K, pressure 22.7 kPa.).

As is seen from the Appendix, supercruise at Mach 1.5 requires less thrust than the fighter mission with sustained turns at Mach 0.9. Vectored thrust has very little influence on performance in the design point. However, the importance increases at lower speed as is seen from Figure 15.9, which shows the turning radius at different Mach numbers. The aircraft is flown at the lower Mach numbers while the thrust is maintained as in the design point. The thrust vector angle φ and the lift coefficient C_L increase as the speed decreases. Note that the lift coefficient in turning flight is $C_L = nC_{L0}$, where $n = a_{max}/g$ is the loading. The lift coefficient must of course not increase beyond what is permissible aerodynamically, see Figure 15.5. The aircraft in Figure 15.9 would therefore stall if flown below Mach 0.7 in 3g turns.
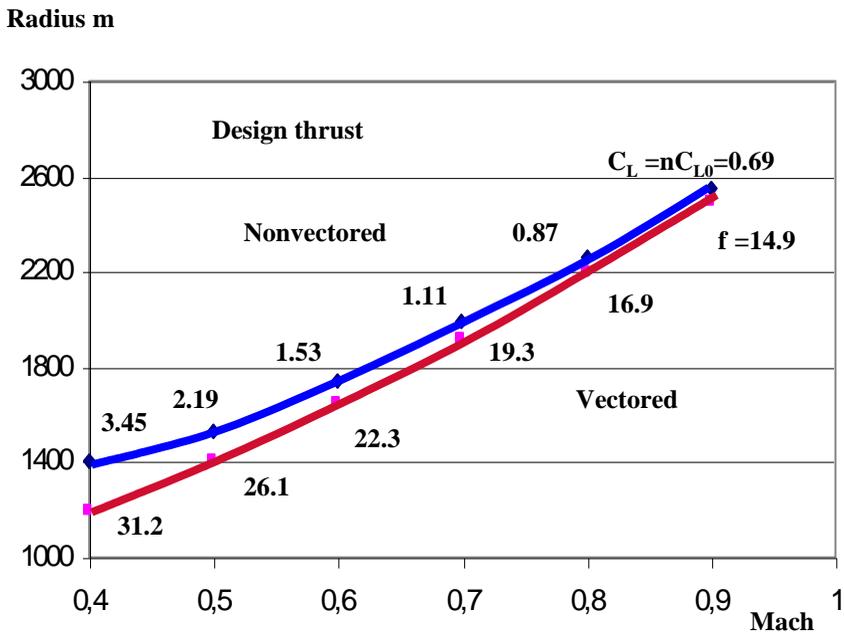
Radius m

Fig. 15.9 Turning radius vs Mach number

The specific excess power (i.e. the speed of climb) of the aircraft as it breaks out of the turn into straight level flight and climbs is 97 m/s. The influence of thrust vectoring on climbing performance is relatively small, a few percentage points at higher speeds than Mach 0.5. The main importance of thrust vectoring is therefore for turning flight at low speed.

Appendix 15

Military aircraft thrust requirements

	Fighter	Supercruise
Atmospheric pressure p [Pa]	22700	22700
Temperature T [K]	216	216
Adiabatic constant γ	1,4	1,4
Mach number M	0,9	1,5
Drag coefficient at zero lift C_{D0}	0,016	0,03
Coefficient in drag-lift relation K	0,2	0,25
Take-off weight m_0 [kg]	18000	18000
Weight at altitude m [kg]	15000	15000
Number of engines N	2	2
Wing loading σ N/m2	3500	3500
Design turning loading n_0	3	1

	Fighter	Super-cruise
Wing area: $S = m_0 g / \sigma$	50,4 m2	50,4 m2
Speed: $V = M\sqrt{\gamma RT}$	266 m/s	443 m/s
Air density at altitude: $\rho = \dfrac{p}{289T}$	0,36 kg/m3	0,36 kg/m3
Zero lift drag coefficient $D_0 = S C_{D0} \rho V^2 / 2$	10.4 kN	54.1kN

Level flight lift coeffient: $C_{L0} = \dfrac{2mg}{\rho V^2 S}$	0,227	0,081
The thrust needed in level flight ($\gamma = 0$) and without vectored nozzle ($\varphi = 0$): $F = D_0 + mgKC_{L0}n_0^2$	70.4 kN	57.2kN
Engine design thrust with two engines	35.2 kN	28.6kN
Maximum SEP vector angle: $\varphi = \arctan(\dfrac{2KC_{L0}\cos\gamma}{1 + 2KC_{L0}\dfrac{F}{mg}\cos\varphi})$	4.6 deg	2.3 deg
Climb angle (iterate with above): $\gamma = \arcsin(\dfrac{F}{mg}\cos\varphi - \dfrac{D_0}{mg} - KC_{L0}(\cos\gamma - \dfrac{F}{mg}\sin\varphi)^2)$	21.8 deg	0.018 deg
Specific excess power SEP=$V\sin\gamma$ with vectored thrust:	98.8 m/s	0.14 m/s
Without vectored thrust	97.3 m/s	0 m/s
Iterate minimum turning radius vector angle: $\varphi = \arctan(2\sqrt{KC_{L0}\dfrac{F\cos\varphi - D_0}{mg}})$	14.9 deg	2.3 deg
Thrust vector loading: $n = \dfrac{F}{mg}\sin\varphi + \sqrt{\dfrac{F\cos\varphi - D_0}{mgKC_{L0}}}$	3.06	1.00

16. DESIGN OF A MILITARY ENGINE

The requirements in a fighter aircraft for acceleration, turning and high speed dictates a high thrust-to-weight ratio. Military engines are therefore designed for high specific thrust per air mass flow. The main differences between military and civilian engines are in the inlet, afterburner and nozzle. The inlet pressure losses may be substantial beyond Mach 2 and inlet distorsion is one of the most troublesome problems. Mixing of the core and bypass streams in an afterburner greatly influencies the performance of the engine. For high speed propulsion the added complexity of a convergent-divergent exhaust nozzle is motivated.

A typical military engine, the RM12 for the Swedish Gripen fighter aircraft, is shown in Figure 16.1 below. It is customary to designate the states in different sections of the engine with numbers. In Figure 16.1, the internationally accepted numbering is used.
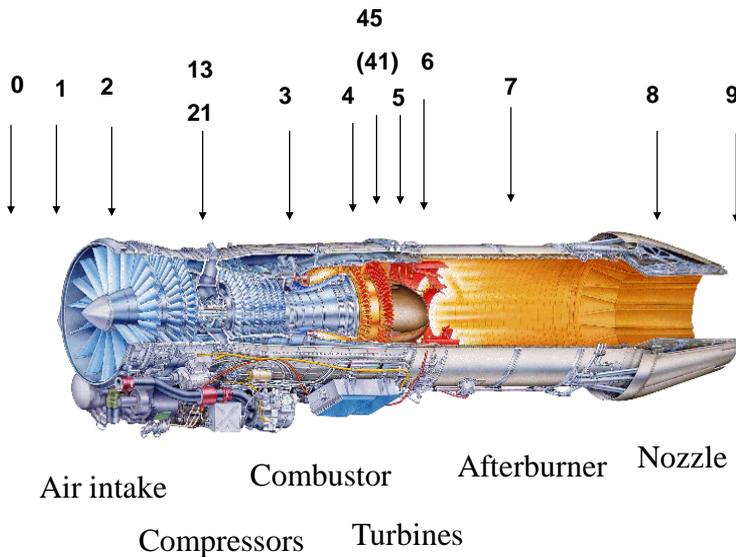
Fig. 16.1 The RM12, a typical military engine

Compared to a civilian engine, the bypass ratio of a military engine is very much lower in order to obtain a high specific thrust. In addition there is a loss of pressure in the inlet in high speed engines. To compensate for those losses the jet must have a high kinetic energy which means a high jet speed. This means that most of the air has to go through the hot core so the bypass ratio should be low.

The **thrust-to-weight ratio** is a common measure of how advanced a military engine is. The requirements in a fighter for acceleration, turning and high speed dictates a high thrust-to-weight ratio. It is seen from Eq. (15.6) that the Specific Excess

Power, that is the acceleration performance, is directly related to the thrust for the same aircraft weight. Increasing the thrust-to-weight ratio of the engine will therefore directly influence aircraft performance.

F/gW_e
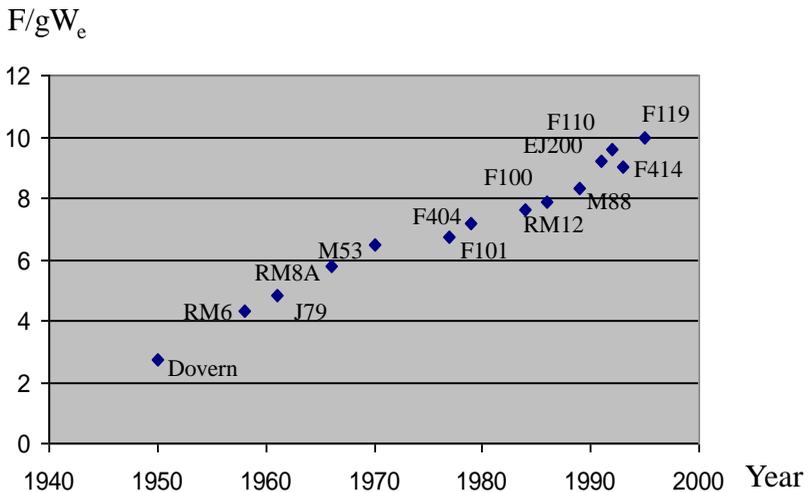
Fig. 16.2 How the thrust-to weight ratio of engines has increased with time

Figure 16.2 shows that the maximum <u>engine thrust-to weight ratio with afterburner has tripled</u> since the beginning of the jet era. The "**Dovern**" was an early Swedish project that never came into production. The **RM6** was a derivative of the RR Avon and used in the Swedish Mach 2 fighter "Draken". The **RM8** was a derivative of the commercial JT8D Pratt & Whitney engine and used to power the Swedish "Viggen" fighter aircraft.

The **J79** was one of the first engines with fully interchangeable modules allowing easier and more flexible maintenance. Interchangeable modules save time and money by reducing spare parts requirements, engine maintenance time, and the degree of skill required by maintenance personnel. The variable stator of the J79 was also one of the most important developments with this engine. The adjustable stator vanes helped the compressor cope with the huge internal variations in airflow from take-off to high supersonic speeds. The J79 powered aircraft such as the F-104 Starfighter and F-4 Phantom. On the Convair 880 airliner, the CJ805 derivative of the J79 engine marked GE's entry into the civil airline market.

Advances in compressor, combustor and turbine knowledge in the 1960s led to a more compact core engine with a single-stage turbine and only two bearing areas versus three, resulting in the GE **F101** engine, selected for the U.S. Air Force's B-1 bomber. Utilizing the same core design as the F101, the **F110** and **F118** engine derivatives were created by adding different fan and afterburner packages to tailor engine performance to the desired aircraft application. The GE F110 engine has been the overwhelming engine choice for the F-14 and F-16 fighters as an alternative to the Pratt & Whitney **F100**, which powers every F-15 ever produced.

The GE **F404** engine powers multiple aircraft from low-level attack to high-altitude interceptors. The **RM12** for the Gripen is an adaptation of the F404 to Swedish single engine aircraft requirements. The **F414** is the U.S. Navy's newest and most advanced technology fighter engine for the F-18. It incorporates advanced technology with the proven design base of its F404 predecessor.

Pratt & Whitney's **F119** engine powers the U.S. Air Force's new air dominance fighter, the F-22. The F119 is the first production engine that features thrust vectoring, which provides the aircraft with exceptional control and maneuverability when performing knife-edge turns. The engine also features advanced stealth technology, which helps to prevent the aircraft from being detected by enemy radar. A derivative of the F119, the **F135**, will power the Lockheed Martin F-35 Joint Strike Fighter.

From the mass flow parameter of Eq. (8.8), it is seen that the areas in the engine and therefore its weight can be decreased by higher Mach numbers in the different components. The weight can also be reduced by increasing the loading in the compressors and turbines, which would decrease the number of stages. Increasing the pressure ratio per stage in the compressor from 1.3 to 1.5 decreases the number of stages from 12 to 8 for an overall pressure ratio of 25. This can be achieved by increasing the tip speed.

The weight of the engine is also directly dependent on the specific strength of the materials**. Fiber-reinforced** components can be designed for minimum weight by providing increased strength in the required direction. The material will then have to be designed together with the component instead as sequentially as with metals. Innovative designs could take advantage of the strength in one direction e.g. by building up the material in the same way as biological materials which are very strong and light-weight.

What weakens materials internally are the dislocations and the grain boundaries. In the very long term it seems possible to design **fault-free materials** with ten times the present strength for the same density compared to to-days materials. Whisker crystals are

possibly the most perfect specimen presently available. In some cases they contain no observable defects at all. Maybe such perfection could be obtained also with bulk materials by building the materials atom by atom.

To reduce the size and weight of an engine, the specific thrust, that is the thrust per mass flow, should be high. An expression for the specific thrust of the bypass engine was given in Eq. (9.19). For a straight turbojet where we let the bypass ratio go to zero and the fan temperature ratio to unity we obtain:

$$\frac{F}{\dot{m}a_0} = \sqrt{\frac{\theta_t - \theta_t / \tau_0\tau_c - \tau_0\tau_c + \tau_0)}{(\gamma-1)/2}} - M \qquad (16.1)$$

The maximum specific thrust is obtained if the compressor pressure ratio is chosen so that:

$$\tau_0\tau_c = \sqrt{\theta_t} \qquad (16.2)$$

Then at M=0:

$$\frac{F}{\dot{m}a_0} = \sqrt{\frac{2}{\gamma-1}}(\sqrt{\theta_t} - 1) \qquad (16.3)$$

It is obvious that the turbine inlet temperature is very important for the specific thrust and therefore the engine thrust-to-weight ratio. Military engines should therefore have high turbine inlet temperatures.

Inlets
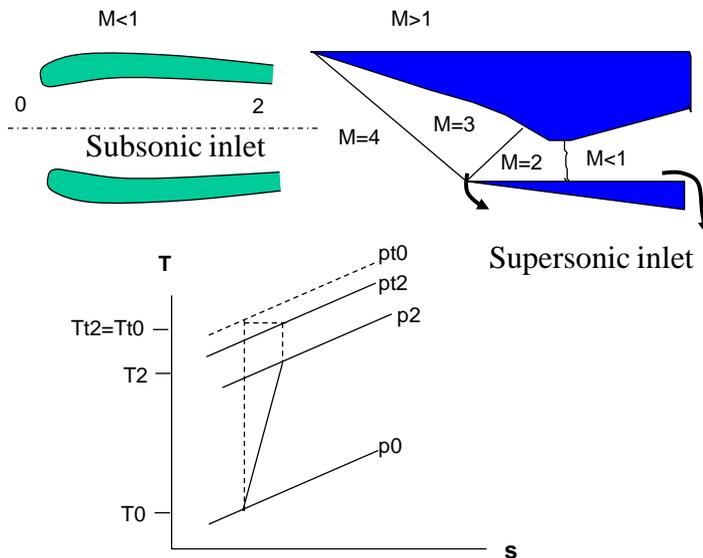
Fig. 16.3 Subsonic and supersonic inlets

One part that is different in military from civilian engines is the inlet, see Figure 16.3. The inlet is usually not part of the engine designer's responsibility but is regarded as a part of the aircraft. However, it influences very much high speed engines. The detailed design of the air intake and internal flow system determines the efficiency with which the air is delivered to the propulsion system. At all flight conditions, the entering air must be decelerated to a low-speed, high-pressure state at the engine compressor face. The air should enter the first stage of the compressor at a Mach number in the region of 0.4-0.5.

When the flight speed is supersonic, losses arise due to compression shocks. Conventional external compression inlets accomplish all of their diffusion outside of the inlet duct through several oblique shocks and a terminal normal shock located at the cowl lip. The number of oblique shocks in the inlet needs to increase with speed and to accomodate them would lead to excessive length and weight. Therefore, due to the inability to increase the number of shocks, the performance of external compression inlets rapidly deteriorates in passing Mach 2 so that higher speed requires **mixed compression inlets** performing some of the compression inside the inlet duct instead of outside.

The requirement to focus multiple oblique shock waves over a wide Mach number range also forces the adoption of two-dimensional geometry for the intake even if this results in a very serious mass penalty due to the inefficient structural design compared to a more rounded cross section.

Variable geometry would be required because at all speeds the shock waves should terminate at the lip of the engine inlet to avoid spillage as shown in Figure 16.3. With a fixed geometry, the inlet area has to be set at its largest required value to swallow the flow at each flight condition. Such an inlet will give more air flow than the engine requires at all other flight conditions. The excess air must then be dumped overboard. Because it has taken part in the compression, the dumped air has a lower momentum than it had in the freestream, which gives rise to an **inlet drag**.

Mixed compression inlets are quite susceptible to a phenomenon known as "**unstart**" or inlet instability. "Unstart" may occur if the free-stream Mach number is reduced. When a disturbance occurs

such as encountering a strong gust, the internal shock system may abruptly move upstream and reposition itself outside the inlet duct. This causes a rapid loss of thrust which may be very dangerous at extremely high speeds. To prevent this, a kind of stability control system is needed such as self-actuating bleed valves.

At low air flows and high Mach numbers, the normal shock can jump in and out of the inlet at relatively low frequencies of 10-20 Hz. This is caused by an interaction with the compressor, the airflow of which can vary very much with pressure at low speeds of rotation. To avoid this so called "**buzz**", a restriction is introduced in the control system to prevent too rapid throttling down of the engine.

The inlet shocks give rise to pressure losses as is shown in Figure 16.4. An empirical relation for the **pressure loss** in a supersonic nozzle (M>1) is according to US military specifications:

$$\frac{p_{t2}}{p_{t0}} = \pi_d = \pi_{d\max}\left[1 - 0.075(M-1)^{1.35}\right] \qquad (16.4)$$

This relation is valid for 1<Mach<4. It is shown as a dashed line in Figure 16.4 and it is seen how the number of shocks has to increase continuously with Mach number to keep down the losses. For higher speeds other relations are needed.
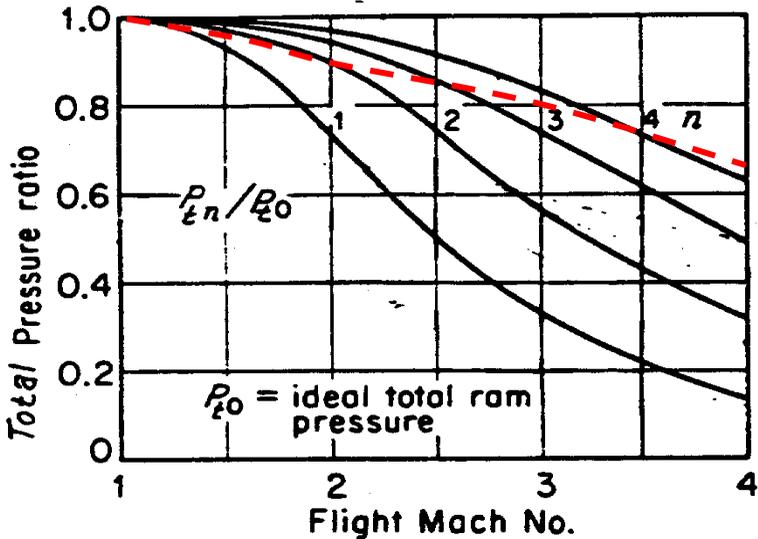
Fig. 16.4 The pressure loss in supersonic inlets

The pressure loss also increases with the angle of attack of the aircraft and the mass flow into the engine.

Inlet **distorsion** is one of the most troublesome problems with inlets, see Figure 16.5. The flow that the compressor receives from the inlet tends to be nonuniform. There may be large variations in pressure and temperature both radially and circumferentially due to e.g. separation of the flow at large angles of attack. The effect of these nonuniformities is to lower the stall margin of the compressor. The real stall margin of a combination of inlet and compressor can only be determined in test rigs. Approximate techniques consist in estimating or measuring the flow from the

inlet and representing it as a combination of radial and circumferential distortion patterns. The patterns can be simulated by inserting screens in the inlet during testing of the engine to determine the stall line.
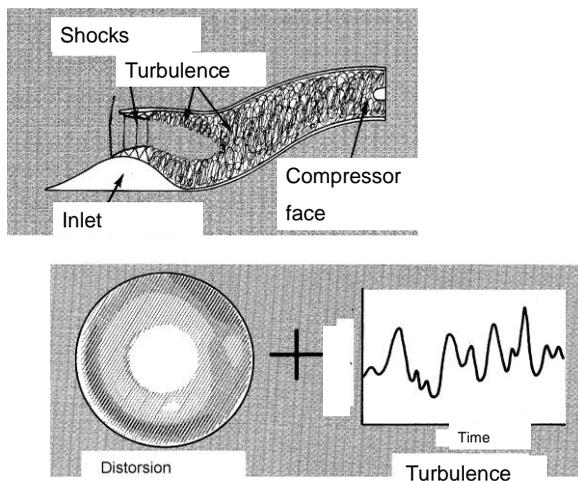
Fig. 16.5 Distorsion patterns in inlets

Afterburner and nozzle

Another important difference between a civilian and a military engine is the afterburner and the nozzle, see figure 16.6. Many military aircraft have need for a large, short-time increase in thrust to be used in such operations as takeoff, climb, acceleration, and combat maneuvers. The afterburner provides the answer to this. In an afterburner, additional fuel is injected directly into the engine exhaust and burned in the tail pipe. Thrust increases of 50 to 80 per cent are achievable by this means in modern engines, but at a large increase in fuel consumption. Afterburning is used in cases where fuel efficiency is not critical, such as when aircraft take off from short runways, and in combat, where a rapid increase in speed may occasionally be required.

The fuel flow needed to raise the temperature to the afterburner temperature can be calculated as in the main combustor as follows:

$$f_a \eta_{ba} h = (1+\alpha+f+f_a)C_{p7}(T_{t7}-298) - (1+\alpha+f)C_{p6}(T_{t6}-298)$$

$$(16.5)$$

Besides giving extra thrust, the afterburner has another very important function, namely to serve as a **mixer** for the core and bypass streams, see Figure 16.6. This greatly influences the performance of the engine and the thermodynamic design. Since the core and bypass streams eject into the same chamber, their outlet pressures are equal.
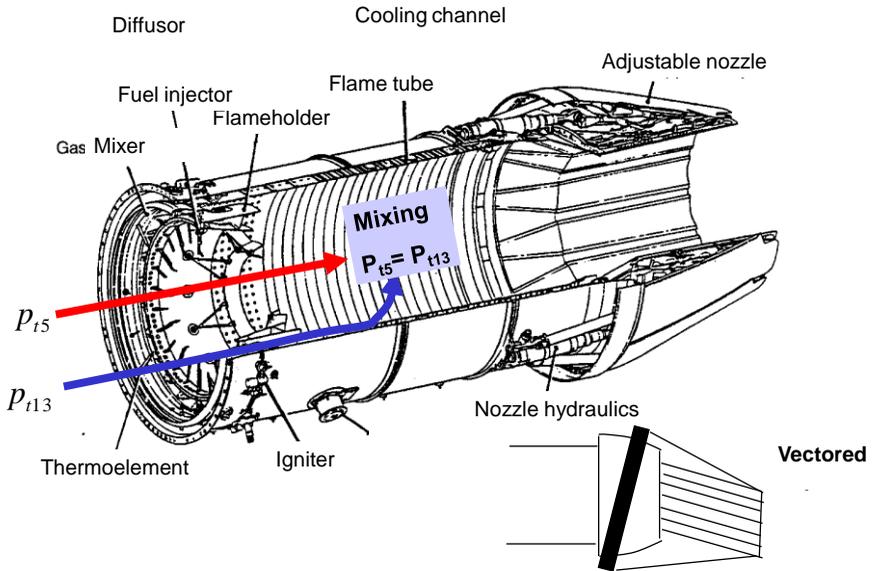
Fig. 16.6 The afterburner and nozzle distinguishes a military engine

$$p_5 = p_{13} = \frac{p_{t5}}{\left(1 + \dfrac{\gamma_t - 1}{2} M_5^2\right)^{\gamma_t/(\gamma_t - 1)}} = \frac{p_{t13}}{\left(1 + \dfrac{\gamma_c - 1}{2} M_{13}^2\right)^{\gamma_c/(\gamma_c - 1)}}$$

$$(16.6)$$

Usually, the design outlet Mach numbers are so low that for simplicity, the core and the bypass streams are assumed to mix at a common stagnation pressure so that:

$$p_{t5} = p_{t13} \qquad\qquad (16.7)$$

This relation is used to match the core and bypass streams and makes it possible to calculate the turbine exhaust temperature.

$$T_{t5} = T'_{t45} \left(\frac{p_{t5}}{p_{t45}} \right)^{(\gamma_t - 1)\eta_t / \gamma_t} = T'_{t45} \left(\frac{p_{t13}}{p_{t45}} \right)^{(\gamma_t - 1)\eta_t / \gamma_t} = T'_{t45} \left(\frac{p_{t13}}{p_{t3}} \frac{p_{t3}}{p_{t4}} \frac{p_{t4}}{p_{t45}} \right)^{(\gamma_t - 1)\eta_t / \gamma_t}$$

$$(16.8)$$

So that:

$$T_{t5} = \frac{T'_{t45}}{\left(\pi_c \pi_b \pi_{th} \right)^{\eta_t (\gamma_t - 1)/\gamma_t}} \tag{16.9}$$

The inside walls of the exit nozzle are shaped so that the exhaust gases continue to increase their velocity as they travel out of the engine. Fighter aircraft have **adjustable nozzles**, allowing the control system to adjust the nozzle to the fuel flow provided by the pilot. The higher the exit velocity of the gases, the more thrust can be generated.

The design of the exhaust system exerts a considerable influence on the performance of the engine. The cross sectional areas of the jet pipe and propelling or outlet nozzle affect turbine entry temperature, the mass flow rate, and the velocity and pressure of the exhaust jet. The use of a vectored nozzle, a thrust reverser (to help slow the aircraft on landing), a noise supressor (to quieten the noisy exhaust jet) or a variable area outlet (to improve the efficiency of the engine over a wider range of operating conditions) make for a more complex exhaust system.

The **net thrust** of the engine is:

$$F = \dot{m}(1+\alpha+f+f_a)V_9 - \dot{m}(1+\alpha)V_0 + A_9(p_9 - p_0) \quad (16.10)$$

And the **gross thrust** is:

$$F_G = \dot{m}(1+\alpha+f+f_a)V_9 + A_9(p_9 - p_0) \quad\quad (16.11)$$

Where"9" signifies the outlet plane of the nozzle and "0" ambient conditions.

Because the nozzle is choked at the throat, the highest possible jet speed would call for **a convergent-divergent** nozzle with **full expansion** i.e. $p_9 = p_0$, see Figure 16.7. For such a nozzle, the jet speed becomes:

$$V_9 = \sqrt{2C_p(T_{t7} - T_9)} \quad\quad (16.12)$$

In reality, the nozzle is not adiabatic and the flow is not axial but three-dimensional and the gas velocity close to the walls is decreased by boundary layers. This may be accounted for by introducing the isentropic **nozzle efficiency:**

$$\eta_j = \frac{T_{t7} - T_9}{T_{t7} - T_{9is}} \quad\quad (16.13)$$
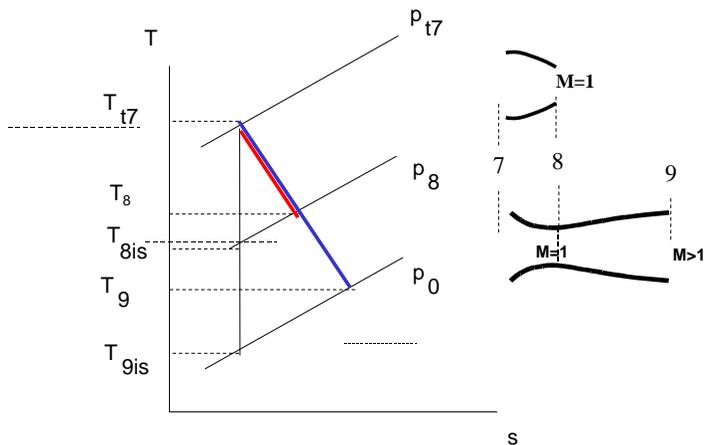
**Fig. 16.7 Expansion in a convergent-divergent
and in a convergent nozzle**

We now obtain:

$$V_9 = \sqrt{2C_p \eta_j (T_{t7} - T_{9is})} \qquad (16.14)$$

Where:

$$T_{9is} = T_{t7} \left(\frac{p_0}{p_{t7}} \right)^{\frac{\gamma-1}{\gamma}} \qquad (16.15)$$

Introducing this into Eq. (16.11), it is seen that the real gross thrust for a full expansion nozzle with $p_9 = p_0$ is the ideal thrust multiplied

with a thrust coefficient C_F , which is proportional to the square root of the nozzle efficiency. This thrust coefficient has to be found from tests with the nozzle. The isentropic nozzle efficiency should be about 0.95 and the thrust coefficient about 0.98.

When the pressure before the nozzle increases beyond a certain value the flow at the nozzle throat at station "8" reaches Mach 1.

Since:

$$\frac{T_{t7}}{T_8} = \frac{T_{t8}}{T_8} = 1 + \frac{\gamma - 1}{2} M_8^{\,2} \qquad (16.16)$$

And $M_8 = 1$ we get the critical temperature

$$T_8 = T_{t7} \frac{2}{\gamma + 1} \qquad (16.17)$$

For an isentropic expansion to the critical pressure:

$$T_{8is} = T_{t7} - \frac{T_{t7} - T_8}{\eta_j} \qquad (16.18)$$

The critical pressure is then:

$$p_8 = p_{t7} \left(\frac{T_{8is}}{T_{t7}} \right)^{\gamma/(\gamma-1)} = p_{t7} \left[1 - \frac{1}{\eta_j} \left(\frac{\gamma - 1}{\gamma + 1} \right) \right]^{\gamma/(\gamma-1)} \qquad (16.19)$$

The nozzle is cut off at station "8" and the area is obtained from:

$$A_8 = \frac{\dot{m}(1+\alpha+f+f_a)}{\rho_8 V_8} \qquad (16.20)$$

where:

$$\rho_8 = p_8 / RT_8 \qquad (16.21)$$

It may be shown that the real throat area A_8 may be obtained by multiplication of the ideal area, obtained from the mass flow parameter of Eq. (8.11), with a nozzle area coefficient, that is:

$$A_8 = C_A \frac{\dot{m}(1+\alpha)\sqrt{C_p T_{t7}}}{p_{t7}\bar{m}} \qquad (16.22)$$

Where the nozzle area coefficient depends on the isentropic nozzle efficiency as:

$$C_A = \left(\frac{2}{\gamma+1-(\gamma-1)/\eta_j}\right)^{\frac{\gamma}{\gamma-1}} \qquad (16.23)$$

For a **convergent nozzle** the exhaust plane is the throat at station 8, see Figure 16.7, where the exhaust velocity is the speed of sound at the critical temperature in the exhaust plane i.e.

$$V_9 = V_8 = \sqrt{\gamma R T_8} \qquad\qquad (16.24)$$

and where $A_9 = A_8$ and $p_9 = p_8$ in Eq. (16.11).
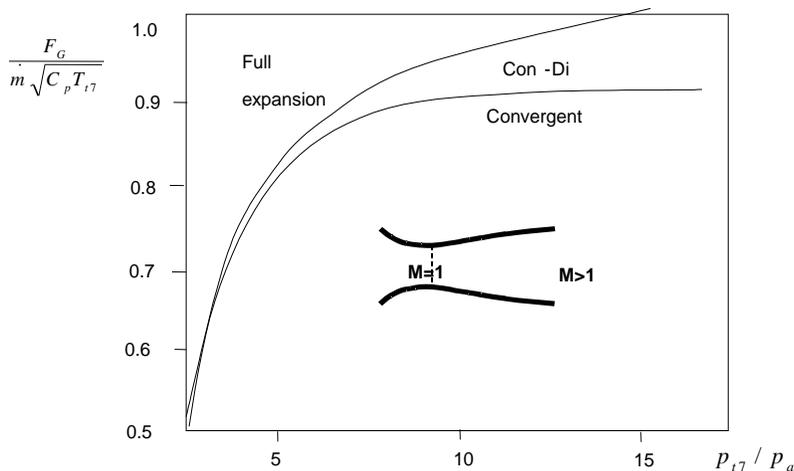
Fig. 16.8 Gross thrust from nozzles

For high speed propulsion it is not uncommon to use convergent-divergent nozzles but usually, the cost and weight is not justified. A simple **convergent nozzle** makes it easier to arrange for variable nozzle areas and thrust reversers and the lower exhaust velocity leads to lower noise levels. Even most military engines operate predominantly at subsonic conditions with only short supersonic dashes and do not need the high jet speed. It is only with engines designed for flight at Mach 2-3 that the added complexity of a convergent-divergent nozzle is motivated.

For pressure ratios over the nozzle up to about 5, experiments show that the convergent nozzle gives as much thrust as a fully expanded convergent-divergent nozzle because of the higher friction losses in the latter, see Figure 16.8.

This means that for civil engines with pressure ratios below 5, full expansion is a good approximation. For military engines with high pressure ratio, full expansion is to be strived for. Consequently, it seems that full expansion nozzles is a good approximation to use in both cases for preliminary design. The specific thrust for such a nozzle is:

$$\frac{F}{\dot{m}(1+\alpha)} = a_0 \frac{1+\alpha+f}{1+\alpha} \sqrt{\frac{2\eta_j}{\gamma_c-1} \frac{C_{pm}}{C_{pc}} \frac{T_{t6}}{T_0}\left[1-\left(p_0/p_{t6}\right)^{(\gamma_m-1)/\gamma_m}\right]} - V$$

(16.25)

Calculation scheme

A calculation scheme for a military engine is given in the Appendix 16 and described in Figure 16.9 below. The main difference from the civilian engine is the mixing of the core and bypass streams that takes place in the afterburner. As with the civil engine, this military engine has been designed for a turbine metal temperature of 1500 K and a turbine inlet temperature of 2000 K at take-off corresponding to just about 1800 K in the design point at 11 km and Mach 0.9.

Highest possible TIT=1800 K.
For a prescribed FPR.
   Make the calculations for various OPR.
   $P_{t5}= P_{t13}$ determines the temperature after the LP turbine
   BPR from the power balance of the LP shaft.
Repeat the calculations for a new FPR.

Chose a suitable combination of FPR and OPR and obtain the Specific thrust:

$$F_{s0} = \frac{F_0}{\dot{m}(1+\alpha)} = \frac{1+f+f_a+\alpha}{1+\alpha} V_j - V$$

Obtain the total mass flow from the required thrust :

$$\dot{m}_{tot} = \dot{m}(1+\alpha) = F_{req} / F_{s0}$$

Fig. 16.9 The calculation scheme (Appendix 16)

The polytropic efficiency of the fan is assumed to be 0.90, of the HP compressor 0.90 and of the turbines 0.88. Those values are

representative for present best technology. The afterburner temperature is assumed to be 2200 K. For simplicity we will assume that $\gamma_c =1.4$ corresponding to a specific heat of 1005 J/kgK before the combustor and $\gamma_t =1.3$ corresponding to a specific heat of 1244 J/kgK after the combustor. In reality γ would vary with the temperature in the different parts of the engine. The gas constant is R=287 J/kgK.

Note that:

- The compressor outlet temperature is well below the restriction of 875 K for the compressor outlet temperature for titanium materials.
- When the fan and core pressure ratios are known, the bypass ratio is immediately obtained. If a certain bypass ratio is required, an iteration is needed from this point.
- The non dimensional specific thrust with afterburner is nearly twice as much as without afterburner. However, the efficiency is very low at 10%.

The choice of the engine parameters Overall Pressure Ratio (OPR), Fan Pressure Ratio (FPR) and Bypass Ratio (BPR) is somewhat arbitrary. To make such a choice, the calculations must be carried out for different values of those parameters. The results of such calculations are shown below.

The general behaviour of the specific thrust and the thermal efficiency with overall and fan pressure ratio is shown in Figure 16.10 for a Mach 0.9 engine.
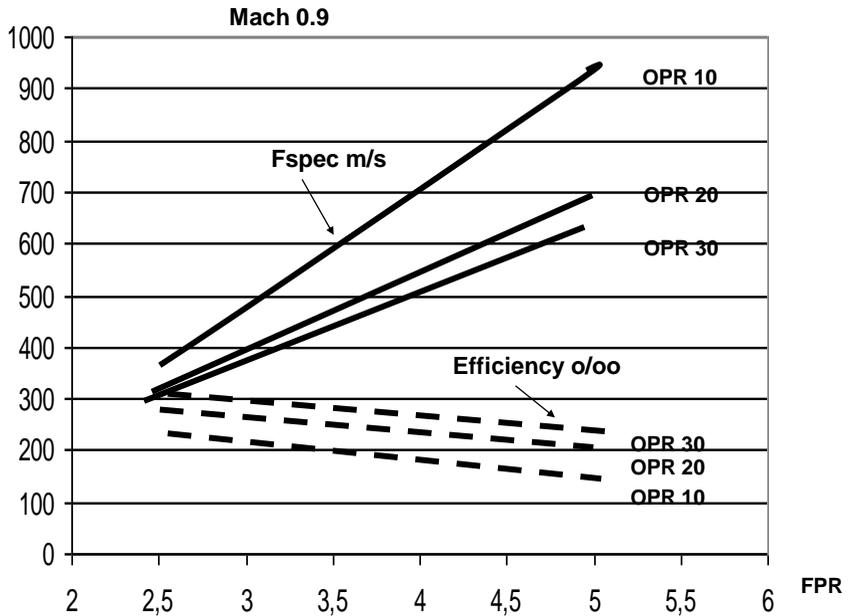
Fig. 16.10 Specific thrust and efficiency versus OPR and FPR

As is seen the FPR and the OPR must be found as a compromise between the wish to have a high specific thrust while also avoiding a low efficiency so as to limit the fuel weight that has to be carried in a mission. One way to weigh this is to use the relative propulsion system weight (the summary of engine and fuel weight).

It is then seen that for long distance aircraft such as commercial airliners, a low fuel consumption, that is a high efficiency, is the dominant requirement while for military aircraft, a low engine weight will be more important.   .

This is the reason for selecting high specific thrust and therefore, as is evident from Figure 16.10, a lower OPR in military engines compared to civilian ones. A high specific thrust engine passes a smaller amount of air and therefore has a lower weight than a low specific thrust engine. It also gives a larger increment in kinetic energy to the air. Therefore, the loss in stagnation pressure in the inlet is proportionally lower, which makes such engines preferable at supersonic speeds where the inlet shock losses are high. The reduction in thrust with forward speed is usually referred to as **thrust lapse** and it is less when the jet speed, that is the specific thrust, is high.

The compressor outlet temperature will increase with Mach number and OPR. To avoid overheating the compressor, the OPR has to be lower for high speed engines. Also, the curves in Figure 16.10 are shifted upwards to higher specific thrusts with Mach number but their shape stays approximately the same, see Figure 16.11. Therefore, a high specific thrust can be achieved with less OPR for higher Mach numbers. For the present design we will chose OPR=30 for the combat engine at Mach 0.9 and OPR=20 for the supercruise engine at Mach 1.5.

Both the combat and supercruise engines have high FPR compared to a civilian engine. This follows from the requirement for high specific thrust in military engines. It is seen from Figure 16.11 that the specific thrust increases significantly with FPR while the efficiency decreases only to a small extent. However, the fan should have **few stages**, typically not more than three. For low speeds one could expect a stage pressure ratio of around 1.6. This restricts the fan pressure ratio to below about 5.

In practise one should chose a lower FPR than that both in the supercruise and the combat engine. As is seen from Figure 16.11, a lower FPR means a somewhat higher efficiency, that is a lower fuel consumption, and this is important in supercruise.
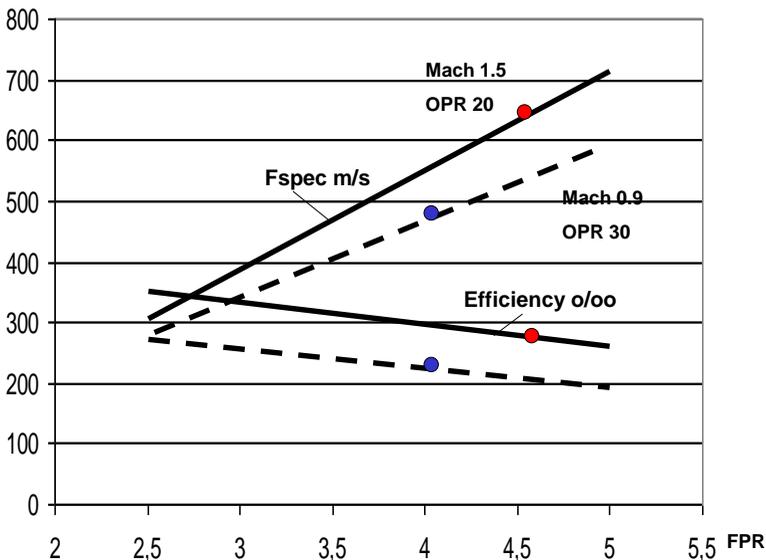
Fig. 16.11 Specific thrust and efficiency versus FPR for different Mach numbers

There is also a trade-off between the FPR and the BPR. Typical variations of fan pressure and bypass ratio are shown in Figure 16.12 below. As the fan pressure ratio is decreased, the bypass ratio is increased and the boost in thrust with afterburning increases. This is important for the combat engine.

As a compromise, we have chosen FPR=4 for the supercruise engine and 4.5 for the combat engine. It is natural to chose a somewhat lower FPR in the supercruise engine because with its lower OPR should also follow a lower FPR. Compared to civilian engines the FPR is high and the BPR is low.
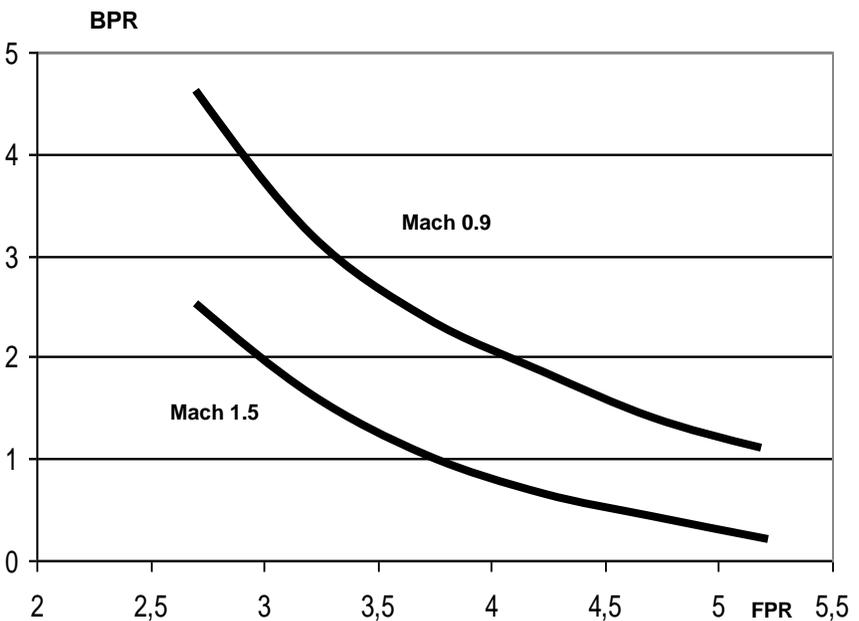
Fig. 16.12 The bypass ratio decreases with fan pressure ratio

The data for the two military engines resulting from Appendix 16 are shown below. It is seen that the combat engine is significantly more powerful than the supercruise engine.

	Combat	Supercruise
Dry thrust	35.2 kN	28.6 kN
A/B thrust	75.5 kN	58.1 kN
FPR	4	4.5
OPR	30	20
BPR	1.18	0.58
Mass flow	61.2	47.1
Diameter	1.15 m	0.73 m

Comparing combat and supercruise engines

Ex 16.1
What is the specific excess power with afterburner (the maximum rate of climb) for the military engine of Appendix 15 at Mach 0.9?

Appendix 16

Military engine design calculations
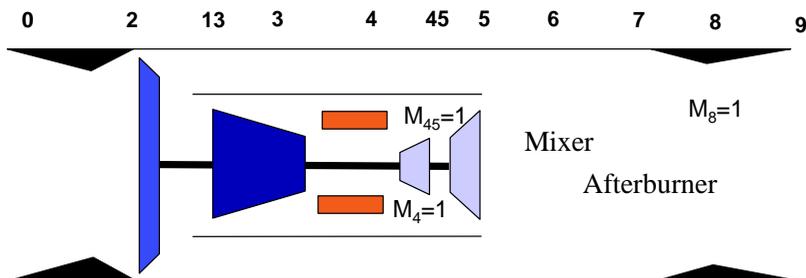
The indata to the calculations are:

Ambient temperature at 11 km T_0 K	216	216
D:o pressure p_0 Pa	2.27E+04	2.27E+04
Adiabatic constant in cold parts γ_c	1.4	1.4
Fan polytropic efficiency η_f	0.9	0.9
Compressor polytropic efficiency η_c	0.9	0.9
Turbine metal temperature T_m K	1500	1500

Turbine Inlet Temperature T_{t4} K	1800	1800
Combustor efficiency η_b	1	1
Fuel heating value h J/kg	4.30E+07	4.30E+07
Specific heat in cold parts C_{pc}	1005	1005
D:o hot parts C_{pt}	1244	1244
Adiabatic constant in hot parts γ_t	1.3	1.3
Turbine polytropic efficiency η_t	0.88	0.88
Nozzle efficiency η_j	0.95	0.95
Afterburner combustion efficiency η_a	0.9	0.9
Specific heat in afterburner C_{pa}	1450	1450
Afterburner temperature T_{ta} K	2200	2200
Pressure recovery in combustion chamber π_b	0.95	0.95
Pressure recovery in afterburner π_b	0.95	0.95
Dry thrust F kN	3.52E+04	2.86E+04
Mach number M	0.9	1.5
Fan pressure ratio π_f	4.5	4
Overall Pressure Ratio π	30	20

A summary of the calculation scheme is given below for Mach 0.9 and 1.5.

Mach	0.9	1.5
Stagnation temperature ratio $\tau_0 = 1 + \dfrac{\gamma_c - 1}{2} M^2$	1.162	1.45
Stagnation pressure ratio $\pi_0 = \tau_0^{\gamma_c/(\gamma_c-1)}$	1.69	3.67
Pressure coefficient in inlet π_d	0.97	0.95
Temperature coefficient in inlet τ_d	1	1
Inlet temperature $T_{t2} = \tau_0 T_0$	251	313
Inlet pressure $p_{t2} = \pi_0 \pi_d p_0$	3.72 E+04	7.93 E+04
Fan pressure $p_{t13} = \pi_f p_{t2}$	1.68 E+05	3.17 E+05
The temperature ratio for the fan $\tau_f = \pi_f^{(\gamma_c-1)/\gamma_c \eta_f}$	1.61	1.55
The temperature after the fan $T_{t13} = \tau_f T_{t2}$	404	486
The pressure ratio of the core compressor $\pi_c = \pi / \pi_f$	6.66	5
Pressure at the compressor outlet $p_{t3} = \pi_c p_{t13}$	1.12 E+06	1.59 E+06
Compressor temperature ratio $\tau_c = \pi_c^{(\gamma_c-1)/\gamma_c \eta_c}$	1.82	1.66
Compressor outlet temperature $T_{t3} = \tau_c T_{t13}$	739	810

Cooling efficiency $\phi = \dfrac{T_{t4} - T_w}{T_{t4} - T_0 \tau_f \tau_c}$ at $T_{t4} = 2000$, $T_w = 1500$, $T_0 = 288$	0.43	0.4
The amount of cooling air $\varepsilon = \dfrac{\dot{m}_c}{\dot{m}} = 0.05 + 0.05 \dfrac{T_{t4\max} - T_m}{T_m - T_{sls} \tau_f \tau_b \tau_c}$	0.088	0.083
The fuel flow $f = \left[(1 + f - \varepsilon)C_{pt}(T_{t4} - 298) - C_{pc}(1 - \varepsilon)(T_{t3} - 298)\right]/\eta_b h$	0.032	0.03
The **power balance** with the HP compressor and HP turbine gives the temperature after the HP turbine from $T_{t45} = T_{t4} - \dfrac{1}{(1 + f - \varepsilon)} \dfrac{C_{pc}}{C_{pt}}(T_{t3} - T_{t13})$	1514	1523
HP turbine pressure ratio $\pi_{th} = \dfrac{p_{t45}}{p_{t4}} = \left(\dfrac{T_{t45}}{T_{t4}}\right)^{\gamma_t/(\gamma_t - 1)\eta_t}$	0.43	0.44
Pressure after the combustor $p_{t4} = \pi_b p_{t3}$	1.06 E+06	1.51 E+06
The pressure after the HP turbine $p_{t45} = \pi_{th} p_{t4}$	4.52 E+05	6.63 E+05
The cooling air is mixed in at constant pressure which gives the temperature after the turbine as $T'_{t45} = \dfrac{\varepsilon}{1 + f} \dfrac{C_{pc}}{C_{pt}} T_{t3} + \dfrac{1 + f - \varepsilon}{1 + f} T_{t45}$	1435	1453

Pressure after LP turbine $p_{t5} = p_{t13}$	1.68 E+05	3.17 E+05
Temperature after LP turbine $$T_{t5} = \frac{T'_{t45}}{\left(\pi_c \pi_b \pi_{th}\right)^{\eta_t (\gamma_t - 1)/\gamma_t}}$$	1173	1238
The **power balance over the LP shaft gives the bypass ratio** $\alpha = (1+f)\dfrac{C_{pt}}{C_{pc}}\dfrac{T'_{t45} - T_{t5}}{T_{t13} - T_{t2}} - 1$	1.18	0.58
The mean specific heat of the exhaust stream is obtained from a simple mass weighting $(1+\alpha+f)C_{pm} = (1+f)C_{pt} + \alpha C_{pc}$ This gives $\gamma_m = 1.34$.	1117	1158
Downstream of the LP turbine the core and the bypass stream mix at constant pressure $p_{t6} = p_{t5} = p_{t13}$	1.68 E+05	3.17 E+05
The mixed temperature $$T_{t6} = T_{t5}\frac{C_{pt}}{C_{pm}}\frac{1+f}{1+\alpha+f} + T_{t13}\frac{C_{pc}}{C_{pm}}\frac{\alpha}{1+\alpha+f}$$	804	1003
Without afterburner, the jet speed is with an ideal convergent-divergent nozzle $$V_j = \sqrt{2\eta_j C_{pm} T_{t6}\left[1 - \left(p_0/p_{t6}\right)^{(\gamma_m-1)/\gamma_m}\right]}$$	828	1029
The speed of sound at 11 km $a_0 = \sqrt{\gamma_c R T_0} = \sqrt{(\gamma_c - 1)C_{pc} T_0}$ The flight speed is 265 m/s at Mach 0.9.	295	295

The specific thrust $$\frac{F}{\dot{m}(1+\alpha)} = a_0 \frac{1+\alpha+f}{1+\alpha} \sqrt{\frac{2\eta_j}{\gamma_c - 1} \frac{C_{pm}}{C_{pc}} \frac{T_{t6}}{T_0} \left[1 - \left(p_0/p_{t6}\right)^{(\gamma_m - 1)/\gamma_m}\right]} - V$$	575	606
The efficiency of the engine is $\eta = \dfrac{FV}{f\dot{m}h}$	0.25	0.33
Total mass flow $\dot{m}_{tot} = F_{dry}/F_s$	61.2	47.1
Core mass flow $\dot{m} = \dot{m}_{tot}/\alpha$	28.1	29.8
Fuel flow in afterburner $f_a = \left[(1+\alpha+f+f_a)C_{pa}(T_{ta}-298) - (1+\alpha+f)C_{pm}(T_{t6}-298)\right]/\eta_{ba}h$	0.13	0.09
The conditions in the afterburner is nearly stoichometric so the specific heat is 1450 J/kg K and $\gamma_a = 1.25$.		
Pressure in the afterburner $p_{ta} = \pi_a p_{t5}$	1.59 E+05	3.01 E+05
The jet speed with afterburner $$V_j = \sqrt{2\eta_j C_{pa} T_{ta} \left[1 - \left(p_0/p_{ta}\right)^{(\gamma_a - 1)/\gamma_a}\right]}$$	1392	1558
The specific thrust with afterburner $$\frac{F}{\dot{m}(1+\alpha)} = a_0 \frac{1+\alpha+f+f_a}{1+\alpha} \sqrt{\frac{2\eta_j}{\gamma_c - 1} \frac{C_{pa}}{C_{pc}} \frac{T_{ta}}{T_0} \left[1 - \left(p_0/p_{ta}\right)^{(\gamma_a - 1)/\gamma_a}\right]} - V$$	1234	1232
Thrust with afterburner $F = \dot{m}_{tot} F_{fs}$	7.55 E+04	5.81 E+04

The inlet area may be found from the equation: $$\frac{\dot{m}(1+\alpha)\sqrt{C_p T_{t2}}}{A p_{t2}} = \frac{\gamma}{\sqrt{\gamma-1}} M_i \left(1+\frac{\gamma-1}{2} M_i^{\,2}\right)^{-(\gamma+1)/2(\gamma-1)}$$ Assuming a Mach number of 0.7	$A_{in}=$ 1.03 D=1.14	$A_{in}=$ 0.42 D=0.73
The critical turbine and nozzle areas are: $$A = \frac{\dot{m}\sqrt{C_p T_t}}{p_t \overline{m}}$$ where $$\overline{m} = \frac{\gamma}{\sqrt{\gamma-1}}\left(\frac{2}{\gamma+1}\right)^{\frac{\gamma+1}{2(\gamma-1)}}$$ Note that the coolant and fuel flows must be taken into account when calculating the areas.	$A_4=$ 0.027 $A_{45}=$ 0.062	$A_4=$ 0.02 $A_{45}=$ 0.045
Nozzle area coefficient: $$C_A = \left(\frac{2}{\gamma+1-(\gamma-1)/\eta_j}\right)^{\frac{\gamma}{\gamma-1}}$$ Nozzle areas:	$C_A=$ 1.035 $A_{8dry}=$ 0.27 $A_{8ab}=$ 0.48	$C_A=$ 1.035 $A_{8dry}=$ 0.12 $A_{8ab}=$ 0.20

The LP-turbine decides the core exhaust Mach number to be $M_5 = 0.3\text{-}0.4$. The bypass Mach number is: $$M_{13} = \sqrt{\frac{2}{\gamma_c - 1}\left\{\left[\frac{p_{t13}}{p_{t5}}\left(1 + \frac{\gamma_t - 1}{2}M_5^2\right)^{\frac{\gamma_t}{\gamma_t - 1}}\right]^{\frac{\gamma_c - 1}{\gamma_c}} - 1\right\}}$$	0.39	0.39
The areas can then be obtained as above using the following mass flow parameter: $$\overline{m} = \frac{\gamma}{\sqrt{\gamma - 1}}M\left(1 + \frac{\gamma - 1}{2}M^2\right)^{-(\gamma + 1)/2(\gamma - 1)}$$	$A_{13} =$ 0.16	$A_{13} =$ 0.05

17. OFF DESIGN AND VARIABLE CYCLES

In on-design all design choices are free to be selected and the corresponding performance may then be determined. In off-design the design choices have already been made and the performance is to be found. Assuming that the engine is operating with the same pressure ratios as at the design point, relatively simple expressions give the performance of the engine but outside of the design pressure ratios, more complicated relations must be found.

Once the engine has been designed, one wants to know how it will work outside of the design conditions. The engine for a military aircraft is required to operate over a much wider range of conditions than a civilian engine. Figure 17.1 shows the throttle settings of a typical military operating cycle and the influence the take-off and full throttle transients have on the life of the engine. For the engines intended for subsonic civil transport the range of operating conditions is relatively small, but for military engines the performance may be critical at widely different operating points. The objective of the off-design analysis is to estimate an engine's performance at conditions different from the design point either in altitude and flight speed or in power setting. The off-design performance of different engines can then be compared to find the engine cycle that is best suited to the specified operating envelope.
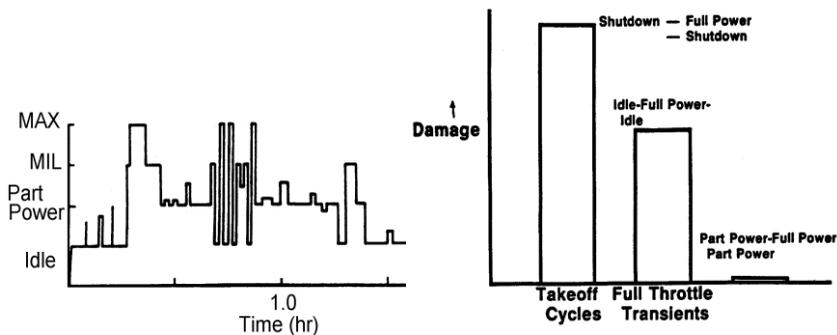
Fig. 17.1 The operating cycle of a military engine

When designing the engine for a specified set of inlet conditions and thrust requirements, it is given specific values of mass flows and pressure ratios. This defines the so called "design point" in the fan and compressor maps, see Figure 17.2 below.

The compressors are the most sensitive parts of the engine. Operation outside of the design point can lead to problems with low efficiency and flow separation. Operating the engine at the design point makes it possible to find relatively simple expressions for the performance of the engine. This is especially interesting for civilian engines because they tend to operate close to the "design point".

The fuel consumption is:

$$\dot{m}_f = f\dot{m} \qquad (17.1)$$

Since the high pressure turbine inlet is choked, we obtain:

$$\bar{m}_4 = \dot{m}_4 \frac{A_4\sqrt{C_{pt}T_{t4}}}{p_{t4}} = \dot{m}(1+f)A_4\sqrt{C_{pt}}\frac{p_{t13}}{p_{t4}}\sqrt{\frac{T_{t4}}{T_{t2}}}\sqrt{\frac{T_{t2}}{T_{t13}}}\frac{\sqrt{T_{t13}}}{p_{t13}} \qquad (17.2)$$

or since $p_{t4}=p_{t3}$ and using Eq. (11.7):

$$\bar{m}_4 = \sqrt{\frac{T_{t4}}{T_{t2}}}\left\{(1+f)A_4\sqrt{C_{pt}}\left(\frac{p_{t2}}{p_{t13}}\right)^{\frac{\gamma-1}{2\eta\gamma}}\frac{p_{t13}}{p_{t3}}\frac{\dot{m}\sqrt{T_{t13}}}{p_{t13}}\right\} \qquad (17.3)$$

The engine is said to be operating at its **design point** if both the fan and the compressor operate at a constant point in the fan and compressor maps, see Figure 17.2 below. Furthermore "f" is a small quantity. In this case, the expression within the brackets is a constant so that at the design point T_{t4}/T_{t2} remains constant.
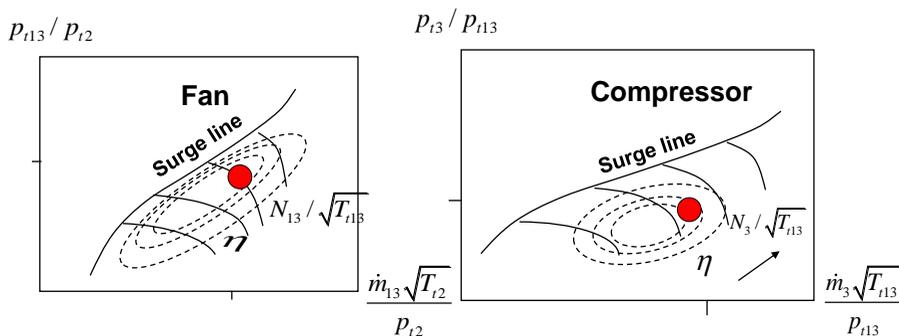
Fig. 17.2 Operating at the design point

The relative fuel flow, f is obtained from:

$$f\eta_b h = (1-\varepsilon)C_{pt}(T_{t4}-298) - C_{pc}(1-\varepsilon)(T_{t3}-298) \quad (17.4)$$

It follows that in the design point where the compressor temperature ratios and T_{t4}/T_{t2} are constant:

$$f \propto T_{t2} \qquad (17.5)$$

and we also obtain from Eq. neglecting the small fuel flow f:

$$\dot{m}_f = f\dot{m} \propto T_{t2}\frac{p_{t4}}{\sqrt{T_{t4}}} = T_{t2}\frac{p_{t3}}{p_{t2}}\sqrt{\frac{T_{t2}}{T_{t4}}}\frac{p_{t2}}{\sqrt{T_{t2}}} \propto p_{t2}\sqrt{T_{t2}} \quad (17.6)$$

The gross thrust with a full expansion nozzle is the mass flow times the jet speed or neglecting the fuel flow using Eq. (16.25):

$$F_G = \dot{m}(1+\alpha)\sqrt{2\eta_j C_{pm}T_{t6}\left[1-\left(p_0/p_{t6}\right)^{(\gamma_m-1)/\gamma_m}\right]} \quad (17.7)$$

Where in the fan design point:

$$\dot{m}_{13} = \dot{m}(1+\alpha) \propto \frac{p_{t2}}{\sqrt{T_{t2}}} \quad (17.8)$$

It is then seen that the bypass ratio is a constant at the design point because:

$$1+\alpha = \frac{\dot{m}_{13}}{\dot{m}} \propto \frac{p_{t2}}{\sqrt{T_{t2}}}\frac{\sqrt{T_{t4}}}{p_{t4}} = const \quad (17.9)$$

From the power balances of the shafts it then follows that T_{t6} is a linear combination of the inlet temperature, the fan and compressor temperatures and the turbine inlet temperature so that:

$$\frac{T_{t6}}{T_{t2}} = k_1 + k_2\frac{T_{t13}}{T_{t2}} + k_3\frac{T_{t3}}{T_{t2}} + k_4\frac{T_{t4}}{T_{t2}} = const \quad (17.10)$$

while:

$$p_{t6} = p_{t5} = p_{t13} \tag{17.11}$$

It can now be seen that the nozzle area is kept constant in the design point because from Eq. (16.22):

$$A_8 = C_A \frac{\dot{m}(1+\alpha)\sqrt{C_p T_{t6}}}{p_{t7}\bar{m}} \propto \frac{p_{t2}}{\sqrt{T_{t2}}} \frac{\sqrt{T_{t6}}}{p_{t13}} = const \tag{17.12}$$

We finally get for the gross thrust:

$$F_G \propto \frac{p_{t2}}{\sqrt{T_{t2}}} \sqrt{T_{t2} \frac{T_{t6}}{T_{t2}} \left[1 - \left(\frac{p_0}{p_{t2}} \frac{p_{t2}}{p_{t13}} \right)^{(\gamma_m - 1)/\gamma_m} \right]} \propto p_0 \frac{p_{t2}}{p_0} \sqrt{\left[1 - \left(\frac{p_0}{p_{t2}} \frac{1}{\pi_f} \right)^{(\gamma_m - 1)/\gamma_m} \right]} \tag{17.13}$$

From these equations the gross thrust and the ram drag and therefore the net thrust can be obtained in the design point for different Mach numbers. Especially, it is possible to calculate the take-off thrust in the design point when the thrust at altitude is known. It can be seen from Eq. (17.13) that the thrust will decrease as the pressure falls with increasing altitude and that it increases with the stagnation pressure ratio, that is with speed. Note that if the nozzle is designed for altitude it expands to a pressure which is below ambient SLS pressure. There is therefore a back pressure

force acting on the exhaust area, which must be subtracted from the gross thrust.

For a given Mach number, T_{t2} is directly proportional to T_0 and p_{t2} to p_0. It is therefore possible to calculate the fuel consumption and the thrust of an engine **for a certain Mach number** at different altitudes if the engine is operating in the design point. The relations are simply:

$$\dot{m}_f \propto p_0 \sqrt{T_0} \tag{17.14}$$

$$\dot{m}_{tot} \propto \frac{p_0}{\sqrt{T_0}} \tag{17.15}$$

$$F = F_G - \dot{m}_{tot} V \propto p_0 \tag{17.16}$$

Note from Eq. (17.16) that even if the gross thrust increases with speed as indicated in Eq. (17.13), the real thrust will sooner or later start to fall because of the increasing inlet momentum.

The turbine is one of the most critical parts in the engine and the turbine inlet temperature determines its life to a large extent. Even if the engine is operating at the design point where T_{t4}/T_{t2} is a constant, the turbine inlet temperature may vary considerably due to variations in the inlet stagnation temperature T_{t2}. For a civilian aircraft, T_{t2} changes relatively little between take-off, climb and cruise but for a military Mach 2 aircraft it may vary between 200 to 400 K. To avoid excessive turbine inlet temperatures at high speed, the engine must be throttled down, leaving the design point. Sometimes, it may also be necessary to operate the engine at higher than the design turbine temperatures. Especially for a

military engine, it is therefore of interest to know how it will behave at conditions different from the design point or what happens if the fuel flow is varied so that T_{t4}/T_{t2} is no longer constant.

Off-design analysis differs from that of on-design. In on-design all design choices are free to be selected and the corresponding performance may then be determined. In off-design the design choices have already been made. The performance of this specific engine is then to be found at flight conditions, throttle settings and nozzle settings other than the design point.

Ideally, an off-design performance analysis should be based on the individual component characteristics obtained from hardware testing. In a preliminary design phase such characteristics do not exist and simplifying assumptions must be made. Typical assumptions are, see Figure 17.3:

- The flow is choked at the high and low pressure turbine inlets and at the exhaust nozzle.
- The component efficiencies and gas properties do not change from their design values.
- Cooling air fractions remain at their design values.

The military turbofan with mixed exhausts is a more complicated case than with separate exhausts as are usual in civil engines. The reason is that with mixed exhausts the balance of flow between the core and the bypass is unknown while with separate exhausts there is a relation between the jet speeds that gives maximum power. However, the process may be significantly simplified by making use of parameters that changes only slightly with varying conditions. Such a method is used here. A complete set of

equations for the performance in supercruise at Mach 1.5 of the engine designed for 3g turns at Mach 0.9 at 11000 m is given in the Appendix 17.

Fuel flow

Choking turbines   Choking nozzle
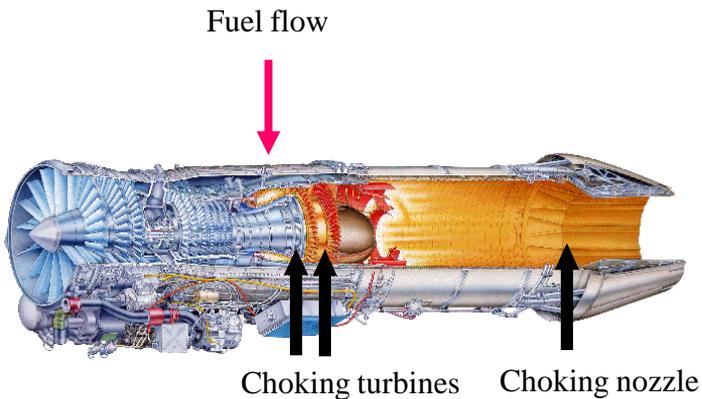
Fig. 17.3 Parameters influencing off-design behavior

The area of the exhaust nozzle is the only adjustable area in the engine and is used to control it together with the fuel setting. The engine will.find the rotor speeds and pressure ratios corresponding to the nozzle setting and the fuel flow. However, the calculations will be easier if we assume a fan pressure ratio and calculate the corresponding.nozzle area. If we want to obtain a specific nozzle area, a reiteration could be made wuth a new fan pressure ratio.

The method we are going to use to calculate off-design behavior is based on the fact that the inlet guide vanes of the turbines behave as choked nozzles with sonic flow at the throat so that for each turbine:

$$\frac{\dot{m}\sqrt{C_p T_{ti}}}{p_{ti} A_i} = \frac{\gamma}{\sqrt{\gamma - 1}} \left(\frac{2}{\gamma + 1} \right)^{\frac{\gamma + 1}{2(\gamma - 1)}} \qquad (17.17)$$

We have assumed before that γ is the same for both turbines and therefore:

$$\frac{\dot{m}_4 \sqrt{T_{t4}}}{p_{t4} A_4} = \frac{\dot{m}_5 \sqrt{T'_{t45}}}{p_{t45} A_{45}} \qquad (17.18)$$

With $\dot{m}$ as the inlet core mass flow and with the coolant air fraction ε:

$$\dot{m}_4 = \dot{m}(1 + f - \varepsilon) \qquad (17.19)$$

$$\dot{m}_5 = \dot{m}(1 + f) \qquad (17.20)$$

$$\frac{p_{t45}}{p_{t4}} = \frac{A_4}{A_{45}} \frac{1 + f}{1 + f - \varepsilon} \sqrt{\frac{T'_{t45}}{T_{t45}}} \sqrt{\frac{T_{t45}}{T_{t4}}} \qquad (17.21)$$

But now:

$$\pi_{th} = \frac{p_{t45}}{p_{t4}} = \left(\frac{T_{t45}}{T_{t4}}\right)^{\gamma_t/(\gamma_t-1)\eta_t} \qquad (17.22)$$

so it follows that the temperature ratio over the high pressure (HP) turbine is obtained from:

$$\left(\frac{T_{t45}}{T_{t4}}\right)^{\gamma_t/(\gamma_t-1)\eta_t-1/2} = \frac{A_4}{A_{45}} \frac{1+f}{1+f-\varepsilon} \sqrt{\frac{T'_{t45}}{T_{t45}}} \qquad (17.23)$$

Since the coolant flow is small, the ratio between temperatures after the HP turbine before and after mixing is near unity. It follows that the temperature ratio over the HP turbine is nearly a constant that is significant for the engine and can be calculated from design values. We may therefore introduce the constant "K" so that:

$$T_{t4} - T_{t45} = (1 - \frac{T_{t45}}{T_{t4}})T_{t4} = KT_{t4} \qquad (17.24)$$

In the first approximation, K can be obtained from the design point:

$$K \cong (1 - \frac{T_{t45}}{T_{t4}})_{des} \qquad (17.25)$$

All the temperatures and pressures may now be calculated as described in Appendix 17. The power of the engine is controlled

by varying the fuel flow. However, it is easier to vary the turbine inlet temperatire and then to calculate the corresponding fuel flow. The fuel flow corresponding to the assumed turbine inlet temperature may now be obtained from a heat balance over the combustor.

All the temperatures and pressures may now be found for a prescribed turbine inlet temperature T_{t4}. The power of the engine is controlled by varying the fuel flow. However, it is easier to vary the turbine inlet temperature and then to calculate the corresponding fuel flow.

Note that when designing the engine, the Mach number in the bypass canal and in the LP turbine exhaust were chosen so as to make the total pressures equal. In off-design behavior, the Mach numbers will deviate from those values and therefore the total pressures will be different while the static pressures will be the same. To simplify the treatment we will, however, continue to assume that the stagnation pressures in the core and bypass canals are equal, that is $p_{t5} = p_{t13}$. The error is not significant as long as the Mach numbers are relatively small. This may not be the case when the engine is pushed to its limits and in such cases it will be necessary to consider the mixing of the two streams in more detail. This will be described in Chapter 18.

Note that the Mach number in the bypass canal changes to accommodate the flow as long as the bypass canal is unchoked.

The core mass flow through the engine and the bypass ratio remains the same independently of the conditions in the nozzle or whether the afterburner is on or not. To adapt to the airflow, the

nozzle area must vary roughly in proportion to the square root of the temperature before the nozzle, see Eq. (17.12).
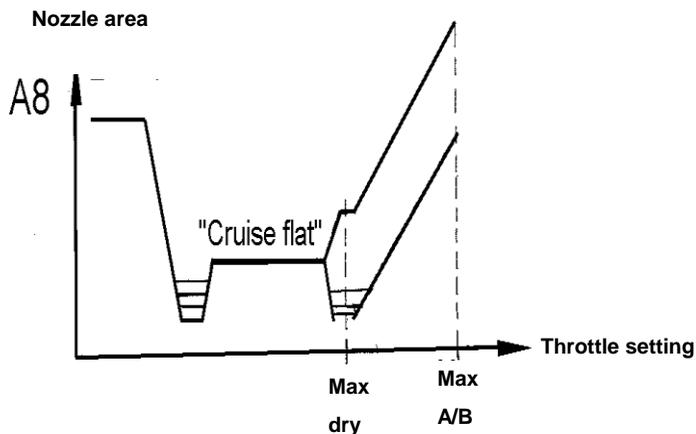
Fig. 17.4 Variation in the nozzle area

We started out assuming a FPR and the final result is a nozzle area that adapts to the resulting mass flow. If we want to obtain a specific nozzle area, a reiteration could be made with a new assumed fan pressure ratio. In this way the nozzle area is used to control the engine. The engine will find the fan rotor speed that corresponds to the nozzle setting and the fuel flow.

When the afterburner is used the nozzle opens up, see Figure 17.4, to ensure that the pressure in the afterburner is the same as the fan pressure.

The equations given before are used to predict the off-design performance of a military engine in Appendix 17. This approach with constant component efficiencies is adequate for preliminary design. However, for detailed design it is usual industrial practice to use "component maps" or "**characteristics**" to increase the accuracy of the results. The preliminary design of the engine is used as indata for the first lay-out of the components such as compressors and turbines. The behavior of the components under different operating conditions and also what limitations there are to their use can then be predicted and used in design and off-design calculations of the engine to increase the accuracy of the design process.

The behavior of the jet engine components under varying operating conditions is the most difficult problem in engine design. The turbine is relatively insensitive to varying flow conditions. It is therefore the fan and compressor that are of most interest.

To understand how a jet engine behaves off-design, it is instructive to study the simple straight turbojet consisting of a compressor and a turbine on a single shaft. The equations governing what happens in the compressor of such an engine can be obtained from the previous equations for the turbofan if the fan is neglected and the nozzle is used as the second choked area instead of the inlet to the low pressure turbine. Neglecting the fuel and coolant flows and the variation of specific heat with temperature, we obtain for the temperature rise in the compressor from Eq. (17.24):

$$T_{t3} = T_{t2} + KT_{t4} \qquad\qquad (17.26)$$

$$\pi_c = (\frac{T_{t3}}{T_{t2}})^{\eta_c \gamma/(\gamma-1)} = (1 + K \frac{T_{t4}}{T_{t2}})^{\eta_c \gamma/(\gamma-1)} \qquad (17.27)$$

$$\frac{T_{t4}}{T_{t2}} = (\pi_c^{(\gamma-1)/\gamma \eta_c} - 1)/K \qquad (17.28)$$

where from Eqs. (17.23) and (17.24) neglecting fuel and cooling air flows and with A_8 as the choked area downstream of the turbine.:

$$(1-K)^{\gamma/(\gamma-1)\eta_t - 1/2} = \frac{A_4}{A_8} \qquad (17.29)$$

From which:

$$K = 1 - \left(\frac{A_4}{A_8} \right)^{1/n} \qquad (17.30)$$

where

$$n = \gamma/(\gamma-1)\eta_t - 1/2 \qquad (17.31)$$

The mass flow through the choked turbine is:

$$\dot{m} = A_4 \frac{p_{t4}\bar{m}_4}{\sqrt{C_{pt}T_{t4}}} \qquad (17.32)$$

where

$$\bar{m}_4 = \frac{\gamma}{\sqrt{\gamma-1}} \left(\frac{2}{\gamma+1} \right)^{\frac{\gamma+1}{2(\gamma-1)}} \qquad (17.33)$$

The non-dimensional mass flow of the compressor based on inlet conditions is then:

$$\frac{\dot{m}\sqrt{T_{t2}}}{p_{t2}} = A_4 \frac{\pi_c \bar{m}_4}{\sqrt{C_{pt}}} \sqrt{\frac{1-\left(A_4/A_8\right)^{1/n}}{\pi_c^{(\gamma-1)/\eta_c}-1}} \qquad (17.34)$$

This equation gives a relation between mass flow and compressor pressure ratio while Eq. (17.27) describes how the pressure ratio depends on the turbine inlet temperature, that is the throttle setting. It therefore describes an operating line of the engine on the compressor characteristics. Each point on the line corresponds to a turbine inlet temperature that is to a power setting.

For prescribed values of the nozzle area, variations in turbine inlet temperature move the operating point away from the design point. The line so obtained in the compressor and fan characteristics is called the operating or working line of the engine, see Figure 17.5.

The arrow indicates the movement of the operating point when increasing the turbine inlet temperature. Typically, the HP compressor operating point varies relatively slightly and the operating point of the fan significantly more. Eq. (17.34) shows that the operating line bends upwards towards the surge line in areas of the compressor map with decreasing efficiency, see Fig.17.5. If the line passes into areas of the map where efficiencies vary significantly then an iteration is necessary to find the exact line. Ideally one would like to control the engine so that the turbine inlet temperature and the compressor pressure ratio are maintained as high as possible without intersecting the surge line.

p_{tout} / p_{tin}
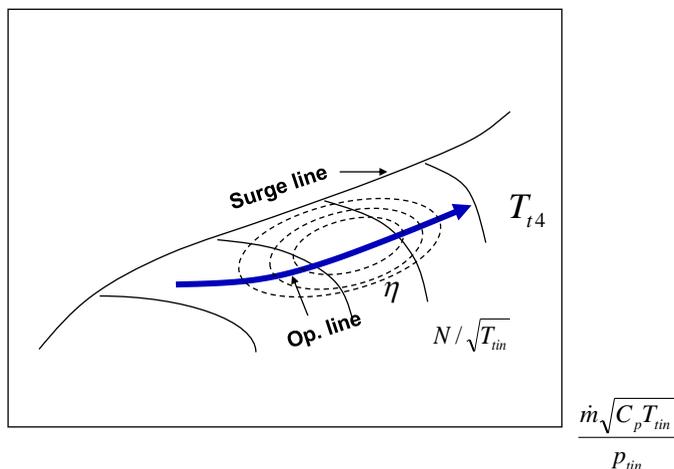
Fig. 17.5 The operating line

Note that the operating line does not require the compressor rotational speed to be selected. Instead, given the working line, the compressor chooses the rotational speed that corresponds to the pressure ratio and mass flow. Reducing the mass flow is equivalent to reducing the rotational speed. Note also from Eq. (17.34) that an increase in the **nozzle area** A_8 will move the whole operating line to lower pressures away from the surge line. Thus, the nozzle may be used to control the engine.

The compressor may surge in the front or in the back stages. At high speeds of rotation, the first stage in the compressor produces a higher pressure than in the design point. Then the density will increase and the axial velocity into the next stage decreases. This effect adds up through the compressor so that the velocity in the back stages becomes too low leading to an increase in flow incidence and surge or stall. Thus the back stages may surge while the first stage is still stable.

If on the other hand, the operating point moves to lower speed of rotations where the pressure is below the design pressure, then the opposite will happen. As the rotational speed is reduced, the pressure rise is decreased. This leads to a decrease in density in the last stages of the compressor. Because the density rise is then smaller than what the compressor was designed for, there is an axial velocity increase in the rear stages. If the speed increases sufficiently, the last stage may choke so that the compressor no longer can swallow the mass flow. This results in a decrease of mass flow and axial flow velocity at the inlet of the compressor eventually leading to surge there. Thus the compressor will surge in the last stages at high speeds and in the front stages at low speed. The mismatch between inlet and outlet increases with the number of stages in the compressor and therefore pressure ratios higher than 20 are not considered practical.

Even when clear of the surge line, if the operating line approaches it too closely, the compressor may **surge** when the engine is accelerated. Figure 17.6 shows what happens during a deceleration and acceleration.

With a rapid increase of the fuel flow, the pressure in the combustion chamber increases. The turbine is not able to swallow all the air so the pressure increases in the compressor. Since the inertia of the rotor prevents the shaft speed to accelerate fast enough, the operating point slides to the left along a speed line and approaches the surge line. The result is an operating line following the upper dashed line in Figure 17.6. On the contrary, with a rapid decrease of the fuel flow, the operating line moves away from the surge line and follows the lower dashed line in Figure 17.6.

p_{tout} / p_{tin}
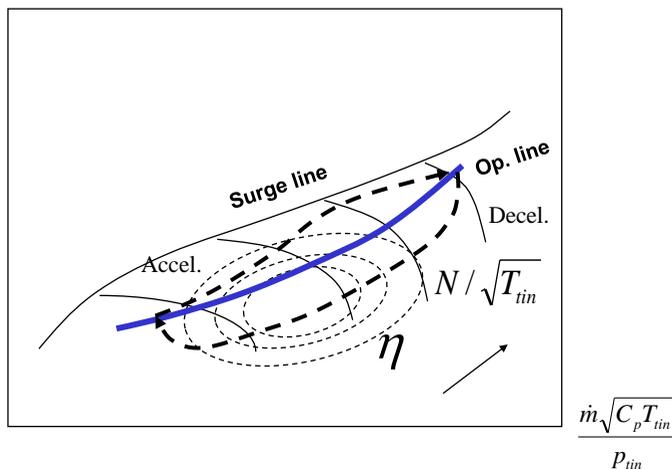
Fig. 17.6 Acceleration and deceleration

A rapid increase of inlet temperature following for instance the firing of a missile while the speed of rotation is maintained may also cause the operating point to approach the surge line. This tendency towards the compressor surge line is a problem with all engines under rapidly varying conditions especially at high altitudes because the operating line has a tendency to move towards higher pressures with **altitude** while the surge line moves down.
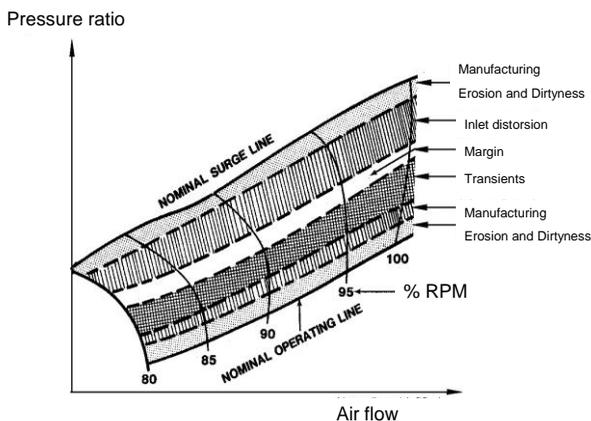
Fig. 17.7 Factors reducing the surge margin

Operating above the surge line is impossible and entering the region is dangerous to the engine and the aircraft. The fan is at a greater level of risk in this respect. Note that inlet flow distorsion, erosion etc may lower the surge line so that the surge margin decreases, see Figure 17.7.

The most significant way of reducing this type of potential surge problems is to **split the compressor** into separate compressors on concentric shafts which may operate at different speeds. The use of multiple shafts has an additional benefit. The front stage of a compressor must not operate with a blade speed which is too high in relation to sonic conditions if the efficiency is to be maintained. However, in the rear stages, because of the higher temperature and speed of sound, the blade speed could be substantially higher without high losses. By splitting the compressor into two or more parts, it is possible to take advantage of this effect by letting the rear compressors rotate faster.

Another method is to **bleed** air from the middle of the compressor into the bypass canal increasing the axial flow velocity in the front stages. This causes a kink in the operating line at low speeds moving it away from the surge line. Bleeding may also be used to temporarily decrease the pressure in the compressor, which lowers the operating line. Bleeding clearly involves a waste of turbine work so it should be used only over the essential parts of the operating line.

An alternative is to use **variable guide vanes** in the front stages to match the flow and the speed. The inventor of this technique was **Gerhard Neumann**, whom we have already met in Chapter 9. Among his milestone achievements for GE was his development of the variable-stator jet engine. By adjustable vanes in the stators, Neumann allowed the engine to increase air pressure in its compressor, for a great improvement in power and performance. Neumann won eight patents and in time saw his design adopted universally.

For an engine with a fixed geometry, the compressor temperature ratio is set by the Mach number at the blade tips. From Eq. (13.8), the so called Euler equation, the temperature ratio of a compressor stage is:

$$\tau = 1 + \lambda \frac{(\gamma-1)M_t^2}{1+(\gamma-1)M_1^2/2}\left(1 - \frac{M_1\cos\alpha_1}{M_t}\left(\tan\beta_2 + \tan\alpha_1\right)\right) \quad (17.35)$$

where:

$$M_t = M_1(\sin\alpha_1 + \tan\beta_1/\cos\alpha_1) \qquad (17.36)$$

With α_1 and β_1 as the flow angles into the rotor and M_1 as the Mach number at the stage inlet.

It is then seen that changing the inlet angle by variable inlet guide vanes makes it possible to adapt the pressure ratios of the fan and compressor to changing conditions.

If several rows of variable guide vanes are used at the front of the compressor, pressure ratios over 15 may be achieved in a single spool. Pressure ratios beyond 20 have rarely been considered practical because of the mismatch between front and end stages.

The approach of Rolls-Royce and Pratt & Whitney has been to use multi-spool configurations while General Electric has favored variable guide vanes. Rolls Royce even uses three spools.

The operating line can also be manipulated by variations of the HP **turbine area**. It is seen from Eq. (17.34) for the operating line that increasing the turbine inlet areas A_4 will move the operating line away from the surge line. The reason it has not been done are

mechanical problems because those parts of the engine are exposed to very high temperatures. An alternative would be to vary the LP turbine area but this has not the same direct effect.

Potential operating benefits of a variable area turbine become apparent when flight at various altitudes and Mach numbers are considered. For mixed flow systems a static pressure match must be maintained in the exhaust system where the cold and hot streams mix. As a turbofan is flown to higher Mach numbers the operating bypass pressure ratio increases. Also limits of compressor and turbine temperatures are reached. This result in difficulties to maintain the required pressure balance and thus fan speed and power must be reduced. Varying the turbine area is one way to facilitate the matching of the core and bypass streams to extend the operation of the engine.

Changing the areas in the nozzle, compressor or turbine to manipulate the operating line in order to avoid surge problems at different operating conditions is just one example of variable geometry in engines.

A long range supersonic transport such as Concord suffers from a fundamental propulsion problem. Its engines are designed to work best at supersonic cruise, which unfortunately means that they are inefficient, noisy and thirsty at low speeds.

Because Concord spends most of its time at supersonic speeds its engines are designed for high exhaust speed. This means less efficiency at low velocities and also more noise because of the shear between the jet and the still air. Furthermore, a supersonic transport is required to fly for long distances over populated areas at subsonic speed so as to avoid the noise from the sonic boom.

The answer is to design an engine with enough variability in its cycle to operate efficiently both at high and low speeds. Such a **variable cycle** engine is also of interest for military applications where the engine has to operate under very variable conditions.

Requirements for take-off, cruise, high-altitude and supersonic operation are different, and ideally, engine cycles should be adjusted for each of these conditions. Since this has not been possible in the past, engine cycle selection for any given propulsion system has necessarily been a compromise. A variable cycle engine, in theory, would allow the propulsion system to be optimized for each specific flight condition. This of course is very simplistic and may not be entirely possible. Variable cycle engines, however, have been studied for many years in an effort to achieve some degree of cycle flexibility.

As Mach numbers increase, designs are driven toward the straight turbojet. To put it simply, subsonic flight requires bypass engines, supersonic flight requires straight turbojets. For aircraft designed to fly mixed missions (at subsonic, transonic, and supersonic flight speeds), it is desirable to have an engine with the characteristics of both a high-bypass engine (for subsonic flight speed) and a low-bypass engine (for supersonic flight speed). The components of the engine must be designed to accommodate the extreme limits of the flow, pressure ratio, and other conditions involved in both high-bypass and low-bypass operation.
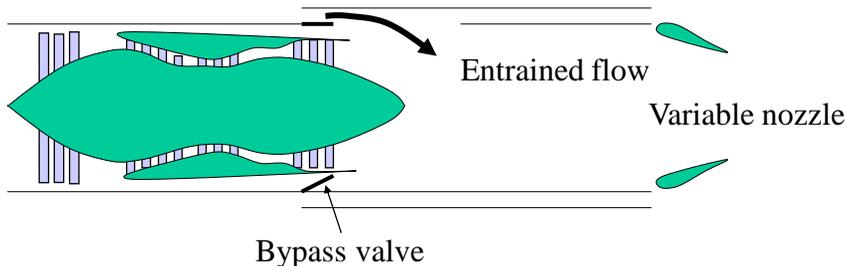
Fig. 17.8 Choked bypass ejector nozzle engine

Various devices have been proposed. For a choked bypass stream and since the inlet of the HP turbine is always choked, the bypass ratio is:

$$\alpha = \frac{\dot{m}_b}{\dot{m}_c} = \frac{A_b}{A_{t4}} \frac{p_{t13}}{p_{t4}} \sqrt{\frac{T_{t4}}{T_{t13}}}$$

(17.37)

Thus the bypass ratio can be controlled by changing the area ratio through **valves in the bypass canal**. There are many different possibilities. One idea is to split the LP compressor into two parts, one driven by the LP turbine, another attached to but separate from

the HP compressor. In its supersonic mode the bypass duct is closed and all of the air pumped through the front block also passes through the HP compressor or through an inner bypass duct, giving a modest bypass ratio. For take-off and subsonic climb, the core is partially closed, reducing the core flow. At the same time the bypass is opened up increasing the overall bypass ratio and reducing the jet velocity.

The engine may be operated at either extreme values of bypass ratio or at any bypass ratio between those extremes by means of a valve in the bypass stream (in conjunction with a variable exhaust nozzle). When the valve is closed, it restricts the flow in the bypass stream to achieve low bypass for supersonic flight. When the valve is open, the bypass is increased to its maximum value for efficient subsonic flight.

The engine could be combined with an ejector nozzle entraining outside free stream air that is mixed with the core jet exhaust, resulting in a slower, cooler exhaust jet that reduces noise, see Figure 17.8. This engine possesses turbofan-like subsonic performance and may also produce a large supersonic jet velocity. It needs a very advanced technology mixer-ejector exhaust nozzle as the ejector airflow is comparable to the primary flow. Its main design difficulty is the long mixer-ejector nozzle which may generate installation problems on the aircraft.

Another concept makes use of a **bypass duct reheat** system. At take-off, the inner exhaust stream is throttled to keep jet noise low. The duct burner is operated at maximum temperature. The velocity of the bypass stream then becomes higher than the inner stream. This inverted velocity profile suppresses noise. For subsonic cruise the engine operates as a moderate bypass ratio turbofan. For

supersonic cruise the inner burner temperature is kept high and the duct burner is again operated.

Auxiliary intake

Variable nozzle

Fan driven by LP compressor
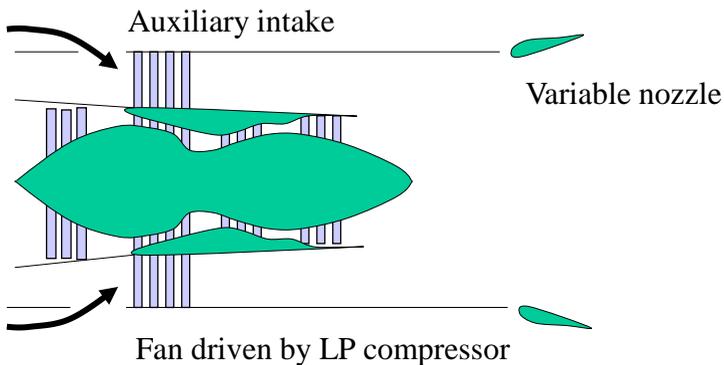
Fig. 17.9 Mid tandem fan

 The **Mid-Tandem Fan**, see Figure 17.9, is equipped with a mid-bypass fan coupled to the secondary body, which allows it to operate with one or two flow paths. For subsonic conditions, the bypass flow enters the engine through two flow paths via both frontal and lateral air inlets, having a bypass ratio of greater than 2. This double flow path, which provides low specific fuel consumption and moderate ejection speeds of about 400m/s, allows noise regulations to be met. For supersonic cruise, the lateral inlets are closed and the variable-pitch guide vanes of the mid-fan reduce the frontal airflow into the bypass duct. This,

decreases the bypass ratio, which is favorable for supersonic conditions. The innovation in this design is the insertion of the fan downstream of the low-pressure compressor. The mid-fan therefore, plays the dual role of supplying the bypass flow in its external section, and also compressing the air in the primary circuit (between the low and high pressure compressors) in its inner section.

The difficulty in all those systems is in finding a "flow multiplier" device, which at take-off and in subsonic operation can significantly increase the air flow adjusted for operation at supersonic speeds. Full authority electronic control systems would be essential in a variable cycle engine to optimize the conditions at variable flight speeds. Turbines and compressors with high efficiency at very variable conditions must also be developed.

Ex 17.1

What is the thrust at take-off with and without afterburner for the combat engine if the pressure is 101 kPa for Sea Level Static (SLS) conditions and the military engine is operating in the design point?

Appendix 17
Off-Design of a military engine

In Chapter 16, an engine was designed for combat at Mach 0.9 at 11 km altitude. Now we will determine its performance in supercruise at Mach 1.5.

| 0 | 2 | 13 | 3 | 4 | 45 | 5 | 6 | 7 | 8 | 9 |

$M_{45}=1$

$M_4=1$

$M_8=1$

Mixer

Afterburner
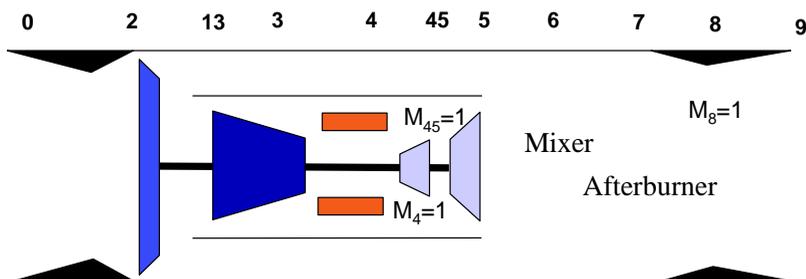
Mach number	1,5	Fuel flow f_0	0,032
Ambient temperature T0 K	216	Combustion efficiency η_c	1
Ambient pressure p0	22700	Fuel heat content h	4,30E+7
Cold parts adiabatic constant γ_c	1,4	Turbine polytropic efficiency η_t	0,88
Hot parts adiabatic constant γ_t	1,3	Nozzle efficiency η_j	0,95

Cold parts specific heat
C_{pc} 1005   HP turbine inlet area A_4 0,0269
Hot parts specific heat
C_{pt} 1244   LP turbine inlet area A_{45} 0,0617
     Combustor pressure loss
Inlet pressure loss π_d 0,97 π_b 0,95
     Constant

Fan polytropic
efficiency η_f 0,9 $K \cong (1 - \dfrac{T_{t45}}{T_{t4}})_{des}$ 0,159

Compressor polytropic
efficiency η_c 0,9   Weight of aircraft m   15000
Cooling flow ε_0 0,088   Number of engines N   2
     Drag of aircraft D   57100

	Off-design Mach 1.5	Design Mach 0.9
Give a turbine inlet temperature matching a throttle setting	1800 K	1800
Assume a fan pressure ratio in order to match a prescribed nozzle area.	2.85	4.5
The relative stagnation temperature at the entrance to the inlet is: $$T_{t0}/T_0 = \tau_0 = 1 + \frac{\gamma_c - 1}{2}M^2$$	1.45	1.16

At supersonic speed there is a pressure loss in the inlet $$\frac{p_{t2}}{p_{t0}} = \pi_d(1-0.075(M-1)^{1.35})$$ so that the pressure p_{t2}	79.3 kPa	37.2
The heat losses in the inlet are neglected so that $T_{t2} = T_{t0}$	313 K	251
The pressure after the fan is p_{t13}	226 kPa.	167
With a polytropic efficiency, the temperature ratio for the fan is $\tau_f = \pi_f^{(\gamma_c-1)/\gamma_c\eta_f}$	1.39	1.61
The temperature is $T_{t13} = T_{t2}\tau_f$	437 K	405
With the **assumed fuel flow** of f_0, the HP compressor temperature is $$T_{t3} = T_{t13} + \left(1+f-\varepsilon\right)\frac{C_{pt}}{C_{pc}}KT_{t4}$$	771 K	739
This temperature is below the limit of 875 K. If it had been higher it had been necessary to limit the fuel flow and the turbine inlet temperature in order not to overheat the engine.		
A **new value of ”f”** may now be obtained from $f\eta_b h = (1+f-\varepsilon)C_{pt}(T_{t4}-298) - C_{pc}(1-\varepsilon)(T_{t3}-298)$	0.03	0.03
This is rather close to the assumed value of 0.032. At this level an **iteration** could be made to find the exact values of "f" and T_{t3}.		
The pressure ratio of the HP compressor is		

$\pi_c = (\dfrac{T_{t3}}{T_{t13}})^{\gamma_c \eta_c/(\gamma_c-1)}$	6.0	6.67
The pressure in the combustion chamber is $p_{t4} = \pi_b \pi_c p_{t13}$	1290 kPa	1060
The core mass flow parameter is $\bar{m}_4 = \dfrac{\gamma_t}{\sqrt{\gamma_t-1}}\left(\dfrac{2}{\gamma_t+1}\right)^{\frac{\gamma_t+1}{2(\gamma_t-1)}}$	1.4	1.39
The core mass flow $\dot{m} = \dfrac{A_4}{1+f-\varepsilon}\dfrac{p_{t4}\bar{m}_4}{\sqrt{C_{pt}T_{t4}}}$	34.1 kg/s	28.1 kg/s
The HP turbine pressure ratio is $\pi_{th} = (1-K)^{\gamma_t/(\gamma_t-1)\eta_t}$	0.43	0.43
The exhaust temperature from the HP turbine is $T_{t45} = T_{t4}(1-K)$	1514 K	1514
The cooling air is mixed in at constant pressure. $T'_{t45} = \dfrac{\varepsilon}{1+f}\dfrac{C_{pc}}{C_{pt}}T_{t3} + \dfrac{1+f-\varepsilon}{1+f}T_{t45}$	1438 K	1435
The stagnation pressures in the core and bypass canals are equal so that the LP turbine exhaust temperature becomes $T_{t5} = \dfrac{T'_{t45}}{(\pi_c \pi_b \pi_{th})^{\eta_t(\gamma_t-1)/\gamma_t}}$	1201 K	1173
A power balance for the LP shaft then gives the bypass ratio $\alpha = (1+f)\dfrac{C_{pt}}{C_{pc}}\dfrac{T'_{t45}-T_{t5}}{T_{t13}-T_{t2}}-1$	1.45	1.18
The mean specific heat of the exhaust stream is		

$C_{pm} = ((1+f)C_{pt} + \alpha C_{pc})/(1+\alpha+f)$	1104 J/kgK	1117
This gives $\gamma_m = \dfrac{1}{1 - R/C_{pm}}$	1.35	1.35
Downstream of the LP turbine the core and the bypass stream mix and the temperature is $T_{t6} = T_{t5}\dfrac{C_{pt}}{C_{pm}}\dfrac{1+f}{1+\alpha+f} + T_{t13}\dfrac{C_{pc}}{C_{pm}}\dfrac{\alpha}{1+\alpha+f}$	794 K	804
The pressure is the same as in the bypass canal, $p_{t6} = p_{t13}$	226 kPa	168
The total mass flow is $\dot{m}_{tot} = \dot{m}(1+\alpha+f)$	83.7 kg/s	61.2
The nozzle mass flow parameter is $\bar{m}_8 = \dfrac{\gamma_m}{\sqrt{\gamma_m - 1}}\left(\dfrac{2}{\gamma_m + 1}\right)^{\frac{\gamma_m + 1}{2(\gamma_m - 1)}}$	1.33	1.33
The nozzle area coefficient: $C_A = \left(\dfrac{2}{\gamma + 1 - (\gamma - 1)/\eta_j}\right)^{\frac{\gamma}{\gamma - 1}}$	1.035	1.035
The nozzle area $A_8 = C_A\dfrac{\dot{m}_{tot}\sqrt{C_{pm}T_{t6}}}{p_{t6}\bar{m}_8}$	0.27 m2	0.27
The design point area is 0.27 so the fan pressure ratio matches the design area setting. If we want to obtain a different **nozzle area**, a reiteration could be made with a **new assumed fan pressure** ratio.		

Without afterburner, the jet speed is $$V_j = \sqrt{2\eta_j C_{pm} T_{t6}\left[1-\left(p_0/p_{t6}\right)^{(\gamma_m-1)/\gamma_m}\right]}$$	866 m/s	828
The flight speed is $V = M\sqrt{\gamma R T_0}$	442 m/s	265
The dry thrust: $F = \dot{m}(1+\alpha+f+f_a)V_j - \dot{m}(1+\alpha)V$	36.4 kN	35.2
Specific excess power $SEP = \dfrac{V(NF-D)}{gm}$	47.2 m/s	0

18. THE LIMITS OF THE TURBOJET ENGINE

Civil aviation will probably remain subsonic and the speed of fighter aircraft has leveled out at around Mach 2. Still there may be a future demand for higher speed for military strike and reconnaissance purposes and for rapid and flexible space travels. The ordinary jet engine is limited to around Mach 3 but with the turboramjet, the turbomachinery is closed down at about Mach 4 and the engine continues to operate as a ramjet. The speed could be further extended to about Mach 6 by a supersonic fan and by precooling with hydrogen.

Historically, the main motivation for aviation has been its ability to produce higher speeds over larger distances than any other means of transportation. It is very probable that this will be so even in the future.

There are some military requirements for higher speed. A Mach 6 aircraft would be able to reach any point on the globe in less than four hours. Such a plane could be of potentially greater use for reconnaissance purposes than high resolution orbiting satellites that can take 24 hours to arrive over the target. Also, it could strike globally within a few hours without the need for refueling or forward bases.

As space exploration proceeds there will also be a growing demand for rapid and flexible access to low earth orbits. The rockets of today will then have to be replaced by high speed space planes using much more advanced propulsion technologies than are now

available. The turbojet could form the core in such new propulsion systems if its speed could be further extended.
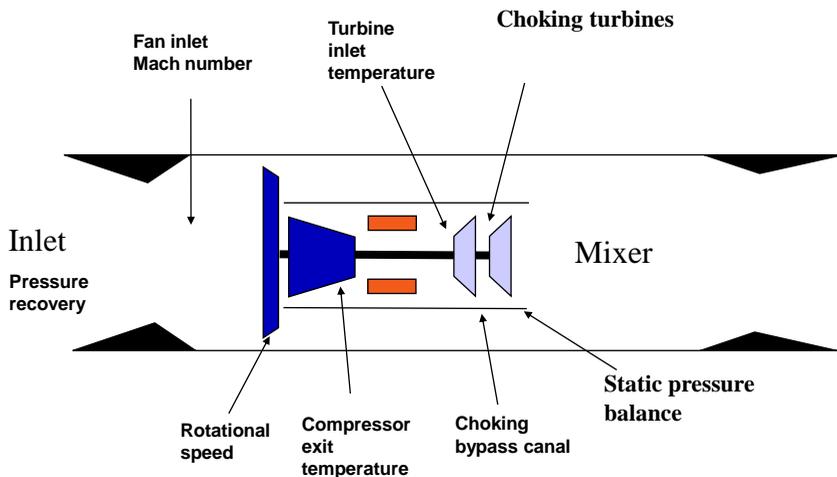
Fig. 18.1 Limitations in the operation of the jet engine

Turbojets are subject to many limitations in the conditions at which they can operate efficiently. Important such limitations are indicated in Figure 18.1 and they mean that the turbojet engine is restricted to speeds at about Mach 3.

One solution to reach higher speeds is to bypass the turbomachinery when it becomes overheated and continue to operate only on the afterburner. This combination of turbojet and ramjet is usually called a **turboramjet**.

Mixing in the afterburner

The analysis of the turboramjet follows that of the turbofan up to the point where we have to consider the mixing of the core and bypass flow. This is more complicated than in the on-design case because the total pressures are now different.

When designing an engine, the Mach number in the bypass canal and in the LP turbine exhaust may be chosen so as to make the total pressures equal. This makes it easier to carry out the design and off-design calculations because the bypass ratio is directly obtained from a power balance over the LP shaft. However, far away from the design point, the Mach numbers in the bypass canal and in the mixer may differ significantly from the design values and the total pressure assumption will no longer be valid. At high flight Mach numbers, the flow in the bypass canal may even become sonic so that the canal is choking.

In reality, the **static pressure** must be the same at the splitter between the two flows. In addition, there is a continuity in mass flow through the core and a power balance over the LP turbine to be satisfied. This makes it possible to calculate the conditions in the exhaust duct and therefore the off-design performance of the engine.

For an assumed fan pressure ratio and turbine inlet temperature, the temperatures and pressures at fan and HP turbine exhaust may be found as in Chapter 16 but from then on the calculations differ. The core inlet mass flow is from the mass flow through the choked HP turbine inlet:

$$\dot{m} = \frac{\dot{m}_4}{1+f-\varepsilon} = \frac{A_4}{1+f-\varepsilon} \frac{p_{t4}\bar{m}_4}{\sqrt{C_{pt}T_{t4}}} \qquad (18.1)$$

where

$$\bar{m}_4 = \frac{\gamma_t}{\sqrt{\gamma_t-1}}\left(\frac{2}{\gamma_t+1}\right)^{\frac{\gamma_t+1}{2(\gamma_t-1)}} \qquad (18.2)$$

For an assumed value of the bypass Mach number M_{13}, the bypass ratio is:

$$\alpha = \frac{\dot{m}_{13}}{\dot{m}} = (1+f-\varepsilon)\frac{A_{13}}{A_4}\frac{p_{t13}}{p_{t4}}\sqrt{\frac{C_{pt}T_{t4}}{C_{pc}T_{13}}}\frac{\bar{m}(M_{13})}{\bar{m}_4} \qquad (18.3)$$

where:

$$\bar{m}(M_{13}) = \frac{\gamma_c}{\sqrt{\gamma_c-1}}M_{13}\left(1+\frac{\gamma_c-1}{2}M_{13}^2\right)^{-(\gamma_c+1)/2(\gamma_c-1)} \qquad (18.4)$$

From the power balance over the LP shaft, the LP turbine exhaust temperature is:

$$T_{t5} = T'_{t45} - \frac{1+\alpha}{1+f}\frac{C_{pc}}{C_{pt}}(T_{t13}-T_{t2}) \qquad (18.5)$$

and the pressure in the LP turbine exhaust is:

$$p_{t5} = p_{t45}\left(\frac{T_{t5}}{T'_{t45}}\right)^{\frac{\gamma_t}{\eta_t(\gamma_t-1)}} \qquad (18.6)$$

Next, from the **static pressure** balance over the splitter between the core and bypass streams, the LP turbine exhaust Mach number can be expressed in the bypass Mach number M_{13} as:

$$M_5 = \sqrt{\frac{2}{\gamma_t - 1}\left\{\left[\frac{p_{t5}}{p_{t13}}\left(1 + \frac{\gamma_c - 1}{2}M_{13}^2\right)^{\frac{\gamma_c}{\gamma_c - 1}}\right]^{\frac{\gamma_t - 1}{\gamma_t}} - 1\right\}} \quad (18.7)$$

Lastly, the continuity of the mass flow in the HP and LP turbines requires that:

$$\dot{m} = \frac{A_4}{1 + f - \varepsilon}\frac{p_{t4}\bar{m}_4}{\sqrt{C_{pt}T_{t4}}} = \frac{A_5}{1 + f}\frac{p_{t5}(M_{13})\bar{m}_5(M_5)}{\sqrt{C_{pt}T_{t5}(M_{13})}} \quad (18.8)$$

The only unknown parameter in this equation is the Mach number M_{13} because M_5 is a function of M_{13} and:

$$\bar{m}_5 = \frac{\gamma_t}{\sqrt{\gamma_t - 1}}M_5\left(1 + \frac{\gamma_t - 1}{2}M_5^2\right)^{-(\gamma_t + 1)/2(\gamma_t - 1)} \quad (18.9)$$

The equations are nonlinear and interdependent so a solution for M_{13} must be found by iteration satisfying Eq. (18.8).

Note that the Mach number in the bypass canal changes to accommodate the flow as long as the bypass canal is unchoked. If the Mach number $M_{13}=1$, then the turbine inlet temperature must be adjusted to match the mass flows.

The mean specific heat of the exhaust stream is obtained from a simple mass weighting:

$$(1+\alpha+f)C_{pm} = (1+f)C_{pt} + \alpha C_{pc} \qquad (18.10)$$

The mean adiabatic constant is then:

$$\gamma_m = \frac{1}{1 - R/C_{pm}} \qquad (18.11)$$

Downstream of the LP turbine the core and the bypass stream mix and the temperature is:

$$T_{t6} = T_{t5}\frac{C_{pt}}{C_{pm}}\frac{1+f}{1+\alpha+f} + T_{t13}\frac{C_{pc}}{C_{pm}}\frac{\alpha}{1+\alpha+f} \qquad (18.12)$$

Finding the common pressure is more complicated. The conservation of momentum means that the impulse function:

$$I = pA + \dot{m}V = pA(1+\frac{\dot{m}V}{pA}) = pA(1+\frac{\rho V^2}{p}) = pA(1+\frac{V^2}{RT}) = pA(1+\gamma M^2) = const$$

(18.13)

Using the relation between total and static pressure, the equation for the mass flow parameter Eq. (8.8) may be rewritten in the form:

$$pA = \sqrt{(\gamma-1)C_pT_t}\,\frac{\dot{m}}{\gamma M\sqrt{1+\frac{\gamma-1}{2}M^2}} \qquad (18.14)$$

Introducing:

$$\Phi = \frac{\gamma^2}{\gamma-1} \frac{M^2}{C_p T_t (1+\gamma M^2)^2} \left(1+\frac{\gamma-1}{2}M^2\right) \qquad (18.15)$$

$$\frac{\dot{m}_5}{\sqrt{\Phi_5}} + \frac{\dot{m}_{13}}{\sqrt{\Phi_{13}}} = \frac{\dot{m}_5 + \dot{m}_{13}}{\sqrt{\Phi_6}} \qquad (18.16)$$

so that:

$$\phi_6 = \frac{\gamma_m-1}{\gamma_m^2} C_{pm} T_{t6} \Phi_6 = \frac{\gamma_m-1}{\gamma_m^2} C_{pm} T_{t6} \left(\frac{1+f+\alpha}{\dfrac{1+f}{\sqrt{\Phi_5}}+\dfrac{\alpha}{\sqrt{\Phi_{13}}}} \right) \qquad (18.17)$$

Then:

$$M_6 = \sqrt{\frac{2\phi_6}{1-2\gamma_m\phi_6 + \sqrt{1-2(\gamma_m+1)\phi_6}}} \qquad (18.18)$$

If $M_6>1$, then the exhaust duct is not able to swallow the air flow from the engine and the turbine inlet temperature T_{t4} must again be adjusted.

Now the total pressure in the exhaust duct is found from the mass flow equation including a pressure loss in the mixer:

$$p_{t6} = \pi_m \frac{(1+f+\alpha)\dot{m}\sqrt{C_{pm}T_{t6}}}{A_6 \bar{m}_6(M_6)} \qquad (18.19)$$

where:

$$\bar{m}_6 = \frac{\gamma_m}{\sqrt{\gamma_m - 1}} M_6 \left(1 + \frac{\gamma_m - 1}{2} M_6^2\right)^{-(\gamma_m+1)/2(\gamma_m-1)} \qquad (18.20)$$

The total mass flow is :

$$\dot{m}_{tot} = \dot{m}(1 + \alpha + f + f_a) \qquad (18.21)$$

where for an afterburner temperature $T_{ta} > T_{t6}$:

$$f_a \eta_a h = (1 + f + f_a + \alpha)C_{pa}(T_{ta} - 298) - C_{pm}(1 + f + \alpha)(T_{t6} - 298)$$

$$(18.22)$$

The nozzle area corresponding to the new conditions is:

$$A_8 = \frac{\dot{m}_{tot}\sqrt{C_{pa}T_{ta}}}{p_{ta}\bar{m}_8} \qquad (18.23)$$

where:

$$p_{ta} = \pi_a p_{t6} \qquad (18.24)$$

$$\bar{m}_8 = \frac{\gamma_a}{\sqrt{\gamma_a - 1}} \left(\frac{2}{\gamma_a + 1}\right)^{\frac{\gamma_a+1}{2(\gamma_a-1)}} \qquad (18.25)$$

The core mass flow through the engine and the bypass ratio remains the same independently of the conditions in the nozzle or whether the afterburner is on or not. The rest of the engine is unaware of the nozzle. The nozzle area must therefore increase

roughly in proportion to the square root of the temperature before the nozzle.

A calculation scheme based on the equations above for the exhaust duct is presented in the Appendix 18 as a complement to the off-design calculation scheme of the military engine in the Appendix to Chapter 17.

The inlet

The inlet duct is perhaps the most critical component in high speed air propulsion systems. It scoops up the propulsive mass flow and delivers it at increased pressure and reduced velocity to the engine. The efficiency of this energy conversion is very important because pressure losses in the inlet can lead to substantial reductions in thrust and specific impulse at high speeds.

The efficiency of the air inlet is very much dependent on the amount of compression which in its turn depends on the permitted Mach number at the inlet to the fan. If this could be increased then the efficiency of the inlet will increase.

At supersonic flight speed, the kinetic energy of the incoming air is converted into pressure in a number of oblique shocks. The number of those oblique shocks in the inlet needs to increase with speed. Flight beyond Mach 2 requires mixed compression inlets performing some of the compression inside the inlet duct instead of outside. For very high speeds, inlets can be designed that perform all the pressure conversion inside the inlet.

Bleed

External compression M=3

External-internal compression M=4

Internal compression M=7
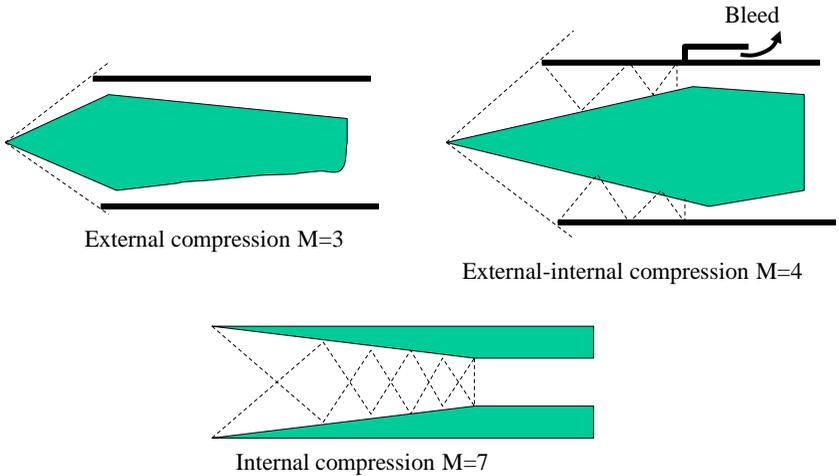
Fig. 18.2 Very high speed inlets

In engines operating over wide speed regimes, the inlet must also be controlled. The engine is only one part of a propulsion system, which includes an inlet and an ejector each producing thrust. A critical problem concerning supersonic flight with air breathing engines is to manage the shocks in the air inlet area without losing too much ram pressure. An example is the **SR-71 Blackbird**, which is powered by two Pratt & Whitney J-58 turbo-ramjets, each developing 15 tons of thrust with afterburning.

The circular air intakes of the SR-71 contain a center body tipped with a conical spike. The spike is movable, forward for takeoff and climb after which, as speed builds up, it moves rearward, controlling the amount of air entering the engine. As it does so, air inlet bypass doors in the side of the nacelle close to establish the correct flow of air through the engine, holding the supersonic shock wave in its critical position within the inlet. The engine itself operates at subsonic speed.

Should the shockwave be expelled from the inlet, a condition known as an **"unstart"** occurs. An unstart in a twin engine aircraft gives rise to a violent yaw where the aircraft pulls to that side where the engine has unstarted. Unstarts have been known to be so violent as to crack a pilot's helmet from the severe yaw of the aircraft. If unchecked, the resulting yaw is described by SR-71 pilots as though the nose and tail are trying to swap ends.

To correct the problem, the spike must be pushed totally forward and adjusted to capture the air properly. An automatic control system senses this problem and repositions the spike in milliseconds with great accuracy even though air loads of up to fourteen tons are acting on the spike.
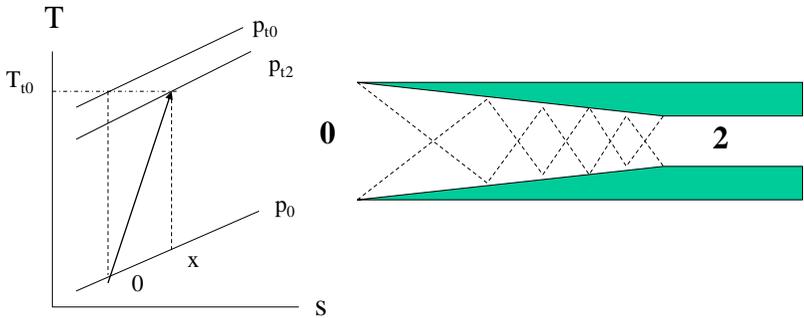
Fig. 18.3 Pressure loss in inlets

 Due to losses in the inlet there is an increase in entropy and a loss in pressure To understand the significance of this, we may introduce the fictitious state "x", see Figure 18.3. The pressure recovery of the inlet can then be written as:

$$\pi_d = \frac{p_{t2}}{p_{t0}} = \frac{p_{t2}}{p_0}\frac{p_0}{p_{t0}} = \frac{p_{t2}}{p_x}\frac{p_0}{p_{t0}} = \left(\frac{T_{t2}}{T_x}\right)^{\frac{\gamma}{\gamma-1}}\frac{p_0}{p_{t0}} = \left(\frac{T_{t0}}{T_x}\right)^{\frac{\gamma}{\gamma-1}}\frac{p_0}{p_{t0}} = \left(\frac{T_{t0}}{T_0}\frac{T_0}{T_x}\right)^{\frac{\gamma}{\gamma-1}}\frac{p_0}{p_{t0}} = \left(\frac{T_0}{T_x}\right)^{\frac{\gamma}{\gamma-1}}$$

(18.26)

However, the total temperature remains the same because there are no heat losses in the inlet:

$$T_{t2} = T_x + \frac{V_x^2}{2C_p} = T_{t0} = T_0 + \frac{V_0^2}{2C_p} \qquad (18.27)$$

so that:

$$T_x / T_0 = 1 + \frac{V_0^2}{2C_p T_0} - \frac{V_x^2}{2C_p T_0} = 1 + (1 - \eta_{ke})\frac{\gamma - 1}{2} M_0^2 \quad (18.28)$$

Where we have introduced the "kinetic efficiency":

$$\eta_{ke} = \frac{V_x^2}{V_0^2} \qquad (18.29)$$

The pressure loss may now be written:

$$\pi_d = \left(\frac{T_0}{T_x}\right)^{\frac{\gamma}{\gamma-1}} = 1 / \left(1 + (1 - \eta_{ke})\frac{\gamma - 1}{2} M_0^2\right)^{\frac{\gamma}{\gamma-1}} \qquad (18.30)$$

The kinetic energy efficiency is decreasing with diffusion in the inlet. A typical variation from experiments taking skin friction into account is [Curran, Murthy p. 502]:

$$\eta_{ke} = 1 - 0.4(1 - \frac{M_1}{M_0})^4 \qquad (18.31)$$

where M_1 is the Mach number after the inlet.

This corresponds approximately to the Military Standard expression of Eq. (16.4), provided that $M_1 / M_0 = 0.435$ where the

kinetic efficiency is approximately 0.96. Beyond Mach 4, Eq. (18.30) could be used.

Note that this means that the Mach number at the fan face is allowed to increase and eventually to become supersonic. This is not allowed with ordinary fans so above about $M_0=2.5$, the Mach number M_1 must be restricted resulting in higher pressure losses.

The pressure after the inlet is:

$$p_{t2} = \pi_d p_{t0} = \pi_d p_0 \tau_0^{\frac{\gamma}{\gamma-1}} \qquad (18.32)$$

while the temperature is:

$$T_{t2} = T_{t0} = \tau_0 T_0 \qquad (18.33)$$

Where:

$$\tau_0 = 1 + \frac{\gamma-1}{2} M_0^2 \qquad (18.34)$$

Performance

Figure 18.4 below shows what will happen with the thrust work efficiency when a turbofan is operated at increasing Mach numbers.
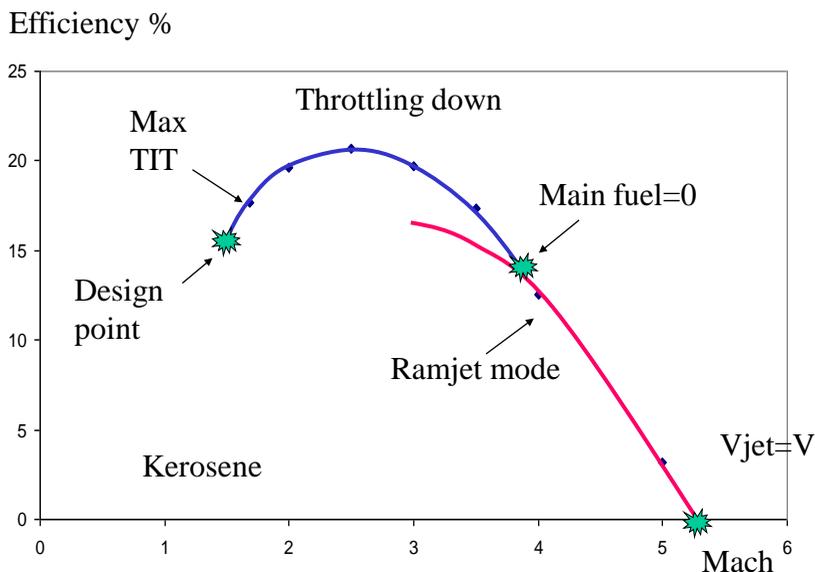
Efficiency %

Fig. 18.4 Turboramjet efficiency versus Mach number

If the engine is operating at the design point at increasing Mach numbers, then T_{t4}/T_{t2} is a constant as explained in Chapter 17. This means that the turbine inlet temperature has to increase gradually with the stagnation temperature (that is flight Mach number) until it reaches its maximum permitted value. After that the fuel flow must be reduced so as to avoid overheating the turbine.

Also in the design point, as seen from the compressor characteristics, the rotational speed of the compressor $N / \sqrt{T_{in}}$ is a constant. But the inlet temperature to the compressor gradually increases with the inlet stagnation temperature. This means that the rotational speed has to increase with flight Mach number until it reaches a maximum permitted value set by the tip Mach number. The restriction is especially critical for the fan, which has a higher diameter and therefore a higher tip speed.

From Eq. (13.8), the temperature ratio of the first stage of the fan is with M_2 as the Mach number delivered by the inlet to the fan:

$$\tau_{f1} = 1 + \lambda \frac{(\gamma - 1)M_t^2}{1 + (\gamma - 1)M_2^2 / 2} \left(1 - \frac{M_2 \cos \alpha_{1f}}{M_t} \left(\tan \beta_{2f} + \tan \alpha_{1f} \right) \right)$$

(18.35)

Where the so called "work factor" $\lambda < 1$.

If the tip Mach number is kept constant at its design value by e.g. using inlet guide vanes to vary the flow angle, then the pressure ratio of the fan will decrease at increasing Mach numbers and move the operating point away from the surge line.

For the case of axial flow at the rotor and stator exits $\alpha_{1f} = \beta_{2f} = 0$, the first stage temperature ratio is recalling that $T_{t2} = T_{t0}$:

$$\tau_{f1} = 1 + \lambda \frac{(\gamma - 1)M_t^2}{\tau_0}$$

(18.36)

Thus, because the fan tip Mach number must stay below its maximum value, there is a restriction on the fan pressure ratio as it is varied so as to meet a certain exhaust area.

The maximum permitted compressor exit temperature will be reached as stagnation temperatures build up in the engine. For ordinary titanium alloys the limit is 875 K, for titanium aluminides it may reach 1150 K but such materials are not yet in general use. When this limit is reached, the overall pressure ratio must be reduced to hold the compressor exit temperature at its upper limit. It is then necessary to move down the operating line by throttling down the engine (reducing turbine inlet temperature) reducing both the mass flow and the pressure ratio. The result is a rapid loss of thrust.

Eventually the gas generator does not make any significant contribution and can he bypassed using a valve arrangement that allows ram air to enter the afterburner directly. The engine then works as a ramjet, that is an engine where all the pressure rise is supplied by the inlet. This happens beyond the Mach number:

$$M_m = \sqrt{\frac{2}{\gamma - 1}(\frac{T_{c\max}}{T_0} - 1)} \qquad (18.37)$$

In this case the turbojet would be isolated from the hot airflow in ramjet mode by blocker doors which allow the airstream to flow around the core engine with small pressure loss.

There is, however, a limit to how fast the engine can fly. According to the momentum principle, the thrust of an airbreathing engine is:

$$F = (\dot{m}_f + \dot{m}_a)V_j - \dot{m}_a V \qquad (18.38)$$

There is therefore (as indicated in Figure 18.4 above) a speed where the thrust, and therefore the thrust efficiency, vanishes. As the fuel flow is small, this happens when the flight speed approaches the jet speed at beyond Mach 5.

The turboramjet represents a combination of turbojet and ramjet, utilizing the turbojet to produce the required thrust for launching and acceleration up to the speeds where the ramjet takes over.
It should be pointed out that the weight disadvantage of the turbomachinery is not significant considering the fact that the weight and size of the variable inlet, the afterburner and its variable nozzle far exceed the weight of the turbomachinery.

The supersonic fan

One limitation for high speed engines is the growing pressure losses in the inlet. This pressure loss in the inlet could be reduced if the relative Mach number leaving the inlet could be increased. Instead of using a long and heavy inlet system to decelerate the inlet air flow to the subsonic speeds required by conventional compressors, a supersonic fan would make it possible to maintain supersonic flow through the inlet. The advantages include much lower inlet system weight but also a lighter compressor with less stages.

The reason why the supersonic fan is so interesting is that for an engine with a fixed geometry, the fan temperature ratio is set by the Mach number at the blade tips. Note that in Eq. (18.35), the tip Mach number is:

$$M_t = M_2(\sin \alpha_{1f} + \tan \beta_{1f} / \cos \alpha_{1f}) \qquad (18.39)$$

For the case of axial flow at the rotor and stator exits, that is $\alpha_{1f} = \beta_{2f} = 0$:

$$M_t = M_2 \tan \beta_{1f} \qquad (18.40)$$

the temperature ratio becomes:

$$\tau_f = 1 + \lambda \frac{(\gamma-1)M_2^{\,2} \tan^2 \beta_{1f}}{1+(\gamma-1)M_2^2/2} \qquad (18.41)$$

where β_{1f} is the relative flow angle into the rotor and M_2 is the axial Mach number delivered by the inlet at the fan face.

In contrast to the subsonic compressor, the Mach number M_2 into the fan is allowed to be supersonic. From Eq. (18.41) for the fan temperature ratio, this means that the temperature ratio of a supersonic stage may be higher than for a subsonic one and could increase with flight speed as M_0 increases. Less stages are then needed in the fan for a given pressure ratio leading to smaller and lighter engines.
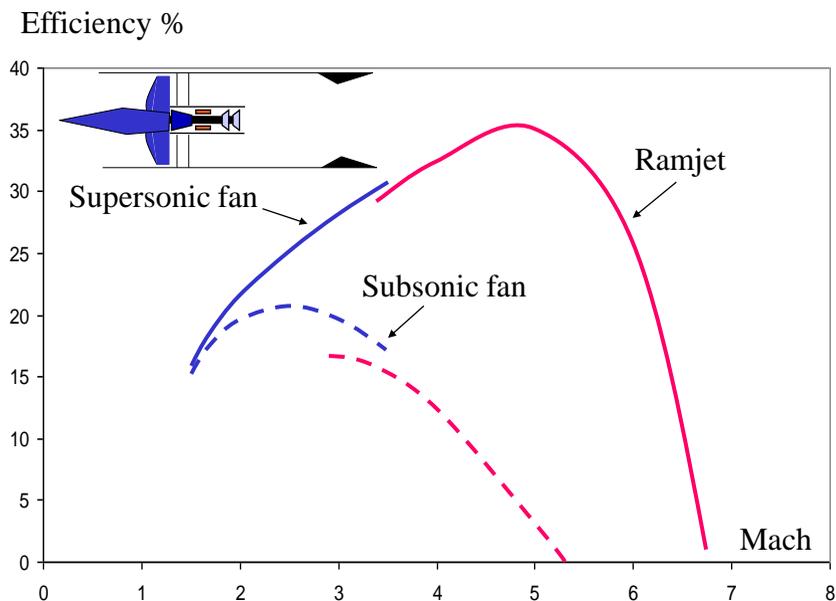
Fig. 18.5 Increased efficiency with a supersonic fan

As is seen from Figure 18.5, the supersonic fan could lead to substantially better thrust work efficiency. However, there are many difficulties.

Thus, the supersonic rotor has to be designed for a certain shock pattern. Variations from this shock pattern will cause great losses. Therefore, for low losses β_{1f} should be nearly constant. To maintain such an angle, the rotative speed of the fan would have to be adjusted as the air speed at the fan face changes with flight speed. There will therefore be a greater matching problem between a supersonic fan and the LP turbine than with a subsonic fan.

It is not uncomplicated to control the tip Mach number because the axial Mach number at the fan face changes with flight speed. It is therefore necessary to match the inlet to the fan to avoid large variations in tip speed and flow angle with flight speed. The inlet Mach number M_2 will have to grow slower than the flight Mach number and the rotating speed of the fan will have to be adjusted so that the flow angle decreases somewhat with flight speed. It is assumed that the fan inlet Mach number can be controlled by variable geometry, bleeding etc.

The fan must also be able to swallow the shock in the transition to supersonic flow. A variable capture and throat area is required to ease the transition to supersonic throughflow within the fan on the runway and to maintain supersonic flow at the fan face throughout the flight.

At low speed the cowl is extended forward so that the flowpath will converge and produce Mach 1 at the throat. As the speed increases to supersonic conditions, a bow shock is formed off the

inlet spike and the cowl is positioned so that the shock is attached to the cowl lip.

As the Mach number becomes supersonic behind the shock, the throat area is set relative to the fan inlet area to achieve the desired fan face Mach number. When the flight Mach number is sufficiently above unity, the flow remains supersonic from the free stream through the rotor and stator of the fan. Thus, the flow in the fan would be sonic at take-off and at low speed, increasing to a value just below the flight Mach number in supersonic flight, then approaching a Mach number of 2 at the fan face in high speed flight. The flow is diffused to subsonic conditions in the stator after the fan before it enters the core compressor.

The first active study of a supersonic compressor took place in Germany around 1935 and a few years later in the US. Axial flow compressor studies were begun there around 1940 by Kantrowitz at NACA. One of the most interesting results of Kantrowitz was that the highest efficiency of his compressor occurred in the transsonic range. This led to the subsequent development at NACA of transsonic compressors. The concept of the supersonic throughflow fan or booster stage before the main compressor was proposed by Antonio Ferri in the 1970's.

Studies have also been conducted at the Von Karman Institute e.g. by Breugelmans. However, problems with shock-boundary layer interaction phenomena and the resulting poor off-design performance have prohibited the use of supersonic stages.

Precooling

A severe restriction on the speed of a jet engine is the maximum permissible temperature of the compressor. Therefore, one way to increase the operating speed of the turbojet would be to use the fuel to cool down the air before the compressor.

Choosing the right type of fuel is indeed crucial to the success of a high speed aircraft. Because various sections of the aircraft will reach very high temperatures, its fuel must both provide energy for the engines and act as a structural coolant extracting destructive heat from the plane's surface.

Conventional kerosene fuels of the JP-type decompose at temperatures above 250 C. They are therefore not able to withstand the heating of the aircraft beyond Mach 2. Advanced JP-type fuels reach thermal stability limits at approximately Mach 3. At very high speeds, even exotic types of kerosene can not absorb enough heat. Endothermic fuels that absorb heat are studied but have practical and economic penalties.

Liquid hydrogen provides more than three times as much energy and absorbs six times more heat per weight than any other fuel. The disadvantage is its low density, which means larger fuel tanks, a larger airframe and more drag.

Most air-burning propulsion systems can be converted to burn hydrogen. In fact, von Ohains first prototype jet engine was running on hydrogen.

As is seen in Figure 18.6, the efficiency of an uncooled turboramjet engine is somewhat lower with hydrogen compared to

kerosene due to the lower value of the adiabatic constant γ. However, because the heating value of hydrogen is so much higher, the fuel consumption is much smaller.
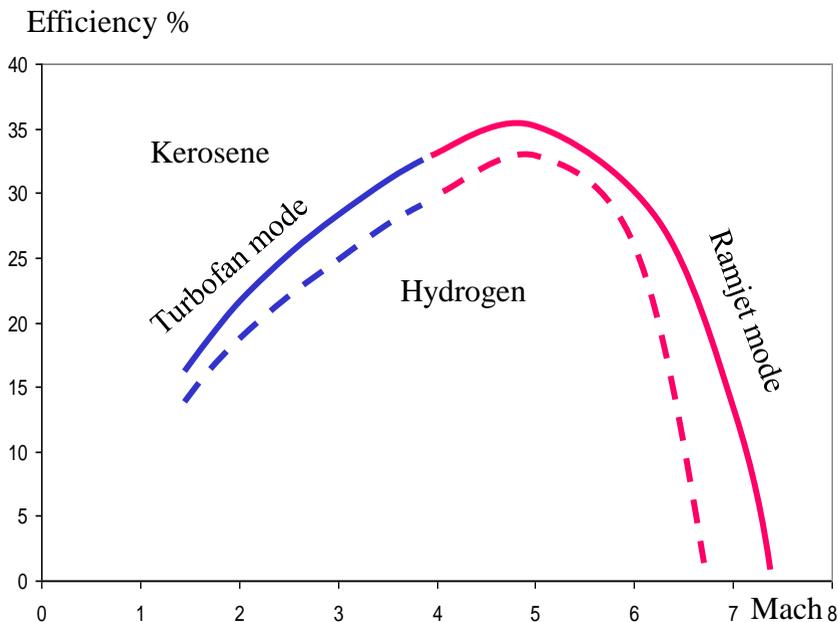
Efficiency %

Fig. 18.6 Decreased efficiency with hydrogen

Heating values for different fuels are:

Kerosene   43 MJ/kg
Methane   50 MJ/kg
Hydrogen   120 MJ/kg

While liquid hydrogen is the fuel of choice for space launch vehicles that accelerate quickly out of the atmosphere, studies have shown that liquid methane is better for an aircraft cruising at Mach

5 to Mach 7. Methane is widely available, provides more energy than jet fuels, and can absorb five times as much heat as kerosene. Compared with liquid hydrogen, it is three times denser and easier to handle.

A favorable property of hydrogen is its heat sink capacity. Effects of precooling with hydrogen are:

- Lower temperature at compressor exit, hence increased Mach capability.
- Increased pressure and flow density in the combustor for a given compressor maximum exit temperature, hence increased engine air flow.
- Lower power demand for compression because the converging pressure lines.
- There is a positive effect on the cycle of heating up the fuel.
- A problem is that icing of the heat exchangers can hardly be avoided below 8 km.
- The relatively low convective heat transfer rates in air leads to a large surface area in the cooler and a relatively large pressure loss of more than 10%. There is also a relatively large weight increase of the engine.
- The inlet size must be increased to accommodate the additional air flow. This also leads to an increased weight and to increased spillage drag at low speed.

Tests on different types of precoolers have been carried out by Tanatsugo et al (IAF-95-s.5.01). The precooler temperature efficiency is defined to be the ratio of the temperature difference between the air inlet and outlet and the temperature difference between air inlet and hydrogen inlet.

$$\eta_p = \frac{T_{t13} - T_{t23}}{T_{t13} - T_{hi}} \tag{18.42}$$

so that the air outlet temperature is:

$$T_{t23} = T_{t13}(1 - \eta_p) + \eta_p T_{hi} \tag{18.43}$$

The air pressure recovery factor is defined to be the ratio of stagnation pressures in the outlet and inlet of the precooler:

$$\pi_p = \frac{p_{t23}}{p_{t13}} \tag{18.44}$$

A "drum" type precooler was found to be the most efficient. The efficiency and the pressure recovery factor for this type of precooler was found to correlate well with the flow rates as follows:

$$\eta_p = \eta_{p0}^{(\dot{m}_a / \dot{m}_{a0})^{0.11} / (f / f_0)^{0.74}} \tag{18.45}$$

$$\pi_p = 1 - (1 - \pi_{p0})(\frac{\dot{m}_a}{\dot{m}_{a0}} \frac{p_{t130}}{p_{t13}} \sqrt{\frac{T_{t13}}{T_{t130}}})^{2.21} (\frac{f}{f_0} \frac{\dot{m}_a}{\dot{m}_{a0}})^{-0.195} \tag{18.46}$$

where "f" is the ratio between hydrogen and the core air mass flow and "0" signifies the design point. Typical values in the design point are efficency 50 % and pressure recovery factor 0.95.
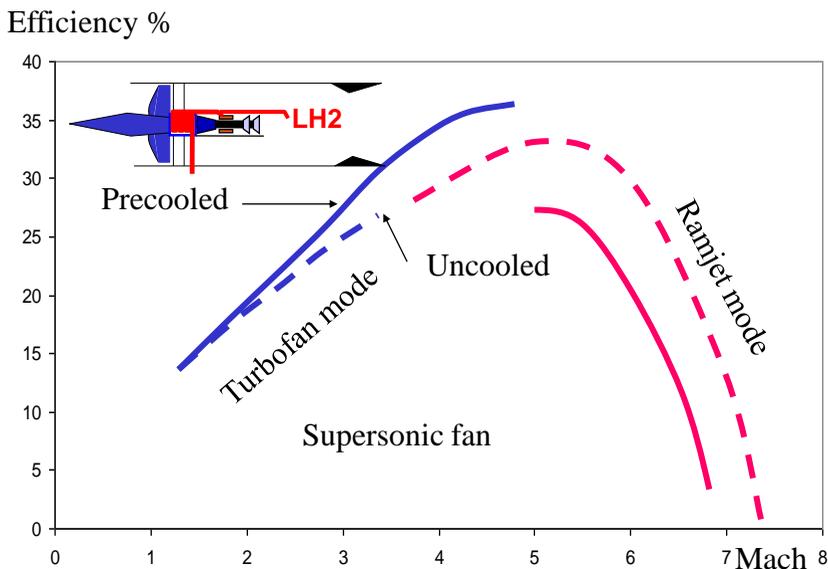
Efficiency %

Fig. 18.7 Increased efficiency with precooling

Using a precooler, it is seen from Figure 18.7 for a hydrogen turboramjet that the range of the turbofan engine is stretched out, which is the main advantage of the cooler. However, if the engine would be operated also as a ramjet, then the advantage of the precooling is much less evident.

One of the main features of a precooled turboramjet is a significant increase in the mass flow due to the lower air temperature. Once the core engine is closed down and the engine continues to operate as an ordinary ramjet, this effect is no longer there. The precooled ramjet cannot swallow as much air as the uncooled one. This

explains the decrease in efficiency in ramjet mode compared to the uncooled engine.

.

Also, to take full advantage of the extended speed as a turbofan, the fan must be made to endure the stagnation temperature. For a precooled compressor, the temperature at the compressor inlet is always cooler than the fan temperature. With sufficient cooling, the fan temperature will be higher than the compressor outlet temperature. The engine can therefore be operated until the limiting fan outlet temperature is reached if it is assumed that this is below the maximum inlet temperature of the cooler. By manufacturing the fan components in a suitable high temperature material (such as reinforced ceramic) the compressor temperature is again critical and it is possible to operate the engine to Mach 5-6.

An alternative would be to use a straight turbojet instead of a turbofan as a core for the turboramjet. However, for applications where high subsonic cruise efficiency is required, the turbofan is universally preferred. It also provides high thrust levels for launching and acceleration. At subsonic speeds, turbofans generally have higher installation drags than turbojets. This drawback is not so severe at higher speeds since the inlet capture area tends to exceed the total frontal engine area.

The weight and bulk of the gas generator for a high speed engine is small compared to the variable inlet, the afterburner and the variable nozzle. If a fan is used, it has to be windmilling at higher speeds, which leads to a blocking in the bypass canal. On the other hand, the turbojet will have to be bypassed at higher speeds using a valving arrangement which allows ram air to enter the afterburner directly. Of course, the same arrangement can be used with a turbofan even if it makes the engine more complicated

Appendix 18
Turboramjet calculation scheme
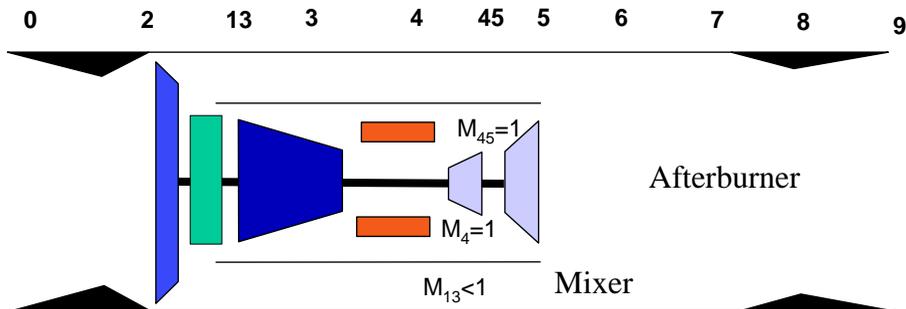
The indata to the calculations are:

Design Mach number M	1.5
Ambient temperature at 11 km T_0 K	216
D:o pressure p_0 Pa	2.27E+04
Adiabatic constant in cold parts γ_c	1.4
Fan design pressure ratio π_{f0}	4.0
Fan polytropic efficiency η_f	0.9

Design fan tip Mach number relative max	0.9
Number of fan stages	2
Hydrogen cooler inlet temperature T_{hi} K	30
Precooler design efficiency η_{p0}	0.5
Design core mass flow m_0 kg/s	33.4
Design hydrogen fraction f_0	0.076
Design precooler pressure recovery factor π_p	0.95
Design fan pressure p_{t130} Pa	3.31E+05
Design fan temperature T_{t130} K	486.3
Hydrogen heat of combustion h J/kg	1.2E+08
Hydrogen heat of vaporization H_{vap} J/kg	5.5E+05
Hydrogen specific heat C_{pH}	14500
Compressor polytropic efficiency η_c	0.9
Compressor max metal temperature T_{cm} K	875
Design air coolant flow fraction ε	0.083
Design gas generator fuel fraction f_{b0}	0.0135
Combustor efficiency η_b	1
Specific heat in cold parts C_{pc}	1005
D:o hot parts C_{pt}	1244
Adiabatic constant in hot parts γ_t	1.3
Turbine polytropic efficiency η_t	0.88
Nozzle efficiency η_j	0.95
Afterburner combustion efficiency η_a	0.9
Specific heat in afterburner C_{pa}	1500
Afterburner temperature T_{ta} K	2700
Pressure recovery in combustion chamber π_b	0.95
Pressure recovery in afterburner π_a	0.95
Pressure recovery in mixer	0.95
HP turbine area A_4 m2	0.0224
LP turbine area A_{45} m2	0.0346
LP turbine exhaust area A_5 m2	0.146
Bypass area A_{13} m2	0.108

| Off-design factor K | 0.088 |
| Design turbine inlet temperature | 1800 |

A summary of the calculation scheme is given below.

Assume coolant flow fraction f_c	0.08
Mach number	2
Stagnation temperature ratio $\tau_0 = 1 + \dfrac{\gamma_c - 1}{2} M^2$	1.8
Design point turbine inlet temperature: $T_{t4} = T_{t4des} \tau_0 / \tau_{odes}$ Use max allowed value in calculations.	2234 2000
Assume $M_{tdes} / M_{tmax} = 0.9$	
Max allowed fan temperature ratio: $\tau_{fd} = (1 + \dfrac{\tau_{0des}}{\tau_0} (\tau_{fdes}^{1/n} - 1)(M_{t\max} / M_{tdes})^2)^n$	1.55
Max allowed fan pressure ratio $\pi_{fd} = \tau_{fd}^{\eta_f \gamma_c / (\gamma_c - 1)}$	3.98
Assumed downrated fan pressure ratio π_{f0} to meet A_{8dry}	3.4
Fan inlet Mach number. Assume that the inlet geometry is varied so that M_2 is 2/3 of free stream value. This is used if below a max value of $M_2 = 2$.	1.33
Stagnation pressure ratio $\pi_0 = \tau_0^{\gamma_c / (\gamma_c - 1)}$	7.82
The kinetic energy efficiency:	

$\eta_{ke} = 1 - 0.4(1 - \dfrac{M_2}{M_0})^4$	0.995
The inlet pressure loss: $\pi_d = \left(\dfrac{T_0}{T_x}\right)^{\frac{\gamma}{\gamma-1}} = 1/\left(1 + (1 - \eta_{ke})\dfrac{\gamma-1}{2}M_0^2\right)^{\frac{\gamma}{\gamma-1}}$	0.986
Inlet temperature $T_{t2} = \tau_0 T_0$	389
Inlet pressure $p_{t2} = \pi_0 \pi_d p_0$	1.75E+5
Fan temperature ratio $\tau_f = \pi_f^{(\gamma_c-1)/\gamma_c\eta_f}$	1.475
The temperature after the fan $T_{t13} = \tau_f T_{t2}$ If $T_{t13} > T_{cm}$ then the fan pressure ratio could be downrated until $T_{t13} = T_{cm}$	573
Fan pressure $p_{t13} = \pi_f p_{t2}$	5.96E+05
Assume efficiency in precooler.	0.515
Assume pressure recovery in precooler	0.96
The temperature after the cooler $T_{t23} = T_{t13}(1 - \eta_p) + \eta_p T_{hi}$	293.5
Pressure after the cooler $p_{t23} = \pi_p p_{t13}$:	5.72E+5

Hydrogen temperature after cooler $$T_H = T_{H0} + \frac{\eta_p C_{pc}}{f C_{pH}}(T_{t13} - T_{H0}) + \frac{H_{vap}}{C_{pH}}$$	299
Compressor exhaust temperature: $$T_{t3} = T_{t23} + (1 + f_{b0} - \varepsilon)\frac{C_{pt}}{C_{pc}} K T_{t4}$$ Design values of fuel and cooling air flows are used throughout. **If $T_{t3} > T_{cm}$ then $T_{t3} = T_{cm}$** **And the turbine inlet temperature is given as:** $$T_{t4} = \frac{C_{pc}}{K C_{pt}} \frac{T_{cm} - T_{t23}}{1 + f - \varepsilon}$$	484
Compressor exhaust pressure: $p_{t3} = p_{t23}(\frac{T_{t3}}{T_{t23}})^{\gamma_c \eta_c /(\gamma_c - 1)}$	2.78E+6
Combustion chamber exhaust pressure: $p_{t4} = \pi_b p_{t3}$	2.64E+06
The fuel flow $$f = (1 - \varepsilon)\left[C_{pt}(T_{t4} - 298) - C_{pc}(T_{t3} - T_H)\right]/(\eta_b h - C_{pt}(T_{t4} - 298))$$	0.015
HP turbine exhaust temperature: $T_{t45} = T_{t4}(1 - K)$	1834
After mixing in cooling air: $$T'_{t45} = \frac{\varepsilon}{1 + f}\frac{C_{pc}}{C_{pt}}T_{t3} + \frac{1 + f - \varepsilon}{1 + f}T_{t45}$$	1716

Pressure after HP turbine: $p_{t45} = p_{t4}\left(\dfrac{T_{t45}}{T_{t4}}\right)^{\gamma_t/(\gamma_t-1)\eta_t}$	1.72E+6
HP turbine mass flow parameter: $\overline{m}_4 = \dfrac{\gamma_t}{\sqrt{\gamma_t-1}}\left(\dfrac{2}{\gamma_t+1}\right)^{\frac{\gamma_t+1}{2(\gamma_t-1)}}$	1.39
The core inlet mass flow: $\dot{m} = \dfrac{A_4}{1+f-\varepsilon}\dfrac{p_{t4}\overline{m}_4}{\sqrt{C_{pt}T_{t4}}}$	55.9
Assume bypass Mach number M_{13}	0.44
Bypass mass flow parameter: $\overline{m}(M_{13}) = \dfrac{\gamma_c}{\sqrt{\gamma_c-1}}M_{13}\left(1+\dfrac{\gamma_c-1}{2}M_{13}^2\right)^{-(\gamma_c+1)/2(\gamma_c-1)}$	0.87
Bypass mass flow: $\dot{m}_{13} = \overline{m}(M_{13})\dfrac{A_{13}p_{t13}}{\sqrt{C_{pc}T_{t13}}}$	73.9
Total mass flow	130
The bypass ratio: $\alpha = \dfrac{\dot{m}_{13}}{\dot{m}}$	1.32

LP turbine exhaust temperature: $$T_{t5} = T'_{t45} - \frac{1+\alpha}{1+f}\frac{C_{pc}}{C_{pt}}(T_{t13} - T_{t2})$$	1370
LP turbine exhaust pressure: $p_{t5} = p_{t45}\left(\dfrac{T_{t5}}{T'_{t45}}\right)^{\frac{\gamma_t}{\eta_t(\gamma_t - 1)}}$	5.77E+5
LP turbine exhaust Mach number: $$M_5 = \sqrt{\frac{2}{\gamma_t - 1}\left\{\left[\frac{p_{t5}}{p_{t13}}\left(1 + \frac{\gamma_c - 1}{2}M_{13}^2\right)^{\frac{\gamma_c}{\gamma_c - 1}}\right]^{\frac{\gamma_t - 1}{\gamma_t}} - 1\right\}}$$	0.4
LP turbine exhaust mass flow parameter: $$\overline{m}_5 = \frac{\gamma_t}{\sqrt{\gamma_t - 1}}M_5\left(1 + \frac{\gamma_t - 1}{2}M_5^2\right)^{-(\gamma_t + 1)/2(\gamma_t - 1)}$$	0.865
LP turbine mass flow: $m_5 = \overline{m}_5\dfrac{A_5 p_{t5}}{\sqrt{C_{pt}T_{t5}}}$	56.0

Continuity of the mass flow requires $\dot{m}_5 = \dot{m}(1 + f_b)$ **If not, assume a new M$_{13}$**	
The mean specific heat of the exhaust stream is obtained from a simple mass weighting $(1 + \alpha + f_b)C_{p6} = (1 + f)C_{pt} + \alpha C_{pc}$	1110
$\gamma_6 = \dfrac{1}{1 - R/C_{p6}}$	1.35
The mixed temperature $T_{t6} = T_{t5}\dfrac{C_{pt}}{C_{p6}}\dfrac{1 + f}{1 + \alpha + f} + T_{t13}\dfrac{C_{pc}}{C_{p6}}\dfrac{\alpha}{1 + \alpha + f}$	964
Afterburner fuel flow: $f_a = (1 + f + \alpha)\left[C_{pa}(T_{ta} - 298) - C_{p6}(T_{t6} - T_H)\right]/(\eta_b h - C_{pa}(T_{ta} - 298))$	0.064
Fix a total fuel flow > f$_a$ +f$_b$	0.079
Cooler efficiency: $\eta_p = \eta_{p0}^{(\dot{m}_a / \dot{m}_{a0})^{0.11}/(f / f_0)^{0.74}}$	0.50

Cooler pressure recovery: $$\pi_p = 1 - (1 - \pi_{p0})(\frac{\dot{m}_a}{\dot{m}_{a0}} \frac{p_{t130}}{p_{t13}} \sqrt{\frac{T_{t13}}{T_{t130}}})^{2.21} (\frac{f}{f_0} \frac{\dot{m}_a}{\dot{m}_{a0}})^{-0.195}$$ **Iterate if necessary.**	0.955
Introducing: $$\Phi_5 = \frac{\gamma_t^{\;2}}{\gamma_t - 1} \frac{M_5^{\;2}}{C_{pt}T_{t5}(1 + \gamma_t M_5^{\;2})^2}\left(1 + \frac{\gamma_t - 1}{2}M_5^{\;2}\right)$$	3.69E-7
and: $\quad \Phi_{13} = \dfrac{\gamma_c^{\;2}}{\gamma_c - 1} \dfrac{M_{13}^{\;2}}{C_{pc}T_{t13}(1 + \gamma_c M_{13}^{\;2})^2}\left(1 + \dfrac{\gamma_c - 1}{2}M_{13}^{\;2}\right)$	1.06E-7
$$\phi_6 = \frac{\gamma_6 - 1}{\gamma_6^2}C_{p6}T_{t6}\Phi_6 = \frac{\gamma_6 - 1}{\gamma_6^2}C_{p6}T_{t6}\left(\frac{1 + f + \alpha}{\dfrac{1+f}{\sqrt{\Phi_5}} + \dfrac{\alpha}{\sqrt{\Phi_{13}}}}\right)$$	0.128
The mixer exhaust Mach number: $$M_6 = \sqrt{\frac{2\phi_6}{1 - 2\gamma_6\phi_6 + \sqrt{1 - 2(\gamma_6 + 1)\phi_6}}}$$ **If $M_6 > 1$, then T_{t4} must be adjusted**.	0.57

Exhaust duct mass flow parameter: $$\overline{m}_6 = \frac{\gamma_6}{\sqrt{\gamma_6 - 1}} M_6 \left(1 + \frac{\gamma_6 - 1}{2} M_6^2\right)^{-(\gamma_6 + 1)/2(\gamma_6 - 1)}$$	1.085
Mixer area $A_6 = A_4 + A_{13}$	0.254
Exhaust duct pressure: $p_{t6} = \pi_m \dfrac{(1 + f + \alpha)\dot{m}\sqrt{C_{p6}T_{t6}}}{A_6 \overline{m}_6}$	4.64E5
Nozzle mass flow parameter: $\overline{m}_8 = \dfrac{\gamma_7}{\sqrt{\gamma_7 - 1}} \left(\dfrac{2}{\gamma_7 + 1}\right)^{\frac{\gamma_7 + 1}{2(\gamma_7 - 1)}}$	1.33
The nozzle area: $A_8 = \dfrac{\dot{m}_{tot}\sqrt{C_{p7}T_{t7}}}{p_{t7}\overline{m}_8}$	0.221
Without afterburner, the jet speed is with an ideal convergent-divergent nozzle $$V_j = \sqrt{2\eta_j C_{pm}T_{t6}\left[1 - \left(p_0/p_{t6}\right)^{(\gamma_m - 1)/\gamma_m}\right]}$$	1049
The speed of sound at 11 km $$a_0 = \sqrt{\gamma_c R T_0} = \sqrt{(\gamma_c - 1)C_{pc}T_0}$$	295
The flight speed	589

The specific thrust $$\frac{F}{\dot{m}(1+\alpha)} = a_0 \frac{1+\alpha+f}{1+\alpha} \sqrt{\frac{2\eta_j}{\gamma_c-1} \frac{C_{pm}}{C_{pc}} \frac{T_{t6}}{T_0} \left[1-\left(p_0/p_{t6}\right)^{(\gamma_m-1)/\gamma_m}\right]} - V$$	466
Dry thrust $F = \dot{m}_{tot} F_{spec}$	60500 N
The dry efficiency of the engine is $$\eta = \frac{FV}{f\dot{m}H} = \frac{V(1+\alpha)F_{spec}}{fH}$$	0.354
The mean specific heat of the exhaust stream with mixing in of hydrogen: $(1+\alpha+f)C_{p7} = (1+\alpha+f_b+f_a)C_{p6} + (f-f_b-f_a)C_{pH}$	1530
$$\gamma_7 = \frac{1}{1-R/C_{p7}}$$	1.23
Temperature in afterburner after mixing in of surplus hydrogen: $(1+\alpha+f)T_{t7} = (1+\alpha+f_b+f_a)T_{ta} + (f-f_b-f_a)T_H$	2650
Pressure in the afterburner $p_{ta} = \pi_a p_{t6}$	4.40E+05
The jet speed with afterburner $$V_j = \sqrt{2\eta_j C_{pa} T_{ta}\left[1-\left(p_0/p_{ta}\right)^{(\gamma_a-1)/\gamma_a}\right]}$$	1814

The specific thrust with afterburner $$\frac{F}{\dot{m}(1+\alpha)} = a_0 \frac{1+\alpha+f+f_a}{1+\alpha} \sqrt{\frac{2\eta_j}{\gamma_c-1} \frac{C_{pa}}{C_{pc}} \frac{T_{ta}}{T_0} \left[1 - \left(p_0/p_{ta}\right)^{(\gamma_a-1)/\gamma_a}\right]} - V$$	1290
Thrust with afterburner	167000
Efficiency with afterburner	0.175
Nozzle mass flow parameter: $\overline{m}_8 = \dfrac{\gamma_7}{\sqrt{\gamma_7-1}} \left(\dfrac{2}{\gamma_7+1}\right)^{\frac{\gamma_7+1}{2(\gamma_7-1)}}$	1.51
The nozzle area: $A_8 = \dfrac{\dot{m}_{tot}\sqrt{C_{p7}T_{t7}}}{p_{t7}\overline{m}_8}$	0.411

19. RAMJETS AND SCRAMJETS

The turboramjet will ultimately be driven towards a straight ramjet at higher speeds. The ramjet and the pulsejet, which may be regarded as a discontinuous ramjet, may operate to around Mach 6 where the inlet temperature becomes too high. The idea behind the scramjet engine is to keep the inlet temperature at a prescribed value by permitting supersonic flow in the combustor. Frictional losses, internal shock control and the difficulties of injecting and burning a fuel in a very high speed flow probably limits the speed of the scramjet to around Mach 10.
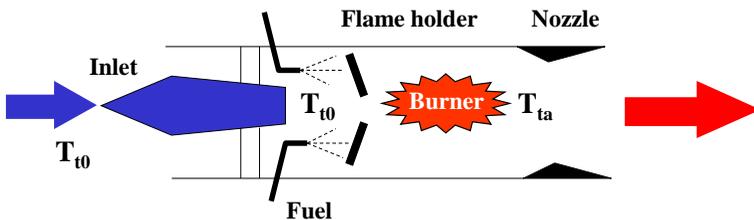
Fig. 19.1 The principle of a ramjet

The ramjet is a very simple device consisting of an inlet, a burner, and a nozzle. It does not have a compressor or a turbine. It has mostly been applied to missile propulsion but it may also be used as a step to more advanced high speed propulsion systems for new types of space launchers.

Rene Lorin of France was in 1913 probably the first to recognize the possibility of using ram pressure for propulsion. **Albert Fono** of Hungary was given a German patent in 1928 on a device with all the elements of a modern ramjet but there is no evidence that any was built. In 1938, the French aeronautical engineer **René Leduc** exhibited a model of a ramjet in Paris that resulted after the war in an experimental aircraft, the Leduc 010. On April 21, 1949, this aircraft was released from a parent aircraft and flew for the first time.

In 1953, France embarked on a project aimed at an aircraft that could fly up to Mach 2, the **Griffon II**. It made use of the first combined cycle engine in which a ramjet was wrapped around a SNECMA Atar engine. The Griffon II established a world record of 1640 km/h in 1959.

the ordinary ramjet can be understood by studying the ideal cycles. The power that is available for propulsion is the jet power added to the kinetic energy of the fuel minus the energy of the inlet flow so that:

$$\dot{E}_j = \frac{1}{2}(\dot{m}_a + \dot{m}_f)V_j^{\,2} + \frac{1}{2}\dot{m}_f V^2 - \frac{1}{2}\dot{m}_f V^2 \qquad (19.1)$$

The internal or thermal efficiency of the engine tells us how much of the chemical and kinetic energy supplied by the fuel we get out as kinetic energy of the jet:

$$\eta_t = \frac{\dot{E}_j}{\dot{m}_f (h + V^2/2)} = \frac{(1+f)V_j^2 - (1-f)V^2}{2f(h + V^2/2)} \qquad (19.2)$$

At the "low" speeds we are talking of, the kinetic energy can be neglected so that:

$$\eta_t = \frac{V_j^2 - V^2}{2fh} \qquad (19.3)$$

The "ideal" jet speed neglecting flow losses is then:

$$V_j^2 = V^2 + 2fh\eta_t \qquad (19.4)$$

The thrust is:

$$F = \dot{m}(V_j - V) \qquad (19.5)$$

and the thrust efficiency:

$$\eta = \frac{FV}{\dot{m}_f h} = \frac{(V_j - V)V}{fh} \qquad (19.6)$$

Thus if we know the thermal efficiency and the fuel consumption, we also know the jet speed and the efficiency.

The ramjet follows the ordinary Brayton cycle for turbojet engines but with all the pressure rise produced by the inlet. For a compressor pressure ratio of unity, we therefore obtain from Eq. (14.42) the simple expression:

$$\eta_{tB} = 1 - \frac{T_0}{T_{t0}} = 1 - \frac{1}{\tau_0} \qquad (19.7)$$

Where from Eq. (8.2) the stagnation temperature is:

$$T_{t0} / T_0 = \tau_0 = 1 + \frac{\gamma - 1}{2} M^2 \qquad (18.1)$$

A heat balance over the combustor gives for the ideal cycle:

$$f = \frac{C_p}{h} (T_{ta} - T_{t0}) = \frac{C_p T_0}{h} (\theta_a - \tau_0) \qquad (19.8)$$

Where:

$$C_p T_0 = \frac{a_0^2}{\gamma - 1} \qquad (19.9)$$

We now get:

$$V_j^2 = V^2 + 2fh\eta_t = V^2 + \frac{2a_0^2}{\gamma - 1} (\theta_a - \tau_0)(1 - 1/\tau_0) \qquad (19.10)$$

So the specific thrust is:

$$\frac{F}{\dot{m}a_0} = \sqrt{\frac{2}{\gamma - 1}(\theta_a - \tau_0)(1 - 1/\tau_0) + M_0^2} - M_0 \qquad (19.11)$$

and the thrust efficiency:

$$\eta = (\gamma - 1)M_0 \frac{\sqrt{\frac{2}{\gamma - 1}(\theta_a - \tau_0)(1 - 1/\tau_0) + M_0^2} - M_0}{(\theta_a - \tau_0)} \qquad (19.12)$$

As is seen there is a maximum speed of the ramjet when the stagnation temperature approaches the combustion temperature somewhere beyond Mach 5. However, the main deficiency of the ramjet is, as is also seen from Eq. (19.11), that it does not produce any thrust from take-off.
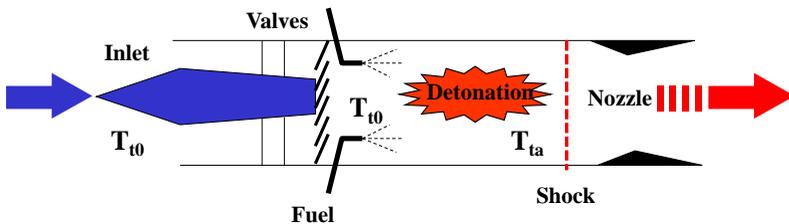
Fig. 19.2 The principle of a Pulse Detonation Engine

An interesting variant of the ramjet is the pulsejet, see Figure 19.2, which may be regarded as a discontinuous ramjet, although with significant differences in its way of operation. A discontinuous ejector effect may be obtained by pulsating combustion like in the German pulsejet **V1** (Vergeltungswaffe I) of the 2nd World War, which used flapper valves in the inlet allowing the air to flow in only one direction. The deflagration wave generated by the explosion in the V1 was not strong enough to cope with the ejector effect of the free stream. Hence the flame blew out at speeds beyond Mach 0.5.

This may be avoided if the combustion is made to take place by detonation, which is proceeding at supersonic speed, instead of explosion, which is a subsonic process. This is the **pulse detonation engine** (PDE).

High frequency (>60 Hz) pulse detonation combustors have been developed by several commercial firms and government laboratories in configurations consistent with aerospace propulsion applications.

As seen in Figure 19.2, air is supplied to the engine through a supersonic inlet. To prevent inlet unstart caused by detonation waves in the combustion chamber requires an interface to prevent the chamber flow from travelling into the inlet. This interface may be a mechanical valved design as was the case in the V1 or it may be achieved through gas dynamics means. The latter is mechanically simpler but may be more complicated to achieve gasdynamically and may limit the operation frequency.

A typical cycle of operation includes initiation and propagation of a detonation shock wave, blowdown of combustion products, filling of purge gas and recharge of reactants. Initially, the valves are open and air is supplied to the detonation chamber together with fuel. Air and fuel are mixed in the buffer zone between the inlet and combustor. The valve is then closed and detonation is initiated by a driver gas with a high temperature. A detonation wave propagates downstream into the nozzle and reflects from the nozzle walls producing a complex flow structure and diffracts outside as a decaying shock creating a toroidal vortex outside the engine. A reflected expansion wave propagates upward toward the closed inlet. This wave then strikes the close valves thrust wall and

rebounds accelerating the combustion products towards the nozzle. At the end of this process, the chamber contains burned products at rest. The valve is then opened sending a shock wave in the burned gases that are blown out of the chamber by the fresh air. Fuel is then introduced, detonation is initiated and the cycle is repeated.

The advantages of PDE's are:
- Theoretically a higher efficiency than a "constant pressure engine"
- Engines can be produced in many sizes and thrust outputs
- They have high thrust to weight ratio (lighter engine, more thrust)
- They are mechanically simple, and have few moving parts.
- The engine can be operated both in air breathing and rocket mode.

The pulse detonation engine promises to provide significant performance advantages over ramjets and turbojets. Jet engines and ramjets follow the so called Brayton cycle where combustion takes place at constant pressure. The PDE may be shown to closely follow the so called **Humphrey cycle** where heat is added at constant volume, see Figure 14.9 reproduced below. The thermal efficiency of that cycle is given in Eqs. (14.46) and (14.47) so that with the detonation temperature T_{td}:

$$\eta_{tH} = 1 - k/\tau_0 \tag{19.13}$$

where:

$$k = \gamma_d \frac{(T_{td}/T_{t0})^{1/\gamma_d} - 1}{T_{td}/T_{t0} - 1} = \gamma_d \frac{(\theta_d/\tau_0)^{1/\gamma_d} - 1}{\theta_d/\tau_0 - 1} \tag{19.14}$$

The pulsating ramjet
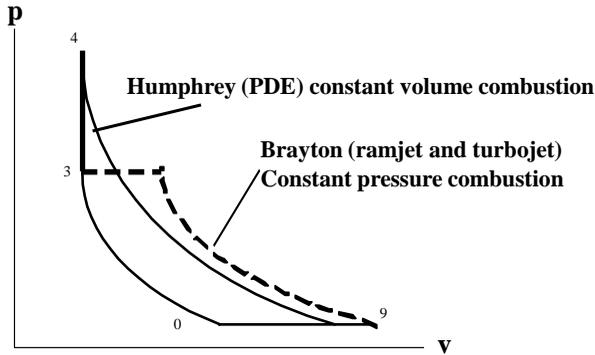
Fig. 14.9 The Humphrey and Brayton cycles

A heat balance over the combustor gives for the Humphrey cycle:

$$f = \frac{C_v}{h}(T_{td} - T_{t0}) = \frac{C_p T_0}{\gamma_d h}(\theta_d - \tau_0) \qquad (19.15)$$

We now get:

$$V_j^2 = V^2 + 2fh\eta_t = V^2 + \frac{2a_0^2}{\gamma - 1}(\theta_d - \tau_0)(1 - k/\tau_0)/\gamma_d \qquad (19.16)$$

So the specific thrust is:

$$\frac{F}{\dot{m}a_0} = \sqrt{\frac{2}{\gamma - 1}(\theta_d - \tau_0)(1 - k/\tau_0)/\gamma_d + M_0^2} - M_0 \qquad (19.17)$$

and the thrust efficiency:

$$\eta = \eta_b \gamma_d (\gamma - 1) M_0 \frac{\sqrt{\dfrac{2}{\gamma - 1}(\theta_d - \tau_0)(1 - k/\tau_0)/\gamma_d + M_0{}^2} - M_0}{(\theta_d - \tau_0)}$$

(19.18)

Note that for $k=\gamma_d=1$ we obtain the efficiency of the ordinary ramjet following the Brayton cycle. For the ramjet the specific thrust is zero at M=0. The PDE, however, gives thrust at M=0. It can therefore be used for take-off.
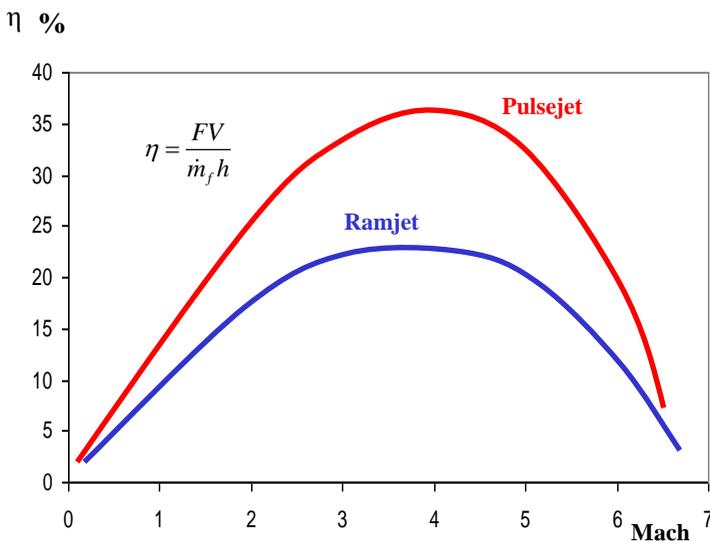
Fig. 19.3 The PDE is more efficient than the ramjet

The typical variation of the **efficiency** for hydrogen powered **ramjets and pulsejets** is shown in Figure 19.3. The pulsejet is shown to be more efficient and therefore has a lower fuel consumption. The efficiency of both the ramjet and the pulsejet increases with speed as pressure builds up in the engine. Soon, however, it starts to decrease due to the shrinking gap between the stagnation temperature and the maximum temperature that may be permitted within the combustion chamber.

At normal supersonic velocities η/M gives a good indication of the thrust variation with the Mach number because it is directly related to the specific impulse I_s, see Figure 19.4.

%

$$\eta / M_0 = \frac{Fa_0}{\dot{m}_f h} = \frac{I_s a_0}{h}$$

Pulsejet
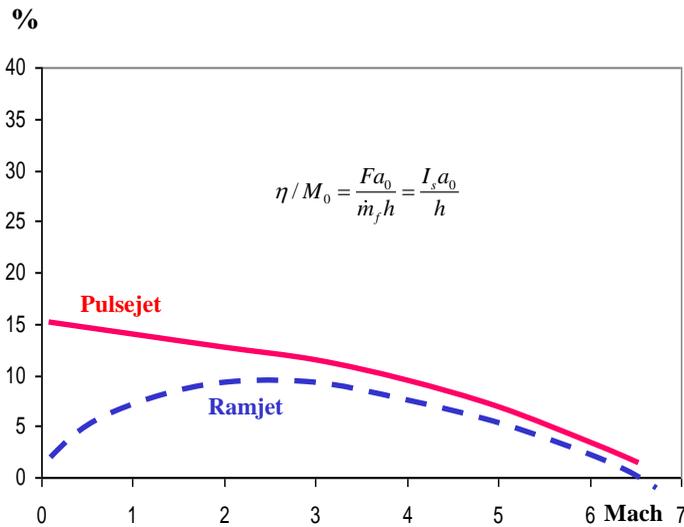
Ramjet

Fig. 19.4 The PDE has thrust at take-off

The main deficiency of the ramjet is immediately obvious, namely that the thrust vanishes at low speed. It is therefore impossible to use it from take-off. It needs another engine to give it the speed

where it can start functioning well, which is above Mach 2. Note also that the thrust of the ramjet has its maximum at a lower speed than the efficiency.

Increasing the combustor entry temperature will eventually result in dissociation of the air during combustion. Part of the internal molecular energy added is then not available for conversion to kinetic energy in the nozzle. Because of this the combustor temperature is limited to below the so called stoichiometric temperature where dissociation increases rapidly. When the stagnation temperature approaches this maximum temperature, there is no room for combustion and the thrust vanishes. There is therefore a maximum temperature for both the PDE and the ramjet that restricts the speed range to not much beyond Mach 6. The maximum Mach number will be:

$$M_{max} = \sqrt{\frac{2}{\gamma - 1}(\frac{T_{ta}}{T_0} - 1)}$$

(8.24)

Pulse detonation based propulsion systems can be combined with a ramjet/scramjet or rocket propulsion cycle where each cycle operates in a different speed range to optimize overall system performance. Thus, it has been suggested that a pulsating jet engine afterburner would be more compact and efficient than a continuous one.

For any of these systems, the requirements for the components external to the detonation tubes are not well understood. The use of an unsteady detonative combustor will have major impacts on those components, which need to be evaluated. The overall system performance is by the same token poorly characterized because of the unknown component performances.

One of the main problems is whether a stable shock system can be established in the inlet without unstarts, the surge-like phenomenon that may occur in high speed aircraft. Inlet losses occur with open inlets where the detonation wave is allowed to travel backwards to be expelled by the inlet. On the other hand, valved inlets tend to stagnate the inlet air flow with high losses as a consequence. More efficient may be to employ a multiple combustor concept, where a rotary valve serves to meter air to different combustors in a continuous manner in such a way that the inlet flow need not be stagnated. This is the so called "wave rotor" described in Chapter 14.

Another problem is the mixing and ignition of the fuel to make detonation possible. Efficient initiation of detonation is a key to engine operation. Special designs will be necessary to enhance fuel/air mixing under flight conditions. The unsteady nature of the process also means that nozzle design is critical.

The Scramjet

In the ordinary ramjet, combustion takes place at very low velocities. This leads to high stagnation temperatures and a restriction on the permitted heat release because the total combustor temperature is limited by materials or by dissociation.
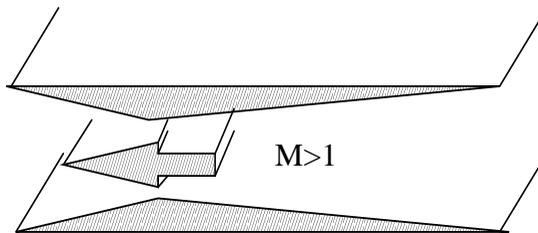
Fig. 19.6 The supersonic ramjet (Scramjet)

A conventional hydrogen fuelled ramjet with a subsonic combustor is capable of operating up to around Mach 5-6 at which point the limiting effects of dissociation reduce the effective heat addition to the air flow resulting in a rapid loss in net thrust.

The idea behind the Supersonic Combustion Ramjet (scramjet) engine, see Figure 19.6, is to avoid the dissociation limit due to the inlet stagnation temperature by permitting supersonic flow in the combustor. Because the flow remains supersonic, its temperature does not increase as dramatically as it does in ramjets hence permitting greater useful heat addition. By this means scramjet engines offer the tantalising prospect of achieving a high specific impulse up to very high Mach numbers.

The scramjet concept was invented in the late 1950s and from 1955-1965 a great deal of progress was made in scramjet propulsion. The interest in the potential of scramjet propulsion was encouraged by early proponents of the technology such as **Antonio Ferri** in the US. The first tests of scramjets in short duration facilities were carried out by **Jim Swithenbank** at the University of Sheffield (England) beginning in the 1960s. A wide variety of scramjets were built and tested, which confirmed the feasibility of supersonic burning.

In the mid-1960s, the US Air Force initiated the Aerospaceplane program, which was intended to develop a single-stage-to-orbit aircraft using scramjet propulsion. There was significant engine development testing in long-duration facilities up to Mach 8.

An experimental aircraft the **X-15** was flown in the US to Mach 6.72 in 1967 but the project was terminated in 1968 because of the technical problems involved especially in mixing and combustion. In the 1970s NASA demonstrated basic scramjet technology with models of hypersonic vehicles in a wind tunnel but it had now become clear that many problems still needed to be confronted.

Testing facilities were still scarce and national attention was firmly fixed on the race to the moon so the program was eventually cancelled.

NASA then embarked on a more modest effort intended to develop a flight-weight scramjet engine for testing on the X-15 aircraft at up to Mach 8. After the cancellation of the X-15 program in 1968 the engine program was restricted toward the testing of two engine modules, a structural evaluator and a performance evaluator. These tests were carried out from 1972 to 1974.

Eventually, advances in materials, structures and other key technology areas led to a resurgence of interest in single-stage-to-orbit vehicles. This interest culminated in a national program, the National Aero Space Plane (**NASP**) in 1986, but this program was also cancelled some years later. Some work was also performed in the former Soviet Union by the Central Institute for Aviation Motors (CIAM), which tested a dual mode ramjet/scramjet in 1992 on the top of a rocket during which the engine operated to a Mach number of 5.5. The same test was carried out some years later in the US.

Scramjets are assumed to be fueled by cryogenic hydrogen or methane instead of a liquid hydrocarbon. The primary reason is to exploit the greater heat release per unit weight of fuels that have a higher ratio of hydrogen to carbon atoms than ordinary fractions of petroleum even though this gain is to be balanced against the higher volume of such fuels. Another incentive for employing a very cold fuel is that it may be used as a heat sink for cooling a very high-speed (and hence very hot) engine and aircraft structure.

The static temperature at the combustor inlet must be limited to a value that prevents excessive dissociation during the heat addition process. It is usually recommended that the static temperature at the combustor inlet be restricted to 1560 K. To keep this temperature the Mach number at the combustor inlet is allowed to increase and become supersonic.

Noting that the total temperature is constant throughout the compression process, it is possible to derive the flight Mach number at which the flow into the combustor becomes supersonic so that the ramjet becomes a scramjet. Let "3" designate the combustor inlet and "0" the engine inlet. Then since the total temperature is a constant throughout the stagnation process

$$T_t = T_0 \left(1 + \frac{\gamma - 1}{2} M_0^2 \right) = T_3 \left(1 + \frac{\gamma - 1}{2} M_3^2 \right) \qquad (19.19)$$

For a ramjet engine, $M_3=0$ so that the static temperature at the combustor inlet equals the stagnation temperature. For a scramjet, $M_3>1$ which means that:

$$T_0 \left(1 + \frac{\gamma - 1}{2} M_0^2 \right) > \frac{\gamma + 1}{2} T_3 \qquad (19.20)$$

Therefore the ramjet becomes a scramjet when:

$$M_0 \rangle \sqrt{\frac{2}{\gamma - 1} \left[\left(\frac{\gamma + 1}{2} \right) \frac{T_3}{T_0} - 1 \right]} \qquad (19.21)$$

It is also seen that the Mach number in the scramjet combustor becomes:

$$M_3 = \sqrt{M_0^2 \frac{T_0}{T_3} - (1 - \frac{T_0}{T_3}) \frac{2}{\gamma - 1}}$$ (19.22)

When the Mach numbers are large this reduces to the "rule-of-thumb":

$$\frac{M_3}{M_0} \approx \sqrt{\frac{T_0}{T_3}}$$ (19.23)

Efficiency is of great importance for the scramjet performance. A simplified way to take flow losses due to friction, shock waves and mixing into account is to use an overall kinetic energy efficiency.

We have earlier introduced the "kinetic efficiency" for the inlet from which the air speed into the combustor, see Eq. (18.29):

$$V_3 = V_0 \sqrt{\eta_{ki}}$$ (19.24)

where from Eq. (18.31) the kinetic efficiency of the inlet is:

$$\eta_{ki} = 1 - 0.4(1 - \frac{M_3}{M_0})^4$$ (19.25)

The combustor Mach number M_3 varies with the flight Mach number according to Eq. (19.22) so that the kinetic efficiency eventually takes on a constant value as the combustor Mach number approaches that given in Eq. (19.23).

Because the Mach number does not vary through the combustor of the scramjet, the relation between the air speed at the combustor exit and inlet is:

$$\frac{V_4}{V_3} = \frac{M_4 a_4}{M_3 a_3} = \sqrt{\frac{T_4}{T_3}} = \sqrt{\frac{T_{t4}}{T_{t3}}} \qquad (19.26)$$

or introducing a kinetic efficiency η_{kc} for the combustor taking into account the momentum losses due to fuel injection and the friction losses:

$$V_4 = V_3 \sqrt{\tau_b \eta_{kc}} \qquad (19.27)$$

where $\tau_b = T_{t4}/T_{t3}$ is the total temperature rise over the combustor. From experiments a kinetic efficiency between 0.65 and 0.75 seems to be realistic.

Lastly, the gases will expand out of the nozzle with a kinetic efficiency η_{kn} around 0.9 so that:

$$V_j = V_0 \sqrt{\tau_b \eta_{ki} \eta_{kc} \eta_{kn}} = V_0 \sqrt{\tau_b \eta_{ke}} \qquad (19.28)$$

Because the gases will accelerate out of the combustion chamber, the total temperature rise over the scramjet combustor is not restricted by the max temperature as in the ramjet but is determined from the heat release of the fuel:

$$\left(\dot{m}_f + \dot{m}_a \right) C_p T_{t4} - \dot{m}_a C_p T_{t3} = \eta_b \dot{m}_f h \qquad (19.29)$$

so that since $T_{t3}=T_{t0}$ and $f=\dot{m}_f / \dot{m}_a$

$$\tau_b = \frac{1}{1+f}\left(1+\frac{\eta_b fh}{C_p T_{t0}}\right) \tag{19.30}$$

where the combustion efficiency would be around $\eta_b=0.9$.

Introducing this expression for τ_b into Eq. (19.28), the specific thrust becomes:

$$\frac{F}{\dot{m}} = a_0 M_0\left[\sqrt{\eta_{ke}(1+f)\left(1+\frac{fh\eta_b}{C_p T_{t0}}\right)}-1\right] \tag{19.31}$$

where the free stream stagnation temperature is:

$$T_{t0} = T_0(1+\frac{\gamma-1}{2}M_0^2) \tag{19.32}$$

At high speed, the fuel burnt contains not only the chemical energy but also a significant kinetic energy. The thrust work efficiency will therefore be:

$$\eta = \frac{FV_0}{\dot{m}f(h+V_0^2/2)} = \frac{a_0^2 M_0^2}{f(h+a_0^2 M_0^2/2)}\left[\sqrt{\eta_{ke}(1+f)\left(1+\frac{fh\eta_b}{C_p T_{t0}}\right)}-1\right] \tag{19.33}$$

It is obvious from these equations that the specific thrust steadily increases with the fuel/air ratio but that this is not so for the

efficiency. In fact, the efficiency will be a maximum for any Mach number at the fuel/air ratio:

$$f_{opt} = \frac{2\sqrt{1-\eta_{ke}}}{(1-\sqrt{1-\eta_{ke}})\eta_b h/C_p T_{t0} - 1 - \sqrt{1-\eta_{ke}}} \qquad (19.34)$$

provided that $f_{opt} < f_s$, the stoichiometric value, which for hydrogen is 0.0291. In fact, most often $f_{opt} > f_s$. If so, the value of f must be kept at the stoichiometric one in the chemical heat release term in Eqs. (19.31) and (19.33) while it can take on any value in the mass addition terms.
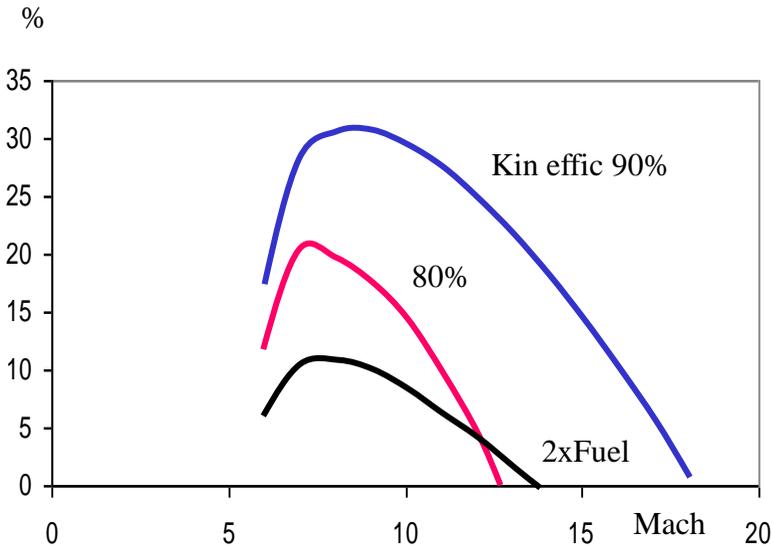
Fig. 19.7 The efficiency of a Scramjet

The variation of the efficiency with the Mach number for a stoichiometric scramjet is shown in Figure 19.7 for two different values of the internal kinetic efficiency η_{kc} η_{kn} provided that the kinetic efficiency of the inlet follows Eq. (19.25). Also shown is the effect of operating the scramjet fuel rich, letting the fuel/air ratio grow above the stoichiometric value.

It is seen from Figure 19.7 that a scramjet is very sensitive to the intake, combustion and nozzle efficiencies. Since the exhaust velocity is only slightly greater than the incoming free stream velocity a small reduction in pressure recovery or the completeness of combustion is likely to convert a net thrust into a small net drag. The component efficiencies are dependent on the detailed physics of poorly understood areas like flow turbulence, shock wave/boundary layer interactions and boundary layer transition.

A relation for the Mach number at which the thrust and efficiency of the scramjet falls to zero may be derived from Eq. (19.33). With $f \geq f_s$ it is found that this maximum Mach number of the scramjet is:

$$M_{max} = \sqrt{\frac{2}{\gamma-1}\left[\frac{\eta_b h f_s}{C_p T_0}\frac{\eta_{ke}(1+f)}{1-\eta_{ke}(1+f)}-1\right]} \qquad (19.35)$$

Note that at high Mach numbers, the kinetic efficiency is approximately independent of the Mach number because of Eq. (19.23).

From experiments, realistic values of the total kinetic efficiency are between 0.65 and 0.75. For such values the maximum speed of the scramjet will be in the range Mach 10 to 15.

One way of prolonging the life of the scramjet besides better efficiencies is to run it fuel-rich at increasing fuel/air ratios even if as is seen in Figure 19.7, this will decrease the overall efficiency. The fuel/air ratio needed to reach a certain maximum Mach number is:

$$f = \frac{1}{\eta_{ke}(1+\frac{\eta_b f_s h}{C_p T_{t0}})} - 1 \qquad (19.36)$$

An extension of this idea is to carry oxidizer on board as well and to burn the excess fuel increasing the mass flow rate. This approach is superior to having a separate rocket engine because it would use the scramjet flow path. Eventually the air flow path could be closed and the engine would operate as a rocket. Such a rocket could also provide thrust to accelerate the engine to a speed where the scramjet could take over.

The scramjet engine is thermodynamically simple but in engineering practice it is perhaps the most complex and technically demanding of all engine concepts. The scramjet is very much dependent on good combustion and low flow losses. Losses due to friction, shock waves and mixing especially in the combustor reduce the efficiency of the engine.

Scramjets have been successfully tested in laboratories since the 1960s, but getting them off the ground is a different matter. One of the main challenges in designing a scramjet is to avoid generating supersonic shockwaves inside the engine. And since a shock wave is created as the fuel is added, something as simple as injecting a stream of fuel becomes very complex.

Those shock waves raise the temperature and pressure inside the engine until oxygen and fuel molecules entering the combustion chamber split into fragments, ignition stops and the engine loses all power. The shock waves can also produce spots of intense heat and high pressure that may destroy the engine.

In order to keep the temperature in the combustion chamber at reasonable values, the Mach number in the chamber must increase with flight speed according to Eq. (19.23). Because the gases then remain for a shorter time in the combustor, the combustion tends to be incomplete which will decrease the efficiency.
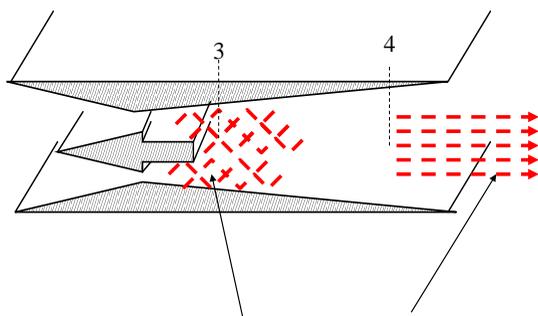
Fuel injection shock waves and incomplete combustion are problems with the scramjet.

Fig. 19.8 Scramjet problems

One of the fundamental physical questions of the scramjet is therefore whether there will be a long enough dwell time in the combustor for the fuel to properly mix and burn. Since the

scramjet impedes the airflow much less than a ramjet, hot gases pass through the engine at many times the speed of sound. So the scramjet's combustion chamber must be long enough to allow the fuel and supersonic air to mix and burn properly. As the air speed inside the engine increases, fuel should be injected progressively closer to the inlet. Even so, the burning gases will remain in a scramjet engine for a few milliseconds at most.

To increase the rate of combustion, the pressure in the combustor could be increased by moving to lower altitudes and higher dynamic pressures but this will increase the heat loads on the vehicle especially in passing the limit for transition to turbulence where the heat loads increase significantly.

Scramjet engines have a relatively low specific thrust due to the moderate combustor temperature rise and pressure ratio. Therefore a very large air mass flow is required to give adequate vehicle thrust/weight ratio. However, at constant free stream dynamic pressure the captured air mass flow is reduced for a given intake area as the Mach number rises.

Consequently the entire vehicle frontal area, see Figure 19.9, is needed to serve as an intake and the entire underside of the tail is an exhaust nozzle. As a result, the engine occupies a large area beneath the vehicle and the need to accommodate a large quantity of fuel means that an all-body shape is most feasible.
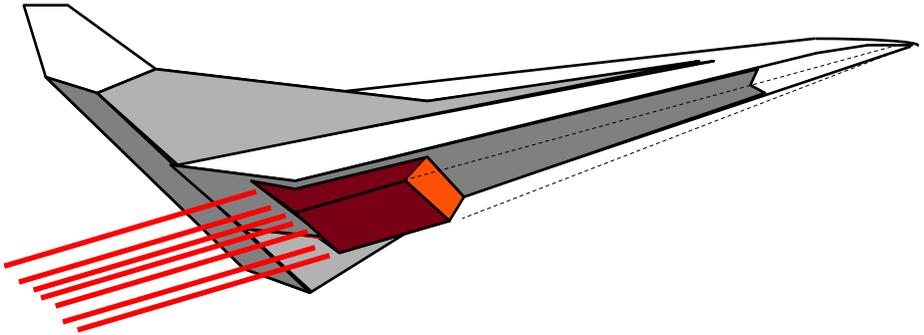
Fig. 19.9 Scramjet vehicle

In order to focus the intake shock system and generate the correct duct flow areas over the whole Mach number range, variable geometries are required. The forebody boundary layer must be carried through the entire shock system, which may upset the intake flow stability. The conventional solution of bleeding the boundary layer off would be unacceptable due to the prohibitive momentum drag penalty.

The vehicle undersurface must be flat in order to provide a reasonably uniform flow field for the engine installation. The flattened vehicle cross section is poorly suited to pressurised tankage and has a higher surface area/volume than a circular cross section with further penalties in structure masses.

The intake and nozzle systems positioned underneath the vehicle generate both lift and pitching moments. Since it is necessary to optimise the intake and nozzle system geometry to maximise the engine performance, it is extremely unlikely that the vehicle will be pitch balanced over the Mach number range. Furthermore, it is not clear whether adequate center of gravity movements to trim the vehicle could be achieved by active propellant transfer.

Clustering several engines into a compact package underneath the vehicle results in a highly interdependent flowfield. An unexpected failure in one engine with a consequent loss of internal flow is likely to unstart the entire engine installation. This would precipitate a large and sudden change in vehicle pitching moment, which would almost certainly be beyond the response capabilities of the propellant transfer system.

The high dynamic pressure trajectory imposes severe heating rates on the airframe. Active cooling of significant portions of the airframe will be necessary with further penalties in mass and complexity.

Ex 19.1

What is the maximum speed of a kerosene and an hydrogen driven ramjet if the stoichiometric temperatures are 2300 and 2700 respectively? The atmospheric temperature is 220 K and γ=1.4.

Ex 19.2

What is the flight Mach number at which the flow into the combustor becomes supersonic so that the ramjet becomes a scramjet. What is this Mach number for the maximum combustor inlet temperature of 1560 K? The atmospheric temperature in the stratosphere may be taken as 220 K and $\gamma=1.4$.

Ex 19.3

If the static temperature at the combustor inlet is to be kept constant at 1560 K the Mach number at the inlet will have to increase continually with flight speed. Derive this relation at very high flight speeds. This constitutes a simple "rule of thumb" for the air speed in a scramjet combustor. The atmospheric temperature is 220 K and $\gamma=1.4$.

Ex 19.4

What will be the fuel/air ratio needed to reach satellite speed (Mach 25) with a scramjet?

The combustion efficiency is 90% and the kinetic efficiency 80%, the heat content for hydrogen 120 MJ/kg and the stoichiometric fuel/air ratio 0.029. The atmospheric temperature is 220 K and the specific heat will increase due to dissociation but an average value may be assumed to be 1500 J/kg K with $\gamma=1.28$.

20. ROCKET ENGINES

The rocket engine is the only contestant for reaching out into space because airbreathing engines like the scramjet are unable to reach sufficient speeds. The rocket thrust is independent of flight speed, inside or outside of the atmosphere. This makes the rocket engine especially well suited for space travels. The gases for the jet of a rocket may be produced from solid or liquid propellants. In the latter, pressurized tanks or turbopumps are used to transport the liquids to the combustion chamber before they are ejected through the nozzle.

Just when the first true rockets appeared is unclear but as is so often the case with the development of technology, the early uses were primarily military. In 1040, some recipes for **gunpowder** mixtures appeared in a printed Chinese book but the date reporting the first use of true rockets was in 1232. Rocket fire-arrows were then used to repel Mongol invaders at the **battle of Kai-fung-fu**. The rockets were huge and apparently quite powerful. According to a report, when the rocket was lit, it made a noise that resembled thunder that could be heard for a long distance. When it fell to earth, the point of impact was devastated for a wide area. Apparently these large military rockets carried incendiary material and iron shrapnel. They may also have included the first combustion chambers, for sources describe the design as incorporating an "iron pot" to contain and direct the thrust of the gunpowder propellant.

Having been exposed to this shock from the ancient Chinese civilization, the **Mongols** acquired rockets of their own and were responsible for spreading them to Europe. Contemporary accounts describe rocket-like weapons being used by the Mongols against Hungarian forces at the battle of Sejo, which preceded their capture of Buda (now known as Budapest) December 25, 1241.

A little later, around 1500, a lesser-known Chinese official named **Wan-Hu** put together a rocket- powered flying chair. Attached to the chair were two large kites, another Chinese invention, and fixed to the kites were around fifty fire-arrow rockets. Not wanting to miss the chance for fame, Wan Hu decided to be his own test pilot. According to reports, he sat in the chair and gave the order to light the rockets. There was a lot of noise and a great burst of flame and smoke, which blocked everyone's vision. No one knows for sure what happened to Wan-Hu…

Rockets first appear in **Arab** literature in 1258, describing Mongol invaders' use of them in order to capture the city of Baghdad. Quick to learn, the Arabs adopted the rocket into their own arms inventory and used them against the European armies during the crusades.

Not later than the year 1300, rockets had found their way into **European** armies. During the Renaissance every army had a rocket corps. Records from 1429 show rockets in use at the French siege of Orleans during the Hundred Years War against the English.

As the 18th Century dawned, European military experts began to take an even more serious interest in rockets. The reason was that they had found themselves on the receiving end of rocket warfare.

As the British, during the Eighteenth Century, began wrestling for control of the riches of India they found themselves frequently engaged against the Mongol forces of Tippoo Sultan of Mysore, who during the two battles of Seringapatam in 1792 and 1799 used rockets against them.

The success of the Indian rocket barrages caught the interest of an artillery expert, Colonel **William Congreve**. He set out to design rockets for use by the British military. The Congreve rockets were highly successful in battle but even with Congreve's work, the accuracy of rockets still had not improved much from the early days. The devastating nature of war rockets was not their accuracy or power, but their numbers. During a typical siege, thousands of them might be fired at the enemy.

All over the world, rocket researchers experimented with ways to improve accuracy. Finally, an Englishman, **William Hale**, developed a technique called spin stabilization. In this method, the escaping exhaust gases struck small vanes at the bottom of the rocket, causing it to spin much as a bullet does in flight. Variations of the principle are still used today.

Rockets were used with success in battles all over the European continent. Powered by black powder charges, rockets served as bombardment weapons, culminating in the 1807 attack on Copenhagen by the British Navy. The Danes were then subjected to a barrage of 25000 rockets which burnt many houses and warehouses.

However, in a war with Prussia, the Austrian rocket brigades met their match against newly designed artillery pieces. Breech-loading cannons with rifled barrels and exploding warheads were

far more effective weapons of war than the best rockets. Especially as the performance of these early rockets was poor by modern standards because the only available propellant was black powder, which is not ideal for propulsion.

Those early rockets were of the solid propellant type, Figure 20.1.

Case

Powder

Nozzle
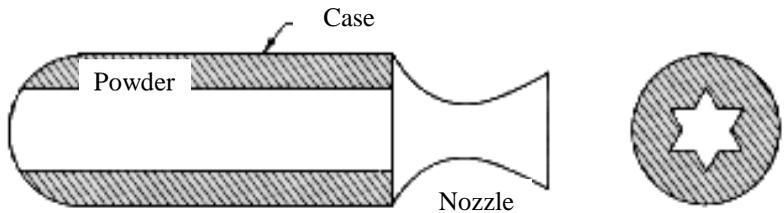
Fig. 20.1 The solid propellant rocket

 The thrust level of a **solid rocket** is determined by the rate of burning of the propellant charge, which is given by the burning **surface area "A_b"** and the **rate "r"** at which it burns, that is:

$$\dot{m} = A_b r \rho_b \qquad (20.1)$$

The burning rate is dependent on the **chamber pressure "p_c"** according to the following empirical relation:

$$r = ap_c^n \qquad\qquad (20.2)$$

This equation is sometimes called **Saint-Roberts law**. While "n" is independent of the temperature of the grain, "a" increases with temperature.

The mass flow produced must balance the mass flow discharged, which is proportional to p_c since the nozzle is choked. It is then found that:

$$p_c = const \left(\frac{A_b}{A_t} \right)^{\frac{1}{1-n}} \qquad\qquad (20.3)$$

Since the burning area is always larger than the throat area, it follows that "n" must always be less than unity or else the pressure will rise to infinite values. Most propellants have a pressure exponent "n" between 0.2 and 0.8.

While the throat area is constant, the burning area varies. A high value of "n" means that small changes in burning area can result in large variations in chamber pressure and mass flow. Disastrous rises in chamber pressure can then occur in a few milliseconds. Small values of "n" are therefore desirable.

It is clear from the above that the thrust is strongly dependent on the burning area. The earliest rockets were of the end burning type. This configuration is neutral with regard to the burning area but

have some other important drawbacks. Chief among those is that the center of gravity shift is large. One therefore prefers other configurations such as the star shaped radial burning area, see Figure 20.1. By suitably choosing the burning area configuration, the thrust can be adjusted to what is required.

This means that the thrust-time function is not amenable to much intentional modification after manufacture, and most missions using solid-rocket motors are designed to take advantage of the predictability of the thrust-time function rather than to regulate thrust during flight. However, it is also clear (see Ex. 20.1) that if the process goes out of control, disastrous thrust variations may occur.

The liquid rocket engine was developed as an answer to these disadvantages of the solid propellant rockets. In addition, liquid-propellant engines have certain other features that make them preferable to solid systems such as a higher attainable specific impulse and the ability to control the thrust level in flight. Thrust termination is easily accomplished with the liquid rocket by simply shutting the propellant valves.

The underline inventor of the liquid rocket engine was **Robert H. Goddard**, an American scientist, who from 1908 to 1945 conducted a wide array of rocket experiments. Goddard's many contributions to the theory and design of rockets earned him the title of father of modern rocketry. His designs and working models eventually led to the German large rockets such as the V-2 of the World War II.

Goddard's interest in rockets began in 1898 when, as a 16-year-old, he read the latest publication of the Brittish science fiction writer H.G. Wells. The book, which so excited Goddard was later

made into a 1938 radio program that nearly panicked the entire nation when it was broadcast.

Goddard started working with rockets in 1915 when he tested solid fuel models. In 1919 he published a paper entitled "*Method of Reaching Extreme Altitudes*." In it he concluded that a rocket would work better in a total vacuum than in the atmosphere. This was against the popular belief that a rocket needed air to push against.

Goddard went on experimenting and on March 16, <u>1926 he flew the first liquid rocket</u>. Fueled by liquid oxygen and gasoline, it flew for only two and a half seconds, climbed 12.5 meters, and landed 56 meters away in a cabbage patch. By today's standards, the flight was unimpressive, but like the first powered airplane flight by the Wright brothers in 1903, Goddard's gasoline rocket was the forerunner of a whole new era in rocket flight.

After this initial success, he flew other rockets in rural Massachusetts until they started crashing in his neighbor's pastures. The local fire marshal declared his rockets as a fire hazard and ended his tests. Charles Lindbergh came to Goddard's rescue by helping him get a grant from the Guggenheim Foundation. With it Goddard moved to Roswell, New Mexico, where he could experiment without endangering anyone. There he developed the first gyro-controlled rocket guidance system and was eventually flying rockets faster than the speed of sound and at altitudes up to 2500 meters.

Liquid-propellant systems carry the propellant in tanks external to the combustion chamber. Most of these engines use a liquid oxidizer and a liquid fuel, which are transferred to the combustion

chamber by pumps or by pressure in the tanks. The two systems are shown in Figure 20.2. The propellants are injected into the combustor in a manner that assures atomization and rapid mixing. There they burn to create a high-pressure and high-velocity stream of hot gases. These gases flow through a nozzle, which accelerates them further, and then leave the engine.
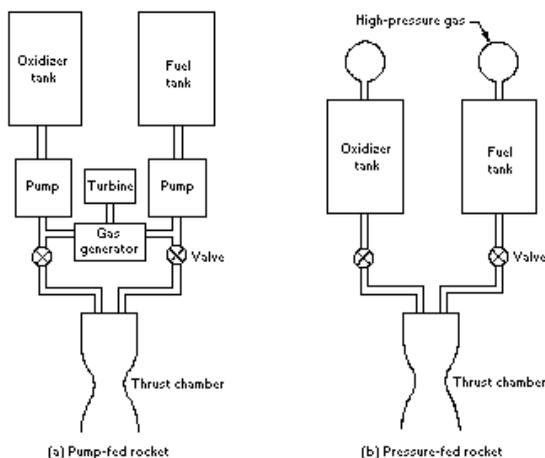
Fig. 20.2 Pump-fed and pressure-fed liquid rocket engines

Hybrid propellant engines represent an intermediate group between solid and liquid propellant engines. One of the substances is solid, usually the fuel, while the other, usually the oxidizer, is liquid. The liquid is injected onto the solid, whose fuel case also serves as the combustion chamber. Such engines have performance

similar to that of solid propellants, but the combustion can be moderated, stopped, or even restarted. It is difficult to make use of this concept for very large thrusts, and thus, hybrid propellant engines are rarely built.

In the **pressure-fed** liquid system, the tanks are pressurized with inertial gases to act against the pressure in the combustion chamber. In this type of engine the fuel and gas tanks are very heavy, which explains why this design principle is only used for smaller rockets with shorter burning times. For liquid hydrogen and oxygen cryogenic propellants, it is not an option at all because of the hydrogen's low density and the corresponding large fuel tank size. On the other hand, removal of the pumping equipment may raise overall reliability.

In the **pump-fed** engine, a gas generator, operated from the main propellants or an auxiliary propellant, drives a turbine which drives pumps to supply fuel and oxidant to the thrust chamber. The pumps have to generate extremely high pressures in order to overcome the pressure that the burning fuel creates in the combustion chamber.

There are three basic ways to arrange the pump fed systems turbine drive gases, see Figure 20.3. In the **staged combustion** or **integrated** cycle a fuel-rich preburner is used to generate the turbine drive gases. Those gases are then injected into the combustion chamber. Fuel is used to cool the main combustion chamber. The result is high pressure (20 Mpa) and high specific impulse. This system is used in the Space Shuttle Main Engine.
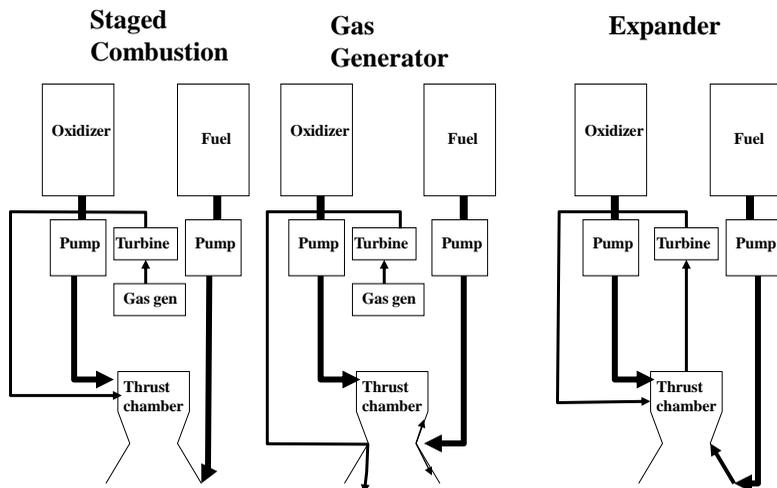
Fig. 20.3 Pump-fed liquid rocket engine cycles

The **gas generator** cycle is used in the Vulcain engine for the European space launcher Ariane 5. Turbine exhaust gases are used to cool the nozzle and are then ejected to boost performance. In this system, the performance is lower due to the lower chamber pressure and the shift in thrust chamber mixture ratio necessary to balance the effect of the fuel-rich turbine exhaust gases.

The **expander** cycle avoids the turbine-drive gas losses of the gas-generator cycle by placing the turbine in series with the thrust chamber, exhausting directly into it. In this cycle there is no combustion upstream of the turbine, the turbine drive gas being the fuel itself after being heated in the thrust chamber cooling jacket.

This limits the turbine inlet temperature which in turn limits the attainable chamber pressure and the specific impulse. As a result, this engine is primarily a space engine where it can exhaust to a vacuum and have a high expansion ratio despite the low chamber pressure.

The typical elements of a liquid rocket engine are shown in Figure 20.4.

LH2 pump   LOX pump   Turbine

90K
50 MPa

30K
50 MPa

Gas generator

Injector plate

Cooling jacket

Combustor
3000K, 40 MPa

Film cooling

Tubular wall

Manifold

Cooling hydrogen
900K

Exhaust at 1000K
4400 m/s
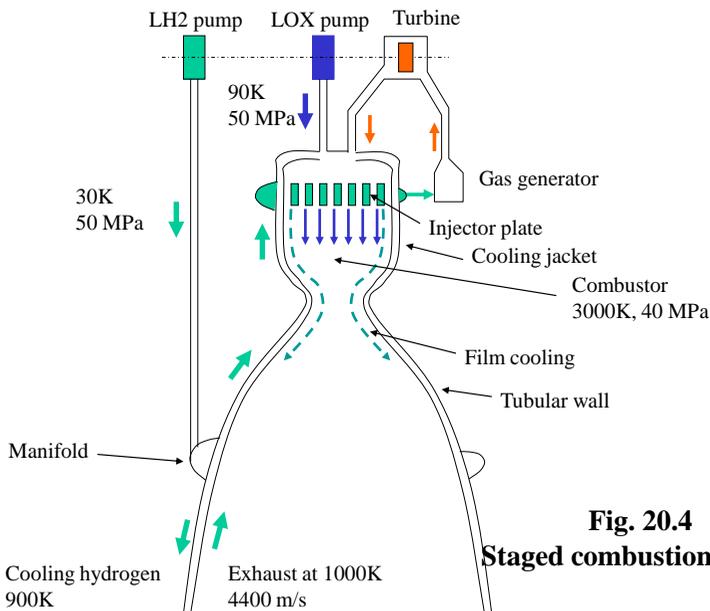
Fig. 20.4
Staged combustion engine

From the outside, a liquid-propellant engine often looks like a maze of plumbing, which connects the tanks to the pumps, carries the coolant flow to and from the cooling jackets, and conveys the pumped fluids to the injector. In addition, engines are generally

mounted on gimbals so that they can be rotated a few degrees for thrust direction control, and appropriate actuators are connected between the engine and the vehicle structure to constrain and rotate the engine.

The **thrust chamber** consists of a main chamber for mixing and burning the fuel and oxidizer, with the fore end occupied by fuel and oxidizer manifolds and injectors and the aft end comprised of the nozzle. Integral to the main chamber is a coolant jacket through which liquid propellant (usually fuel) is circulated.

The function of the **injector** is to introduce the propellants into the combustion chamber in such a way that efficent combustion can occur. There are different types of injectors. A common type is the impinging stream injector with which the oxidizer and fuel are injected through a number of separate holes so that the resulting streams intersect with each other. The fuel stream will impinge with the oxidizer stream and both will break up into small droplets.

When gaseous oxygen is used as the oxidizer, and a liquid hydrocarbon is used as fuel, the impingement of the liquid stream with the high velocity gas stream results in diffusion and vaporisation, causing good mixing and efficient combustion. A disadvantage of this type of injector is that extremely small holes are required for small engine flow rates and the hydraulic characteristics and equations normally used to predict injector parameters do not give good results for small orifices. The small holes are also difficult to drill, especially in the soft copper used.

Injection pressure drops of 500 to 1000 kPa or injection vclocities of 20 to 30 m/sec are usually used in small liquid-fuel rocket engines. The injection pressure drop must be high enough to

eliminate combustion instability inside the combustion chamber but must not be so high that the tankage and pressurization system used to supply fuel to the engine is penalized

The **combustion chamber** is where the burning of propellants takes place. This chamber must be strong enough to contain the high pressure and the high temperature resulting from the combustion process. Because of the high temperature and heat transfer, the chamber and nozzle are usually cooled. The chamber must also be of sufficient length to ensure complete combustion before the gases enter the nozzle.

The combustion chamber is a critical component of the engine, because of the high output and accordingly high pressures. Pressures of over 20000 kPa and temperatures of more than 3000 K cause a great deal of heat strain on the combustion chamber and call for effective cooling. Copper combustion chambers are often used, in the outside of which cooling channels are milled. This technology was developed very early on in Germany and is used in all engines of this kind today.

A parameter describing the chamber volume required for complete combustion is the **characteristic chamber length**, L*, which is given by

$$L^* = V_c / A_t \qquad\qquad (20.4)$$

where "V_c" is the chamber volume (including the converging section of the nozzle), and "A_t" is the nozzle throat area. For gaseous oxygen/hydrocarbon fuels, an L* of 1 to 3 m is appropriate. L* is in fact a substitute for determining the chamber residence time of the reacting propellants.

To reduce losses due to the flow velocity of gases within the chamber, the combustion chamber cross sectional area should be at least three times the nozzle throat area. This ratio is known as "**contraction ratio**" and it determines the diameter of the combustion chamber.

Heat transfer presents a critical problem for rocket engine designers. Various approaches have been considered, including
* Radiative cooling: radiating heat to space or conducting it to the atmosphere.
* Regenerative cooling: running cold propellant through the engine before exhausting it.
* Boundary-layer cooling: aiming some cool propellant at the combustion chamber walls.
* Transpiration cooling: diffusing coolant through porous walls.

The combustion chamber must be able to withstand the internal pressure of the hot combustion gases. The combustion chamber must also be physically attached to the cooling jacket and, therefore, the chamber wall thickness must be sufficient for welding or brazing purposes. Since the chamber will be a cylindrical shell, the working **wall stress** is given by

$$\sigma = \frac{pD}{2t_w} \qquad\qquad (20.5)$$

where "p" is the pressure in the combustion chamber (neglecting the effect of coolant pressure on the outside of the shell), "D" is the mean diameter of the cylinder, and "t_w" is the thickness of the cylinder wall.

A typical material for cooled combustion chambers is copper, for which the allowable working stress is about 6E7 N/m2. This limit gives the minimum thickness. Actually the thickness should be somewhat greater to allow for welding, buckling, and stress concentration.

Cooled rocket motors have provision for **cooling** some or all metal parts coming into contact with the hot combustion gases. The injector is usually self-cooled by the incoming flow of propellants. The combustion chamber and nozzle definitely require cooling.

A **cooling jacket** permits the circulation of a coolant, which, in the case of flight engines is usually one of the propellants. The cooling jacket consists of an inner and outer wall. The combustion chamber forms the inner wall and another concentric but larger cylinder provides the outer wall. The space between the walls serves as the coolant passage. The nozzle throat region usually has the highest heat transfer intensity and is, therefore, the most difficult to cool.

Equation (20.5) can also he used to calculate the wall thickness of the cooling jacket. Here again, the value of t_w will be the minimum thickness since welding factors and design considerations (such as O-rings, grooves, etc.) will usually require walls thicker than those indicated by the stress equation.

The **energy release** per unit chamber volume of a rocket engine is very large, and can be 250 times that of a good steam boiler or five times that of a gas turbine combustion chamber. It is apparent, therefore, that the cooling of a rocket engine is a difficult and exacting task.

The largest part of the heat transferred from the hot chamber gases to the chamber walls is by **convection**. The amount of heat transferred by **conduction** is small and the amount transferred by **radiation** is usually less than 25%, of the total. The chamber walls have to be kept at a temperature such that the wall material strength is adequate to prevent failure. Material failure is usually caused by either raising the wall temperature on the gas side so as to weaken, melt, or damage the wall material or by raising the wall temperature on the liquid coolant side so as to vaporize the liquid next to the wall. The consequent failure is caused by the sharp temperature rise in the wall caused by excessive heat transfer to the boiling coolant.

Once the wall material of an operating rocket engine begins to fail, final burn-through and engine destruction are extremely rapid. Even a small pinhole in the chamber wall will almost immediately open into a large hole because the hot chamber gases (2000-3000 K) will oxidize or melt the adjacent metal, which is then blown away exposing new metal to the hot gases.

Exotic metals and difficult fabrication techniques are used in today's space and missile rocket engines, providing the lightweight structure absolutely required for efficient launch and flight vehicles. Expert machine and welding work is essential to produce a safe and useable rocket engine.

The function of the **nozzle** is to convert the chemical-thermal energy generated in the combustion chamber into kinetic energy. The nozzle converts the slow moving, high pressure, high temperature gas in the combustion chamber into high velocity gas of lower pressure and temperature. Since thrust is the product of mass and velocity, a very high gas velocity is desirable.

The principal requirement for a nozzle is that it be able to produce an optimum flow of the exhaust gas from combustion chamber pressure to exterior pressure, a function that is accomplished by proper contouring and sizing. The contour is initially convergent to a "throat" section. The velocity of the exhaust gas in this region is equal to the local velocity of sound, and the throat cross-sectional area controls the mass discharge rate (and hence the operating pressure). Beyond the throat, the channel is divergent and the flow accelerates to high supersonic speeds with a corresponding pressure decrease. Contours are often carefully designed so that shock waves do not form.

The problem of the conventional nozzle shape is that it is only optimized for a fixed operational point. Since the atmospheric pressure decreases constantly while the rocket is climbing but the flow conditions within the nozzle remain the same, the engine's performance during flight changes accordingly.

Engines with **aerospike nozzles,** Figure 20.5, pioneered by Rocketdyne engineers in the 1950s, try to avoid this problem. With aerospike engines, the hot gases are not guided along the inside of the engine nozzle, but stream along the outer surface of a nozzle ramp, which has an open side to the atmosphere. The ramp serves as the inner wall of the bell nozzle, while ambient atmospheric pressure serves as the invisible outer wall.
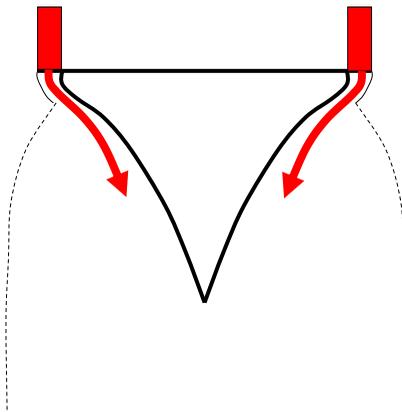
Fig. 20.5 Aerospike nozzle

This design is supposed to avoid an overexpansion on the ground and allows a variety of nozzles with big area proportions and appropriate specific impulses in vacuum. The aerospike can self-compensate for decreasing atmospheric pressure as the vehicle ascends, keeping the engine's performance very high throughout the entire trajectory.

Instead of a circular combustion chamber with a narrow slot-shaped opening, which is almost impossible to construct, a line of small single combustors is used. They form a kind of circular combustion chamber. Each of these single combustion chambers

has to be supplied with fuel via a central turbopump. The so called linear aerospike is a special case of this type of engine. Here the combustors are arranged in a linear configuration, enabling a better integration with the vehicle and reducing the tail drag.

Desirable properties of **propellant combinations** for liquid engines are low molecular weight and high temperature of reaction products for high exhaust velocity, high density to minimize tank weight, low hazard factor (e.g., corrosivity and toxicity), and low cost. **Liquid oxygen** is widely used because it is a good oxidizer for a number of fuels giving high flame temperature and low molecular weight and because it is reasonably dense (its density is 1140 kg/m3) and relatively inexpensive. It is liquid only below minus 183 C, which somewhat limits its availability, but it can be loaded into insulated tanks shortly before launch and replenished or drained in the event of launch delays.

Liquid fluorine or **ozone** are better oxidizers in some respects but involve more hazard and higher cost. The low temperatures of all of these systems require special design of pumps and other components, and the corrosivity, toxicity, and hazardous characteristics of fluorine and ozone have thus far prevented their use in operational systems.

Other oxidizers that have seen operational use are **nitric acid** (HNO3) and **nitrogen tetroxide** (N2O4), which are liquids under ambient conditions. While they are somewhat noxious chemicals, they are useful in applications where the rocket must be in a near ready-to-fire condition over an extended period of time, as in the case of long-range ballistic missiles. Systems of this sort also find application on longer duration flights such as those involving the

Space Shuttle Orbital Maneuvering System and the Apollo Lunar Module.

Combinations of oxygen or fluorine as oxidizer and hydrogen or methane as fuel make especially attractive fuel mixtures for rockets. Under normal atmospheric conditions, these substances are in a gaseous state. One cannot remedy the low density by increasing the pressure, because the required tank structures would end up being too heavy. The answer is to liquify the fuels by cooling them down. This is why these kinds of fuels are also called cryogenic fuels.

Among the **cryogenic** fuels the combination of liquid oxygen (LOX) as oxidizer and **liquid hydrogen** (LH2) as fuel deserves a special mention. Both components are easily and cheaply available. The fuel is environmentally friendly, non-corrosive and has the highest efficiency of all non-toxic combinations. To liquefy, hydrogen has to be cooled to a temperature of minus 253 C. Its boiling point is 20 K, only just above absolute zero on the temperature scale. During this process its density increases to above 70 kg/m3.

The rocket pioneers knew about the advantageous performance of this fuel combination for rocket technology but since there were difficulties in handling liquid hydrogen, their knowledge could not be put into practice. However, from the beginning liquid oxygen was used as an oxidizer.

The exhaust velocity is determined by the combustion temperatures and the molecular weights of reaction products. Liquid hydrogen is usually the best fuel from the standpoint of high exhaust velocity, and it might be used exclusively were it not

for the cryogenic requirement and its low density. Such hydrocarbon fuels as alcohol and kerosene are often preferred because they are liquid under ambient conditions and denser than liquid hydrogen.

In practice, a variety of choices of propellants have been made in major systems. In flights where cryogenic propellants can be utilized (e.g., ground-to-earth-orbit propulsion), liquid oxygen is usually used as the oxidizer. In first stages either a hydrocarbon or liquid hydrogen is employed, while the latter is usually adopted for second stages.

Certain propellant combinations are **hypergolic**, that is they ignite spontaneously upon contact of the fuel and oxidizer. The easy start and restart capability of hypergolics make them ideal for spacecraft maneuvering systems. Also, since hypergolics remain liquid at normal temperatures, they do not pose the storage problems of cryogenic propellants. Hypergolics are highly toxic and must be handled with extreme care.

Hypergolic fuels commonly include **hydrazine**, monomethyl hydrazine (MMH) and unsymmetrical dimethyl hydrazine (UDMH). The oxidizer is typically nitrogen tetroxide (N_2O_4) or nitric acid (HNO_3). **UDMH** is used in many Russian, European, and Chinese rockets while **MMH** is used in the orbital maneuvering system and reaction control system of the Space Shuttle orbiter.

Certain liquid chemicals can be made to form hot gas for thrust production by decomposition in a rocket chamber. The most common such **monopropellants** are hydrogen peroxide and ethylene oxide. When such a liquid is passed through a platinum

catalyst mesh it decomposes into hot steam and oxygen. These gases can then be ejected to develop thrust. Engines of this kind have comparatively low exhaust velocity, but have the advantage of simplicity, require only one tank in the vehicle and can be readily turned on and off. Since they are adaptable to repetitive operation they find application in various control systems where efficiency of propellant utilization is of minor importance. Their performance, however, is inferior to that of bipropellants or modern solid propellants.

The use of more than two chemicals as propellants in rockets has never received a great deal of attention, and is not considered advantageous at present. Occasionally a separate propellant is used to operate the gas generator, which supplies the gas to drive the turbopumps of liquid rockets.

During a **combustion** process the mass of each element remains the same. Consider the reaction of **hydrogen with oxygen:**

$$2H_2 + O_2 \rightarrow 2\,H_2O \qquad\qquad (20.6)$$

This equation states that two kmol of hydrogen react with one kmol of oxygen to form two kmol of water. This also means that 4 kg of hydrogen react with 32 kg of oxygen to form 36 kg of water. The stoichiometric mixture ratio is then O/F=8.

Similarly for the reaction of **kerosene with oxygen**:

$$C_{12}H_{26} + 12.5\,O_2 \rightarrow 12\,CO + 13\,H_2O \quad (20.7)$$
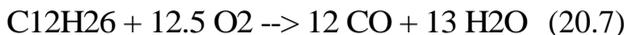
Given that the molecular weight of $C_{12}H_{26}$ is 170 and that of O_2 is 32, we have a mixture ratio of O/F = (12.5 x 32) / 170 = 2.35, which is typical of many rocket engines using kerosene, or RP-1, fuel.

The above combustion reactions are examples of **stoichiometric** mixtures. That is there is just enough oxygen present to chemically react with all the fuel. The highest flame temperature is achieved under these conditions. However, it is often desirable to operate a rocket engine at a "fuel-rich" mixture ratio. The mixture ratio is defined as the mass flow of oxidizer divided by the mass flow of fuel.

It should be pointed out that in the combustion process there will be a **dissociation** of molecules among the products. That is, the high heat of combustion causes the separation of molecules into simpler constituents, which are then capable of recombining. In the reaction of kerosene with oxygen, the true products of combustion will be an equilibrium mixture of atoms and molecules consisting of C, CO, CO_2, H, H_2, H_2O, HO, O, and O_2. Dissociation has a significant effect on flame temperature.

Sample values of adiabatic flame temperature, average molecular weight, and specific heat ratio for some common rocket propellants at various mixture ratios and pressures are given in Table 20.1. The adiabatic flame temperature T_c is the temperature achieved by a combustion process that takes place adiabatically, that is, with no heat entering or leaving the system. It is the maximum temperature that can be achieved for the given reactants.

Ox/Fuel	O/F	Pc kPa	Tc K	M	Gamma
LOX/LH2	5.0	2500	3220	11.7	1.21
		5000	3280	11.8	1.21
		7500	3310	11.8	1.21
		10000	3330	11.8	1.21
	6.0	2500	3380	13.3	1.2
		5000	3470	13.4	1.2
		7500	3510	13.5	1.2
		10000	3550	13.5	1.2
Nitrogen tetroxide/	2.1	2500	3220	21.7	1.23
Dimethyl-Hydrazine		5000	3270	21.8	1.23
		7500	3300	21.8	1.23
		10000	3320	21.9	1.23
	2.6	2500	3320	23.4	1.22
		5000	3400	23.5	1.22
		7500	3440	23.6	1.22
		10000	3480	23.7	1.22

Table 20.1

As is seen, the chamber pressure also has some effect on the combustion process. Increasing the pressure tends to increase the adiabatic flame temperature and molecular weight. The result is an increase in jet velocity, that is in specific impulse.

In order to compare a variety of fuel combinations and rockets, the most important quantity is the **specific impulse**, which determines the thrust per kilogram of emitted fuel per second. For a rocket engine this is the same as the exhaust velocity.

The enthalpy difference between the combustion chamber and the exhaust conditions may be used to find the **ideal exhaust velocity** as the difference between the enthalpy released in the thrust chamber and the enthalpy of the exhaust gases according to:

$$V_j = \sqrt{2(h_{tc} - h_0)} \qquad (20.8)$$

If the state of the gas is assumed to be "frozen" during the expansion through the nozzle that is that the specific heat C_p remains constant then:

$$V_j = \sqrt{2C_p(T_{tc} - T_0)} \qquad (20.9)$$

where the specific heat is given by $C_p = \Re/M$, in which $\Re = 8314$ is the universal gas constant and M is the molecular weight of the gas.

The **ideal specific impulse** is often used as a measure on the performance of the system and is given by the jet velocity in full expansion to ambient pressure as:

$$I_{s0} = \sqrt{\frac{2\gamma}{\gamma - 1} \frac{\Re T_c}{M} \left[1 - \left(\frac{p_0}{p_c} \right)^{\frac{\gamma - 1}{\gamma}} \right]} \qquad (20.10)$$

The mass flow through the nozzle follows the following equation:

$$\dot{m} = \frac{\bar{m}_t A^* p_{tc}}{\sqrt{C_p T_{tc}}} \qquad (20.11)$$

where A^* is the nozzle throat area and the mass flow parameter is as in Eq. (8.11).

The nozzle throat cross-sectional area may be computed if the total propellant flow rate is known and the propellants and chamber pressure have been chosen. "T_{tc}" is the combustion chamber flame temperature in degrees K, which is dependent on the operating conditions such as the mixture ratio between oxidizer and fuel.

Full expansion to the surrounding pressure would require a very long nozzle. In reality, the nozzle is shortened so that the exhaust pressure is higher than the surrounding pressure. This means that the jet speed is lower than at full expansion and also the thrust. This is partly compensated by the back pressure in the exhaust plane.

The **real specific impulse** for a rocket engine is now given by:

$$I_s = \frac{F}{\dot{m}} = \frac{F}{A^* p_{tc}} \frac{A^* p_{tc}}{\dot{m}} = \frac{F}{A^* p_{tc}} \frac{\sqrt{C_p T_{tc}}}{\bar{m}_t} = C_F C^* \quad (20.12)$$

The parameter:

$$C^* = \frac{\sqrt{C_p T_{tc}}}{\bar{m}_t} \qquad (20.13)$$

is a **characteristic velocity** that depends on the thermochemical properties of the propellant reaction products and the burning temperature that is usually assumed to be constant. Using the well known expressions for the specific heat and the mass flow parameter, the characterisitc velocity is:

$$C^* = \frac{\sqrt{\gamma \Re T_{tc} / M}}{\gamma \sqrt{\left(\dfrac{2}{\gamma+1}\right)^{(\gamma+1)/(\gamma-1)}}} \qquad (20.14)$$

The thrust of a rocket engine is given by the equation:

$$F = C_F A^* p_{tc} \qquad (20.15)$$

where the so called **thrust coefficient** "C_F" depends on thermochemical properties and increases somewhat with the ratio between chamber and external pressure. Typical values are 1.6-1.7. The theoretical value for "C_F" at any altitude is:

$$C_F = \sqrt{\frac{2\gamma^2}{\gamma-1}\left(\frac{2}{\gamma+1}\right)^{(\gamma+1)/(\gamma-1)}\left[1-\left(\frac{p_e}{p_{tc}}\right)^{(\gamma-1)/\gamma}\right]} + \varepsilon \frac{p_e - p_0}{p_{tc}} \quad (20.16)$$

where the subscript "c" signifies chamber, "e" exhaust and "0" atmospheric conditions and where the nozzle area expansion ratio for a prescribed exhaust pressure p_e is from Eq. (8.12):

$$\varepsilon = \frac{A_e}{A^*} = \frac{\left(\dfrac{2}{\gamma+1}\right)^{\frac{1}{\gamma-1}}\left(\dfrac{p_{tc}}{p_e}\right)^{\frac{1}{\gamma}}}{\sqrt{\dfrac{\gamma+1}{\gamma-1}\left[1-\left(\dfrac{p_e}{p_{tc}}\right)^{\frac{\gamma-1}{\gamma}}\right]}} \qquad (20.17)$$

The ambient pressure reduces the thrust of the engine. Optimum thrust for a given ambient pressure is obtained when the expansion ratio is such that $p_e = p_0$. Unfortunately, because the ambient pressure decreases with altitude, there is no such optimum expansion ratio. It is therefore important to state whether specific impulse is the value at sea level or in a vacuum.

The expansion ratio for expansion to ambient pressure will increase with altitude. In vacuum the optimum expansion ratio would have to become infinite. Therefore one sometimes utilizes extendible nozzles to adapt to decreasing pressure.

From the equation for specific impulse we see that high chamber temperature and pressure, and low exhaust gas molecular weight results in high ejection velocity, thus high thrust. Thus, we can see why liquid hydrogen is very desirable as a rocket fuel.

There are a number of losses within a rocket engine, the main ones being related to the inefficiency of the chemical reaction (combustion) process, losses due to the nozzle, and losses due to the pumps. Calculated values of specific impulse are therefore about 10% higher than those attained in practice.

Unlike the fuel combinations liquid oxygen-kerosene or nitrogen tetroxide- unsymmetrical dimethyhydrazine (UDMH), which generate specific impulses between 3000 m/ s and 3400 m/s in a vacuum, the cryogenic combination liquid oxygen-liquid hydrogen can reach up to 4500 m/s. This high specific impulse makes this fuel combination very attractive and explains why engines using this fuel are frequently used for high performance missions in spaceflight.

The list of all hydrogen-oxygen cryogenic engines, which have been developed up until today, is relatively long. The best-known is the Space Shuttle Main Engine (**SSME)**. This engine has a vacuum thrust of 2090 kN and a specific vacuum impulse of 4500 m/s. The fuel- mass stream of 470 kg/s, (which is needed when the engine is operating), is supplied by two turbopumps with an output of 70 MW. The three engines, which are needed for the main stage of the Space Shuttle system, have a combined output of more than 27000 Megawatts, which corresponds to about 30 conventional nuclear power plants.

The **Vulcain** engine of Ariane 5, the European launch rocket, is a further example of successful engine technology using cryogenic fuels. It supplies a vacuum thrust of 1150 kN and has a specific vacuum impulse of 4200 m/s. During its burn time of 570s, the engine uses a fuel mass flow of 306 kg/s, which is supplied by the fuel turbo pumps with an output of 15 MW.

Ex. 20.1

Assume that a solid rocket motor is of the internal burning tube type with the initial diameter of the burning surface one third of the case diameter. A typical value of the Pressure Exponent is n=0.2. What would be the ratios of chamber pressure (i.e. thrust) at start and end of the burning? What happens if the Pressure Exponent is raised to 0.8? Compare this to the end burning type.

Ex. 20.2

The F-1 engines of the Saturn V first stage operated at a combustion chamber pressureof 6500 kPa and a temperature of 3570 K. The propellant was kerosene of $C_{12}H_{26}$ of a molecular weight of 170 and liquid oxygen at a 2.26 mixture ratio and the nozzle was adapted to operate at sea level. Calculate the ideal sea level specific impulse. Assume $\gamma = 1.20$.

Ex 20.3

A rocket engine uses liquid hydrogen and liquid oxygen propellants. It operates at a mixture ratio of 6 at a combustion chamber pressure of 10 MPa. Calculate the area of the exhaust nozzle throat if the thrust at sea level is to be 100 tons. The engine is designed for full expansion at sea level. What is the specific impulse at sea level and in vacuum?

21. COMBINED ENGINES

Air-breathing engines have several advantages over rockets but no airbreathing engine is capable of operating all the way up to space velocities. A rocket engine will always be required for the final ascent to orbit. The main problem in very high speed propulsion is to find the right combination of airbreathing and rocket engines and to merge them into one single system.

?? M<6

Air

Scram 6<M<15

Air

Rocket M>15
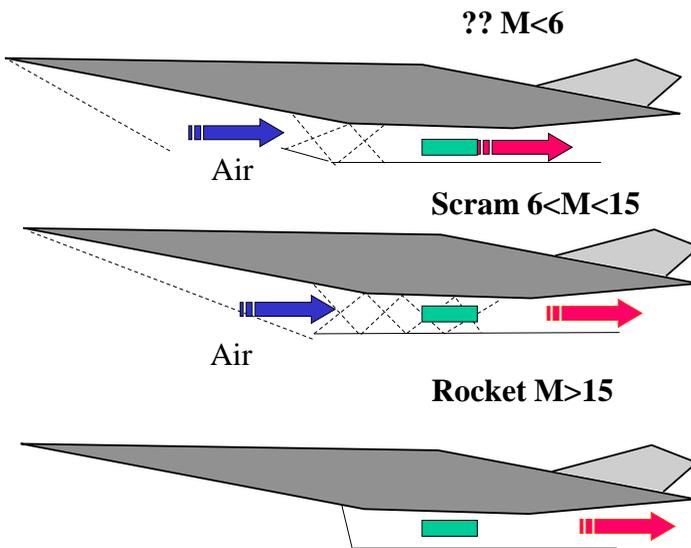
Fig. 21.1 Spaceplane propulsion phases

Because the airbreathing engines use oxygen from the atmosphere, they require less propellant (carrying only the fuel, but no oxidizer) resulting in lighter, smaller and cheaper launch vehicles. To produce the same thrust, air-breathing engines require less than one seventh the propellant that rockets do. Furthermore, because air-breathing vehicles rely on aerodynamic forces rather than on rocket thrust, they have greater maneuverability. Flights can be aborted, with the vehicle gliding back to Earth and missions can also be more flexible with horizontal landing and starting. The problem is to find a suitable propulsion system for such spaceplane.

To reach satellite speed, a spaceplane must be able to operate to Mach 25. As described in Chapter 19, **scramjets** can operate at very high speeds through maintaining a supersonic flow in the combustor. The upper speed limit of scramjets has yet to be determined, but theoretically it is in the range of Mach 15 to 20. For higher speeds than about Mach 15 a rocket engine is the only alternative.

Thus, the propulsion system of a spaceplane would probably include a scramjet and a rocket. The scramjet can not be used below Mach 6. The rocket could but to take advantage of the lower propellant consumption one would prefer an airbreathing alternative.

There are several possibilities. We have already described some of them. The **turboramjet**, which was analyzed in detail in Chapter 19, has a high efficiency but is rather heavy. An uninstalled turbojet has a thrust/weight ratio of around 10 but this falls to below 5 when intake and nozzle systems are added while a rocket

engine is above 60. It is also difficult to integrate a turbojet with a scramjet and rocket. It would probaby have to operate in parallell.

The **Pulse Detonation Engine** of Chapter 19 is a simple device that can be combined with a scramjet and a rocket but it is still not clear if it can be realized.

An alternative to the turboramjet for boosting the ramjet to high speed is the **turboramrocket**. The pure turboramrocket, see Figure 21.2, consists of a low pressure ratio fan driven by an entirely separate turbine employing LOX/LH2 combustion products from a separate combustor.

Fuel Oxidizer
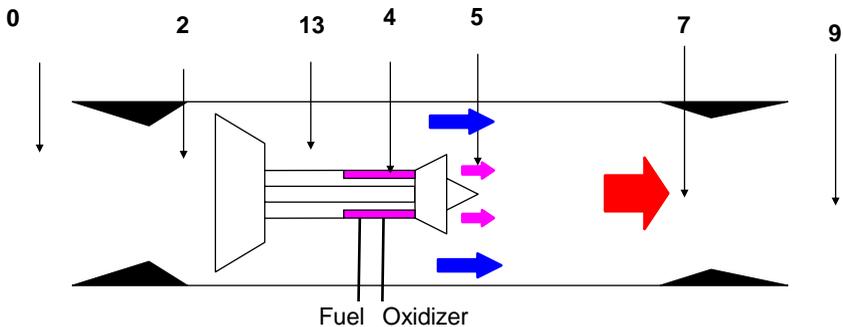
Fig. 21.2 In the Turboramrocket, the rocket exhaust gases are used to drive the turbine for the fan

As there is no compressor, the temperature limit of overheating

the compressor is removed though there remains a temperature problem with the fan. Due to the separate turbine working fluid the matching problems of the fan with the turbine are easier than in the turbofan since the fan can in principle be operated anywhere on its characteristic. In practice this involves designing the engine at reduced non-dimensional speed and hence pressure ratio to give room for increased tip speed of the fan at higher Mach numbers. To avoid choking the fan outlet guide vanes, a low pressure ratio fan with few stages is selected, which permits operation over a wider flow range.

The turboramrocket is considerably lighter than the turboramjet. However, the low cycle pressure ratio reduces the specific thrust at low Mach numbers. In conjunction with the preburner liquid oxygen flow this also results in a poor efficiency compared to the turboramjet.

A potential advantage is that the separate combustor could be used as a rocket engine after the ram engine is overheated and closed down. The turbine exhaust gases, containing a high percentage of unburnt fuel, can be mixed with the compressed air and burnt adding considerably to the energy content of the jet.

The performance of the turboramrocket can be obtained from the equations given for the turboramjet with compressor pressure ratio unity and with constant values on the combustor pressure and temperature. In the limit when the stagnation temperature approaches the max allowed fan material temperature, the engine is then again reduced to a ramjet.

Air turboramrockets have been successfully demonstrated but they lack the operating efficiency of the turboramjet over a wide range of Mach numbers and have not been introduced for operational use so far.
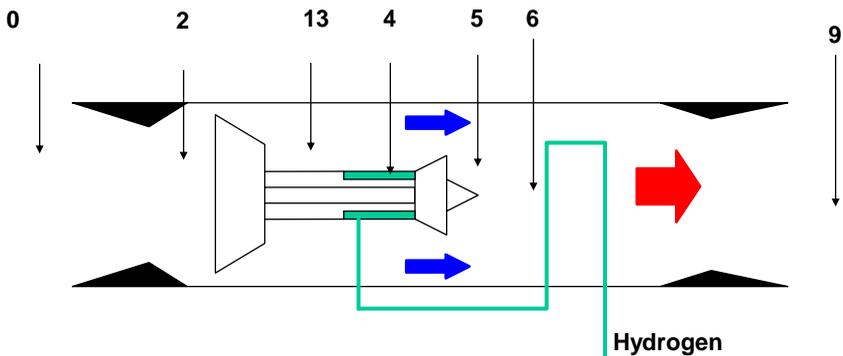
Fig. 21.3 In the Turboramexpander, the heated fuel is used to drive the turbine

 The **turboramexpander** or expander cycle turboramrocket, see Fig. 21.3, is a variant of the turboramrocket whereby the separate combustor working fluid is replaced by high pressure regeneratively heated hydrogen warmed in a heat exchanger located in the exhaust duct. Hydrogen is heated in the afterburner to a high temperature, expanded through the turbine driving the compressor and then burnt in the afterburner.

Due to heat exchanger metal temperature limitations, the afterburner temperature, that is the turbine entry temperature, is quite low at around 950K. The low afterburner temperature is a severe restricion but can be avoided with a second afterburner after the heat exchanger.

The turboramexpander exhibits a moderate improvement in efficiency compared with the pure turboramrocket due to the elimination of the liquid oxygen flow. However this is achieved at the expense of additional pressure loss in the air ducts and the mass penalty of the heat exchanger.

The fuel to air ratio of hydrogen is from a heat balance over the first afterburner:

$$f_{a1} = \frac{C_{pa}}{h}(T_{ta1} - T_{t6}) \qquad (21.1)$$

For a certain heat exchanger efficiency, the heat exchanger outlet temperature, that is the hydrogen turbine inlet temperature, is:

$$T_{H4} = T_{H0} + \eta(T_{ta1} - T_{H0}) \qquad (21.2)$$

 The turbine outlet temperature is from the work balance between the compressor and the turbine :

$$T_{H5} = T_{H4} - \frac{C_{pc}}{f_{a1}C_{ph}}(T_{t13} - T_{t2})$$ (21.3)

In the turbine, the hydrogen expands to the fan outlet pressure so that:

$$p_{H4} = p_{t13}\left(\frac{T_{H4}}{T_{H5}}\right)^{\gamma_h/\eta_t(\gamma_h-1)}$$ (21.4)

This means that a relation can be found between the hydrogen pressure and the fan pressure ratio.

If the hydrogen flow is neglected compared to the air flow then:

$$p_{t6} = p_{t13}$$ (21.5)

and:

$$T_{t6} = T_{t13}$$ (21.6)

The rest of the equations are as for the turboramrocket.

All the previous engines are based on turbomachinery to provide thrust for take-off, which makes for heavy weight and difficulties to integrate them with the rocket engine required for the highest speeds. The idea of the **ramrocket,** or the **ejector rocket** as it is

sometimes called, is to make a ramjet provide thrust at take-off by using a rocket engine to pull air into an ejector duct, see Figure 21.4.
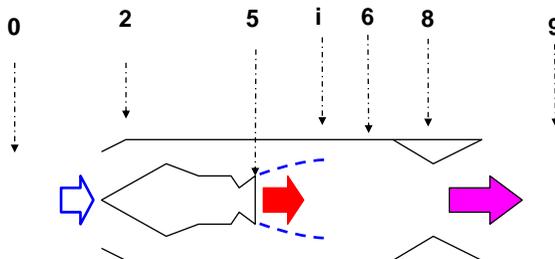
Fig. 21.4 In the Ramrocket thrust at take-off is produced by an ejector rocket

The basic idea of the ejector is to multiply the rocket mass flow by drawing in a supplementary mass flow from the surrounding atmosphere. The pressure of that flow is raised to a value between that of the ambient and the rocket flow. Ejectors are mechanically simple and the main advantage of this engine is its low weight. It is also the system that is easiest to integrate with a scramjet.

In the so called **strutjet**, the scramjet injector struts serve as both ejector nozzles entraining air at low speeds and as rocket

combustion chambers for the final ascent. The drawback is that the efficiency is rather low at low speeds.

In contrast to the jet engine, the ramrocket is running at a constant core rocket engine combustor temperature and pressure. Another difference from the jet engine is in the core flow exhaust, which is supersonic in nature. If the rocket exhaust static pressure exceeds the bypass duct static pressure, the pressure of the rocket exhaust stream will gradually adjust to the bypass pressure by passing through expansion fans attached to the nozzle lip.

If on the other hand the rocket exhaust static pressure is lower than the bypass duct static pressure, oblique shock waves will move into the nozzle and bring the core pressure up to the bypass pressure.

Those events may be modelled by assuming that the primary and secondary flows are at static pressure equilibrium at the mixer inlet plane "i" behind the splitter and not at the splitter lip "5" itself as with the jet engine. This means that the flow areas of the two streams are varying while the sum of them is fixed by the exhaust duct area. Note that for any ejector effect to occur, the static pressure at the mixer inlet must be below the ambient pressure p_0 .

For an assumed value of the secondary air flow Mach number M_{ai} in the inlet plane, the mass flow parameter is:

$$\bar{m}(M_{ai}) = \frac{\gamma_a}{\sqrt{\gamma_a - 1}} M_{ai} \left(1 + \frac{\gamma_a - 1}{2} M_{ai}^2 \right)^{-(\gamma_a + 1)/2(\gamma_a - 1)} \qquad (21.7)$$

With a common static pressure for the rocket and air flow in the mixer inlet plane, the core rocket exhaust Mach number is:

$$M_{ri} = \sqrt{\frac{2}{\gamma_r - 1}\left\{\left[\frac{p_{tr}}{p_{ta}}\left(1 + \frac{\gamma_a - 1}{2}M_{ai}^2\right)^{\frac{\gamma_a}{\gamma_a - 1}}\right]^{\frac{\gamma_r - 1}{\gamma_r}} - 1\right\}} \quad (21.8)$$

where the rocket chamber total pressure is known.

Since the total pressure and temperature are the same in the mixing inlet plane and in the rocket nozzle throat, it follows from the mass flow equation that the rocket exhaust area in the mixing inlet plane is given by:

$$\frac{A_{ri}}{A^*} = \frac{\bar{m}_r(1)}{\bar{m}_r(M_{ri})} \quad (21.9)$$

and the air flow area in the mixing inlet plane:

$$\frac{A_{ai}}{A^*} = \frac{A}{A^*} - \frac{A_{ri}}{A^*} \quad (21.10)$$

where the relation between the total exhaust area and the throat area is assumed to be known as a design value.

The mass flows per unit area are:

$$\frac{\dot{m}_a}{A_{ai}} = \frac{p_{ta}\bar{m}_{ai}}{\sqrt{C_{pa}T_{ta}}} \quad (21.11)$$

and

$$\frac{\dot{m}_r}{A^*} = \frac{p_{tr}\bar{m}_r(1)}{\sqrt{C_{pr}T_{tr}}}$$ (21.12)

where the temperature and pressure are known from the air inlet and chamber conditions.

Now the bypass ratio is:

$$\alpha = \frac{\dot{m}_a}{\dot{m}_r} = \frac{A_{ai}}{A^*}\frac{\dot{m}_a/A_{ai}}{\dot{m}_r/A^*}$$ (21.13)

The specific heat and adiabatic constant in the mixing inlet plane is then obtained from a mass weighting and the total temperature in the mixing plane from an energy balance.

The Mach number in the mixing inlet plane is obtained as in the turboramjet, see Eq. (18.18). For this Mach number in the mixing inlet plane, the mass flow parameter can be calculated. For a constant flow area in the mixer, a mass balance between the inlet and outlet mixing plane gives the total pressure in the outlet mixing plane "6". This Mach number also gives the static temperature and therefore the static pressure. This static pressure must satisfy the conservation of momentum over the mixer, which means that:

$$p_m A(1+\gamma_m M_m^2) = p_i A_{ai}(1+\gamma_a M_{ai}^2) + p_i A_{ri}(1+\gamma_r M_{ri}^2)$$ (21.14)

If that is not the case, then a new value of the inlet air Mach number will have to be assumed.

Calculations will show that the mixing plane is very often choked so that $M_m=1$. As the flight Mach number increases, however, the air inlet plane may choke so that $M_{ai}=1$. Then the outlet mixing plane will unchoke and the Mach number there may be iterated until the conservation of momentum over the mixer is satisfied.

Once the conditions in the mixer plane are determined, the performance of the ramrocket may be calculated as for the jet engine. The engine may be provided with an afterburner in which case the afterburner fuel flow is added to the rocket fuel flow.

Thrust augmentation ratio
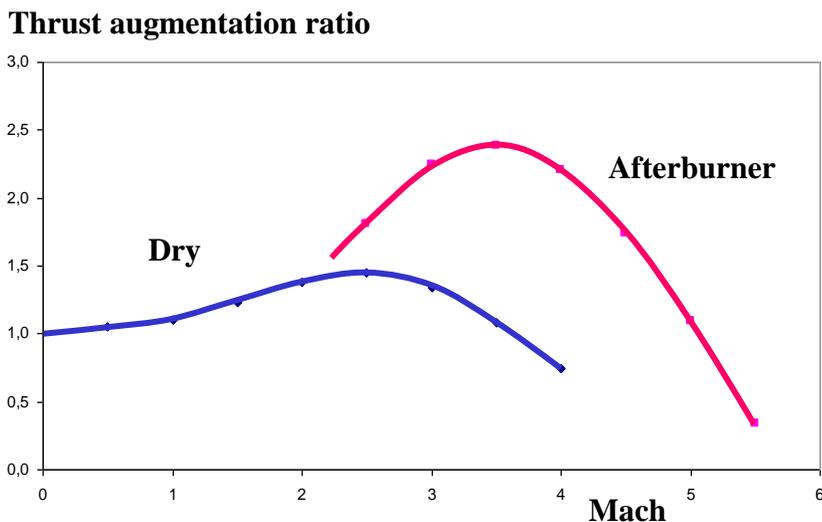
Fig. 21.5 The ratio between the ramrocket thrust and the rocket thrust.

Results from such a calculation for a hydrogen/oxygen rocket engine with a ram duct/ rocket throat area ratio of 10:1 is shown in Figure 21.5. The augmentation ratio is defined as the ratio between the ramrocket thrust and the rocket thrust.

Obviously, the ejector has the potential to significantly increase the thrust above that of the rocket alone. Also, in contrast to the ramjet, it can provide static thrust and can therefore be used from take-off. The increase of the thrust with Mach number after take-off would also help to overcome the transsonic drag rise.

The air mass flow will increase rapidly with speed as pressure builds up in the inlet. Afterburning does not give a positive thrust contribution until the air mass flow has increased so much that the mixer temperature falls below the stoichiometric combustion temperature. This happens at about Mach 2. Afterburning then gives a significant increase in thrust.

A somewhat different picture is obtained if we choose to compare the efficiency instead of thrust, see Figure 21.6.

From an efficiency point of view, the afterburner does not give any positive contribution until above Mach 4. It is also seen that the efficiency of the engine is rather low compared to the precooled turboramjet, see Figure 18.7.

Like in all airbreathing engines, the inlet air momentum tends to grow more rapidly than the jet momentum so that the thrust vanishes. This happens also for the ramrocket but the maximum speed may be significantly increased by the afterburner. As the thrust falls below that of the rocket engine, the air duct should be

closed down and the engine continues as an ordinary rocket engine.
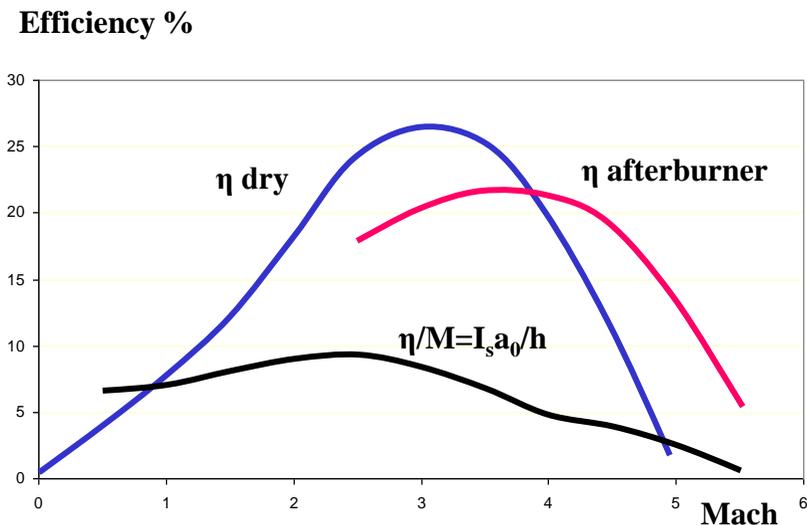
Efficiency %

Fig. 21.6 The efficiency of a ramrocket with and without afterburner.

The efficiency of a rocket engine could be increased at low speed by using atmospheric air as the oxidizer instead of carrying the oxygen in a separate tank. One way to do this is to liquify the air by precooling it. This is the so called **LACE (Liquified Air Cycle Engine),** see Figure 21.7.

In this engine, the air is cooled down in heat exchangers by liquid hydrogen into a liquid state. The liquid air is then pumped to a rocket-like combustion chamber along with the hydrogen. This

engine is an example of an engine combining airbreathers and rockets.

Since oxygen is taken from the air and since the air contains nitrogen that adds to the exhaust mass flow rate, the performance of the LACE is better than that of a rocket engine.
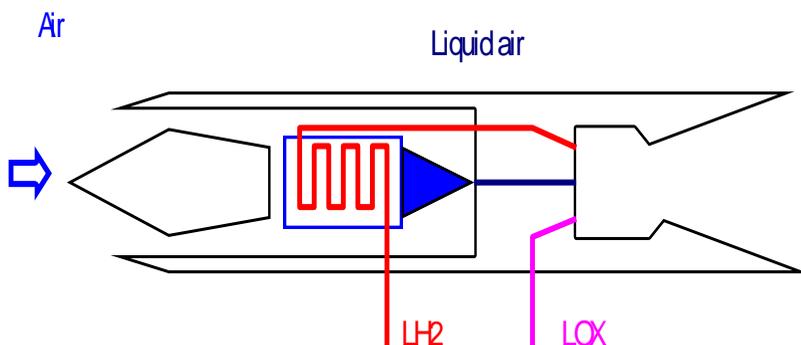
Fig. 21.7 Liquid Air Combustion Engine (LACE)

Liquid air cycle engines were first proposed by the Marquardt company in the early 1960's. The simple LACE engine exploits the low temperature and high specific heat of liquid hydrogen in order to liquefy the inlet air stream in a specially designed condenser. Following liquefaction the air is relatively easily pumped up to such high pressures that it can be fed into a conventional rocket combustion chamber.

The main advantage of this approach is that the air breathing and rocket propulsion systems can be combined with only a single nozzle system required for both modes. This results in a mass saving and a compact installation. Also the engine is in principle capable of operation from sea level static conditions up to perhaps Mach 6-7. When the temperature in the inlet becomes too high for liquefaction one could switch over to a liquid oxidizer and continue as a rocket.

The air inlet conditions may be calculated as for other high speed engines. The hydrogen burnt in the combustion chamber is used to produce a certain amount of liquid air while the balance of the oxygen used in the combustion chamber is supplied from a separate source. Air contains 3.76 parts of nitrogen for each part of oxygen. Then in the reaction between oxygen and hydrogen, water is formed according to the following reaction:

$$x(3.76N_2 + O_2) + (1-x)O_2 + 2H_2 \rightarrow x3.76N_2 + 2H_2O \quad (21.15)$$

The relative mass flows are now:

$$\frac{\dot{m}_a}{\dot{m}_j} = \frac{x(3.76 \bullet 28 + 32)}{x3.76 \bullet 28 + 36} \quad (21.16)$$

$$\frac{\dot{m}_{O_2}}{\dot{m}_j} = \frac{2 \bullet 16}{x3.76 \bullet 28 + 36} \quad (21.17)$$

$$\frac{\dot{m}_{H_2}}{\dot{m}_j} = \frac{2 \bullet 2}{x3.76 \bullet 28 + 36} \quad (21.18)$$

The enthalpy of the inlet air although partially given to the hydrogen, is introduced in the combustion chamber in its entirety so the enthalpy of the gases in the combustion chamber is:

$$h_{tc} = \dot{m}_a / \dot{m}_j C_{pa} T_{t0} + \dot{m}_{H_2} \dot{m}_j / h \qquad (21.19)$$

Where the heating value of hydrogen is h=120 MJ/kg.

The jet mass flow is for a constant combustion chamber pressure:

$$\dot{m}_j = \bar{m} \frac{A_t p_{tc}}{\sqrt{C_{pc} T_{tc}}} = \dot{m}_{j0} \sqrt{\frac{h_{tc0}}{h_{tc}}} \qquad (21.20)$$

The air and hydrogen flows may now be calculated.

The condenser efficiency is dependent on the mass flows of air and hydrogen. A typical expression is:

$$\eta_p = \frac{T_{t0} - T_{air}}{T_{t0} - T_{hi}} = \eta_{p0}^{(\dot{m}_a / \dot{m}_{a0})^{0.85} (\dot{m}_{H_2} / \dot{m}_{H_2 0})^{0.74}} \qquad (21.21)$$

where "0" signifies the properties in the design point.
The relative amount of air "x" may now be found so that Eq. (21.21) is satisfied with the air cooled down to its liquification point (80 K) by liquid hydrogen (30 K).

In the condenser, the liquid hydrogen is first evaporated and then heated. The hydrogen temperature after the condenser is:

$$T_H = T_{H0} + \frac{\dot{m}_a}{\dot{m}_{H_2}} \frac{\eta_p C_{pc}}{C_{pH}} (T_{t13} - T_{H0}) + \frac{h_{vap}}{C_{pH}} \qquad (21.22)$$

Note that the efficiency must always be so high that the leaving hydrogen temperature is lower than the incoming air temperature.

The jet velocity is with expansion to the atmosphere:

$$V_j = \sqrt{2h_{tc}\left[1 - \left(\frac{p_0}{p_c}\right)^{\frac{\gamma-1}{\gamma}}\right]} \qquad (21.23)$$

The thrust is:

$$F = \dot{m}_j V_j - \dot{m}_a V \qquad (21.24)$$

and the specific impulse:

$$I_s = \frac{\dot{m}_j V_j - \dot{m}_a V}{\dot{m}_{H_2} + (1-x)\dot{m}_{O_2}} = \frac{V_j - V\dot{m}_a/\dot{m}_j}{\dot{m}_{H_2}/\dot{m}_j + (1-x)\dot{m}_{O_2}/\dot{m}_j} \qquad (21.25)$$

The efficiency is:

$$\eta = I_s \frac{V}{h + V^2/2} \qquad (21.26)$$

The rocket engine is obtained with x=0.
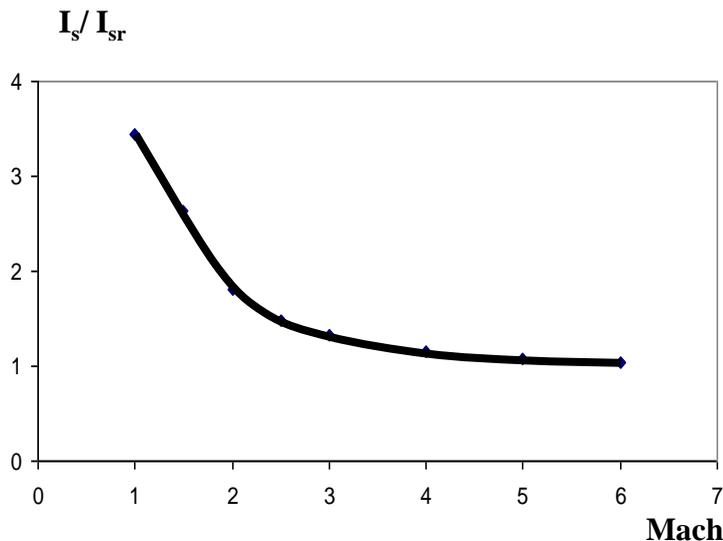
Fig. 21.8 The specific impulse of a LACE compared to a rocket

 In essence, the LACE is a type of rocket engine and its efficiency at moderate speeds is low compared to airbreathing engines. As is seen from Figure 21.8, it has a significantly better specific impulse than the ordinary rocket engine at low speeds but this advantage decreases rapidly as the stagnation temperature builds up in the condenser.

One challenge of the simple LACE engine is the obvious need to prevent clogging of the condenser by frozen carbon dioxide and water vapor. The air pressure within the condenser also affects the latent heat of vaporisation and the liquifaction temperature and consequently has a strong effect on the fuel/air ratio.

At high Mach numbers the fuel flow may need to be increased further, due to heat exchanger metal temperature limitations exacerbated by hydrogen embrittlement limiting the choice of tube materials. To reduce the fuel flow it is sometimes proposed to employ slush hydrogen and recirculate a portion of the coolant flow back into the tankage. However, the handling of slush hydrogen poses difficult technical and operational problems.

By terminating the cooling process before the vapor boundary (80K), a very large saving in the required coolant flow is obtained. This would leave sufficient hydrogen to power a high pressure ratio turbocompressor able to compress the airflow up to typical rocket combustion chamber pressures. An example of this type of engine was the Rolls Royce RB545 designed for the HOTOL space plane.

In a more complex variant of this cycle, a lower fuel flow can be achieved by a helium loop interposed between the 'hot' airstream and the 'cold' hydrogen stream. The work output of the helium loop provides the power to drive the air turbocompressor. Employing helium as the working fluid permits superior heat resisting alloys for the precooler and also results in more optimally matched turbine stages.

The specific impulse divided by the orbital speed at earth surface of the different low speed engines below Mach 6 is compared in Figure 21.9.

The **Pulse Detonation Engine** of Chapter 19 seems to be a very advantageous alternative. It has a high specific impulse and a low weight. It can produce thrust from take-off and it is mechanically

simple and it might be possible to integrate it with a scramjet or a rocket. Potentially, this may be one of the most promising alternative engines but it is still in its infancy.

$$I_s / V_0$$
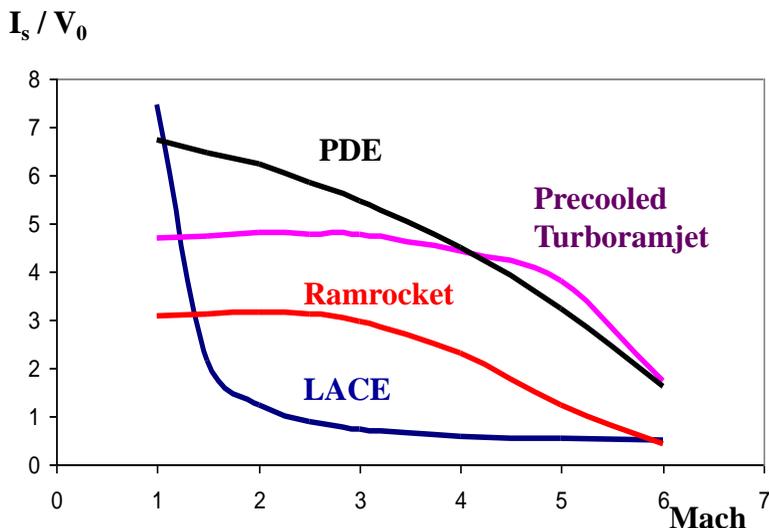
Fig. 21.9 Specific impulse of engines for speeds below Mach 6

With precooling the **turboramjet** and its variants, the turboramrocket and the turboramexpander, could be extended to Mach 6 with a high specific impulse. The problem is the high weight of the turbomachinery. The turbomachinery may also be difficult to integrate with a scramjet and a rocket.

As regards the specific impulse, the **ramrocket** seems not to be able to compete with the precooled turboramjet because of its low pressure ratio in the expander version. Its advantage is that it may

be easy to combine it with a rocket for continued flight and also that it has a low weight.

Finally, the **LACE** may also be easy to integrate with a rocket but it has a low specific impulse compared to other airbreathing engines.

I_s / V_0
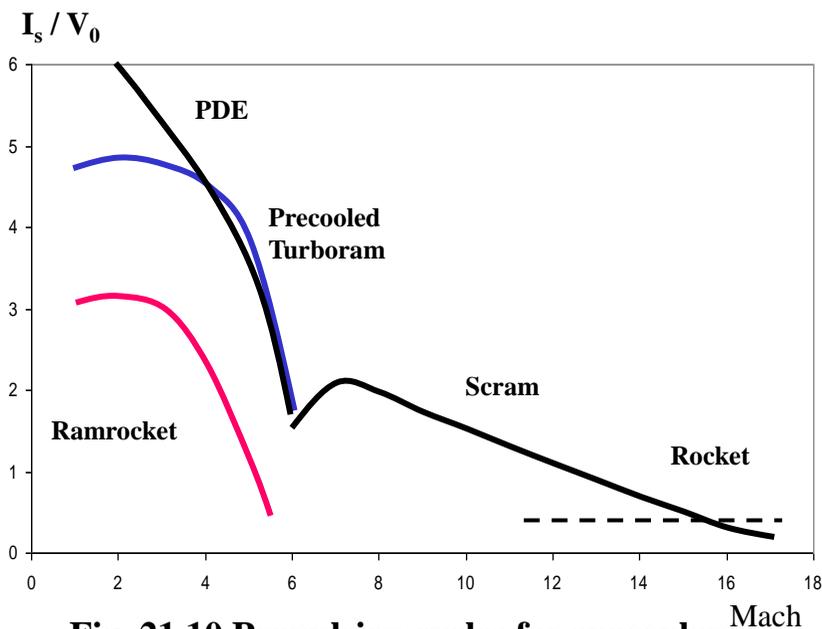
Fig. 21.10 Propulsion cycles for spaceplanes

In summary, there are at least three different phases in the propulsion of a spaceplane, see Figure 21.10. For low-speed operation below Mach 6, the combined-cycle engine would probably operate like an ejector ramjet or a precooled turbojet (or a Pulse Detonation Engine). Between Mach 6 and Mach 15, there are two alternatives, either the rocket or the scramjet. Above Mach 15, a rocket engine must be used.

As the aircraft accelerates, the engine should be converting from cycle to cycle by varying the configuration and geometry of its air passages. This requires a rather elaborate control system and a complex mechanical integration with the vehicle. The forward part of the lower fuselage would actually be the engine intake while the rear of the fuselage would function as an exhaust nozzle. The rocket engine must be integrated into the airbreathing engine nozzle otherwise the base drag penalty of a separate nozzle system would cripple the vehicle performance.

Ex 21.1

To what flight speeds would the stoichiometric scramjet with fuel/air ratio f=0.029 be superior to the liquid hydrogen/liquid oxygen rocket engine with a specific impulse of 4500 m/s?

The specific heat will increase due to dissociation but an average value may be assumed to be 1500 J/kg K with γ=1.28. The speed of sound is taken to be 300 m/s. The heating value of hydrogen is 120 MJ/kg and the total kinetic efficiency 0.75 and the combustion efficiency 0.9. The atmospheric temperature is 220 K.

22. FLYING INTO SPACE

The rocket is presently the dominant vehicle for space travels. However, a winged airbreathing single stage spaceplane would have many advantages because it could take off and land on conventional runways. Airbreathing engines would be a necessity in such a spaceplane in order to keep down the propellant consumption and increase the payload fraction. Variations with speed of the specific impulse of the engines and the lifting capacity of the wings will make the trajectories of spaceplanes very different from rockets.
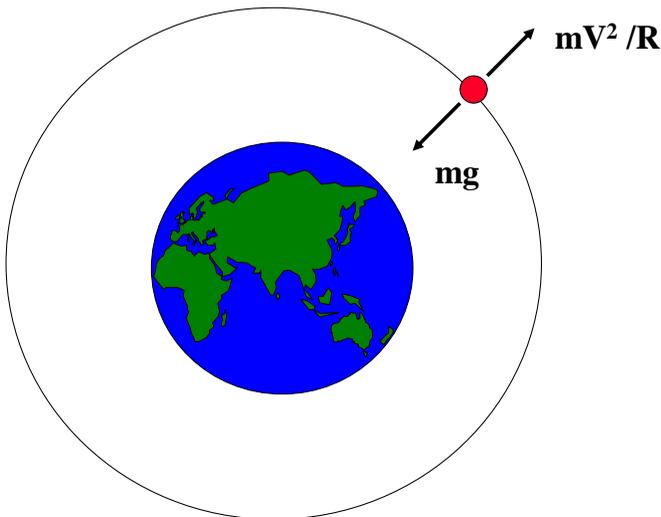
Fig. 22.1 Satellite orbit

In order to enter into a satellite orbit close to a planet one needs to reach the so called **circular velocity**. It may be obtained from the balance between centrifugal and gravitational forces at the distance R from the center of the earth, see Figure 22.1, where the gravitational constant is g:

$$V = \sqrt{gR}$$

(22.1)

This velocity is very high, nearly 8 km/s. Until the end of the 1800´s one had no idea how such velocities could be reached but then in 1898 an elementary school teacher in a small town outside Moscow, the Russian <u>Konstantin E. Tsiolkovsky (1857-1935) proposed the idea of space exploration by rockets</u>. Being independent of the atmosphere, this type of engine is ideal for space flight.

In his numerous writings Tsiolkovsky proposed liquid propellants, the multistage rocket and space stations. In his later years, he gained appreciation for his work, becoming a favorite of Stalin and was allowed to explain his ideas about space flight to respectful though probably confused masses at a May 1 celebration in the Red Square.

The speed that may be reached with a given amount of propellants was first derived by Tsiolkovsky in 1895 for a straight-line rocket motion with constant exhaust velocity. This is nowadays called the **Tsiolkovsky equation** and it forms the basis for rocket flight. Tsiolkovsky stated that the speed and range of a rocket were limited only by the exhaust velocity of the escaping gases.

The fundamental physical principle involved in rocket propulsion was formulated by Newton. According to his third law of motion, the rocket experiences a force that is the mass flow of the exhaust multiplied by the jet velocity. The definition of the specific impulse as the thrust per propellant flow gives:

$$F = \dot{m}_p I_s \tag{22.2}$$

Note that the specific impulse with this definition is equal to the exhaust velocity. In engineering circles, notably in the United States, the specific impulse is often given in seconds obtained by dividing the exhaust velocity with g=9.81.

The equation of motion is:

$$F = m\frac{dV}{dt} = -I_s\frac{dm}{dt} \tag{22.3}$$

With Eq. (22.2), we now obtain:

$$-\frac{dV}{I_s} = \frac{dm}{m} \tag{22.4}$$

which can be integrated to give the relation between cutoff and initial mass:

$$\frac{m_c}{m_0} = e^{-V/I_s} \tag{22.5}$$

or the cut-off velocity:

$$V_c = I_s \ln \frac{m_0}{m_c} \tag{22.6}$$

This is the so called **Tsiolkovsky rocket equation**. It shows why high exhaust velocity (specific impulse) has historically been a driving force for rocket design. The cut-off weight, which includes the payload weight, depends strongly upon the exhaust velocity of the rocket engine, that is the specific impulse.

The rockets in Tsiolkovsky´s time were of the solid propellant type. A typical specific impulse for a solid propellant is below 2500 m/s. This is not sufficient for space travels and a more powerful engine was needed. The answer was the liquid rocket engine. In a report he published in 1903, Tsiolkovsky had suggested the use of liquid propellants for rockets in order to achieve greater range but the real inventor of the liquid rocket engine was the American Robert Goddard, see Chapter 20.

Besides inventing the liquid rocket engine, Robert Goddard also stated that **multistage** or step rockets were the answer to achieving high altitudes and the velocity needed to escape Earth's gravity. The idea is that the launch vehicle carries multiple stages, which are left behind as they burn out. In this way, the inert components of the burnt out stages are not carried to final velocity, which saves energy.

From the rocket equation for the n:th stage the ratio between cut off mass and initial mass is:

$$\frac{m_{pn}}{m_{0n}} = 1 - e^{-\Delta V_n / I_{sn}} \tag{22.7}$$

With the propellant ratio:

$$f_n = \frac{m_{pn}}{m_{0n} - m_{0n+1}} \tag{22.8}$$

the ratio between cutoff mass and initial mass in each stage is:

$$\frac{m_{0n+1}}{m_{0n}} = 1 - \frac{1}{f_n}(1 - e^{-\Delta V_n / I_{sn}}) \tag{22.9}$$

The overall cutoff to initial mass ratio is then:

$$\mu = \prod_1^N \left[1 - \frac{1}{f_n}(1 - e^{-\Delta V_n / I_{sn}}) \right] \tag{22.10}$$

subject to the restriction that:

$$V = \sum_1^N \Delta V_n \tag{22.11}$$

If the specific impulse and the propellant ratio are the same in all stages, then the cutoff mass ratio is a maximum when the velocity increase is the same in all stages. It can then be seen that the payload is always higher for a multistage rocket compared to a single stage where $V_1 = V$.

Using separate stages has other advantages. It turns out that a rocket engine is most efficient when the exhaust gases exit its nozzle at the prevailing atmospheric pressure. At low altitudes, where air pressure is high, this effect favors a short nozzle. However, in the near vacuum of the upper atmosphere, a longer

nozzle is more effective. Staging thus allows the use of nozzles that work reasonably well even as the craft climbs through progressively thinner air.

The Rumanian-born **Hermann Oberth** wrote, in 1923, a highly prophetic book: "*The Rocket into Interplanetary Space*" in which he proved that flight beyond the atmosphere might be possible. In another 1929 book called "*The Road to Space Travel*" Oberth proposed liquid-propelled and multistage rockets. Those books enthralled many with dreams of space flight, including a German teenager, **Wernher von Braun**, who read the first book in 1925. Five years later, von Braun had joined Oberth and was assisting with rocket experiments.

By the age of 22 von Braun had earned his doctorate in physics. Two years later he was directing Germany's military rocket development program. The Germans took Goddard's ideas and turned them into real weapons. The rocket researchers quickly outgrew their facilities at Kummersdorf on the outskirts of Berlin and in 1936 operations were transferred to the remote island of **Peenemuende** on Germany's Baltic coast.

Due to the work of the early pioneers and a host of rocket experimenters, the potential of rocket propulsion was at least vaguely perceived prior to World War II, but there were many technical barriers to overcome. Development was accelerated during the late 1930s and particularly during the war years. Under von Braun, the Germans perfected the large liquid-fueled rocket which culminated in a long range ballistic missile, the Vergeltungswaffe number two, **V2** for short. The V2 was the first successful, long range ballistic missile, and Wernher von Braun is credited as its principal developer.

After two failed attempts, <u>on October 3, 1942, a third V2</u> roared aloft from Peenemuende, followed its programmed trajectory perfectly, and landed on target 190 kilometers away. This launch can fairly be said to mark the beginning of the space age.

The V2 rocket was small by today's standard but at the time, it was the largest rocket vehicle ever made, being 14 m long, 1.6 m in diameter and developing 25 tons of thrust. The main advances in propulsion that were involved in it were the development of pumps, injectors, and cooling systems for liquid-propellant engines.

The V2 achieved its great thrust by burning a mixture of liquid oxygen and alcohol at a rate of about one ton every seven seconds. Once launched, the V2 was a formidable weapon that could devastate whole city blocks.

As World War II drew to a close, von Braun led his contingent of several hundred rocket scientists and engineers into American lines. Other German scientist ended up in the Soviet Union and in France. The **Viking** engines designed in France for the Ariane 1-4 is based on a German war time design.

In June, General Eisenhower sanctioned the final series of V2 launches in Europe. Watching each of the three V2s which rose from a launch site at Kuxhafen was <u>a Russian Army colonel,</u> **<u>Sergei Korolev</u>**<u>.</u> Ten years later, Korolev would be hailed as the Soviet Union's chief designer of spacecraft and the individual responsible for building the Vostok, Voshkod and Soyuz spacecraft, which since 1961 carried all Soviet cosmonauts into

orbit. He would become von Brauns great competitor in the space race.

Korolev (1907-1966) was the founder of the Soviet space program. Involved in the pre-WWII studies of rocketry in the USSR, Korolev like many of his colleagues went through Stalin's prisons and later participated in the search for rocket weapons in occupied Germany. His incredible energy, intelligence, his belief in the prospects of the rocket technology, managerial abilities and almost mythical skills in handling the decision-making process made him the head of the first Soviet rocket development centre. He deserves the highest credits for turning the rocket weapon into an instrument of space exploration and making the Soviet Union the world's first space-faring nation.

On October 4, 1957, the world was stunned by the news of an Earth-orbiting artificial satellite launched by the Soviet Union. Called **Sputnik** I, the satellite was the first successful entry in a race for space between the two superpower nations. Less than a month later, the Soviets followed up its success with the launch of a satellite carrying a dog named Laika on board. Laika survived in space for seven days before being put to sleep before the oxygen supply ran out.

The Soviets had clearly taken the lead in the space race and they crowned their success with the first manned space flight on April 12, 1961. On this day, the Soviet Union orbited the 5 ton Vostok spacecraft carrying the cosmonaut **Yuri Gagarin**, a Russian air force major. His flight lasted 1 hr and 48 minutes. He was later killed in an airplane accident in 1968.

A few months after the first Sputnik, the United States followed the Soviet Union with a satellite of its own. The von Braun team had developed what was essentially a super-V2 rocket, named after the U.S. Army arsenal where it was being designed, the Redstone.

In 1956, the Army Ballistic Missile Agency was established at the Redstone Arsenal under von Braun's leadership to develop the Jupiter intermediate range ballistic missile. A version of the Redstone rocket, known as the Jupiter C, was used on January 31, 1958, to launch America's first satellite, Explorer I. Three years later, it launched Alan Shepard and Virgil Grissom on suborbital space flights, paving the way for John Glenn's first orbital flight.

In October of 1958, the United States created the National Aeronautics and Space Administration (NASA). **NASA** became a civilian agency with the goal of peaceful exploration of space for the benefit of all mankind. In 1961, President Kennedy committed the US to being first on the Moon and NASA's Marshall Center was charged with developing the gigantic rockets which would take the US there.

The **Saturn rockets** developed at Marshall to support the Apollo program and to honor President Kennedy's pledge are the most powerful space launch vehicles ever. The Saturn V served as the workhorse of the Apollo Moon launches. Its first stage developed over 30 MN of thrust and burned about 14 tonnes of propellant per second for 2.5 minutes. It used five 680 tons of thrust liquid-propellant engines in the first stage.

Soon, astronauts orbited Earth on long duration missions and landed on the Moon. Robot spacecraft traveled to the planets.

Space was suddenly opened up to exploration and commercial exploitation. Satellites made it possible to investigate the world, forecast the weather, and to communicate instantaneously around the globe. As the demand for more and larger payloads increased, a wide array of powerful and versatile rockets had to be built.

Since the earliest days of discovery and experimentation, rockets have evolved from simple gunpowder devices into giant vehicles. The two most well known are the European **Ariane** and the American **Space Shuttle**. Ariane is today the world's most successful commercial satellite launcher with about half the world market. It is a highly reliable liquid hydrogen/liquid oxygen propelled launcher combined with two giant solid strap-on boosters. It is launched from the Kourou Space Center in French Guiana by Arianespace, the first space transportation company in the world, composed of a consortium of European aerospace companies.

America's Space Shuttle, as the Space Transportation System (STS) is commonly known, is a reusable launching system. After each flight, its main components, except the external propellant tank, are refurbished to be used on future flights. The space shuttle is launched with two solid propellant rocket boosters and three cryogenic liquid hydrogen/liquid oxygen main rocket engines.

Current launchers are generally multi-stage expendable rockets, a concept originally developed for the early space race. In a way, the situation is like the railways for ground transportation at the end of the 1800s. The vehicle is running along a prescribed trajectory between two end stations. For rapid and comfortable access to space, engineers have long dreamt of building a more flexible

system around an aircraft that could reach satellite speeds, that is the so called circular velocity, which for the earth is Mach 25.

The **spaceplane** concept is not really new. In fact, the general idea has been around for more than 50 years. Tsiolkovsky pointed out in 1929 that the altitude of an aircraft does not have to be limited to the atmosphere if rocket propulsion was used. This inspired rocket enthusiasts in the Soviet Union and led to development of experimental and military rocket planes during the 1930's.
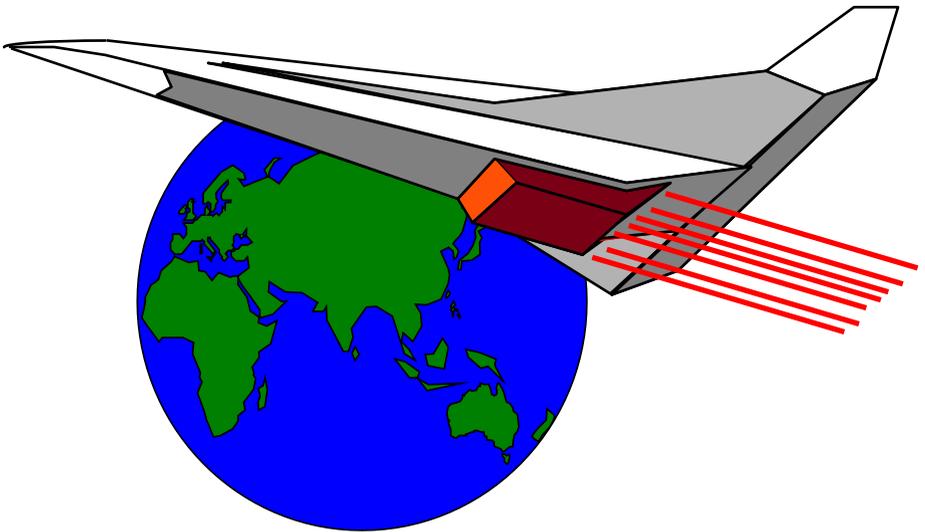
Fig. 22.2 The spaceplane would give a more flexible space access

In 1944, two German scientists, **Eugen Sänger** and **Irene Bredt**, proposed a concept for a hypersonic rocket-powered aircraft that

could bomb the US. Such an aircraft would ascend to approximately 40 km before turning off its engines and coasting back to the edge of the atmosphere. There, it would again fire its air-breathing engines and skip back into space. The craft would repeat this process of skipping motion along the edge of Earth's atmosphere much like a stone skipping across water, until it reached its destination.

Their work influenced the shape of the US **X-1**, the first rocket-powered airplane to break the sound barrier on October 14, 1947. Later on, the **X-15** program made nearly 200 flights from 1959 through 1968 and reached Mach 6.7, the highest speed up till now in a manned aircraft. From it and the US Air Force **Dyna-Soar** program technologies followed that led to the Space Shuttle. The most recent US research effort was the high-profile National Aerospace Plane (**NASP**), or X-30, which was cancelled in 1994 due to budget cuts. The motivation for NASP was that it would make possible very short flight times from the west coast of the US to Japan.

The US is not the only country interested in spaceplanes. Britain has developed several spaceplane concepts, some of which date to the 1950s. Japan began research into spaceplane technology in 1987. The European Space Agency has had similar thoughts and Germany in the 1990s embarked on the later to be cancelled Sänger concept of a two-stage spaceplane.

NASA began a three-pronged technology demonstration programme in 1994. The **DC-X**, Delta Clipper, made four successful flights demonstrating its vertical landing capability. However, testing ended July 31, 1996, when the vehicle toppled and exploded after its fourth flight. The **X-33** lifting-body concept

was called Venture Star. It had a new aerospike engine and would launch vertically but land like an airplane. The **X-34** was a single-engine rocket with short wings and a small tail surface capable of flying at Mach 8. It was to be carried aloft aboard an L-1011 aircraft. Both were terminated at the end of the 1990's.

It is only with **wings** that something similar to air traffic can be achieved in space. 0ne of the main advantages of the wings is that they help in lifting the vehicle. With a vertically launched rocket, the engine must give an acceleration higher than one "g" for lift-off. With winged vehicles it is only necessary to have enough thrust to accelerate on the runway to make the take-off run sufficiently short. A typical value for horizontally take-off airplanes is g/2 or less than half of what is required for vertical take-off. The thrust required from the engines is therefore less to the same extent. Wings also make the vehicle more suited for recovery, allowing an efficient cruise home followed by a conventional landing. For real reusability and flexibility and for decreased thrust, winged spaceplane vehicles will be necessary.

But if a winged airbreathing spaceplane would have many advantages, there are also many problems. One is that contrary to the rocket it must stay within the atmosphere during its ascent to space. This means that the airframe heating and loading are higher. At high speeds the flow is at **stagnation temperature** at several points on a supersonic vehicle. Large temperature gradients in the compression region between the detached shock wave and the vehicle surface is a major cause of aero-thermodynamic heating. Heating also occurs in the hypersonic wakes at the base of the vehicle.
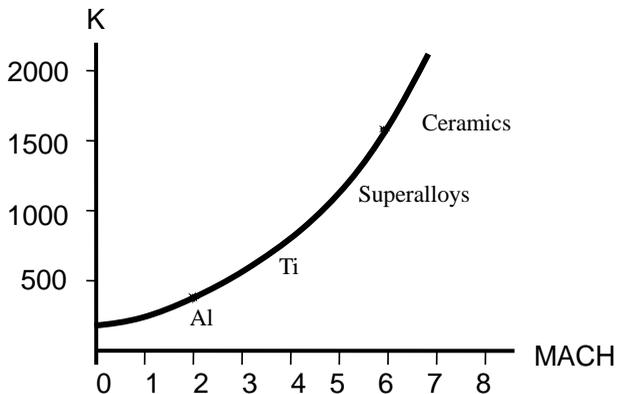
Fig. 22.4 Stagnation temperature and materials

The stagnation temperatures will be very high compared to what typical materials can endure, see Figure 22.4. The hypersonic aircraft will have to be wrapped in a heat-resistant, flexible skin possibly composed of exotic ceramics composites. Since large cockpit windows would enable heat to radiate into the cockpit, small porthole-type windows would only be used on takeoffs and landings. The pilot would rely on video displays connected to external sensors.

The mass of propellants needed to reach a given speed is given by the Tsiolkovsky equation. For spaceplanes, this must be modified taking air drag and gravity into account.

Thus the equation of motion is with α as the angle to the horizontal:

$$F - D - mg\sin\alpha = ma \qquad (22.12)$$

Introducing the specific impulse:

$$I_s = \frac{F}{\dot{m}_p} = \frac{F}{-dm/dt} \qquad (22.13)$$

We now obtain:

$$F = m\frac{dV}{dt}(1 + \frac{D}{mg}\frac{g}{a} + \frac{g}{a}\sin\alpha) = -I_s\frac{dm}{dt} \qquad (22.14)$$

The cut-off weight including payload that could be lifted to a certain velocity V is then:

$$\frac{m_c}{m_0} = 1 - \frac{m_p}{m_0} = \exp(-\int_{V_0}^{V}\frac{dV}{\eta_f I_s}) \qquad (22.15)$$

where the "flight efficiency" is:

$$\eta_f = 1/(1 + \frac{D}{gm}\frac{g}{a} + \frac{g}{a}\sin\alpha) \qquad (22.16)$$

and where V_0 is the tangential velocity of the earth at the launch point. This velocity is 465 m/s at the earth's equator (Kourou) and 410 m/s at Cape Canaveral. At the poles, of course, $V_0=0$. This means that there is a clear advantage with launch sites close to the equator.

The "flight efficiency" includes losses because of gravity and air drag. In vacuum without gravity, its value would be unity resulting in the original Tsiolkovsky equation.

It is seen from Eq. (22.16) that the gravitational losses are reduced by increasing the acceleration thus reducing the time the gravity acts on the vehicle. Unfortunately, there is a limit to what the human body can endure. One does not want to get much over 10 g for any length of time. As a rule of thumb, a reclining pilot can tolerate 5 g without permanent harm for about six minutes and 10 g for about three.

For a spaceplane the **flight efficiency** could be rewritten:

$$\eta_f = 1/(1 + \frac{D}{L}\frac{L}{gm}\frac{g}{a} + \frac{g}{a}\sin\alpha) \qquad (22.17)$$

A high Lift-to-Drag ratio L/D is obviously very important for high flight efficiency. A type of vehicle that have been proposed to maximize the L/D is the "**waverider**". **Nonwieler**, 1963, devised this concept as a supersonic or hypersonic vehicle, which has an attached shock wave all along its leading edge. Because of this, the high pressure under the vehicle can not leak to the top surface resulting in higher lift. The vehicle appears to be riding on top of its shock wave-hence the term waverider. This is in contrast to

conventional vehicles where the shock wave is detached from the body.

Optimized waveriders have been shown to have very high L/D values. According to **Kuchemann**, 1978, in a fundamental text on aircraft design, an upper limit for the L/D for conventional vehicles is described by the relation:

$$L/D = 4(M+3)/M \qquad (22.18)$$

while optimized waveriders could reach:

$$L/D = 6(M+2)/M \qquad (22.19)$$

The modified Tsiolkovsky equation (22.15) above is useful to understand what is required from the engines for a spaceplane. The higher the flight efficiency and the higher the specific impulse of the engine, the higher is the cut-off mass fraction. The hydrogen/oxygen propellant combination is invariably chosen for spaceplanes because of a higher specific impulse than other alternatives despite the structural penalties of a low density fuel.

For a space plane, flying along a trajectory with a radius of curvature R, a balance of forces perpendicular to the flight path gives:

$$m\frac{V^2}{R} = mg\cos\alpha - L \qquad (22.20)$$

so that

$$\frac{L}{mg} = \cos\alpha - \frac{V^2}{gR} \qquad (22.21)$$

and

$$\eta_f = 1/(1 + \frac{D}{L}\left(\cos\alpha - \frac{V^2}{gR}\right)\frac{g}{a} + \frac{g}{a}\sin\alpha) \qquad (22.22)$$

The speed-altitude band where flight sustained by aerodynamic forces is technically possible is called the flight corridor. Usually it is assumed that the vehicle flies at a constant **dynamic pressure** q. If q is too small, the wing area required for lift may become very large. Also, to keep up thrust, q should be as high as possible. Therefore, one would like to fly at the highest possible q without the structural forces and the drag of the vehicle becoming excessive. A typical value may be q=50 kPa.

In such a trajectory, there is a unique relation between the flight speed and the altitude. The variation with altitude of the ratio of the static atmospheric pressure p to the sea level pressure p_{sl} is approximately:

$$\frac{p}{p_{sl}} = e^{-h/h_0} \qquad (22.23)$$

where the so called scale height h_0 =6670 m.

Using the perfect gas law and the speed of sound as a function of temperature, we can then derive an expression for the altitude as a

function of Mach number for a trajectory with constant dynamic pressure. With $\rho = \dfrac{p}{RT}$ and $a_{\mathrm{O}} = \sqrt{\gamma RT}$ we obtain

$$M = \sqrt{\frac{2q}{\gamma p_{sl} e^{-h/h_0}}} \qquad (22.24)$$

This gives the variation of Mach number with altitude in a constant-q trajectory. The **flight angle** in this trajectory is with the acceleration a=dV/dt:

$$\sin \alpha = \frac{1}{V}\frac{dh}{dt} = \frac{a}{V}\frac{dh}{dV} = \frac{a}{a_0^2}\frac{dh}{d(M^2/2)} = \frac{2ah_0}{a_0^2 M^2} \quad (22.25)$$

The flight angle is then seen to be very small for most of the trajectory. In fact, the spaceplane will stay within the stratosphere throughout all of its flight.

This makes the trajectory of an airbreathing spaceplane very different from that of a rocket. For rockets without wings, L/D is very small. Rockets must therefore rise out of the atmosphere as fast as possible as shown in Figure 22.5. Maximum dynamic pressure is reached after about one minute. When the rocket reaches about 200 km altitude, the angle is tilted down so as to minimize gravity losses during acceleration. The winged spaceplane flies at a relatively low altitude until it reaches a speed where the rocket engines has to take over for the final boost into space.
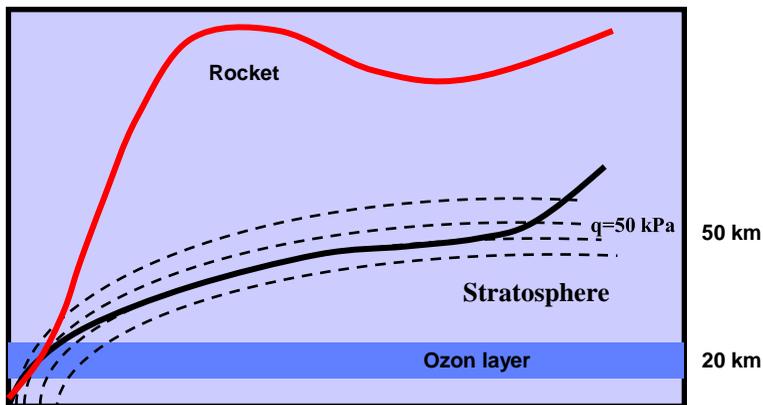
Fig. 22.5 Spaceplane and rocket trajectories

To compare different combined propulsion systems one may introduce an **effective specific impulse** such that:

$$\frac{V}{I_{eff}} = \int_{V_0}^{V} \frac{dV}{\eta_f I_s}$$

(22.26)

This reduces the Eq. (22.15) to the original Tsiolkovsky relation of Eq. (22.5). Typically, the effective specific impulse is about 3500 m/s for a single stage rocket with a vacuum specific impulse of 4500 m/s.

From the variations of the specific impulse with Mach number in Figure 20.10, the efficient specific impulses in m/s for the different airbreathing engine alternatives as compared to the rocket engine are:

Turbo/scram/rocket	5700
Ramrocket/rocket	5500
Rocket	3500

Obviously, the difference between the available airbreathing alternatives is relatively small but they are much superior to the rocket engine. However, it must be recognized that although the airbreathers can produce a higher cut-off mass as seen from Eq. (22.15), their structural mass including wings, engines etc is also higher than that of a rocket so the payload mass lifted into orbit relative to take-off mass is not that much higher. In this context, it should also be noted that the ramrocket-scram-rocket combination may in fact be marginally better than the engine based on the precooled turbojet because of the lower weight of the rocket engine compared to the turbojet.

Ex 22.1

Calculate the velocity of an artificial satellite orbiting the earth in a circular orbit if the radius of the earth is 6375 km.

Ex 22.2

Compare the ideal payload mass ratios for single stage, two stage and three stage to orbit rockets if all stages have a propellant ratio of 0.9 and a structural to take-off mass ratio of 0.1. The specific impulse is 4500 m/s and there are no flight losses.

Ex 22.3

Calculate the altitude at which a space plane enters satellite speed (Mach 25) f it flies at a dynamic pressure of 50kPa.

23. INTERPLANETARY FLIGHT

Travelling in space requires very different engines from getting there. Fortunately, the orbits of the planets are all more or less in the same plane called the ecliptic. Elliptic orbits are the most efficient to transfer from one circular orbit to another in the ecliptic plane. Nuclear and electrical rocket engines are more advantageous than the chemical ones for space travels because of their larger specific impulse.
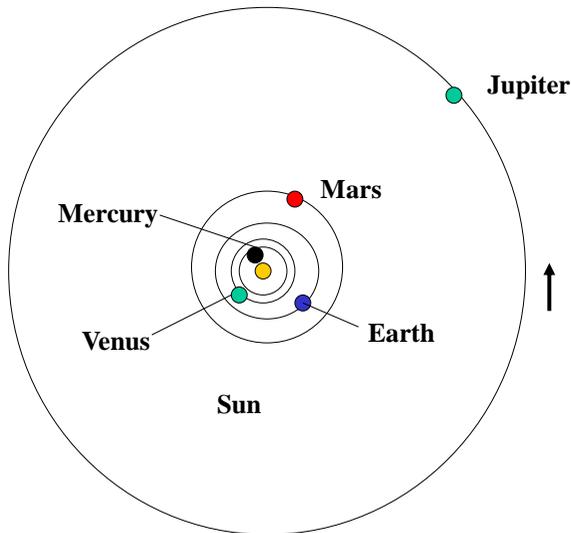
Fig. 23.1 The inner solar system

The solar system consists of the Sun and the nine planets Mercury, Venus, Earth, Mars, Jupiter, Saturn, Uranus, Neptune and Pluto. The masses are very unevenly distributed. The Sun contains 99.85% of all the matter in the solar system and Jupiter contains more than twice the matter of all the other planets combined. The planets, Venus, Earth, and Mars have significant atmospheres while Mercury has almost none. Those planets also have a compact, rocky surface like the Earth's. The other planets are all gigantic compared with Earth, but they are of a gaseous nature although some or all of them might have small solid cores.

The **orbits** of the planets are ellipses with the Sun at one focus, though all except Mercury and Pluto are very nearly circular. Some characteristics of the planets and their orbits are given in Table 23.1.

The orbits of the planets are all more or less in the same plane (called the **ecliptic** and defined by the plane of the Earth's orbit). The ecliptic is inclined 7 degrees from the plane of the Sun's equator. Pluto is a special case in that its orbit is the most highly inclined (18 degrees) and the most highly elliptical of all the planets. Because of this, for part of its orbit, Pluto is closer to the Sun than is its inner neighbor Neptune. All the planets move in the same direction (counter-clockwise looking down from above the Sun's north pole). All but Venus, Uranus and Pluto rotate around their axes in that same sense. The axis of rotation for most of the planets is nearly perpendicular to the ecliptic. The exceptions are Uranus and Pluto, which are heavily tipped on their sides.

Numerous smaller bodies also inhabit the solar system such as the satellites of the planets, the main **asteroid belt** between the orbits of Mars and Jupiter and the many small icy bodies in the Kuiper

belt beyond Neptune. There are also the comets, small icy bodies which come and go through the solar system in highly elongated orbits and at random orientations to the ecliptic.

Table 23.1 Characteristics of the planets

Planet	Solar distance a	Eccentricity e	Radius	Surface gravity
Mercury	0.39	0.206	0.38	0.367
Venus	0.72	0.007	0.97	0.866
Earth	1	0.017	1	1
Mars	1.52	0.093	0.53	0.383
Jupiter	5.20	0.048	11.20	2.648
Saturn	9.55	0.055	9.47	1.405
Uranus	19.2	0.047	3.75	0.957
Neptune	30.09	0.009	3.50	1.527
Pluto	39.5	0.247	1.10	0.815

1. The Earth's mean distance from the Sun is the so called Astronomical Unit (1 AU=1.496E11 m).
2. The greatest and smallest distances of a planet from the sun are:
   Max $R=a(1+e)$
   Min $r=a(1-e)$
3. The radius of the Earth is 6.378E6 m. The surface gravity is 9.81 m/s^2.

The Sun's nearest known stellar neighbor is a red dwarf star called Proxima Centauri, at a distance of 4.3 light years away. One light year is the distance the light travels in one year. The whole solar system, together with the local stars visible on a clear night, orbits

the center of our home galaxy, a spiral disk of 200 billion stars called the **Milky Way**.

Our galaxy, one of billions of galaxies known, is traveling through intergalactic space. The Milky Way has two small galaxies orbiting it nearby, which are visible from the southern hemisphere. They are called the Large Magellanic Cloud and the Small Magellanic Cloud. The nearest large galaxy is the Andromeda Galaxy. It is a spiral galaxy like the Milky Way but it is four times as massive and is two million light years away.

The solar system by volume appears to be an empty void but far from being nothingness, it includes various forms of energy as well as interplanetary dust and gas. Interplanetary dust consists of microscopic solid particles. Interplanetary gas is a tenuous flow of gas and charged particles, protons and electrons, which stream from the Sun and is called the **solar wind**. The solar wind can be measured by spacecraft, and it has a large effect on comet tails. It also has a measurable effect on the motion of spacecraft. The speed of the solar wind is about 400 kilometers per second in the vicinity of Earth's orbit.

Spaceflight started with the first photos of the far side of the moon by the Soviet spacecraft **Luna 3** in 1959. **Mariner 2** was the first successful probe to fly by Venus in December of 1962, and it returned information which confirmed that Venus is a very hot (500 degrees C) world with a cloud-covered atmosphere composed primarily of carbon dioxide.

Mariner 4 reached Mars in 1965 and took the first close-up images of the Martian surface as it flew by the planet. The probe found a cratered world with an atmosphere much thinner than

previously thought. **Pioneer 10** was the first spacecraft to fly by Jupiter in 1973 and Pioneer 11 became the first probe to study Saturn in 1979. **Voyager 2** flew by Uranus in 1986, and by Neptune in 1989.

It took some time for people to realize that the Earth was not the centre of the universe. For nearly two thousand years after his death in 322 BC, the Greek thinker Aristotle was regarded as the ultimate authority on many aspects of science. This was unfortunate because Aristotle tended to favour theory before experiment, which discouraged people from making observations of the real world.

However, in the late 1500's scientists started to challenge the Aristotelian methods. The science of applied mechanics based on experiments was pioneered by the Italian scientist **Galileo Galilei**. In 1590, he wrote a treatise on motion that disputed nearly every assumption made by Aristotelian physics. Aristotle had stated that the speed of a falling body was directly proportional to its weight. Galileo found that if he dropped two balls of similar material but different weights off the Leaning Tower of Pisa, they would hit the ground at the same time. This proved that acceleration was a natural constant.

In 1632, Galileo also published his "*Dialogue*", reconciling the earth's motion, based on **Johannes Kepler's** (1571-1630) proof of the solar system, with man's experience in everyday life of a stationary earth. At a time when the Church based its position on the thought that the earth was the center of the universe those ideas were controversial. Galileo, was threatened with torture and put under guard. Nontheless, the heliocentric ideas gained in the end

and contrary to the fears of the bishops people continued to believe in God even in a heliocentric universe.

Galileo's law of uniform acceleration, its application to falling bodies and his proof that the planets moved around the sun, called for a unified science of physics and astronomy. This was achieved by **Isaac Newton** and his concept of gravity as a natural force. Based on Galileo's work, Newton, beginning in 1687 introduced his laws of motion and gravity. Calculus, invented independently by Newton and **Gottfried Leibniz** (1646-1716), plus Newton's laws of motion are the mathematical tools needed to understand the motion of bodies in gravitational fields.

Newton's universal law of gravitation tells us that the gravitational attraction is inversely proportional to the square of the distance so that the gravity constant varies as:

$$g = g_0 \, \frac{r_0^2}{r^2} \qquad\qquad (23.1)$$

This law was the focus of a heated debate in the British Royal Society in 1693, where Newton was challenged by his nemesis **Robert Hooke** (known for Hooke's law in solid mechanics). Hooke maintained that he had found the inverse-square law before Newton. As a result, Newton had a nervous breakdown that lasted for nearly a year. After his recovery, Newton announced that he had found the law in 1666 well before Hooke's claimed date of 1679. Because of his reputation this was accepted. The controversy may have contributed to Newton's decision to leave science in 1696 to take up a position at the British Mint where he advanced to director in 1699. He had had an earlier encounter with Hooke

about the nature of light after which he devoted himself to astrology for several years.

With the help of Newtons and Leibniz theories, astronomers in the 1700's were able to explain to a large extent how the universe worked. Foremost among them was the French astronomer and mathematician **Lagrange**. He has given name to the Lagrange (sometimes called Libration) points which are positions of equilibrium for a body which is acted upon by two other bodies. Those points are at the third vertex of an equilateral triangle formed with the other two bodies. This means that a satellite can be placed in a stable position with respect to for instance the Earth and the Moon or the Sun and the Earth.

Newton also devised general laws for bodies acted upon by forces, see Chapter 2. It follows from those laws that if a body is left to itself close to a gravitational center, the angular momentum and the total energy (the summary of the kinetic and potential energies) will remain constant so that with " $\overline{V}$ " as the orbit velocity vector and "R" as the distance from the centre of gravity:

$$\overline{V}R = const \qquad (23.2)$$
and
$$\frac{\overline{V}^2}{2} + \int_{R_0}^{R} gdR = const \qquad (23.3)$$

From those equations one can find the trajectories of bodies in space using Newton's law of gravity of Eq. (23.1). Eq. (23.3) is following Leibniz often called the **vis-viva** or living force integral.

For a circular orbit at distance "R_0" from a center of gravity with gravity constant "g_0" at surface radius "r_0", the speed is:

$$V_0 = \sqrt{g_0 \frac{r_0^2}{R_0}} \tag{23.4}$$

It is interesting to note that the circular speed is lower in orbits further away from the earth because of the lower gravity. Thus, one might think that it would be easier to reach more distant points. This is not so, however, because the energy that must added to the spacecraft to reach the orbits increases with the distance.

If the velocity is increased above that of the circular orbit, the spacecraft will move into an elliptical trajectory around the center of gravity. This is called a **Hohmann trajectory**. For the elliptic trajectory to reach a farthest distance with radius "R_1", the velocity closest to the gravity center at radius "R_0" must be increased by:

$$\Delta V_0 = \sqrt{\frac{g_0 r_0^2}{R_0}} \left(\sqrt{\frac{2}{R_0 / R_1 + 1}} - 1 \right) \tag{23.5}$$

The velocity in the farthest point of the elliptic trajectory is lower than the circular velocity at that distance. To enter into the new circular orbit, the velocity must again be increased by:

$$\Delta V_1 = \sqrt{\frac{g_0 r_0^2}{R_0}} \left(1 - \sqrt{\frac{2}{R_0 / R_1 + 1}} \sqrt{\frac{R_0}{R_1}} \right) \sqrt{\frac{R_0}{R_1}} \tag{23.6}$$

Low Earth Orbit (LEO) is where most space activity takes place. It is at an altitude of approximately 400 km. Observation satellites and space stations fly there. Hohmann transfer trajectories can be used to reach orbits further out in space. Geosynchronous Earth Orbit (GEO) is an orbit at altitude 36000 km above the equator, and is popular for communications satellites because the orbit period is 24 hours. Since the Earth's rotation period is also 24 hours, the satellite sits above one point on the Earth's surface. Geosynchronous Transfer Orbit (GTO) has its low point (perigee) at 400 km altitude and its high point (apogee) at 36000 km. As its name implies, it is used to transfer from LEO to GEO. In this case, the vehicle is first lifted to LEO and accellerated to circular velocity there before being accellerated into GTO and circularized in GEO.

Interplanetary Hohman trajectories are shown in Figure 23.2 for the Earth-Mars and Earth-Venus cases. For Earth-Mars, the spacecraft is first accellerated from the Earth orbital velocity of 29.8 km/s to 32.8 km/s. This takes it into an elliptical orbit that touches that of Mars, where its velocity is 21.5 km/s. It must then be accelerated to the Mars orbital velocity of 24.1 km/s to enter into Mars gravitational field. The total change of velocity required, the so called delta-V is 5.6 km/s.

To go to Venus we must accelerate opposite to the direction of Earth's revolution around the Sun, thereby decreasing the orbital energy at aphelion to the extent that the new orbit will have a perihelion equal to the distance of Venus's orbit.
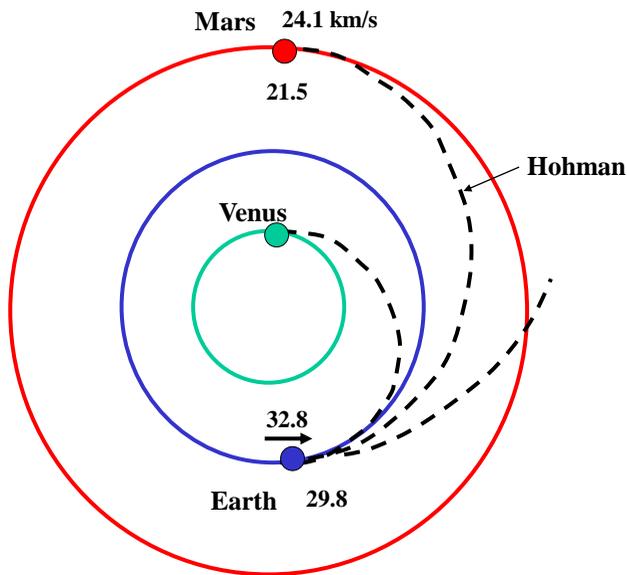
Fig. 23.2 Hohman transfer orbits to Mars and Venus

Now assume that we are in a parking orbit around the earth at radius "R_1". From Eq. (23.3), in order to extend the elliptic trajectory into infinity, that is escaping the earth's gravity, and reach a velocity "V_∞" there relative to the earth, we need to give the spacecraft an injection velocity:

$$V_1 = \sqrt{V_\infty^2 + V_{esc}^2} \tag{23.7}$$

where the so called **escape velocity** is:

$$V_{esc} = \sqrt{2g_0 \frac{r_0^2}{R_1}}$$
(23.8)

For escaping from LEO where $R_1 = r_0$ the escape velocity is 11.2 km/s and we require an excess velocity of 3 km/s to enter the Hohmann transfer to Mars. To leave Earth and enter into the Mars transfer orbit, we could first accelerate to 11.2 km/s and when we are sufficiently far away, the excess of 3 km/s could be added. The total delta-V is then 14.2 km/s. However, it would be better to combine the two propulsive periods and accelerate directly to Hohmann transfer velocity. The injection velocity that must be given to the spacecraft is then from Eq. (23.7) 11.6 km/s. There is therefore a general advantage in combining propulsive periods.

To be captured into a planetary orbit, the spacecraft must decelerate relative to the planet using a retrograde rocket burn or some other means. To land, the spacecraft must decelerate even further using a retrograde burn to the extent that the lowest point of its orbit will intercept the surface. If there is an atmosphere, final deceleration may also be performed by aerodynamic braking.

A Hohmann transfer orbit is the most efficient intermediate orbit to transfer from one circular orbit to another and it is guaranteed to take the smallest amount of delta-V possible. Unfortunately a Hohmann orbit also takes the maximum amount of transit time. For the Earth-Mars Hohmann mission, the transit time is 260 days.

The other drawback is that there are only certain times that one can depart for a given mission, the so-called "Synodic period" or **Hohmann launch window**. The reason is that the departure and destination planets have to be in the correct positions. For the Earth-Mars Hohmann mission, the Hohmann launch windows

occur only every 26 months. Venus launch opportunities occur about every 19 months. There is of course a similar launch window for the return flight from Mars to Earth. Once arrived at Mars one would have to wait for 441 days for the right return date and the total round trip would take 970 days or nearly three years.

Clearly, such trip times are rather impractical. Shorter times can be achieved by increasing the injection velocity so as to extend the transfer ellipse and crossing rather than touching the new planet's orbit, see Figure 23.2. A flight time to Mars of 70 days requires an excess velocity of 12.3 km/s and a total injection velocity of 16.6 km/s. Entering Mars orbit requires 20.7 km/s. After a 12 days stay at Mars, the conditions for a return flight are right and the total mission is then only 154 days or about five months. By doubling the velocity requirement, the total mission time has been reduced from three years to five months. One can trade more delta-V for less trip time down to a lower limit of about two days, where continuous acceleration of 1 g is applied but the delta-V is forbidding at about 500 times greater than the Hohmann minimum.

Gravity assist is a technique to facilitate many missions to the outer planets. A trip to Jupiter is illustrated in Figure 23.3. A ship leaving the Earth for some distant planet can go faster on less fuel by dropping first toward Venus. As the spacecraft comes into Venus gravitational influence, it falls toward the planet, increasing its speed toward maximum at closest approach. The spacecraft passes by Venus since its velocity is greater than Venu's escape velocity. It leaves the Venus environment carrying an increase in angular momentum stolen from Venus. This technique is repeated twice when passing Earth, thus gaining sufficient velocity to enter a Jupiter transit orbit.
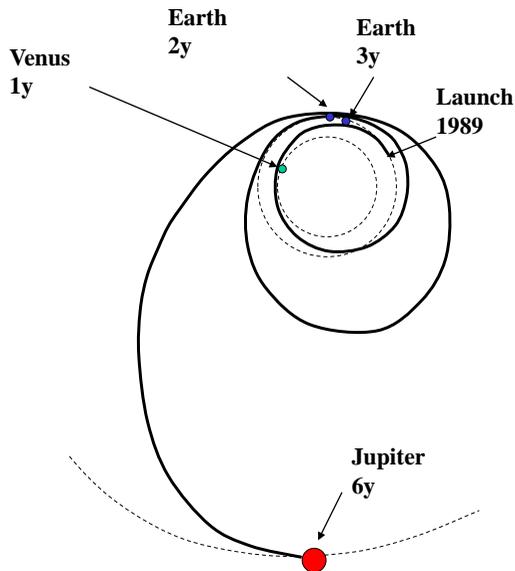
Fig. 23.3 A travel to Jupiter

The final weight relative to the initial weight that can be transported in a trajectory requiring a certain delta-V is given by the Tsiokovsky equation:

$$\frac{m_f}{m_i} = \exp(-\frac{\Delta V}{V_j})$$ (23.9)

It is obvious then that for missions with high delta-V, we need high jet velocities to be able to transport a sufficient final weight. For a rocket engine, the jet velocity is the same as the specific impulse, that is the thrust divided by the mass flow. Two

alternatives to the conventional chemical rocket engine are currently under consideration for space travels, the nuclear propulsion engine and the electrical propulsion engine. Both of these engines are more advantageous than the traditional chemical engine because of the larger specific impulse.

The traditional and most practical approach to the design of a **nuclear thermal** propulsion rocket is the use of a solid-core, heat-exchanger nuclear reactor, see Figure 23.4.
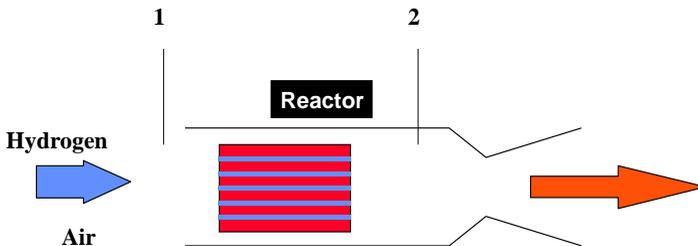
Fig. 23.4 Nuclear engines are heavy but have a large specific impulse.

 In this design the propellant, liquid hydrogen, is pumped through all extra-core components for cooling. After all the components have been cooled, the propellant is pumped through the reactor core to be heated to a temperature determined by the material

limits of the core, and expanded through the nozzle to produce thrust. Typically the core material limits the exhaust temperature to 2500 to 3000 K.

The two main features that lead to the advantages of a nuclear thermal rocket over a chemical one are the enormous energy available per unit mass of fission (or fusion) fuel, and also that in a nuclear thermal system the energy producing medium is separate from the thrust-producing propellant. This allows nuclear systems to use propellants of low molecular weight.

This provides nuclear thermal systems with a greater specific impulse (Isp) than chemical ones. The greater specific impulse of the nuclear rocket allows it to carry a larger payload into space, and to accomplish its missions in a reduced time span. The other advantage of a high specific impulse is that the spacecraft can attain transfer orbits that reduce travel time to the destination.

A chemical rocket can achieve a specific impulse of approximately 4500 m/s, while a solid core nuclear rocket can reach a specific impulse of approximately 9000 m/s. For long duration missions or manned missions to a planet, such as Mars, the nuclear engine is more advantageous to use than the chemical one because of the higher specific impulse.

To analyze the performance of a nuclear thermal engine, we note that the shear force on a length element "dx" in the canal through which the propellant passes while heated is:

$$dF_s = c_f \frac{1}{2} \rho V^2 \pi D dx = c_f \frac{1}{2} \gamma p M^2 \pi D dx \qquad (23.10)$$

where c_f is a friction coefficient.

From Eq. (18.13) the momentum of the flow is with $A = \pi D^2/4$:

$$I = pA(1 + \gamma M^2) \qquad (23.11)$$

The change in momentum is balanced by the shear on the fluid so that:

$$p_1(1 + \gamma M_1^2) - p_2(1 + \gamma M_2^2) = \int_0^L c_f \, 2\gamma p M^2 \frac{dx}{D} \qquad (23.12)$$

Neglecting the fluid velocity at the inlet and taking the shear force as the average of the upstream and downstream values gives the chamber pressure:

$$p_{t2} = p_{t1} \frac{\left(1 + \dfrac{\gamma - 1}{2} M_2^2\right)^{\gamma/(\gamma-1)}}{1 + \gamma M_2^2 (1 + c_f \dfrac{L}{D})} \qquad (23.13)$$

The thermal energy transferred to the propellant medium over an elemental length element dx in one of the canals is:

$$\dot{m} C_p \, dT_t = h(T_w - T_t)\pi D dx \qquad (23.14)$$

Introducing the Stanton number $St = hA/\dot{m}C_p$ and noting that according to the "Reynolds analogy" $St = c_f/2$ and assuming that the power density distribution within the reactor is such that the temperature difference between the wall and the fluid is a constant, we obtain:

$$T_{t2} = \frac{T_{t1} + T_{wm}\, 2c_f L/D}{1 + 2c_f L/D} \tag{23.15}$$

The total exhaust temperature from the canal, and the inlet temperature "T_{tc}" to the nozzle, is therefore determined by the limiting wall temperature "T_{wm}", which occurs at the end of the canal.

The exhaust velocity from the engine, that is its specific impulse, is:

$$I_s = V_j = \sqrt{\frac{2\gamma}{\gamma-1} R T_{t2} \left[1 - \left(\frac{p_0}{p_{t2}} \right)^{(\gamma-1)/\gamma} \right]} \tag{23.16}$$

This means that the specific impulse of the engine is expressed in the Mach number at the end of the canal.

Because the weight of the nuclear reactor is very high we would like to obtain as much thrust as possible from a given cross section of the reactor. To calculate the thrust we need the mass flow through the canal. From Eq. (8.8) this is:

$$\dot{m} = \frac{A p_{t2}}{\sqrt{C_p T_{t2}}} \frac{\gamma}{\sqrt{\gamma-1}} M_2 \left(1 + \frac{\gamma-1}{2} M_2{}^2 \right)^{-(\gamma+1)/2(\gamma-1)} \tag{23.17}$$

Since the thrust is the mass flow times the jet speed, we obtain the following expression for the thrust per unit cooling flow area:

$$\frac{F}{A p_{t1}} = J(M_2)\gamma \sqrt{\frac{2}{\gamma-1} \left[1 - \left(\frac{p_0}{p_{t2}} \right)^{(\gamma-1)/\gamma} \right]} \tag{23.18}$$

where:

$$J(M_2) = M_2 \frac{\sqrt{1 + \frac{\gamma - 1}{2} M_2^2}}{1 + \gamma M_2^2 (1 + c_f \frac{L}{D})} \qquad (23.19)$$

For expansion into a vacuum as in space, maximum thrust density is obtained for a Mach number that makes the J-function a maximum, namely:

$$M_2 = \frac{1}{\sqrt{1 + \gamma c_f L/D}} \qquad (23.20)$$

so the thrust density becomes:

$$\frac{F}{A p_{t1}} = \frac{\gamma}{\sqrt{(\gamma - 1)(1 + \gamma + 2\gamma c_f L/D)}} \qquad (23.21)$$

and the specific impulse is, recognizing that $T_{t1} \ll T_{wm}$:

$$I_{s0} = V_{j0} = \sqrt{\frac{4\gamma}{\gamma - 1} \frac{\Re}{M} T_{wm} \frac{c_f L/D}{1 + 2 c_f L/D}} \qquad (23.22)$$

where $\Re = 8314$ Nm/kmol K the universal gas constant and "M" is the molecular weight of the propellant.

It is interesting to note that a flow of pure hydrogen, owing to its extraordinarily low molecular weight, will have a high specific impulse even when heated to relatively modest temperatures, see Eq. (23.22). This is the basis for the nuclear engines.

It is also seen in Figure 23.5 that the thrust density decreases with the L/D ratio while the specific impulse increases. In other words, an increase in specific impulse leads to higher weight for a given thrust.
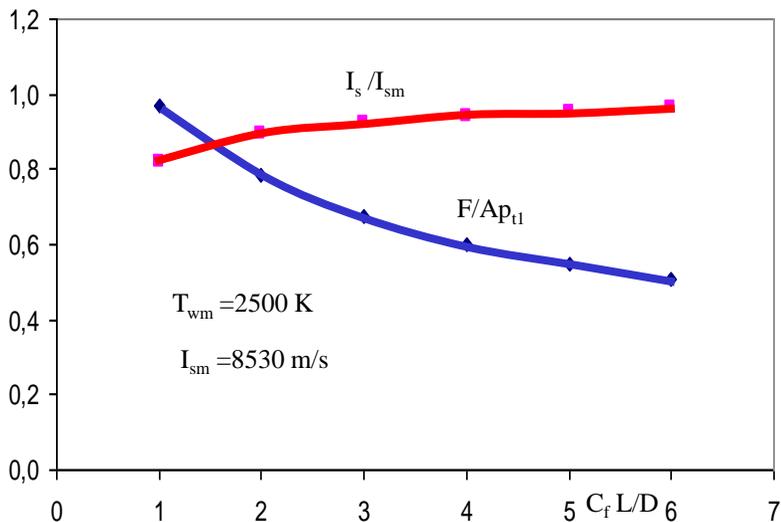
Fig. 23.5 Specific impulse and thrust for a nuclear engine

There are indications that it might be possible to design nuclear engines with thrust-to-weight ratios that could provide sufficiently high acceleration. From 1955 through 1973, the US invested $1.5 billion in the development of <u>nuclear rocket engines</u>. As an example of record performances during this **NERVA** program, one engine reached a thrust of 930 kN, a thermal power of 4100 MW at a specific mass of 2.3 kg/MW and exhaust velocities of 8400

m/s compared to 4500 m/s in the best chemical rocket engines. This would give a thrust/weight ratio of about 10. The real value is probably less than half of that because of radiation shields and other equipment.

The weights that need to be minimized are the neutron absorbing material of the core, neutron moderating components, highly enriched uranium fuel, a neutron-reflector to minimize neutron losses from the core, and the overall core dimensions.

One of the most important aspects of the engine is the fuel it uses. The main consideration to be taken into account in the selection of the reactor fuel material is that the material must have adequate strength at high temperature.

Examples of some materials with very high melting temperatures are:

- Hafnium Carbide   4170 K
- Tantalum Carbide   4140 K
- Graphite   3900 K
- Tungsten   3640 K

The fuel material should also include a low neutron-absorption cross-section, high thermal conductivity, compatibility with high-temperature uranium, compatibility with hot hydrogen, and low mass and molecular weight.

The main problem of nuclear rockets is the heating of engine components by nuclear radiation emanating from the core. Since the core power and power density are high and the system size is minimized, the resulting neutron and x-ray leakages are high.

These leakages are the cause of the heating of the components and can only be counteracted by efficient cooling of all components.

Other methods of using the fission reactor have been proposed to avoid the severe materials problem while transferring heat to the gas directly by the extremely hot reactor walls. One possibility might be to contain the hot fissioning fuel in a **gaseous** state within a transparent wall of fused silica. Hydrogen propellant flowing outside the silica wall is heated by radiation and exhausts through the nozzle. Exhaust velocities of between 16000 to 20000 m/s is said to be possible, which would correspond to hydrogen temperatures of 4500 K.

Another concept is a **uranium plasma** contained by the hydrodynamic flow pattern of the hydrogen propellant. Because no solid material is in the core, the potential exhaust velocities could reach 50000 m/s. Containing the fuel is a major obstacle, however.

One could also place gaseous fissile material in the center of an open reactor retaining it in position by **magnetic** means. Then the propellant gas would be heated by radiation from the hot gaseous fissile material without the interposition of a solid wall. Feasibility of such a device is still a subject of investigation.

The greater specific impulse of the nuclear rocket allows it to carry a larger payload into space, and to accomplish its missions in a reduced time span. For a manned mission to a distant planet like Mars a nuclear propulsion system seems to be more advantageous in terms of propulsive power than a chemical system.

One interesting advantage of the nuclear engine for aircraft use is that if we use the surrounding air for the jet, then there is no fuel

consumption and the range of an aircraft is in principle unlimited. Such a nuclear airbreathing engine could be very heavy and still accelerate a spaceplane to circular speeds. In principle it is therefore a very interesting alternative as a spaceplane engine. One may also consider combinations where air or liquid oxygen is burnt with hydrogen preheated in a nuclear reactor. Such an engine could operate as a non-nuclear chemical air-assisted rocket inside the atmosphere and as a nuclear rocket outside the atmosphere.

The **electric propulsion** system is an alternative to the nuclear thermal propulsion system. Although its total thrust is lower than that of the nuclear rocket, the electrical engine can provide sufficient thrust to propel a spacecraft during planetary missions such as the manned exploration of Mars.

The main difference between an electrical system and a nuclear or chemical system is that the exhaust particles of the rocket are not accelerated by heat energy, but by electrical energy. This accounts for electrical propulsion systems reaching higher exhaust velocities than any of the other available propulsion systems. An electrical engine is also benefited by test results, which show that it is highly efficient in transforming power into thrust.

Study and development of elecrical engine systems has been going on for a long time. The first to describe scientifically the possibility of electric space propulsion was **Robert Goddard** in 1906. Goddard mentioned the possibility of accelerating electrically charged particles to very high velocities without the need for high temperatures. **Hermann Oberth** devoted one chapter of his book "*Wege zur Raumschiffahrt*" (1929) to various problems of electric propulsion systems. After World War II, **Ernst Stuhlinger**, a German rocket scientist then in the US,

argued that lighter-weight electric propulsion systems would make planetary trips more feasible than they were with chemical propulsion.

However, only after 1957 actual small scale experiments were conducted in government laboratories and many independent companies mainly in the USA. At that time it was realized that electric propulsion was not limited to the electrostatic or ion thrusters envisioned in the earlier years, but could be extended to electrothermal and electromagnetic systems. The first space tests of an electric thruster, involving an electrostatic ion engine, were made in mid 1964. Such ion engines are now used for the control of satellites and as primary propulsion of deep space probes. The large number of successful missions that have already employed an electric propulsion system supports its feasibility for long duration space missions.

The flexibility with respect to the power source makes electric propulsion a candidate for a great range of mission applications. The significant and on-going improvements in the specific mass of power subsystems have been a major factor in the acceptance of electric propulsion.

At present electric propulsion systems derive their power from photovoltaic solar arrays but fission nuclear power sources could also be used for outer planetary missions where the available solar power is too low. At the mean distance of the earth from the sun, one square meter receives 130 W of solar radiation. At the distance of Venus, this amount is 240 W and at Mars 55 W. Of this perhaps 10 % may be taken up by solar panels. A 10-kilowatt Mars spacecraft relying on solar power would require a solar panel area

as large as about 2000 m2 so manned spaceships to Mars and beyond would probably require a nuclear reactor. Solar-powered ion thrusters are restricted to the inner solar system, where sunlight is abundant. It is estimated that a nuclear powerplant for electric propulsion including reactor, heat exchangers, coolers and turbine generator could be built at a specific power of 300 W/kg.

The electric power is used to ionize and accelerate the propellant, via a variety of methods. Of these, several are technologically mature enough to be used on spacecraft, including the resistojet, the arcjet, the electron bombardment thruster (particularly the xenon ion thruster), the Hall thruster and the pulsed plasma thruster. Other devices such as Magneto Plasma Dynamics thrusters, and pulsed induction thrusters have not progressed beyond laboratory studies.

In the **resistojet**, a resistive electric heater is used to add heat to a gas stream. Temperature limits of the materials used limit the jet velocity of resistojets to less than 10 km/s for hydrogen. Since the storage of hydrogen is difficult, ammonia has been used as an alternative. Jet velocities of 3.5 km/s have been reached but the efficiency of this type of thruster begins to drop rapidly as the jet velocity is raised because of the energy required to decompose the propellant. Typical efficiencies of resistojets are at 40 %. The efficiency is that part of the power produced by the system that is transformed into jet power.

Jet velocity limitations imposed by materials can be overcome by adding heat directly to the gas in a high intensity **arc**. In this manner the temperature can be raised to perhaps 10000 K and jet velocities of 10-30 km/s can be reached. At these temperatures,

appreciable dissociation and ionization of the gas occurs, absorbing energy that cannot be recovered in the nozzle. This reduces the efficiency of **arcjets** to 20-40 %.

Within the various systems of electrical propulsion that have been developed, the one that currently best satisfies the requirements of a propulsion system for a long duration space mission is the **ion propulsion system**. Besides having the best efficiency (around 60 %) among the electric propulsion systems, this type of electrical rocket is one of the most developed systems currently available.

In the various devices for **ion propulsion**, each molecule of propellant is ionized. It is then possible to accelerate the charged molecules, or ions, to very high velocities through a nozzle by means of an electric field. The performance of such an ion engine is very good with values of specific impulse estimated to be as high as 200 km/s. However, the amount of electric power required is very large, so the weight of the power-generating equipment becomes a major obstacle to an efficient vehicle.

The gas used for propellant in this type of engine is either the gases argon or xenon, or the vaporized form of mercury or cesium. The ionization chamber to which the power supply is connected is the site of particle acceleration. The propellant is pumped into the ionization chamber where it is passed over heated metal grids that ionize it. The electrical field between the grids accelerates the positive ions of the propellant. A neutralizer, which is also connected to the power supply, fires electrons at the accelerated fuel particles. The purpose of these electrons is to counteract the positive charge of the particles, and to assure that the exhaust of the rocket is electrically neutral. Otherwise it would be attracted back to the spacecraft's positive surfaces and cancel out the thrust.

Optimistic estimates of electric-power-supply weight show that the power unit would weigh about one ton for each Newton of thrust produced. Therefore, an ion rocket can accelerate itself only very slowly.

Ion thrusters take a lot of energy, partly to ionize the materials, but mostly to accelerate the ions to the extremely high speeds. Exhaust speeds of 50 km/s are not uncommon. There is also a problem with the relatively short life of the thruster. The ions often hit the grids on their way through the engine, which leads to the decay of the grids, and their eventual failure. Smaller grids lower the chance of these accidental collisions, but decrease the amount of charge they can handle, and thus lower the acceleration.

The **Hall thruster** is a type of ion thruster that was used for decades for station keeping by the Soviet-Union. It uses the Hall effect to accelerate ions to produce thrust. The Hall effect is a potential voltage difference on opposite sides of a thin sheet of conducting or semiconducting material through which an electric current is flowing, created by a magnetic field applied perpendicular to the Hall element. A Hall thruster typically operates at around 50–60% thrust efficiency and provides jet velocities from 12–18 km/s.

Magnetoplasmadynamic (MPD) thrusters use the Lorentz force (a force exerted on charged particles by magnetic and electrical fields in combination) to generate thrust. Thus an electron will be accelerated in the same linear orientation as the electrical field. MPD thrusters may operate in steady state mode or in pulsed, quasi-steady mode. They have been under development since the

late 1960's in Russia and in the US, where several variations of the primary concept were investigated.

In a self field MPD thruster, the arc current created between a central cathode and an annular peripheral anode ionizes the propellant and induces an azimuthal magnetic field. The generated Lorentz body force compresses and accelerates a quasi-neutral plasma along the central axis. Because the self-induced magnetic field is only significant at very high power, low power MPD thrusters often resort to an externally applied magnetic field.

The great scalability of MPD thrusters allows them to cover an impressive range of operating parameters from a few kW to several MW of power, from a few mN to several hundred N of thrust and from 20 to 50 km/s of jet velocity. MPD thrusters, in particular self-field thrusters, are most efficient at high power and can perform with up to 40% of efficiency.

Despite its potential advantages, the development of MPD thrusters remains hindered by longstanding cathode erosion problems limiting their life to a few hundred hours at best.

The properties of the different space based engines are summarized in Table 23.2.

Table 23.2 Properties of different electrical engine types

Engine type	Jet velocity km/s	Efficiency percent
Chemical	2-5	
Nuclear thermal	8-9	
Resistojet	4-10	40
Arcjet electrothermal	10-30	20-40
MPD	20-50	40
Hall	12-18	50-60
Ion	40-50	60

The Tsiolkovsky rocket equation relates the ratio of final mass and initial mass to the specific impulse, that is the exhaust velocity. The final mass contains the payload "m_{pl}", which is supposed to include vehicle dry mass, and the weight of the thrust-producing system "m_t":

$$\frac{m_t + m_{pl}}{m_0} = e^{-\Delta V / V_j} \qquad (23.23)$$

so that:

$$\frac{m_{pl}}{m_0} = e^{-\Delta V / V_j} - \frac{m_t}{m_0} \qquad (23.24)$$

With the propellant mass "m_p", the initial mass is:

$$m_0 = m_{pl} + m_p + m_t \qquad (23.25)$$

For electrical rockets the power, and associated mass increases directly with the exhaust velocity and takes up a dominating part of the dry mass.

If the the thrust-producing system has a power per kg of weight of "α" W/kg, then the power is:

$$P = \alpha m_t \qquad (23.26)$$

If the propulsion system was operating for itself at the power "P" and if all of its available energy were converted to kinetic energy, then it would reach the velocity delta-V required by the mission in a **characteristic time**:

$$t_c = \frac{(\Delta V)^2}{2\alpha} \qquad (23.27)$$

A chemical rocket engine may have a power density of 1 MW/kg, which means that the characterisitic time for the Mars orbit at delta-V of 5600 m/s would be 16 seconds. For the nuclear NERVA system of 500 kW/kg the characteristic time is 50 seconds. By contrast, a solar array or a nuclear generator producing 50 W/kg would have a characteristic time of 3 months.

If the efficiency in transforming the power into jet power is "η", then the mass of propellants used can be obtained from:

$$m_t = \frac{P}{\alpha} = \frac{\dot{m}V_j^2}{2\alpha\eta} = m_p \frac{V_j^2}{2\alpha\eta t} = m_p \left(\frac{V_j}{\Delta V}\right)^2 \frac{t_c}{\eta t} \qquad 823.28)$$

If this is used in Eq. (23.24), it is possible to deduce the following equation for the payload ratio where $v = V_j/\Delta V$ and $\tau = t/t_c$:

$$\frac{m_{pl}}{m_0} = e^{-1/v} - \frac{v^2}{\eta\tau}\left(1 - e^{-1/v}\right) \qquad (23.29)$$

Figure 23.6 shows this function for the Earth-Mars mission with delta-V 5600 m/s for t=6 months and α=100 W/kg and η=0.5. As is seen the function has a maximum for a certain jet speed to delta-V ratio. Electric propulsion concepts are typically chosen that operate at or near this optimum for a given mission.
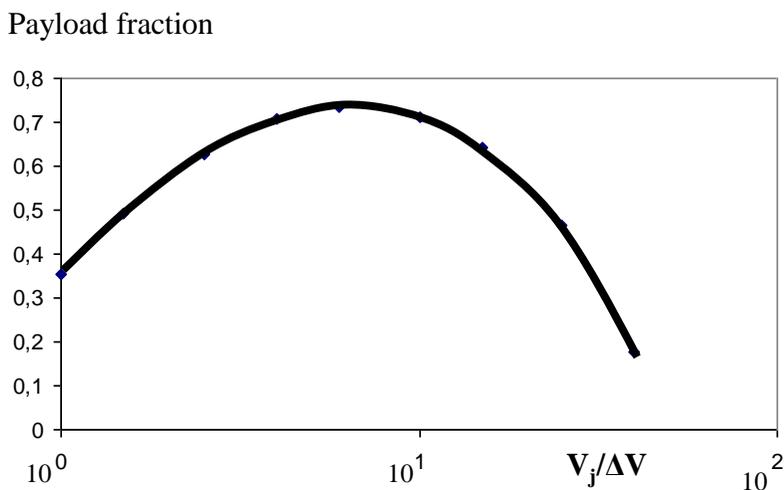
Payload fraction

Fig. 23.6 Earth-Mars mission payload fraction

The conditions for maximum payload ratio can be obtained by differentiating Eq. (23.29) with respect to v and putting the result to zero. This will lead to the following relation:

$$\eta\tau = 2v^3(e^{1/v}-1)-v^2 \qquad\qquad (23.30)$$

This relation is shown in Figure 23.7. Note that this line approaches $\eta\tau=2v^2$ with increasing values of "v", that is $t=V_j^2/\eta\alpha$. The operating time of an electrical propulsion system is therefore approximately equal to the square of the jet velocity divided by the specific power and the efficiency. Thus with a high jet velocity, the operating time must also be high.
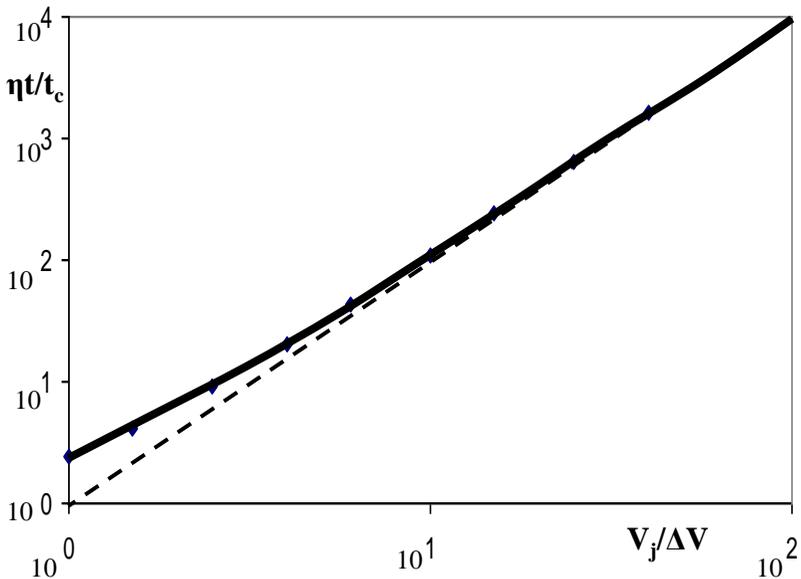
Fig. 23.7 Optimum non-dimensional time of operation

The final mass will be:

$$m_f = m_0 e^{-1/v} \qquad\qquad (23.31)$$

and the mass of the thrust-producing system:

$$m_t = m_f - m_{pl} \qquad (23.32)$$

The total power then follows from Eq. (23.26).

Now, the propellant mass is:

$$m_p = m_0 - m_f \qquad (23.33)$$

The thrust is:

$$F = \dot{m}V_j = \frac{m_0}{t}\left(1 - e^{-\Delta V/V_j}\right)V_j \qquad (23.34)$$

Using the approximation that $t = V_j^2/\eta\alpha$, the terminal acceleration is then simply:

$$a_f = \eta\alpha/V_j \qquad (23.35)$$

Thus the acceleration is very small and not more than about two or three times 10^{-4} g.
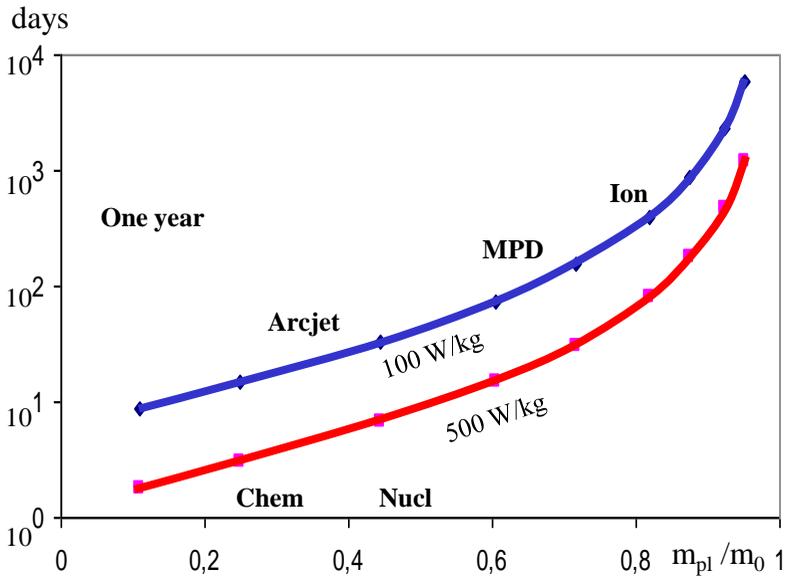
Fig. 23.8 Operating time with optimum payload

Eqs. (23.29) and (23.30) can be used to calculate how the payload depends on the jet velocity and the operating time for an electrical system. Figure 23.8 compares the performance of chemical, nuclear and electric propulsion for the Mars orbit transfer mission for one moderate and one relatively high specific power density. It is seen that electric propulsion enables large payload masses but at propulsion operating times measured in months rather than minutes as with chemical and nuclear propulsion.

In summary, electric propulsion provides much lower thrust levels than chemical and nuclear propulsion, but at much higher jet velocities. This means that they must work for a longer period to produce a desired change in trajectory or velocity. However, the higher jet velocity enables them to carry out a mission with relatively little propellant and, in the case of a deep-space probe, to build up a high final velocity.

Low thrust systems follow interplanetary orbits that look nearly the same as the coasting paths of high-thrust vehicles. The primary drawback is the additional time needed to spiral out from Earth orbit, which may take as long as the transfer from the escape point to Mars. Because of the lower gravity of Mars, the spiralling in to Mars takes about 1/3 the time of spiralling out from Earth. However, the comparative total trip times required for chemical and electric propulsion are extremely mission-specific. As the mission delta-V increases, electric propulsion trip times may become shorter than those for chemical propulsion despite the long acceleration period.

24. THE FUTURE OF PROPULSION

For the nearest future, the priority will be to maximize the efficiency of flight operations in order to meet the demands of a sustainable and lean society. However, speed will continue to be the main motivation for flight and spaceplanes at Mach 15 and higher may be demonstrated in the 2030-2050 period. Key propulsion technologies would be pulse detonation engines or light weight turboramjets combined with scramjets and rockets. Magnetohydrodynamics could increase the efficiency of very high speed engines and "phantom" aircraft bodies could reduce air drag. Hydrogen will gradually be introduced as a fuel. Light weight electric power supplies will make the electric rocket very interesting for flight in the solar system. Radio waves and magnetic fields may become key technologies further into the future.

There is a growing public concern about emissions and their effect on the global atmosphere. Aviation provides only a few percent of the emissions and over the past 20 years, aircraft fuel consumption per flight has been reduced by 30-40%. However, new reductions are harder and harder to achieve. Therefore, with the current growth of air transportation, the amount of fuel burnt and the emissions of green-house gases such as CO_2 and water will increase.

The strongest force shaping the present world is the demand for **efficiency**, largely driven by economy but increasingly also by environmental issues. Products will have to be designed to optimize the total environmental impact of the products over their

life cycle. New and efficient designs will have to be found to conserve scarce resources such as fuel.

As we enter the "Information Age," the power of computer simulation and the integration of existing computer-based modelling technologies will allow complementary, and conflicting, needs to be considered together. For example how a new aircraft would fit new airports, how new aircraft capabilities would match new operating procedures and deliver environmental improvements, how congestion could be relieved by new aircraft capabilities that work in a new air traffic control regime etc. In this way, it will point the way to more efficient and optimized systems.

A lot of new technologies will have to be developed to assure the functionality of the product throughout the life cycle. Better **health monitoring**, more efficient servicing, and improved performance can also reduce operating costs and increase safety.

What is needed specifically for aircraft engines is to merge a condition monitoring system and a dynamic predictive model performing damage assessments in real time with a product data base into a diagnostic system which may interact with an electronic technical manual containing maintenance planning, tracking and scheduling. A further step into the future would be adding the interactive control of adaptive components to obtain a truly cost optimized operation of the product. It is easily seen that most of this is centered especially on sensors and information technologies.

Information technologies may have large influence in order to optimize the performance of engines especially at varying conditions. Some examples of such technologies are given below:

- Smart sensors, distributed controls, optical FADEC.
- Active control of blade clearances.
- Individual inlet guide vane distortion control
- Smart structures air seals and recamberable fan blades.
- Real time corrective damping of stall, vibrations and combustor oscillations.
- Self-balancing magnetic bearings
- Inlet object detection and nozzle erosion monitoring
- Artificial intelligence diagnostic systems
- Real time calculation of component life usage
- Adjusting combustor pattern to the monitoring of turbine stress and temperatures

All electric engines could be lighter through the elimination of gear boxes, hydraulics and oil systems. Adaptive components would increase efficiency. Operating costs could decrease through active condition monitoring and control. Intelligent controls could be used to predict and diagnose component failures, optimize engine performance in flight and allow more efficient maintanence and overhaul planning.

The engines of the future will have very high pressure ratios and therefore small flowpath sizes leading to increased losses. To counteract this, optical sensors could measure the gap between the blade and the casing and actively adjust the casing diameter. This would improve turbine efficiency significantly.

Individual inlet guide vane control based on local pressure measurement could dynamically adjust the compressor distortion tolerance and increase the stall margin.

Smart structures would involve layers of piezoelectric or electrostrictive materials dispersed within a structure supplying distributed forces. Smart structures could also be used for active damping of vibrations and to alleviate stall. Combined with optical sensors, the stabilization of combustion oscillations could allow the combustor to operate at otherwise unstable fuel to air ratios. Active and predictive systems to control engine surge could reduce life-cycle cost, increase mission flexibility and relieve pilot workload.

Electromagnetic bearings would remove the need for oil systems. It would be possible to compensate out of balance forces with electric fields applied to the bearings.

Smart distributed controls that could think for themselves would allow continuous optimization of the engine variables in response to engine degradation as well as real time calculation of component life usage.

Artificial intelligence diagnostic systems are considered a significant future enhancement to the jet engine support and maintenance. The control system could be designed to give maintenance personnell access to expert data bases and information on tools and assembly details.

Lean burning is a way to reduce emissions but needs active burning control to ensure that blow-outs do not occur.

Development of a finely adjustable burner could adjust the combustor pattern so as to obtain the optimum conditions.

Efficiency and safety and the gradual refinement of existing technologies will be the priorities for the near future. Still, the major prerogative of flight is to provide for **higher speed**, that is shorter travelling times over wider ranges. Any person who has spent twenty hours on a flight to Australia may be forgiven for wanting more speed.

However, there is a limit to flight speeds over the earth. Assume that the flight consists of an accelleration to a certain velocity, a cruise at that velocity and a deceleration of the same size as the acceleration. The time to fly a certain distance "s" if the acceleration and deceleration is "a" and the end speed "V" would then be:

$$t = 2\frac{V}{a} + \frac{s - 2\frac{V^2}{2a}}{V} = \frac{V}{a} + \frac{s}{V} \tag{24.1}$$

Obviously, to shrink the flight time, we should use the highest possible acceleration. However, there is a maximum value for the passengers' comfort. For this maximum acceleration, differentiating with respect to "V" gives the end velocity, which makes the flight time a minimum:

$$V = \sqrt{a_{max}s} \tag{24.2}$$

The minimum flight time then becomes:

$$t_{min} = 2\sqrt{\frac{s}{a_{max}}} \qquad\qquad (24.3)$$

This means that there is no cruise phase i.e. the flight consists of an accelleration to "V" followed by a deceleration to zero velocity. This is the so called bang-bang principle that one follows intuitively when moving between obstacles as fast as possible.

Now, the distance could be so large that "V" reaches the circular speed. If we continue the acceleration beyond this point we will enter into an elliptical orbit that leaves the atmosphere. This should be avoided because we would then have to circle the earth before coming back for a descent. Furthermore, air breathing engines will not function outside of the atmosphere.

We should therefore restrict the velocity to below the circular one at about V_c=7900 m/s. The minimum flight time is then:

$$t_{min} = \frac{V_c}{a_{max}} + \frac{s}{V_c} \qquad\qquad (24.4)$$

Assuming a maximum acceleration level of half a "g", a flight from Europe to Australia would then take about 70 minutes.

This is the shortest time we can ever hope for and it requires hypersonic speeds. Such speeds will also be required for cheap and frequent travels to space.

When can we expect to make such travels? Using the logistic technique based on historical data, see Figure 24.1, it seems probable that propulsion systems for flight at about Mach 15 and

higher could be demonstrated in the 2030-2050 period. At this time the first aerospace planes will emerge based on mixed airbreathing and rocket propulsion. Pure air breathing aerospace planes could not be expected until in the 22nd century.
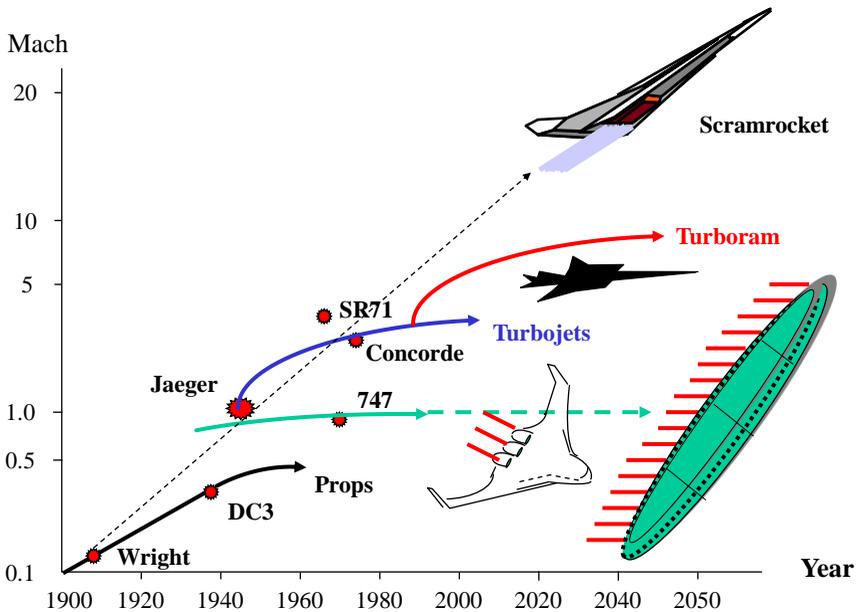

Fig. 24.1 The future of airbreathing propulsion

Key propulsion technologies for spaceplanes will be **Pulse Detonation Engines** or light weight **turboramjets** combined with **scramjets** and **rockets**. To compete with the PDE, the turbojet needs to come down in size and weight. Fortunately, during the

next few decades, a revolutionary jump is expected in the thrust-to-weight ratio of the jet engines thanks to the introduction of new materials and new designs. Fiber reinforcements applied to ring rotors, blades and static structures will eliminate the need for heavy rotating disks. Weight reductions will also result from reducing the number of compressor and turbine stages and compacting the combustor and exhaust nozzle. Advancements in high through-flow technology combined with swept airfoil aerodynamics and improved computational design codes will produce very compact compression systems.

Further on, radically new engine concepts may emerge, which are more efficient than those based on the PDE or the turbojet. We may get some clues to such systems from the physical principles involved. Presently, there is only one method to obtain sufficient thrust for flight and that is through the reaction force of a jet. To obtain a jet one needs a flux of matter and to accelerate the jet one must supply energy continuously to it and transform that energy into kinetic energy of the gas molecules. One therefore also needs a flux of energy or power. Matter and power are the two prime necessities to achieve thrust.

The most efficient way to get the matter needed for the jet is obviously to take it from the surrounding air instead of transporting it on the vehicle. The spaceplanes of the future will therefore rely on air breathing engines.

Each transformation of energy on the way to the jet involves losses and this costs weight. Therefore, the power source should be as close to the jet as possible. The closest the energy source could get to the jet is obviously to use the jet itself as a source of energy. Reactions involving the jet, chemical or other, is therefore to be

preferred because it leads to the lowest weight for a given amount of power.

Alternative ways to transport the power to a jet, by electrical or magnetic fields, mechanically as with the propeller, by heat transfer as in a nuclear engine or by microwaves are all heavier than the chemical reaction of a fuel with the jet. It is probable, therefore, that future engines will continue to rely on that principle.

As an example, the best chemical rocket engines we have today give about 10 MW of jet power for each kg of engine while a nuclear rocket engine, where the propellant is heated externally, is expected to give only 0.5 MW/kg.

What could then be achieved using airbreathing chemical reaction engines? As we have seen above, the specific impulse is the most important measure of the performance of space flight systems. A high specific impulse means a lower propellant consumption and lighter and simpler vehicles.

Taking the kinetic energy of the propellants into account, the specific impulse can be written:

$$I_s = \frac{F}{\dot{m}_p} = \eta_e(\frac{h}{V}+\frac{V}{2}) \qquad (24.5)$$

The relation between the theoretically ultimate propulsion system (engine thrust power efficiency $\eta_e=1$) and the best systems we know today (PDE or turboramjet, scramjet, rocket) is shown in Figure 24.2 with hydrogen as the fuel.
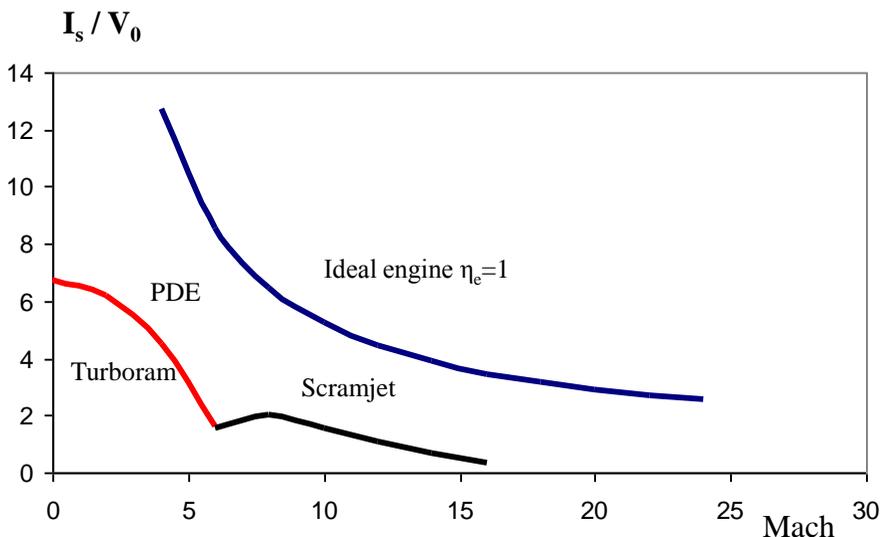
Fig. 24.2 Limits to airbreathing propulsion

The degree of closeness to the ultimate machine is a measure of the total efficiency of the engines so it seems that we are still far from the ultimate limit. This makes it probable that new types of engines could be invented especially at lower speed.

With Eq. (22.15), the maximum cut-off weight that could be lifted into orbit is:

$$\frac{m_c}{m_0} = \exp(-\int_0^{V_0} \frac{V dV}{\eta_e \eta_f (h + V^2/2)}) \qquad (24.6)$$

The cut-off weight includes payload and dry weight of the vehicle. Assuming constant efficiencies, the maximum possible cut-off weight ratio is then:

$$\left(\frac{m_c}{m_0}\right)_{max} = \frac{1}{(1 + V_0^2/2h)^{1/\eta_e \eta_f}} \qquad (24.7)$$

The higher the efficiency and the higher the heating value of the propellant, the higher is the cut-off weight ratio. Obviously, the ideal propulsion system is the one where there are no losses whatsoever so that $\eta_e = \eta_f = 1$. For a satellite orbit with the velocity $V_0 = 7900$ m/s and hydrogen fuel at $h = 120$ MJ/kg the maximum cut-off weight ratio is 0.79, which is higher than commercial airplanes of today at around 0.5. Thus, there is at least a theoretical possibility that spaceplanes may evolve to become as comfortable as todays aircraft if sufficiently efficient propulsion systems can be found. The systems we have today can at best achieve a cut-off ratio around 0.1 in satellite orbit.

The propulsive efficiency is highest if the jet speed is close to the flight speed. In order to maximize the propulsive efficiency throughout the flight, the jet speed will therefore have to be adapted to the flight speed. At low Mach numbers, the low jet speed must be compensated for by a high mass flow. This means that the new engines must be variable geometry machines. Of

course, 100 % propulsive efficiency can never be reached. The thrust would then vanish because it is proportional to the difference between the jet speed and the flight speed.

New concepts such as **magnetohydrodynamics** could perhaps be used to increase the efficiency of very high speed engines. At such speeds, the compression temperature in the inlet would be so high that the air becomes a plasma. Magnetohydrodynamics could be employed to produce electricity from this plasma, thus cooling down the air so that burning could take place. The electricity could then be resupplied at the end of the engine to produce a more energetic jet, see Figure 24.3.
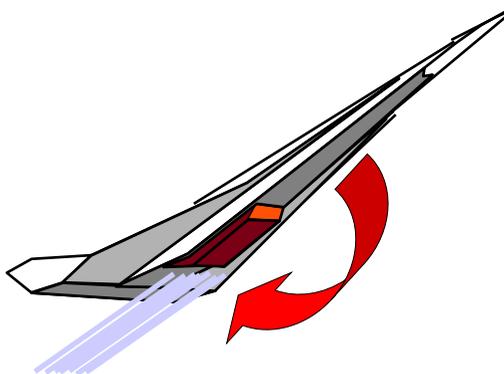
Fig. 24.3 Magnetohydrodynamic airbreathing vehicle

To increase the transported mass, one would also like to increase the flight efficiency in Eq. (24.7). Reducing the drag of the aircraft will directly lead to a higher flight efficiency. The **laminar flow** technologies now being developed are part of this work. Recently, there has also been a great deal of interest in the possibility of using an ionized gas (a **plasma**) to reduce drag. Russian researchers have shown that the drag of a supersonic aircraft could be reduced by 30% or more by forming a plasma in the air stream before the aircraft by a microwave beam.

Ionized boundary layer

Phantom body

Virtual nose
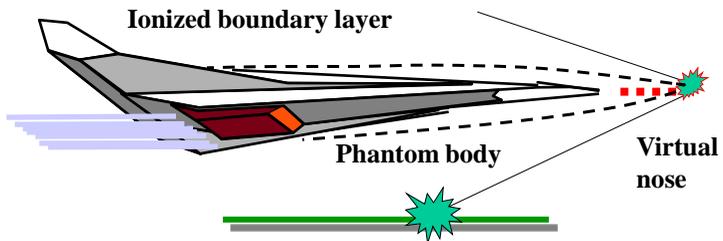
Fig. 24.4 Drag reduction through electricity

There are even indications that plasmas might influence airflow at subsonic speeds. If that is the case, tiny plasma generators could replace control surfaces such as ailerons and flaps. Aircraft of the future might not need any moving control surfaces at all. Plasma could also provide a invisibility shield for stealth aircraft.

In the 1960s and 70s, aerospace engineers experimented with forward-facing jets as a way to slow planetary probes as they entered the atmosphere. To their surprise, they found that the jets actually produced thrust in the direction of flight. The jets were heating the air and deflecting the flow away from the vehicle, effectively giving it a more streamlined shape.

In this way one could create a "**phantom**" aircraft body with reduced air drag by the employment of force or heat fields. This new phantom body must be in conformance with the area rule as described in Chapter 8. The heat and force fields must therefore be distributed very carefully and must extend well ahead and behind the aircraft to insure a properly shaped phantom body.

Without any losses, the power required to create the "phantom" body is the drag reduction multiplied by the flight velocity. This power is a significant part of the propulsive power supplied by the engine. Not only must methods be found to deliver such large quantities of power to the flow field around the aircraft but means must also be found to extract power from the air in a controlled manner to maintain a properly shaped "phantom" body. Irregularities and gradients in the local power distribution makes this very difficult. Moreover, it must be possible to change the shape of the phantom body as the flight velocity changes.

A summary of the possibilities to use magnetohydrodynamics for flight purposes is given in Figure 24.5.
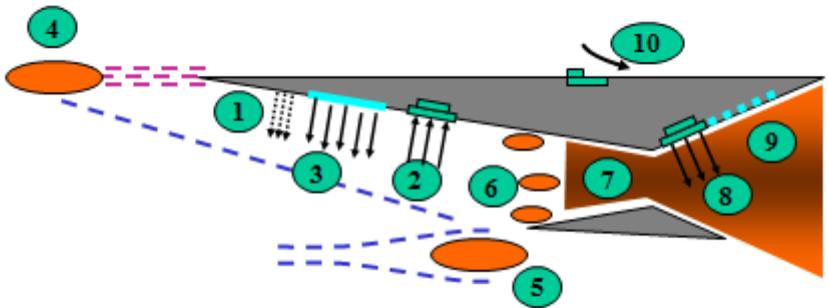
Fig. 24.5 Magnetohydrodynamic airbreathing vehicle

1. At M>12 the flow is seeded with an alkali metal such as cesium and thermally ionized. For M<12 artificial ionization is required. The cost for ionization determines design and performance.
2. MHD power is extracted from the flow. addition/extraction

3. MHD power is used for ion or electronic beam injection for inlet shock flow control.

4. Laser or ion beams are used for energy addition for drag reduction, steering and shock flow control.

5. Dito virtual cowl for air capture increase.

6. Dito flow preconditioning at Mach 4-6 (ram/scram transition)
7. Plasma/MHD enhanced mixing, flame spreading, and ignition control.
8. MHD power addition to the flow after the combustor to produce a more energetic jet.
9. Thrust vectoring.
10. Aircraft drag reduction using plasma actuator to control the boundary layer.

Distributing the thrust over the surface of the aircraft thereby making use of the so called **Coanda effect** is another possibility to decrease the drag of aircraft. In 1910 a young Romanian engineer, named **Henri Coanda,** tested a plane he had built powered by the worlds first jet engine of which he was the inventor. The engine was not a turbojet based on the gas turbine as later invented by Frank Whittle and Von Ohain, but had a gasoline engine driven centrifugal compressor, a combustion chamber and a nozzle.

Coanda placed metal plates between the hot jet gases and the plywood fuselage in order to protect it from the heat. However, instead of the jet being deflected away it attached onto the plates, ran along them and set his plane afire. For a long time this phenomenon of the burning gases and flames attaching to the fuselage remained a great mystery. After studies which lasted more than 20 years, (carried out by Coanda and other scientists) it was recognized as a new aeronautical effect and was named after him.

The Coanda effect is the tendency of a jet of fluid to attach itself to a surface. The velocity of the jet immediately evacuates the molecules between it and the wall. This low pressure region cannot be relieved by ambient inflow as ambient air is on the other side of

the jet and so the jet quickly deflects toward and runs along the wall. The lower pressure along the wall means that the pressure drag of the aircraft decreases. Also, the average pressure across a Coanda jet is lower than the average pressure across an unbounded jet. This means that the average velocity at any point in the Coanda jet is higher than in a conventional jet. Therefore, it should be possible to use this effect to increase the thrust of a jet.

The **Bielefeld-Brown effect** is an electromagnetic force exerted on a capacitor when it is charged with electricity. Although all capacitors experience some type of internal force when charged with a high-voltage, **Thomas Townsend Brown** discovered in the 1950's that a capacitor utilizing capacitive plates of different geometric sizes could accelerate the surrounding air when charged. This **ion-wind** technology has been demonstrated to require large amounts of power and provide relatively little thrust but by applying a high-voltage at the surface of a vehicle, it could be possible to create an electromagnetic Coanda effect.

Whatever the thermodynamics of the future engine, the heat content of the fuel is seen from Eq. (24.7) to be very important for increasing the dry weight fraction. **Hydrogen** is the most energetic fuel we know of today and seen over several centuries, the world seems indeed to be moving slowly and inevitably towards it**,** see Figure 24.6.

The hydrogen content in the fuels we have used has consistently increased from wood over coal, oil and gas. The problem for flight applications is the low density of hydrogen. However, significant density increases are possible with gelled hydrogen. A 10% density increase is possible with 10% added ethane or methane. These gellants are introduced into the hydrogen as frozen particles.

Also, metallic hydrogen has been produced in small quantities at extreme pressures and may very well be the ultimate fuel in the long term.
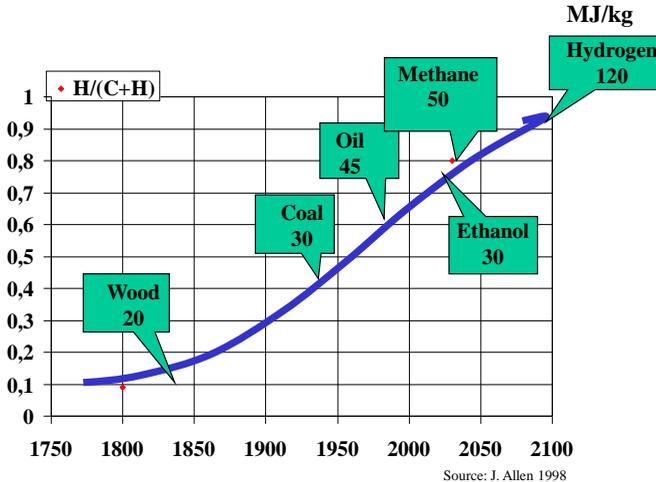
Fig. 24.6 Hydrogen in our future

There is therefore much that speaks for hydrogen as a future fuel. In the long run this may favour **fuel cells** over gas turbines but less so for aviation than for energy production. Fuel cells have now reached a power density of about 2 MW/m3. Assuming that the required compressor power is about 2 MW/ton thrust, the engine volume for a large aircraft with 100 ton of thrust would be prohibitively high. This may change in the future because fuel cells are developing very rapidly. Still it is probable that combustion directly in the jet fluid will remain more weight efficient than any other known process such as large fans powered by fuel cells.

Hydrogen has a heat content of 120 MJ/kg. To increase the heat content beyond that value, new chemical compounds must be developed with high energy density and low molecular weight. If certain molecules are torn apart, they will give up large amounts of energy upon recombining. It has been proposed that such unstable fragments, called free radicals, could be used as a fuel. The difficulty is, however, that these species tend to recombine as soon as they are formed. Hence, a central problem in their use is development of a method of stabilization. Atomic hydrogen is the most promising of these substances. Spin-polarized **atomic hydrogen** has been produced in laboratories, but its lifetime decreases drastically with density due to an increase in recombination collisions.

The most exotic of all fuels would be **antimatter,** which can be thought of as the mirror image of normal matter. An antiparticle has identical mass as normal matter but opposite charge and spin. Upon annihilation with matter, antimatter offers the highest energy density of any material currently found on Earth. When a particle and an antiparticle come in close contact, they annihilate each other through a series of interactions and their rest mass is converted entirely into energy. Approximately 42 milligrams of antiprotons (about 0.6 cubic centimeters in the form of antihydrogen) have an energy content equal to the 750 tons of fuel and oxidizer stored in the Space Shuttle External Tank. Small amounts of antimatter could also be used for initiating and maintaining fission or fusion reactions in rockets.

As for flights in the solar system, past spacecraft development has focused on propellants, which are expelled by the energy generated on board the vessel as in electric rockets. The primary consideration in obtaining useful thrust from such ion or plasma

rockets is the construction of **light weight electric power supplies**.

However, some proposed spacecraft designs would use energy that is not carried on board. This energy would be transmitted to the spacecraft in the form of a radio frequency or laser beam, thus greatly reducing the mass of the spacecraft. Solar power satellites can be built to convert solar radiation into electrical power, which is then converted to **microwaves,** which are captured by a receiver on the electrically propelled spaceship.

A number of schemes have been proposed to employ radiation from the Sun to obtain propulsive power for a space ship. Solar propulsion schemes fall into two categories. In one, the radiation pressure of solar rays would be used to supply thrust on a large, lightweight surface attached to the space ship. This device has been called a **solar sail**. The other approach is to use the solar rays to heat a hydrogen gas, which is then expelled through a nozzle to produce thrust. In both of these approaches the weight of mechanism relative to the thrust obtained is likely to be so large as to severely limit the usefulness of solar propulsion.

Most planets in the Solar System have magnetic fields that extend into space like a giant bubble. For example, the Earth lies at the heart of such a magnetic bubble, which occupies a volume at least a thousand times greater than the planet itself. This magnetosphere protects life on Earth from the Solar wind and from potentially deadly solar flares, unlike Mars and the Moon which lack their own magnetospheres.

In addition to providing shielding from Solar radiation, a **magnetosphere** can work like a space sail because the Solar wind

pushes on it constantly. A 15 km-wide miniature magnetosphere around a spacecraft at the Earth's distance from the Sun would feel enough Solar pressure (1 to 3 Newtons of force) to accelerate a 200 kg spacecraft to 80 km/s in only three months.

The force exerted on a magnetosphere increases with its size, as the Solar wind has more to push against. Magnetospheres that move further away from the Sun naturally expand as the Solar wind pressure decreases, for the same reason that a balloon inflated at sea level will expand in the less dense air of higher altitudes. However, the solar wind pressure declines by the same factor that the cross section of magnetospheres increases. Hence, the propulsive thrust would remain the same whether the spacecraft is near the Sun or in the outer reaches of the Solar System.

For rapid movements in space more thrust are needed than what can be provided by electrical or external propulsion. The **nuclear salt water rocket** is a radically new concept for propulsion in space. The fuel would be a solution of uranium salt in water. This fuel would be injected into the reaction chamber to create a critical mass. It is basically a continuously detonating nuclear reaction with water as propellant. The advantage is that this is the only known propulsion system that combines high exhaust velocity with high thrust. It has an estimated exhaust velocity of 60000 meters per second (as compared with perhaps 4500 m/s for a chemical rocket). It is estimated to produce a thrust of almost 1000 tons and to have a power output of 400 gigawatts.The disadvantage is of course that it expells highly radioactive nuclear fission products directly into space.

Variable specific impulse magnetoplasma rockets or **VASIMRs** is another hypothetical form of spacecraft propulsion that uses radio waves and magnetic fields to accelerate a propellant. VASIMRs bridge the gap between high-thrust low-specific impulse propulsion systems and low-thrust high-specific impulse systems, being capable of functioning in either mode simply by adjusting its parameters of operation.

The propellant, usually hydrogen, is first ionized by radio waves and then guided into a central chamber surrounded by magnetic fields. The ions spiral around the magnetic field lines with a certain natural frequency and by bombarding them with radio waves they are heated to ten million K. A magnetic nozzle converts the spiralling motion into axial motion, driving the hydrogen ions out the back of the rocket and producing thrust.

The radio waves and magnetic fields could be produced by electricity, which would almost certainly be produced by nuclear fission. By adjusting the manner of heating and a magnetic choke, a VASIMR can control the exhaust rate. Closing the choke shifts the rocket into high gear. It reduces the number of ions exiting the drive (thus producing less thrust), but keeps their temperature high (thus increasing specific impulse). Opening the choke has the reverse effect. A spacecraft would use low gear to climb out of planetary orbit, and high gear for interplanetary cruise.

The method of heating plasma used in a VASIMR was originally developed as a result of research into nuclear fusion. One possible future enhancement of the VASIMR system may be to promote fusion among the atoms of the propellant. This could provide a great deal of extra heating, and therefore provide even greater thrust than the electrical input into the system would otherwise

allow. A VASIMR-powered spacecraft could be launched with only enough fuel to get to its destination, such as Mars, and then pick up more hydrogen upon arrival to serve as fuel for the return trip home. Another benefit of hydrogen fuel is that hydrogen is the best known radiation shield, so the fuel for the VASIMR engine could also be used to protect the crew from the harmful effects of radiation exposure during the flight.

Nuclear fusion is cleaner than fission and it is a more exciting prospect with its higher energy density and specific impulse. However, scientists are still struggling to prove that such a device can offer more energy output than input, let alone making the device small enough to be sent into deep space. There are two principle schemes for providing the confinement necessary to contain a fusion reaction, **inertial** and **magnetic**. These confinement schemes result in two very different propulsion system designs.

Because of the difficulty of "igniting" fusion reactions, several schemes have been proposed to simplify or reduce the energy requirements of the fusion ignition process. One scheme uses **muons.** The muon is a sort of heavy electron, that can replace the electron in a hydrogen atom (or molecule). The resulting "atoms" are able to approach each other more closely. This in turn increases the probability of fusion. An alternative ignition method uses a small amount of **antimatter** (anti-protons) to trigger a sub-critical fission reaction. The fission energy then ignites the fusion fuels.

Studies suggest that the primary benefit of fusion propulsion is the potential for fast piloted missions to a wide variety of planetary targets (e.g., Mars, Jupiter, Saturn). A fusion powered spacecraft

could accomplish a 60- to 100-day round-trip Mars mission carrying 100 metric tons of payload. Piloted 5-year round-trip missions to Jupiter and Saturn also appear to be feasible.

Due to the large velocity capability and moderately high thrust levels which may be available from fusion powered spacecraft, they are not as affected by launch windows as existing systems. In addition, missions such as transporting large bulk cargo payloads, moving asteroids etc could become feasible with advanced fusion propulsion systems.
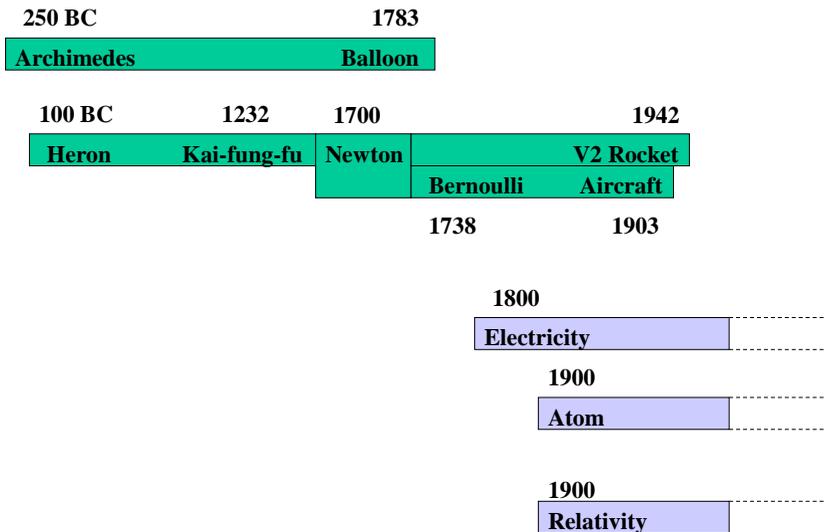
Fig. 24.7 Sometimes it takes a long time

Far into the future, as yet unheard of schemes for propulsion may appear. It took about two thousand years from the first discoveries before Archimedes principle and the reaction principle were applied to practical propulsion concepts. Among the more recent scientific discoveries, electricity, which was born in the 1800's will probably be of great importance in the future, for instance for manipulating ionized gases within engines and around aircraft. Atomic energy as fission or fusion may produce the large amount of power required for interplanetary flight.

The understanding of gravity is still rudimentary despite the work of Newton and Einstein. In an aeroplane, lift is obtained by deforming the aerodynamic flow field with a wing. In a balloon, lift is achieved by the bouyancy effect. Some day, it might be possible to do something like that with the gravitational or magnetic fields but as of today we do not understand how this could be done.

No prospects are now apparent for propulsion based on **antigravity**, because the negation or reversal of the gravitational attraction of matter would violate basic physical laws as presently understood. Awaiting the discovery of a new class of physical phenomena, the notion of antigravity remains in a state similar to that of the perpetual motion machine.

A **space drive** can be defined as an idealized form of propulsion where the fundamental properties of matter and spacetime are used to create propulsive forces anywhere in space without having to carry and expel a reaction mass. Such an achievement would revolutionize space travel as it would circumvent the need for propellant.

Different hypothetical space drives have been analyzed to identify the specific problems that have to be solved to make such schemes plausible. They include the possibility of creating a local gradient in a background scalar property of space (such as gravitational potential) by the juxtaposition of diametrically opposed field sources across the vehicle.

Although Einstein's theory of special relativity forbids objects to move faster than light within spacetime, it is known that spacetime itself can be warped and distorted although it takes an enormous amount of matter or energy. As an analogy, even if there were a speed limit to how fast a pencil could move across a piece of paper, the motion or changes to the paper is a separate issue. In the case of the **wormhole**, a shortcut is made by warping space (folding the paper) to connect two points that used to be separated.

It is also unknown how fast spacetime itself can move. The **warp drive** is like one of those moving sidewalks in an airport. Although there may be a limit to how fast one can walk across the floor (analogous to the light speed limit), you may find yourself on a moving section of floor that moves faster than you can walk (analogous to a moving section of spacetime). In the case of the warp drive, this moving section of spacetime is created by expanding spacetime behind the vehicle (analogous to where the sidewalk emerges from underneath the floor), and by contracting spacetime in front of it (analogous to where the sidewalk goes back into the floor).

In summary, the history of propulsion is a history of power density. The engines propelling aircraft and rockets are the most powerful of all machines produced by mankind. It took us many hundred years to build the Wright Flyer, which at 25 W/kg vehicle

mass, gave us about the same performance as a bird but still much less than the insects. Since then we have reached to a level of about 20000 W/kg in liquid rockets like the Ariane. The systems of the future will require still higher power densities.

25. ANSWERS TO THE EXERCISES

Answer 3.1

A typical bumblebee has a weight of 175 mg, a wing length of 13 mm, a wing area of 50mm^2 and a wing beat angle of 114° with a frequency of 150 periods/s. The air density on a standard day is 1.225 kg/m^3 . Calculate the lift coefficient it requires.

From Eq. (3.11), the **lift coefficient** is:

$$C_L = \frac{4}{\Phi \sin \Phi / 2} \frac{mg}{\rho \omega^2 b^2 S}$$

The bumblebee requires a lift coefficient of $C_L = 5.7$ compared to the theoretical maximum of $C_L = 2$ for steady flow.

Answer 5.1
What would be the power density of a gull flying at twice the minimum drag speed if the wing span is one meter and the weight 0.4 kg? The lift-to-drag ratio of a gull is (L/D=10). Air density is 1.225 kg/m3 and the Oswald factor e=0.85.

From Eq. (4.13):

$$\frac{\dot{W}}{m} = \frac{\dot{W}_{d0}}{2m}\left(v^3 + \frac{1}{v}\right)$$

Where from Eq. (4.14):

$$\frac{\dot{W}_{d0}}{m} = 2g\sqrt{\frac{mg}{\pi e \rho \lambda b^2}}$$

The lift-to-drag ratio of a gull is $\lambda = (L/D) = 10$ from Fig. From Eqs. Air density is 1.225 kg/m3 and the Oswald factor e=0.85. The specific power becomes 29 W/kg.

Answer 5.2

What would be the wing span of a man weighing 100 kg flying at minimum power assuming that he can reach the lift-to-drag ratio of a gull (L/D=10) and has a specific power of 3 W/kg. Air density is 1.225 kg/m3 and the Oswald factor e=0.85. What would be the flight speed?

The wing span required can be obtained from Eq. (5.10) as:

$$b = \frac{4g}{3^{3/4}\left(\dot{W}_{min}/m\right)}\sqrt{\frac{mg}{\pi e \rho \lambda}}$$

where λ=L/D is the maximum lift to drag ratio. This gives a wing span of 62 m.

From Eqs. (4.14), (4.15) and (4.16) the speed at minimum power is 2.6 m/s or 9.5 km/h from:

$$V_{p0} = \frac{\sqrt{3}}{2}\frac{\lambda}{g}\frac{\dot{W}_{min}}{m}$$

Answer 5.3

The Mars atmosphere is mostly CO2 and is at about 1/100 the density of the Earth. The gravity is 0.38 times that of Earth. What would be the wing span of a Mars flyer compared to one on Earth?

From the equation for the wing span, the wing span will be 2.3 times larger.

Answer 6.1

Accelerating an airplane to take-off speed is risky. To keep the speed down, the lift coefficient should be high which can be achieved with a high angle of attack. On the other hand there is an angle beyond which the aircraft stalls. The Wright Flyer weighed 340 kg with the pilot. Its wing span was 12 m and the wing area was 46 m2. What would be the take-off speed required to avoid stall?

To avoid stall, the lift coefficient should be below 1.6.The air density is assumed to be 1.225 kg/m3. From Eq. (6.11) the take-off speed is:

$$V_{to} = 1.2 \sqrt{\frac{2mg}{\rho S C_{L\max}}}$$

This gives a take-off speed of 10.3 m/s which is much lower than modern standard.

Answer 6.2

Another indication of the standard of technology is wing loading, which is a measure of the sofistication of the wings. The wing loading of the Wright Flyer was 72 N/m2. What is the wing loading required for a modern aircraft at take-off when the standard take-off speed is 90 m/s?

The modern aircraft would have a wing loading of 5512 N/m2 compared to the Wright Flyer at 72.

Answer 7.1

Tip speed is most important in suppression of noise and for that reason the tip Mach number is limited to below 0.85. What is the limit of the flight Mach number if the advance ratio is to be chosen for maximum performance?

The advance ratio for maximum performance is around $J=3\pi/4$ from Eq. (7.13). From Eq. (7.14) the tip speed will be:

$$V_{tip} = V\sqrt{1+\left(\frac{\pi}{J_{opt}}\right)^2}$$

If the tip Mach number is to be below 0.85 then the flight Mach number is to be below about M=0.51.

Answer 8.1

The stagnation temperature equation, together with the isentropic relation can be used to measure the flight speed of aircraft from the stagnation pressure in a Pitot-tube. Assume that an aircraft is flying at a speed of 700 km/h in air with a temperature of 15 C and a pressure of 101.4 kPa. What is the pressure measured by a Pitot-tube relative to the aircraft if the adiabatic constant is 1.4 and the ideal gas constant 287 J/kg K?

The Mach number at 700 km/h is 0.57 and the stagnation temperature ratio 1.065 from Eq. (8.2):

$$T_{t0}/T_0 = \tau_0 = 1+\frac{\gamma-1}{2}M^2$$

The total pressure becomes 126.5 kPa from Eq.(7.22):

$$T / p^{(\gamma-1)/\gamma} = const$$

Answer 8.2

A jet engine is flying at an altitude of 11 km where the ambient temperature is 216 K. What is the maximum speed if the maximum temperature in the titanium compressor is 875 K and the maximum turbine inlet temperature 1900 K while the maximum combustion temperature is 2300 K?

The maximum Mach number of a jet engine is from Eq.(8.24):

$$M_{max} = \sqrt{\frac{2}{\gamma-1}(\frac{\theta_t}{\tau_c}-1)}$$

Where with Eq.(8.19):

$$\theta_t = \frac{T_{t4}}{T_0}$$

The absolute speed limit of the turbojet is at τ_c=1 that is ramjet mode. The max Mach number is 6.2 due to the turbine and 6.9 due to the combustor.

The limit due to the compressor is given by Eq.(8.26):

$$M_{max} = \sqrt{\frac{2}{\gamma-1}(\theta_{cm}-1)}$$

Where $\theta_{cm}=T_{cm}/T_0$. The max Mach number is then 3.9 due to the compressor.

Answer 9.1

It is common to operate a civil engine at its design point, where it will have the same pressure ratio at all conditions. The material temperature at the compressor outlet must stay below the maximimium permitted, which for titanium is at 875 K, in all conditions. What is the maximum design pressure ratio for an engine operating in cruise at 10 km altitude and Mach 0.85 where ambient temperature is 223 K if at take-off in Sea Level Static standard atmosphere the temperature is 288 K? Is cruise or take-off the most critical for the compressor? The adiabatic constant for air is 1.4

In cruise, from ram pressure the compressor inlet temperature is 255 K while at SLS the compressor inlet temperature is 288 K. It is therefore at SLS we risk an overheating of the compressor and in order to avoid that, the max allowed overall pressure ratio is 49.

Answer 9.2
Compare the nondimensional specific thrust and the efficiency for a straight turbojet and a turbofan with bypass ratio 8 at conditions and overall pressure ratio as in Ex 9.1. The turbine inlet temperature is 1560 K.

the specific thrust of the bypass engine is from Eq.(9.19):

$$F_{spec} = \sqrt{\frac{\theta_t - \theta_t/\tau_0\tau_f\tau_c - \tau_0(\tau_f\tau_c - 1) + \alpha(\tau_0 - 1)}{(1+\alpha)(\gamma - 1)/2}} - M$$

The total **efficiency** is from Eqs. (9.20) and (9.21):

$$\eta = (\gamma - 1)(1 + \alpha)M \frac{F_{spec}}{\theta_t - \tau_0 \tau_f \tau_c}$$

Hence:

BPR	F_{spec}	η	
0	2.8	0.27	Military
8	0.6	0.53	Civil

Answer 9.3
Calculate values on the curves in Fig. 9.2 for the overall pressure ratio of Ex. 9.1 to verify the trend shown. The turbine inlet temperature is 1560 K and the specific heat is 1005 J/kgK.

BPR	0	2	4	6	8
η	0.27	0.39	0.46	0.50	0.53
F_{spec}	2.79	1.36	0.95	0.74	0.60

Answer 9.4

Assume that we want to design an engine for max specific thrust. Calculate the variation of total compression ratio at Mach numbers 0, 1 and 2 to show that an engine requires much less pressure ratio at high speeds. The turbine inlet temperature is 1560K and the ambient temperature is 223 K.

The total compression temperature ratio that maximizes the specific thrust is with Eq. (9.22):

$$\tau_f \tau_c = \frac{\sqrt{\theta_t}}{\tau_0}$$

From Eq. (9.22) and (8.2):

Mach	OPR
0	30
1	16
2	4

Answer 9.5

Calculate the variation of the nondimensional specific thrust and the efficiency with overall pressure ratio for a turbofan with bypass ratio 1 to verify the general behaviour of Fig. 8.3. The turbine inlet temperature 1560 K. Assume Mach 2 conditions with ambient temperature 223 K.

From Eqs. (9.19) to (9.21):

OPR	1	5	10	15	20	25	30
η	0,35	0,49	0,55	0,58	0,61	0,63	0,64
F_{spec}	1,13	1,28	1,21	1,12	1,05	0,97	0,90

Answer 9.6

Calculate the variation of fan pressure ratio with bypass ratio at Mach numbers 1 and 2 to verify the curves in Fig. 9.4. The turbine inlet temperature is 1560K. The overall pressure ratio is designed for max specific thrust at Mach 1, see Ex. 9.4.

The relation between fan pressure ratio and bypass ratio is from Eq. (9.24):

$$\alpha + 1 = \frac{\theta_t - \theta_t / \tau_c - \tau_0 \tau_f (\tau_c - 1)}{\tau_0 (\tau_f - 1)}$$

Mach 1

FPR	2	3	4
BPR	6.4	2.7	1.4

Mach 2

FPR	2	3	4
BPR	2.4	0.7	0.14

Answer 10.1

Subsonic aircraft typically fly at an altitude of 10 km at Mach 0.85. What would be the altitude of a Mach 2 aircraft flying at the same dynamic pressure as the subsonic aircraft?

The flight altitude for a given dynamic pressure is from Eq. (10.7):

$$h = h_0 \ln \gamma \frac{p_0 M^2}{2q}$$

The altitude of a Mach 2 aircraft will be 22.3 km.

Answer 11.1

The fuel fraction would be somewhat lower for a supersonic aircraft because of a heavier structure. Compare the range if the useful fuel fraction is 0.4 for a Mach 0.85 aircraft and 0.35 for a Mach 2 aircraft.

The fuel fraction is from the Brequet equation, Eq. (11.1):

$$f_{cr} = \frac{m_{fcr}}{m_{0cr}} = 1 - \exp(-\frac{gR}{h\eta L / D})$$

From Fig. 11.7, the lift-to-drag ratio of the Mach 1 aircraft is 18 and for the Mach 2 aircraft about 10. From Eq. (11.1), the range of the Mach 2 aircraft is then 47 % of the subsonic aircraft.

Answer 12.1

A jet engine has a maximum allowed turbine inlet temperature of 1700 K. What is the operating temperature at cruise conditions

with M=0.85 at 11 km altitude where the temperature is 216 K if the ambient temperature at take-off is 293 K?

The turbine inlet temperature in the design point is proportional to the total inlet temperature. The total inlet temperature at altitude is 247 K so the turbine inlet temperature in the design point becomes 1434 K.

Answer 12.2

It must be checked that the New Civil Engine designed in Appendix 11 can be used in all climates. What is the maximum ambient air temperature for which the engine can be used without overheating the compressor if its last stages are made from titanium aluminides that can take 1150 K?

For given pressure ratios, the compressor outlet temperature at take-off is directly proportional to the total inlet temperature. The engine was designed to have a compressor outlet temperature of 995 K at the total inlet temperature 255 K. With operation in the design point, the overall temperature ratio would remain constant. The maximum ambient take-off temperature without overheating the compressor would then be 295 K or +22 C, which is but marginally higher than the standard sea level temperature +15 C!

Answer 13.1

The New Civil Engine was designed in Appendix 12 to give a compressor outlet temperature of 995 K at altitude. A deterioration of compressor performance takes place during

the life time of the engine due to erosion, dirt etc. Assume that the polytropic efficiency of the HP compressor falls from 92 to 85 %. What would be the compressor outlet temperature at altitude and at SLS +15 C?

The temperature ratios of the fan and the booster are 1.16 and 1.42. The HP compressor pressure ratio is 16. The temperature at the core compressor outlet i.e. the cooling air temperature increases from 995 to 1067 K due to the decrease in polytropic efficiency and at SLS it rises to 1205 K, which is above the permitted temperature 1150 K. This means that the use of the engine in different temperatures is severely limited.

Answer 13.2

Assume as in Ex 13.1 that for some reason the core compressor efficiency is reduced from 92 to 85%. How does that influence the HP turbine metal temperature. A rule of thumb for materials limited by creep is that a temperature increase of 10 K halves the creep life. What is the metal temperature?

The cooling system was designed to give a max metal temperature of 1500 K for max take-off temperature 2000 K. Design compressor outlet temperature is 995 K at total inlet temperature 255 K so the total design temperature ratio is 3.9. The ambient design take-off temperature is 288 K so the cooling system efficiency is 0.57. In the design case where the coolant temperature is 995 K, the metal temperature is 1340 K. With an eroded compressor the coolant temperature rises to 1067 K from Ex 12.1 and the metal temperature becomes 1381 K that is 41

degrees higher. The creep life will decrease by $2^{4.1}$ that is by 17 times.

Answer 16.1

What is the specific excess power with afterburner (the maximum rate of climb) for the military engine of Appendix 15 at Mach 0.9?

The thrust with afterburner is 76 kN from Appendix 15. The Specific excess power SEP=Vsinγ with the angle iterated from:

$$\gamma = \arcsin(\frac{F}{mg}\cos\varphi - \frac{D_0}{mg} - KC_L(\cos\gamma - \frac{F}{mg}\sin\varphi)^2) \quad (15.8)$$

where without vectored thrust φ=0.

With data and equations from Appendix 14, the SEP is 252 m/s and the climb angle is 72 deg.

Answer 17.1

What is the thrust at take-off with and without afterburner if the pressure is 101 kPa for Sea Level Static (SLS) conditions and the military engine is operating in the design point?

From Appendix 17, the jet speed in the design point is 828 m/s and the total mass flow is 61.2 kg/s so the gross thrust in the design point becomes 50.7 kN. The ambient pressure is 22.7 kPa, the fan inlet pressure 37.2 kPa and the fan pressure ratio 4.5. The nozzle adiabatic constant is 1.35. The ambient pressure at SLS is 101 kPa.

The gross thrust is from Eq. (17.13):

$$F_G \propto p_{t2}\sqrt{\left[1-\left(\frac{p_0}{p_{t2}}\frac{1}{\pi_f}\right)^{(\gamma_m-1)/\gamma_m}\right]}$$

From Eq. (17.13), the gross thrust is 110 kN. However, the nozzle is designed for altitude and expands to 22.7 kPa which is below ambient SLS pressure. There is therefore a back pressure on the nozzle of 78.3 kPa whose area is 0.27 m2 so the net thrust becomes 89 kN. The take-off acceleration is then 1 g.

Answer 19.1

What is the maximum speed of a kerosene and an hydrogen driven ramjet if the stoichiometric temperatures are 2300 and 2700 respectively? The atmospheric temperature is 220 K and γ=1.4.

The max Mach number where the thrust vanishes can be obtained from Eq. (19.3):

$$M_{max} = \sqrt{\frac{2}{\gamma-1}(\frac{T_{ta}}{T_0}-1)}$$

From Eq. (18.3), the max Mach numbers are 6.9 and 7.5.

Answer 19.2
What is the flight Mach number at which the flow into the combustor becomes supersonic so that the ramjet becomes a scramjet. What is this Mach number for the maximum combustor inlet temperature of 1560 K? The atmospheric temperature in the stratosphere may be taken as 220 K and γ=1.4.

The Mach number at which the ramjet becomes a scramjet combustor is from Eq. (19.21):

$$M_0 = \sqrt{\frac{2}{\gamma-1}\left[\left(\frac{\gamma+1}{2}\right)\frac{T_3}{T_0}-1\right]}$$

This Mach number is M=6.1.

Answer 19.3
If the static temperature at the combustor inlet is to be kept constant at 1560 K the Mach number at the inlet will have to increase continually with flight speed. Derive this relation at very high flight speeds. This constitutes a simple "rule of thumb" for the air speed in a scramjet combustor. The atmospheric temperature is 220 K and γ=1.4.

At high speed, from Eq. (19.23), the Mach numbers in the scramjet combustor follows the "rule-of-thumb":

$$\frac{M_3}{M_0} \approx \sqrt{\frac{T_0}{T_3}}$$

T_3=1560 and T_0=220 gives with Eq. (18.23) the result

$$\frac{M_3}{M_0} \approx 0.38$$

Answer 19.4

What will be the fuel/air ratio needed to reach satellite speed (Mach 25) with a scramjet?

The combustion efficiency is 90% and the kinetic efficiency 80%, the heat content for hydrogen 120 MJ/kg and the stoichiometric fuel/air ratio 0.029. The atmospheric temperature is 220 K and the specific heat will increase due to dissociation but an average value may be assumed to be 1500 J/kg K with γ=1.28.

The fuel/air ratio needed to reach a certain maximum Mach number with a scramjet is from Eq. (19.36):

$$f = \frac{1}{\eta_{ke}(1+\dfrac{\eta_b f_s h}{C_p T_{t0}})} - 1$$

The fuel/air ratio becomes 0.13 which is more than four times higher than the stoichiometric value.

Answer 20.1

Assume that a solid rocket motor is of the internal burning tube type with the initial diameter of the burning surface one third of the case diameter. A typical value of the Pressure Exponent is n=0.2. What would be the ratios of chamber pressure (i.e. thrust) at start and end of the burning? What happens if the Pressure Exponent is raised to 0.8? Compare this to the end burning type.

The chamber pressure in a solid propellant rocket engine follows from Eq. (20.3):

$$p_c = const \left(\frac{A_b}{A_t} \right)^{\frac{1}{1-n}}$$

From the relation between pressure and area ratio of Eq. (20.3), the pressure and the thrust is 4 respectively 243 times larger at end of burning than at ignition! With end burning, the pressure and the thrust is constant throughout.

Answer 20.2

The F-1 engines of the Saturn V first stage operated at a combustion chamber pressureof 6500 kPa and a temperature of 3570 K. The propellant was kerosene of $C_{12}H_{26}$ of a molecular weight of 170 and liquid oxygen at a 2.26 mixture ratio and the nozzle was adapted to operate at sea level. Calculate the ideal sea level specific impulse. Assume $\gamma = 1.20$.

Given: O/F = n x 32 / 170 = 2.26 we obtain n = 12 and a chemical reaction.
$C_{12}H_{26} + 12\ O_2 \longrightarrow 12\ CO + 12\ H_2O + H_2$
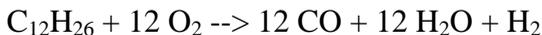
The average molecular weight of exhaust gases is:

$M = (12 \times 28 + 12 \times 18 + 1 \times 2) / (12 + 12 + 1) = 22.2$

The ideal specific impulse of a liquid rocket engine is from Eq. (20.10):

$$I_{s0} = \sqrt{\frac{2\gamma}{\gamma-1} \frac{\Re T_c}{M} \left[1 - \left(\frac{p_0}{p_c} \right)^{\frac{\gamma-1}{\gamma}} \right]}$$

Eq. (20.10) gives Is=2835 m/s.

Answer 20.3

A rocket engine uses liquid hydrogen and liquid oxygen propellants. It operates at a mixture ratio of 6 at a combustion chamber pressure of 10 MPa. Calculate the area of the exhaust nozzle throat if the thrust at sea level is to be 100 tons. The engine is designed for full expansion at sea level. What is the specific impulse at sea level and in vacuum?

From Table 19.1 we get for O/F = 6 and Pc= 10000 kPa a combustion chamber temperature Tc = 3550 $^\circ$ K, the adiabatic constant $\gamma = 1.20$ and the molecular weight M = 13.5.
The nozzle area expansion ratio for a prescribed exhaust pressure p_e is from Eq. (20.17):

$$\varepsilon = \frac{A_e}{A^*} = \frac{\left(\dfrac{2}{\gamma+1}\right)^{\frac{1}{\gamma-1}}\left(\dfrac{p_{tc}}{p_e}\right)^{\frac{1}{\gamma}}}{\sqrt{\dfrac{\gamma+1}{\gamma-1}\left[1-\left(\dfrac{p_e}{p_{tc}}\right)^{\frac{\gamma-1}{\gamma}}\right]}}$$

The expansion ratio becomes 11.9 for full expansion at sea level.

The thrust coefficient at any altitude is from Eq. (20.16):

$$C_F = \sqrt{\frac{2\gamma^2}{\gamma-1}\left(\frac{2}{\gamma+1}\right)^{(\gamma+1)/(\gamma-1)}\left[1-\left(\frac{p_e}{p_{tc}}\right)^{(\gamma-1)/\gamma}\right]} + \varepsilon\frac{p_e - p_0}{p_{tc}}$$

The thrust coefficient 1.64 from Eq. (20.16) gives a throat area of 0.061 m2 from Eq. (20.15), $F = C_F A^* p_{tc}$, and an exhaust area of 0.72 m2. The diameter is 0.96 m.

The real specific impulse for a rocket engine is from Eq. (20.12):

$$I_s = C_F C^*$$

where the characteristic velocity is from Eq. (20.14):

$$C^* = \frac{\sqrt{\gamma \Re T_{tc} / M}}{\gamma \sqrt{\left(\dfrac{2}{\gamma+1}\right)^{(\gamma+1)/(\gamma-1)}}}$$

From Eq. (20.12) and (20.14) the specific impulse at sea level is 3630 m/s and in vacuum 3890 m/s.

Answer 21.1
To what flight speeds would the stoichiometric scramjet with fuel/air ratio f=0.029 be superior to the liquid hydrogen/liquid oxygen rocket engine with a specific impulse of 4500 m/s?
The specific heat will increase due to dissociation but an average value may be assumed to be 1500 J/kg K with γ=1.28. The speed of sound is taken to be 300 m/s. The heating value of hydrogen is 120 MJ/kg and the total kinetic efficiency 0.75 and the combustion efficiency 0.9. The atmospheric temperature is 220 K.

The specific impulse is the specific thrust divided by the fuel/air ratio. From Eq. (19.31), the specific impulse is:

$$\frac{F}{f\dot{m}} = \frac{a_0 M_0}{f}\left[\sqrt{\eta_{ke}\left(1+f\right)\left(1+\frac{fh\eta_b}{C_p T_{t0}}\right)} - 1\right]$$

Introducing the values of the parameters, the scramjet engine will be superior to the rocket (I_S=4500 m/s) up to about Mach 13.

Answer 22.1

Calculate the velocity of an artificial satellite orbiting the earth in a circular orbitclose to the earth if the radius of the earth is 6375 km.

The circular velocity is from Eq. (22.1):

$$V = \sqrt{gR}$$

The gravity constant is 9.81 m/s2 so the circular velocity becomes 7908 m/s.

Answer 22.2

Compare the ideal payload mass ratios for single stage, two stage and three stage to orbit rockets if all stages have a propellant ratio of 0.9 and a structural to take-off mass ratio of 0.1. The specific impulse is 4500 m/s and there are no flight losses.

The final to take-off mass ratio of a multistage rocket is from Eq. (22.10):

$$\mu = \prod_{1}^{N}\left[1 - \frac{1}{f_n}(1 - e^{-\Delta V_n / I_{sn}})\right]$$

From Eq. (22.10) the single stage rocket has a cutoff ratio of −1.3 %, the two stage rocket 2.8 % and the three stage tocket 3.6 %. Thus the single stage rocket will not be able to reach orbital speed.

Answer 22.3

Calculate the altitude at which a space plane enters satellite speed (Mach 25) f it flies at a dynamic pressure of 50kPa.

Using q=50 kPa and M=25, the altitude is found from Eq. (22.24) to be 43 km, which means that the whole flight to space will take place within the stratosphere.

Further Reading

There are a number of books available for those wishing a deeper knowledge of aerospace vehicles and propulsion. They include:

J.D. Anderson, A History of Aerodynamics, Cambridge University Press, 1997.

J.D. Anderson, Introduction to Flight, McGraw Hill, 2000.

H. Cohen et al, Gas Turbine Theory, Addison Wesley Longman Ltd. 1998.

N.A. Cumpsty: Jet propulsion, Cambridge University Press, 1997 (reprinted 1999).

E.T. Curran and S.N.B. Murthy, editors, Scramjet Propulsion, AIAA Progress in Aeronautics and Astronautics, Volume 189, 2000.

W.D. Heiser and D.T. Pratt et al, Hypersonic Airbreathing Propulsion, AIAA Education Series, 1994.

D.K. Huzel and D.H. Huang, Design of Liquid-Propellant Rocket Engines, AIAA Progress in Aeronautics and Astronautics, Volume 147, 1992.

J.L. Kerrebrock, Aircraft Engines and Gas Turbines, 2nd ed., Massachusetts Institute of Technology, 1992.

J.D. Mattingly et al, Aircraft Engine Design, AIAA Education Series, 1987.

S.N.B. Murthy and E.T. Curran, High-Speed Flight Propulsion Systems, AIAA Progress in Aeronautics and Astronautics, Volume 137, 1991.

S.N.B. Murthy and E.T. Curran, Developments in High-Speed-Vehicle Propulsion Systems, AIAA Progress in Aeronautics and Astronautics, Volume 165, 1996.

G.C. Oates, Aerothermodynamics of Gas Turbine and Rocket Propulsion, AIAA Education Series, 1988.

D.P. Raymer, Aircraft Design: A Conceptual Approach, AIAA Education Series, 1989.

G.P. Sutton, Rocket Propulsion Elements, John Wiley & Sons, 1986.

P.P. Walsh and P. Fletcher, Gas Turbine Performance, Blackwell Science, 1998.

A. Azuma, The Biokinetics of Flying and Swimming, 2nd Ed., AIAA Educ. Series, 2006.